Exploring the seasonal dynamics of Australian temperate grasslands through phenocam imagery, remote sensing and field data

Christopher J. Watson

A thesis submitted for the degree
Doctor of Philosophy (Science)

Climate Change Cluster
School of Life Sciences
University of Technology Sydney
2017

Certificate of Original Authorship

I certify that the work in this thesis has not previously been submitted for a degree nor has it been submitted as part of requirements for a degree except as fully acknowledged within the text.

I also certify that the thesis has been written by me. Any help that I have received in my research work and the preparation of the thesis itself has been acknowledged. In addition, I certify that all information sources and literature used are indicated in the thesis.

This research is supported by an Australian Government Research Training Program Scholarship.

Signature of Student:

Date: 19/5/2017

Acknowledgements

I would like to express my sincere thanks to my supervisor, Professor Alfredo Huete. He has taught me a great deal about the research process and I am indebted to him for being willing to share his time, wisdom and knowledge of remote sensing.

I also thank Rainer Rehwinkel (NSW OEH) for sharing his time and transmitting his enthusiasm for grassland ecology. His mentorship, training and help in obtaining field sites was invaluable.

Acknowledgement is due to the following organisations for financial support: the UTS Climate Change Cluster, and Australian Wildlife Conservancy grant. Travel funds were granted by the UTS Faculty of Science. This research was supported by an Australian Government Research Training Program Scholarship.

The use of field sites would not have been possible without the permission and ongoing assistance of several people: Dr Sally Power for access to the DRI-GRASS facility, Michael Mulvaney, Greg Baines and Don Fletcher; Peter Saunders and Brett Peden; Tobias and Lawrence Koenig; and David and Judith Watson.

Technical and moral support was provided by past and present post-docs and students of the Huete lab, particularly Zunyi Xie who has set the pace throughout this journey. I also thank members of the Forbes lab 'Shut Up and Write' team, fellow students of the School of Life Sciences, and Dr Andy Leigh, Professor Derek Eamus and Dr Brad Murray for their constructive feedback at various stages. This research would not have been possible without the assistance of the excellent UTS technical and administrative staff and undergrad volunteer, Nicole Laurie.

Sincere thanks are due to my OEH team leaders Terry Brill and Lucian McElwain for continuing to support my studies throughout a period of organisational change.

Finally, thanks to Shari and Izzy for their unwavering support and waggly tail, respectively.

Table of Contents

List of Tables

List of Figures

Abbreviations

ACT	Australian Capital Territory
ANPP	Aboveground Net Primary Productivity
BOM	Bureau of Meteorology
BRDF	Bidirectional Reflectance Distribution Function
C_3	photosynthetic system that uses three carbon molecules; cool season active
C_4	photosynthetic system that uses four carbon molecules; warm season active
CAI	Cellulose Absorption Index
CO_2	Carbon dioxide
ETM+	Enhanced Thematic Mapper plus
EVI	Enhanced Vegetation Index
fAPAR	fraction of Absorbed Photosynthetically Active Radiation
FOV	Field Of View
(f)BG	(fraction of) background substrate
(f)NPV	(fraction of) Non Photosynthetic Vegetation
(f)PV	(fraction of) Photosynthetic Vegetation
Gcc	Green Chromatic Coordinate
LAI	Leaf Area Index
MODIS	Moderate resolution Imaging Spectroradiometer
MSS	Multiscanner System
NDVI	Normalized Difference Vegetation Index
$NDVI_{705}$	Red-edge Normalized Difference Vegetation Index
NIR	Near Infra-Red
NSW	New South Wales
OLI	Operational Land Imager
Phenocam	Time-lapse camera used for monitoring land surface phenology
RGB	(of images, or image capture systems) Red, Green, Blue
ROI	Region of Interest
SWIR	Short-Wave Infra-Red
UTS	University of Technology Sydney
VI	Vegetation Index
WSU	Western Sydney University

Abstract

Management of temperate grasslands in south-eastern Australia is critical to support biodiversity conservation and agriculture under altered rainfall and warming conditions of future climates. Remote sensing is a common tool for monitoring vegetation but the dynamics of temperate grasslands present some unique challenges to conventional remote sensing methods. Land surface phenology—changes in large-scale vegetation dynamics—can improve the characterisation of temperate grasslands but the bulk of research in this field occurs in deciduous systems that show predictable vegetation changes. This research aims to explore drivers of grassland phenology and quantify the vegetation response by using field measurements, spectral instruments, time-lapse 'phenocams' and satellite data.

A series of controlled experiments explored the fundamental expression of grassland characteristics. Spectral ($NDVI_{705}$ vegetation index) and biophysical (fractional cover) response of grassland mesocosms was investigated through manipulation of species, density and disturbance. C_3 and C_4 species showed distinctive phenology profiles, density treatments demonstrated a logical increase in $NDVI_{705}$ from low- to high-density, and recovery of grasslands from disturbance was quantified. Standing litter, a common feature of Australian grasslands, strongly suppressed reflectance-based vegetation indices.

To investigate grassland response to changes in rainfall quantity and timing, phenocams collected sub-daily imagery from rainfall exclusion plots. Five treatments were assessed: ambient rainfall, increased rainfall, decreased rainfall, summer drought and extreme events. The Green Chromatic Coordinate index (g_{CC}) showed dynamic response to rainfall in all treatments. Increasing quantities of rainfall resulted in significantly higher productivity throughout the year. Grassland productivity increased during cooler months from extreme events, but was equivalent to ambient rainfall during summer months. Summer drought unexpectedly drove higher g_{CC} during non-drought periods, which was attributed to exotic forb invasions following disturbance.

Field research was conducted on native and exotic C_3- and C_4-dominated grasslands in the South Eastern Highlands bioregion. Floristic surveys showed high variation in species richness and condition throughout the year, with highest detection of native

species during summer months. Sites comprising multiple dominant species with overlapping phenophases showed a complex relationship with land surface phenology. Comparison of satellite NDVI (MODIS Terra, Landsat ETM+/OLI), phenocam and field variables showed that satellites and phenocams were equivalent at estimating green cover but the higher temporal capacity of phenocams allowed more precise definition of greening/browning trends.

Dynamic knowledge of field conditions is essential for validating remote sensing phenology studies. This research develops a greater understanding of non-conventional phenology and provides practical tools to improve management of temperate grasslands.

Chapter 1: Introduction

The research that forms the basis for this thesis is multidisciplinary in nature, with its main components being grassland ecology, remote sensing and phenology. This introduction provides an overview of these different components, and explains how they relate to one another in the context of the individual research projects.

Grasslands are a dominant biome, both globally and within Australia. Chapter 1 describes the importance and ecology of Australian grasslands, particularly in temperate south-eastern Australia. Section 1.3 identifies the key threats and challenges facing grasslands within temperate Australia, and outlines the need for appropriate monitoring and management to meet these challenges.

Remote sensing is now a common tool used to provide information on the vegetated landscape and forms a key part of this thesis. Section 1.4 highlights the different methods by which remote sensing can be used to gather information on vegetation, and gives some examples of relevant remote sensing studies that have been conducted in Australia and throughout the world.

Phenology is the study of seasonally-recurring events and has been used for centuries as a form of environmental monitoring. Section 1.5 outlines the concepts of phenological research, discusses the reasons for the recent increase in popularity of this discipline, and demonstrates what methods are used to study phenological variables.

These components are brought together in the context of how remote sensing of phenology can be used to provide information about Australian temperate grasslands. Section 1.6 provides conceptual models of the factors that impact grassland phenology.

Finally, the introduction will provide clear aims of the thesis, and provide direction to subsequent chapters.

1.1 TERMINOLOGY

The terminology regarding grasses and grasslands can be ambiguous, as commonly-used words have precise meanings in this field. For example, the term 'pasture' implies land that is grazed by domestic stock, whereas 'grassland' is a more generic term that may include natural systems as well as pasture. Some terms have different or interchangeable meanings in different countries, or even regions within the same country. The following words are used frequently throughout this thesis, and some guidance is provided on their usage.

The International Forage and Grazing Lands Terminology Committee has developed standard definitions of terms to enable accurate communication within and between countries (Allen *et al.* 2011). While useful for agricultural practitioners, these definitions have a clear bias towards grazing systems over natural systems. For example, a productive exotic grass species may be seen as beneficial by a grazier and termed 'improved pasture', but the same plant may be viewed as a weed in a conservation reserve. As such, some of the following terms are defined according to the aforementioned committee and are indicated (§). Others are synthesised from a combination of ecological and agricultural sources (as in Tremont and McIntyre 1994) and incorporate a more balanced definition that includes multiple needs and priorities.

Grassland: Land dominated by a ground cover of grasses, graminoids and forbs, with a notable absence of woody species.

Native grassland: Areas that contain predominantly native grass and forb plants, and are largely devoid of trees and shrubs (Benson 1994); also 'treeless communities dominated by native perennial grasses and forbs as well as some annuals' (Groves and Whalley 2002).

Temperate grassland: Grassland within distinct geographic and rainfall zones defined by Moore and Perry (1970) – refer to Section 1.3.

Natural temperate grassland:

A grassland community of high conservation value that occurs within the South Eastern Highlands bioregion of the Australian

Capital Territory (ACT) and New South Wales (NSW), and is listed under the *Environmental Protection and Biodiversity Conservation Act 1999.*

Native pasture: Natural ecosystem dominated by indigenous or naturally-occurring grasses and other herbaceous species, used mainly for grazing by livestock and wildlife[§].

Improved pasture (also exotic pasture):

Non-native pasture that may include exotic grasses and other introduced pasture species such as legumes.

Rangelands: Land on which the indigenous vegetation is predominantly grasses, graminoids, forbs or shrubs that are grazed or have the potential to be grazed[§]. In Australia, rangeland tends to refer to arid and semi-arid regions rather than temperate regions.

Native: Indigenous to a region.

Exotic/Introduced: Non-indigenous to a region.

Invasive plant: A species that readily colonises land to the detriment of native ecosystem function and other land uses.

Weed: A native or exotic plant (though usually exotic) that causes a loss in utility (e.g. grazing productivity) or native ecosystem function.

Grass: Plant species from the Poaceae family[§].

Graminoid: A grass or grass-like plant (e.g. sedges or rushes).

Forb: Any herbaceous non-graminoid.

Shrub: A woody plant having multiple stems arising near the base[§].

C_3 plants: Vegetation that utilises the C_3 photosynthetic pathway. These plants tend to predominate in cooler, mesic environments.

C_4 plants: Vegetation that utilises the C_4 photosynthetic pathway. These plants tend to predominate in areas of higher temperatures. They have a higher water use efficiency, thus also tend to dominate more arid environments.

Ecological community:

A group of interacting species in a unique habitat.

Botanical composition:

The relative proportions of the plant components in a canopy above a defined sampling height[§].

Sward: A population or a community of herbaceous plants characterised by a relatively short habit of growth and relatively continuous ground cover[§], used mostly in a grassland management context.

1.2 Grasslands: Characteristics, Uses and Threats

Grasslands are the most extensive biome on earth, occupying an area of approximately 40% of the earth's vegetated surface (White, Murray, *et al.* 2000, O'Mara 2012). Although precise definitions vary in detail (Gibson 2009), common characteristics of grasslands include a composition of almost exclusively ground level flora, with minimal woody plants, dominated by species of the family Poaceae. Extensive grasslands are found in every continent except for Antarctica and include the great prairies of North America, the eastern Eurasian steppe of Mongolia, China and Russia, the Argentine pampas, managed meadows of Europe, and the extensive grasslands of the Serengeti. They cover a wide range of climatic zones, ranging from tropical moist climates to dry and cool environments (Campbell *et al.* 1997).

Grasslands provide a range of ecosystem services, acting as repositories of biodiversity, providing high rates of carbon sequestration, and performing critical cycling of nutrients (White, Murray, *et al.* 2000, Jones and Donnelly 2004, Fry *et al.* 2013). They provide anthropocentric services including ecotourism and recreation, particularly in Africa, as well as producing biomass for biofuels (Gibson 2009). The most significant service that

grasslands provides is a food source for large herbivores (Groves and Whalley 2002). This grass-grazer relationship is present in all grassland environments and suggests that the evolution and continued presence of grasslands depends on this interaction (Coughenor 1985). This relationship has extended to domestic animals such as cattle and sheep, and as a result grazing agriculture has impacted native grasslands throughout the world. Threats to grasslands that have emerged as a direct result of grazing are habitat fragmentation, altered disturbance regimes, and increased levels of invasive species (Gibson 2009, Williams and Morgan 2015). Nevertheless, grazing-based agriculture is a major process in most parts of the world and provides economic benefit and food to millions of people.

The growing awareness of climate change has brought attention to new threats to grassland biomes that act independently of, or are exacerbated by, human activities. Increased atmospheric carbon dioxide is expected to globally increase plant productivity, change vegetation community structure, and increase the abundance of woody plants (Kulmatiski and Beard 2013, Volder *et al.* 2013). Increased temperatures and evaporation rates are predicted to cause less water availability, alter seasonal timing of key events (phenology), increase wildfire frequency, and provide competitive advantage for certain species (Pitman *et al.* 2007, Dostálek and Frantík 2011). Changes in rainfall regimes will differ by region, but will generally result in altered quantity, seasonality and frequency, leading to more extreme rain events and subsequent changes to ecosystems (IPCC 2014). When all these factors are taken in combination, the short-term and long-term effect on grassland vegetation is extremely difficult to predict (Williams, Marshall, Morgan, *et al.* 2015). In part, this is due to grasslands' characteristics of responding quickly and dynamically to environmental drivers (Petrie *et al.* 2011). Likely impacts to grassland biomes include increased levels of fire and other disturbance (Dunlop and Brown 2008), a decrease in available moisture and increase in periodic drought (Williams, Marshall, Morgan, *et al.* 2015), increases in weed invasions (Howden *et al.* 1999, Hughes 2000) and widespread changes in species composition and ecosystem function (Fay *et al.* 2008, Baldocchi 2011, IPCC 2014). Being able to more accurately predict the effects of climate change on grassland is critical for global food security (O'Mara 2012), but also for retaining the immense biodiversity that these lands contain. The latter is of particular concern, given that only

7.6% of the world's grasslands are managed under protected areas, one-third of which are in Africa (Gibson 2009).

1.3 Australian Temperate Grasslands

Fossilised pollen of grass species have been found in Australia dating back to the Eocene period, some 40 million years ago (MacPhail and Hill 2002). However, the fossil record does not show significant grassland presence until the beginning of the Pleistocene period, 2.5 million years ago (Gott *et al.* 2015). As in most parts of the world, grasslands co-evolved with large grazing herbivores; in the case of Australia, these were predominantly macropods such as kangaroos. When Aboriginal people arrived in the country some 50,000 years ago, grasslands would have been commonplace in many regions—in fact treeless vegetation covered most of south-eastern Australia as little as 20,000 years ago (Hill 2004). Aboriginal land management, in the form of regular fire disturbance (so-called 'firestick farming'), ensured the ongoing succession of grasslands and the periodic rejuvenation of the grasses and forbs. However for the last 12,000 years, grasslands generally have been restricted to areas where the dominant tree species, *Eucalyptus*, does not occur (Petherick *et al.* 2013). These trees are typically excluded through the restriction of seedling establishment and growth. This occurs in environments where frequent fire or seasonal frosts occur, where soils impede tree seedling establishment, such as the cracking clay soils of north-western New South Wales, or where humans or animals prevent it (Gott *et al.* 2015).

According to some definitions, Australia has the highest land area of grassland at 6.6×10^6 km^2, with 85.4% of the country classified as grassland (White, Murray, *et al.* 2000). However, a more conservative definition that excludes the extensive savannahs of the country's north places the grassland proportion at a more modest, but still significant, 37% of the total continental area (Lymburner *et al.* 2011; Figure 1.1a).

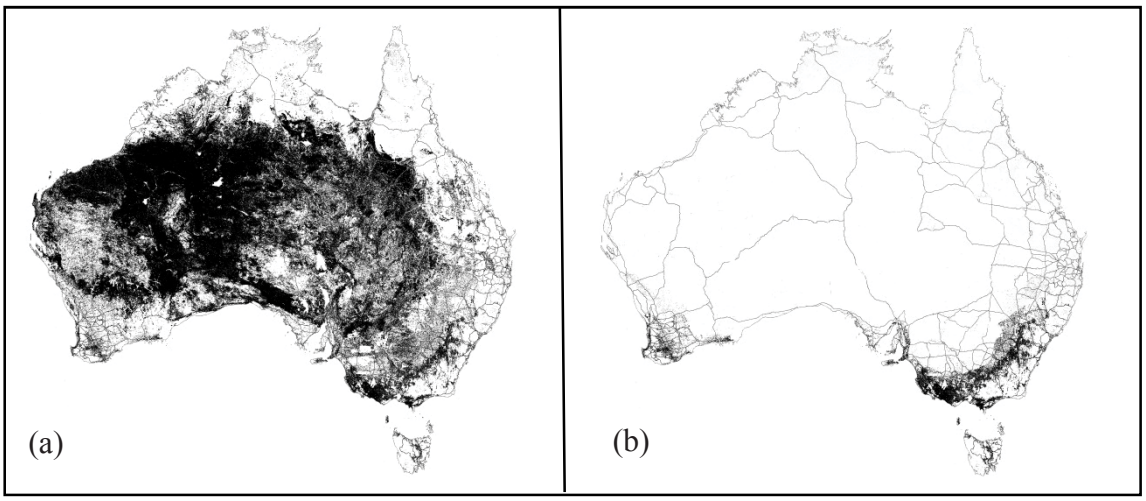

Figure 1.1. Area of Australia occupied by (a) all grasslands, and (b) temperate grasslands (black shading; adapted from Lymburner et al. 2011).

Four major grassland zones are identified in the Australian landscape (Moore and Perry 1970, Groves 1979, 1994); these are detailed in Table 1.1. Tussock grasslands of the temperate zones, the main focus of this thesis, represent only a small fraction of the total (Figure 1.1b), but are proportionally important in the context of food production and biodiversity. Moore and Perry define these 'temperate grasslands'—as is termed throughout this thesis—as being located in New South Wales, Victoria and parts of South Australia, where rain falls mainly in winter or year-round, and are dominated by tussock species of the genera *Themeda*, *Poa*, and *Austrostipa* (Moore and Perry 1970). This temperate grassland subset is within their classification of 'subhumid grasslands of southern Australia', but excludes the tropic subhumid grasslands of Queensland and the montane subalpine grasslands of south-eastern Australia.

Table 1.1. Classification of Australian grasslands (Moore and Perry 1970), with updated taxonomy.

Grassland type	Description
Arid tussock grassland	Areas of Mitchell grasses or *Astrebla* species extensively distributed in inland Queensland, Northern Territory and northern Western Australia in a zone receiving between 200 and 500 mm average annual rainfall and characterised by predominately summer rain
Arid hummock grassland	Dominated by the genus *Triodia* in areas with less than 200 mm average annual summer and/or winter rainfall. They cover over 20% of Australia and most of arid Australia
Coastal grassland	Dominated by the genera *Sporobolus* and *Xerochloa* and confined to the tropical summer-rainfall region of the northern coastline.
Sub-humid grassland ***(1) Tropical grassland***	Dominated by *Dichanthium* and *Eulalia* and sometimes by *Bothriochloa* and *Heteropogon* in eastern and northern Queensland in regions with mostly summer rain.
(2) Temperate grassland	With an irregular distribution north of Adelaide around the zone of 500–1000 mm average annual winter and/or summer rainfall of south-eastern Australia to northern New South Wales. Dominant genera are *Poa, Rytidosperma* and *Austrostipa.*
(3) Subalpine grassland	Confined to the cold and wet mountain regions of the Monaro region of southern New South Wales and north-eastern Victoria. Dominant genera are *Poa* and *Rytidosperma.* These grasslands are similar in many respects to some of the New Zealand tussock grasslands.

1.3.1 Characteristics of Australian temperate grasslands

Native temperate grasslands have several distinctive features that define how they shape the landscape and respond to biotic and abiotic drivers. Groves and Whalley (2002) identify four functional floristic components that contribute to the species composition of temperate grasslands:

1. C_3 grasses, such as *Poa*, *Rytidosperma*, and *Austrostipa* genera, which grow most vigorously in spring and autumn when temperatures are lower and the day length is shorter. These grasses, particularly, *Rytidosperma* and *Austrostipa* will dominate more disturbed environments in the absence of annual or exotic species (Moore 1970).
2. C_4 grasses, such as *Themeda triandra*, which grow best in summer and retain the capability to respond to summer rains. *T. triandra* is considered a climax community in many locations and is indicative of a high-quality native grassland (Lazarides 2002, Rehwinkel 2007).
3. A suite of perennial and annual native forbs that occupy the intertussock spaces, providing most of the floral diversity of the grassland. These forbs typically flower during mid to late spring and are often inconspicuous at other times of the year.
4. Exotic grasses and forbs resulting from continuous grazing and subsequent changes in nutrient distribution.

In addition, other researchers have identified key characteristics of south-eastern temperate grassland that help in understanding the nature of these unique ecosystems.

The ongoing presence of grasslands in many locations is driven by land management and climate. Continuous grazing restricts the establishment of woody seedlings, even in the absence of fire. In addition, many grasslands are located in frost hollows, where cold air drains from higher elevations and kills or retards developing tree seedlings (Wearne and Morgan 2001).

Maintenance of the distinct tussock/intertussock structure is driven by ecosystem processes that impede the development of full canopy cover, namely fire or grazing.

Periodic fires have been shown to maintain diversity in *Themeda* grasslands, with vegetation diversity being maintained even when exposed to annual fires (Stuwe and Parsons 1977, Robertson 1985, Lunt and Morgan 2002). In the absence of fire, the ecological condition worsens: unburnt *Themeda* swards show lower native species diversity and higher numbers of exotic species when left unburnt for more than a decade (Morgan and Lunt 1999). Most native grassland species resprout after fire (as opposed to germinating from seed), hence in the absence of invasive species the community structure after fire is relatively unchanged. There are few studies of other grassland types' response to fire, though it has been suggested that *Poa*- and *Rytidosperma*-dominated grasslands may show a different response to *Themeda* grasslands (Williams *et al.* 2006, Prober *et al.* 2007).

Temperate grass leaves grow and senesce within a year and remain attached to the plant after death (Morgan 2015). As such, temperate grasslands have a significant fraction of their biomass retained as standing dead litter (Morgan and Lunt 1999). This dead material contributes to the spread of fire within grassland, but when left unburnt can shade out emergent forbs and ultimately result in plant death (Morgan and Lunt 1999).

Despite occurring in temperate zones with distinct seasons, rainfall quantity and seasonal variability is a primary driver on annual cover, biomass, flowering and botanical composition (Morgan and Williams 2015). Like other grasslands around the world (e.g. Hill 2013), Australian temperate grasslands are highly dynamic in space and time and respond quickly to environmental conditions (Morgan and Williams 2015). Because temperate grasslands contain different functional floristic components—some of which have differential responses to environmental drivers—the dynamics and species interactions within these grasslands are complex.

The matrix of agricultural grazing and natural grassland is a global phenomenon due to the domestication of livestock and the grass-grazer relationship (Gibson 2009), but is particularly evident in temperate Australia. As such, temperate grasslands occupy a continuum along an ecological gradient from native to modified to exotic-dominated (Hill *et al.* 2006). Pastoral land use is not only important from a food production perspective, but also from an historical and cultural perspective.

1.3.2 Temperate grasslands for food production

The temperate grasslands of south-eastern Australia were managed by indigenous land managers for thousands of years prior to European settlement. Indigenous people mostly used grassland forbs as food sources, rather than the grasses themselves (Gott 1982), but used fire management as a way of ensuring the ongoing viability of these food sources (Gammage 2011).

Upon British colonisation, the south-eastern temperate grasslands were viewed as attractive grazing lands, particularly for sheep (Gott *et al.* 2015). Most parts of the south-east were stocked with sheep by the mid-1830s, and by 1850, Australia's sheep population numbered 3 million (Pearson and Lennon 2010). Shortly thereafter, the degradation of grazing lands from overstocking and hard-hooved livestock was evident and the community composition of many grasslands began to change. Large numbers of exotic species became common throughout the landscape, either through deliberate introductions as exotic pastures or through accidental release. Pasture improvement through application of artificial fertilisers became common around 1930. This resulted in the increased productivity of exotic pasture species that out-competed native grasses which are adapted to Australia's nutrient poor soils. Moore (1970) provides an accurate representation of temperate grassland compositional change under grazing regimes that broadly describes ecosystem change from native perennial climax species to native perennial disturbance-tolerant species through to annual exotic species.

Despite the increased levels of invasive and exotic species, primary productivity of grasslands within the temperate region is very high, relative to the rest of the country. Currently, temperate grasslands of south-eastern Australia continue to support extensive grazing operations, particularly cattle production for meat and dairy and sheep production for meat and wool. The proportion of meat and wool production occurring in south-eastern Australia relative to the rest of Australia is presented in Table 1.2. Over 60% of the $28 billion annual economic value of these industries is contributed from temperate areas. This is due to the moderate climate that enables grass productivity year-round, thereby supporting higher stock carrying capacity. The production of high-quality wool in these regions is attributed to the consistent pasture quality. Lazarides (2002) notes that the pasture grasses of the temperate regions are generally more

palatable and nutritious than those of other regions due to more fertile soils, less severe climate, and rainfall that is more reliable.

Table 1.2. Proportion of meat, dairy and wool production on temperate grasslands in Australia (collated from the Australian Bureau of Agricultural and Resource Economics and Sciences 2013).

Commodity	Animals (millions)	Proportion in temperate south-eastern Australia	Approximate economic value (AUD billion/year)
Sheep (wool)	37.68	51.5%	$0.98
Sheep (meat)			$0.53
Cattle (dairy)	1.42	89.3%	$11.61
Cattle (meat)	9.02	31.7%	$3.88
		Total Value	$17.0
		Total Economic Proportion (against national figures)	60.33%

Currently, the landscape in these temperate areas is a matrix of exotic and native pastures with isolated pockets of undisturbed native grasslands. While exotic pastures are still commonly employed—and in fact are proving difficult to remove from the landscape for conservation purposes (Zerger *et al.* 2011)—the value of native pastures is increasingly recognised as part of sustainable land management practices (Wong and Dorrough 2015). Native grasses, particularly those that possess the C_4 photosynthetic pathway, have the ability to produce leaf matter throughout the year, unlike many exotic species that senesce in summer (Crosthwaite 1995). Furthermore, native grasses are more resilient to drought, and do not require artificial fertilisers in order to thrive (Dunin *et al.* 1978, Ross 1999, CSIRO 2011).

The challenges to temperate grasslands in a food production context relate mostly to potential decreases in productivity resulting from by climate change impacts. These include increased levels of invasive species, higher temperatures and evaporation rates, more variable rainfall, and more extreme events such as droughts and storms (Hennessy *et al.* 2007). These impacts are likely to have some predictable effects, such as the overall loss of productivity despite the 'CO_2 fertilisation effect', but many of the ecological and seasonal impacts are difficult to forecast. For this reason, it is important

to understand grassland productivity and function on a large scale such that informed adaptation strategies can be prepared.

1.3.3 Temperate grasslands for native biodiversity

On a global scale, temperate grasslands represent the most poorly protected biome, with just 4% of the world's temperate grasslands awarded some level of protection (United Nations Environment Programme 2008, Henwood 2010). In south-eastern Australia, it is estimated that of the 470,000 ha of temperate grassland that was present before European settlement, only 5,800 ha (1.2%) remain in 'natural' condition (Williams and Morgan 2015). Of these, most exist in small, fragmented areas that have been excluded from continuous or high-impact grazing such as cemeteries, road/rail reserves, and travelling stock routes (Lunt 1997, Ross 1999).

One of the key features of temperate grasslands is the diverse array of forbs that grow in the intertussock spaces between the grasses. These forbs are a major contributor to the biodiversity of these areas, and comprise the majority of the species richness (Tremont and McIntyre 1994). As such, temperate grasslands can be extremely species rich, with native species richness of up to 25–35 species/m^2 having been reported (Kirkpatrick 1999, Scott and Morgan 2012). In terms of native fauna, temperate grasslands are home to a number of endemic fauna species, particularly reptiles, birds, and invertebrates (Williams, Marshall, and Morgan 2015). The grassland earless dragon *(Tympanocryptis pinguicolla*) and striped legless lizard (*Delma impar*) are two reptiles that are temperate grassland specialists. The plains-wanderer (*Pedionomus torquatus*) is one of the world's most threatened birds (Jetz *et al.* 2014) and as a grassland specialist is a flagship species for temperate grassland conservation. Quails, button-quails and dryland shorebirds also rely on this habitat. Some overlooked animals that have their last refuge in temperate grasslands are invertebrates. The golden sun moth (*Synemon plana*) and the Perunga grasshopper (*Perunga ochracea*) are examples of such threatened species. Regrettably, many grassland mammal species are already extinct.

The primary threats to the biodiversity and ecological function of native grasslands as identified in a recent summary (Morgan and Williams 2015) are:

- agriculture (including fertilisation, introduction of exotic species, and overgrazing/overstocking);
- habitat fragmentation;
- continual habitat loss (land clearing);
- weeds and feral animals;
- inappropriate disturbance regimes (particularly lack of fire); and
- climate change.

The majority of these threats will have predictably negative effects on natural systems, with most contributing to a direct loss of habitat, or the ecological degradation of that habitat through invasive species and/or other disturbance. Climate change presents an extra dimension to these threats, as the pathways through which it will affect temperate systems are broadly unknown. There is a paucity of experimental studies that test climate change impacts on Australian grasslands. The few that have been conducted highlight the complexity of climate-vegetation interactions. Generally, both herbaceous and woody C_3 species are thought to benefit more from the CO_2 fertilisation effect than C_4 species (Morgan *et al.* 2011) though higher temperatures and more extreme rainfall regimes may modulate this. Some studies using free air carbon enrichment (FACE) and warming to manipulate natural environments have suggested the opposite: that *Themeda triandra* as a C_4 species may increase in dominance as increased CO_2 and higher temperatures negatively impact the co-dominant C_3 species *Rytidosperma caespitosa* (Williams *et al.* 2007). Although uncertainty remains, it is clear that climate change will exacerbate many of the existing threats to temperate grasslands (Dunlop and Brown 2008).

There is a pressing need to understand and improve the conservation of these remnant grasslands through an understanding of their ecology, response to climatic drivers, and interaction with herbivores. In a complementary fashion, there is also an urgent need to undertake restoration works to increase the quality of native grasslands in this region, and to monitor the progress of these restorations in the midst of a changing climate.

1.3.4 Challenges in managing temperate grasslands

The current challenge of managing temperate grassland is two-pronged: to ensure that grassland productivity is sufficient to ensure adequate livestock production and food security for coming decades, and to ensure the improved biodiversity and increased sustainability of native grassland communities. While these challenges seem directly opposed to one another, in fact they require a similar approach: long-term monitoring of vegetation dynamics. It is also essential to co-monitor climatic variables to avoid drawing erroneous conclusions: for example that a decrease in vegetation quantity is due to land management rather than a drought event.

The monitoring of grazing lands has traditionally been relatively straightforward. Vegetation quantity is the primary variable of interest, although to some extent the composition of the pasture is important—particularly if weeds are a significant contributor. Monitoring of grasslands for conservation is more complex. Usually, some estimation of vegetation condition is required, which relates to the structure, quantity and composition of vegetation species (Sharp 2006, Seddon *et al.* 2011). However, a precise definition of vegetation condition has been difficult for land managers to agree upon (Keith and Gorrod 2006).

Most assessments of grassland condition are conducted through fieldwork: on-ground assessments of species composition, abiotic components, and biophysical parameters (e.g. Rehwinkel 2007). However, grasslands are by their nature spatially and temporally heterogeneous, and point-source field measurements only apply to the immediate area and the immediate time that they are taken. To adequately characterise a large area, multiple samples in space and time are needed, which requires a large investment in resources (Psomas *et al.* 2011).

From a regional scale and greater, the management of grassland resources faces an additional problem in that the majority of grasslands occur on private lands (NSW Natural Resources Advisory Council 2010). On private lands, access for inventory and monitoring may be restricted; and therefore large areas of grassland may be unknown. It has been recognised that in this situation, grassland managers need reliable data across multiple landscape units to support regional management strategies (Moran et al 1997).

A conventional solution to this challenge is to use remotely-sensed data collected from satellites or aircraft. Remote sensing offers a more efficient complement to the collection of field data, and an opportunity to gather ecologically-relevant information over large geographical areas. It is regarded as an efficient and accurate method of collecting consistent information about the vegetated landscape (Peterson *et al.* 2002).

1.4 Remote Sensing of Vegetation

Fundamentally, remote sensing is the collection of electromagnetic energy by a sensor, and using the characteristics of this energy to identify properties and patterns at the earth's surface (Ustin *et al.* 2004). Conventional sensors can be integrated into a satellite, mounted on an airborne platform (such as from a helicopter), or used as hand-held devices at canopy or ground level, thus being able to provide information about the surface of the earth at many different scales. Remote sensing is used for a wide variety of applications, and increasingly in ecological studies (Pettorelli *et al.* 2005). Remote sensing is currently used in an ecological context to:

- provide land cover and vegetation mapping (Kokaly *et al.* 2003, Lymburner *et al.* 2011, Youngentob *et al.* 2011);
- locate and map invasive species (Kalapos 1994, Hestir *et al.* 2008, Kandwal *et al.* 2009, Gavier-Pizarro *et al.* 2012);
- estimate productivity (Brinkmann *et al.* 2011; Gu, Wylie and Bliss 2013; Donald *et al.* 2010);
- determine vegetation density and structure (Coops *et al.* 2004, Wood *et al.* 2012);
- study potential climate change impacts (Donohue *et al.* 2009); and
- track phenological changes (Ahl *et al.* 2006, Soudani *et al.* 2006, Jenerette *et al.* 2010).

Objects of different composition are identified spectrally by comparing their reflectance characteristics at different wavelengths (Xie *et al.* 2008). Early remote sensing technologies, particularly satellite-based sensors, used a few broad wavelength bands in the visible and infrared ranges to collect data. The earliest Landsat-based sensor, the Multispectral Scanner System (MSS), collected four spectral bands from the 0.5 μm–1.1 μm range of the spectrum. Those sensors that use only a few wavebands are known

as multispectral sensors. Throughout the years, these technologies have improved to increase the number of bands (spectral resolution), the level of ground detail (spatial resolution) and the re-visit time (temporal resolution). The current generation of sensors in use are termed 'hyperspectral' as opposed to multispectral, as they can detect hundreds of discrete bands across the spectrum. This provides a much greater discriminatory ability and higher sensitivity than multispectral systems (Hansen and Schjoerring 2003, Glenn *et al.* 2005, Lawrence *et al.* 2006), but requires more computing resources for analysis (Xie *et al.* 2008). Furthermore, many of the bands co-vary in the information that they provide, resulting in redundant wavelength bands (Blackburn 2007). The majority of ground-based sensors currently used (e.g. spectroradiometers) are hyperspectral in nature, while satellite systems are still dominated by multispectral sensors. Though hyperspectral sensors for satellite and airborne platforms are increasing in popularity, the high cost of acquiring and processing hyperspectral imagery is still an impediment to widespread use (Gavier-Pizarro *et al.* 2012).

Currently there are many satellite-based sensors that are available to provide data on the earth's surface. With all sensors, there are trade-offs between spectral, spatial and temporal resolution that are pertinent to the data needs of the user. Much of this satellite data is becoming more accessible, through its release by data custodians or through ecological networks that link remote sensing experts with other ecologists (e.g. TERN-Auscover in Australia). This accessibility is resulting in development of novel methodology and applications that are further increasing the utility of remotely-sensed data (Reed *et al.* 2009).

1.4.1 Vegetation spectral signatures

Vegetation spectral signatures are determined by an integrated combination of leaf biochemistry and canopy structural properties. This includes factors such as photosynthetic pigments, water content, nitrogen concentration, specific leaf area, leaf area index, leaf angle distribution and canopy architecture (Asner *et al.* 2008). The spectral signature of photosynthetic vegetation is very distinct and is illustrated in Figure 1.2 (from Chuvieco and Huete 2009). The typical pattern is a low reflectance in the visible portion of the spectrum (0.4–0.7 μm) due to the high absorbance of light in

these wavelengths by chlorophyll and other photosynthetic pigments. The green wavelengths (0.5–0.6 μm) are reflected more than others in this portion—hence why healthy foliage appears green—but red light (0.6–0.7 μm) is highly absorbed for photosynthesis. Reflectance in the near infrared band (NIR; 0.7–1.1 μm) is very high; the light in this portion is not used for photosynthesis and is scattered as a result of canopy architecture and the intercellular structure of the plant. Absorbance in the short-wave infrared (SWIR; 1.1–2.5 μm) is strongly influenced by water absorbance features, and plant dry matter (Ustin *et al.* 2004, Vohland and Jarmer 2008). The large difference in reflectance between the adjacent red and NIR regions is termed the red edge (Dawson and Curran 1998), and is routinely used to gather information about vigour, health, or stressed condition of plants (Coops *et al.* 2004, Mutanga and Skidmore 2004a, Campbell *et al.* 2007, Govender *et al.* 2007).

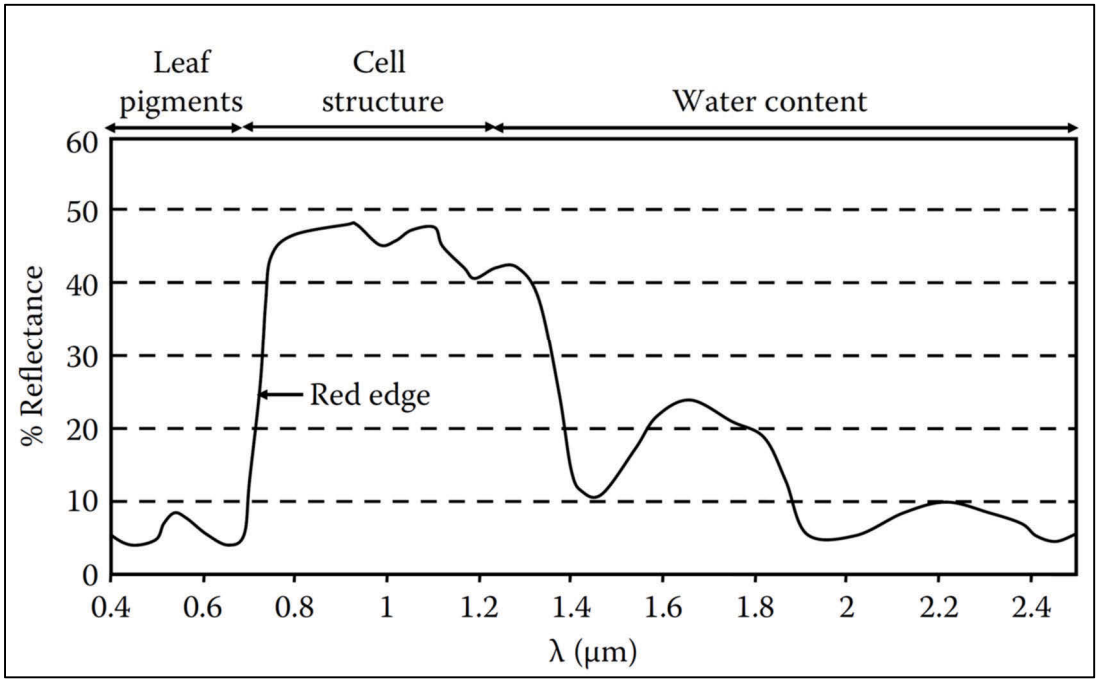

Figure 1.2. Typical vegetation reflectance spectrum, indicating the primary contributors to spectral characteristics (from Chuvieco and Huete 2009).

1.4.2 Vegetation indices

Biophysical characteristics, such as leaf area index (LAI), biomass, chlorophyll content, and fraction of absorbed radiation (fAPAR) are among the most important vegetation parameters for ecological studies (Qi *et al.* 1995, Yang *et al.* 1998, Lu *et al.* 2003).

They provide direct information about the amount and condition of vegetation in a given area, which is the primary driver for global energy and carbon fluxes (Si *et al.* 2012). A common method to relate biophysical parameters to spectral response is through the use of vegetation indices (VIs). VIs are spectral transformations of two or more wavelength bands designed to enhance the contribution of vegetation properties (Asner *et al.* 1998, Huete *et al.* 2002). They are a representation of photosynthetic activity, or 'greenness' of a scene, and are a composite of leaf area, chlorophyll content, and canopy cover/structure (Glenn *et al.* 2008). A good VI should have a predictable response for biophysical parameters over a range of growing conditions, should normalise external effects such as viewing geometry, and normalise internal effects such as soil background (Huete *et al.* 1994). Over the past decades, dozens of VIs have been developed for different environments and purposes. The most common include the Normalized Difference Vegetation Index (NDVI) (Rouse *et al.* 1974, Tucker 1979); the Enhanced Vegetation Index (EVI) (Huete *et al.* 2002) and the Soil Adjusted Vegetation Index (SAVI) (Huete 1988). These were generally developed for use with multispectral systems, and are known as broad-band VIs. With the advent of hyperspectral sensors, narrow-band VIs have been developed that utilise ratios from single wavelength bands. While hyperspectral indices can track specific signals accurately (Rahman *et al.* 2003), narrow-band VIs do not always outperform broad-band VIs (Goel *et al.* 2003).

With the understanding that VIs are a representation of biophysical parameters, researchers are increasingly using time-series VI measures as an indication of how these parameters change over time, and how this relates to the drivers of ecosystems.

1.4.3 Challenges to remote sensing of Australian temperate grassland

Australian vegetation presents a number of challenges to traditional remote sensing methods (Datt 1998, Goodwin *et al.* 2005). The primary issue at a landscape scale is the canopy architecture of the dominant tree genus, *Eucalyptus*. Unlike in many broadleaf ecosystems (where many remote sensing methods were developed), eucalypts have pendulous leaves that render the canopy semitransparent (Greaves and Spencer 1993, Kumar 1998), and mixes the tree signal with that of the understory vegetation (Goodwin *et al.* 2005). This is particularly true for 'two-canopy systems', such as savannahs or open woodlands, that remain one of the biggest challenges for remote sensing (Hill *et*

al. 2011). As grasses comprise a significant component of the understory across various biomes (e.g. Tozer *et al.* 2010), understanding the grass response is critical not only to 'pure' grasslands, but to the successful assessment of other grassy ecosystems.

Australia's climate is typified by periods of low rainfall as a result of the El Niño Southern Oscillation (McAlpine *et al.* 2009). These droughts, together with the low nutrient content of many soils, have shaped the evolution of the vegetation on the continent (Specht 1969). Many plants have adaptations to reduce moisture loss (e.g. leaves with thick epidermis or waxy cuticles) or to increase moisture gathering capacity (e.g. deep taproots). As herbaceous species such as grasses do not always have the mechanisms to survive over very long drought periods, they tend to be responsive to rainfall events, and can re-sprout or germinate quickly to repopulate an area, particularly after fire (Tremont and McIntyre 1994). As such, grasslands show a high variability in condition and species composition between seasons and years. This dynamic state makes it difficult to track ecological trends via remote sensing and impossible to compare satellite to field data if not collected concurrently (Gao 2006).

Australia shows less distinct seasonal variation when compared to other temperate environments, which makes traditional seasonal metrics such as 'start of season' more difficult to define. In Australia, tropical grasslands and savannahs contain a majority of C_4 species, and their phenology is mostly driven by wet season rainfall amount and timing (Williams *et al.* 1997). In contrast, temperate grasslands often include a mix of native and exotic C_3 and C_4 species and can be extremely dynamic in response to changes in climate (Vohland and Jarmer 2008). Montane grasslands are impacted by winter snowfall and may show seasonal profile more typical of northern hemisphere temperate vegetation types. Arid and semi-arid rangelands are also highly responsive to rainfall drivers, and their ecosystem dynamics have an annual or ephemeral vegetation component (Lewis *et al.* 2001, Greenville *et al.* 2009).

While there is a long history of remote sensing of vegetation in Australian environments (Foran 1987, Pech and Davis 1987), researchers in the past have tended to focus on woody vegetation types (Zerger *et al.* 2011). Australian scientists have explored remote sensing as a tool for estimating deforestation and regrowth (Kuhnell *et al.* 1998), conducting community and habitat classification (Goodwin *et al.* 2005) and assessment

of forest health and species richness (Coops *et al.* 2004, Waring *et al.* 2006). Non-woody vegetation studies are more limited, but have included pasture productivity studies, particularly in rangeland systems (e.g. Donald et al., 2010; Hill, Donald, Hyder, and Smith, 2004), fuel loading investigations for bushfire hazard reduction (Paltridge and Barber 1988, Dilley *et al.* 2004, Martin *et al.* 2009, Verbesselt, Hyndman, Newnham, *et al.* 2010), and vegetation recovery after fire (Greenville *et al.* 2009, Levin *et al.* 2012). Lu and colleagues used time series data to separate woody from non-woody cover and generate seasonal maps of each fraction (Lu *et al.* 2003).

A small number of published Australian studies have used remote sensing techniques to acquire information on temperate grasslands. Early use of Landsat imagery from the Monaro district of the Southern Tablelands found limited success in separating native from modified grasslands (Benson 1994), though separating grassland from woody vegetation was possible. The same conclusion was reached for the derived grasslands of the Riverine Plain (Benson *et al.* 1997). More recently, the work of Zerger and colleagues suggests that optimal sites for temperate grassland rehabilitation may be identified by Landsat-estimated soil nutrient content, as native species are unlikely to outcompete exotic species where nutrient content is high (Zerger *et al.* 2011).

Integrating fieldwork with remote sensing is crucial to provide validation of remote sensing data, confirm relationships between remote sensing products and field characteristics, and to fully explain changes in remote sensing signals (Cheng *et al.* 2006). Further work, however, is required to effectively integrate the two approaches for mapping and monitoring vegetation condition (Lawley *et al.* 2015).

Many of the ecologically-based remote sensing studies of grasslands have been commissioned by state or federal departments and published as government reports (e.g. Agrecon 2004, 2005; Environmental Research & Information Consortium 2001). This has coincided with a rise in the conservation profile of herbaceous communities, such as grasslands, and an increased need to identify and map these communities to enable resource allocation and informed land management decisions (Vickery *et al.* 1997). The bulk of this work has been conducted in the Monaro district of the NSW and ACT Southern Tablelands where conservation and agricultural values of grassland is high. The results of floristic surveys of temperate grassland areas have indicated that most

high quality remnants occur in small patches of public land, such as travelling stock routes, roadsides and cemeteries (Groves 1965, 1979, Benson *et al.* 1997, Maguire *et al.* 2012), though larger areas are likely to occur on inaccessible private land (Barlow 1998). As such, the fragmented nature of temperate grasslands presents a spatial issue for the detection of homogenous grassland types. While Landsat sensors (30 m x 30 m pixels) may be suitable for detecting small, fragmented grasslands, sensors that have coarser spatial scales may be less reliable.

The results of remote sensing efforts to date have yielded some distinctions, particularly with extreme examples of the grassland continuum (i.e. strongly exotic versus strongly native) using data from the Landsat Thematic Mapper (TM) and Enhanced Thematic Mapper Plus (ETM+) sensors (R. Rehwinkel, pers. comm.).Given that the objective of governments is often to map vegetation communities, and that the ability to spectrally separate different native communities remains challenging, other mapping methods such as annual aerial photography are being explored (Maguire *et al.* 2012). However, aerial photographs have the disadvantage of being 'snapshot' images, and do not account for seasonal fluctuations showing differences in ecosystem dynamics and vegetation condition. Time-series satellite imagery has presented a potential solution, with frequent satellite revisit times being able to capture changes in dynamic systems (e.g. Petus, Lewis and White 2013).

1.5 Phenology: Definition, History and Current Relevance

1.5.1 Conventional methods for estimating phenology

Phenology is the study of seasonal events, and is one of the oldest methods of monitoring environmental change. Phenology has experienced an increase in popularity in recent years, as it is directly applicable to monitoring climate change impacts (Schwartz 1999, Hughes 2000, Parmesan and Yohe 2003). Examples of phenological variables that are currently studied include bird migration timing, plant phenophase (such as leaf-out, flowering and fruiting), and amphibian breeding activity (Peñuelas *et al.* 2004). Plant phenology monitoring has been conducted in Europe and Asia for centuries (Fitter and Fitter 2002), and usually involves the monitoring of emergence,

leaf unfurling, flowering, fruiting and senescence of single plants or small patches at discrete locations. This has been a basis of several 'citizen science' programs (e.g. Project Budburst in the USA; PlantWatch in Canada), and has been central to the development of phenology networks that have been established across the world (e.g. the US National Phenology Network; Betancourt *et al.* 2007). The limitations of point-source phenology monitoring, however, are that the results are only applicable to a discrete location or range, there may be inconsistencies between observers, and that the observation frequencies may be irregular (Menzel 2002).

Understanding the seasonal patterns of vegetation provides a fundamental understanding of terrestrial ecosystems and how they respond to basic drivers. Vegetation phenology is directly related to productivity; can be used as an accurate expression of long-term change; is a key input for climate models and feedbacks; can be used to detect disturbances; and can indicate the dominant vegetation type.

1.5.2 Contemporary and novel methods for studying phenology

1.5.2.1 Repeat digital photography ('phenocams')

Another method for monitoring vegetation phenology is through "near surface" methods. These are designed to monitor a larger area than traditional phenology monitoring methods, and can be accomplished through the use of digital time-lapse photography or webcams (Richardson *et al.* 2009). These 'phenocams' are often used in conjunction with eddy-covariance monitoring towers, which can be used to validate the phenology signal through the time-series measurement of gross primary productivity (Richardson *et al.* 2007, Xiao *et al.* 2009, Moore *et al.* 2017). Phenocams typically use conventional red-green-blue ('RGB') sensors (e.g. Crimmins *et al.* 2008; Richardson *et al.* 2007) as are found in consumer-grade digital cameras. This restricts the analysis of the image to visible wavebands, though vegetation dynamics have been successfully captured through novel methods (Graham *et al.* 2010, Hufkens *et al.* 2012). Some phenocams have been engineered to be multi-band (i.e. include visible and NIR bands), and can therefore approximate more common satellite VIs, such as NDVI (Nagler *et al.* 2012). In order to capture larger scenes, phenocams typically capture oblique imagery. Near surface methods such as phenocams offer the advantage that the sensor can be

positioned to focus on a particular scene, and are cost-effective methods for monitoring select community-scale areas.

Phenocams are becoming more commonly used in ecological research and have been successfully used to describe vegetation dynamics in a variety of biomes around the world, including broadleaf forests (Richardson *et al.* 2007, 2009, Nagai *et al.* 2011, Sonnentag *et al.* 2012), conifer forests (Ide and Oguma 2010, Bater *et al.* 2011, Sonnentag *et al.* 2012), mixed forests (Ahrends *et al.* 2008, Henneken *et al.* 2013) semiarid scrub (Kurc and Benton 2010), tropical savannah (Alberton *et al.* 2014, Moore *et al.* 2017), alpine grasslands (Migliavacca *et al.* 2011, Ide and Oguma 2013, Julitta *et al.* 2014), and suburban parks and gardens (Crimmins and Crimmins 2008, Nijland *et al.* 2014). As phenocam research is in its infancy, these studies continue to explore the effect of camera type, image format, geometry and index use on phenocam response.

1.5.2.2 Satellite remote sensing

The use of satellite-based remote sensing to detect vegetation phenology is termed 'land surface phenology' (de Beurs and Henebry 2004). It offers the potential to track the expression of phenology patterns at landscape to global scale, and—critically—is able to retrospectively obtain historical phenology data through satellite data archives (Reed *et al.* 2009). While many historical remote sensing studies have stressed the importance of taking seasonal spectral characteristics into consideration, or have used multi-date imagery to assist in spectral separation of land cover types (e.g. Agrecon 2005; Glenn *et al*. 2005), true time-series remote sensing studies are relatively recent. To generate accurate phenology profiles, imagery is required that offers sufficient temporal sampling to allow the detection of changes amidst seasonal variation in the scene (de Beurs and Henebry 2005). This has only been possible due to the long-term deployment of certain satellites, and the development of methods to fuse data from older sensors with newer ones. Table 1.3 summarises the specifications of several of the more commonly used satellite-based sensors that have time-series capability.

Table 1.3.Summary detail of common satellites used for remote sensing of vegetation phenology (from Reed, Schwartz and Xiao 2009).

Satellite	Sensor	Operation	Resolution	Frequency
Landsat	MSS	1973–1985	79 m	18 days
Landsat	TM	1984–present	30 m	16 days
Landsat	ETM+	1999–present	30 m	16 days
SPOT	Vegetation	1999–present	1 km	1–2 days
NOAA	AVHRR	1982–present	8 km	twice monthly
NOAA	AVHRR	1989–present	1 km	biweekly
Terra	MODIS	2000–present	250 m, 500 m, 1 km	1–2 days
Aqua	MODIS	2002–present	250 m, 500 m, 1 km	1–2 days
Envisat	MERIS	2002–present	300 m	1–3 days

1.5.2.3 Phenology metrics and phenological profiling

The use of VIs from satellites with high temporal resolution allows tracking of phenology metrics, such as ‘green-up’ (start of season), ‘brown-down’ (end of season), and length of season (Zhang *et al.* 2003, Fontana *et al.* 2008, Schmidt *et al.* 2012). These metrics aim to estimate key markers such as onset of greening, onset of senescence, timing of the peak of the growing season, and growing season length based on the analysis of the VI curve (de Beurs and Henebry 2010). Figure 1.3 shows an example NDVI phenology curve with metrics as presented in Chandola *et al.* (2010).

Phenology metrics can be tracked from year to year and related to climatic variables (Peñuelas *et al.* 2004, Cleland *et al.* 2007, Chandola *et al.* 2010), though are often location-specific (Schwartz *et al.* 2002). While this has most utility in northern hemisphere biomes with distinct seasonal patterns, phenology studies using satellite data have been used to highlight productivity differences in the tropics and in less seasonally-distinct regions (Saleska *et al.* 2007, Huete *et al.* 2008, Schmidt *et al.* 2012).

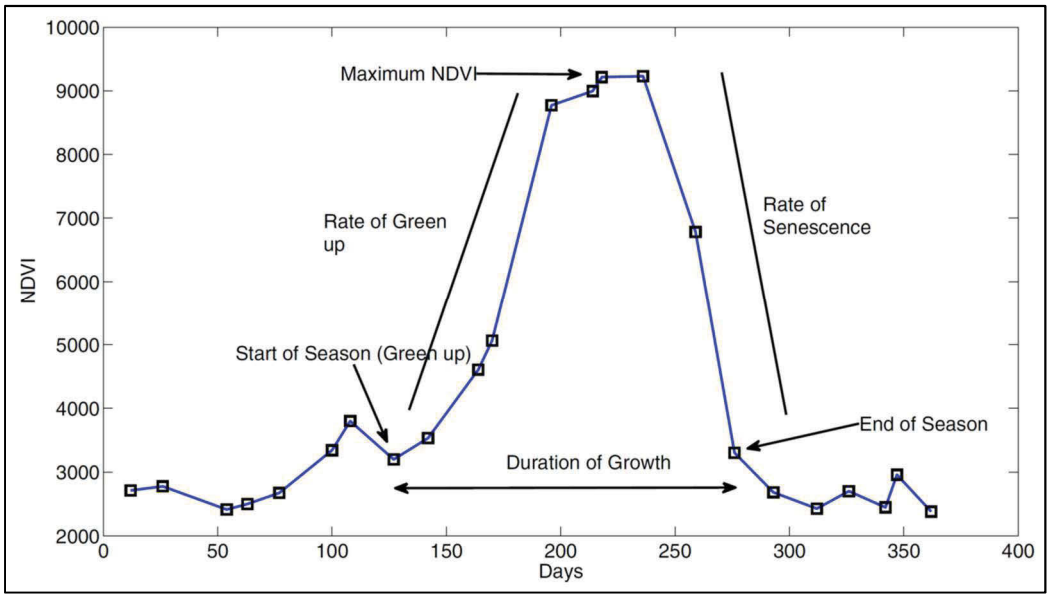

Figure 1.3. An NDVI phenology profile, illustrating examples of common phenology metrics (from Chandola *et al.* 2010).

Several options exist for comparing phenology metrics derived from vegetation indices, and can be classified into: threshold-based, derivative-based, smoothing functions-based, and model fitting-based (de Beurs and Henebry 2005). Each of these comparative methods have their advantages and disadvantages, for example, smoothing algorithms can be used to reduce spurious data points, but hold the danger of introducing artefacts and suppressing natural variations of the time-series (Fontana *et al.* 2008). Methods for deriving phenology metrics for Australian grassland types are likely to be different from those used for northern hemisphere temperate biomes, and alternative key indicators will need to be adapted or developed.

When examining ecosystem change through time-series data, it is important to consider seasonal change, driven by rainfall and temperature, gradual change (e.g. trends in rainfall), and abrupt trend change, such as from a major disturbance (Verbesselt, Hyndman, Newnham, *et al.* 2010). Statistical methods suitable for separation of entire phenology curves (rather than just comparison of metrics) are also diverse and techniques are specific to location and vegetation type. Time-series similarity measures determine the difference in phenology cycles between years or locations. Lhermitte and colleagues have reviewed methods that are used to compare time-series cycles (Lhermitte *et al.* 2011). Users are cautioned to consider data characteristics (collection frequency, contamination, spatial resolution), time-series characteristics (correlation,

temporal resolution, missing values), and ecosystem characteristics (phenology patterns, baseline, and dynamics) in order to select an appropriate method.

Phenology profiles were first used in conjunction with satellite sensors to differentiate agricultural crops, as these have distinct and well-understood growing periods (e.g. (Odenweller and Johnson 1984, Sakamoto *et al.* 2010). Although natural systems are much more complex, phenology-based information has been successfully used to differentiate different vegetation types such as warm-season versus cool-season grassland (Peterson *et al.* 2002, Davidson and Csillag 2003), identify plant invasions (Underwood *et al.* 2003, Andrew and Ustin 2008), separate woody from non-woody vegetation (Lu *et al.* 2003), assess the timing and impact of insect infestation (Nagler *et al.* 2012) and improve vegetation classification maps (Vickery *et al.* 1997, Lymburner *et al.* 2011). Several studies have used land surface phenology to identify land use change—usually related to agricultural practices—either through abrupt or gradual changes (Reed *et al.* 1994, de Beurs and Henebry 2005). Geerken and colleagues used time-series similarity to classify rangeland types and condition (Geerken *et al.* 2005). An application that is in its early stages is the concept of phenology forecasting (White and Nemani 2006). This approach uses deviations from historical data with uncertainty bounds, and may be used to provide predictions of insect outbreaks, pollen release, fire danger and crop conditions.

Although land surface phenology has been used in different applications and geographical areas, the field is still in its infancy and there are many opportunities for advancement. The main areas for improvement that have been identified are the long-term continuity of sensors and the inability to validate historical data (Reed *et al.* 2009), the need to scale between plant level and landscape level (de Beurs and Henebry 2010, Hufkens *et al.* 2012), deriving comparable phenology metrics (Fisher *et al.* 2006), and the often weak relationship between ground and satellite observations (Badeck *et al.* 2004, Ahl *et al.* 2006, Soudani *et al.* 2012).

1.5.3 Phenology research in Australia

Most research into phenology has been conducted in the northern hemisphere where seasonal changes are predominantly temperature-driven and vegetation growing season

is well-defined and predictable. Chambers (2009) reports that 28,115 studies of the 28,671 published on phenology (98%) are based on northern hemisphere data sets. In other parts of the world phenological changes may be more subtle however the importance of minor variation should not be underestimated.

Phenology studies have been limited in Australia—perhaps due to the high climatic variability that produces subtle phenology changes. Australia also lacks long-term datasets that are key for trend detection in phenology (Gallagher *et al.* 2009). A lack of phenological data in Australia has been cited as a focus of future climate change research in this country (Howden *et al.* 2003, Hennessy *et al.* 2007, Chambers 2009).

Unlike the northern hemisphere, the passing of the seasons is followed less closely in temperate south-eastern Australia. Some of the more obvious phenological markers include the flowering of *Acacia* species in the early spring, the vibrant flowering of the exotic but widespread *Jacaranda* species in late spring, and the summer return of cuckoo species that spend winter in northern Australia (Entwistle 2014). Farmers and graziers in this region are more attuned to phenology markers; the country's only long-term phenology records come from agricultural records (Koch 2010). An understanding of seasonal cycles has long been required for the planting and harvesting of crops, pest control and the timing of lambing to coincide with spring pasture growth (Entwistle 2014). Understandably, many of the early phenology studies in Australia relate to pasture production (Biddiscombe *et al.* 1953, Williams 1961).

Contemporary phenology studies—most of which have a distinct focus on climate change impacts—can be categorised into a few subject areas and are driven by a few key research groups in this field. The movement of certain migratory birds has shown a trend of earlier arrivals and later departures and has been correlated with temperature and rainfall variables (Norment and Green 2004, Beaumont *et al.* 2006, Chambers 2008, Green 2010). The timing of breeding and egg-laying of native birds has been noted to be either earlier or later depending on the region (Gibbs 2007, Chambers *et al.* 2008).

Changes in plant phenophase are also highly dependent on region and species. Most studies investigate impacts on flowering time, as flowering is usually conspicuous and easy to monitor. The flowering time of native plants in the south-east has been shown to

have shifted earlier or later depending on species (Keatley *et al.* 2002). Flowering of grassland species has also been shown to be responsive to warming in Tasmania (Hovenden 2007), with warmer temperatures resulting in an average earlier flowering time. In south-eastern alpine regions, some species showed earlier flowering times with warmer temperatures (Gallagher *et al.* 2009). Two alpine plant species showed a very strong relationship between flowering and date of snow melt (Green 2010). Only one study refers to fruiting phenophases: wine grapes were observed to have matured earlier, in an apparent correlation with warmer temperatures (Webb *et al.* 2011). Studies of phenological changes in vegetation (leaf growth and senescence) are also limited. An investigation into leaf phenology showed that leaf flushing in a variety of Australian tropical species occurs as a precursor to seasonal rainfall (Williams *et al.* 1997).

Remote sensing is being increasingly utilised in the global phenology domain, however Australia has received little attention in this regard. This may be due to the dominance of biomes within Australia that are either subtle in their seasonal changes or have a high variability in the timing of phenological events—both examples are challenging to traditional phenology methods. The few satellite-based phenology projects that have been conducted in Australia have been focussed on arid and semi-arid zones, where land surface phenology is driven by moisture—typically rainfall—and is somewhat predictable. These studies include:

- combining Landsat and MODIS satellite data to enhance spatio-temporal resolution in northern savannahs (Schmidt *et al.* 2012);
- using MODIS data to investigate vegetation phenology and groundwater in the Great Artesian Basin (Petus *et al.* 2013); and
- investigating the temporal dynamics of the Northern Australian Tropical Transect (Ma *et al.* 2013).

Collation of the limited available phenocam data in Australian ecosystems has shown the diverse range of drivers and responses of vegetation phenology across country (Moore *et al.* 2016). While this data demonstrates phenocam deployment in rainforests, savannahs and temperate evergreen forests, it also highlights the need for additional

phenocam data to understand the phenology of these complex systems. More recently, phenocams and eddy-covariance flux towers were used to assess the difference between understory and overstory dynamics in an Australian tropical savannah (Moore *et al.* 2017). This study provided much needed insights into grass and tree phenology in a mixed system but, like satellite phenology research, is limited to the Australian tropics.

There is a clear need for increased research in phenology of various Australian biomes, and an obvious potential in using remote sensing tools for this purpose. However, the Australian studies that have been published demonstrate the differences between Australian ecosystems and northern hemisphere biomes, and the need to develop appropriate phenological methods for Australian systems (Broich *et al.* 2015).

1.6 Conceptual Models of Grassland Phenology

The following diagrams represent conceptual models of phenological changes that occur under typical and disturbed conditions and specifically relate to the reflectance properties that are detected using remote sensing tools. These models are used to identify important areas of focus for this project and demonstrate feedbacks and interactions within these variables. The primary mechanisms that have been identified to alter spectral reflectance—and hence vegetation indices and phenology profiles—are changes in species composition, rainfall, and disturbance. Ultimately, effects on spectral reflectance relate to changes in biophysical characteristics of vegetation (Asner 1998).

Species composition is a major influence on spectral reflectance. Every species presents a range of biophysical parameters that are have characteristic reflectance properties; these may be unique or may overlap with other species. It is the unique signatures that are exploited by researchers attempting to detect particular species using remote sensing methods (e.g. Dehaan *et al.* 2007; Pengra, Johnston and Loveland 2007). Figure 1.4 identifies the key biophysical parameters that are associated with an individual species. For each species present, these parameters change seasonally depending on photosynthetic type and response to temperature and rainfall, For example, a species with conspicuous flowers will have a different spectral reflectance during flowering times versus when it is vegetative (Underwood *et al.* 2003, Huang and Asner 2009). This model illustrates that even in a hypothetical monoculture, phenological changes

will be apparent in the spectral profile. In grassland with many different species, each species may change differently, resulting in a complex integrated response. Herbaceous species will also have a more dynamic response to these drivers than woody species do, resulting in faster and more extreme changes for individual species as well as community composition (Petrie *et al.* 2011).

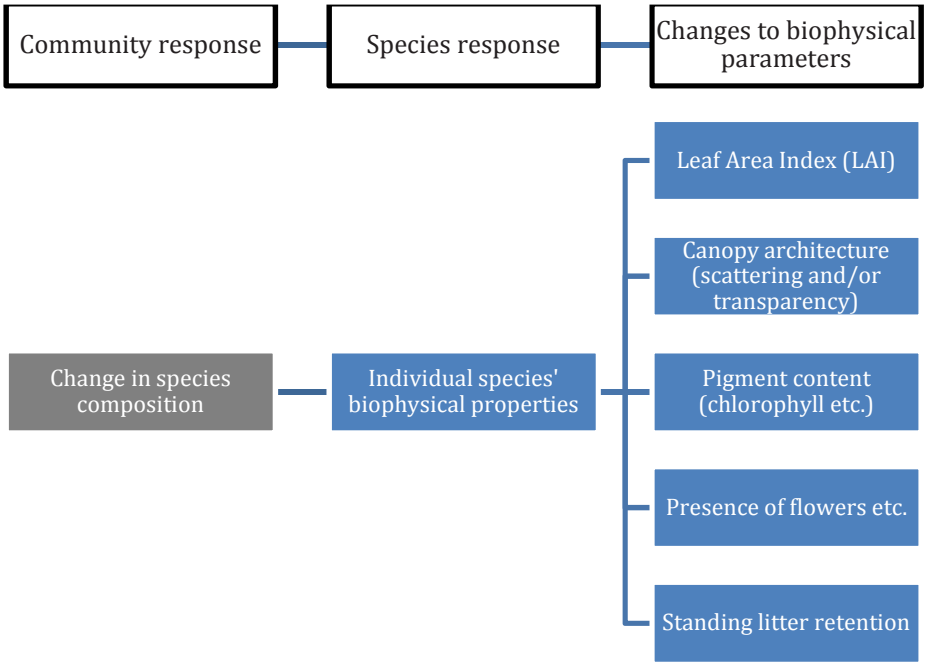

Figure 1.4. Conceptual model: how biophysical properties of individual species contribute to changes in spectral reflectance. These parameters are not static, but change in response to climatic variables, adding an additional temporal component to this figure.

Figure 1.5 shows the effect that rainfall and drought have on vegetation by detailing the driver, effect, community response and changes to biophysical parameters. In each case, change in species composition is a likely community response, and the suite of biophysical changes shown in Figure 1.4 is relevant. Other effects, such as increased vegetation vigour, promote more a more linear response, such as increased leaf area index (LAI). A change in fractional cover is a common biophysical response and refers to the proportion of an area covered by photosynthetic vegetation, non-photosynthetic vegetation, and background substrate (Guerschman *et al.* 2009).

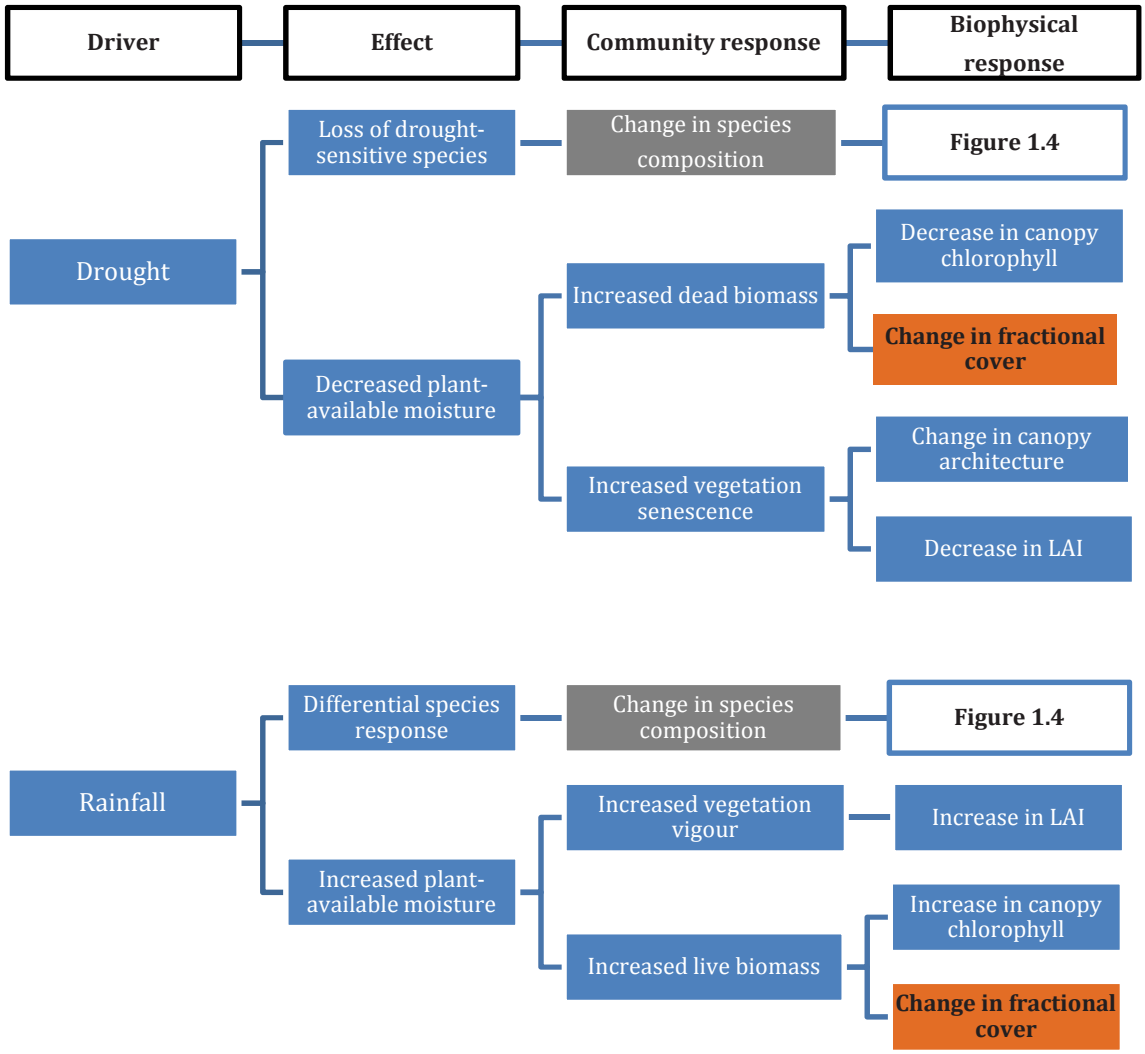

Figure 1.5. Conceptual model: rainfall and drought effects, community response and expected changes to biophysical parameters.

Disturbance events bring about the most abrupt changes in grassland structure and function (Verbesselt, Hyndman, Zeileis, *et al.* 2010). Figure 1.6 and Figure 1.7 show the impacts of common grassland disturbance events—fire, weed invasions, grazing and scalping (the removal of vegetation and surface soil)—on the community response and the vegetation biophysical parameters. It is important to note that changes to community composition are likely after all disturbances, as are changes to the proportions of fractional cover. In addition, disturbances are likely to cause feedback loops; for example, a weed invasion may result in less grazing by livestock, which leads to greater quantities of dead vegetation and higher risk of fire. Fire then provides another disturbance which may make the area more vulnerable to weed invasions, and the cycle continues.

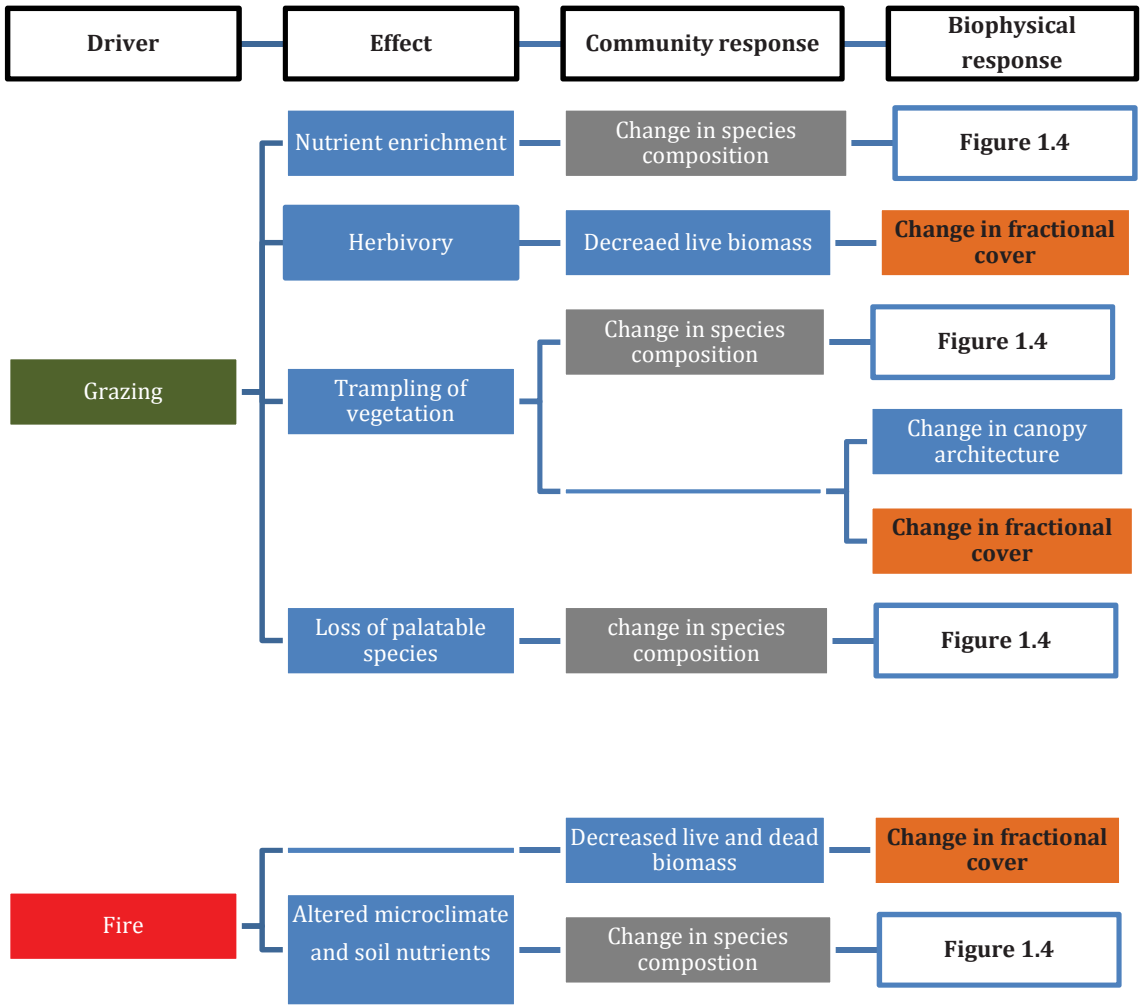

Figure 1.6. Conceptual model showing how disturbance events change vegetation biophysical parameters (grazing and fire).

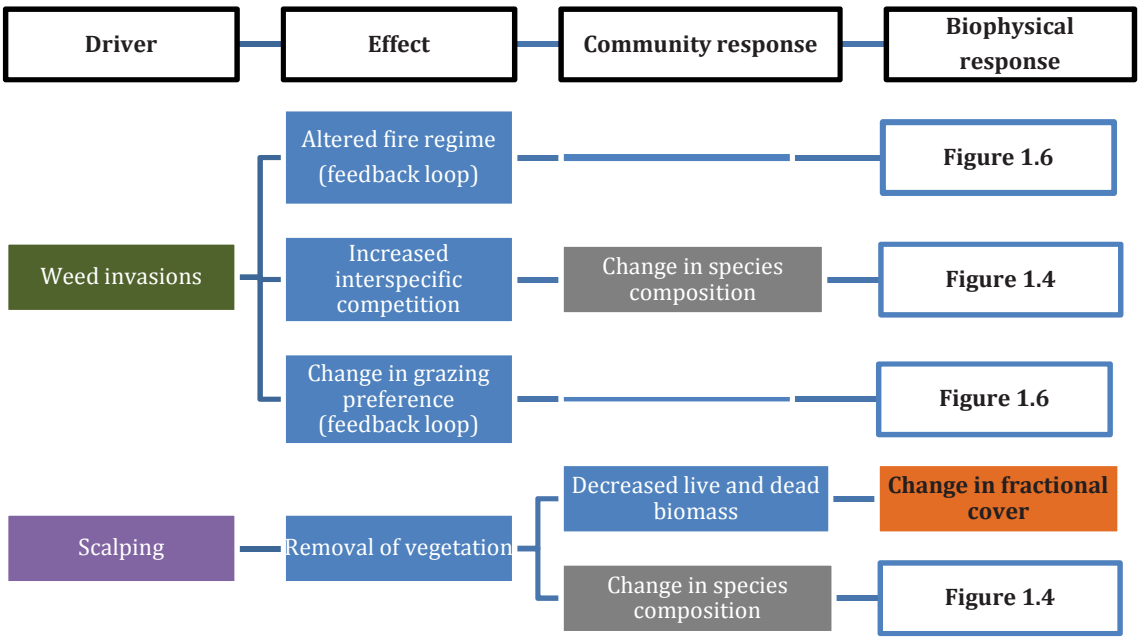

Figure 1.7. Conceptual model showing how disturbance events change vegetation biophysical parameters (weed invasions and scalping).

1.7 Thesis Aims and Research Questions

The broad research questions that this thesis aims to answer are:

- How do climate, biophysical factors and species composition interact to influence temperate grassland phenology?;
- How do different temperate grassland functional types differ in their phenology?;
- How do phenological estimates change with different spatial and temporal scales?; and
- What is the capability of satellite-based and near-surface sensors to accurately quantify grassland phenological variables?

1.8 THESIS STRUCTURE

This research project is designed to use complementary and comparable methods in laboratory and field experiments to control particular variables. This will be used to build an understanding of the contribution of each variable to the grassland phenology profile. This thesis is structured such that each chapter covers a small suite of variables that contribute to and build our understanding of grassland phenology.

Chapter 2 details an experiment conducted in controlled laboratory conditions to investigate the impacts of fractional cover and species composition in native grassland mesocosms. This experiment was conducted over a year, and was designed to control for factors such as density and species, while minimising the effects of variables such as climate and sensor geometry, as is found in natural environments. In particular, Chapter 2 explains the effect of standing litter on the phenological profile, and highlights how species composition of grassland can impact land surface phenology.

Chapter 3 details the effects of different rainfall regimes on temperate grassland, in this case an improved pasture. This experiment utilised rainfall exclusion shelters over 1 m^2 grassland plots to mimic rainfall regimes of altered quantities and timing. The effect on vegetation was monitored through time-lapse digital cameras ('phenocams') that were subsequently processed to generate a 'greenness' index for each image. The results of longitudinal image analysis of different rainfall treatments were compared with daily soil moisture values and rainfall data. This provides a baseline of information to prepare climate adaptation strategies to secure the future of Australia's grazing industries.

Chapter 4 investigates how the community structure of the four grassland functional types changes throughout the year, and the how the phenology of dominant species contribute to land surface phenology over an annual cycle. This chapter provides a 'field-level' understanding of how grassland species change throughout the seasons and how grassland types are differentially affected by abiotic drivers such as climate.

Chapter 5 examines how estimates of land surface phenology taken at different temporal and spatial scales detect temperate grassland phenology signatures. This chapter compares different methods of estimating vegetation dynamics: conventional

phenology estimates (biomass samples, pasture height and vegetative cover), contemporary near-surface remote sensing (phenocams), and traditional satellite remote sensing. This comparison provides a basis for determining where satellite estimates of phenology may or may not be viable, and the potential for scaling satellite-based observations to field conditions. This chapter also assesses the utility of phenocams in a temperate grassland system.

Chapter 6 provides a synthesis of the findings of the overall research project and suggests future recommendations for this area of research. It discusses the role of remote sensing in phenological studies and the advantages that different methods provide. Chapter 6 concludes with a discussion of how multiple remote sensing tools can improve management of Australian temperate grasslands and contribute to our understanding of Australian phenology.

Chapter 2: The effect of species composition and fractional cover on spectrally-derived phenology in Australian grasslands

2.1 INTRODUCTION

Temperate grasslands in south-eastern Australia represent a mosaic of diverse land uses, species composition, and ecological conditions because of their historical and current coexistence with pastoral agriculture and urbanisation (McDougall and Kirkpatrick 1994, Ross 1999). Many native grassland communities are listed as threatened under Australian state and federal legislation, however the economic and cultural importance of livestock production in the region is high (Williams, Marshall, and Morgan 2015). The need for informed management of temperate grassland in this region is important to maintain or improve the ecological integrity and pasture production values under changing climatic conditions. Of particular interest is the relative dominance of species that use C_3 or C_4 photosynthetic pathway. C_3 species are more productive in cooler climates, whereas C_4 species have a greater advantage in warmer, dryer conditions (Baldocchi 2011). The relative response shown by C_3 and C_4 grasses to increased CO_2, higher temperatures and modified rainfall regimes of future climates will have major impacts to both ecological condition and agricultural productivity (Körner 2006, Morgan *et al.* 2011).

2.1.1 Remote sensing and temperate grassland management

Satellite-based remote sensing is now a commonly used tool for consistently assessing vegetation characteristics at a landscape scale (Huete 2012). Remote sensing methods have been used in a grassland context both within Australia and internationally to identify land cover types (Price *et al.* 2002, Geerken *et al.* 2005), determine land use change (Henebry 1993, Wylie *et al.* 2002), estimate primary productivity (Psomas *et al.* 2011, Gu *et al.* 2013), assess vegetation cover (Liu *et al.* 2007, Guerschman *et al.* 2009, Zhang *et al.* 2009) and quantify ecological threats (Akiyama and Kawamura 2007). Traditionally, this data acquisition has been conducted through spectral classification, where differences in the spectral reflectance of vegetation types relate to differences in

biophysical (e.g. canopy architecture, leaf area index) or biochemical (e.g. pigmentation) parameters. The use of vegetation indices (VIs), which take advantage of the differential reflectance of light wavelengths by vegetation, have shown considerable accuracy in quantifying biomass, leaf area index, and vegetative fractional cover (Weiser *et al.* 1986, Xie *et al.* 2008, Guerschman *et al.* 2009). The Normalized Difference Vegetation Index (NDVI; Tucker, 1979) and the Enhanced Vegetation Index (EVI; Huete *et al.*, 2002) are among the most used VIs, although numerous VIs have been developed that are optimised for different applications and sensors. These VIs can be generated from satellite-based sensors as well as ground-based spectral measurements.

Identifying and characterising temperate grassland communities via remote sensing methods in south-eastern Australia is challenging (Eco Logical Australia 2009). Efforts are confounded by the dynamic response of grassland species to temperature and rainfall, which results in rapid changes to species composition and green/dead vegetative proportions. The high contribution of standing dead litter to Australian temperate grasslands can obscure the contribution of the green vegetation fraction, a feature that is known to impact spectral signals (van Leeuwen and Huete 1996, Nagler *et al.* 2000). Attempts to acquire grassland information in the spectral domain have been limited in number as well as success due to the spectral similarity of many grassland communities (Benson 1994, Environmental Research & Information Consortium 2001, Agrecon 2005). As a consequence, most grassland classification conducted by government organisations is currently conducted through annually-collected aerial photography analysis (Maguire *et al.* 2012). While this provides high quality information on grassland spatial extent it is a 'snapshot' at one moment in the year and provides no additional information on ecosystem function, productivity or quality.

2.1.2 Land surface phenology and vegetation dynamics

A complementary source of information on vegetation dynamics is through time-series patterns of vegetation growth. When this information is gathered from a mixture of vegetation types, such as a pixel from a satellite sensor that may cover several square metres, it is termed 'land surface phenology' (de Beurs and Henebry 2004). Phenology is the study of recurring seasonal events and is one of the oldest forms of vegetation

monitoring (Aono and Kazui 2008). Leafing and flowering times of individuals and groups of plants are commonly used in phenology studies, such as those that provide evidence of climate warming (Caradonna *et al.* 2014). In contrast, land surface phenology examines larger spatial scales, and uses vegetation growth to provide an indication of landscape-scale vegetative dynamics. When vegetation indices are measured over time, the resultant phenology profile is a greenness signature that is analogous to primary productivity over the measured area (Reed *et al.* 1994). Recent development of phenological methods have included applications to separate C_3/C_4 functional types (Wang *et al.* 2013), identify land cover classes (Lymburner *et al.* 2011), and detect ecosystem change (Nagler *et al.* 2012). There has also been discussion regarding the need for vegetation phenology data to improving carbon and energy balance models (Peñuelas *et al.* 2009, Richardson *et al.* 2012).

The incorporation of phenological data has the potential to improve the classification and characterisation of temperate grassland types, monitor land use change, track restoration efforts or degradation, and estimate productivity. However, the vegetation dynamics of temperate grasslands in south-eastern Australia show different phenology patterns from northern hemisphere deciduous ecosystems where the majority of phenology studies have taken place. As such, there is a fundamental need to understand the drivers behind Australian temperate phenology signals before phenological methods can be applied to landscape-level management. This is best investigated in a controlled environment to limit the extraneous variability that natural systems exhibit. In particular, vegetation indices can be affected by changes in soil type, soil moisture, species composition, plant water content and canopy architecture (Jones and Vaughan 2010), which need to be carefully controlled to ensure they do not confound the target variables.

In this experiment, time-series spectral measurements of grassland mesocosms are used to determine the influence that photosynthetic and non-photosynthetic vegetation has on grassland phenology. Vegetative fractional cover is used as the response variable as this is commonly used for assessing grassland quality (Guerschman *et al.* 2009, Zhang *et al.* 2009) and can be measured non-destructively. Fractional cover refers to the aerial proportion of photosynthetic vegetation (f_{PV}) and non-photosynthetic vegetation (f_{NPV}) (White, Asner, *et al.* 2000), with the remainder constituting background substrate (fBG).

These relative proportions determine important ecosystem features like rates of carbon and nutrient exchange and heat fluxes. Fractional cover estimates are also used to estimate grassland vegetation condition (Purevdoj *et al.* 1998) and are crucial for providing land management information, such as estimates of productivity, fire frequency and erosion control (Guerschman *et al.* 2009). Nadir digital photography is used to provide a quantitative estimate of cover, as this method has proven to provide good fractional cover estimation of grassland systems (Przeszlowska *et al.* 2006).

2.1.3 Aims

This chapter investigates how spectral reflectance and VIs are impacted by species composition and vegetative fractional cover under controlled sensor/illumination geometry and in the absence of rainfall effects. A pilot study was conducted to determine appropriate VIs and assess spectral reflectance features of leaf and canopy level scenes. The preliminary results of this study was published as part of the 2013 IEEE Geosciences and Remote Sensing Society conference proceedings (Watson *et al.* 2013) and is reproduced in part here.

The aims of this experiment were to:

- investigate differences in phenology patterns due to grass species and C_3/C_4 photosynthetic functional type;
- determine how vegetation density affects spectral estimates of phenology in grasslands; and
- quantify the proportional impact of photosynthetic vegetation and standing litter on spectral indices and phenology estimates.

2.2 METHODS

2.2.1 Canopy reflectance spectra

This study used two grass species, *Themeda triandra* Forssk. (*Themeda*; C_4 grass) and *Poa labillardierei* Steud. (*Poa*; C_3 grass). These species are perennial caespitose (tussock) grasses that are common in grassland communities throughout temperate south-eastern Australia. These species are indicators of high quality temperate grasslands (Rehwinkel 2007) and are readily available from specialist native nurseries. Year-old potted plants were grown in a glasshouse and provided with adequate water, nutrients and pest control. Plants were moved within the greenhouse every two weeks to ensure subtle differences in light and temperature did not influence a particular group of plants. The glasshouse temperature and humidity were automated to represent ambient temperature conditions in Sydney (-33.883647 N, 151.199202 E). Temperature was recorded constantly with a Priva E-measuring box (Priva, De Leir, The Netherlands) for the study period and is presented as mean monthly maximum, mean monthly minimum and mean monthly temperature in Figure 2.1. Generally, the temperature followed typical seasonal patterns for the Sydney region, with a cool winter (June 2013–August 2013), followed by increasing temperatures through spring (September 2013–November 2013), and warm temperatures being maintained through summer (December 2013–February 2014). For the period of the study, autumn temperatures (March–April 2014) also remained high.

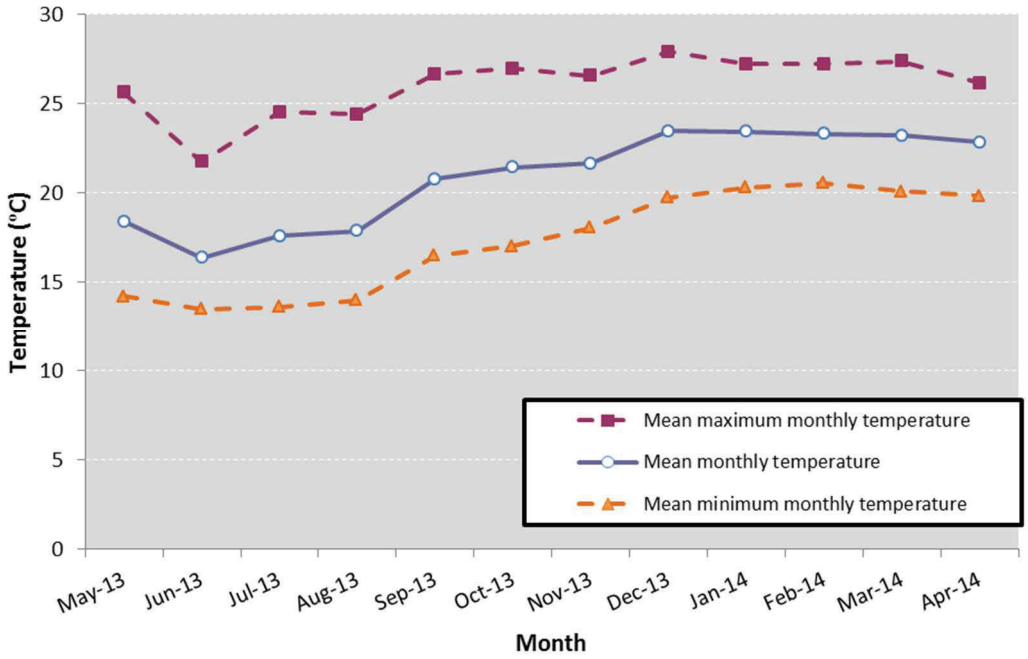

Figure 2.1. Mean temperature, mean maximum temperature and mean minimum temperatures (°C) of the study glasshouse, measured monthly from May 2013 to April 2014.

For each species, three density treatments were used to assess the influence of vegetation quantity on grassland phenology. These treatments of low density (16 plants per m^2), medium density (32 plants per m^2), and high density (64 plants per m^2) replicated a common range of vegetation densities found in natural south-eastern Australian grassland systems. The approximate dry biomass per plant was assessed at 25 g, hence the approximate biomass per treatment is 200 g/m^2 (low density), 400 g/m^2 (medium density) and 800 g/m^2 (high density). Biomass was not measured for each mesocosm due to the non-destructive nature of this experiment.

For each species, two manipulative treatments of fractional cover were modified at the start of the experiment to test extremes of cover types that are encountered in natural systems. The first treatment, termed 'drought', involved water-stressing plants such that all green foliage had senesced, representing grassland conditions under drought stress. These plants had no photosynthetic vegetation (0% f_{PV}); all the vegetation was non-photosynthetic. The second treatment, termed 'resprout' involved the removal of all non-photosynthetic foliage so that only live vegetation remained (as close as practical to 0% f_{NPV}). This represents grassland vegetative resprouting following a disturbance event such as fire (Morgan 2015), or the broad scale clearing of ground-level vegetation

for pasture preparation or weed control (also known as 'scalping'). Both treatments were initiated in June 2013 and were allowed to recover throughout the experiment. These fractional cover treatments were measured at the medium-density level of 32 plants/m^2 and were compared to the control treatments at the same density.

To replicate the vegetative structure of a grassland for spectral measurement, individual potted plants were placed together as a mesocosm. The mesocosms comprised a modular 0.25 m^2 frame that allowed experimentation with density and species arrangements (Figure 2.2). Individual grass plants were selected at random, placed within the frame and covered with a 2 cm layer of dry dark soil. For spectral measurements, the mesocosm was placed within a dark box to minimise stray light and was illuminated obliquely with two 1000 W tungsten-quartz lamps in a dark room (Figure 2.3), as recommended by the spectroradiometer manufacturer (Analytical Spectral Devices 1999). The mesocosms were mounted on a rotating platform, which was rotated for six sequential readings (i.e. 0º, 45º, 90º, 135º, 180º, and 270º) to account for differences in bidirectional reflection characteristics.

An Analytical Spectral Devices spectroradiometer (ASD Inc., Boulder, CO, USA), FieldSpec FR Pro; range 350–2500 nm; maximum spectral resolution of 10 nm, was used to collect canopy-level hyperspectral reflectance data from each grass mesocosm. Each spectrum represents the average of 30 scans. The spectroradiometer probe (25º viewing angle) was positioned at nadir 1.3 m above the subject, allowing for an integrated viewing diameter of 44 cm. Reflectance was calculated used a Spectralon™ reference panel measured in the same plane as the target.

Spectral measurements were taken once every month between May 2013 and April 2014 to generate annual profiles of vegetative phenology for each species, density and fractional cover treatment group. Five replicate mesocosms with different individual plants were recorded for each treatment.

Figure 2.2. Grassland mesocosm design, with dark soil and low-density *Poa* control treatment.

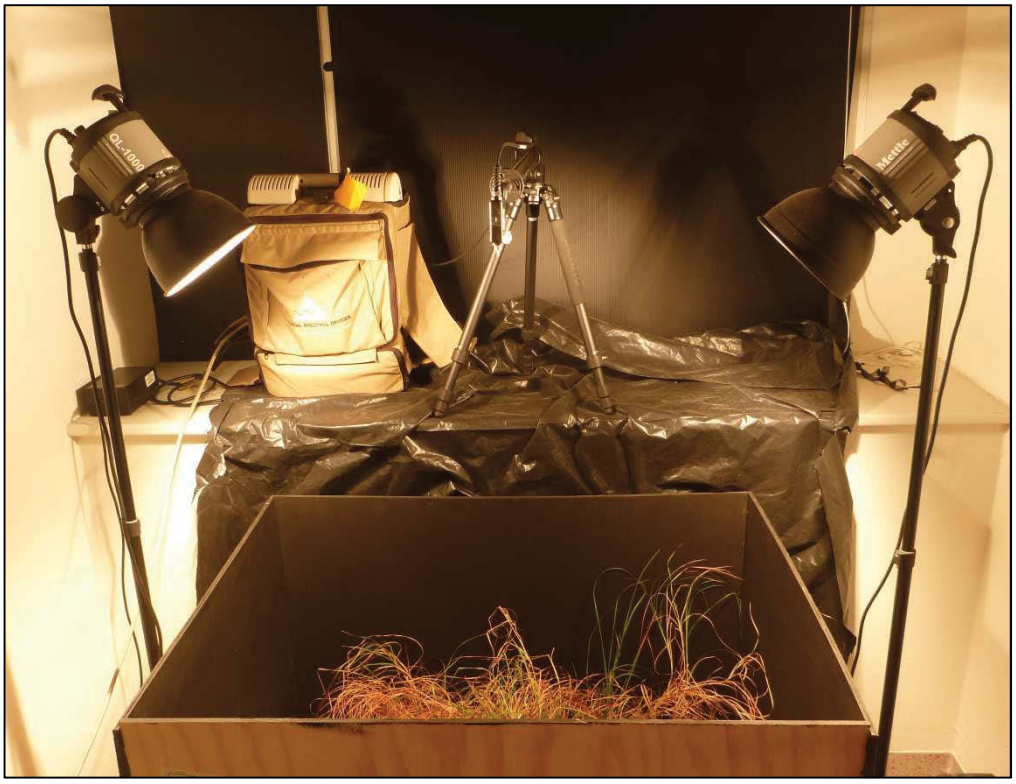

Figure 2.3. Grassland mesocosm under 2 x 1000 W oblique tungsten-quartz lamps during spectroradiometer measurements.

Fractional cover of each scene within the viewing diameter of the spectroradiometer was estimated through digital photography (Panasonic Lumix TS-4), and was processed for fractional components: photosynthetic vegetation (f_{PV}), non-photosynthetic vegetation (f_{NPV}), and background (fBG) using manipulation of colour thresholds in Adobe Photoshop™ CS5 version 12.0.4 (example shown in Figure 2.4). Replicate photographs were taken between repeat spectral measurements to ensure adequate repeatability of this method. An average relative percentage difference between replicates was less than 4% for all fractions.

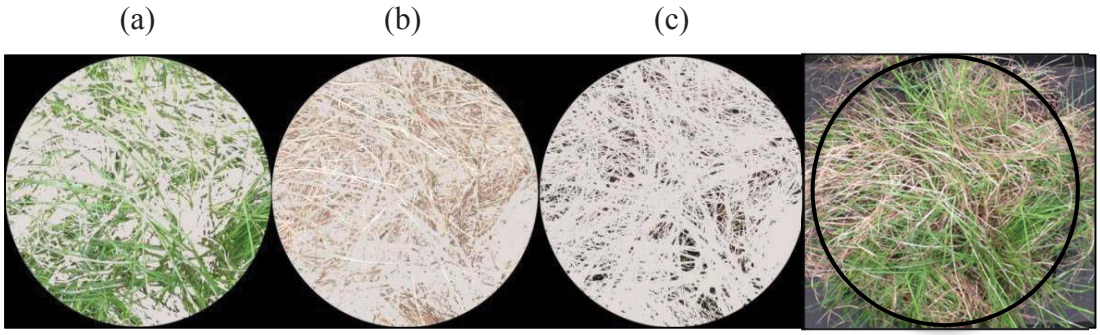

Figure 2.4. Separation of nadir photograph into (a) photosynthetic, (b) non-photosynthetic and (c) background fractional cover components.

2.2.2 Leaf-level reflectance spectra

Leaf-level spectra were taken using the ASD FieldSpec Pro in conjunction with a LI-COR 1800-12 integrating sphere, as detailed in the pilot study (Watson *et al.* 2013). Spectral measurements of green (photosynthetic) and senesced (non-photosynthetic) leaf material were taken using narrow-leaf methods specified by Daughtry, Biehl and Ranson (1989). Typical leaf-level spectra of live and dead foliage from each species are presented in Figure 2.5.

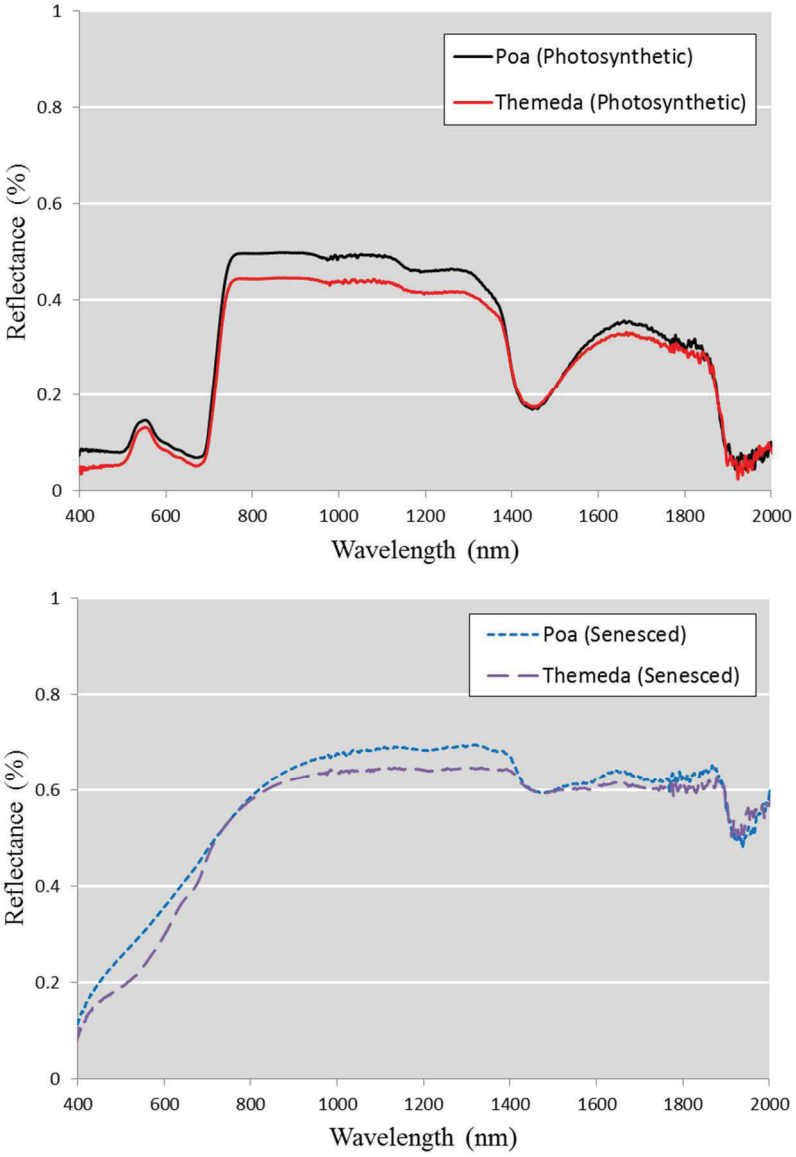

Figure 2.5. Leaf-level typical spectra (400–2000 nm) of photosynthetic (top) and senesced (bottom) *Poa* and *Themeda* leaves

As part of the pilot study, reference spectra were taken from canopies with a high level of f_{PV}, which approximate plant condition at the start of the 'resprout' treatment, and those with a high level of f_{NPV}, which approximate plant condition at the start of the 'drought' treatment (shown in Figure 2.6).

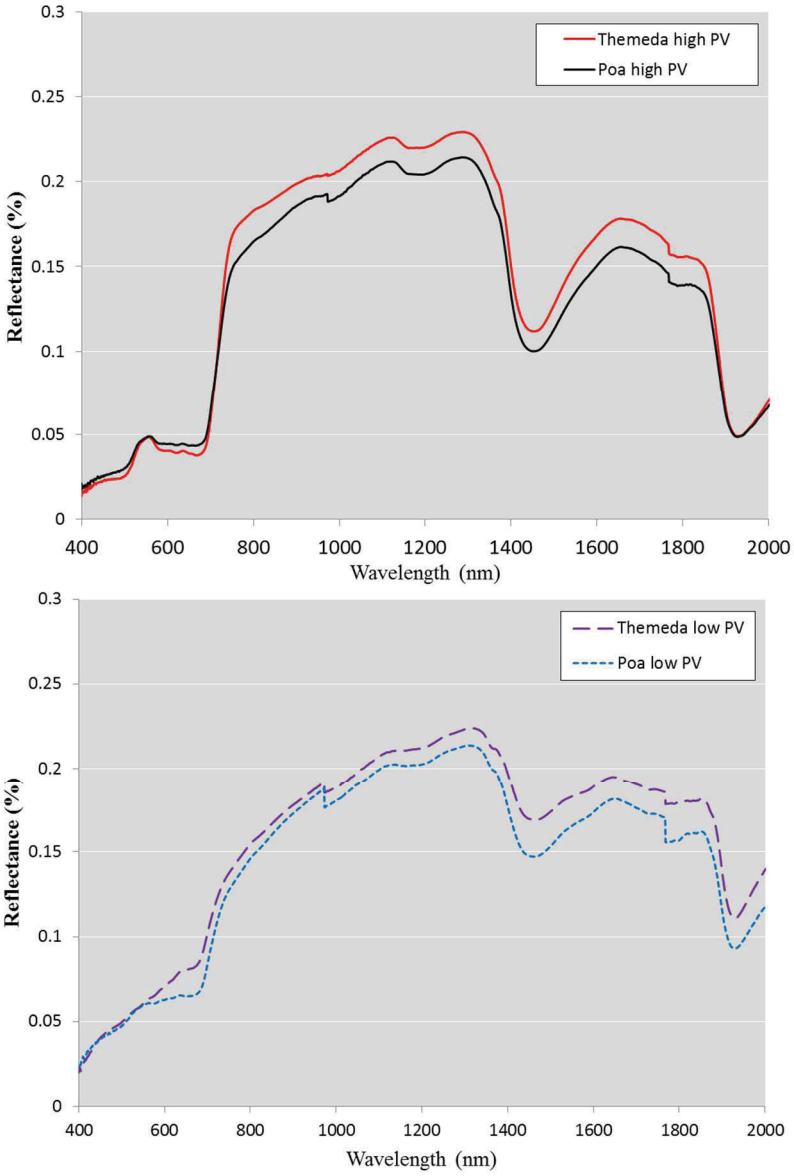

Figure 2.6. Canopy-level reference spectra (400–2000 nm) of *Poa* and *Themeda* medium-density canopies with high f_{PV} (top) and low f_{PV} (bottom).

2.2.3 Spectral indices

In the pilot study (Watson *et al.* 2013), a range of conventional narrow-band and broad-band VIs were tested to determine the optimal VI for estimating vegetative cover in temperate grasslands. The best agreement with f_{PV} was found to be the red-edge NDVI (Equation 2.1; Pearson's correlation coefficient $r = 0.95$). This VI is also termed $NDVI_{705}$ and utilises the sensitivity of the red-edge—the boundary of the red and near infrared wavelengths—to changes in canopy cover, gap fraction and senescent vegetation (Gitelson and Merzlyak 1994). This index is unitless and has a theoretical

range of between -1 and 1, with higher values representing higher vegetation greenness. In practice, however, values tend to be between 0 and 0.6.

$$NDVI705 = (\rho750 - \rho705)/(\rho750 + \rho705) \quad (2.1)$$

(Gitelson and Merzlyak 1994)

The best agreement with f_{NPV} (r = 0.826) was found to be the Cellulose Absorption Index (CAI; Equation 2.2), which uses cellulose-sensitive absorbance regions in the 2000–2200 nm range (Daughtry *et al.* 1996). This index has been successfully used in savannahs and croplands to quantify f_{NPV} (Nagler *et al.* 2003, Guerschman *et al.* 2009).

$$CAI = 0.5(\rho2200 - \rho2000/\rho2100) \quad (2.2)$$

(Daughtry *et al.* 1996)

2.2.4 Chlorophyll content

Relative chlorophyll content of grass leaves was measured monthly between November 2013 and April 2014 using a Minolta SPAD-502 chlorophyll meter (Minolta Co Ltd., Osaka, Japan). This instrument uses the spectral reflectance features of chlorophyll pigments at 650 nm and 940 nm to estimate chlorophyll content at the leaf level. This method has been shown to provide an accurate relative estimate of chlorophyll content (Víg *et al.* 2012). The benefit of this method is that it is non-destructive, can be used *in-situ* and is able to measure the chlorophyll content of thin leaves, such as grasses. Leaves were measured in three locations, between the midpoint of the leaf and the tip, to account for the tip-down maturation of grass leaves. The leaf midrib could not be excluded from the measurement due to the small size of the leaf relative to the measurement port. Ten leaves for each time/treatment were measured in this manner resulting in thirty measurements per time/treatment. Instrument availability prevented this measurement from being taken for the duration of the experiment.

2.2.5 Spectral processing and analysis

Spectra visualisation and processing was conducted with ViewSpec Pro version 6.0 (ASD Inc., Boulder, CO, USA). Data processing and analysis was undertaken using the

R software package (R Core Team 2013). Locally Weighted Scatterplot Smoothing (LOESS) curves were used to assist in visualisation of data trends (Cleveland 1979). In all statistical tests, the level of significance was set at $p < 0.05$.

2.3 RESULTS

2.3.1 Fractional cover and vegetation indices

The $NDVI_{705}$ (Gitelson and Merzlyak 1994) demonstrated a strong relationship with f_{PV} across all species, treatments and time measurements (Figure 2.7; Pearson's $r = 0.846$). The same relationship calculated separately showed a higher correlation for each species (Figure 2.8, *Themeda:* $r = 0.928$, *Poa:* $r = 0.916$). Given this strong relationship, it is reasonable to suggest that the time series measurements of $NDVI_{705}$ accurately reflect changes in f_{PV}. Several other narrow and broadband NDVI-based indices also demonstrated a strong positive correlation with f_{PV}, as did 'RGB' indices that are applied to colour digital imagery. These correlations are presented in Appendix A.

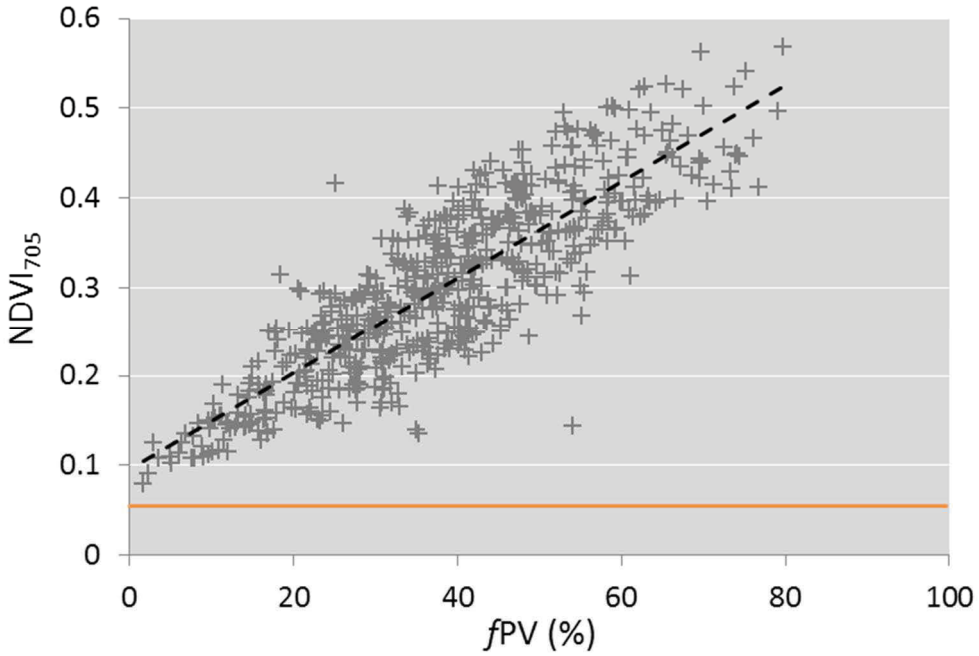

Figure 2.7. Pearson's correlation of f_{PV} with $NDVI_{705}$ for all treatments over all months ($r = 0.730$). The orange horizontal line represents the average bare soil $NDVI_{705}$ value of 0.084.

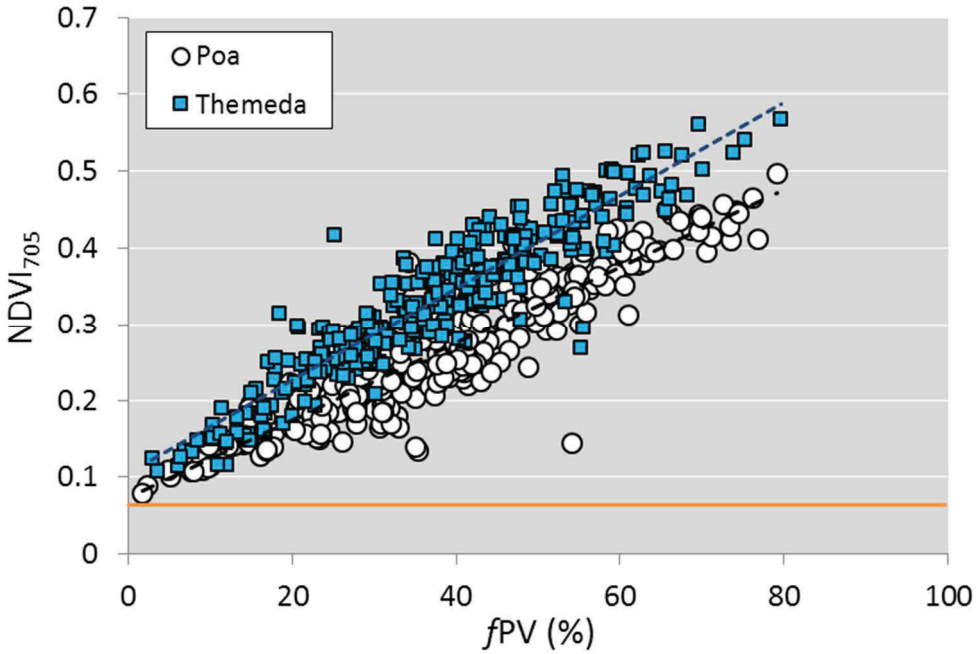

Figure 2.8. Pearson's correlation of f_{PV} with $NDVI_{705}$ for all treatments over all months, separated by species (*Themeda:* $r = 0.928$; *Poa:* $r = 0.916$). The orange horizontal line represents the average bare soil $NDVI_{705}$ value of 0.084.

Despite being strongly correlated in the pilot study (Watson *et al.* 2013), the CAI was found to be only moderately correlated with f_{NPV} when compared across all measurement times and treatments (Pearson's $r = 0.619$). This was not improved when analysed individually by species (Figure 2.9; *Themeda:* $r = 0.619$; *Poa:* $r = 0.618$).

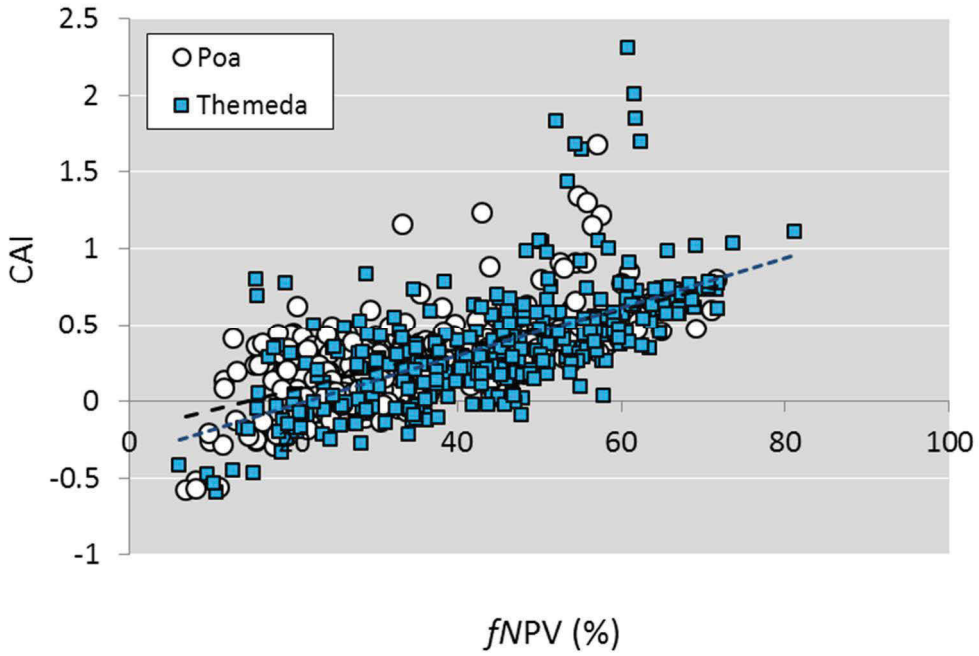

Figure 2.9. Pearson's correlation of f_{NPV} with CAI for all treatments over all months, separated by species (*Themeda:* $r = 0.619$ and. *Poa:* $r = 0.618$).

Phenology metrics of each treatment including mean $NDVI_{705,}$ peak $NDVI_{705,}$ month of peak, minimum $NDVI_{705,}$ month of minimum $NDVI_{705}$, and $NDVI_{705}$ amplitude can be used to identify similarities and differences within the groups. These metrics are presented in Table 2.1. Throughout this experiment the lowest recorded $NDVI_{705}$ mean value was 0.102 (*Poa* drought treatment, June 2013) and the highest recorded $NDVI_{705}$ value was 0.569 (*Themeda* control, October 2013). The mean $NDVI_{705}$ of bare soil was 0.084.

Table 2.1. Summary of phenology metrics of *Poa* and *Themeda* mesocosms at low, medium or high density, and for control, drought or resprout treatments (mean values; n = 5). Shaded rows are *Themeda* (C_4) treatments; unshaded rows are *Poa* (C_3) treatments.

	Average value	Peak value	Peak months	Min. value	Min. month	Amplitude
***Themeda* Control Low Density**	0.377	0.461	May/Oct	0.246	Apr	0.215
***Themeda* Control Medium Density**	0.429	0.540	Oct	0.300	Apr	0.240
***Themeda* Control High Density**	0.460	0.547	May/Oct	0.345	Apr	0.202
***Themeda* Drought Medium Density**	0.322	0.421	Sep	0.182	May	0.239
***Themeda* Resprout Medium Density**	0.457	0.567	Sep	0.315	Apr	0.252
***Poa* Control Low Density**	0.310	0.392	Aug	0.235	Mar	0.157
***Poa* Control Medium Density**	0.366	0.440	Jul	0.286	Mar	0.154
***Poa* Control High Density**	0.397	0.463	Aug	0.298	Feb	0.165
***Poa* Drought Medium Density**	0.271	0.349	Oct	0.187	Jun	0.162
***Poa* Resprout Medium Density**	0.414	0.519	Jul	0.299	Feb	0.220

2.3.2 Differences in phenology by species

To illustrate the primary phenological differences between the two species, Figure 2.10 provides a comparison of the $NDVI_{705}$ phenology profiles of *Themeda* and *Poa* medium-density mesocosms. The profile of *Themeda* showed a high greenness at the commencement of the experiment ($NDVI_{705}$ = 0.529) which declined and stayed consistently low during the winter months at approximately 0.420. During October, this rose again to a maximum value of 0.540 before steadily decreasing in the summer and autumn months to 0.300. The average *Themeda* $NDVI_{705}$ throughout the course of the experiment was 0.429. The amplitude (difference between highest value and lowest value) was 0.240. This pattern was demonstrated by all density treatments. In contrast,

the *Poa* profile was notably more moderate throughout autumn, winter and spring, with a fairly consistent $NDVI_{705}$ of between 0.384 and 0.440 (maximum in July). This decreased to a minimum of 0.286 in March but increased again after March as temperatures became cooler. One of the more evident and consistent differences was that the *Poa* profile peaked earlier in spring, and decreased rapidly with the onset of warm temperatures. *Poa* had a lower average mean $NDVI_{705}$ of 0.366 with a smaller inter-annual variability (amplitude) than *Themeda*.

One of the most marked differences between the two profiles is that *Poa* profile is more cyclical across the break in annual period, whereas *Themeda* demonstrates a strong disconnect: the mean $NDVI_{705}$ during May is high (0.531), while after one year, the April $NDVI_{705}$ is low (0.302).

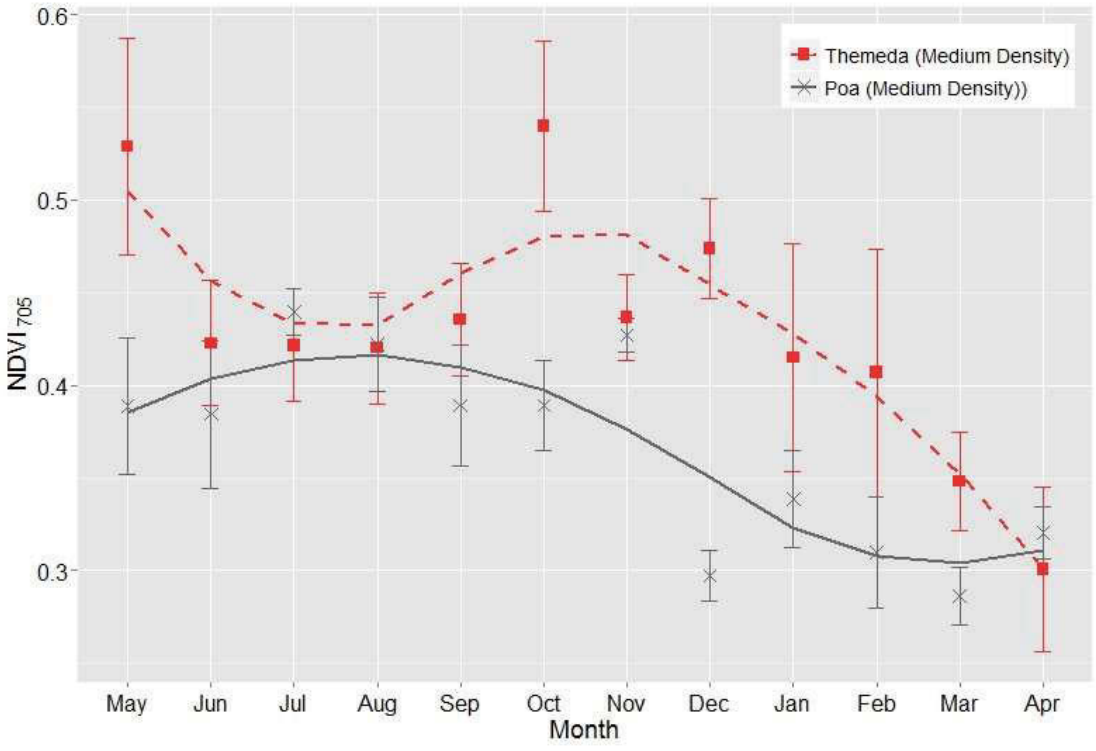

Figure 2.10. Mean monthly $NDVI_{705}$ values (± 1 s.d.) for medium-density *Themeda* and *Poa* mesocosms (n = 5). The trend line for each series is represented by a LOESS fitted curve (span = 0.8).

2.3.3 *Differences in phenology by plant density*

The phenology patterns of low, medium and high density *Themeda* mesocosms showed similar shapes (Figure 2.11) with a low period during the winter months, maxima in May and October, and a steady decline from December into the summer and autumn. Increased densities showed a predictable higher $NDVI_{705}$ throughout, with the high density treatment averaging 0.460 compared to the low density 0.377. The medium- and high-density values tended to be similar to one another at higher $NDVI_{705}$values (e.g. in May, October and December), suggesting a saturation point had been approached. When compared with the raw fractional cover data, it was apparent that the f_{PV} values reached a natural maximum at 80%. As such, it is considered that the f_{PV} rather than the index was saturated, and results at the higher end of the $NDVI_{705}$ scale are valid. The amplitudes of the curves were comparable between density treatments.

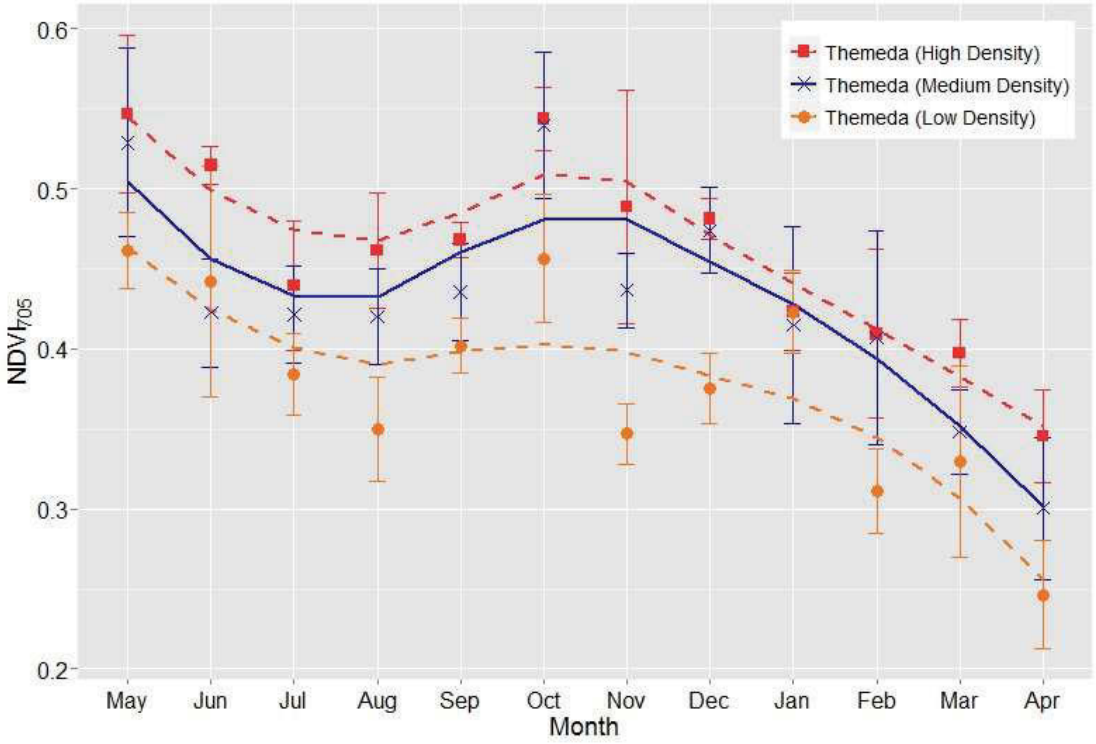

Figure 2.11. Mean monthly $NDVI_{705}$ (± 1 s.d.) phenology for low-, medium- and high-density *Themeda* mesocosms (n = 5). The trend line for each series is represented by a LOESS fitted curve (span = 0.8).

Likewise, the different *Poa* density mesocosms all showed similar phenology patterns (Figure 2.12), with the $NDVI_{705}$ peaking in the winter and early spring months then

declining in summer. The greenness values rose with increasing plant density: the low density treatment had an average $NDVI_{705}$ of 0.310 and the high density treatment averaged 0.397.

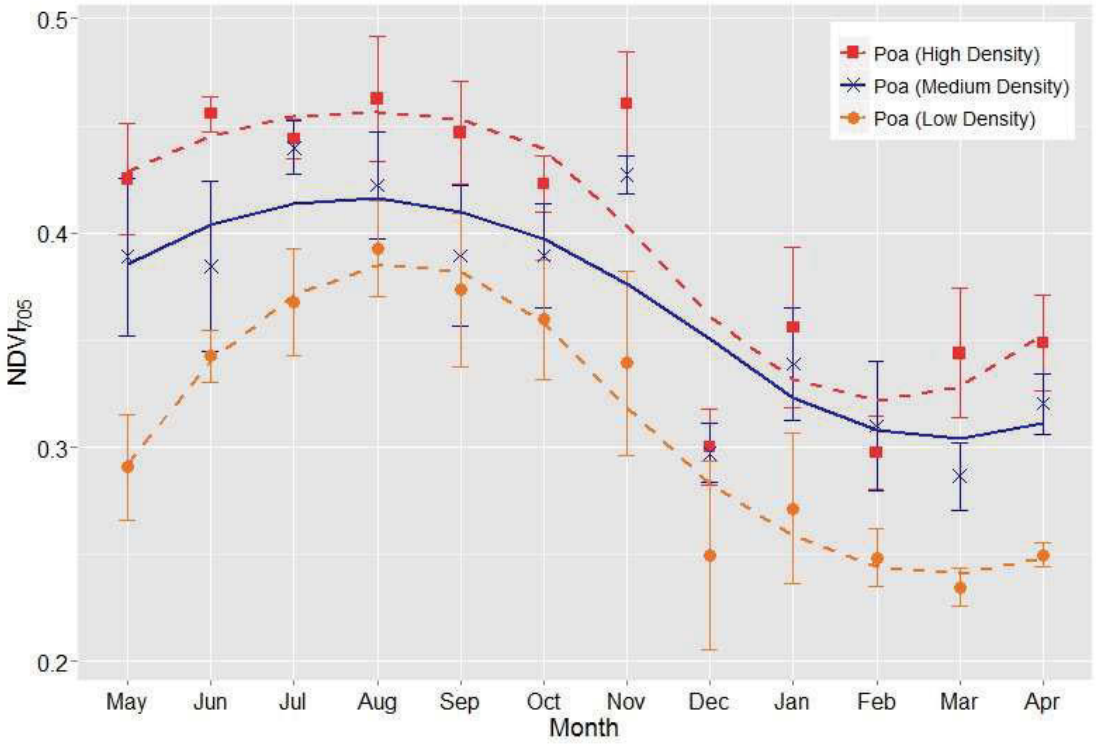

Figure 2.12. Mean monthly $NDVI_{705}$ (± 1 s.d.) phenology for low-, medium- and high-density *Poa* mesocosms (n = 5). The trend line for each series is represented by a LOESS fitted curve (span = 0.8).

The strong relationship between f_{PV} and $NDVI_{705}$ was maintained across all density treatments for both *Poa* (Figure 2.13) and *Themeda* (Figure 2.14) control groups.

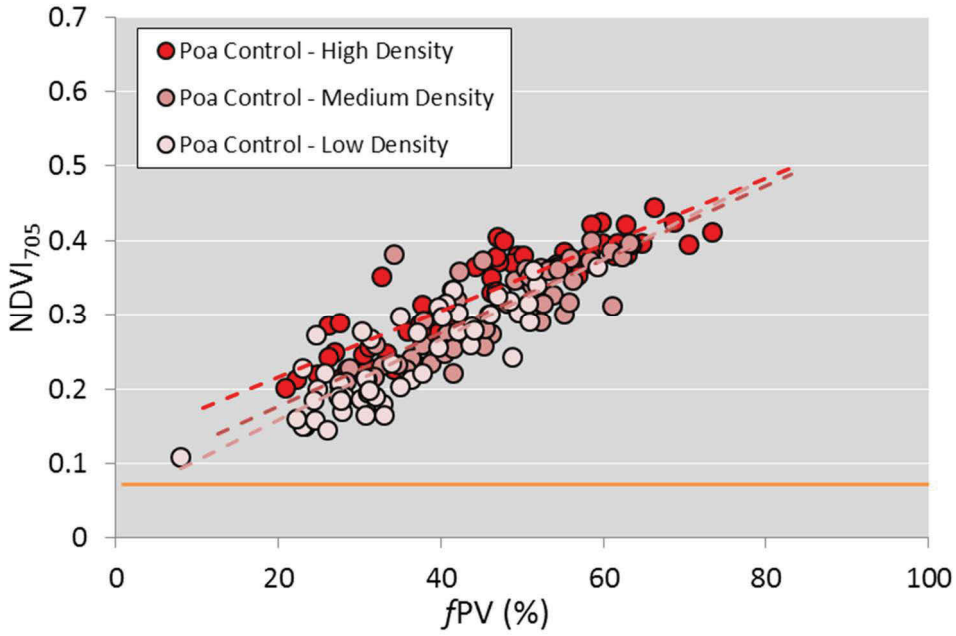

Figure 2.13. Pearson's correlation of f_{PV} with $NDVI_{705}$ for *Poa* control treatments, separated by density. The orange horizontal line represents the average bare soil $NDVI_{705}$ value of 0.084.

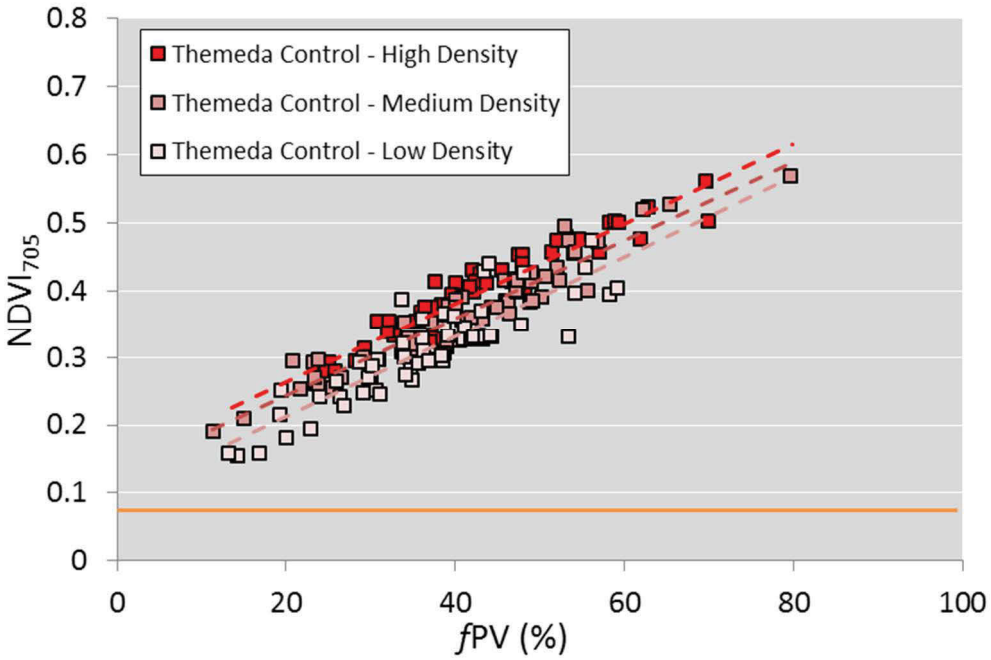

Figure 2.14. Pearson's correlation of f_{PV} with $NDVI_{705}$ for *Themeda* control treatments, separated by density. The orange horizontal line represents the average bare soil $NDVI_{705}$ value of 0.084.

2.3.4 Differences in phenology due to treatment

The drought treatment involved stressing the plants such that no green vegetation was present, and then monitoring the recovery throughout the year. *Themeda* plants in the drought treatment exhibited consistently low $NDVI_{705}$ values through the winter months of June and July ($NDVI_{705} < 0.355$) before recovery and more vigorous growth of new foliage in spring (Figure 2.15). However these drought treatment plants reached a peak $NDVI_{705}$ one month earlier than the controls, and maintained a lower VI throughout the duration of the experiment (annual average $NDVI_{705}$ of 0.322 compared with the control annual average $NDVI_{705}$ of 0.429). *Poa* plants (Figure 2.16) showed a faster recovery response than *Themeda*, but also maintained a greenness level much lower than the control plants (annual average $NDVI_{705}$ of 0.271 compared with an annual average $NDVI_{705}$ of 0.366 in controls). Unlike the *Themeda* treatments, *Poa* peaked two months later than the control treatment.

The resprout treatment involved the removal of all standing litter from the mesocosms to mimic the state of green vegetation resprouting after a major disturbance (e.g. fire, broad scale clearing). The treatment then monitored the maturation of the 'resprouted' grass plants throughout the year. At the starting point, the resprout treatment for both species had a greater $NDVI_{705}$ than control treatments, which comprised both standing litter and green vegetation. Following the initial state of 100% photosynthetic vegetation, the green leaves matured and senesced throughout the year, continually reducing the $NDVI_{705}$, even as new green foliage was produced. In the *Themeda* treatment, an increased greenness was observed relative to the control throughout winter and spring, and remained higher than controls until October (Figure 2.15). At this point, controls and resprout treatments contained similar fractions of PV and NPV to one other, a state which remained comparable until the end of the experiment. In contrast, *Poa* resprout treatments showed a consistent decline in $NDVI_{705}$ from the commencement but maintained higher values than the control until late summer (February) when the treatment returned to dynamic equilibrium (Figure 2.16).

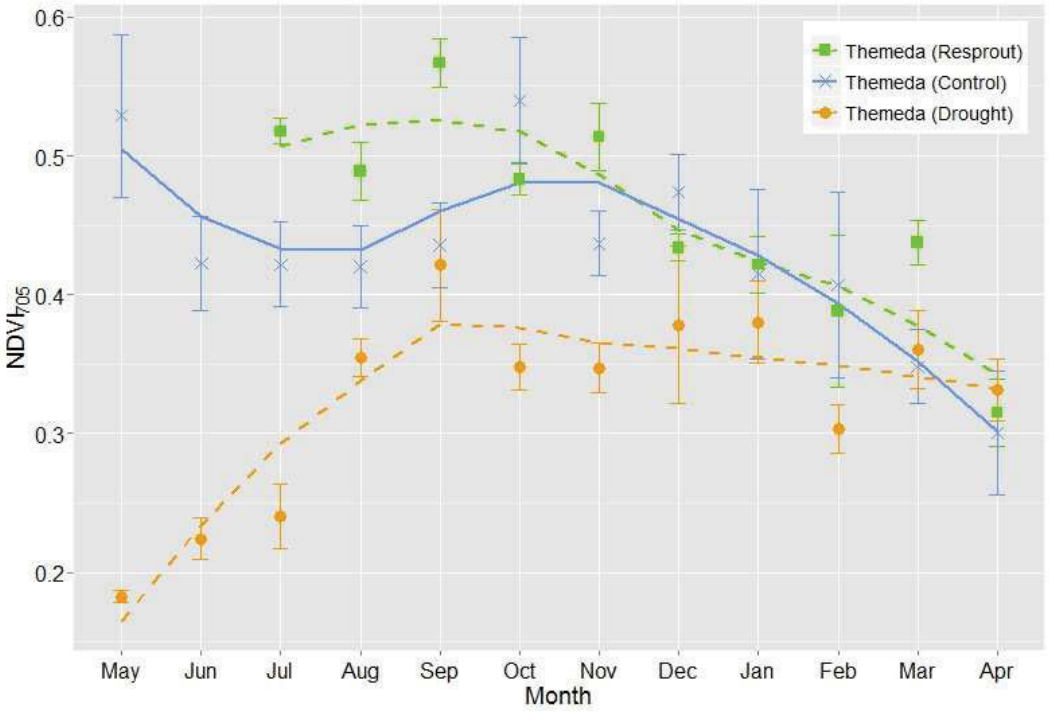

Figure 2.15. Mean monthly $NDVI_{705}$ (± 1 s.d.) phenology for *Themeda* control, drought and resprout treatments at medium density. The trend line for each series is represented by a LOESS fitted curve (span = 0.8).

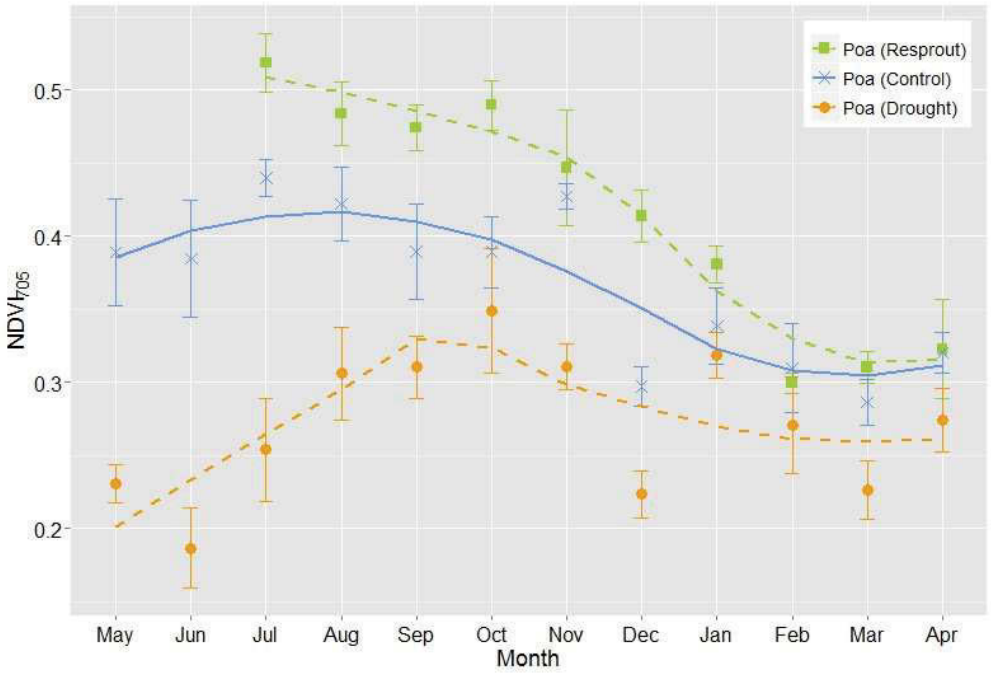

Figure 2.16. Mean monthly $NDVI_{705}$ (± 1 s.d.) phenology for *Poa* control, drought and resprout treatments at medium density. The trend line for each series is represented by a LOESS fitted curve (span = 0.8).

Control and resprout treatments for both *Poa* (Figure 2.17) and *Themeda* (Figure 2.18) mesocosms maintained the strong relationship between f_{PV} and $NDVI_{705}$. In each case, the resprout treatment had the higher correlation coefficient (*Poa*: $r = 0.971$, *Themeda*: $r = 0.960$). For both species, the drought treatments exhibited a weaker relationship between these two variables (*Poa*: $r = 0.678$, *Themeda*: $r = 0.796$).

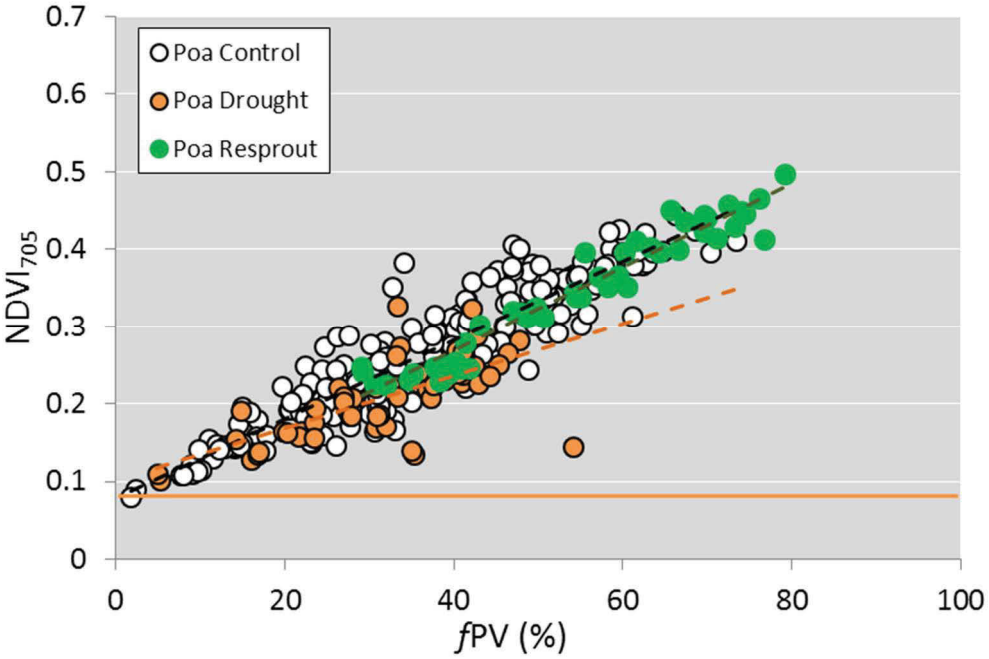

Figure 2.17. Pearson's correlation of f_{PV} with $NDVI_{705}$ for *Poa* medium-density mesocosms, separated by treatment (control $r = 0.809$, drought $r = 0.698$, resprout $r = 0.971$). The orange horizontal line represents the average bare soil $NDVI_{705}$ value of 0.084.

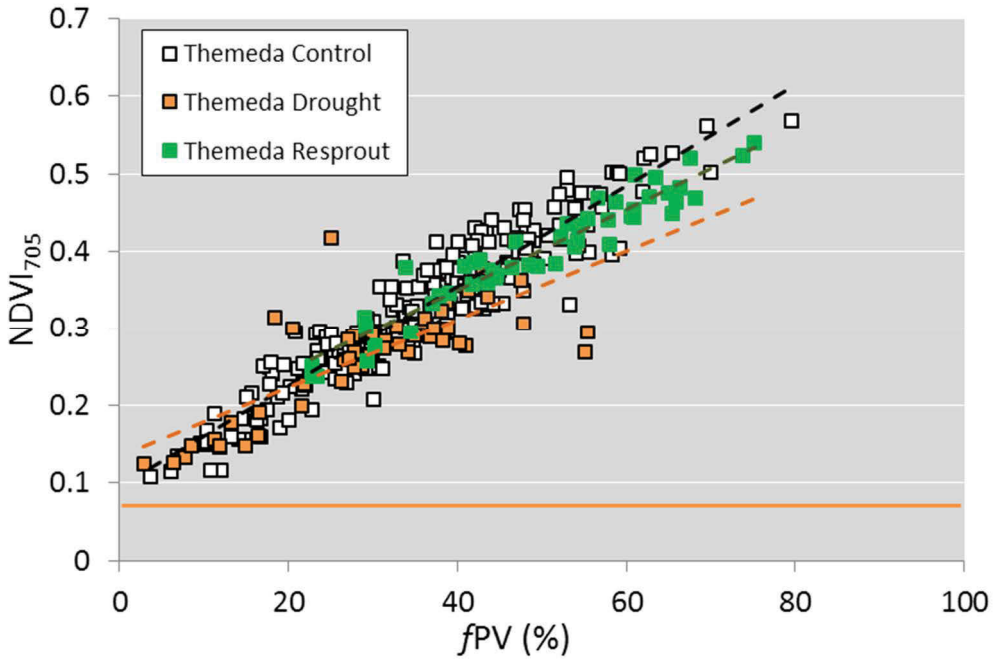

Figure 2.18. Pearson's correlation of f_{PV} with $NDVI_{705}$ for *Themeda* medium-density mesocosms, separated by treatment (control $r = 0.951$, drought $r = 0.796$, resprout $r = 0.960$). The orange horizontal line represents the average bare soil $NDVI_{705}$ value of 0.084.

2.3.5 Removal and addition of litter

Plants in the resprout treatment had all non-photosynthetic material removed. Spectral reflectance readings were taken before and after the removal and converted to $NDVI_{705}$ values. The results show a significant increase from controls for both species (paired t-test; *Poa* $p < 0.001$; *Themeda* $p < 0.001$), despite the fact that the physical quantity of photosynthetic material in the mesocosm had not changed (July control versus July resprout, Figure 2.15, Figure 2.16). It was apparent that the litter quantity affected $NDVI_{705}$ response, so a supplementary experiment was set up to quantify this response. This experiment involved the removal of standing litter from a mixed vegetation scene, and the replacement of increasing quantities of litter (100 g, 200 g, 400 g, and 800 g per square metre) to determine the effect on the $NDVI_{705}$ values.

The soil used in this study had a mean $NDVI_{705}$ of 0.084 with a standard deviation of 0.0029. In natural systems, it is more common for grasslands to have a background layer of senesced vegetation still attached to the plant rather than a large amount of visible soil (Morgan and Lunt 1999). To evaluate how litter would impact a soil

background, increasing amounts of grass litter were added to bare soil, and the spectral reflectance response was recorded. Data was analysed using the Kruskal-Wallis non-parametric analysis of variance due to non-normal distribution of the data. Post-hoc comparisons of treatments were conducted using Dunn's test.

The $NDVI_{705}$ response of the addition of increasing quantities of *Poa* and *Themeda* litter to bare soil is illustrated in Figure 2.19. In both species, there was a significant ($p < 0.05$) difference in VI response between treatments (*Themeda*: $\chi^2 = 21.19$, $p = 0.0002$; *Poa*: $\chi^2 = 20.70$, $p = 0.0003$). The addition of 100 g/m^2 of *Poa* litter to bare soil results in a significantly lower $NDVI_{705}$, though there is no further decrease when more litter is added. At higher quantities of *Poa* litter (400 and 800 g/m^2), the $NDVI_{705}$ is still significantly lower than that of bare soil.

The addition of low quantities of *Themeda* litter (100 and 200 g/m^2) to bare soil decreased the $NDVI_{705}$, though this was only significant at 200 g/m^2. Adding more litter resulted in an $NDVI_{705}$ significantly greater than that of bare soil.

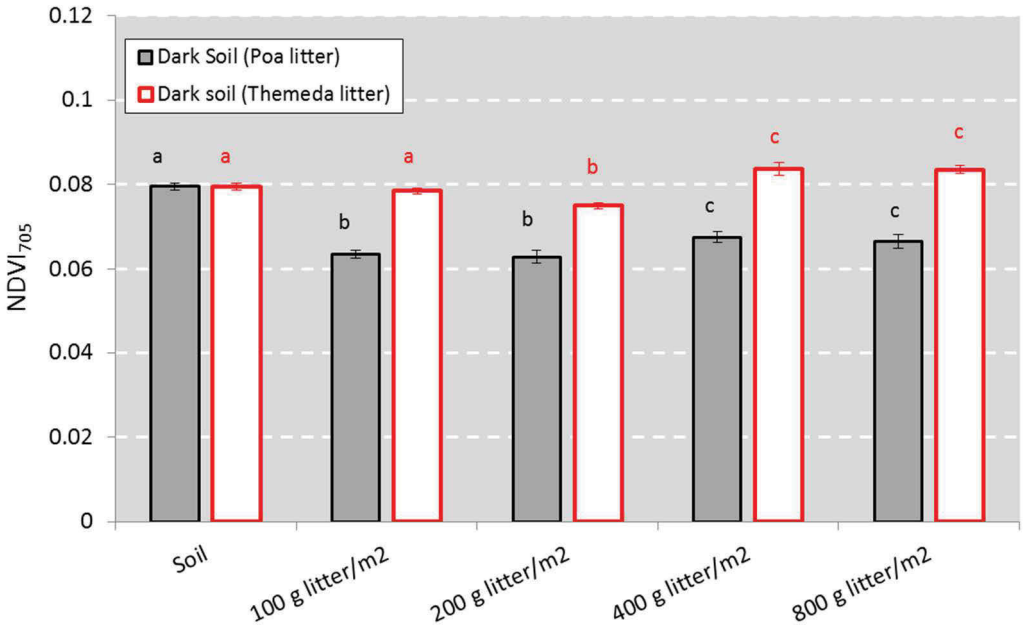

Figure 2.19. $NDVI_{705}$ (± 1 s.d.) response to addition of increasing quantities of *Themeda* (grey) and *Poa* (white) litter to bare soil. Means with the same letter are not significantly different within each species (Dunn's test at $p < 0.05$).

To investigate the effects of litter on a vegetated scene, five replicates of medium-density (32 plants/m^2) mesocosms were established for each species. Initial spectral measurements were taken with existing quantities of green vegetation and standing litter. All standing litter was then removed (as in the 'resprout' treatment), weighed, and the mesocosm reflectance taken. Increasing quantities of litter (100 g/m^2, 200 g/m^2, 400 g/m^2 and 800 g/m^2) were added to the mesocosms to determine the effect of litter on the spectral reflectance, with spectral readings taken at every interval. Care was taken to not obscure the green vegetation with the litter; that is, the litter replaced the contribution of the background soil rather than obscuring the green vegetation. Finally, the highest quantity of litter was added on top of the plants ('overlain'), to test for the effect of obscuring photosynthetic material. This sequence is presented in Figure 2.20. Data was analysed using the Kruskal-Wallis non-parametric analysis of variance due to non-normal distribution of the data. Post-hoc comparisons of treatments were conducted using Dunn's test.

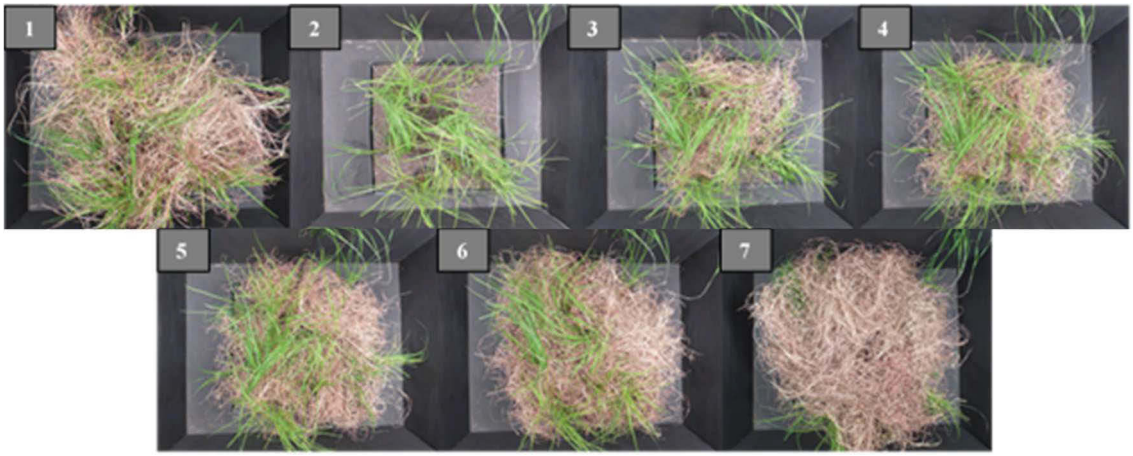

Figure 2.20. Photographs of sequence of litter measurements taken: (1) mixed PV/NPV scene, (2) removed litter, (3) 100 g/m^2 litter, (4) 200 g/m^2 litter, (5) 400 g/m^2 litter, (6) 800 g/m^2 litter and (7) 800 g/m^2 overlain litter.

Kruskal-Wallis analysis showed a significant different between litter treatment for both species (*Themeda:* $\chi^2 = 29.25$, $p < 0.001$; *Poa*: $\chi^2 = 19.01$, $p = 0.004$). Post-hoc analysis between treatments showed that the initial removal of litter significantly increased the $NDVI_{705}$ in both *Poa* and *Themeda* mesocosms. In *Poa* mesocosms, $NDVI_{705}$ increased from 0.195 to 0.269, with an average of 66.3 g of litter removed per mesocosm. In *Themeda* mesocosms, the increase was from 0.215 to 0.350, and equated to an average

of 76.2 g of litter. An alternate way of quantifying litter contribution is that adding 11.6 g *Poa* litter per m^2 increases the $NDVI_{705}$ by 0.01 units. The same $NDVI_{705}$ increase is obtained with 5.6 g of *Themeda* litter per m^2.

Increasing quantities of re-applied litter was found to decrease the $NDVI_{705}$ value in both *Poa* and *Themeda* mesocosms (Figure 2.21 and Figure 2.22), though the effect was more linear with *Themeda*. *Themeda* showed a consistent decrease of 0.01 units for every 49.1 g/m^2 (s.d. = 17.4) of litter applied, whereas *Poa* exhibited a more variable range (64.0 g/m^2 litter; s.d. = 48.9).

The largest decrease in $NDVI_{705}$ in both species was found when litter was placed to obscure the green vegetation, as this greatly decreased the fraction of green vegetation visible in the scene and increased the proportional reflectance of near infrared wavelengths.

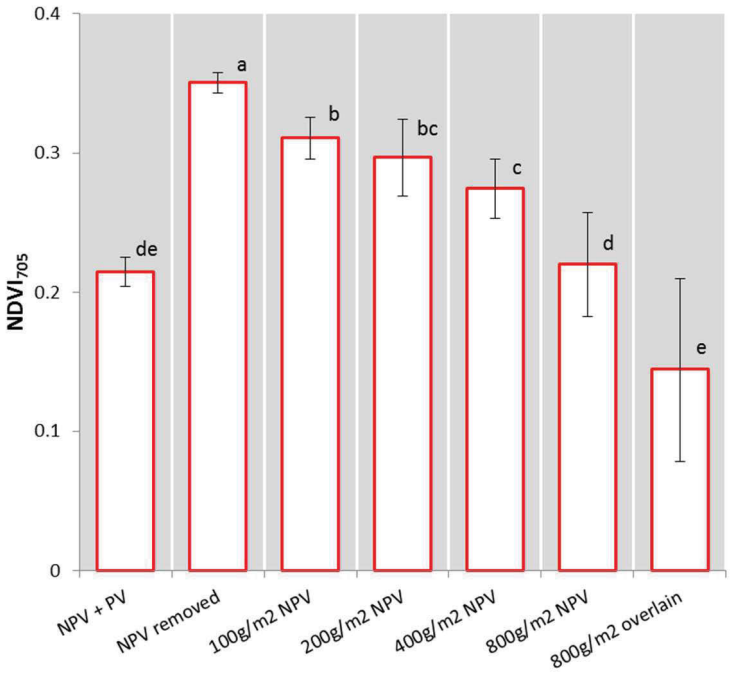

Figure 2.21. *Themeda* mesocosm mean $NDVI_{705}$ response (± 1 s.d.) to removal and replacement of increasing quantities of non-photosynthetic vegetation (NPV), or standing litter. Means with the same letter are not significantly different (Dunn's test at $p < 0.05$).

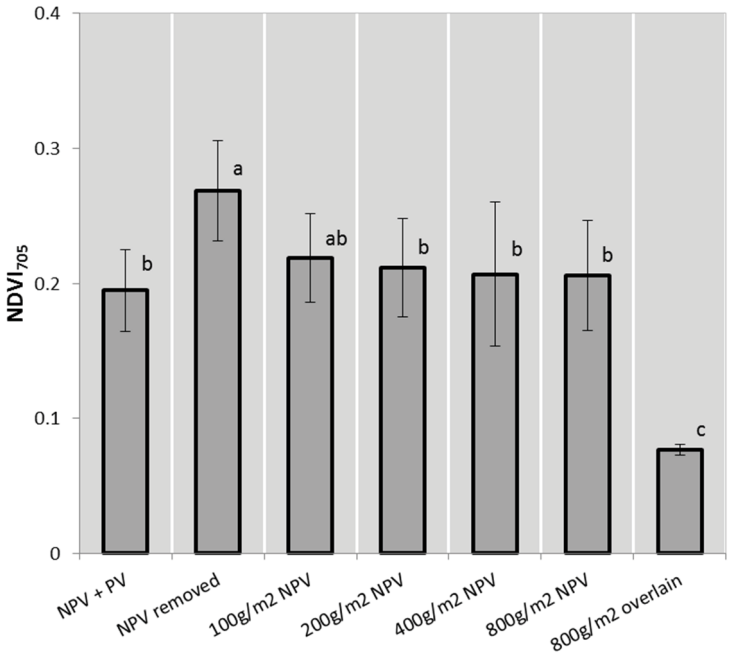

Figure 2.22. *Poa* mesocosm mean $NDVI_{705}$ response (± 1 s.d.) to removal and replacement of increasing quantities of non-photosynthetic vegetation (NPV), or standing litter. Means with the same letter are not significantly different (Dunn's test at $p < 0.05$).

2.3.6 Chlorophyll content

Chlorophyll content, as represented by SPAD values, were measured between November 2013 and May 2014 (Figure 2.23). Analysis of SPAD data was performed using 2-factor ANOVA with Tukey's HSD post-hoc test. In general, each treatment exhibited a high variance in chlorophyll content and there were no consistent significant differences between treatment types. As such, all treatments were grouped by species and comparisons of chlorophyll content made over time. SPAD values were observed to vary significantly for both species with time (*Themeda*: $F = 3.923$, $p = 0.0017$*; Poa:* $F = 10.23$, $p < 0.0001$), indicating that chlorophyll content was not constant over the study period.

Poa chlorophyll content was found to be significantly lower than *Themeda* ($F = 106.36$, $p < 0.0001$). Monthly mean SPAD values ranged between 34 and 36.3 for *Themeda* and 29 and 33.5 for *Poa,* however there was no consistent temporal pattern that matched observations of vegetation growth. A small but significant interaction effect between species and sampling time was observed ($F = 2.82$, $p = 0.15$). This suggests that the

temporal response of SPAD values differed between species; that is the chlorophyll concentration of each species had a different magnitude of change at different times of the year.

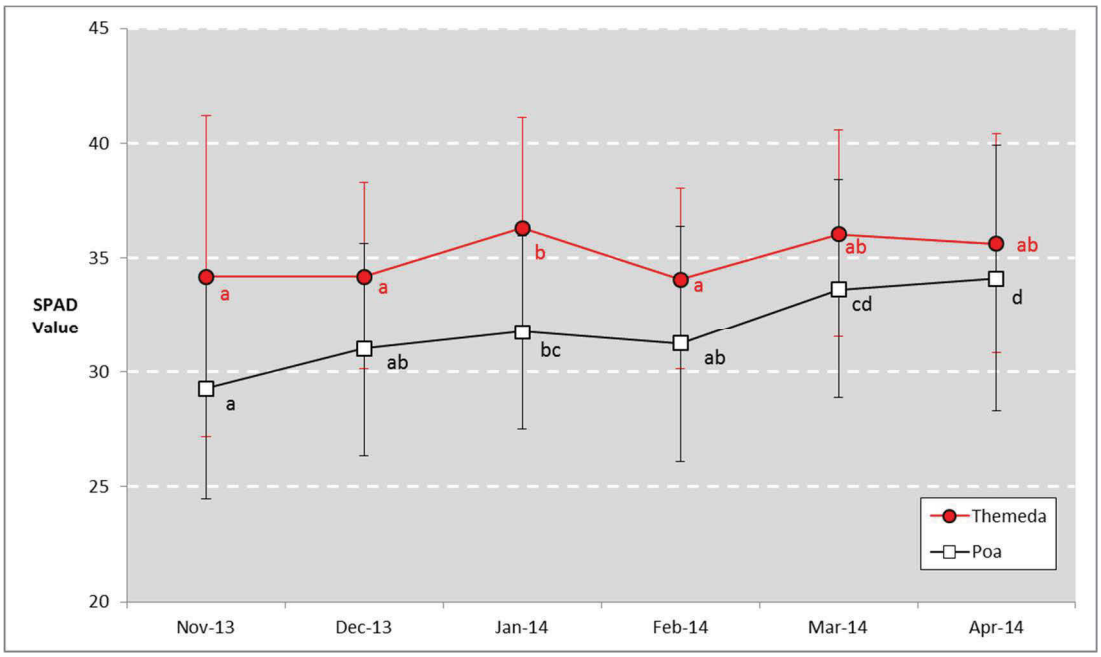

Figure 2.23. Leaf-level chlorophyll content (SPAD values) for *Poa* and *Themeda* between November 2013 and April 2014. Means with the same letter are not significantly different within each species.

2.4 DISCUSSION

2.4.1 Phenological differences between species

The difference in *Poa* and *Themeda* phenology patterns are evident in this controlled experiment, which was independent of the quantity and seasonal patterns of rainfall. In temperate Australia, the growth of C_3 grasses such as *Poa labillardierei* tends to be greater through the cooler months, with reduced growth and increased senescence apparent in warmer temperatures (Morgan and Williams 2015). This is evident with *Poa* in this experiment: higher greenness is evident during the cooler months (June to October), with a sharp decline in $NDVI_{705}$ in the warmer months brought on by increased senescence and lower production of green vegetation. In the final month of the experiment, when temperatures were cooler, a renewal in productivity and an

increase in greenness was observed. Some perennial C_3 plants are classified as year-round perennials (Rose and Rose 2012) because they are able to sustain low levels of growth even at less favourable growing times, which is apparent with *Poa* plants in this experiment.

C_4 grasses in temperate Australia grow more favourably than C_3 grasses during the summer months due to higher light use efficiency at warmer temperatures (Ehleringer *et al.* 1997, Morgan and Williams 2015). This was apparent in these results, with a distinct productive season (October to February) and less active season (June–August) for the C_4 *Themeda* grasses. Frost is a major driver of vegetation dynamics in *Themeda triandra*; foliage rapidly senesces when exposed to sub-zero temperatures and minimal green vegetation is retained on the plant (Robinson and Archer 1988). While frost effects clearly drive vegetation phenology in areas where temperatures are sufficiently low, similar and consistent phenology patterns in this species were observed despite the relatively moderate conditions in which these plants were grown.

Poa had a cyclical intra-annual pattern, whereas *Themeda* did not. While *Themeda* showed an increased $NDVI_{705}$ in the summer months, values decreased sharply through late summer to autumn. Given these plants had adequate water and other resources, a more expected pattern would have been sustained $NDVI_{705}$ through summer, and a decline only in cooler seasons. It is likely that this decline in greenness and corresponding misalignment in annual cycles is due to an enhanced contribution of standing litter. This senescence was attributed to several days of very high temperatures following the high-growth period in October. The effect of litter is further discussed in Section 2.4.4.

While replication of other C_3 and C_4 species is required to directly assess the reproducibility of phenology profiles according to photosynthetic type, it is encouraging that the key features of the phenology profiles of the C_3 and C_4 grasses were as expected. C_3 grasses had higher greenness in winter than summer, and C_4 peak values during warmer times of the year and distinctly poorer growth in the winter. With only minor variation, the density treatments of each species showed similar patterns. This provides assurance that the observed profiles are reflective of actual vegetation biophysical changes.

2.4.2 Phenological differences between density treatments

Poa plants had a lower greenness than *Themeda* plants due to the combined effects of lower f_{PV} and lower mean chlorophyll content. Because of this difference, it is not appropriate to directly compare $NDVI_{705}$ values between species groups. While it is feasible to compare values for intra-species treatments, patterns of phenology rather than $NDVI_{705}$ metrics present a more appropriate method for inter-species trend comparison.

The average annual $NDVI_{705}$ followed a predictable increase with increasing vegetation density for both species. The average annual $NDVI_{705}$ of *Themeda* increased from 0.337 at low densities through 0.397 at medium densities to 0.431 at the highest density measured. Average annual *Poa* $NDVI_{705}$ values increased from 0.272 at low densities, to 0.328 at medium densities and 0.363 at high densities. For both species, this order was observed consistently from month to month: in 10 out of 12 months for *Themeda* and 11 out of 12 months for *Poa.*

Vegetation indices have been successfully used for estimating vegetation density in other parts of the world (Karnieli *et al.* 2013). As has been demonstrated in field- and laboratory-based grassland experiments (e.g. Hansen and Schjoerring 2003; Mutanga and Skidmore 2004) increasing vegetation quantity results in increased VI for both species. However, particularly for *Themeda*, vegetation density reaches an upper threshold where f_{PV} does not increase, and the difference in VIs between high and medium densities is not significant. This is confirmed by the representation of fractional cover with increasing densities, which is invariant at these same times. It would be suitable, therefore to use $NDVI_{705}$ and similar indices as indicators of vegetation cover in the field, with the understanding that plant density increases are not detectable beyond a certain point due to an equilibrium of f_{PV} and f_{NPV} being reached.

2.4.3 Phenological differences between treatments

The phenological patterns of the ‘drought’ and ‘resprout’ treatments illustrate how grassland vegetation develops as systems recover from disturbed states. In both treatments, we see a slow reversion of the vegetation to the control state as the

proportion of green vegetation to standing litter returns to a dynamic equilibrium. For the drought treatments, the mesocosms start at a state of 0% green vegetation (May 2013) and a corresponding low $NDVI_{705}$. As the plants recover and start to grow, f_{PV} increases as the new green vegetation emerges beyond the standing litter. Rates of growth and $NDVI_{705}$ increase will be different for C_3 and C_4 species depending on the recovery season; in this example the C_3 *Poa* shows a faster recovery than C_4 *Themeda* because the 'recovery' component of the experiment commenced in the winter months where temperatures favour C_3 growth over C_4 (Murphy and Bowman 2007). Both species' drought treatment $NDVI_{705}$ approached that of the control within six months, but remained lower than the controls throughout the experiment. Rather than indicating that drought inhibits the recovery and production potential of grasses, this lower $NDVI_{705}$ value may result from the increased fraction of standing litter that is present on the plants (see Section 2.4.4).

Plants in the 'resprout' treatment started with 100% green vegetation to mimic resprouting following a disturbance event such as fire or broad scale clearing. The $NDVI_{705}$ of the initial state exceeded the control treatment for both species, but decreased as leaves started to senesce from the leaf tips and the f_{NPV} increased. As further leaves grew, matured and senesced, the VI for the resprout treatment approached that of the control groups for both species. The *Themeda* resprout treatment returned to a similar value as the control treatment only four months after the start of the experiment, whereas the *Poa* resprout group maintained an elevated $NDVI_{705}$ over the control group for eight months. This may be due to the seasonal timing of the start of the treatment. As a C_4 grass, *Themeda* is less active in the winter months when the experiment started and leaves are likely to senesce faster than they grow. On the contrary, *Poa* is in an active growth period during winter months and will be producing net green vegetation until the summer, thus maintaining greater levels until higher temperatures promote leaf senescence. A different result may be expected if this part of the experiment commenced at another time of year (e.g. in the middle of summer).

2.4.4 Effect of litter on vegetation index

The contribution of standing litter is known to have confounding effects to vegetation indices and estimates of biophysical characteristics, though the magnitude and direction

of change is dependent on soil type, stage of senescence of vegetation, and position of litter (Huete and Jackson 1987, van Leeuwen and Huete 1996). The removal of the NPV from both *Themeda* and *Poa* plants treatment led to a higher $NDVI_{705}$, indicating that senescent vegetation has a negative influence on VI value. Both species are caespitose in form, and as such have NPV and PV both represented in upper and lower strata. As such, there is likely a combination of two effects: a masking effect of standing litter overlaying green vegetation and a dilution effect of litter on the red to near-infrared reflectance signal. A similar response to drying was seen by Cristiano and colleagues for the C_3 grass *Dactylis glomerata* in controlled mesocosm studies (Cristiano *et al.* 2010). Because litter has high reflectance of both red and infrared wavelengths, increasing quantities of litter will naturally decrease VI values of a scene that normalise these wavelengths. In the case of grasses that exhibit different parts of the plant growing and senescing concurrently, this may create an artificial drop in VI immediately following the peak growth period. Put another way, when the active growth period commences, a large quantity of green foliage is produced. Particularly in the summer months when conditions are hot, a fraction of this foliage will start to cure and brown. This net increase in f_{NPV} will reduce the VI, even though the active growth of the plant continues. As other authors have cautioned (Nagler *et al.* 2000), using VIs to estimate productivity may result in underestimated productivity if the effects of plant litter are neglected. This is likely to be a significant issue in Australian grasslands that tend to have a high proportion of litter throughout the year (Morgan and Lunt 1999). This is a major difference to northern hemisphere temperate grassland systems where the majority of senescence is confined to one part of the year.

As increasing quantities of litter were added to bare soil, the response of $NDVI_{705}$ changed depending on the species of litter applied. Application of a small quantity (100 g/m^2) of *Poa* litter decreased the $NDVI_{705}$ of bare soil, but no further decrease was apparent with higher quantities of litter. In fact at higher litter application rates the $NDVI_{705}$ increased, though was still significantly below the $NDVI_{705}$ of bare soil. Application of low quantities of *Themeda* litter had a smaller effect of decreasing $NDVI_{705}$ below that of bare soil. However, when higher quantities of litter were added, $NDVI_{705}$ was increased to a value above the bare soil. As grassy ecosystems in temperate Australia usually have a dense litter layer rather than bare soil (Morgan and Lunt 1999, Morgan 2015), these results have an influence on the quantification of

phenology parameters and ability to compare phenology metrics between systems. While some researchers have highlighted that increasing quantities of litter in a canopy may cause VIs to approach that of bare soil (Tucker and Sellers 1986), this result suggests that litter can suppress the VI below that of bare soil. As a bare soil VI is reasonably considered the zero-point of a phenology profile, phenology metrics where litter is abundant may be lower than a similar ecosystem with less or no standing litter. This will have an impact on some widely used phenology metrics (e.g. VI maxima, VI minima, large integral), and may restrict the ability to compare phenological values between systems that have different quantities of litter present. However, other metrics (e.g. small integral, amplitude, start of season, end of season, length of season) will be largely unaffected. For higher quantities of litter, the *Poa* $NDVI_{705}$ is below that of bare soil, however the *Themeda* $NDVI_{705}$ is above that of bare soil. This differential response to species of litter suggests that this impact may be relevant for some grassland types and not others.

Where there is a mix of green vegetation and litter present, *Themeda* showed a more pronounced effect to the addition of litter to the mesocosm, exhibiting a significant reduction in $NDVI_{705}$ with increasing amounts of litter. The exponential relationship that is displayed suggests that a threshold is reached at which additional litter no longer contributes to a decrease in vegetation index. In this experiment, that threshold for *Themeda* has not been reached and must be greater than 800 g/m^2 of litter. *Poa* showed a less consistent result. While adding a small quantity of litter significantly decreased the VI, analysis showed no significant difference between the quantity of background litter and a limit of 400 g/m^2 of litter, beyond which no more reductions occurred. This may be due to the architecture of the dried leaves of each species; Themeda tends to curl when dried, producing a tangled mat of litter, whereas *Poa* is more two-dimensional, or filiform, in nature. This may result in more infrared scattering from *Themeda* litter, making the $NDVI_{705}$ signal more sensitive to litter quantity. Other researchers have noted the potential response and overlapping nature of litter (Nagler *et al.* 2000), but little confirmatory research has been conducted in specific systems. Both *Poa* and *Themeda*, however, show a significant change in $NDVI_{705}$ when a) all NPV was clipped and removed from the mesocosm, and b) when litter was overlain over the vegetation to obscure it. In a natural grassland system, the obscuring effect is likely to be a major contributor, particularly early in the growing season at locations

that have a high proportion of standing litter. This could feasibly result in an underestimate of the start of the growing season, as new growth will take some time to emerge past the litter layer.

The negative impact of litter on $NDVI_{705}$ may also be visible in the apparent failure of *Themeda* drought treatments to recover from the initial drought stress. Despite plants being observed to establish green vegetation during the winter months, they retained a large proportion of NPV which consequently retarded their apparent recovery in the $NDVI_{705}$ data. Native grasses can survive for long periods under drought conditions (Hodgkinson and Miller 2005) and are often reliant as pasture when exotic species have succumbed to drought stress. Understanding how plants recover from drought is critical for Australia, where droughts are common and projected to increase (Hennessy *et al.* 2007), hence further research into grass resilience under drought stress is necessary.

2.4.5 Chlorophyll content

Chlorophyll content differed between species but the range of SPAD measurements were quite large at each treatment. Part of this may be due to an inherent limitation of chlorophyll measurements using the SPAD method. The only leaves that were large enough to be measured by the SPAD were fully expanded leaves of both species. Smaller and partially expanded leaves were too thin to accurately cover the measurement window and were excluded from measurement. These excluded leaves can make up a substantial fraction of the total vegetation at certain times and chlorophyll content changes as grass leaves mature and expand from the leaf apex to the base (Prioul *et al.* 1980). Chlorophyll content varied significantly over time, but these changes did not correspond to observations in plant and leaf growth at particular times. In spite of this, the contribution of chlorophyll content to phenological variability appears low when compared to the contribution of vegetative cover. Further investigations into chlorophyll variation, which is known to affect NDVI-type vegetation indices (Tucker and Sellers 1986), may need to be conducted using destructive methods or a greater sample size to gain a complete picture of how total canopy chlorophyll changes seasonally.

2.4.6 Application to natural systems

Caution should be taken when applying these results to natural systems because of the inherent simplicity of the conditions under which this experiment was conducted. Controlled conditions were necessary in this case to test the required parameters, but rely on artificially uniform mesocosms that differ from natural temperate grasslands in many ways. Australian temperate grasslands are rarely uniform in age or species composition. Their composition includes native and exotic forbs growing in the interstices between grass tussocks (Tremont and McIntyre 1994) which was not simulated here. Climatic conditions are more extreme in natural systems, which would result in more pronounced greenness minima in particular: *Themeda* browns in response to frosts and *Poa* senesces in summer heat and low rainfall conditions. Rainfall timing and quantity has a great impact on most Australian environments, and seasonal response to rainfall is a primary driver of growth and abundance in C_3 and C_4 grasses (Murphy and Bowman 2007). This impact was minimised within this study as plants were provided with adequate water at all times. Also, native grasslands are exposed to a myriad of other stressors, such as pests and diseases, grazing and competition, all of which were excluded or reduced in this experiment.

In addition, the majority of remote sensing studies are conducted using satellite-based sensors, which can be variable in atmospheric effects and viewing/illumination geometries (Bhandari *et al.* 2011). These inconsistencies can generate noise in the data, which is limited in our controlled setting due to the consistent illumination and short distance between the scene and the sensor. Further data processing, filtering and quality control will naturally be required for satellite application. Different soil types across landscape-scale studies may necessitate the use of alternative vegetation indices that minimise the contribution of the soil reflectance component (e.g. the soil-adjusted vegetation index, SAVI, Huete 1988).

2.4.7 Future work and recommendations

The need for controlled conditions in this case has allowed for the expression of phenological characteristics of common C_3 and C_4 grass species that would be difficult in to conduct in non-controlled conditions. This improved understanding of grassland

phenology drivers can be applied to future studies of grassland ecosystems using satellite or ground-based remote sensing methods, which can be used to improve the knowledge and management of these dynamic systems. Validation of these findings in relevant ecosystems under natural conditions are addressed in Chapter 5 of this thesis.

While the two examples of a C_3 grass and a C_4 grass within this study exhibited phenology trends that are consistent with the expectation for each photosynthetic type, these responses cannot be extrapolated for all C_3 and C_4 temperate grasses. Repeating this study with other dominant temperate species, such as *Microlaena stipoides* (C_3), *Rytidosperma caespitosum* (C_3), and *Bothriochloa macra* (C_4), would provide more information on the consistency of C_3 and C_4 phenology between species.

This study used fractional cover, a repeatable but non-destructive measure, as the main biophysical response variable. Vegetative biomass—the dry mass of vegetation per unit area—is an important biophysical parameter and can also be used to determine patterns of vegetation dynamics. In this case, repeated destructive biomass sampling was not feasible as the number of plants needed for adequate replication would have exceeded space requirements and budget. While vegetation indices can be used to estimate photosynthetic biomass as well as photosynthetic fractional cover (Ratana *et al.* 2005), these relationships are species-specific and should be empirically tested if accurate estimates of biomass are required.

The soil used in this experiment was a dark brown native topsoil, similar to surface soil conditions in many areas of temperate Australia. However, different soil types are known to alter spectral reflectance characteristics and alter the spectral reflectance contribution of photosynthetic and non-photosynthetic vegetation (Huete 1988). Future research should test soils of different composition and colour to determine if the results presented here are repeatable for different soil types.

At the start of the experiment, *Themeda* plants showed a high greenness, which is atypical for C_4 plants in the cooler months. It is possible that the nursery had grown these plants in warmer conditions, or had removed some of the standing litter to make the plants appear more attractive to customers. While this does not appear to have affected overall patterns of phenology throughout the experiment, it is recommended

that future studies acclimatise plants to experimental conditions for at least six months to exclude potential legacy effects.

In this experiment, $NDVI_{705}$ was used as the primary response variable, as it showed the best relationship with photosynthetic fractional cover in the pilot study (Watson *et al.* 2013). However, other vegetation indices, particularly narrow- and broad-band NDVI, also showed strong relationships with fractional cover ($r > 0.80$; Appendix A), hence the conclusions drawn using $NDVI_{705}$ could be extended to other vegetation indices, particularly for sensors that do not have hyperspectral capabilities.

2.5 Conclusion

This study used a narrow-band vegetation index, the $NDVI_{705}$, to test the effect of grass species, density and fractional cover on the vegetative phenology of controlled grassland mesocosms. This experiment showed that the $NDVI_{705}$ had a strong relationship with vegetative fractional cover over a range of cover types for both species, and is a suitable index for hyperspectral assessments of temperate grassland vegetation cover. Other NDVI-type narrow- and broad-band indices also showed good relationships with photosynthetic fractional cover (Appendix A). Over the course of one year, species that represent C_3 and C_4 functional types showed differences in their phenological profiles that reflect different periods of vegetation growth and senescence in the two species. *Poa* treatments had high greenness in winter and early spring, whereas *Themeda* treatments showed peak greenness in later spring and summer. Increasing plant density for both species increased the VI as expected, but differences in density did not change the phenology profile, showing that phenology patterns are consistent regardless of vegetation density. Fractional cover treatments that mimicked drought and post-disturbance vegetation resprouting showed differences in phenophase timing and magnitude of $NDVI_{705}$, with the resprout treatment exhibiting higher greenness than the drought or control groups. This is due to this treatment's lack of standing litter, as non-photosynthetic vegetation was found to decrease $NDVI_{705}$ under repeated measures. This represents a potential source of error in estimating productivity and cover of Australian temperate grasslands, which typically have high standing litter quantities throughout the year. Chlorophyll content varied between species but did now show any consistent temporal differences. These influences of fractional cover,

functional type and vegetation density on grassland phenology can be used to improve the accuracy and design of studies that use remote sensing to assess complex grassland ecosystems.

Chapter 3: The effect of rainfall regime on the phenology and productivity of Australian temperate pasture

3.1 Introduction

3.1.1 Grazing agriculture in temperate Australia

Grazing of sheep and cattle in south-eastern Australia has been an important part of Australia's economic and cultural heritage since British colonisation in 1788. Grazing-based agriculture (meat, wool, and dairy products), contributes approximately $16 billion per annum to Australia's economy, including beef ($7.3 billion), dairy products, ($4 billion), sheep meat ($2.2 billion), and wool ($1.9 billion) (Australian Bureau of Agricultural and Resource Economics and Sciences 2013, Australian Bureau of Statistics 2014). These industries are pivotal to Australia's economic growth and export sectors and thus critical to Australia's future prosperity (Stokes *et al.* 2008, Australian Bureau of Agricultural and Resource Economics and Sciences 2013). Over the last 200 years, most grazed landscapes have experienced a sequence of increased grazing pressure during climatically favourable periods followed by prolonged drought periods that result in high disturbance to surface soils and vegetation quality (McAlpine *et al.* 2009). Given the importance of grazing industries to Australia's food and economic security, there is a clear need to understand how the source of these industries—grasslands—respond to climatic conditions. Projected pasture-related challenges for the grazing industry include declines in pasture productivity, reduced forage quality, increased weed invasions, more frequent droughts and more intense rainfall events (Stokes and Howden 2010, CSIRO 2011, Scott *et al.* 2014). The primary factor that links all these challenges is the quantity and distribution of rainfall.

Grazing landscapes in temperate Australia are a mosaic of different pasture types, ranging from improved pastures (deliberately sown exotic species) to native grasslands. Between these two extremes are grazing lands that contain a mixture of native and exotic species. Sometimes this is deliberately facilitated through sowing of exotic species in native grassland—termed pasture cropping—to obtain the dual-benefit of high-quality exotic pastures and drought-resistant native grasses (Williams, Marshall,

and Morgan 2015). More often, mixed pastures are a result of long-term invasions of exotic species into native pastures, their spread assisted by changes in nutrient fluxes caused by long-term livestock impacts, chemical fertilisation, altered fire regimes, and other land management practices. Now, the majority of temperate grasslands contain a significant quantity of exotic species (Benson 1994). Australian temperate grasslands in an undisturbed state tend to be dominated by *Themeda triandra*, a C_4 summer-growing species, with many subdominant C_3 and C_4 grass species (Rehwinkel 2007). However most pastures are highly disturbed, and contain a mix of C_3 grass and forb species that are most active in the cooler months, and C_4 grasses that are more active in the warmer months (Murphy and Bowman 2007, Williams, Marshall, and Morgan 2015).

In temperate grassland biomes throughout the world, rainfall is the primary driver of productivity (Sala *et al.* 1988, Sala 2001) and up to 90% of the variability in production can be accounted for by annual precipitation (Campbell *et al.* 1997). As such, grasslands can be sensitive to subtle changes in water supply, which can often cause major changes in ecosystem structure and function (Sala *et al.* 1992). It is not surprising given the importance of grazing agriculture around the world that research into rainfall effects on grassland productivity has been prominent.

3.1.2 Climate: perspectives in temperate south-eastern Australia

Like many terrestrial biomes (Churkina and Running 1998), the temperate areas of Australia exhibit seasonal variation in climatic variables. Rainfall is the primary driver for growth of vegetation in Australia's south-east (Morgan and Williams 2015). The mean rainfall in this region of Australia is relatively consistent throughout the year, with some parts having no dominant rainfall season, and other parts having a slightly higher winter rainfall. However, the inter-annual and intra-annual rainfall variability throughout south-eastern Australia is high (Murphy and Timbal 2008). Australia regularly experiences lengthy droughts, the causes of which are partially influenced by the variable El Niño Southern Oscillation and Pacific Decadal Oscillation and partially influenced by factors as yet unknown (McAlpine *et al.* 2009). The south-east is regularly impacted by this variation—the so called 'big dry' drought of 2001–2007 is a recent reminder of the economic, social and ecological impacts of rainfall variation (Cai *et al.* 2009). Throughout the period 1997–2006, only two years exceeded the mean

annual rainfall of the past 50 years. The ‘big dry’ had a seasonal component as well; most of the rainfall decline occurred in the autumn months of March to May (Murphy and Timbal 2008).

Most reliable sources suggest that there is a continued long-term drying and warming trend evident in Australia, with indications that Australia has been drying for at least the past 5000 years (Schulmeister and Lees 1995). Since 1910, the average annual temperature of Australia has increased by 0.9 degrees, with the most warming having occurred since 1950 and in the east of the country (CSIRO 2011). The number of hot days (> 35 °C) and hot nights (> 20 °C) have increased during this time, as have declines in the frequency of cold days. Likewise, most of eastern and south-western Australia has become dryer (CSIRO and Bureau of Meteorology 2015).

A greater awareness of the likely impacts of climate change on human activities and natural systems has led to widespread global modelling to estimate and refine predictions of future climates. While different models predict different magnitudes of change, predictions of temperature variables are consistent on the direction and general trends of change. The Intergovernmental Panel on Climate Change 2014 report provides the most recent synthesis of future climate predictions (IPCC 2014). Maximum and minimum temperatures will rise in all locations throughout the globe, with the highest rates of temperature change being concentrated to the polar regions. A global surface temperature increase of 2 ºC is confidently predicted by 2081–2100, with the magnitude of further warming to be impacted by carbon emission scenarios (IPCC 2014). This suite of models also predicted that extremes of temperature (e.g. heatwaves) are likely to occur with increasing frequency.

Changes in precipitation regimes may have more severe impacts on ecosystems than that of temperature change or CO_2 increase (Weltzin and McPherson 2003, Garbulsky *et al.* 2011). Predicting changes in the quantity and timing of rainfall is more challenging than other climate variables, as changes in rainfall will be more spatially heterogeneous and less predictable (Knapp *et al.* 2008, Beier *et al.* 2012). Nevertheless, an intensification of the global water cycle has been acknowledged that includes changes in annual precipitation amounts, seasonal timing, variability and frequency of extreme events (Seneviratne *et al.* 2010, Min *et al.* 2011, IPCC 2014). In fact, despite

the disagreement of many models at regional and local scales, most models are consistent in predicting more intensified intra-annual precipitation; that is, rainfall events that are less frequent but deposit more rain per event (Easterling *et al.* 2000, Hennessy *et al.* 2007). Changes in these precipitation events can influence a myriad of ecosystem processes including carbon cycling and storage (Harper *et al.* 2005).

3.1.3 The future climate of south-eastern Australia

3.1.3.1 Temperature

The warming trend that Australia is experiencing is expected to continue, and is likely to be consistent with the global warming mean (Hennessy *et al.* 2007). Further warming of 0.6–1.5 ºC is expected by 2030, and 1.0–3.0 ºC by 2070. Warming trends are expected to be less in the south, especially in winter. There will be an increased frequency of extreme high daily temperatures and a decrease in the frequency of cold extremes, including frosts (CSIRO and Bureau of Meteorology 2015).

3.1.3.2 Rainfall

Precipitation is likely to decrease in southern Australia, caused by the contraction of the rainfall belt to more southern latitudes. This will be particularly pronounced in the winter and spring (Hennessy *et al.* 2007, Stokes and Howden 2010), with some sources also predicting autumn rainfall declines (Howden *et al.* 2003). The direction of precipitation change in other months is uncertain and model-dependent, however the overall annual average rainfall in southern Australia is confidently forecast to decrease (CSIRO and Bureau of Meteorology 2015). Extremes of precipitation are likely to increase (Hennessy *et al.* 2004, 2007, Kharin *et al.* 2007, Reisinger *et al.* 2014), though may be less pronounced where total rainfall decreases are predicted. Southern Australia is likely to experience seasonal shifts in rainfall as well as increased extreme events (Zeppel *et al.* 2014).

3.1.3.3 Drought

In a general sense, climate predictions emphasise greater variability and increased incidence of extreme events (Howden *et al.* 2003). This classification includes fires, floods and droughts.

There is an increased risk of drought in south-eastern areas of Australia, with some researchers demonstrating a 20–40% increase of drought frequency by 2030 (Mpelasoka *et al.* 2008). Despite seasonally variable rainfall changes (i.e. some seasons may experience more rainfall than currently), there is a predicted net increased moisture deficit due to increased temperatures and increased evaporation (Kirono and Kent 2011). Water availability will also be greatly affected by changes in vegetation and surface-atmosphere feedbacks (Donohue *et al.* 2009). Overall, this equates to longer periods of time in drought conditions for the south-east of Australia (CSIRO and Bureau of Meteorology 2015).

3.1.4 Anticipated impacts to pasture production in southern Australia

The impacts of climate change to pasture production are anticipated to be complex due to the interacting factors of increased atmospheric CO_2, increased temperatures, variability in quantity and timing of rainfall, and soil nutrient availability (Fischer *et al.* 1997, Suter *et al.* 2002). This is particularly true in south-eastern Australian pastures as many contain both C_3 and C_4 pasture species that have differential seasonal responses to these drivers. Hence, ecological processes of competition and exclusion between these functional types add an extra level of complexity.

Impacts of potential climate change scenarios can be monitored through experimental research, observations, or models (Reyer *et al.* 2013). Controlled experiments tend to be relatively small in scale. They provide accurate data for a specific region and a local set of conditions, hence the application of their results may be limited to similar locations or conditions. Observations can be small in scale or can be continental- or global-scale, made through remote sensing and climate data sources. While such large-scale observations may be appropriate for global estimates or cross-biome studies, they may not have the required levels of sensitivity for specific scenarios, or may need to undergo

several iterations of refinement before the data matches with validated information. Hence, reconciling the results of experimental research and remote sensing observations and models can be difficult (see also Chapter 5), and different approaches may yield different results. The following section presents a summary of effects that are predicted for changes in temperature, atmospheric carbon dioxide concentration on pasture production, and integrated changes on plant communities. The explicit effects of rainfall are presented in Section 3.1.5.

3.1.4.1 Temperature and CO_2 impacts on pasture production

Warmer temperatures during cool seasons could benefit pastures in south-eastern Australia by increasing the length of the growing season and reducing frost damage (Stokes and Howden 2010). However, accelerated growth in winter may deplete soil moisture stocks and reduce the capacity for spring growth. In warmer seasons, increased heat stress and higher evaporative demand would likely have negative effects on all pasture types. In turn, pastures with mixed C_3/C_4 species may favour an increase in C_4 species (Williams *et al.* 2007, Cullen *et al.* 2008), which tend to be less palatable to stock and of a lower forage quality (Ehleringer *et al.* 1997, Cullen *et al.* 2009). For the most productive C_3 exotic pastures, heat stress and moisture deficit reduces their growth and quality (Waller and Sale 2001), which will become more pronounced and result in greater losses under hotter, dryer conditions.

The CO_2 'fertilisation effect' suggests that vegetation productivity increases in the presence of elevated CO_2, which is a result of reduction of water use per unit of carbon assimilated (Campbell *et al.* 1997). While it is expected that C_3 species will obtain more benefit than C_4 species from this effect (Ehleringer *et al.* 1997), results can be unpredictable when considered in concert with other variables such as temperature, moisture, and soil nutrient content (Shaw *et al.* 2002, Suter *et al.* 2002). Temperate C_3 pasture response to increased CO_2 has shown that modelled plant production was mostly attributed to the effects of moisture savings, rather than photosynthesis itself (Volk *et al.* 2000). There is some evidence that C_4 grasses may be less responsive to increases in CO_2 than C_3 grasses (Owensby *et al.* 1993, Morgan *et al.* 2004, Nelson *et al.* 2004), although C_4 prairies have been reported to increase above- and below-ground productivity under elevated CO_2 and water stress (Owensby *et al.* 1997, Moran *et al.*

2011). In the absence of water stress, a greenhouse-based mixed C_3/C_4 pasture showed a net increase in productivity under enriched CO_2 conditions (Campbell *et al.* 1997).

Modelled results of C_4 pasture species in south-eastern Queensland suggests that increased CO_2 is likely to have beneficial effects on the growth and productivity of C_4 species, with a greater advantage in dry years than wet years. Increased temperature in combination with elevated CO_2 further increased productivity due to the increase in the length of the growing season. However, when drier conditions were modelled (as is predicted), pasture production was reduced compared to current conditions (Howden *et al.* 1999). An Australian study that modelled the integrated effect of carbon dioxide, rainfall and temperature change across south-eastern Australian pastures (Cullen *et al.* 2009) found that potential increases from carbon dioxide and temperature effects were offset by moisture deficits. The greater the decrease in rainfall, the more apparent the loss in productivity.

3.1.4.2 Integrated climate impacts on demographic change

Demographics and community composition is less commonly studied than production-based variables, but often shows site- or period-specific results. In a New Zealand study, a C_4 grass population had a differential response depending on the degree of CO_2 enrichment (Campbell *et al.* 2007). In Australia, a population of C_4-dominant *Themeda* was unaffected by experimental warming and CO_2 enrichment, while the C_3 *Rytidosperma* was reduced in abundance (Williams *et al.* 2007). Likewise in US tallgrass prairie, cover and relative proportion of C_4 species was unchanged under elevated CO_2 but C_3 grass abundance decreased (Owensby *et al.* 1999). These results provide some context to the conflicting views that C_3 species will benefit more than C_4 from higher CO_2 (Wand *et al.* 1999), but C_4 species are better suited to warmer temperatures (Howden *et al.* 2008). This conflict highlights the need to continue studying these interactions in different biomes.

Prolonged drought conditions in US grasslands have been implicated in species compositional change and weed invasions (Scott *et al.* 2010, Moran *et al.* 2014). Weed invasions reduce the amount of productive land and have also been highlighted as a key threat to Australian systems that will be exacerbated under climate change (Scott *et al.*

2014). Weeds can be more problematic under higher disturbance regimes, as exotic annual species have an advantage in perturbed systems (Fry *et al.* 2013). As most Australian grassland systems comprise perennial species, they are particularly sensitive to such scenarios.

3.1.4.3 Integrated climate impacts on phenology

Changes in rainfall and moisture availability in other biomes have shown complex phenological changes that can have far-reaching consequences for ecosystem functioning (Peñuelas *et al.* 2004). Impacts of climate change on the phenology of pasture species are less-frequently studied. In particular, the response of phenology to changes in climate variability is poorly understood compared to the change in mean climate (Reyer *et al.* 2013).

Vegetation green-up is a fundamental phenological event that is likely to be impacted by climate change. The dynamics of photosynthetic vegetation is perhaps the best integrative measure of ecosystem functioning (Jobbagy and Sala 2000). The observed active period of photosynthetic vegetation refers to the growing season. Decreases in the number of cool days would increase the period that C_4 grasses are active, thereby lengthening their growing season. Conversely, higher temperatures would limit the photosynthetic efficiency of C_3 grasses (Murphy and Bowman 2007). Flowering time is a key phenophase for grassland dynamics. One experiment conducted in Tasmania under elevated CO_2 and infrared warming showed that warming had an accelerated effect on flowering time, and elevated CO_2 had little impact, though the effect was species-dependent (Hovenden, Wills, *et al.* 2008). Plants that flower in response to rainfall such as the Australian wallaby grasses (Groves and Whalley 2002) will have their flowering times and reproductive capacity impacted by any changes in rainfall regime.

The need for further research into how grasslands will respond to climate change is essential to maintain food security and develop adaptation strategies. It has been recognised that strategies for adaptive grazing management should be a priority (Stafford Smith *et al.* 2007) and that extra initiatives into fire regime management should be implemented (Pitman *et al.* 2007). However, the lack of research in this area

is limiting to informed progress. Researchers have demanded more experimental research, given the degree of uncertainty around the relationship between CO_2, temperature and rainfall, and the impact on pasture growth and productivity under Australian conditions (Howden *et al.* 2003, Harle *et al.* 2007). In the absence of Australian studies, we are obliged to look to temperate systems elsewhere to assess how Australian temperate grasslands might respond to changes in rainfall regimes.

3.1.5 Grassland response to rainfall: global lessons

3.1.5.1 Components of rainfall change

Globally, research into rainfall effects on vegetation has been prominent and there is a large body of research literature investigating the effects of variability in rainfall (Weltzin and McPherson 2003). A recent synthesis of this field (Zeppel *et al.* 2014) highlights three interrelated components of rainfall change:

1. overall quantity of rainfall;
2. frequency of extreme rainfall events; and
3. seasonal precipitation regimes.

While the quantity of rainfall is a primary driver in many systems (Campbell *et al.* 1997), the frequency of extreme precipitation events and changes to seasonal precipitation regimes can impact the quantity and timing of plant growth, and impact on phenological timing (Zeppel *et al.* 2014). An increase in extreme rainfall events refers to a situation where the same volume of rainfall occurs, but in larger events at less frequent intervals. A reduction in rainfall frequency is equivalent to an increase in extreme events.

While most ecosystems are sensitive to precipitation change (Weltzin *et al.* 2003), grasslands attract substantial attention due to their aforementioned importance in grazing systems and food production (O'Mara 2012). Grasslands have a greater sensitivity to change than other vegetation types (Knapp and Smith 2001) and their low growth form makes experimental rainfall modification relatively straightforward. An analysis of precipitation modification experiments showed that 46% of 95 experiments globally had been conducted on grasslands (Beier *et al.* 2012).

In temperate grasslands around the world, several research groups have demonstrated that increased precipitation promotes plant growth and productivity (Lane *et al.* 1998, Huxman *et al.* 2004). However, studies that incorporate precipitation frequency and timing into their experimental design are restricted to a few well-studied regions.

3.1.5.2 Temperate grassland response to changes in rainfall frequency

The US Great Plains constitute one of the most extensive and well-studied temperate grasslands in the world. These large expanses of prairie cross a mesic to semi-arid climatic gradient. Results from over a decade of research into precipitation regimes have concluded that reduced rainfall frequency (but same total volume) in a mesic C_4 grassland led to decreased soil moisture and a reduction in aboveground net primary productivity (ANPP; Knapp *et al.* 2002), a result that was subsequently confirmed by Fay and colleagues (Fay *et al.* 2003). This follow-up study also showed an increased root to shoot ratio under more intense rainfall regimes. Interestingly, the location of this research is water-limited and extreme events usually increase production in water-limited environments (Knapp *et al.* 2001). Further studies have suggested that this assumption is too simplistic, as extreme event factors interact with total rainfall quantity (Fay *et al.* 2008). Hence a more complex model is required to predict whether an increase or decrease in productivity will occur under different rainfall regimes.

In contrast to the mesic grassland, a semi-arid C_4 grassland under similar reduced rainfall frequency demonstrated an increase in ANPP (Heisler-White *et al.* 2008, 2009). An intermediate site on this mesic to semi-arid gradient was established to confirm the relationship between productivity and rainfall frequency. This intermediate site showed an unexpected result: highly positive productivity as a response to more extreme rainfall events (Heisler-White *et al.* 2009).The non-linear responses shown in these studies demonstrate the strong sensitivity of temperate grasslands to extreme growing season rainfall regimes and highlight the inherent complexity in these biomes.

Also in the USA, Zhang and colleagues (2013) performed a cross-biome study using MODIS EVI satellite data. While other biomes including arid grasslands showed a drop in ANPP with reduced rainfall frequency, mesic grasslands did not. Elsewhere in the

world, coarse-scale satellite remote sensing has been used to investigate the relationship between productivity and rainfall regimes. Some research suggests that more frequent, less intense and evenly-distributed rainfall will enhance productivity of temperate grasslands (Fang *et al.* 2005). When modelling the cumulative effects of rising CO_2, temperatures and precipitation forecasts, Parton and colleagues predicted all global grassland types to increase in productivity, with the additive effect of CO_2 and climate change showing a significant increase in net primary productivity in mesic areas (Parton *et al.* 1995). In water-limited *Themeda*-dominated South African C_4 grasslands, interactions with precipitation and ANPP were highly complex, with event size important at the driest site, spacing of events important at the wettest sites, and neither important at an intermediate site (Swemmer *et al.* 2007). In a Spanish grassland (Miranda *et al.* 2009), reducing rainfall quantity through a shelter experiment reduced grass productivity, but changing event size had little effect. A mesic grassland in the UK was exposed to drought and drought/downfall treatments in combination with increased winter rainfall (Fry *et al.* 2014) The more extreme regime resulted in lower species richness and vegetative cover but overall the grassland displayed resistance to changes in rainfall.

3.1.5.3 Temperate grassland response to seasonal changes in rainfall

There have been few experimental studies of the effect of seasonal redistribution of rainfall on grasslands. In a long-term rainfall modification experiment in a northern California grassland, effects of rainfall redistribution were very strongly dependent on seasonality (Suttle *et al.* 2007). The results showed that extending the rainy season into spring resulted in an increase in plant productivity but supplemental water during the wet winter had minimal effect. The treatment that extended the rainy season into spring brought about an unexpected trophic cascade: in the first year of the study, nitrogen-fixing forbs showed the largest increase, whereas the second year showed a pulse of annual grasses. By the fourth year, the built-up grass biomass had suppressed other species' establishment success and led to species richness collapse.

A less-dramatic result in composition was shown in a nine-year observational study in the Czech Republic: increases in winter rainfall led to increases in some grasses, and declines in rosette-based forbs (Dostálek and Frantík 2011). This result conflicted with

studies from other temperate regions that reported increases of annual plants in response to spring and autumn rains (Winkler and Klotz 1997, Matesanz *et al.* 2009). Though small in number, these studies on seasonal rainfall distribution highlight the importance of long-term observations and likely vegetation community changes under different rainfall regimes.

Given the level of complexity and differential responses shown at site-dependent scales, several researchers have expressed concern on the scarcity of data in different biomes and the need to increase our understanding on rainfall-vegetation relationships (Weltzin *et al.* 2003, Knapp *et al.* 2008, Zeppel *et al.* 2014). In particular, the impact of extreme precipitation and altered seasonality has been identified as a key research gap (Beier *et al.* 2012, Zeppel *et al.* 2014), particularly in mesic grasslands (Swemmer *et al.* 2007).

3.1.6 Near-surface phenology as a monitoring tool

Vegetation productivity in grasslands has traditionally been assessed by harvesting aboveground biomass (all plant parts) or phytomass (leaves) after a known period of growth. Typically this is aggregated from the start of the growing season to either the peak of the growing season or time of harvest, whichever is most appropriate (Lauenroth *et al.* 1986, Paruelo *et al.* 2000). By this method, an estimate of quantity of carbon fixed to aboveground vegetation over a known time per unit area (productivity) can be obtained. This method captures the integrated quantity of productivity over the period and is particularly useful in circumstances where vegetation growth is unidirectional and relatively constant. In environments where vegetation is more dynamic—such as those with highly variable rainfall—a method that estimates vegetation dynamics (both greening and senescence) more regularly may add value to these studies.

The use of time-lapse digital photography for estimating vegetation dynamics has become more common in the past decade, with the lower costs of digital cameras facilitating use by researchers in the climate and plant sciences. Time-lapse cameras are used to monitor seasonal vegetation dynamics, or phenology, and are often termed ‘phenocams’. Phenocams are a form of near-surface remote sensing and have been used to monitor phenology in several distinct biomes: broadleaf forests (Richardson *et al.*

2007, 2009, Nagai *et al.* 2011, Sonnentag *et al.* 2012), conifer forests (Ide and Oguma 2010, Bater *et al.* 2011, Sonnentag *et al.* 2012), mixed forests (Ahrends *et al.* 2008, Henneken *et al.* 2013) semiarid scrub (Kurc and Benton 2010), tropical savannah (Alberton *et al.* 2014), alpine grasslands (Migliavacca *et al.* 2011, Ide and Oguma 2013, Julitta *et al.* 2014), and suburban parks and gardens (Crimmins and Crimmins 2008, Nijland *et al.* 2014). These studies have generally praised the ability of phenocams to detect changes in vegetative phenology and promoted their future use in ecological research.

Conventional satellite remote sensing utilises vegetation indices for monitoring vegetation dynamics, such as the Normalized Difference Vegetation Index (NDVI; Tucker and Sellers 1986) and the Enhanced Vegetation Index (EVI; Huete *et al*. 2002). Similar to satellite remote sensing, phenocam vegetation indices are calculated from the red, green and blue (RBG) image brightness values to give an integrated 'greenness' value of the image. This greenness is linked to biophysical characteristics, as plant canopy reflectance in visible wavelengths (400–700 nm) is predominantly influenced by chlorophyll and photosynthesis-related pigments (Sims and Gamon 2002, Gitelson *et al.* 2003). This vegetation index can subsequently be used for time-series visualisation and analysis to determine how the greenness changes over time. Common indices used within the literature include the green chromatic coordinate (Sonnentag *et al.* 2012) and the excess green index (Richardson *et al.* 2007). Both of these indices utilise the concept of normalising the green brightness channel relative to other channels to minimise the effects of illumination and increase the contribution of green pigments.

Phenocams have several advantages over satellite remote sensing, particularly for smaller-scale measurements. They can be programmed to take high frequency (sub-daily) images, they are less impacted by cloud or atmospheric effects, and can be manually positioned to capture specific individuals, species or communities (Ide and Oguma 2010, Mizunuma *et al.* 2013, Julitta *et al.* 2014). Some studies even report a better accuracy for RGB indices than infra-red indices such as NDVI (Mizunuma *et al.* 2013, Nijland *et al.* 2014). Phenocams also have advantages over traditional phenophase estimates or radiometric sampling of vegetation function in that they provide a continuous measure, can cover a large spatial area, require minimal resources

and produce estimates of phenophase (particularly vegetative phenophase) that are less vulnerable to subjectivity than visual estimates (Richardson *et al.* 2007).

Although some of the pioneering research using phenocams was conducted on agricultural areas (Adamsen *et al.* 1999), this technology has not been used extensively to examine pasture vegetation dynamics. The only similar example in the literature is webcam-based phenological research conducted on grazed peatland pastures (Sonnentag *et al.* 2011), however the subject of the research was the physical parameters of a dominant invasive weed, rather than the pasture itself. Digital photography has been used as a method for estimating ANPP (Paruelo *et al.* 2000), but this research project did not have a temporal component to it, which is a key feature of phenology studies.

This research project uses 13 months of sub-daily phenocam images to record changes in temperate grassland phenology and productivity trends in response to the modification of rainfall regimes. It represents the first use of phenocams to examine differences in vegetation dynamics between experimental treatments. Rainfall modification was conducted at the DRI-Grass study site (Power *et al.* 2016): a rainfall modification experiment located at the Hawkesbury Institute of the Environment, Western Sydney University (WSU).

3.1.7 Aims

The aims of this research are to:

- determine how differences in the quantity and timing of rainfall impacts vegetation dynamics and phenology;
- determine how individual species phenophase responds to rainfall regimes; and
- assess the ability of phenocams to estimate vegetation dynamics in temperate grasslands.

3.2 MATERIALS AND METHODS

3.2.1 Study site and climatic variables

The study was conducted at the Hawkesbury campus of Western Sydney University (WSU) located near Richmond, New South Wales approximately 50 km north-west of Sydney (33.608139 S, 150.737222 E). This area is on the Cumberland Plain at the foot of the Blue Mountains and broadly comprises extensive agricultural lands (grazing and turf farms), rural residential properties and open *Eucalyptus* woodland.

The climate of this region is temperate with hot summers and cool winters. The average annual maximum temperature is 24.1 °C and the average annual minimum is 11.0 °C (Table 3.1). The mean maximum daily temperature of the summer months ranges between 28.5 °C and 30.0 °C, and dips to a low of 17.6 °C in the winter (July). Minimum daily temperatures frequently reach below freezing in the winter; the average minimum daily temperature is 3.6 °C in July. The area has a mean annual rainfall of approximately 800 mm, measured on campus from 1881 to 2015 (Table 3.1). The seasonal distribution of rainfall is shown in Figure 3.1, with approximately double the rainfall in the summer months (December–February) than winter/early spring (July–September). Note that these mean values are used as an overview only, and are highly variable from year to year.

Table 3.1. Mean monthly minimum and maximum temperatures taken from Richmond RAAF base, 3 km from the study site (1993–2015) and mean monthly rainfall, taken from WSU Hawkesbury (1883–2015).

	Jan	Feb	Mar	Apr	May	Jun	Jul	Aug	Sep	Oct	Nov	Dec	Avg.
Mean maximum temperature (°C)	30.0	29.0	26.9	23.9	20.7	17.9	17.6	19.8	22.8	25.2	26.9	28.5	24.1
Mean minimum temperature (°C)	17.6	17.7	15.6	11.5	7.5	5.1	3.6	4.4	8.0	10.9	14.1	16.0	11.0

	Jan	Feb	Mar	Apr	May	Jun	Jul	Aug	Sep	Oct	Nov	Dec	Tot.
Mean monthly rainfall (mm)	95.6	95.6	87.6	68.6	57.4	60.6	44.8	42.8	42.6	56.9	73.4	76.0	802

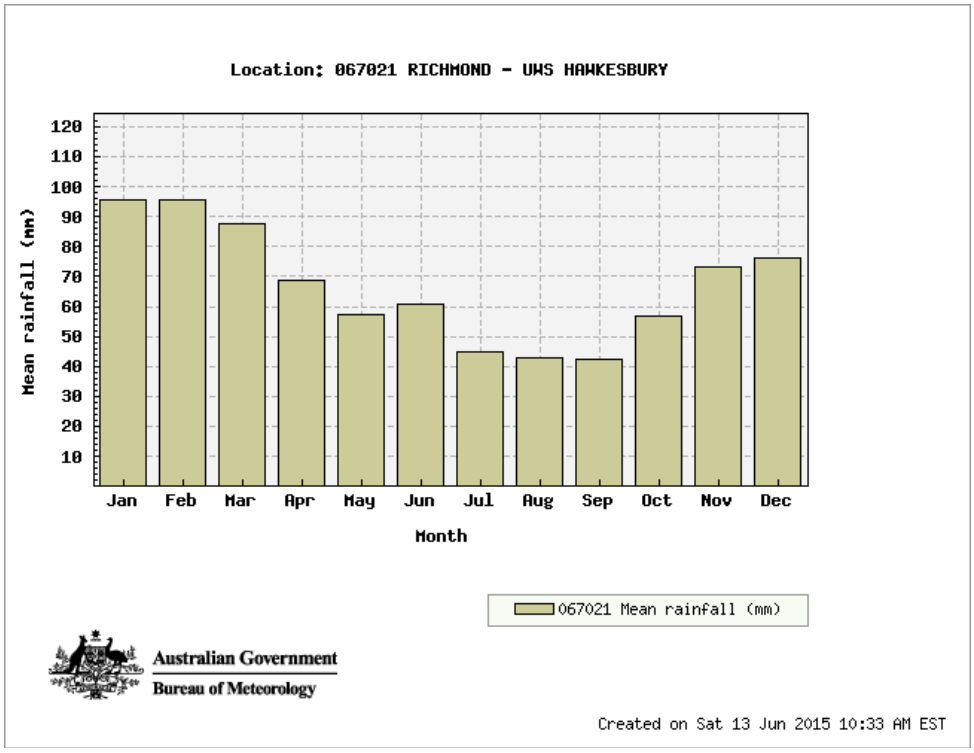

Figure 3.1. Average monthly rainfall measured at WSU Hawkesbury 1883–2015 (formerly known as UWS Hawkesbury). Figure courtesy of the Australian Bureau of Meteorology.

Rainfall for the experimental period is presented in Figure 3.2. This period was slightly wetter than average, with 1066.8 mm of rainfall throughout the experimental period, as compared to the long-term equivalent average of 870.5 mm. The rainfall was highly variable, with more than half of the total rainfall falling in only three months (December 2014, January 2015 and April 2015). The period of April 2014 to November 2014 was particularly dry, with the exception of the months of August 2014 (much wetter than average) and October 2014 (average rainfall). The summer months of December 2014 and January 2015 were extremely wet. February 2015 was more consistent with the long term average, and March 2015 was much drier. April 2015 was much wetter than average.

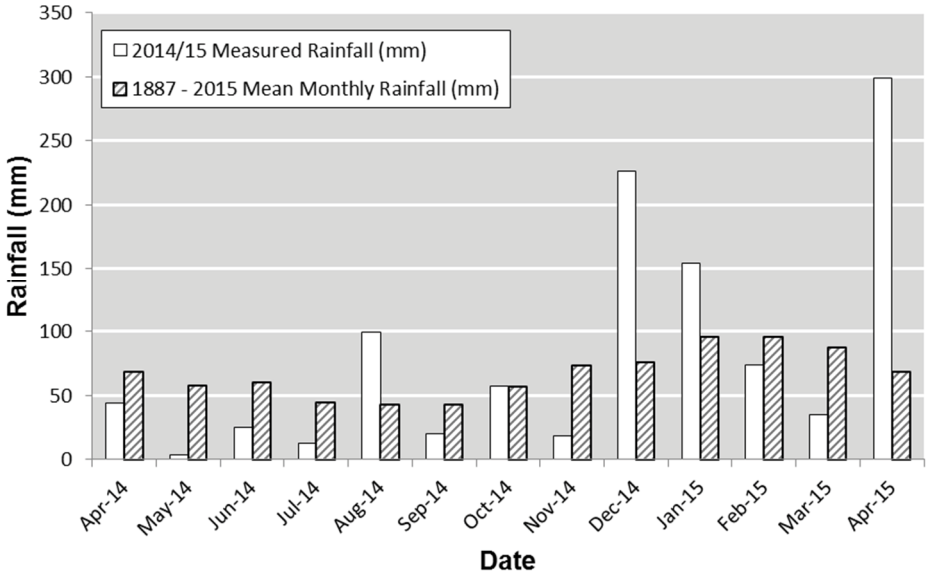

Figure 3.2. Total monthly rainfall for the experimental period (April 2014–April 2015) and the long-term monthly average (1883–2015).

Soil moisture was measured in 30 plots in the larger network, and an average soil moisture time-series data set for each treatment was used. The average soil moisture for ambient treatments as compared with daily rainfall is presented in Figure 3.3. In general, the ambient soil moisture followed the rainfall very closely, with even small rainfall quantities (>1 mm) promoting a detectable increase in soil moisture. Sequential days of rain led to sustained periods of high soil moisture, but due to the sandy nature and high drainage capability of the soils, large rainfall events did not increase the soil moisture beyond a threshold of 24% volumetric water content. Mean soil moisture for all treatments is presented in Figure 3.4.

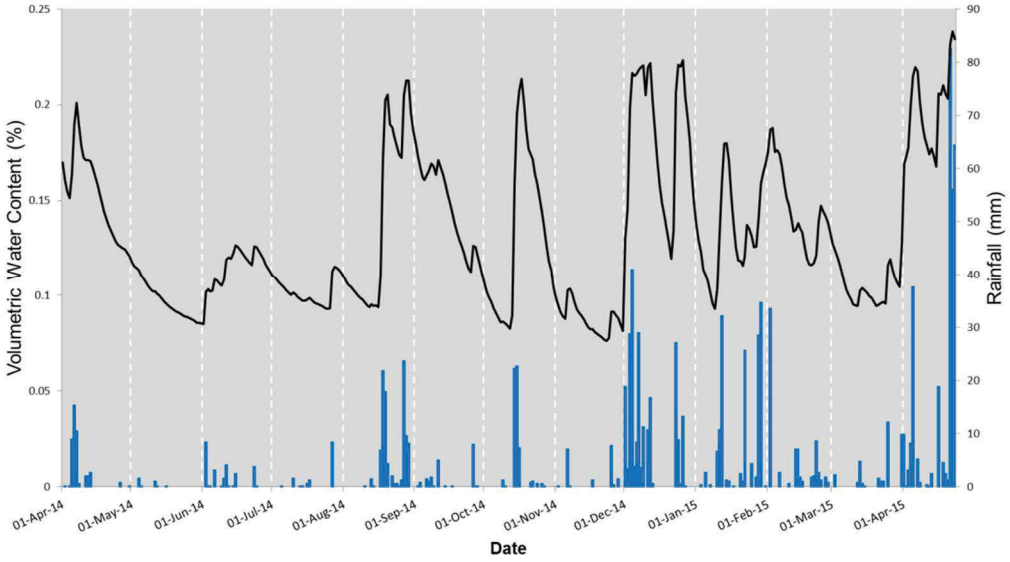

Figure 3.3. Average soil moisture (%v/v) of ambient rainfall treatments (primary y-axis; black line) and daily rainfall (secondary y-axis; blue bars) throughout the experimental period (April 2014–April 2015).

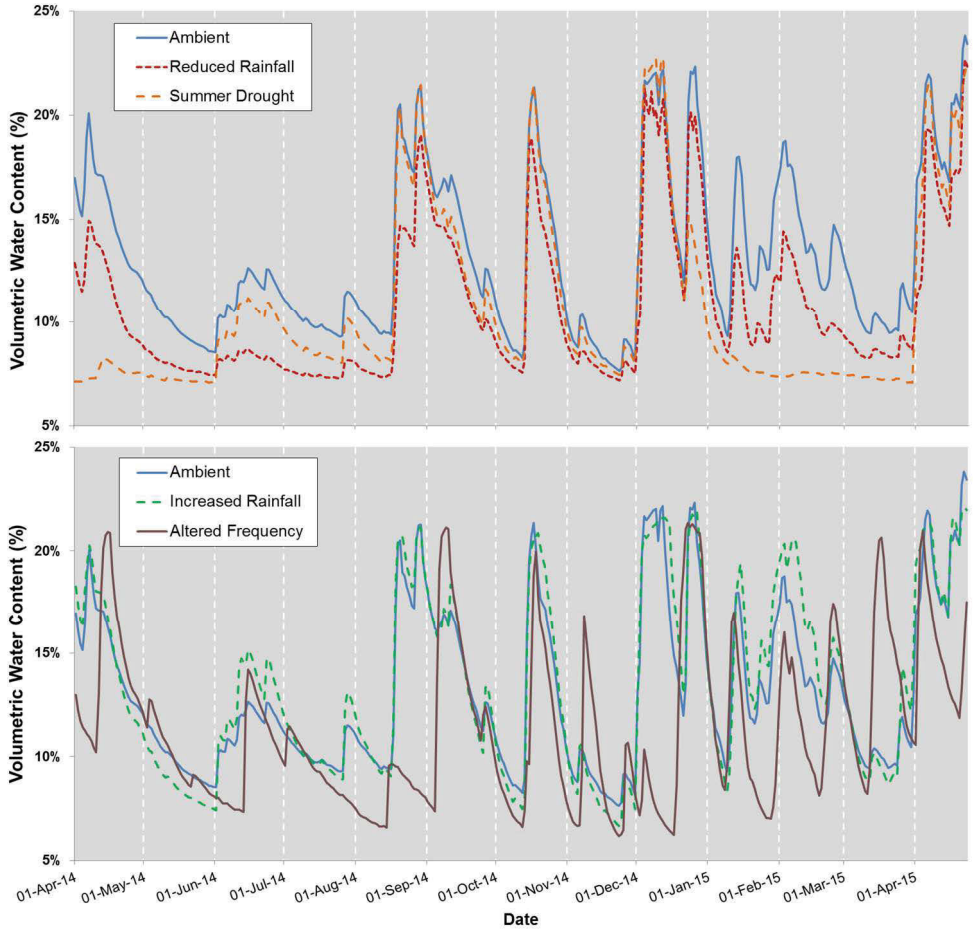

Figure 3.4. Average soil moisture (% v/v) for all treatments: top (ambient, reduced rainfall, summer drought) and bottom (ambient, increased rainfall and altered frequency).

The soils of the study site are described as Blackendon sand, a formation unique to the WSU Hawkesbury campus and identified during a campus survey by Walker in the 1950s (Aiken 2004). While technically poorly described, Blackendon sand is a red podzolic sandy soil with increasing clay at depth, and displays good drainage. Clarendon sand (Walker 1960), a similar formation, is present on the boundary of the study site. This soil type has a higher clay fraction, exhibits poorer drainage and can facilitate a perched water table.

The study was conducted on an improved mixed C_3/C_4 pasture that has been periodically grazed by domestic livestock (mostly cattle) since at least the early 1980s. Pasture crops such as lucerne (*Medicago sativa*) were grown in the paddock in the 1960s, but a detailed land use history prior to this time is not available. Grass and forb species present at the location are predominantly exotic, and common species recorded during the experimental period are presented in Table 3.2. Several species of native and exotic weed species are present amongst the pasture grasses, with some native grasses present, but very few native forbs. Over 62 species have been identified since the DRI-Grass project commenced (Power *et al.* 2016).

Table 3.2. Common vascular plant species found within the DRI-Grass plots, separated by life form (graminoids/forbs) and photosynthetic functional type (C_3/C_4). Exotic species are indicated with (*); pasture weeds are indicated with (^). Dominant species are in bold. Species identified as weeds follow Richardson, Richardson and Shepherd (2011).

Graminoids		**Forbs**
C_4	C_3	
Axonopus fissifolius*	*Avena sativa**	*Bidens pilosa*^*
Bothriochloa macra	*Briza* spp.*	*Commelina cyanea*^
Cymbopogon refractus	*Bromus* spp.*	*Conyza bonariensis*^*
Cynodon dactylon	*Dichelachne* sp.	*Echium plantagineum*^*
Digitaria ramularis	*Cyperus sesquiflorus*^*	*Euchiton sphaericus*
***Eragrostis curvula**^*	***Microlaena stipoides***	***Hypochaeris radicata**^*
Paspalidum flavidum	*Lolium perenne**	*Lotus corniculatus*^*
Paspalum dilitatum*	*Poa annua**	*Medicago sativa**
Setaria parviflora*	*Vulpia myuros**	*Ornithopus compressus**
Sporobolus sp.*		*Oxalis corniculata*^*
		Plantago lanceolata^*
		Senecio madagascariensis^*
		Sida rhombifolia^*
		Sonchus oleraceus^*
		Verbena bonariensis^*
		Vicia sativa^*
		Wahlenbergia sp.

3.2.2 Experimental design

The DRI-Grass rainfall exclusion experiment (Power *et al.* 2016) was established at WSU in June 2013 and had been running for 10 months at the time this experiment commenced. The rainfall exclusion shelters are located on grassland, and were set up in a block design over an area of 1200 m^2. The shelters are 2.5 m x 1.9 m in dimension (4.75 m^2) and constructed of steel tubing frame with a UV-transparent acrylic roof, angled at 20° from horizontal (Figure 3.5). The experimental plot is 2.0 m x 1.8 m (3.6 m^2) and smaller than the shelter so that windblown rainfall and external effects were minimised. The experimental plot was surrounded by a 300 mm deep root barrier so that plants within the plot could not extract moisture or be subject to belowground competition from outside of the plot. Within the experimental plot is an area of 1 m x

1 m (1 m^2). This smaller plot is designed to further minimise external effects and is used for biomass harvesting and the phenological observations for the current study (Figure 3.6). The grassland species composition was not controlled within the plots; the experiment was designed to mimic a natural grazing system.

Figure 3.5. The network of rain exclusion shelters used in the DRI-Grass experiment.

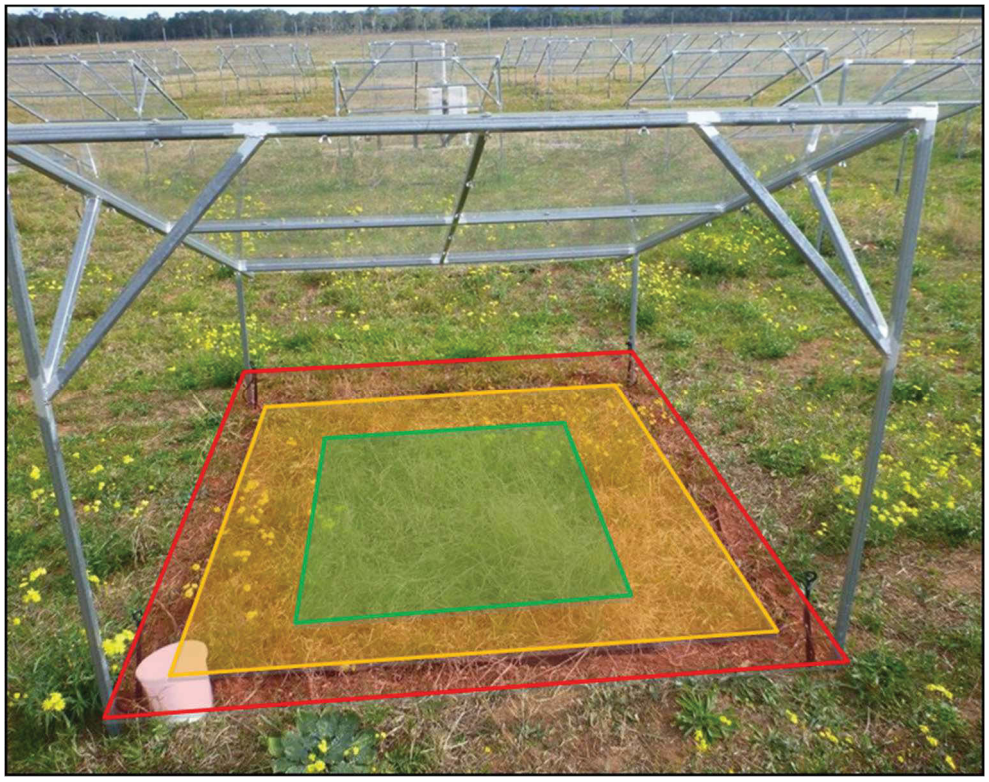

Figure 3.6. The experimental regions with in the plot: area covered by shelter (red; 4.75 m^2), experimental plot (yellow; 3.6 m^2) and harvesting/phenology plot (green; 1 m^2).

Ambient rainfall was measured with a 0.2 mm resolution tipping bucket rain gauge (ICT, Armidale, Australia), and redistributed with an automated irrigation system according to treatment. Irrigation of each plot was individually controlled by a Campbell Scientific CR1000 data logger with SDM-CD16AC relay controllers (Campbell Scientific, Logan, Utah, USA). Soil moisture was measured using a TDR CS616 soil moisture sensor (Campbell Scientific, Logan, Utah, USA), which integrates the soil moisture from the surface to 15 cm depth.

Six replicates of six rainfall treatments were used for the broader DRI-Grass project. For the current study, three replicates of five treatments were used because of limited equipment availability. The five treatments that were investigated are detailed in Table 3.3.

Table 3.3. Description of the rainfall modification treatments used.

Treatment	Description
Ambient	Rainfall was delivered at the same rate and frequency as measured ambient rainfall.
Increased rainfall	Rainfall was delivered at 150% of the quantity of measured rainfall, but frequency did not change.
Reduced rainfall	Rainfall was delivered at 50% of the quantity of measured rainfall, but frequency did not change.
Altered frequency	Rainfall was delivered less frequently, in more extreme events. One pulse of water was delivered once every three weeks, however the total quantity each three-week period did not change from ambient.
Summer drought	Rainfall was eliminated in the summer months (17 December 2014 to 17 March 2015) to simulate a prolonged summer drought.

3.2.3 Phenology observation with repeat digital photography

At each site, a Wingscapes™ time-lapse RGB camera ('phenocam') was installed to capture the vegetation changes at a high temporal capacity. These phenocams are contained in a weatherproof housing with a solar panel to supplement battery power. These cameras are of a 'black box' design, with proprietary hardware, and no adjustable white balance or exposure settings. In spite of this, Wingscapes™ phenocams have performed favourably when compared with more complex phenocam systems (Sonnentag *et al.* 2012) and given their relatively low cost are suited to applications where multiple fields-of-view are required or where power is not readily available.

The phenocam was mounted on the elevated edge of each shelter, 1.4 m above ground level, and was angled at 20° from horizontal, parallel to the shelter (refer to Figure 3.7). While nadir camera views are often used for vegetation growth studies *(e.g. Adamsen et al.* 1999), the shelter structure only allowed for an oblique view, which has also been shown to be effective (Kurc and Benton 2010). The field-of-view (FOV) of the camera incorporated the entire experimental plot, though this was restricted in some cases by movement of the camera or the FOV being obscured.

Figure 3.7. Wingscapes™ phenocam mounted to rain exclusion shelter. The camera is angled at 20° from horizontal on the same plane as the shelter roof.

Sub-daily images were captured over a period of 13 months, from 1 April 2014 to 30 April 2015, with the exception of the summer drought treatment that started later (24 May 2014) due to technical issues. The phenocams were programmed to capture photographs at hourly intervals between 9:00 and 15:00 Australian Eastern Standard Time. Pilot studies using these cameras showed that images captured outside this period were either too dark or too variable to be consistently utilised for phenology purposes. This time-filtering is in agreement with similar studies (Sonnentag *et al.* 2012, Klosterman *et al.* 2014). For image analysis, only noon (12:00) images were used to reduce variability from sun-angle effects. No standardisation of colour was used through the use of a reference card, as can be found in some other camera-based projects (Migliavacca *et al.* 2011, Sonnentag *et al.* 2011), due to the practical limitations of the equipment configuration. In this study, the card could not be mounted in the same plane as the target; preventing the card from becoming contaminated from dust and plant material was impractical; and the card could not be mounted from the camera without interfering with the image collection and other experimental elements. As all cameras were from the same manufacturer and from the same batch, it was assumed that the sensors within each camera were all similar to one another, and that

any sensor drift would a) be negligible over the course of one year, and b) occur at the same rate in all cameras.

In addition to the fifteen phenocams installed on the treatments, one camera was also installed over a patch of representative bare soil as a reference to monitor changes in background soil qualities over the study period.

Total aboveground biomass was harvested on two occasions throughout the 13-month period: in the middle of the study (September 2014) and at the end (late March 2015). The harvesting was not conducted as part of this study, but is presented here as it necessarily resulted in a change in vegetation.

3.2.4 Image processing and analysis

Viable images were processed using ImageJ open source image processing software (Abràmoff *et al.* 2004). For each image, a region of interest (ROI) was described that corresponded with the 1 m^2 plot. Average image brightness values were processed from the area bounded by this ROI (Figure 3.8). Multiple ROIs were not taken in this experiment (compared to phenocam studies in Chapter 5) as it was the integrated plot response that was of primary interest rather than different regions within the plot.

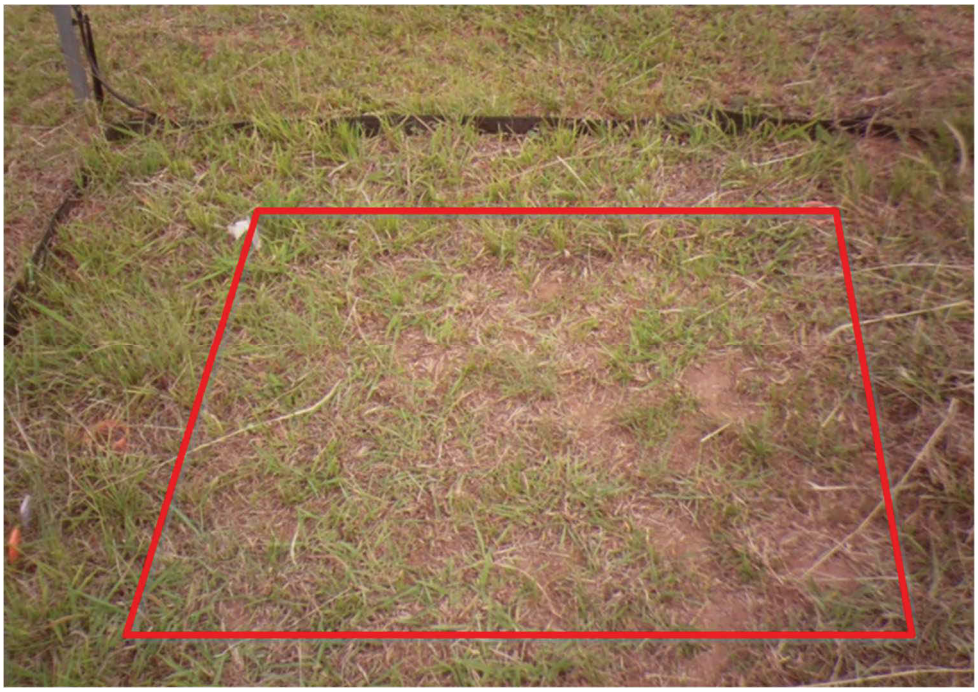

Figure 3.8. Representative phenocam image showing the area of the phenology plot in red.

This study used the green chromatic coordinate (g_{CC}) as the RGB vegetation index to monitor vegetation greenness. The g_{CC} is presented as Equation 3.1 and is the relative brightness of the green fraction as compared to the sum of the red, green and blue fractions (Gillespie *et al.* 1987, Sonnentag *et al.* 2012). The g_{CC} is a unitless index that pilot studies suggest ranges between 0.25 (no green vegetation) and 0.5 (abundant green vegetation) in grassland systems. A variety of phenocam-based studies have used this index over other indices because of its robustness to variations in image brightness due to time of day or shadowing, and its dynamic response to changes in plant biophysical variables (Ide and Oguma 2010, Sonnentag *et al.* 2012, Julitta *et al.* 2014).

$$g_{CC} = \frac{G}{R + G + B} \tag{3.1}$$

To calculate the g_{CC} for each region, images were separated into their red, green and blue channels, and the pixel brightness of each channel was computed for each image region of interest (ROI). Figure 3.9 shows images of g_{CC} values at various quantities of photosynthetic and non-photosynthetic grass cover with a colour filter to emphasise differences in g_{CC}.

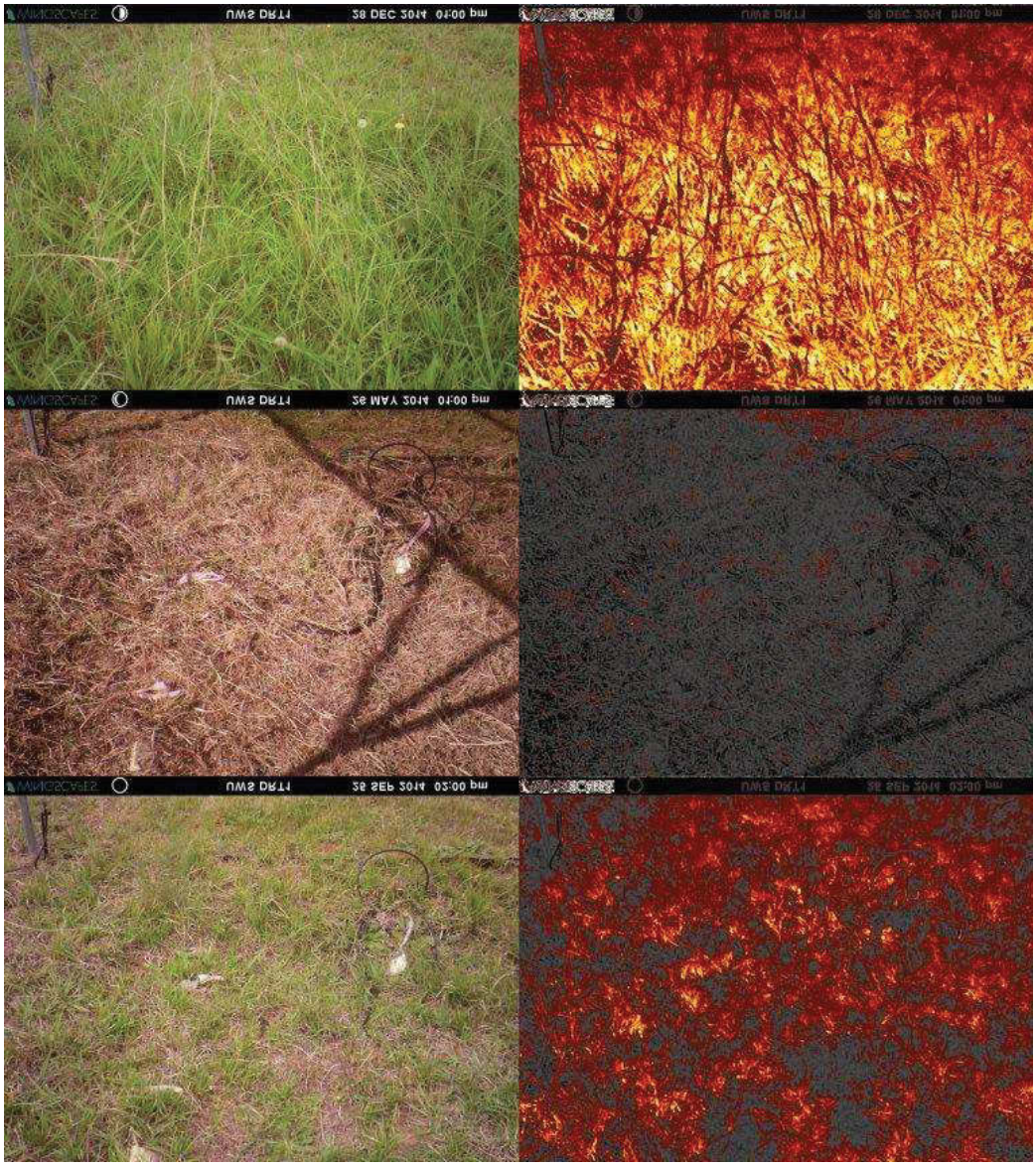

Figure 3.9. Corresponding phenocam images—RGB (left) and g_{CC} values (right) for different levels of photosynthetic vegetation cover. High greenness is expressed in December 2014 (top), low greenness in May 2014 (middle), and moderate greenness in September 2014 (bottom). For the g_{CC} images, darker colours (grey/black) represent lower g_{CC} values, brighter colours (yellow/white) represent higher g_{CC} values, and reds represent intermediate g_{CC} values.

Data summary and graphical interpretation was conducted with the R software package (R Core Team 2013). Midday (12:00) g_{CC} values were used to establish a daily time series, or phenology profile. Images that were fogged or where the experimental plot was obscured were removed from the analysis, thereby removing obvious outliers. This filtering allowed for the use of raw g_{CC} values rather than fitted curves as is common in some phenocam research.

The integrated value of vegetation indices (i.e. the calculated area under the VI phenology curve) is a theoretical representation of productivity (Goward *et al.* 1985, Running and Nemani 1988). This method has been used successfully to estimate ANPP in grassland biomes (Zhang *et al.* 2013, Moran *et al.* 2014), though these examples use satellite-derived indices such as the EVI and the NDVI. Here, the integrated g_{CC} (ig_{CC}) is used as an estimate of productivity and a method for comparing vegetation dynamics between treatments. As the calculation of ig_{CC} required a data series with no gaps, gap filling was undertaken where necessary using linear interpolation. The soil g_{CC} mean value of 0.3076 was used as a baseline for this calculation; therefore the ig_{CC} represents the area between the g_{CC} profile and the soil baseline. This is explained further and illustrated in Section 3.3.4.

The ig_{CC} data was non-normally distributed for all groups (Shapiro-Wilks test for normality, $p < 0.01$). As such, Kruskal-Wallis non-parametric statistical tests were conducted to assess differences between treatments, at a threshold of $p < 0.05$. If a significant difference between treatments was present, Dunn's post-hoc test was conducted to determine which treatments were significantly different at $p < 0.05$.

3.2.5 Phenophase observations

The assessment of key phenophase dates was conducted for all species where specific phenophase (e.g. commencement of flowering/fruiting, end of flowering) could be reliably confirmed in the imagery. After examination of all treatment plots, it was determined that commencement of flowering date was the only phenophase that could be accurately identified. End-of-flowering dates were difficult to assess due to large quantities of biomass present at this time, and fruits tended not to be conspicuous enough to be accurately resolved in the images.

3.3 RESULTS

3.3.1 General phenocam observations

The g_{CC} phenology profiles generated from phenocam data showed obvious and dynamic response to rainfall events and correlated well with seasonal growth patterns observed in the field. In particular, increases in g_{CC} corresponded precisely with major rainfall events. Throughout the experimental period, five distinct and complete greening/browning cycles (modes) were identified (Figure 3.10). These five modes were observed for all treatments where data was available and corresponded with the following dates:

- Mode 1: 6 April 2014–29 May 2014
- Mode 2: 30 May 2014–15 August 2014
- Mode 3: 16 August 2014–10 October 2014
- Mode 4: 11 October 2014–22 November 2014
- Mode 5: 23 November 2014–7 April 2015

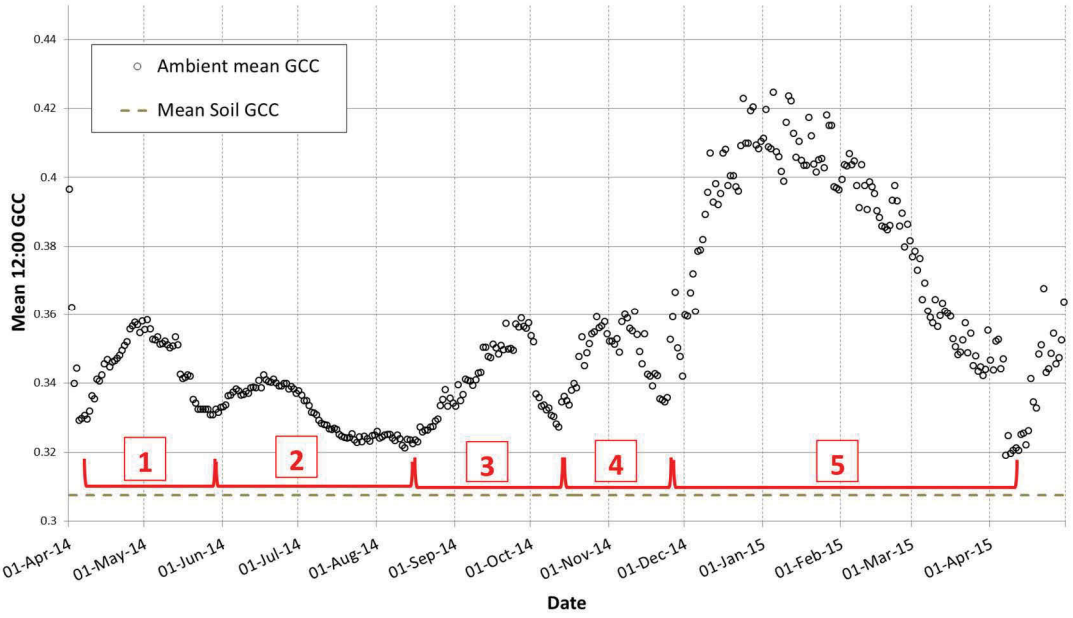

Figure 3.10. Phenology profile of the average ambient rainfall treatment (n = 3), indicating five distinct periods of greening and senescence (modes). Harvesting occurred near the end of mode 3 and mode 5, creating a drop in g_{CC}.

More so than other projects using phenocam monitoring (see Chapter 5), the protection from the rain exclusion shelters, less severe winter temperatures and regular monitoring contributed to a large proportion of images being viable for analysis. Non-viable images were caused by lens fog (1.5%), FOV obscured (0.1%) and camera failure (5.7%). This resulted in minimal gaps in the data series, with over 90% of images being used.

The g_{CC} has been found to correlate well to grass biophysical parameters, specifically with fractional cover (Appendix A); and photosynthetic biomass in (Chapter 5 and Paruelo, Lauenroth and Roset 2000). It has been found to perform more consistently than other common RGB greenness indices (Sonnentag *et al.* 2012) and is regularly used in digital image analysis of vegetation change (Ide and Oguma 2010, Mizunuma *et al.* 2013, Julitta *et al.* 2014). Given that it also corresponds well with measured rainfall events and field observations of greenness, the g_{CC} is considered appropriate here for assessing vegetation dynamics.

3.3.2 Growth response to rainfall/soil moisture

When all treatments were measured across the entire monitoring period, the integrated g_{CC} (ig_{CC}) was found to have a strong relationship with total rainfall (Pearson's $R^2 = 0.8116$), indicating that approximately 80% of the variation in productivity can be explained by rainfall quantity (Figure 3.11). However, when separated into seasonal components, this relationship was not found to be consistent. A very strong relationship (Pearson's $R^2 = 0.97$) was present between rainfall and productivity in the summer months, when both rainfall and productivity were high. However, this relationship was much weaker during all other months (Figure 3.12). Differences in the relationship strength between productivity and rainfall were also observed when the data was split into modal groups (not presented).

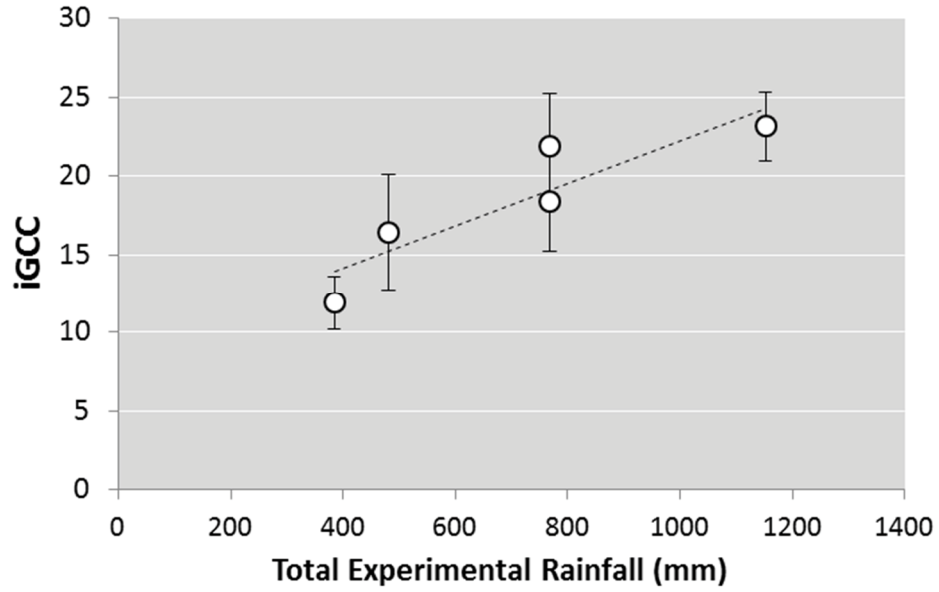

Figure 3.11. Relationship between total productivity (ig_{CC} ± 1 s.d.) and total experimental applied rainfall (mm) for all treatments throughout the study period. The dashed line is a linear trend (Pearson's $R^2 = 0.8116$).

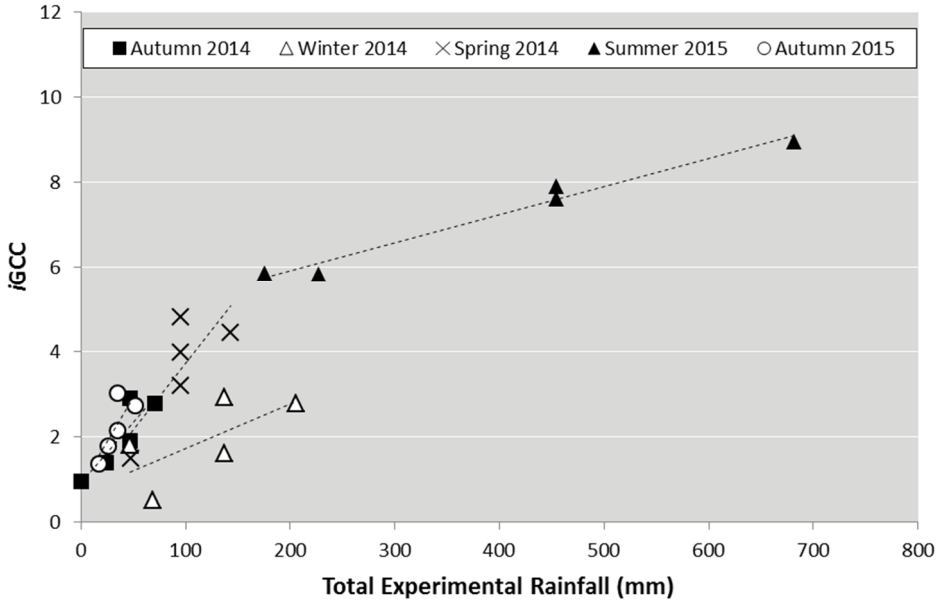

Figure 3.12. Relationship between productivity (ig_{CC} ± 1 s.d.) and total rainfall (mm), separated by season. The productivity/rainfall relationship was strong during periods of high rainfall and high productivity (Summer 2015 Pearson's $R^2 = 0.97$), but poorer at other times (Autumn 2014 Pearson's $R^2 = 0.79$; Winter 2014 Pearson's $R^2 = 0.45$; Spring 2014 Pearson's $R^2 = 0.63$; Autumn 2015 Pearson's $R^2 = 0.62$).

Rainfall was only moderately correlated with soil moisture content (Pearson's $R^2 = 0.75$). This is particularly evident in the different treatments. The reduced rainfall treatment (50% reduction in rainfall) results in a proportional reduction in mean soil moisture of approximately 65% of ambient. However, the increased rainfall treatment (50% increase in rainfall) only resulted in a mean soil moisture content 105% of ambient.

Soil moisture content (mean soil moisture and integrated soil moisture) was poorly correlated with ig_{CC} for the total monitoring period, harvest and seasons (not presented).

3.3.3 Qualitative comparisons: annual phenology profiles

Average phenology profiles for each treatment are presented in Figure 3.13 to illustrate the general trends in greenness throughout the experimental period. Greenness from April 2014 to mid-August 2014 was relatively low, though the first two small greening modes occurred during this time. Most treatments experienced their lowest recorded g_{CC} values in August. Greenness started to increase in late August, but decreased when biomass was harvested in early October—close to the local peak of this greening mode. The growth response to harvesting resulted in a small g_{CC} peak that quickly declined in most treatments. The dominant period of growth commenced in mid-November and steadily increased to a broad peak in early- to mid-January. This peak was followed by equally steady decline until late March and another harvesting event. Post-harvesting saw another sharp increase in greenness until the experiment's conclusion.

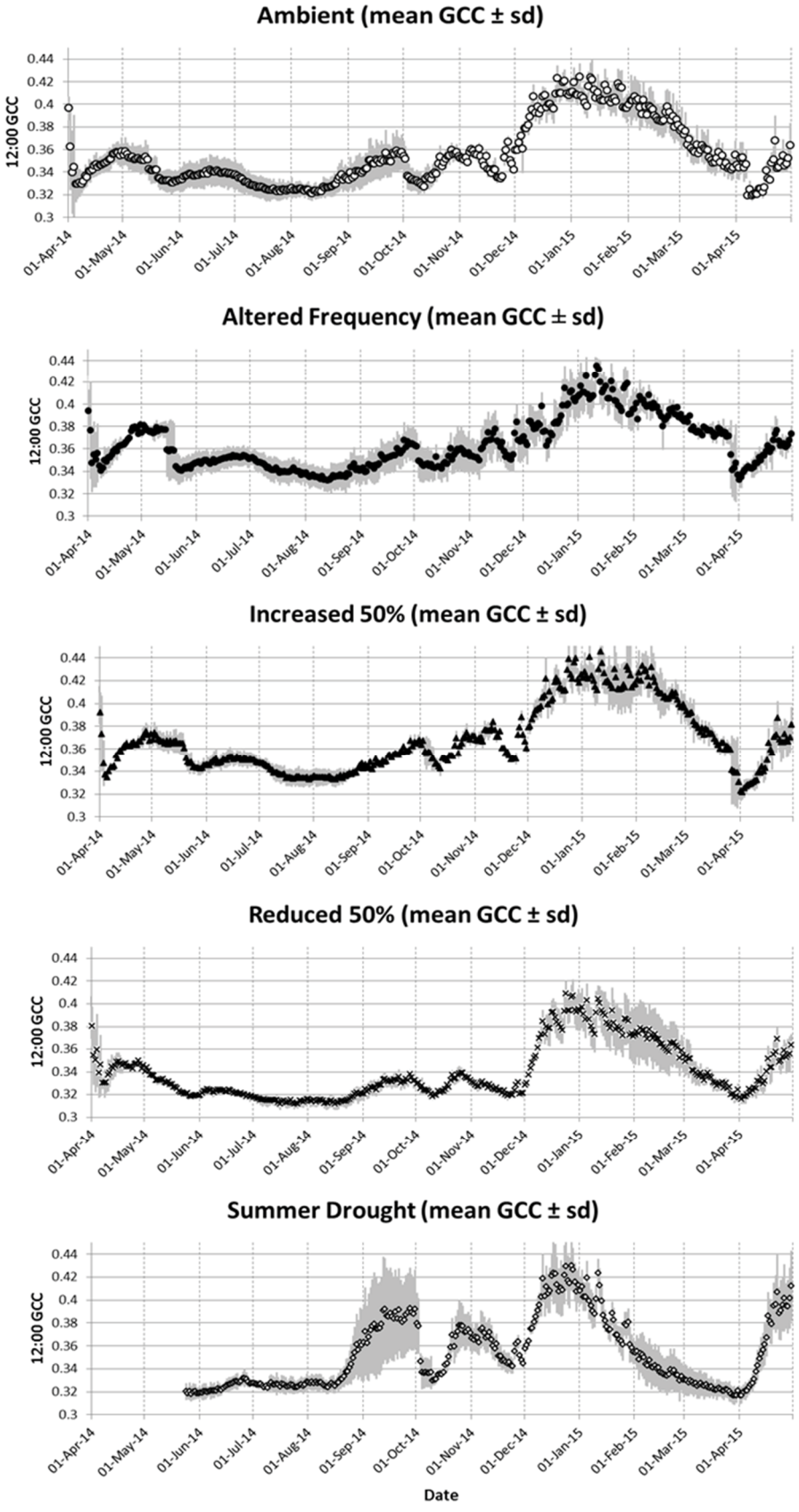

Figure 3.13. Phenology profiles of mean 12:00 g_{CC} values (± 1 s.d.) for all rainfall modification treatments (n = 3).

The g_{CC} of bare soil fluctuated between 0.301 and 0.318. Variations in soil g_{CC} also corresponded with rainfall events with wetting of the soil increasing the g_{CC}. This effect has the potential to impart g_{CC} fluctuations on imagery where soil is a large fractional component, but would be negligible where soil contributes a small fractional component. In all photographs, green vegetation and/or non-photosynthetic vegetation dominate the scene, and soil comprises a small fraction. The highest soil fraction observed in all images was approximately 20%. More so than other treatments, the phenocam that was monitoring bare soil had several hardware issues and resulted in an incomplete data series. For these reasons, the mean value of soil g_{CC} (0.3076) is used as the baseline.

3.3.3.2 Changes in rainfall quantity

The treatments that involved only changes to rainfall quantity, reduced rainfall and increased rainfall, generally showed a predictable pattern when compared to the ambient treatment. Throughout the observational period, the g_{CC} trend followed the pattern of reduced rainfall < ambient < increased rainfall (Figure 3.14). The only exception to this occurred during times of high rainfall, specifically the end of September and mid-December through January. At these times, ambient g_{CC} approached the increased rainfall treatment g_{CC}, but the reduced rainfall treatment remained lower. Greenness response was also similar for a short period after harvesting events, which tended to lower g_{CC} values to a comparable level for all treatments.

The timing of phenology markers were very similar between the treatments, with the key features being five obvious growth periods (modes) and a steep linear green-up during the month of December. The only discernible difference in timing was that the reduced rainfall treatment had a slightly earlier peak at mode 5 than the ambient and increased treatments. The peak of the reduced treatment was not as broad, and the following slope of decreasing g_{CC} was steeper, indicating a faster period of senescence.

The increased rainfall treatment was consistently higher than ambient and reduced rainfall treatments. This means that not only does increased rainfall promote higher levels of greenness, but that it can extend the growing season under certain circumstances.

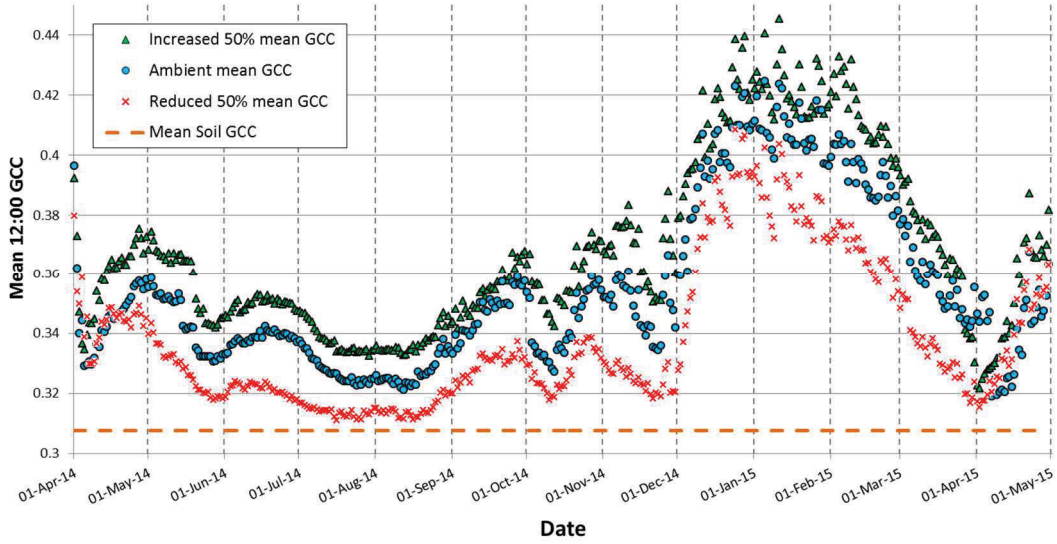

Figure 3.14. Phenology profiles of mean 12:00 g_{CC} for three treatments: reduced rainfall, ambient and increased rainfall. The mean soil g_{CC} is indicated by the dashed horizontal line.

3.3.3.3 Changes as a result of summer drought

The summer drought treatment was not given water between 17 December 2014 and 17 March 2015, a period of three months. During this imposed drought, the most striking difference occurs between this treatment and the ambient (Figure 3.15). Both treatments peak at approximately the same g_{CC} (~ 0.425) in response to high rainfall in early December, but the drought treatment g_{CC} quickly drops as drought is imposed and vegetation wilts and senesces. This results in a very narrow peak of mode 5, quite different to the broad peak shown by the ambient treatment.

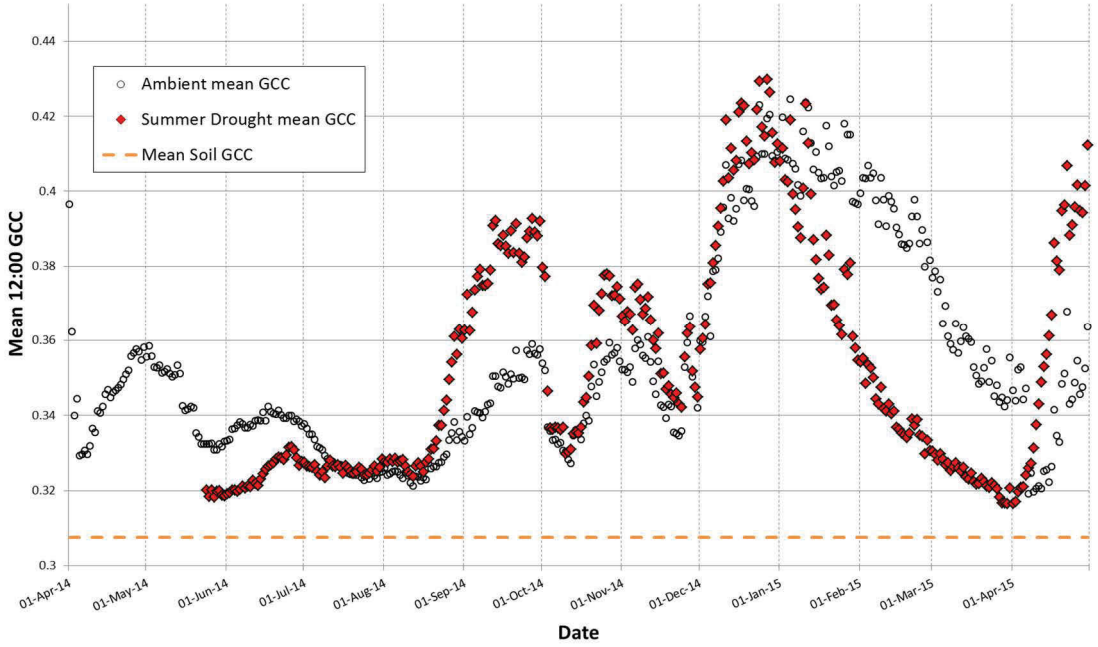

Figure 3.15. Phenology profiles of mean 12:00 g_{CC} for ambient and summer drought treatments. The mean soil g_{CC} is indicated by the dashed horizontal line.

Through the winter months, the mean g_{CC} of the summer drought treatments was considerably lower than ambient. However, with the first spring rainfall (mode 3), the drought treatment rapidly increased to peak at a much higher greenness than ambient (g_{CC} maximum = 0.390 in the drought treatment versus 0.360 in the ambient treatment). A destructive harvesting event occurred at this time, however the same phenomenon was observed following post-harvest greening (mode 4). On this occasion, the mean maximum g_{CC} was 0.375 for the drought treatment and 0.360 for the ambient treatment. Notably, these two drought peaks showed a higher g_{CC} than even the increased rainfall treatment. Another greening event at the end of the observational period was recorded to have an even greater difference, although this mode is incomplete. At the end of April 2015, following post-harvest greening, the mean maximum g_{CC} of the drought treatment was 0.412, compared with the ambient treatment of 0.368. Although the g_{CC} is different, the soil moisture of the two treatments is equivalent during these periods, and this phenomenon is a clear indicator of drought influence on vegetation.

With respect to timing, the three peaks of modes 3, 4 and 5 appear to occur earlier in the drought treatment than the ambient treatment. However, this is difficult to resolve as disturbances disrupt the phenology curve at mode 3 (harvest) and mode 5 (drought

treatment). While again difficult to quantify, it appears that the peak of mode 2 occurs later in the drought treatment than in the ambient treatment. This is during the winter when the drought g_{CC} is less than ambient g_{CC}.

3.3.3.4 Changes from rainfall frequency reduction

The altered frequency treatment simulates a reduction in the frequency of rainfall events while keeping the overall rainfall volume equal. In this case, rainfall from every 3-week period was withheld and deposited in one event.

Throughout early April to mid-August 2014, the altered frequency treatment was consistently greener than ambient (Figure 3.16). The mean g_{CC} maximum at mode 1 was 0.382 for the altered frequency plots and 0.358 for the ambient plots. At mode 2, this value was 0.354 for altered frequency treatments and 0.342 for ambient treatments. This difference between the two treatments was consistent throughout this period. From mid-August 2014 through to March 2015, the two treatments were very similar and did not exhibit the differences seen in the drier winter months. At no time was the altered frequency treatment g_{CC} consistently lower than the ambient treatment g_{CC}.

While a delay in phenological timing could reasonably be expected due to the periodic withholding of water, no discernible differences in peak timing were observed for any modes. However, the greening of modes 4 and 5 was more gradual in the altered frequency treatment, and more abrupt in all other treatments. In mode 5, a slight delay in browning during March 2015 was observed. The greening shape and peak of mode 4 was less distinct in the altered frequency treatment because of higher variability within the treatment around this time.

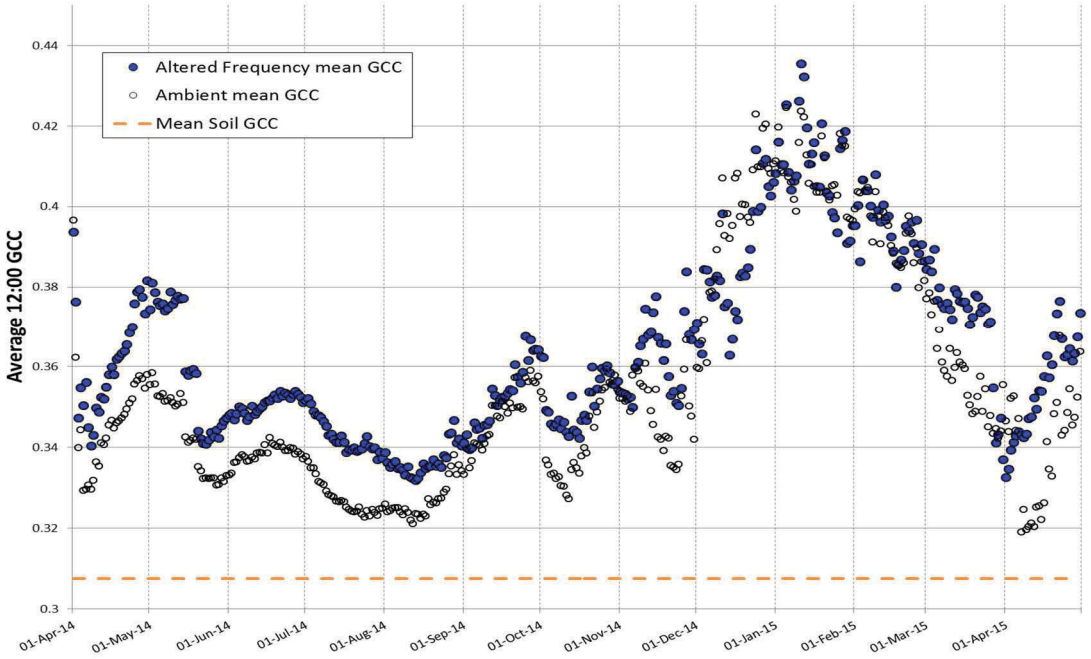

Figure 3.16. Phenology profiles of mean 12:00 g_{CC} for ambient and altered frequency treatments. The mean soil g_{CC} is indicated by the dashed horizontal line.

3.3.4 Total and seasonal differences in productivity

The integrated g_{CC} (ig_{CC}) between the phenology curve and the mean soil g_{CC} (0.3076) is used to estimate the overall productivity of the treatment (refer to Figure 3.17). Treatment data was analysed using the non-parametric Kruskal-Wallis test due to non-normal distribution of ig_{CC} data. Post-hoc comparisons of treatments were conducted using Dunn's test at a threshold of $p < 0.05$.

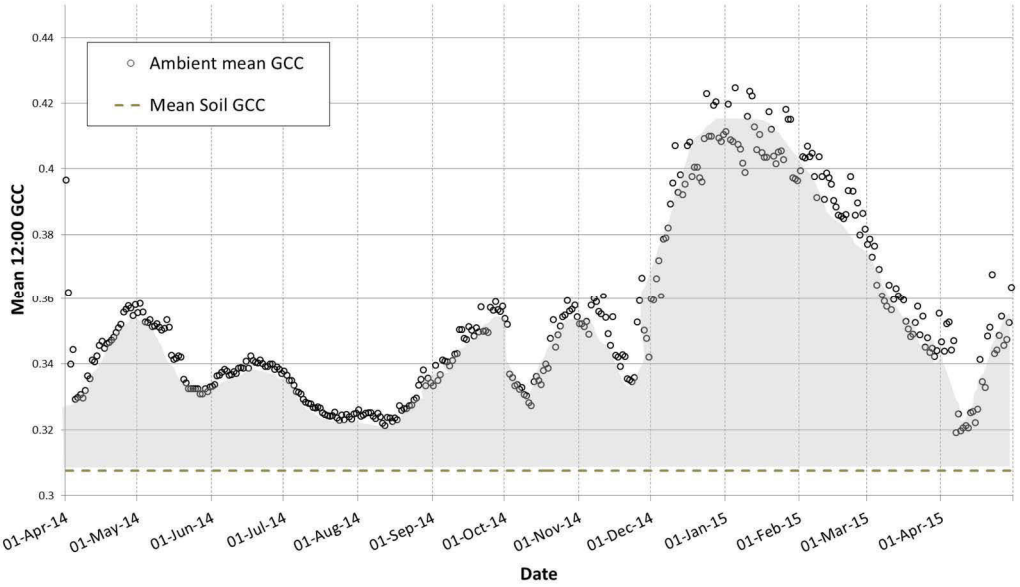

Figure 3.17. Mean g_{CC} phenology profiles of the ambient treatment illustrating the integrated g_{CC}, or ig_{CC} (shaded region). This integrated region between the g_{CC} curve and the soil baseline (dashed line) is analogous to aboveground net primary productivity.

3.3.4.1 Total productivity

When integrated g_{CC} is used as an analogue for productivity across the whole observational period, the treatments show a significant difference in mean ig_{CC} ($\chi^2 = 10.23$, $p = 0.037$). The increased and reduced rainfall treatments showed, respectively, greater and less productivity than ambient, as would be expected (Figure 3.18). The altered frequency treatment had a higher mean than ambient (mean $ig_{CC} = 21.9$ versus 18.4), though these were not significantly different from one another. Likewise, the drought treatment mean ig_{CC} was lower (mean $ig_{CC} = 16.4$), though not significantly different from the ambient treatment.

While this provides information about the total annual productivity, Section 3.3.3 demonstrated that the treatments exhibit differential responses at different times of the year, depending on environmental and climatic conditions. One advantage of taking high-frequency measurements is that data subsets can be examined separately to determine how different seasonal and climatic factors affect vegetation growth patterns.

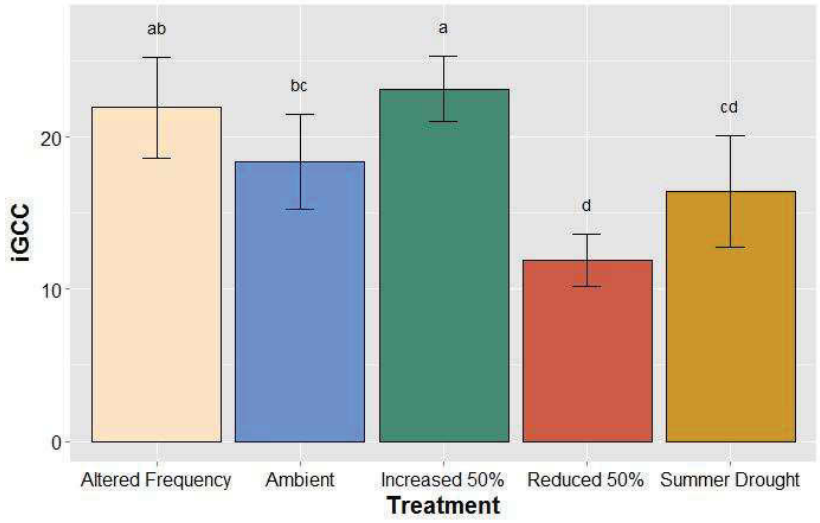

Figure 3.18. Mean igCC (± 1 s.d.) by treatment for the full experimental period. Means with the same letter are not significantly different between each treatment (Dunn's post-hoc test $p < 0.05$).

3.3.4.2 Productivity by season

Further information can be obtained by examining the seasonal trends of the treatments throughout the year.

The g_{CC} data was subset into different seasons (Autumn 2014, Winter 2014, Spring 2014, Summer 2015 and Autumn 2015) and the seasonal productivity (ig_{CC}) calculated for each treatments (Figure 3.19). The summer drought treatment was not included in the Autumn 2014 analysis due to insufficient data.

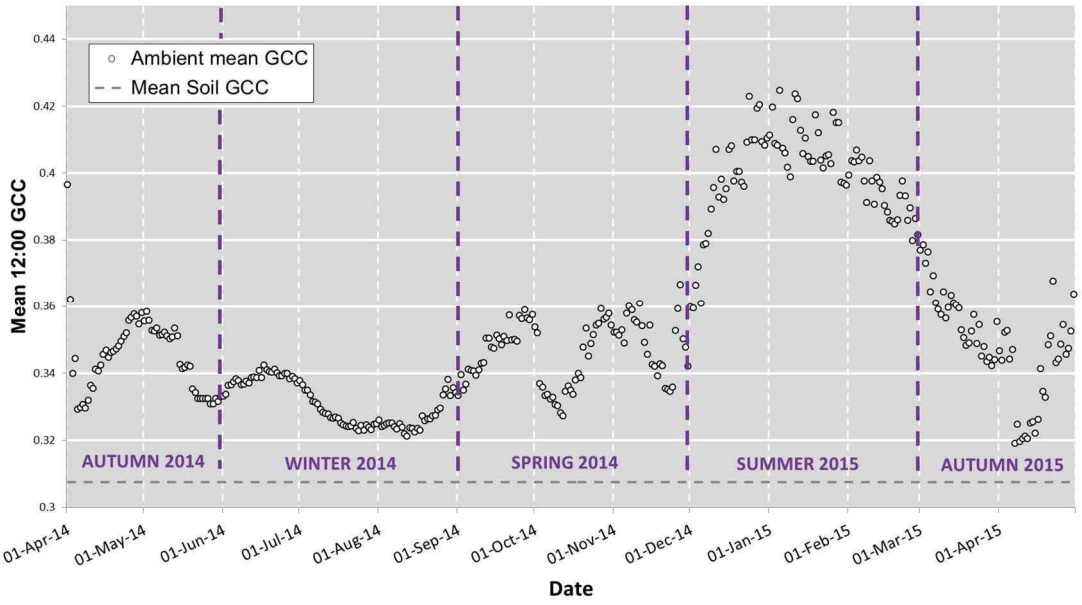

Figure 3.19. Phenology profile of mean ambient treatment, separated into seasons (Autumn 2014, Winter 2014, Spring 2014, Summer 2015 and Autumn 2015). The horizontal dashed line represents the mean soil g_{CC} value.

Total seasonal rainfall data was also separated into seasonal components and presented as Table 3.4. This table can be used as a reference point to identify the moisture conditions when examining the seasonal productivity trends. Rainfall was very low during Autumn 2014. Although the winter rainfall in 2014 was similar to average, it was unevenly distributed. October had average rainfall, whereas September and November had very little rainfall. Summer was extremely wet: almost double the annual average for this period. The Autumn 2015 period saw approximately double the typical rainfall.

Table 3.4. Seasonal rainfall (mm) by season for the experimental period (April 2014–April 2015) and long-term average (1883–2015).

	Seasonal Rainfall 2014–15 (mm)	**Long-term Average Seasonal Rainfall (mm)**
Autumn 2014	47.25	126
Winter 2014	136.92	148.2
Spring 2014	95.13	172.9
Summer 2015	454.23	267.2
Autumn 2015	333.24	156.2
Total	**1066.77**	**870.5**

Autumn 2014 showed a significant difference in productivity between treatments ($\chi^2 = 9.256$, $p = 0.026$), which is displayed in Figure 3.20. The altered frequency and the increased rainfall treatments were similarly high (mean $igCC = 2.9$ and 2.8, respectively), and were significantly greater than both the ambient (mean $igCC = 1.9$) and reduced rainfall (mean $igCC = 1.4$) treatments. The summer drought treatment was not included in this analysis because of insufficient data.

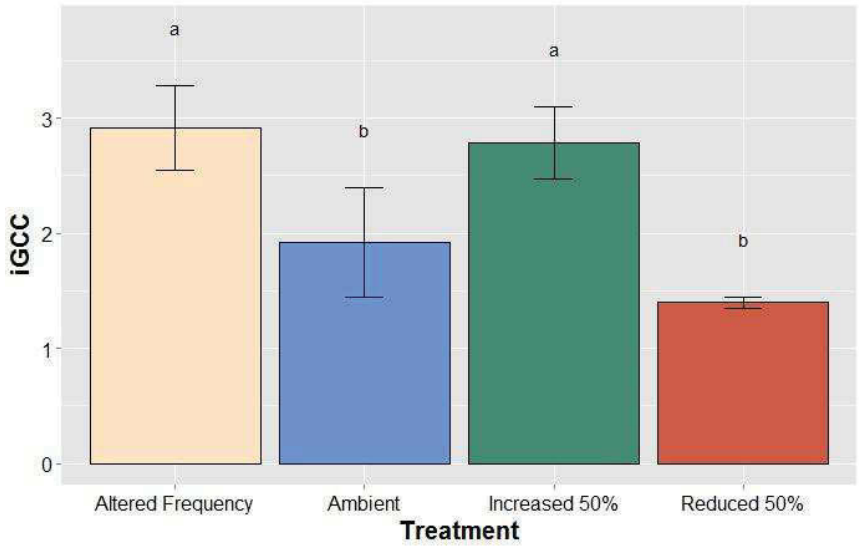

Figure 3.20. Mean $igCC$ (± 1 s.d.) by treatment for Autumn 2014 (1 March 2014–31 May 2014). Means with the same letter are not significantly different between each treatment (Dunn's post-hoc test $p < 0.05$).

Winter 2014 also showed a significant difference between treatments (Figure 3.21; $\chi^2 = 10.567$, $p = 0.032$) with similar trends to the Autumn 2014 data. Inter-treatment variability was higher, however, particularly for the altered frequency and ambient plots. The altered frequency treatment had the highest mean productivity (mean $igCC = 2.9$), with the increased rainfall treatment only slightly lower (mean $igCC = 2.8$). The reduced rainfall treatment was extremely low, (mean $igCC = 0.5$) and dropped proportionally more than all other treatments when compared to the previous season. At this stage, the reduced rainfall soil moisture content was extremely low, and did not exceed 8.5 % v/v between 1 June 2014 and 15 August 2014. Although more productive (mean $igCC = 1.6$), the summer drought treatment was not significantly different to the reduced rainfall treatment, nor was it significantly different to the ambient treatment.

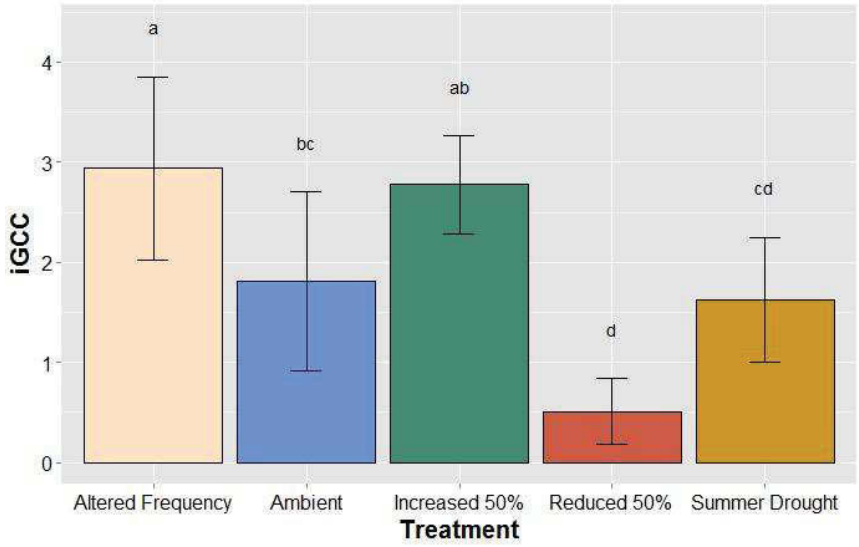

Figure 3.21. Mean $igCC$ (± 1 s.d.) by treatment for Winter 2014 (1 June 2014–31 August 2014). Means with the same letter are not significantly different between each treatment (Dunn's post-hoc test $p < 0.05$).

No significant difference between treatments was observed for Spring 2014 (data not shown). This is likely due to high variation within the small number of replicate plots. Nevertheless, the summer drought treatment showed the highest mean productivity (mean $igCC = 4.8$). This is a highly responsive trend difference for this treatment, which has productivity between the reduced rainfall and the ambient treatments in other seasons. This increased productivity is due to the increased gCC peaks in modes 3 and 4, seen in Figure 3.15.

No significant difference between treatments was observed for Summer 2015 (data not shown). This season had a high rainfall, and represents the bulk (45%) of the total annual productivity. Summer 2015 also shows the most even growth and the most consistent variability within the five treatments. Despite the wet conditions, the increased rainfall treatment still had the highest mean productivity (mean ig_{CC} = 8.9). The ambient and altered frequency treatments were only slightly less productive (mean ig_{CC} = 7.9 and 7.6, respectively). Despite being without water for most of the season, the summer drought treatment did not show as dramatic a decrease as would be expected, as the drop in g_{CC} throughout the drought period was modulated by very high productivity in early December. In fact, the mean productivity of this treatment is still slightly higher than that of the reduced rainfall treatment (mean ig_{CC} = 5.9 versus 5.8).

The productivity during Autumn 2015 (Figure 3.22) showed a similar pattern to Autumn 2014 and Winter 2014. The differences between the treatments were significant (χ^2 = 10.433, p = 0.034), with the altered frequency having the highest mean ig_{CC} of 3.0. This was significantly higher than the ambient treatment (mean ig_{CC} = 2.1). As is typical for other seasons, the summer drought treatment (mean ig_{CC} = 1.8) and the reduced rainfall treatment (mean ig_{CC} = 1.4) had the lowest productivity.

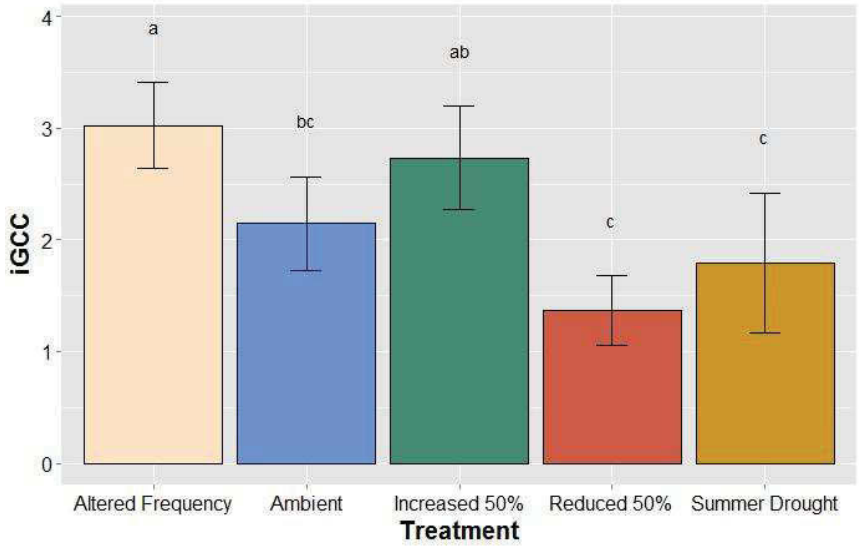

Figure 3.22. Mean ig_{CC} (± 1 s.d.) by treatment for Autumn 2015 (1 March 2015–30 April 2015). Means with the same letter are not significantly different between each treatment (Dunn's post-hoc test $p < 0.05$).

The trends that were observed from the seasonal analysis of ig_{CC} data provide more information than the total analysis. We see an increasing productivity trend with treatments of increasing rainfall quantity (reduced rainfall < ambient rainfall < increased rainfall). However, more subtle differences are present in the treatments that mimic changes in rainfall frequency and seasonality. The altered frequency treatment tends to be more productive than the ambient treatment, but this trend is more apparent in seasons when rainfall is low (e.g. Autumn 2014, Winter 2014), though occasionally when rainfall is higher (e.g. Autumn 2015). The summer drought treatment tends to show similar productivity to the ambient treatment at times when drought conditions are not imposed. The exception to this is in spring, when the productivity of summer drought plots is unexpectedly higher than ambient plots. Summer drought productivity also tends to have a higher mean ig_{CC} than the reduced rainfall plots, even when drought conditions are imposed, however this difference is not significant for any season. Variability within treatments is an indication that differences in community composition and vegetation response is occurring. High variability is present during spring for both the altered frequency plots and the summer drought plots. High within-plot variability is also observed for all treatments during throughout autumn 2015.

3.3.4.3 Productivity by drought regime

For drought regime, ig_{CC} data was split into two periods: when summer drought was imposed ('drought' period; 17 December 2014–17 March 2015) and outside of the drought period ('no drought' period; 1 April 2014–16 December 2014 and 18 March 2015–30 April 2015). Figure 3.23 illustrates the drought period in the context of an ambient treatment phenology profile.

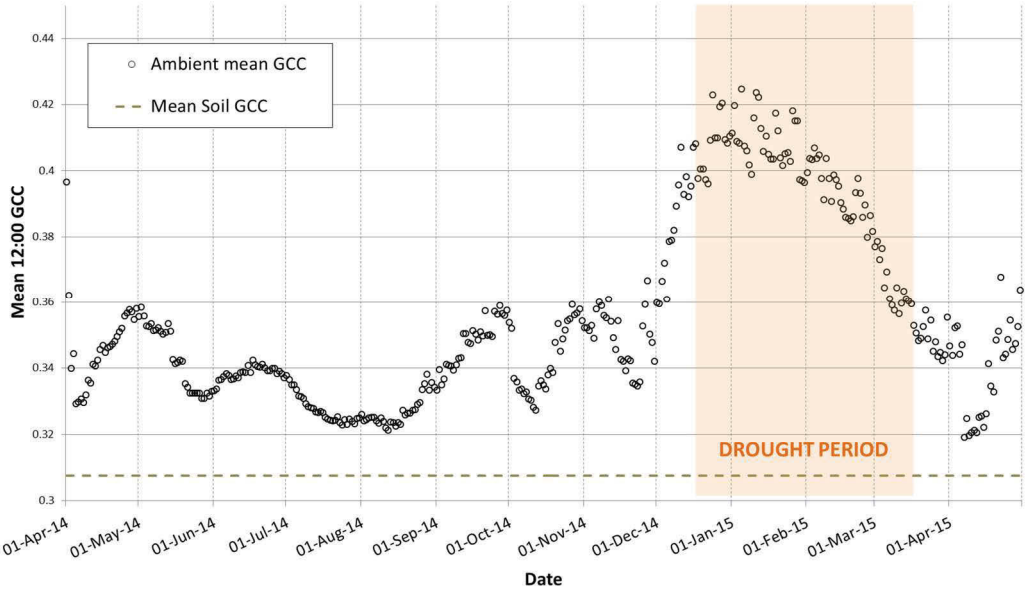

Figure 3.23. Phenology profile of mean ambient treatment with the 'drought' period shaded (17 December 2014 to 17 March 2016). The horizontal dashed line represents the mean soil g_{CC} value.

No significant difference in productivity was present between treatments during the 'drought' period (Figure 3.24). This is unexpected, as the summer drought treatment received no water during this time while the other treatments were exposed to the wettest months of the experiment. Reasons for this are discussed in Section 3.4.3, but the relatively high inter-treatment variability during this time (see Figure 3.13) may have contributed to the lack of statistical resolution.

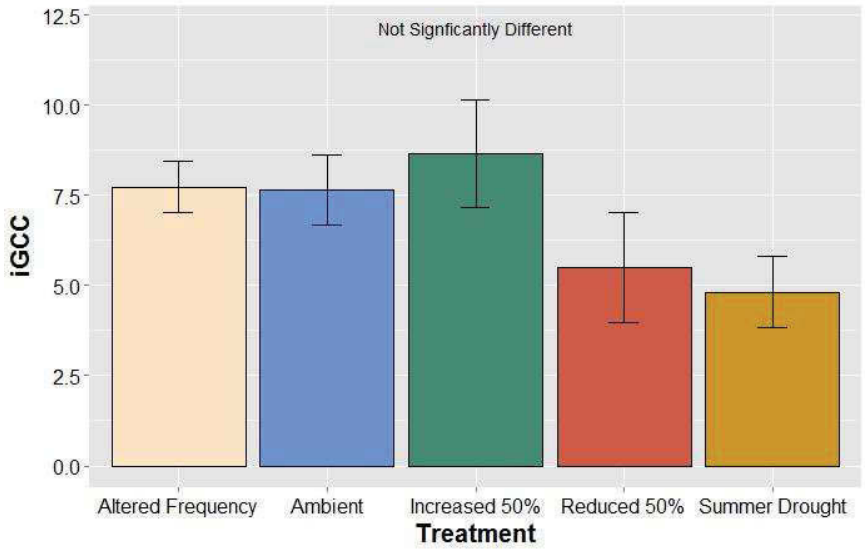

Figure 3.24. Mean ig_{CC} (± 1 s.d.) by treatment for 'drought' period (17 December 2014 to 17 March 2015).

During the 'no drought' period, productivity differences between the treatments were significant ($\chi^2 = 9.900$, $p = 0.042$; Figure 3.25). While the increased rainfall treatment, ambient treatment and reduced rainfall treatment showed the usual pattern of decreasing productivity, the summer drought treatment showed the most surprising result. This treatment (mean $ig_{CC} = 11.22$) was almost identical to the altered frequency treatment (mean $ig_{CC} = 11.23$), and more productive than the ambient treatment (mean $ig_{CC} = 10.34$), though the difference between these treatments was not significant.

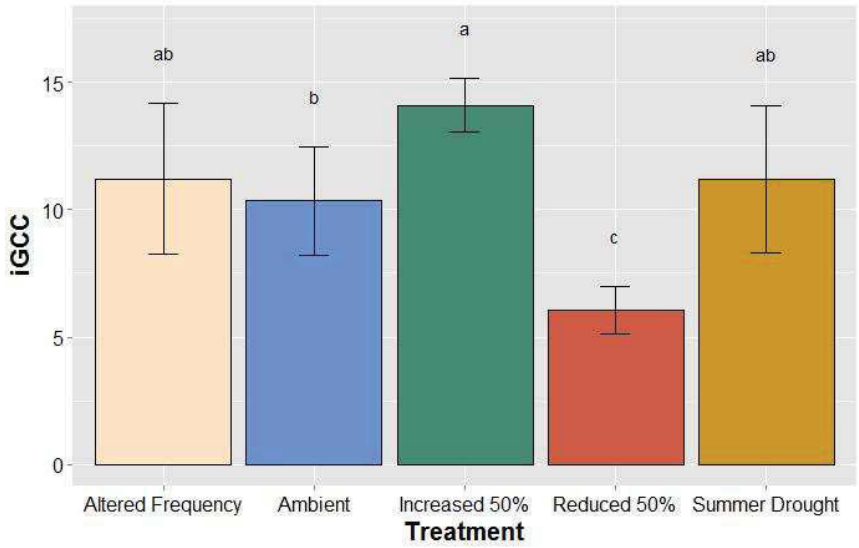

Figure 3.25. Mean ig_{CC} (± 1 s.d.) by treatment for 'no drought' period (1 April 2014–16 December 2014 and 18 March 2015—30 April 2015). Means with the same letter are not significantly different between each treatment (Dunn's post-hoc test $p < 0.05$).

The trends from separating the drought data into 'drought' and 'no drought' periods are illustrative for the summer drought treatment, but do not reveal further information than the seasonal data for the other treatments.

Analysis of the productivity of individual growth period (modes) was also conducted. Modal productivity showed similar trends to seasonal productivity. Analysis of treatment productivity separated by harvest period was conducted and showed similar trends to other results. These analyses are presented in Appendix B.

3.3.5 Phenophase differences between treatments

The date of flowering commencement for identified species was recorded across all treatment plots (Table 3.5). Commencement of flowering times for six species could be identified through the phenocam images. The most widespread species were: *Hypochaeris radicata* (8 of 15 plots), *Paspalum dilatatum* (6 of 15 plots), *Cymbopogon refractus* (5 of 15 plots) and *Senecio madagascariensis* (3 of 15 plots). Two other species were only found in one plot each. Many other species were present in the plots (see Table 3.2), however these did not have conspicuous flowers that could be identified through the images.

Table 3.5.Flowering start dates of species able to be identified through phenocam imagery.

Treatment	Replicate	Species	Flowering Start Dates
Ambient	1	(none)	
	2	(none)	
	3	*Hypochaeris radicata* *Paspalum dilatatum*	24 Jan 2015 15 Jan 2015
Altered Frequency	1	*Paspalum dilatatum*	26 Jan 2015
	2	*Hypochaeris radicata* *Paspalum dilatatum*	27 Dec 2014 17 Jan 2015
	3	*Cymbopogon refractus*	13 Dec 2014 < > 17 Jan 2015*
Drought	1	*Hypochaeris radicata* *Cymbopogon refractus*	15 Dec 2014 10 Jan 2015
	2	*Plantago lanceolata* *Hypochaeris radicata* *Paspalum dilatatum*	9 Dec 2014 22 Nov 2014 13 Jan 2015
	3	*Verbena bonariensis*	21 Oct 2014
Increased Rainfall	1	*Hypochaeris radicata* *Senecio madagascariensis*	19 Aug 2014 15 Feb 2015
	2	*Hypochaeris radicata* *Senecio madagascariensis* *Paspalum dilatatum*	6 Oct 2014 26 Jan 2015 25 Jan 2015
	3	*Hypochaeris radicata* *Cymbopogon refractus* *Senecio madagascariensis*	11 Nov 2014 2 Jan 2015 13 Jan 2015
Reduced Rainfall	1	*Paspalum dilatatum*	26 Jan 2015
	2	*Cymbopogon refractus*	23 Dec 2014
	3	*Hypochaeris radicata* *Cymbopogon refractus*	4 Dec 2014 4 Jan 2015

* Note: Precise date not resolved due to camera failure

Due to the different composition of species within each plot, little replication of species within each treatment was found: some species were only found in one plot of the treatment, and others were not found in certain treatment plots. Two plots had no observable flowering at all.

For the four most widespread species, two had relatively consistent flowering start dates across all treatments, both of these being C_4 grasses. *Cymbopogon refractus* commenced flowering consistently in early January, between January 2 and January 10, across three different treatments. *Paspalum dilatatum* had a broader flowering start date: from January 13 to January 26, 2015. There was no obvious difference in flowering commencement of C_4 grass species between treatments.

A treatment-based anomaly was observed for the flowering of *Hypochaeris radicata*, a common exotic forb. While this species had a broad start-of-flowering threshold (22 November 2014–24 January 2015), the increased rainfall treatment showed the earliest flowering commencement dates, including three plots that commenced flowering during winter/spring (19 August 2014, 6 October 2014 and 11 November 2014). Another anomalous observation was made with regard to *Senecio madagascariensis*. Flowering of this species was observed in all three increased rainfall plots, with no flowering observed in any other treatments.

3.4 Discussion

3.4.1 Effects of change in rainfall quantity

In temperate grasslands, inter-annual variation in biomass production is regarded to be primarily determined by inter-annual variation in precipitation quantity (Campbell *et al.* 1997, Sala 2001). However, while this may be true at regional scales, the relationship may not hold true at local scales (Swemmer *et al.* 2007). In the current experiment, total rainfall accounts for approximately 80% of the variation in productivity (as estimated by ig_{CC}) across all treatments. However, when broken down into seasons, or periods of growth, the accuracy of this model becomes much more variable. During the summer, where rainfall and vegetation growth were both high, the relationship between rainfall and ig_{CC} was very strong (Pearson's $R^2 > 0.95$) however at other times this relationship was much weaker (e.g. Winter 2014 Pearson's $R^2 = 0.11$). Given that agricultural production is seasonally-based, particularly in grazing systems, the need for accurate seasonal and local predictors is of great importance.

The qualitative observations of g_{CC} phenology profiles showed a consistent trend of increasing greenness with increasing rainfall throughout the year. That is, the reduced rainfall treatment consistently showed the lowest greenness, the ambient treatment had intermediate greenness, and the increased rainfall treatment had the highest greenness. This trend indicates that the system is rainfall-limited and that for most times throughout the year, a threshold limit to greenness has not been reached. However,

ambient and increased rainfall treatment g_{CC} values approached one another in the higher-rainfall periods of early spring and summer. At these times, soil moisture content was similar between the two treatments. This observation was supported by the analysis ig_{CC} as a proxy for productivity. At all segmentation fractions (harvest periods, seasons, etc.) the same trend of increasing productivity with increasing rainfall was observed in mean ig_{CC} values. However, this was not statistically significant at all segmentation fractions, which may either reflect convergence to a rainfall-limited threshold value during those seasons, or simply a low detection power of the statistical analysis (see Section 3.4.6).

The observations from this experiment showed that rainfall quantity changes produced only minor modifications to the shapes of phenology profiles. These differences included a skewed greenness distribution and possible earlier greenness peak, but generally differences were minor. This suggests that changes in rainfall quantity may yield predictable responses in the increase or decrease of productivity. However, there may be specific seasonal thresholds beyond which dramatic responses occur, such as the dramatic drop in greenness observed in the reduced rainfall treatment in Winter 2014. This may be most applicable to areas that are approaching those seasonal thresholds already, and where further rainfall decreases are predicted for the future.

The effect of rainfall on temperate grassland growth in other parts of the world have concluded that ANPP response to rainfall quantity is dictated by the water holding capacity of the soil (Sala *et al.* 1988, Lane *et al.* 1998), which determines the soil moisture content (Volder *et al.* 2013). Favourable years (more rainfall) may promote greater productivity on certain soil types, but unfavourable years (less rainfall) may promote greater productivity on other soil types, particularly where water is less limiting. In the current study, this concept can be extended to favourable and unfavourable seasons, as several growth patterns occur within one season. Although it refers to a temperature-driven system, this separation of seasons has also been suggested in British temperate grasslands where diverging responses to rainfall occur according to season (Morecroft *et al.* 2004).

Most of south-eastern Australia is water-limited, which suggests that primary production will benefit from increased rainfall, and decrease under lower rainfall

conditions. Given that climatic forecasts predict decreasing rainfall quantities in the autumn, winter and spring (IPCC 2014, CSIRO and Bureau of Meteorology 2015), lower productivity during these periods is likely. Autumn and winter rainfall also serves to improve soil moisture for spring growth (Cai *et al.* 2009), hence a decrease in winter rainfall may precipitate a greater moisture deficit in early spring.

3.4.2 Effects of change in rainfall frequency

Understanding how vegetation productivity responds to extreme rainfall patterns is crucial for assessing the impacts of climate change on terrestrial ecosystems (Zeppel *et al.* 2014). With more extreme rainfall predicted for south-eastern Australia (Hennessy *et al.* 2007, Reisinger *et al.* 2014), there are substantial consequences for pasture production in this region. Many scientists have acknowledged that an intensification of the water cycle is occurring, but it still remains to a) identify likely vegetation response and b) design appropriate adaptation strategies for future climates (Howden *et al.* 2008, Cullen *et al.* 2009, CSIRO 2011, Rickards and Howden 2012).

In the altered frequency treatment, higher greenness than ambient was observed throughout the cooler periods, and equivalent greenness to ambient was observed through the warmer, wetter months. No wholesale changes to timing of vegetative phenology was observed, although some increases in greenness tended to be more moderate (i.e. less steep) in the altered frequency treatments than others. This moderation was contrary to expectations; a periodic pulse of rainfall would logically result in a periodic greening, however this was not observed. Presumably if the event size and interval between events results in a steady supply of plant-available water, pulses in growth may not necessarily occur.

This phenomenon of reduced rainfall frequency resulting in higher productivity has also been observed in water-limited temperate grasslands in the USA (Heisler-White *et al.* 2008). In these studies, the productivity response of vegetation to changes in rainfall frequency has been shown to be related to the moisture state of the environment: xeric environments tend to respond more positively to extreme precipitation (i.e. higher productivity), whereas mesic environments tend to respond negatively (Knapp *et al.* 2001, 2008, Heisler-White *et al.* 2009). As an example, very little water will be

available to the plant following small rainfall events, as much of it will have evaporated before the rooting zone is reached. As the event size increases, the loss to evaporation will be proportionally less and more water will be available to plants. After a certain threshold, larger rainfall events will result in water loss through percolation through the soil column beyond the rooting zone (Weltzin *et al.* 2003). Hence, for xeric systems where evaporation is high, more water would be available to biota with larger events, whereas mesic systems would have proportionally less water available with less frequent rainfall (Knapp *et al.* 2008).

Soil characteristics (particularly water-holding capabilities) have an impact on this model (Lane *et al.* 1998). Sandy soils allow faster infiltration, so less water is lost to evaporation, but more plant-available water is lost through percolation beyond the rooting zone. Soils with more clay or loam restrict infiltration, so will lose more water to evaporation but retain more within the rooting zone (Sala *et al.* 1988). The relationship of these properties to climate type is known as the inverse texture effect (Noy-Meir 1973), and promotes a 'crossover point' of mean annual precipitation. Either side of this point provides a water-holding (and by extension, productivity) advantage to coarse-textured or fine-textured soil.

Measurement of the soil moisture over the study period showed that mean soil moisture was much lower for the altered frequency treatment than the ambient treatment for all seasons. Soil water-holding capacity (c.f. texture) has been identified as an important variable in ANPP (Epstein, Lauenroth, and Burke 1997) when considered on a regional scale. In the absence of temperature and soil texture variation at local scales, a positive relationship would be expected between soil moisture and productivity. However our experiment found only a moderate correlation between these variables, both overall and within seasons. Soil moisture was only measured to 15 cm, and some deep-rooted perennial grasses may have accessed soil moisture lower than this. However, this result provides a new perspective on the relationship between soil moisture and ANPP for Australian temperate grassland systems. It also highlights the need for more research on plant-soil water relations in these environments.

The interactions between the xeric/mesic nature of the grassland biome and the soil properties have a large impact on whether changes in extreme events have a positive,

negative or neutral impact on productivity. For each ecosystem there is likely to be an optimum distribution of precipitation event sizes and intervals between them (Swemmer *et al.* 2007). In the temperate pasture of this experiment, this optimum distribution is closer to the altered frequency treatment than the ambient treatment—at least over the course of the study period. However, because we see differential seasonal effects, this concept can be extended to seasonal climatic conditions rather than annual climatic conditions. It is clear that the continuation of this study is required to determine the full suite of seasonal conditions under which enhanced productivity is observed.

Thus far, only productivity response to changes in rainfall frequency has been considered, but changes to species composition are likely as well. Consideration needs be given to the types of species that are responding to moisture in different seasons. In cooler months, C_3 plants are more likely to take advantage of available moisture. In the case of the altered frequency treatments, perhaps certain functional types (C_3 annuals, for example) are more responsive to rainfall pulses seen in the altered frequency treatment, but are less responsive to consistently low rainfall of the ambient treatment in these winter months. While an obvious species shift was not observed in the phenocam imagery, the resolution is insufficient to register changes of this nature. Extending this research over different years will confirm conditions under which reduced rainfall frequency results in higher productivity. This should be integrated with high-frequency (e.g. monthly) vegetation surveys to determine which plant functional types are responding during this time.

It is generally agreed that future climate in south-eastern Australia will involve intensification of the hydrological cycle: an increase in rainfall event size and a reduction in event frequency (CSIRO and Bureau of Meteorology 2015). The results of this study suggest that under some circumstances, particularly when rainfall is low, an increase in grassland productivity may be observed as a result of reduced rainfall frequency. This is more likely in cooler, drier seasons, but confirmation of this trend is required.

This conclusion should be put in context of other studies that have found complex interactions between rainfall event size, quantity and interval (e.g. Fay *et al*. 2008; Zhang *et al*. 2013). Here, we use ambient rainfall with a constant interval and relative

event size, a regularity that is unlikely to occur in natural rainfall events. More long-term observations are required to determine if this trend is consistent in years of different climatic variability. In addition, it should be considered that more extreme events are likely to result in negative impacts such as increased runoff (particularly where surface soils are dry) and increased soil erosion (CSIRO and Bureau of Meteorology 2015). These impacts result in lower soil moisture and less grazing land, respectively, and may offset any potential productivity benefits.

3.4.3 Effects of drought events

Future climate predictions for south-eastern Australia indicate that droughts are likely to increase in severity and duration (CSIRO and Bureau of Meteorology 2015). For a country such as Australia that already experiences regular and lengthy droughts, this is a serious prospect for agricultural production in coming decades.

The results of the summer drought treatment show a predictable sharp decrease in greenness and corresponding loss of productivity during the time that the drought was in effect (17 December 2014 to 17 March 2015). This result was expected, but illustrates the dramatic effect that drought can have on healthy ecosystems and soil moisture, and the speed at which vegetation senescence can occur. In contrast, outside of the drought period, the summer drought plots exhibited very different behaviour. Over the non-drought period, productivity of the summer drought treatment was significantly higher than ambient treatments, despite the fact that both treatments were receiving equal quantities and distribution of rainfall during this time. The phenology profile suggests that the increased seasonal and overall productivity was attributed to large greenness peaks at modes 3 and 4. The same phenomenon was observed after mode 5, in April 2015. The review of phenocam imagery allowed an explanation of this: that the drought plots had been subject to invasion from a variety of exotic forbs. The weed invasion caused a dramatic community change that occurred in all drought plots and was not evident in other treatments. Droughts are well known to promote weeds; exotic plants that typically have fast establishment times and are able to take advantage of the lack of competition following drought conditions (Richardson *et al.* 2011). Several field observations have documented weed invasions to temperate grasslands following major droughts (Scott *et al.* 2010, Moran *et al.* 2014).

This abrupt change in community composition was unexpected and clearly reinforces the prediction that prolonged and more frequent droughts will provide more opportunities for weed invasion (Scott *et al.* 2014). This will result in lower productive land for grazing and greater costs relating to weed control and eradication. With weeds estimated to cost agricultural producers over $3.5 billion annually (Sinden *et al.* 2004), increases in drought frequency and extent will result in a significant inflation of this cost.

This observation also serves as a reminder that a higher vegetation index, or greenness, is not always reflective of a more positive situation. Although the greening of the Sahel region of Africa following several droughts is often cited as an example of ecosystem resilience (Dardel *et al.* 2014), ground data indicates large ecological shifts have occurred and that the vegetation is more impoverished than the pre-drought condition (Herrmann and Tappan 2013). When using satellite or near-surface remote sensing (such as phenocams), the need for ground validation, particularly of anomalous or unexpected results, is critical.

Like the altered frequency treatment, the impacts of drought may be more or less severe depending on annual rainfall quantity and soil texture. In a European temperate grassland, biomass reduction was reported for low-rainfall sites following drought, but experimental drought actually increased biomass in higher-rainfall locations (Gilgen and Buchmann 2009). However, even the low rainfall treatment in Gilgen and Buchmann's study is higher than the annual rainfall of the DRI-Grass location, and the drivers in European temperate grasslands are very different to those in south-eastern Australia.

During the drought period, a large and significant decline in greening and productivity was evident. At this stage of the experiment, the plots were dominated by C_4 grasses, species that have a higher water use efficiency than C_3 species, and tend to be more resistant to drought effects (Ghannoum *et al.* 2011). As the drought effects on these plants were dramatic, droughts occurring at other times of year—when C_3 plants are more dominant—will be even more damaging. The key message, obvious though it may be, is that the direct impacts of extended and more regular droughts on grassland

ecosystems will be senescence and death of vegetation and large losses in pasture production. When droughts reoccur before an ecosystem has recovered, the likelihood of widespread community change impacts on plant mortality is even more pronounced (Anderegg *et al.* 2013).

3.4.4 Observed changes in species composition and phenophases

Through this experiment, most of the biomass production occurred during the summer months, when temperature and rainfall were both high. Field observations, confirmed with phenocam image review, indicated that C_3 grass and forb species were dominant during the cooler months, however C_4 grasses such as *Cymbopogon refractus* and *Paspalum dilatatum* were extremely vigorous during the warmer months. This pattern of C_3/C_4 dominance in cool/warm seasons respectively was observed for all treatments. This is a typical pattern for mixed pastures such as this, but the high levels of rainfall in the warmer months is a key driver of high levels of C_4 productivity (Volder *et al.* 2010), as was the case in summer 2014/15.

The drought impact on community composition has already been discussed (Section 3.4.3), with particular reference to weed invasions. However, more subtle changes in rainfall quantities and distribution can result in long-term species compositional change (Bates *et al.* 2006, Suttle *et al.* 2007). While the resolution of phenocam images may be insufficient to monitor this over time, ongoing species monitoring at the plot level is critical to determine the interactions between different functional groups. Groups that are predicted to have differential response to rainfall change include C_3 versus C_4 (Cristiano *et al.* 2012), grasses versus forbs (Dostálek and Frantík 2011), native versus exotic (Scott *et al.* 2014), deep-rooted versus shallow-rooted (Morecroft *et al.* 2004) and annual versus perennial (Dostálek and Frantík 2011). In addition there is growing evidence that rainfall regime from the current year is likely to result in community change during the following year (Sherry *et al.* 2012, Dudney *et al.* 2016).

Phenological changes in vegetation communities are widely predicted in response to changes in rainfall (Reyer *et al.* 2013), though remain a major data gap in current research. Widespread changes to plant phenology in response to drought was reported in an oak forest (Misson *et al.* 2011) but similar studies are rare in other biomes. The

current study observed changes in the magnitude of phenology curves (i.e. greenness), but did not observe substantial changes in the timing of vegetation phenology. Changes in the integrated phenology of the plot (i.e. through community change) may be visible in the short-term, but any changes in vegetative phenology of individual species are likely to take many years to resolve. The seasonality of plant available water has been shown to influence the distribution of C_3 and C_4 grasses at larger scales (Winslow *et al.* 2003, Flanagan 2009), though its effect on C_3/C_4 distribution at smaller scales remains to be seen.

Such experiments also present the opportunity to explore traditional phenology—changes in flowering and fruiting times. This experiment identified minor phenological differences in flowering times of two exotic forb species which suggests that increased rainfall may promote earlier or more vigorous flowering of unwanted species. However, the camera resolution and angle of viewing was not ideal for this purpose. While the lack of species consistency between experimental plots makes exhaustive comparisons impossible, comparison of flowering and fruiting time of the primary species would be extremely valuable for demographic studies. It is recognised that traditional monitoring of phenology can be extremely time-consuming (Tuanmu *et al.* 2010) but may be an appropriate value-adding service if the plots are attended regularly.

3.4.5 Assessment of phenocam utility

This phenocam-based approach used an RGB vegetation index, the green chromatic coordinate (g_{CC}), to monitor vegetation dynamics at a high temporal frequency. While several studies have used a similar approach to investigate and monitor changes in ecosystems (e.g. Ide and Oguma 2010; Richardson *et al.* 2007), this is the first study that has used this approach in an experimental setting to assess vegetation growth differences between experimental treatments.

Based on field observations and correlations with rainfall and soil moisture, the g_{CC} provides an accurate assessment of grassland vegetation dynamics. Although unable to correlate integrated g_{CC} with measured biomass, the observed greening and productivity trends closely match field observations and rainfall patterns. The setup of the phenocam

in this experiment ensured a consistent camera angle relative to the pasture. This allows the magnitude of g_{CC} change to be directly compared between phenocams.

In the last decade, the use of phenocams to conduct ecological and phenological research has increased. Primarily, this is due to the ability to collect a continuous record without a human operator. Imagery collected with phenocams also has a critical advantage over alternative methods: the ability to subset the data spatially and temporally. In the broader rainfall exclusion experiment, assessment of productivity through destructive harvest was conducted twice annually. However, productivity estimates using phenocam-based indices are able to be subset to any desired timeframe: over the total period, biannually, by season, or by growth period. Many phenocam studies are interested in investigating the green-up period, which can be easily extracted from phenocam data, even where there are several growth periods in one year. This is not to say that phenocam-based estimates of greenness or productivity negate the need for ground measurements. Rather, with appropriate validation, phenocams allow the coverage of a wider geographical area or greater replication.

The high spatial resolution afforded by phenocams provides the capability to investigate different areas of the data (image) independently. As such, specific regions of interest (ROIs) within the same image can be defined and compared. Such capability has been used to differentiate the phenology of different species (Alberton *et al*. 2014; Nagai *et al*. 2011) and even quantify phenology timing down to the pixel level (Julitta *et al.* 2014).

Despite the considerable advantages that phenocams provide, throughout the course of this experiment several features were identified that could contribute to data contamination or loss. These factors relate to the quality of the data and are discussed below.

3.4.5.1 Shadowing

Shadowing was present in many photos due to the proximity of the shelter framework, the shelter roof, and the phenocam itself. The g_{CC} was selected as an appropriate vegetation index as it is known to be relatively invariant to changes in illumination

effects (Sonnentag *et al.* 2012), however some suppression of g_{CC} from shadows is still known to occur (Crimmins and Crimmins 2008). This effect is visible in the centre right panel of Figure 3.9.

Analysis of one month of g_{CC}-processed imagery (not presented) compared images on sunny days (shadows) with cloudy days (no shadows). The results showed that although shadowed images did have a lower g_{CC} (mean 0.3399 compared to 0.3369) this difference was minor. Shadowing effect on bare ground lowered the g_{CC} by 0.05 units (typically from 0.3 to 0.25) but had no effect on g_{CC} when vegetation was present. The shadows, therefore, only affect imagery where they intersect with bare ground, which is relatively rare in the image time-series.

For this study, the shadows in the images were retained instead of being manually removed. While this results in minor dampening of the 'true' g_{CC} value, the removal of the shadows via colour threshold methods introduces an extra element of uncertainty and potential error. As the shadowed portion of the image was never greater than 10%, and this only affected images that had a higher proportion of bare soil, this was considered an acceptable level of uncertainty in the data.

3.4.5.2 Viewing geometry

The relative angles of the illumination source and the sensor has an impact known as anisotropy that will impact reflectance characteristics of the target (Jones and Vaughan 2010). In our case, the camera angle remains constant in all plots but the sun angle changes continuously throughout the day and with the seasons. Sun angle has been found to provide a minor impact on g_{CC} (see Chapter 5), however to be conservative only noon (12:00) photographs were used. The change in sun angle due to the earth's tilt on its axis has not been taken into account, but the effect is expected to be negligible.

The most apparent impact that illumination has is the change in shadows throughout the year. The shadowing impact on g_{CC} has already been discussed and, with the exception of images with very low vegetation cover, has been determined to have a low impact on image g_{CC}.

3.4.5.3 Soil signal

Changes in soil moisture are known to affect certain vegetation indices; robust spectral indices have been developed in the satellite domain that correct for this (Huete 1988). The g_{CC} of bare soil fluctuated in response to rainfall, with values of 0.30 typical at low soil moisture and values up to 0.32 occurring immediately after rainfall. Because of this fluctuation, the average value (g_{CC} = 0.3076) was used as a baseline throughout this experiment.

Attempts to correct for this soil moisture anomaly proved difficult because of the different proportions of background fraction for each image. For images that contained a high proportion of soil (e.g. 20%), the g_{CC} may be artificially inflated when soil moisture content is high. However when the background fraction was close to zero (i.e. ~ 100% of the image was comprised of green or senesced vegetation), changes to the soil colour had no impact on the overall g_{CC}. Fortunately, this imposes an element of self-correction: during times of high rainfall, where the variant soil g_{CC} may impact the g_{CC} of the scene, vegetation growth was high and soil contribution was negligible. The images that exhibited the highest proportion of background soil were on occasions when conditions were dry and the soil was relatively invariant. In this case, no correction was made, with the acknowledgement that the g_{CC} minima of low-rainfall treatments, the only treatment with a significant quantity of bare soil, may be marginally inflated when rainfall has occurred and when greenness values are very low.

While negligible in this case, soil g_{CC} variation may have a greater impact on studies where more background soil is present throughout the year, or where the soil has a particularly large change in g_{CC} with moisture conditions. This should be assessed on a case-by-case basis depending on individual soil types.

3.4.5.4 Technical issues

Like most pieces of technical equipment, the phenocams used in this study were not infallible. Moisture incursion (lens fogging) and hardware failure resulted in the loss of some data but an overall capture rate of > 90% is considered more than sufficient to observe trends. Additional weatherproofing would further improve this capture rate.

A range of phenocams have been used in ecological studies from inexpensive 'webcams' to professional-grade cameras. In a comparative study, the Wingscapes™ product used in this study showed no difference to higher-quality phenocams (Sonnentag *et al.* 2012), and offered the advantage of lower cost; hence more replicates could be used. One disadvantage of this product is that it is a 'black box' as far as technology and customisable settings are concerned (Sonnentag *et al.* 2012), with very few options able to be modified by the user. However, when used in a consistent setting in conjunction with an appropriate vegetation index, this does not seem to present a major problem.

Over time, the sensors within digital cameras have been known to degrade, which can compromise the integrity of time-series imagery. One study in Japan observed a decay in colour consistency that occurred gradually over 8 years (Ide and Oguma 2010), though sensor drift was not evident until almost three years into the observations. While sensor degradation is likely to differ between camera models and—reasonably—more inexpensive phenocams may experience degradation faster than more expensive ones, our study used new cameras from the same manufacturing batch over the span of one year. Visual inspection of images could not discern any noticeable changes between invariant objects (e.g. shelter framework) from the beginning of the study to the end, and it is not believed that sensor drift has impacted these results. Nevertheless, future studies should attempt to incorporate some form of colour reference, despite the acknowledged limitations that these entail (Migliavacca *et al.* 2011).

From a digital photography perspective, RAW image format is the only scientifically justified file format (Verhoeven 2010), one that is not supported by Wingscapes™ phenocams. Other image formats (e.g. JPEG) can result in spatial or colour compression that can potentially lead to information loss (Stevens *et al.* 2007). This position though continues to be challenged, with JPEG and uncompressed formats showing no significant differences in data quality from RAW format counterparts (Pekin and Macfarlane 2009, Sonnentag *et al.* 2012). The extensive use of alternative file formats amongst researchers using phenocams suggests that file format, while still an important consideration, is not an impediment to obtaining accurate results.

3.4.5.5 Overall assessment

Overall, phenocams represent a novel and accurate method of exploring vegetation dynamics and phenology. It has been suggested that the development of inexpensive, instrument-based approaches for field measurement is necessary to advance phenology monitoring (Morisette *et al.* 2009). The use of phenocams in an experimental setting is a step in this direction and provides an excellent opportunity to obtain high-frequency data that is difficult to obtain using other methods. The increasingly widespread use of open-source image processing software also facilitates the sharing of methods to improve the speed and accuracy of image processing. Phenocams also provide several value-adding services, like the ability to revisit anomalous observations, and to validate trends visually (Richardson *et al.* 2007). However, factors that can affect data quality should be understood, and considered on a case-by-case basis to ensure the validity and integrity of the phenocam data.

3.4.6 Limitations and recommendation for future research

Due to equipment cost and availability, this study was limited to three replicate phenocams per treatment. Ultimately, this is a low number of replicates when working with heterogeneous grassland, as subtle differences in species composition can result in unwanted variation within treatments. As such the statistical power is low in this experiment, particularly when data is subset to seasonal periods and shorter timeframes (< 90 data points). With three replicates, the data is not normally distributed and less powerful non-parametric statistical tests have to be employed. However, the trends are promising even where non-significant differences were observed and provide opportunities for future research. It has to be recognised that in natural conditions where variability is high, more replication is needed to increase the confidence in statistical tests. In the absence of simply obtaining more resources for extra equipment, future experiments can focus more replications on fewer treatments.

Field validation of remotely-sensed vegetation dynamics is important to ensure that the observed trends are accurate representations of conditions (Reed *et al.* 2009). In this experiment, an element of validation is obtained through photographic data capture and the ability to visually confirm greening and browning trends. However, validation of

productivity estimates is much less straightforward. Simulation research on grassland productivity highlights the complexity and variability in conducting field-based productivity estimates, in particular the difficulty in accounting for changes in vegetation between harvests (Lauenroth *et al.* 1986). Even simple unimodal monoculture systems do not accurately capture translocation of resources from belowground to and from aboveground (e.g. as a result of plant stress), or loss of vegetation from the system (e.g. from herbivory) (Scurlock *et al.* 2002). As a result, grassland productivity estimates using different methods can vary markedly—by up to five times (Singh *et al.* 1975, Long *et al.* 1989). In the current experiment—with complex multimodal dynamics that include several species—harvesting at 6-monthly intervals cannot accurately reflect the vegetation dynamics estimated by the phenocams. For future experiments, a much greater degree of replication is required to allow for monthly (or even more frequent) harvesting and accurate validation of productivity estimates.

While rainfall is the most direct driver on temperate grassland productivity and vegetative phenology (Sala 2001), it must be acknowledged that rainfall is only one element of the overall climate change effect. Temperature and CO_2 concentrations will also have their own impacts; some of these are known, some are unknown. These factors will also interact with rainfall regimes to impact plant-available soil moisture. Higher temperatures will promote greater moisture loss through increased evaporation which will be further increased for areas with predicted lower humidity (CSIRO and Bureau of Meteorology 2015). It is possible that evaporative loss will be so high that even where increases in rainfall are predicted, a net loss in soil moisture will result. On the other hand, some evidence suggests that increased atmospheric CO_2 may offer the possibility of moisture deficit savings in grasslands (Volk *et al.* 2000). As such, the results of this experiment should be considered in conjunction with potential changes imparted by CO_2 and temperature interactions.

While the DRI-Grass experimental plots have been established since 2013, the research project described in this chapter only ran for 13 months. This is a relatively short time frame, and is insufficient to take into account long-term ecological effects of rainfall regime changes. Some ecosystems may have strong resilience to climatic changes, and ecological change may only occur after many years (Bates *et al.* 2006). In less-resilient

biomes, changes may be apparent within the first year, but cascading effects may result in ecosystem instability for several years until equilibrium is restored. Such an effect was observed in a rainfall redistribution experiment on a northern Californian grassland (Suttle *et al.* 2007). While some interesting ecosystem responses have already been observed in the DRI-Grass treatments, the long-term effects on our temperate grassland systems will only be fully revealed after many years of monitoring. In addition, the south-eastern part of Australia is typified by a variable climate. The year that this research was conducted was an unusually dry winter and a very wet summer. Hence, conclusions on vegetation response can only be drawn for these conditions, and a variable response may be observed if, for example, a dry summer occurs in future years. Ongoing monitoring at this research facility will ensure that the grassland response to a range of climatic conditions is recorded.

Precipitation exclusion experiments are inherently complex and invariably result in 'dilemmas' that dictate the experimental variables and artefacts that occur from a shelter-type design (Beier *et al.* 2012). One such dilemma is a trade-off between realistic and imposed experimental conditions. Here, the project infrastructure was deliberately established on a natural grassland to ensure that results and findings could be directly applied to natural systems. However, the heterogeneity of Australian temperate grasslands means that the species composition at the start of the experiment may be subtly—or more obviously—different between treatment plots. This is a different strategy to controlling the species composition from the start of the experiment (e.g. Fay *et al.* 2008). In the dilemma between exercising control versus representing reality, each strategy has its advantages and disadvantages. In our case, a non-consistent plant community will result in a more integrated response of vegetation rather than being able to identify specific responses from individual species. This strategy is more appropriate for mixed pasture systems where this importance is less on individual species and more on the integrated pasture response. However, adequate replication is required to provide a representation of the variety of plant community.

Beier (2012) provides a comprehensive summary of recommendations for future rainfall modification experiments. The DRI-Grass project addresses many of these data gaps, and will continue to collect data over the coming years. Phenocams offer a value-adding service to rainfall modification experiments at a modest cost, however over-replication

is recommended to ensure hardware failure and vegetation variation does not limit the applicability of the findings.

3.5 CONCLUSION

Changes in rainfall regime and the occurrence of more extreme events such as drought have been identified as a major threat to Australia's grazing economy, as much remains unknown about future climate effects on pasture productivity. This experiment used a network of time-lapse digital cameras (phenocams) to quantify the effect of different rainfall treatments on a mixed grassland in temperate south-eastern Australia. Rainfall treatments were designed to alter either the quantity or timing of rainfall events within a rainfall shelter design. The phenocam images were processed to the green chromatic coordinate (g_{CC}), a vegetation index that has been successfully used to track changes in vegetative phenology in many biomes. The integral of the g_{CC} was used as an estimate of aboveground net primary productivity. Five growth periods (modes) were identified throughout this 13–month experiment, which is in sharp contrast to unimodal or (rarely) bimodal patterns observed in northern hemisphere phenology studies.

The results showed that in treatments that involved changes in rainfall quantity, the variables of greenness and productivity followed a predictable pattern. Seasonally, as well as over the course of the experiment, higher volumes of rainfall produced consistently higher greenness values and higher levels of productivity. This is indicative of this system being water-limited at some times of the year but in other seasons approaching a water limiting threshold where increased rainfall did not result in significantly greater productivity. Soil moisture changes were not commensurate with rainfall regime. A reduction of rainfall to 50% of ambient resulted in a mean soil moisture content 65% of ambient, and an increase of rainfall to 150% of ambient resulted in only a 105% increase in soil moisture. This is likely due to the high drainage capability of the sandy soils at this location, and reinforces the concept that the water-holding capacity of soils may dictate the extent to which changes in rainfall quantity will affect productivity. In this ecosystem, the impacts of rainfall reduction on soil moisture are more apparent than those due to rainfall increase.

Two treatments investigated the effects of altering rainfall timing. The summer drought treatment imposed a three-month drought, consistent with predictions for south-eastern Australia to experience harsher and longer droughts in coming decades. During the drought period, this treatment showed a dramatic drop in greenness as vegetation wilted and senesced, and significantly lower productivity than the ambient treatment. However, outside the drought period, productivity was not significantly different to ambient, and in fact greatly exceeded it at several times. Upon examination of the phenocam images it was apparent that the increased greenness was caused by the invasion of exotic forbs that occurred at each of the drought treatment plots following the drought event. This illustrates a critical warning: that extended droughts will not just reduce productivity for the drought period, but can reduce ecosystem resilience such that undesirable species may increase in abundance. This finding also acts as a caution to remote sensing scientists that 'greener is not always better', and ground validation is necessary to confirm greening trends.

The 'altered frequency' treatment is analogous to the intensification of the hydrological cycle that is predicted to occur in south-eastern Australia. At some times of the year—particularly the warmer months where rainfall was high—the greenness of this treatment closely mirrored the ambient treatment, though was slightly more productive. In cooler and dryer months, the altered frequency treatment was consistently and significantly more productive than ambient. This finding is consistent with research from other temperate grasslands around the world where water is limited, though was unexpected in our case due to the much lower soil moisture content in altered frequency plots.

Impacts on phenophase, such as flowering and fruiting times were difficult to monitor across treatments due to the heterogeneity of species composition. However, the flowering of one exotic forb, *Hypochaeris radicata*, commenced earliest in the increased rainfall plots. Another exotic forb, *Senecio madagascariensis,* was only observed to flower in the increased rainfall plots. While not conclusive, these observations suggest that in regions where increased seasonal rainfall is predicted for future climates, there may be some unexpected negative impacts to offset the likely increases in production.

This is the first research study that used phenocams to monitor experimental changes in vegetation dynamics. The method and the vegetation index used provided an accurate assessment of greening and browning changes that would be time-consuming to collect with traditional field measurements. An obvious advantage of high-frequency phenocam data is the ability to segment the data into specific time periods and enable the resolution of seasonal or monthly productivity trends that destructive harvesting may not be able to resolve. Phenocams also offer the advantage of creating a visual record, so that anomalies can be revisited and inspected at a later date. Image quality issues such as shadowing, sun angle and filtering were not considered to have a great impact on the overall findings, but require assessment on a project-by-project basis to reduce noise in the data and improve overall accuracy.

Validation of the imagery was not possible in this experiment as the harvesting timing and number of experimental units had been established prior to commencement. Although biannual harvesting is sufficient for some studies, the multimodal nature of the pasture as detected through the phenocams suggest that more fine resolution harvesting would be required to accurately validate the phenocam estimates of productivity. Future experiments should consider the modality of the ecosystem and consider this *a priori*.

Ecosystem change from rainfall experiments may take several years to fully resolve, and this experiment represents only one year of a long-term project. In addition, this project was conducted in a region that has highly variable climatic conditions, and further observations are required under a range of seasonal climatic states to completely understand the grassland response to rainfall. However, results obtained thus far show changes to grassland productivity, phenology and community composition that are valuable clues into how grazing agriculture may be affected by future rainfall regimes. From these results, and results from other manipulation experiments across the world, it is clear that the interaction between rainfall quantity, rainfall event size, and soil type is a complex one, and further work is required to disentangle these factors under varying climatic conditions. Although rainfall is only one of a number of changing factors that affect grassland ecosystems, these results provide additional insight into the type of adaptation strategies that will be required to ensure Australia's food security in coming decades.

Chapter 4: Seasonal changes in temperate grassland species dynamics and phenophase: a floristic study

4.1 Introduction

Temperate grasslands are often described as 'dynamic' vegetation types; they are comprised of many different species that change rapidly in response to environmental variables (Tremont 1994, Lunt and Morgan 1999, Eddy 2002). While some grassland communities have a single dominant species that remains constant, others have species compositions that change between seasons and from year to year. This dynamic nature is thought to increase the resilience of grasslands (Fry *et al*. 2013), but presents challenges in understanding larger-scale ecological processes.

Because grassland components change more quickly than, for example, forested ecosystems, grasslands can be viewed as early indicators of external drivers. Species changes may be indicative of short- or long-term climatic factors, fire regimes, or grazing impacts. Monitoring these changes, either through remote sensing (Petrie *et al.* 2011) or field surveys (e.g. Vivian and Baines 2014) is critical for identifying these changes. Increasingly, land surface phenology—the integration of vegetative phenology across a large area—is being used for ecological monitoring purposes (Bradley and Mustard 2008; Keenan *et al.* 2014). Given the complexity of grassland dynamics, it is clear that a strong understanding of grassland community compositional change is necessary to provide context to land surface phenology information.

4.1.1 Monitoring changes in grassland species richness

Species richness—the number of species in an ecosystem—is a fundamental ecological monitoring variable. It has been linked to ecosystem resilience, condition, restoration, degradation and disturbance (Prober, Thiele and Lunt 2007; Vickers, Gillespie and Gravina 2012; Williams *et al.* 2006). Monitoring the abundance and phenophases of individual species can provide important information as to the dynamics of key species, and can thus explain their contribution to land surface phenology.

In ecosystems dominated by woody species, species richness remains relatively constant throughout the year. However in ecosystems dominated by herbaceous species, or in non-woody vegetation layers (e.g. groundcover) species richness can change markedly as annual species germinate, grow and senesce through the year. In some species, senescent plants may leave residual aboveground parts, but others can leave no evidence of their former presence. In temperate Australian grasslands, some species are only conspicuous when flowering—after which, aboveground parts wither, leaving only belowground tubers. In addition, species may be eliminated from an area through preferential grazing. Species richness at any given time—or at least species richness as determined by traditional botanical survey—is thus dependent on the phenophase, life history strategies and ecology of the suite of species present. Monitoring species richness throughout the year is important to determine ideal times for ecological monitoring or validation of remote sensing measurements. This is particularly true in grasslands, as different functional types may have different seasonal patterns of species richness. For example, annual plants are more likely to have greater species richness in the Australian spring whereas plants that utilise the C_4 photosynthetic pathway will be more abundant in the summer.

While the dynamic nature of grasslands in temperate Australia is regularly highlighted, there are few examples of studies in the literature that confirm the species dynamics through frequent floristic survey. Some exceptions occur: in a study of grasslands in the northern tablelands of New South Wales, Tremont made general ecological observations on a monthly basis, but only made formal surveys twice within a year (Tremont 1994). A disturbance-based investigation on grassland ecology on the New England Tablelands surveyed species richness every three months (Li *et al.* 2006). Stuwe and Parsons surveyed across spring and summer, but recognised the importance of sampling outside this period for detecting other species (Stuwe and Parsons 1977). Chan surveyed weekly phenology of dominant species in grasslands of the Australian Capital Territory (Chan 1980), but did not survey full floristic details. A report to the ACT Commissioner for Sustainability and the Environment monitored the species mix of several grasslands at three targeted occasions over one year (Hodgkinson 2014). Many long-term grassland surveys are surveyed once per year, but repeated in the same month each year for consistency (e.g. Lunt and Morgan 1999; McIntyre and Martin

2002; Vivian and Baines 2014). More regular flora surveys are required to adequately capture changes in species composition throughout the year.

4.1.2 Monitoring changes in grassland condition

Ecosystem 'condition' generally refers to the heath or well-being of the community, but a precise definition remains vague (Keith and Gorrod 2006). Nevertheless, 'condition' is now an accepted form of valuing an ecosystem and is embedded in Australian state and federal legislation (Department of the Environment 2016). A common broad approach to assessing condition is related to the integrity of the structure, composition and function of that ecosystem (Hnatuik *et al.* 2009, Department of Environment Climate Change & Water 2011), often as compared to a 'benchmark' or representative example of an undisturbed community.

Changes in ecosystem condition are typically long-term; they relate to ecosystem restoration or degradation that occurs over many years. However, the question of how measures of ecosystem condition change on a seasonal basis has not been explicitly addressed. This may be because in many Australian ecosystems, the dominant vegetation types such as *Eucalypt* woodlands are woody, evergreen, long-lived, and are relatively invariant to seasonal changes.

The dynamic nature of grasslands makes the concept of condition at any point in time more uncertain. The factors used to assess condition (e.g. native species richness, vegetation cover, exotic species presence) will change in grassland much faster than other ecosystems. Given that the structure and composition of grasslands can change rapidly—even from week to week—there is a need to investigate how this impacts estimates of condition. Understanding how seasonal changes affect condition measures may also help inform optimal monitoring times for long-term condition assessments; conversely, ignorance of short-term condition changes may undermine long-term monitoring strategies.

There is a variety of methods to monitor grassland condition (Seddon *et al*. 2011). Many of these use the biomass or cover of grass as the defining variable (Sharp *et al.*

2015). However, in Australian temperate grasslands, a primary indicator of condition is the richness and abundance of native forbs. A Floristic Value Score (FVS) method has been developed that provides a greater weighting to sensitive species, and is reflective of the true conservation value of the grassland (Rehwinkel 2007). This method was designed to monitor long-term changes in grassland condition, however has potential to investigate seasonal changes of condition.

4.1.3 Grassland phenology

The phenology of select south-eastern Australian grasslands has been described by several authors. Most of these studies have either focused on a combination of flowering and vegetative phenology (Biddiscombe *et al.* 1953, Williams 1961, Groves 1965, Chan 1980). Some studies investigated only flowering phenology (e.g. Tremont 1994), particularly where it related to climate change impacts (Hovenden *et al.* 2008).

For the majority of these studies, the vegetatively dominant species of the ecosystem has been the focus, as dominant species will proportionally contribute the most towards total ecosystem function. As an extension of this, the dominant species will provide the greatest contribution to land surface phenology. Understanding individual species contribution to land surface phenology is essential to enable scaling between field and remote sensing sources.

4.1.4 Land surface phenology of grasslands

As detailed in Chapter 1, land surface phenology refers to large-scale phenology observations, as opposed to traditional point-source phenological observations (de Beurs and Henebry 2004). These large-scale observations are typically associated with time-series imagery of a vegetated scene collected from satellite remote sensing or a time-lapse phenology camera ('phenocam'). The change in vegetative phenology is represented as a time-series 'greenness' vegetation index (VI), such as the Normalized Difference Vegetation Index (NDVI; Rouse *et al*. 1974), Enhanced Vegetation Index (EVI; Huete *et al*. 2002) or Green Chromatic Coordinate (g_{CC}; Sonnentag *et al*. 2012).

How the VI changes through time is dependent on changes in vegetation biophysical characteristics, such as Leaf Area Index, aboveground biomass and chlorophyll content (Glenn *et al.* 2008). In turn, the biophysical characteristics of individual species are affected by their inherent phenology and how they respond to environmental drivers (e.g. climate, herbivory). For example, a grass plant may decrease canopy chlorophyll content and lose photosynthetic biomass due to winter senescence (phenology), but an environmental driver such as a long drought may produce a similar effect. It is important to determine how species respond to environmental drivers before taking remote data at face value.

Depending on the scale of capture, an image used to quantify land surface phenology will contain several to many thousands of individual plants, likely comprised of many species. Each individual plant within an image time-series has its own phenophase signature: a seasonal pattern of growth and development that may include emergence, foliage growth and senescence, flower production and fruit development (Hudson 2010). Individual species phenophase will result in changes in VI relative to the changes in their biophysical characteristics.

Land surface phenology measures will be further impacted by the change of species composition through time, as the proportion of each species will affect their contribution to the vegetation signal. In particular, land surface phenology will be impacted by changes in the canopy species as the effect of understory species may be reduced or eliminated if the canopy is closed. In this section, 'canopy' refers to the uppermost vegetation that can be observed by the sensor. This may include trees (in a forest), grasses (in a grassland), shrubs (in a heathland), or a mixture of any of these where mixed strata occur (e.g. in a savannah). Grassland ecosystems present a unique challenge to the interpretation of land surface phenology. Unlike woody ecosystems such as forests, temperate grassland canopies typically contain a mix of annual and perennial C_3 and C_4 herbaceous species that can respond dynamically and differentially to seasonal drivers and environmental conditions.

Consequently, the land surface phenology response at any given time will be dictated by three on-ground factors:

a) The biophysical characteristic of each species (i), which is in turn impacted by:

    i. the inherent phenological characteristics of each species (PSi);

    ii. the response of each species to environmental drivers (ERi); and

b) The relative proportion of each species to the community composition ($Prop(i)$).

This can be conceptually represented as:

$$LSP = \Sigma \frac{(PSi+ERi)}{Prop(i)} \quad (5.1)$$

4.1.4.1 Species phenophase

Changes in plant phenophase in temperate environments is most commonly driven by temperature and photoperiod (Crimmins *et al.* 2008). Changes in phenophase will impact the vegetation index in different ways depending on the specific index. However, the typical response is an increasing VI with increased quantity and quality of green vegetation, such as through plant growth and leaf expansion (Asner 1998; Glenn *et al*. 2008). Conversely, decreases in VI will result from leaf loss, decreases in chlorophyll content (or senescence), or obscuring of green vegetation with non-photosynthetic parts, including seed heads, flowers, or standing litter (van Leeuwen and Huete 1996, Nagler *et al.* 2000). Chapter 2 showed that a relative increase in non-photosynthetic (i.e. senesced) vegetation decreased indices that differentially use red and near infra-red fractions of the electromagnetic spectrum, such as NDVI and EVI. The magnitude of VI increase or decrease will also depend on the viewing geometry of the sensor and illumination source (Bhandari *et al.* 2011).

4.1.4.2 Environmental drivers

Environmental drivers refer to any external factor that can alter a phenological signature. This includes weather factors, such as rainfall, temperature and cloud cover. It also includes land management factors such as grazing, mowing or vegetation clearing. These environmental conditions may result in an *actual* change to land surface

phenology; for example, cold temperatures may induce leaf senescence that results in a VI decrease. However, they may also result in an *apparent* change to land surface phenology; for example, grazing removes plant biomass that results in a VI decrease that is not directly a result of plant phenology.

Environmental conditions can induce rapid changes in apparent or actual phenology, and is particularly the case in grasslands. In temperate grassland systems, frosts can induce widespread senescence in *Themeda*-dominated grasslands. Rainfall following a drought will promote the rapid growth of annual grasses and forbs, and high temperatures can result in widespread wilting and/or plant death.

4.1.4.3 Community composition

Changes in land surface phenology signatures may occur through ecological interactions that change community species composition (Figure 4.1). This was observed in Chapter 3, where the invasion of exotic forbs in drought-impacted treatments altered land surface phenology as compared to the control treatments. Different ecosystems have variable species mixtures and different rates of compositional change. Ecosystems with long-lived species, like forests, have a relatively consistent canopy species mix due to the slow turnover of individual plants. Grasslands, on the other hand have a complex mixture of annual and perennial species. Their dynamic nature means that species turnover is fast, with high year-to-year variability in species composition possible from one year to the next (Vivian and Baines 2014). Complexity is added in that, because of their short community stature, all grassland species contribute to land surface phenology. In contrast, a closed forest would only have the canopy tree species contributing to the land surface phenology signature as the understory plants are not visible to the sensor.

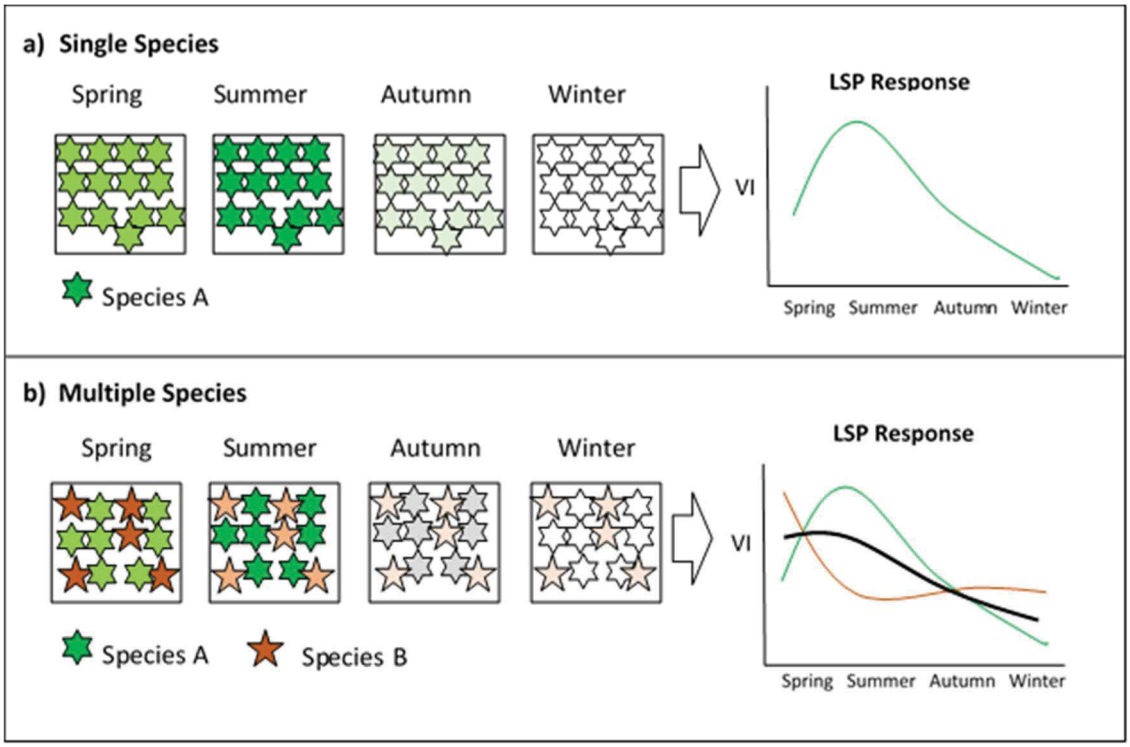

Figure 4.1. Conceptual diagram of land surface phenology where the vegetation is a) comprised of a single species (✸) and b) comprised of multiple species (★and✸) with different phenophase patterns. Darker colours represent higher greenness, with white representing low greenness. The resultant phenology profile is presented on the right: green and red lines represent the profiles for species A and species B, respectively. The black line is the integrated land surface phenology profile of species A and B.

Perennial communities maintain a relatively consistent composition (Ceballos *et al*. 2010), whereas communities dominated by annual species may be very quick to change (Suttle *et al.* 2007). In addition, deciduous communities are more likely to show rapid change than coniferous communities (Hmimina *et al*. 2013; Huete 2012).

4.1.5 Aims

Grassland systems are typified by dynamic and rapid changes in species composition and biophysical characteristics of individual species. Understanding how these elements change throughout the year is essential for planning and conducting grassland surveys for remote sensing validation or ecological monitoring. Likewise, this understanding will be integral in the interpretation of remotely-sensed land surface phenology patterns.

This project aims to:

- identify the species present at each site and determine how temperate grassland species composition changes throughout the year;
- determine any differences in plant functional group dynamics between native- and exotic-dominated grasslands;
- asses how grassland condition changes seasonally, and to identify optimal times for conducting grassland monitoring;
- assess how the phenophase of dominant species changes through the course of the year, and
- identify how seasonal grassland changes are likely to impact land surface phenology estimates.

4.2 MATERIALS AND METHODS

4.2.1 Study region

4.2.1.1 General description and range

The study area is in the South Eastern Highlands region of New South Wales (NSW) and the Australian Capital Territory (ACT), and is approximately bounded by the towns of Bungendore (35.2500° S, 149.4500° E), Gungahlin (35.1831° S, 149.1330° E), and

Bredbo (35.9420° S, 149.2009° E) (Figure 4.2). This region was selected because it has distinct seasonal differences in temperature that promotes phenological variation. Crucially, this region contains several types of native and exotic grasslands within a similar climate envelope.

The predominant land uses in the region are agriculture, specifically native and exotic pasture for meat (sheep and cattle) and wool production. Aside from grassland, natural vegetation types are mostly closed to open *Eucalyptus* woodland with a grassy understory. Development is typically limited to scattered rural centres, with the city of Canberra (population 388,000) representing the only major urban centre. Pre–1788, the majority of this region was expansive grassland and grassy open woodland (Chan 1980) but most of this has been cleared or modified for agriculture and urban development. Regeneration of woody vegetation is naturally limited through parts of the region due to cold winters and frost valleys restricting the establishment of tree seedlings (Wearne and Morgan 2001). As such, it is these naturally treeless areas that have become dominated by grasses. Historical indigenous 'fire-stick' land management, that involved regular burning of grasslands to facilitate the regeneration of wild food plants, also contributed to the sustained grassland in the region (Gammage 2011, Gott *et al.* 2015). In the ACT, relatively large areas of mixed-condition grasslands have been conserved in government reserves, whereas the reserved grasslands in NSW are generally confined to small (< 50 ha) high-quality remnants in areas where livestock grazing is prevented or reduced (Williams and Morgan 2015).

Kangaroos were historically the dominant vertebrate grazer within the region. Although livestock (sheep and cattle) and introduced species (rabbits and goats) are now abundant, kangaroos remain the dominant native vertebrate herbivore and represent the main source of biomass removal in areas ungrazed by livestock. In certain areas, kangaroos can be found at very high densities and occasionally have numbers reduced through culling (ACT Territory & Municipal Services 2010).

Figure 4.2. Map of study region, with approximate boundary in red.

4.2.1.2 Soil and Climate

The climate of this region is characterised by warm summers (December–February) with maximum daily temperatures frequently reaching 35 ºC. Winters (June–August) are cold, with daily minimum winter temperatures frequently below 0 ºC (Figure 4.3). The intermediate seasons of spring and autumn are cooler than coastal areas of south-eastern Australia. Rainfall is relatively consistent throughout the year, with a mean of between 30 mm and 90 mm per month (see Figure 4.4), and an annual average of 650 mm. There is a slight north to south gradient of decreasing average maximum and minimum temperatures, however the patterns of temperature and rainfall are consistent across the study region. Several weather stations were used to capture the most complete data sets of long-term and current climate variables across the study region as individual stations within the region contained data gaps. Note that these mean values are used for overview purposes only and it should be noted that both rainfall and temperature can vary markedly from year to year.

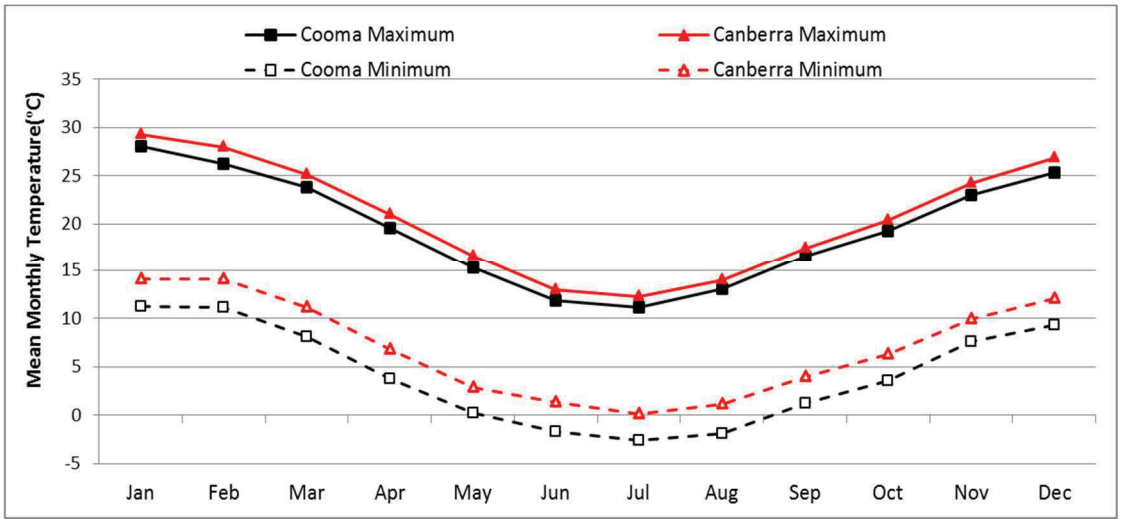

Figure 4.3. Mean monthly minimum temperatures and mean monthly maximum temperatures (ºC) at the northern (Canberra) and southern (Cooma) extent of the study region. Average temperatures are reported by the Australian Bureau of Meteorology (BOM) between 1997 and 2014.

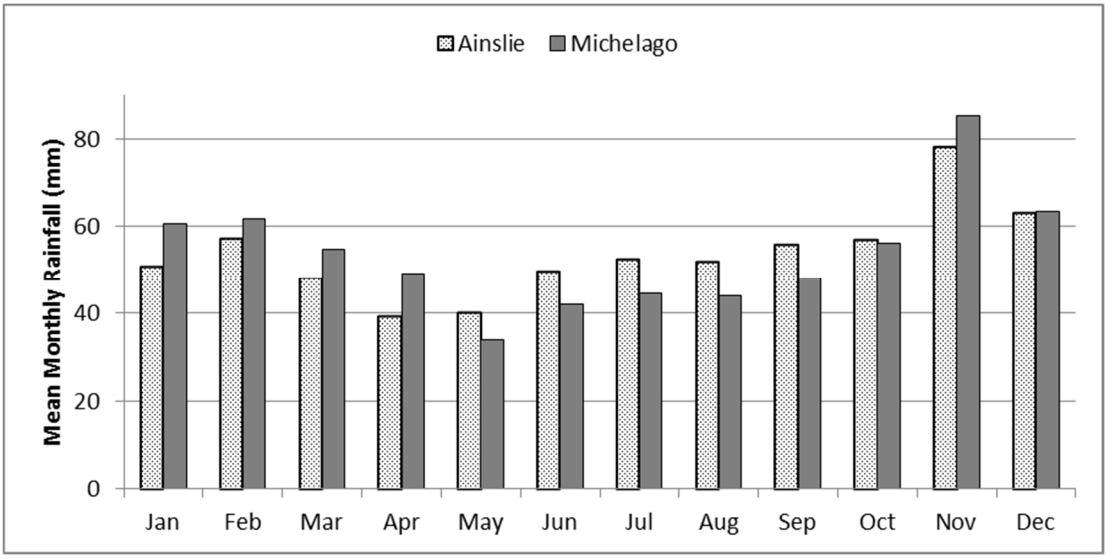

Figure 4.4. Mean monthly rainfall (mm) near the northern (Ainslie) and southern (Michelago) extent of the study region. Average rainfall values are reported by BOM between 1985 and 2014.

The soils of the study region are generally acidic, of low to moderate soil fertility, and are often deficient in key plant nutrients such as phosphorus, sulfur and molybdenum (Clements *et al.* 2003). The topography of the area is that of rolling hills, with flat river valleys and some taller hills (to 2100 m) towards the south of the study region. In general, areas of improved pasture (that is; with a significant exotic component and/or supplemented with fertiliser) are found on the valley floors and floodplains. Native grasslands and grassy woodlands are located on the foothills and hillsides, and denser woodland is found at higher altitude. Few pastures in the region are artificially irrigated.

4.2.1.3 Weather Patterns During Study Period

The study period comprised one year from 1 May 2014 to 30 April 2015. Climate data was gathered from the Australian Bureau of Meteorology (BOM) that has several stations throughout the study region. Rainfall data was gathered from the Canberra National Botanic Gardens weather station with the long-term average taken from 1896–2014. Temperature data was gathered from the Tuggeranong station from 1996 to 2014. These stations contained the most complete rainfall and temperature data from the stations within the study region.

Early 2014 (Australasian summer) consisted of below-average rainfall which limited growth in most grasslands. February to April 2014 was a period of higher than average rainfall; autumn rains following the dry period brought growth to most grassland types, which gives an indication of conditions when the study period began. Figure 4.5 illustrates the rainfall for the study period compared with the long-term average (1968–2014). May 2014 had low rainfall, followed by high rainfall in June. The months July through to November were all slightly below average in rainfall. December and January had high rainfall (~160% of average), whereas February, March and April 2015 were lower (60% of average for Feb and March, < 20% for April). The total rainfall for the study period was 633.8 mm compared with the long-term annual average of 700.7 mm.

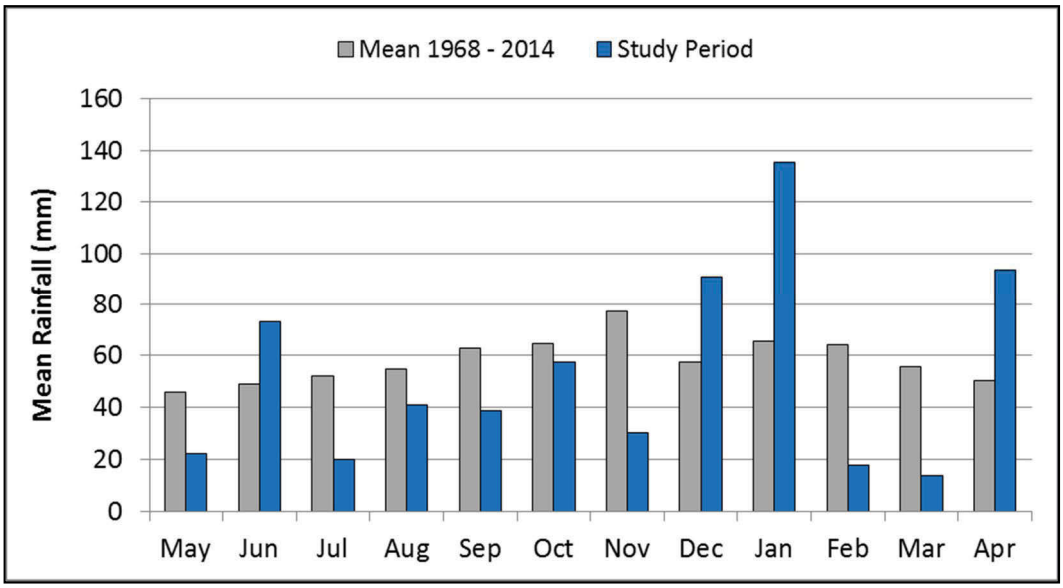

Figure 4.5. Monthly rainfall (mm) at the Australian National Botanic Gardens BOM station for the study period compared with the long-term average (1968-2014).

Monthly temperatures throughout the study period were generally typical, with minor deviations from the average shown in Figure 4.6. Mean maximum temperatures from spring to early summer (September to December) were consistently higher than average. The mean monthly maximum for November 2014 was much hotter (3 degrees) than the long-term average. January and April 2015 mean monthly maximum temperatures were more than 2 degrees cooler than average. Overall, the mean maximum temperate of the study period was 18.9 ºC as compared with the recent average of 20.8 ºC. These conditions led to relatively good seasonal grassland

productivity throughout the study period, with the exception of some sites that saw vegetation wilt and senesce in summer.

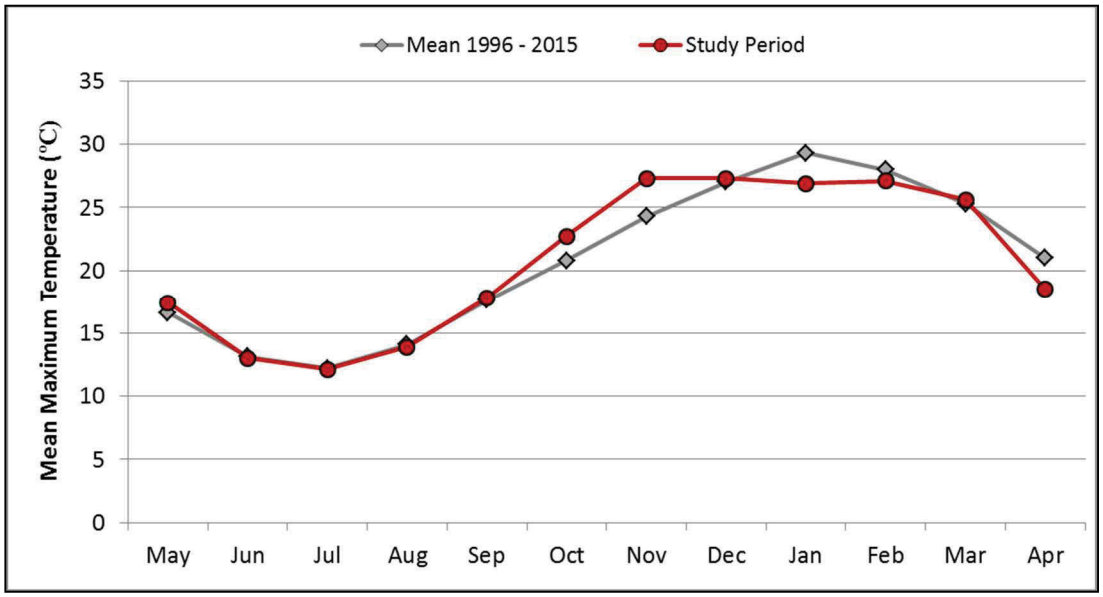

Figure 4.6. Monthly mean maximum temperature (ºC) at the Tuggeranong BOM weather station for study period compared with the recent average (1996–2014).

4.2.2 Study Sites

For this experiment, three replicate areas of four distinct perennial grassland types were selected. To be eligible for selection, sites had to meet a strict set of criteria to ensure the full suite of data could be collected at each location throughout the year. These criteria included:

- relatively homogenous cover of the selected grassland type;
- consistent land management throughout the study period;
- a grassland area greater than 20 hectares, with adequate coverage in all dimensions to incorporate a minimum of one MODIS pixel;
- permission to access the site at all stages of the experiment; and
- being undisturbed by human activities (e.g. vehicles, buildings, roads, etc.)

Sites were grouped based on the C_3/C_4 and native/exotic status of the dominant perennial grass species, with three replicates of each type. Site groups were selected

based on important grassland types in the region, including those that are used for conservation purposes, and others that are used for grazing agriculture. Sites within each category were not required to have the same dominant species *per se*, but rather be dominated by the same functional group (e.g. native C_4 grass). This dominance is designated by the terminology used throughout this part: C_4 Native, C_4 Exotic, C_3 Native and C_3 Exotic. However, it should be acknowledged that these functional groups are not monocultures and all contain some elements of different plant types (e.g. all sites contain some exotic C_3 forbs). In addition, the contribution of different functional groups can change with season and climate.

Locations of each site are shown in Figure 4.7. Sites were selected with the assistance of local experts and were monitored three months prior to the commencement of the experiment to ensure that the site was representative of the required type. This was necessary because grasslands can change in species composition and structure relatively rapidly, and a significant change in these elements may reduce the usefulness of the experimental units. As it was, some sites did show a difference in grass species throughout the study period, but not in sufficient abundances to affect overall outcomes.

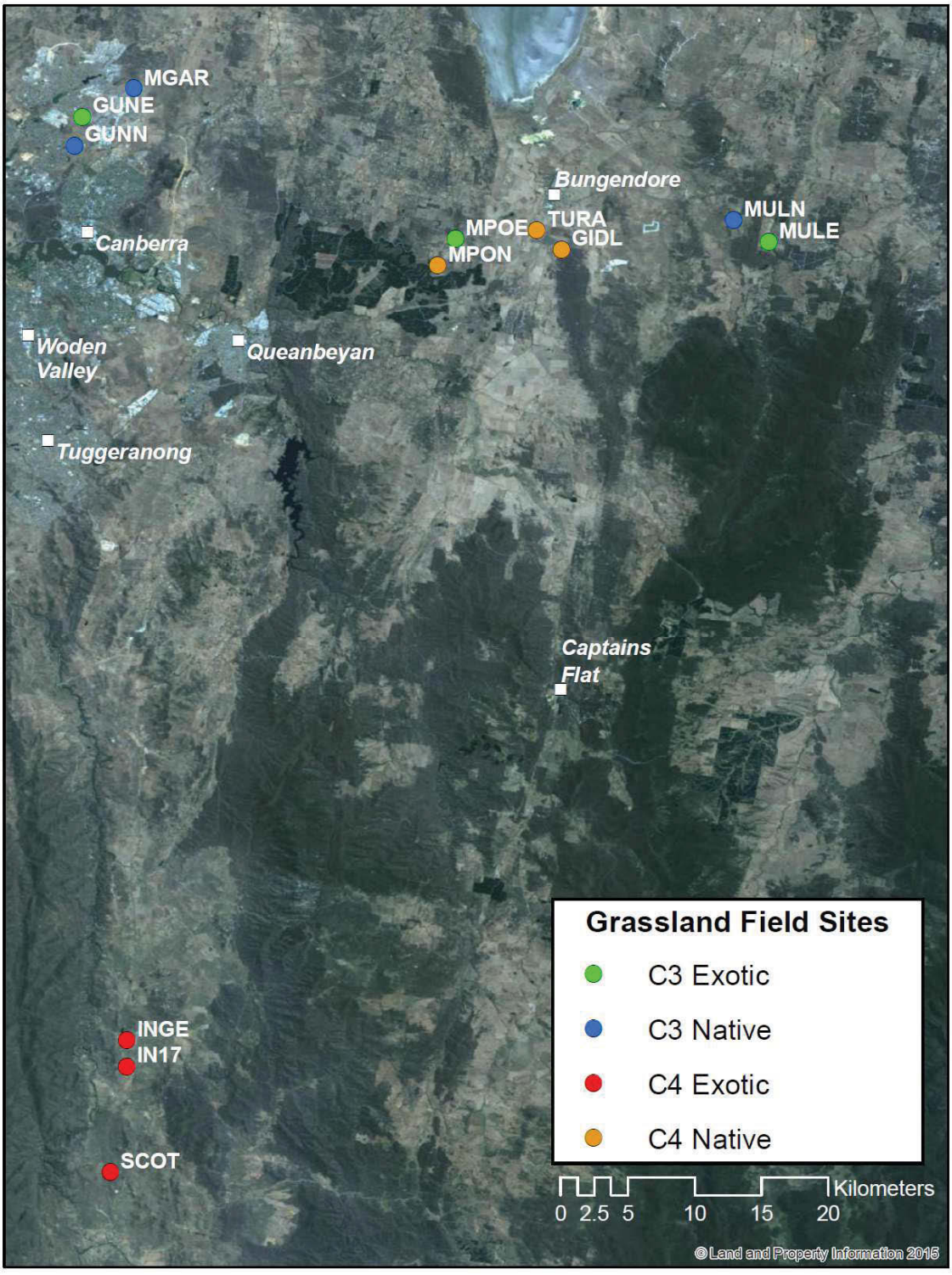

Figure 4.7. Location of temperate grassland field sites.

A summary of each site is provided in Table 4.1, with a fuller description presented in Table 4.2. Photographs of the native-dominated sites are presented as Figure 4.8, with photographs of exotic-dominated sites included as Figure 4.9.

Table 4.1. Summary of temperate grassland field sites.

Field Site Name	Field Site Code	Grass Dominance	C_3/C_4 Dominance
Mullunggari Nature Reserve	MGAR	Native	C_3
Gungaderra Grassland Reserve (native paddock)	GUNN	Native	C_3
Mulloon Creek Natural Farms (native paddock)	MULN	Native	C_3
Gidleigh Travelling Stock Reserve	GIDL	Native	C_4
Turallo Nature Reserve	TURA	Native	C_4
Millpost Farm (native paddock)	MPON	Native	C_4
Mulloon Creek Natural Farms (exotic paddock)	MULE	Exotic	C_3
Gungaderra Grassland Reserve (exotic paddock)	GUNE	Exotic	C_3
Millpost Farm (exotic paddock)	MPOE	Exotic	C_3
Scottsdale Bush Heritage Reserve	SCOT	Exotic	C_4
Ingelara Farm	INGE	Exotic	C_4
Ingelara Paddock 17	IN17	Exotic	C_4

At each site, the following activities were conducted:

- permanent installation of at least one time-lapse phenology camera with sub-daily image capture;
- monthly floristic surveys at three 20 x 20 m locations;
- monthly harvesting of aboveground biomass in six 1 x 1 m quadrats;
- monthly assessment of pasture height at 20 locations; and
- monthly measurement of fractional cover (percent green vegetation, brown vegetation and bare soil) at 100 step-point locations.

Figure 4.8. Photographs of native-dominated temperate grassland field sites: (a) Turallo Nature Reserve, (b) Gidleigh Travelling Stock Reserve, (c) Millpost Farm (native paddock), (d) Gungaderra Grassland Reserve (native paddock), (e) Mullunggari Nature Reserve, (f) Mulloon Creek Natural Farms (native paddock). Photographs were taken in January–February 2015.

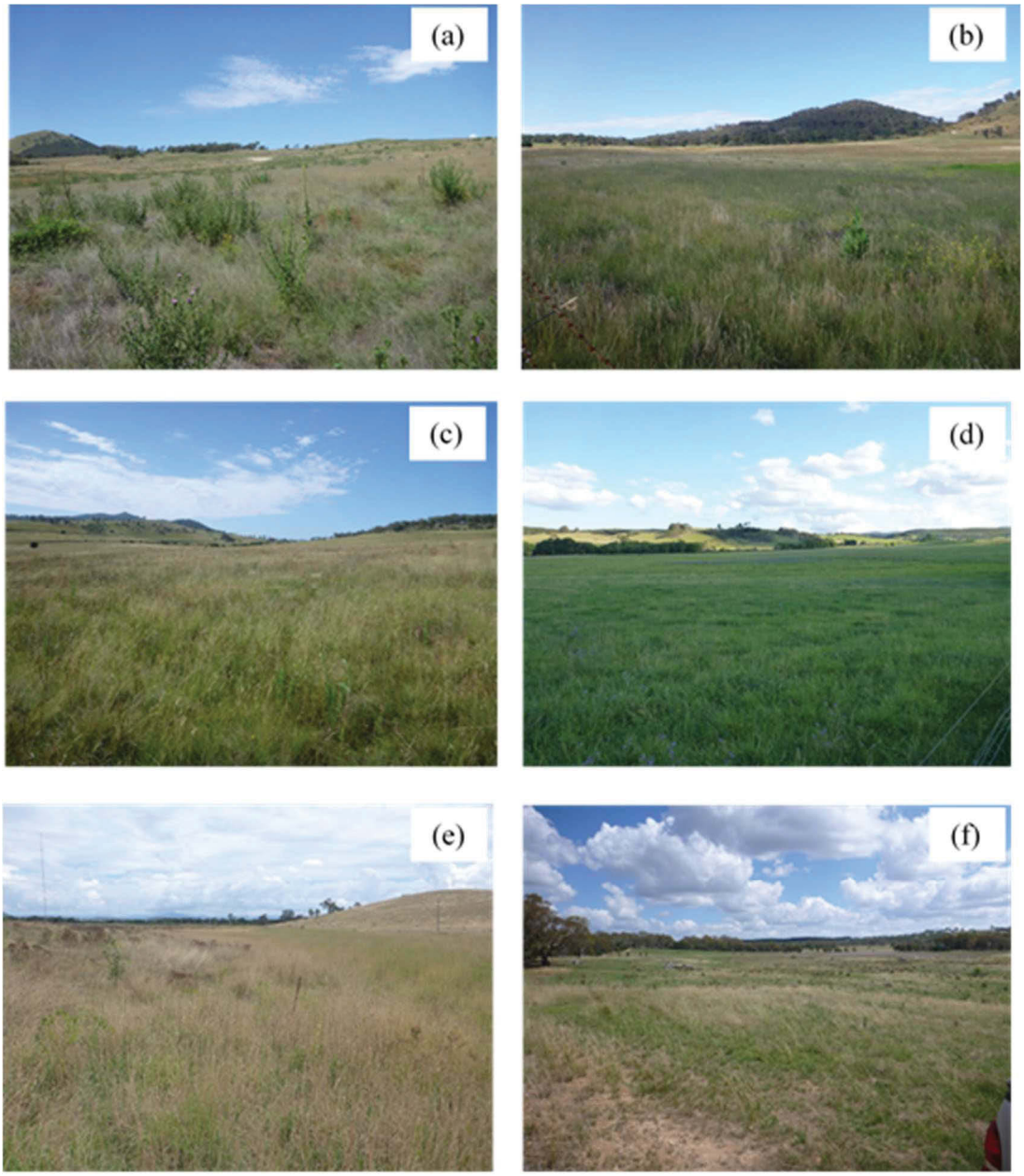

Figure 4.9. Photographs of exotic-dominated temperate grassland field sites: (a) Scottsdale Bush Heritage Reserve, (b) Ingelara Farm, (c) Ingelara Paddock 17, (d) Mulloon Creek Natural Farms (exotic paddock), (e) Gungaderra Grassland Reserve (exotic paddock), (f) Millpost Farm (exotic paddock). Photographs were taken in January–February 2015.

Table 4.2. Description of field sites. Shaded cells represent C_4-dominated sites; white cells represent C_3-dominated sites.

Site name	Code	Location (Dec.Degrees)	C_3/C_4	Dominance	Grazing pressure	Dominant genera	Nearest town	Area	Floristic Composition	Tenure
Mullunggari Nature Reserve	MGAR	-35.17377, 149.15075	C_3	Native	Moderate (kangaroos)	*Rytidosperma, Austrostipa*	Gungahlin	48 ha	Native/exotic forbs and grasses	Nature Reserve
Gungaderra Grassland Reserve (native paddock)	GUNN	-35.20961, 149.13885	C_3	Native	Moderate (kangaroos)	*Rytidosperma, Austrostipa*	Gungahlin	35 ha	Native and exotic forbs (particularly *Hypochaeris*); mostly native grasses	Nature Reserve
Mulloon Creek Natural Farms (native paddock)	MULN	-35.27538, 149.57024	C_3	Native	Light (cattle)	*Rytidosperma, Austrostipa*	Bungendore	24.1 ha	Very diverse mix of native and exotic forbs and grasses	Private Land

Site name	Code	Location (Dec.Degrees)	C_3/C_4	Dominance	Grazing pressure	Dominant genera	Nearest town	Area	Floristic Composition	Tenure
Gidleigh Travelling Stock Reserve	GIDL	-35.29711, 149.45078	C_4	Native	Light (horses, sheep)	*Themeda*	Bungendore	15.5 ha	Very diverse in native forbs; few exotics	Travelling Stock Reserve
Turallo Nature Reserve	TURA	-35.2983, 149.47868	C_4	Native	Light (sheep)	*Themeda*	Bungendore	23.4 ha	Very diverse in native forbs	Nature Reserve
Millpost Farm (native paddock)	MPON	-35.29873, 149.36943	C_4	Native	Heavy (sheep)	*Themeda*	Bungendore	17.5 ha	Extremely diverse in native forbs; few exotics	Private Land

Site name	Code	Location (Dec.Degrees)	C_3/C_4	Dominance	Grazing pressure	Dominant genera	Nearest town	Area	Floristic Composition	Tenure
Mulloon Creek Natural Farms (exotic paddock)	MULE	-35.27643, 149.59981	C_3	Exotic	Heavy (cattle)	*Phalaris, Festuca, Dactylis*	Bungendore	26.3 ha	Exotic pasture grasses with some exotic legumes.	Private Land
Gungaderra Grassland Reserve (exotic paddock)	GUNE	-35.20252, 149.10452	C_3	Exotic	Light (kangaroos, wallabies)	*Phalaris*	Gungahlin	25 ha	Exotic pasture grasses and sedges	Nature Reserve
Millpost Farm (exotic paddock)	MPOE	-35.3126, 149.33973	C_3	Exotic	Heavy (sheep, rabbits)	*Festuca, Dactylis, Phalaris*	Bungendore	12.4 ha	Mostly exotic grass/legumes with some native grass species	Private Land

Site name	Code	Location (Dec.Degrees)	C_3/C_4	Dominance	Grazing pressure	Dominant genera	Nearest town	Area	Floristic Composition	Tenure
Scottsdale Bush Heritage Reserve	SCOT	-35.90046, 149.1482	C_4	Exotic	Light (kangaroos)	*Eragrostis*	Bredbo	46 ha	Exotic grass, scattered exotic annual forbs with some small areas of native forbs	Nature Reserve
Ingelara Farm	INGE	-35.82609, 149.15601	C_4	Exotic	Heavy (cattle)	*Eragrostis*	Bredbo	14.3 ha	Exotic perennial grass with annual exotic forbs and grasses	Private Land
Ingelara Paddock 17	IN17	-35.84286, 149.13597	C_4	Exotic	Moderate (cattle/ kangaroos)	*Eragrostis*	Bredbo	26.6 ha	Exotic perennial grass with annual exotic forbs and grasses	Private Land

.

4.2.3 Floristic surveys

A monthly survey of the floristic composition of each site was conducted between May 2014 and April 2015. The survey was conducted in accordance with a method commonly used in vegetation surveys in NSW and adapted for temperate grassland ecosystems (Rehwinkel 2007, Hnatuik *et al.* 2009, Department of Environment Climate Change & Water 2011). This method involved surveying a square 20 x 20 m plot for all vascular plants. Three replicates of 20 x 20 m plots were surveyed per site per month. The location of these plots was fixed throughout the study period.

The cover and abundance of each species was scored based on a modified Braun-Blanquet scale (Poore 1955, Rehwinkel 2007). This 7-point scale attributes a value to each species based on the combined abundance (number of individuals) and percentage cover class (refer to Table 4.3). For quantification of vegetative cover, Braun-Blanquet values were transformed into per cent cover for different functional group categories (e.g. native forbs, exotic grasses, etc.) (McNellie *et al.* 2017). While this type of transformation has acknowledged limitations, it allows useful grouping of the data on a numerical scale and avoids difficulties associated with the analysis of ordinal data (Ricotta and Feoli 2013).

Table 4.3. Modified Braun-Blanquet Scale used for floristic surveys.

Braun-Blanquet Score	**Cover/Abundance Criteria**	**Transformed Cover** (after McNellie *et al.* 2016)
r	< 5% cover and solitary (< 4 individuals)	0.05%
+	< 5% cover and few (4-15 individuals)	0.05%
1	< 5% cover and numerous (> 15 individuals)	0.5%
2	5% – < 25% cover	15%
3	25% – < 50% cover	38%
4	50% – < 75% cover	63%
5	75% or greater cover	88%

Species were categorised into one of two functional forms: graminoids (including grasses, sedges and rushes), and forbs (herbaceous non-graminoids). As grasses were the dominant graminoid, the term 'grass' is used generically for graminoids within this chapter. Species were identified as native or exotic, following PlantNET (Royal Botanic Gardens and Domain Trust 2016). Any species that could not be accurately classified as native or exotic was classified as 'unknown' and excluded from that component of the analysis. Senesced or dead plants were included in the census if they were able to be identified. However many grassland species die back to belowground parts, and cannot be identified during floristic surveys.

No native woody shrubs were found within the sampling zones, and trees were excluded from the sampling protocol. One species of fern, *Cheilanthes austrotenuifolia*, was included in the 'forbs' group for simplicity, as was the exotic species *Hypericum perforatum* (St John's wort), which is nominally a shrub. Species and common names are consistent with the Australian Plant Name Index (www.anbg.gob.au/apni).

4.2.4 Grassland condition assessment

Grassland condition was assessed using the Floristic Value Score (FVS) method (Rehwinkel 2007, 2014). The FVS has been developed and tested by temperate grassland experts in New South Wales and is widely used by government agencies and private consultants to assess temperate grassland condition in the South Eastern Highlands bioregion of NSW (Hodgkinson 2014, Vivian and Baines 2014, Department of the Environment 2016).

The FVS is a weighted score that relates each recorded flora species to a known sensitivity status. Species that are known to be of low sensitivity (i.e. are regionally common and increase under disturbance) are weighted lower. Species that are known to be of high sensitivity (i.e. native species that are regionally rare and are known to decrease under disturbance) are weighted higher. The cover/abundance of individual species also impacts the FVS, with higher cover/abundance scores contributing a higher

weighting. As different species are apparent throughout the year, the FVS can change accordingly.

By prescribing threshold values, the FVS can be used to place grassland sites into condition classes. Following the classes prescribed in the method, a FVS below 5.0 represents low condition; between 5.0 and 6.5 represents medium condition; and above 6.5 represents high condition (Rehwinkel 2014). However, this method assumes surveys are conducted at the optimum time of year. As this is not always practical, the Australian Commonwealth legislation for Natural Temperate Grasslands of the South Eastern Highlands varies the condition threshold values based on the time of year of sampling (Department of Environment 2016). These values are presented in Table 4.4, and are used within this chapter. We designated 'favourable sampling time' to be from December to February, and 'other sampling time' to be the remainder of the year.

Table 4.4. Condition classes based on Floristic Value Score and time of year in which survey was undertaken (Department of Environment 2016).

	Floristic Value Score	
	Favourable sampling time (December–February)	Other sampling times (March–November)
Low	0–4.99	0–2.99
Moderate to High	5–6.49	3–6.49
High to Very High	6.5 +	6.5 +

The mean FVS and species richness from the three plots per site is used in analysis and calculations.

4.2.5 Phenophase of dominant species

Phenophase refers to the state of growth and development of a plant and is typically used to describe stages of leaf growth, flowering and fruiting (Menzel *et al.* 2006). At each survey location, a phenophase category was assigned to each dominant species

(refer to Table 4.5). Dominant species were defined as those that had a Braun-Blanquet score of 2 or more (5%–25% cover or higher) at 2 or more consecutive months throughout the year. Only dominant species were selected for this analysis as less dominant species (< 5% cover) occupy a small proportion of the site area and are unlikely to significantly impact overall land surface phenology.

While it is acknowledged that phenophase is often variable in natural systems, each phenophase category was attributed based on the dominant phenophase at the survey time.

Table 4.5. A description of the phenophase characteristics used for grassland monitoring.

Phenophase	Symbol	Description
Vegetative	V	Photosynthetic leaves present, some non-photosynthetic leaves may be present. No flowering or fruiting structures present.
Flowering	Fl	Flowering structures present; anthers evident.
Fruiting	Fr	Flowering structures absent; fruits evident.
Post-fruiting	P	Flowering and fruiting structures senesced but retained on the plant. Photosynthetic leaves present.
Senescent	S	All vegetation is non-photosynthetic.
Absent	X	Species is not recorded

4.3 RESULTS

4.3.1 Annual species richness

A total of 192 species were recorded across all sites throughout the sampling period. Of these, 90 species (46.9%) were native and 90 species (46.9%) were exotic. Twelve species (6.2%) were unable to be identified to species level and their native/exotic status could not be determined. The native-dominated sites had a total of 159 species recorded (82 native, 68 exotic and 9 unknown), whereas the exotic-dominated sites recorded 115 species (40 native, 70 exotic and 5 unknown). A total of 59 grass species and 133 forb species were recorded across all sites. Table 4.6 shows the species richness recorded by plant functional type (i.e. grass/forbs and native/exotic). Figure 4.10

illustrates the total number of native, exotic and unknown species. Figure 4.11 illustrates the total number of species recorded at all sites, separated by functional group. A full list of species recorded at each site is presented in Appendix C.

Table 4.6. Total number of flora species identified at native-dominated, exotic-dominated and all sites.

	Total species	Native species	Exotic species	Unknown species	Grasses	Forbs	Native Grasses	Exotic Grasses	Native Forbs	Exotic Forbs
Native-dominated sites	159	82	68	9	53	106	28	20	54	48
Exotic-dominated sites	115	40	70	5	29	86	9	17	31	53
All sites	192	90	90	12	59	133	30	22	60	68

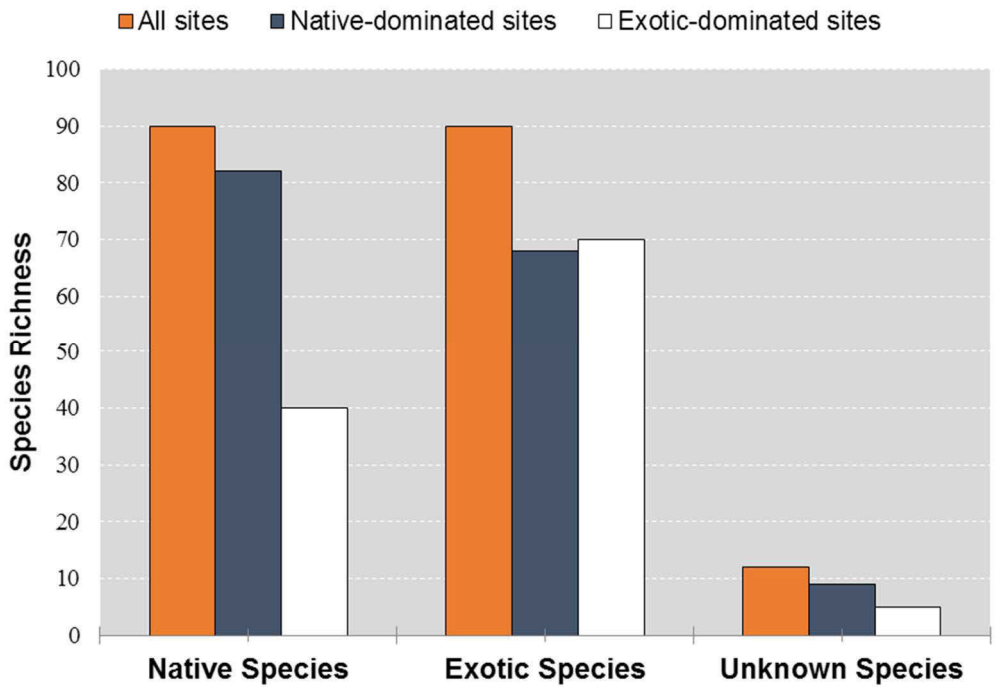

Figure 4.10. Total number of native, exotic, and unknown flora species recorded at temperate grassland sites. Data is grouped by: all sites (orange bars) native-dominated sites (dark bars) and exotic-dominated sites (white bars).

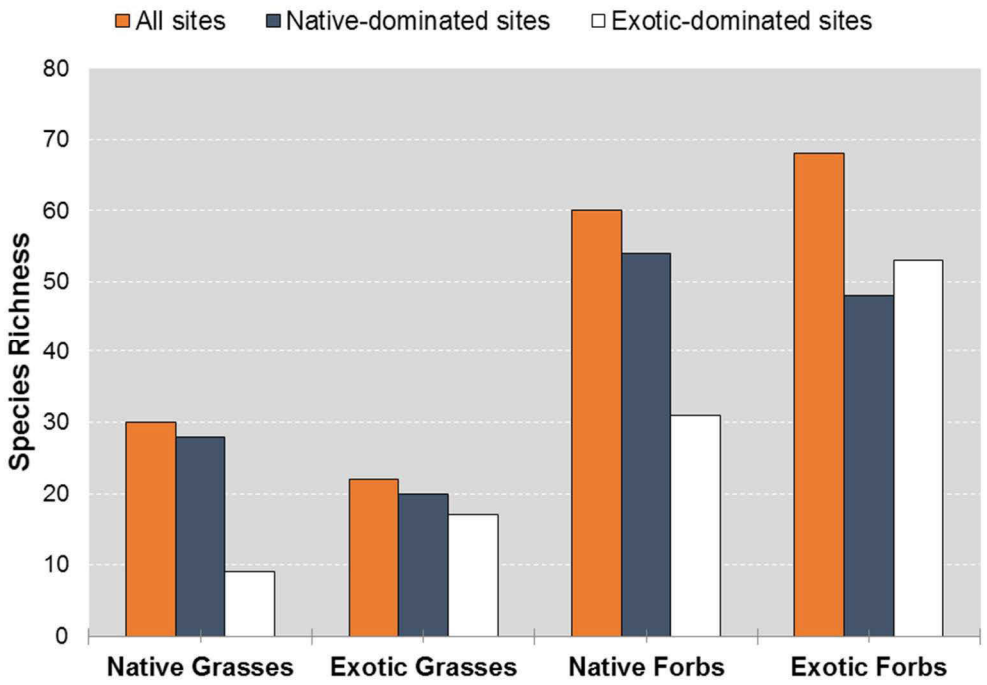

Figure 4.11. Total number of flora species recorded at temperate grassland sites in four functional groups: native grasses, exotic grasses, native forbs and exotic forbs. Data is grouped by: all sites (orange bars) native-dominated sites (dark bars) and exotic-dominated sites (white bars).

Native-dominated sites had a higher annual species richness (mean = 68.3) than exotic sites (mean = 40.5), with higher numbers of native forbs and native grass species. Exotic-dominated sites had similar numbers of exotic forbs and grasses as the native-dominated sites, however had low richness of native forbs and grasses.

The native-dominated C_4 grasslands MULN and TURA had the highest annual species richness with 99 and 73 species, respectively. The exotic-dominated C_3 grasslands MULE and GUNE had the lowest species richness, with 18 and 21 species, respectively. Annual species richness for each site is presented in Table 4.7.

Table 4.7. Annual species richness by plant functional group at each site.

Site	Total	Native	Exotic	Unknown	Grasses	Forbs	Native Grasses	Exotic Grasses	Native Forbs	Exotic Forbs
MGAR	64	34	28	2	22	42	12	8	19	20
GUNN	44	13	29	2	15	29	4	10	9	19
MULN	99	49	46	4	36	63	19	14	30	32
GIDL	59	38	19	2	18	41	10	7	28	12
TURA	73	47	25	1	25	48	15	10	27	15
MPON	71	46	24	1	15	56	10	5	30	19
Native Average	**68.3**	**37.8**	**28.5**	**2.0**	**21.8**	**46.5**	**11.7**	**9.0**	**23.8**	**19.5**
MULE	18	0	18	0	4	14	0	4	0	14
GUNE	21	7	12	2	10	11	1	7	6	5
MPOE	39	13	24	2	20	19	7	12	6	12
SCOT	56	18	37	1	8	48	3	5	15	32
INGE	53	10	41	2	15	38	3	11	7	30
IN17	56	14	38	4	11	45	2	7	12	31
Exotic Average	**40.5**	**10.3**	**28.3**	**1.8**	**11.3**	**29.2**	**2.7**	**7.7**	**7.7**	**20.7**

4.3.1.1 Exotic versus native species richness

Native-dominated sites contained the highest species richness of native grass and forb species. However some native-dominated sites were surprisingly low in native species, such as GUNN, with only 13 native species recorded throughout the year.

Exotic-dominated sites had a higher proportion of exotic species than native-dominated sites. They did not always have the highest exotic species richness as many exotic sites were dominated by only a few species.

4.3.2 Seasonal changes in species richness

Average species richness per month is presented in Figure 4.12. Species richness changed throughout the year as different species progressed through their life cycle and responded to ecological pressures. The highest average species richness across all sites was in January with over 31 species recorded per site. The winter months all recorded an average of less than 20 species per site. Native-dominated sites recorded higher species richness than exotic-dominated sites. The average species richness in native dominated sites remained consistently above 35 between October and February. In contrast, the shape of the curve of exotic-dominated sites showed a more distinct peak in species richness. This occurred in January, when average richness reached 26.

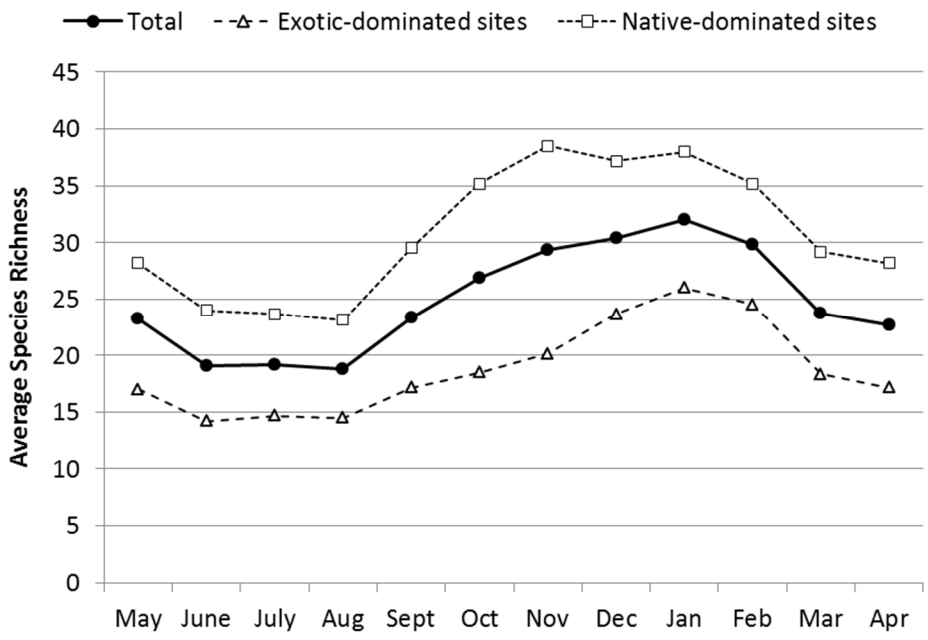

Figure 4.12. Average species richness by month, as measured at all sites, native-dominated sites, and exotic-dominated sites.

Figure 4.13 illustrates the proportion of species at each site detected in each month, relative to each site's annual total. As an example, a site that records 10 species throughout the year but only 5 species in June will have a detection frequency of 50% for that month. Given the variety of species richness throughout the different field sites, this method provides a standardised measure of relative species richness. This is of particular usefulness as it can direct sampling effort to seasons of optimum efficiency,

i.e. when detection frequency is highest. January was the month with the highest detection frequency for both native-dominated and exotic-dominated sites. During January, an average of 65% of species was detected at exotic-dominated sites, whereas an average of 55% of species was detected at native-dominated sites. A consistently low proportion of species (< 40%) was detected in the winter months (June to August) at all sites.

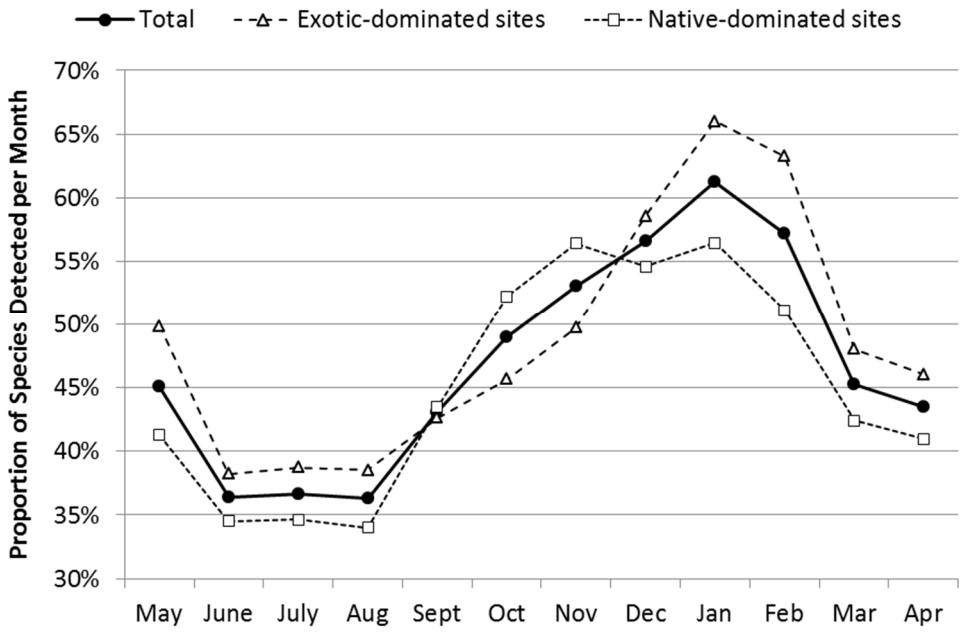

Figure 4.13. Average proportion of species detected per month. This value is represented as the average proportion of the annual species richness for each site.

4.3.3 Seasonal changes by functional group: richness, detection frequency and cover

Separating data into functional groups provides further resolution in elucidating ecological changes throughout the year. This is conducted by examining the changes in species richness, species detection frequency, and vegetative cover over time. Figure 4.14 presents the patterns of average species richness for each month. Figure 4.15 presents the annual patterns of average detection (as explained in Section 4.3.2). Figure 4.16 presents the annual patterns of average vegetative cover, as calculated by summing the transformed Braun-Blanquet scores for each functional group. In each

group of figures, data is separated into native-dominated sites and exotic-dominated sites.

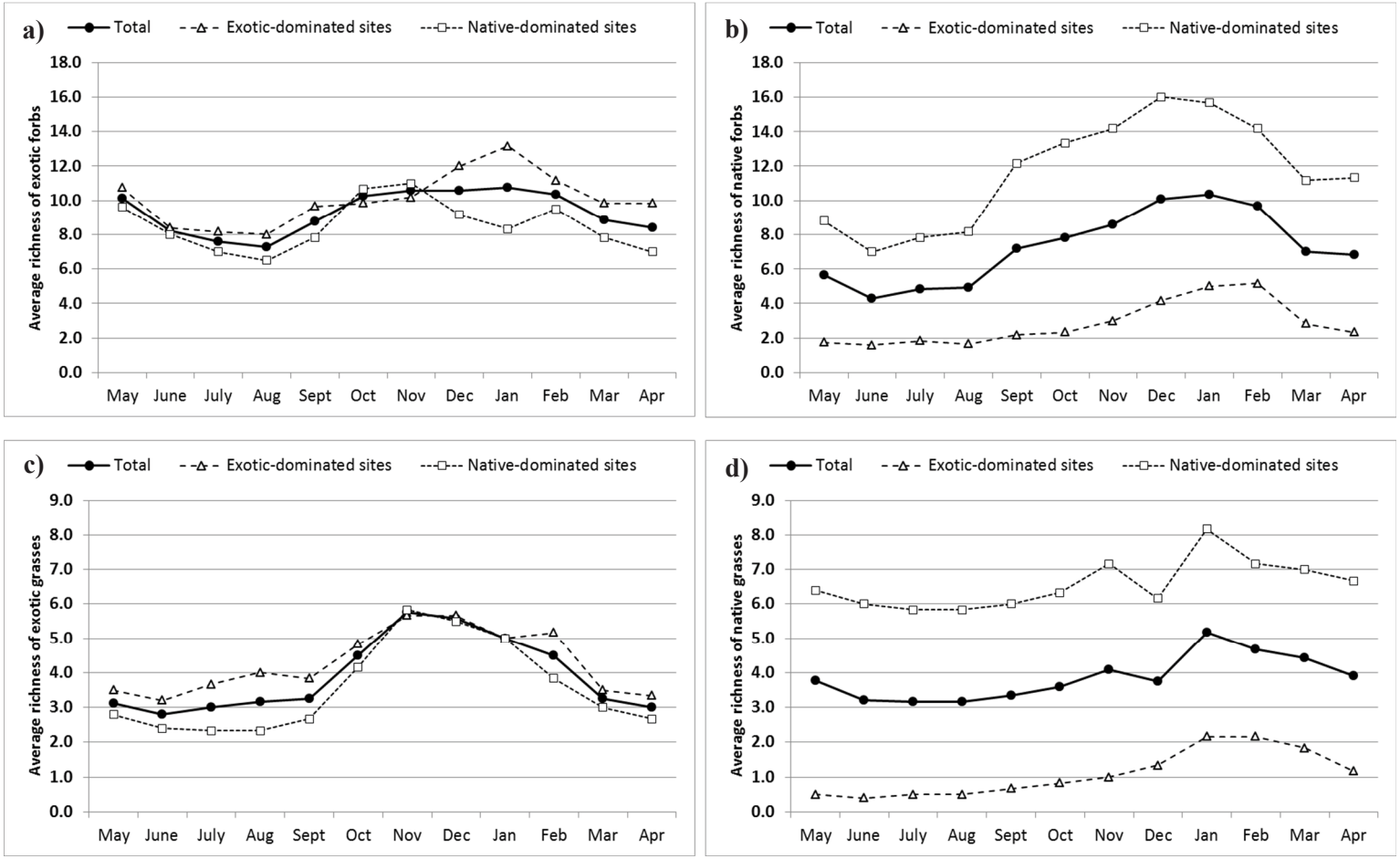

Figure 4.14. Time-series from May 2014–April 2015 of average species richness by functional group: a) exotic forbs, b) native forbs, c) exotic grasses, d) native grasses.

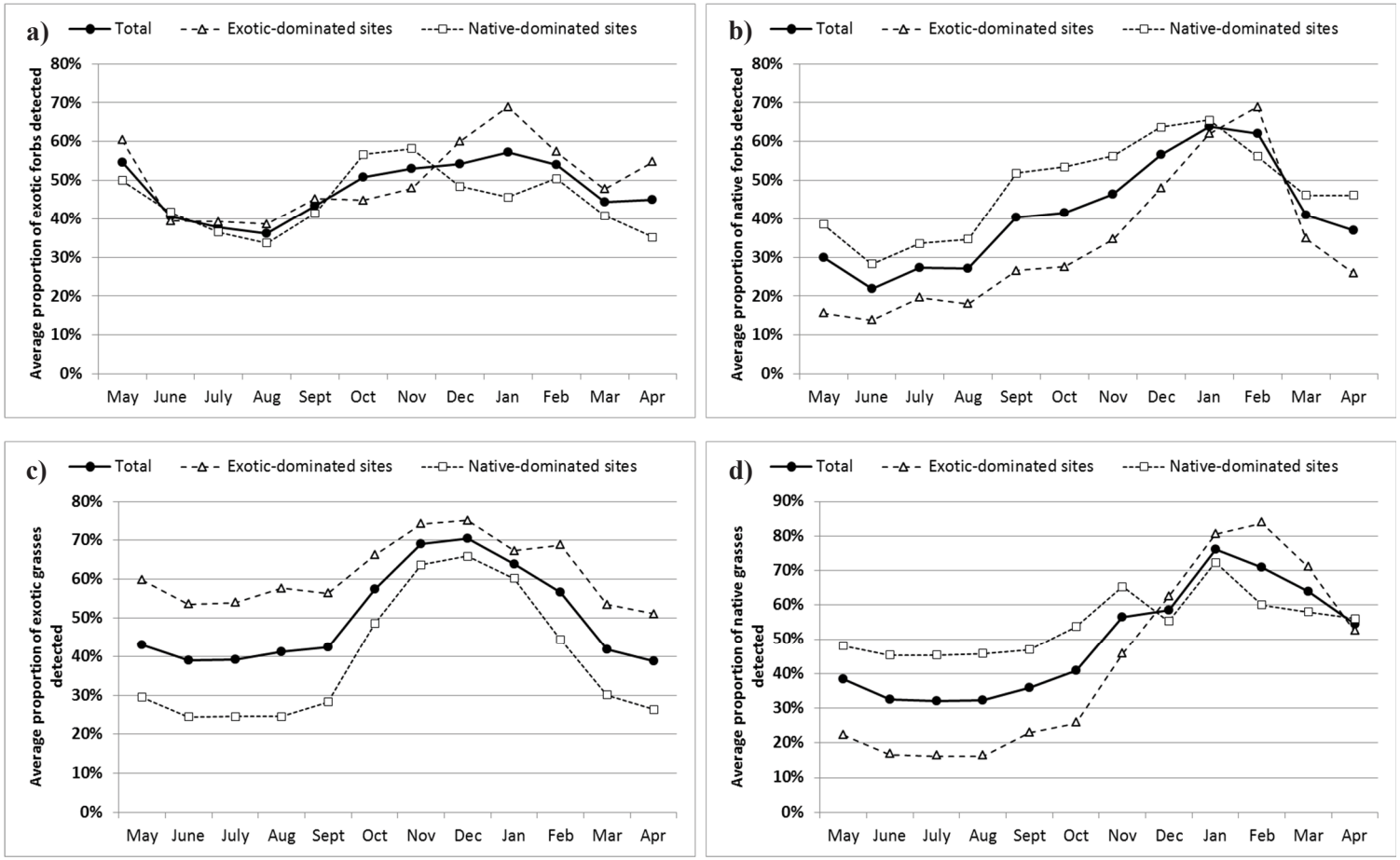

Figure 4.15. Time-series from May 2014–April 2015 of average proportion of species detected per month for each functional group; a) exotic forbs, b) native forbs, c) exotic grasses, d) native grasses.

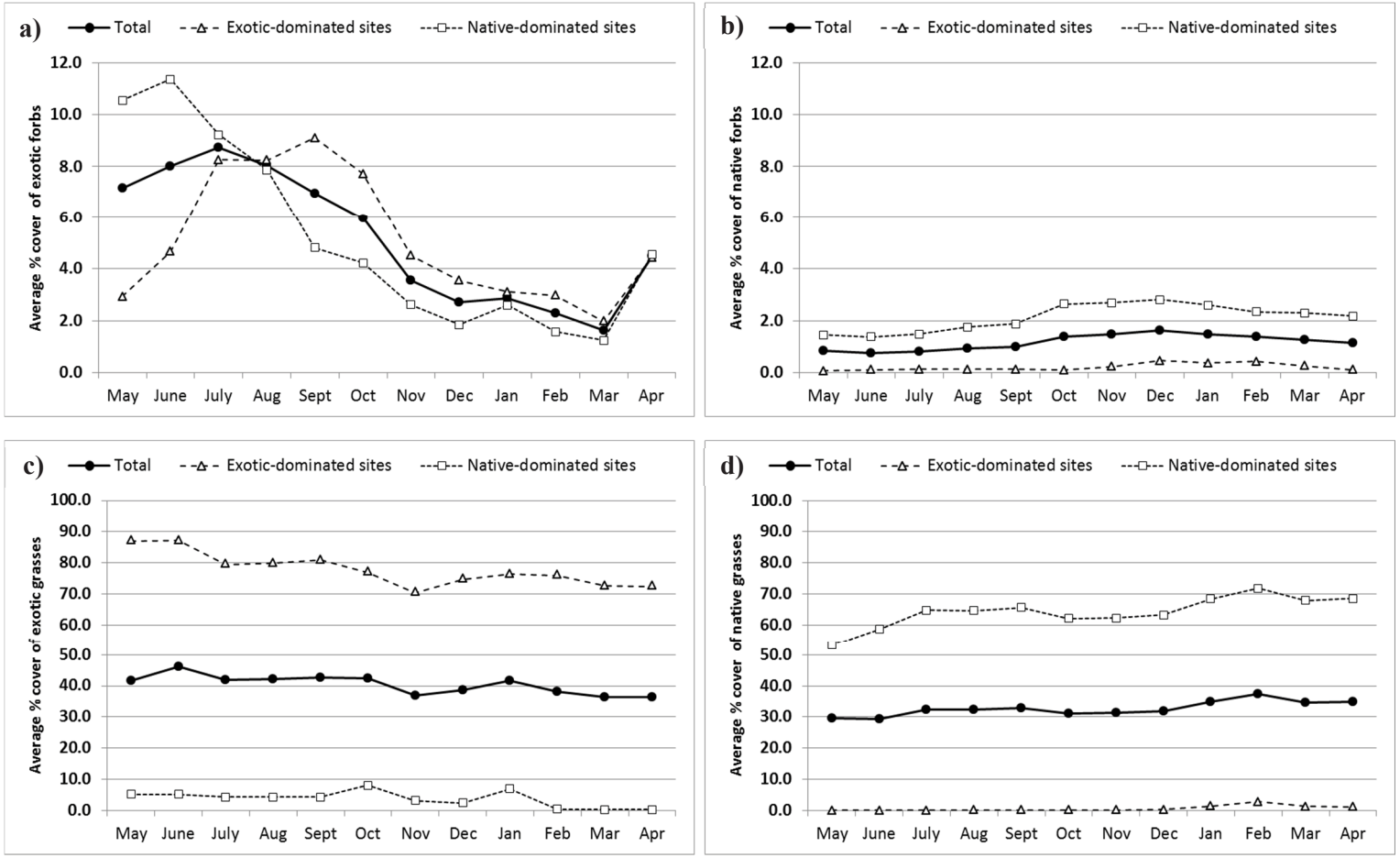

Figure 4.16. Time-series from May 2014–April 2015 of average proportion of vegetative cover for each functional group; a) exotic forbs, b) native forbs, c) exotic grasses, d) native grasses.

4.3.3.1 Native forbs

Native forbs require specific attention, as they are often used as direct indicators of grassland condition. They also represent the most potential for change in species richness, as forbs are less likely to retain aboveground senescent material as grasses or exotic forbs regularly do—hence are likely not to be recorded outside of peak times. Over all sites, native forbs have the highest average species richness in January. However, native-dominated sites showed a different pattern to exotic-dominated sites. At native-dominated sites, species richness of native forbs peaked in December, whereas at exotic-dominated sites the native forb species richness peaked in February.

For native-dominated sites, the highest proportion of native forbs present was in January, when an average of 61% of native forbs was detected. In exotic-dominated sites, the highest proportion of native forbs was detected in February (69%). Native forbs were least likely to be detected through the cooler months (May to August), with only 22%–30% of native forbs being observed during this time.
Average native forb cover was consistently low throughout the year, below 3%. At exotic-dominated sites, average native forb cover was very low and peaked in December (0.5%). This was slightly higher for native-dominated sites (2.8%), which also peaked in December.

4.3.3.2 Exotic forbs

Exotic forb richness was relatively consistent throughout the year, with an average between 7 and 11 species. Many common exotic forbs retain seed heads and other dead material aboveground throughout the year, hence are consistently present in the species count. At exotic-dominated sites, exotic forb species richness peaked in January. In native-dominated sites, the peak was earlier in November, and showed a lower species richness. This pattern was consistent with proportion of exotic forbs detected throughout the year which also peaked in November for native-dominated sites (58%) and in January for exotic-dominated sites (69%).

Exotic forb cover was highly variable throughout the year, with the average for all sites ranging between 1.6% and 8.7%. Native-dominated sites showed high exotic forb cover in the cooler months, peaking in June at 11.4%. Exotic forb cover was lower in warmer months (December–March), being consistently below 3%. Exotic forb cover in exotic-dominated sites peaked in September (9.1%).

4.3.3.3 Native grasses

Native grass richness followed a similar seasonal pattern for native- and exotic-dominated sites, with low richness in winter and reaching a maximum in January. However, native-dominated sites had a much greater richness (average maximum of 8.2 species at peak time) than exotic-dominated sites (average maximum of 2.2 species at peak time).

Detection frequency was quite high during peak times, with over 70% of native grasses detected in January for both native- and exotic-dominated sites. This was slightly lower in winter for native-dominated sites (approximately 45% throughout), but was very low in winter for exotic-dominated sites, where less than 20% of native grasses were found.

Cover of native grasses was consistently high in native-dominated sites, with an average of between 53.3% and 71.8% throughout the year. However, exotic-dominated sites had an extremely low cover of native grasses, with a maximum average cover of 2.8% (February).

4.3.3.4 Exotic grasses

The pattern of average richness of exotic grasses is similar for native- and exotic-dominated sites, peaking in November (average 5.8 species). Seasonal patterns of detection frequency are also similar, with highest detectability in November and December. However, native-dominated sites are markedly lower, particularly in winter.

Cover of exotic grasses at exotic-dominated sites was extremely high, ranging between 70% and 90% at all times throughout the year. Native-dominated sites, however, had a low cover of exotic grasses, with two minor peaks in October (8%) and January (7%).

4.3.4 Seasonal changes in grassland condition

Grassland condition is represented by the Floristic Value Score (FVS). Figure 4.17 illustrates the mean annual FVS for each site. The native-dominated C_4 sites had the highest FVS (range: 22.6–25.1). Two out of the three native-dominated C_3 sites had an average FVS of more than 5 (7.6 and 11.4). All the exotic-dominated grassland sites had average FVS of below 5.

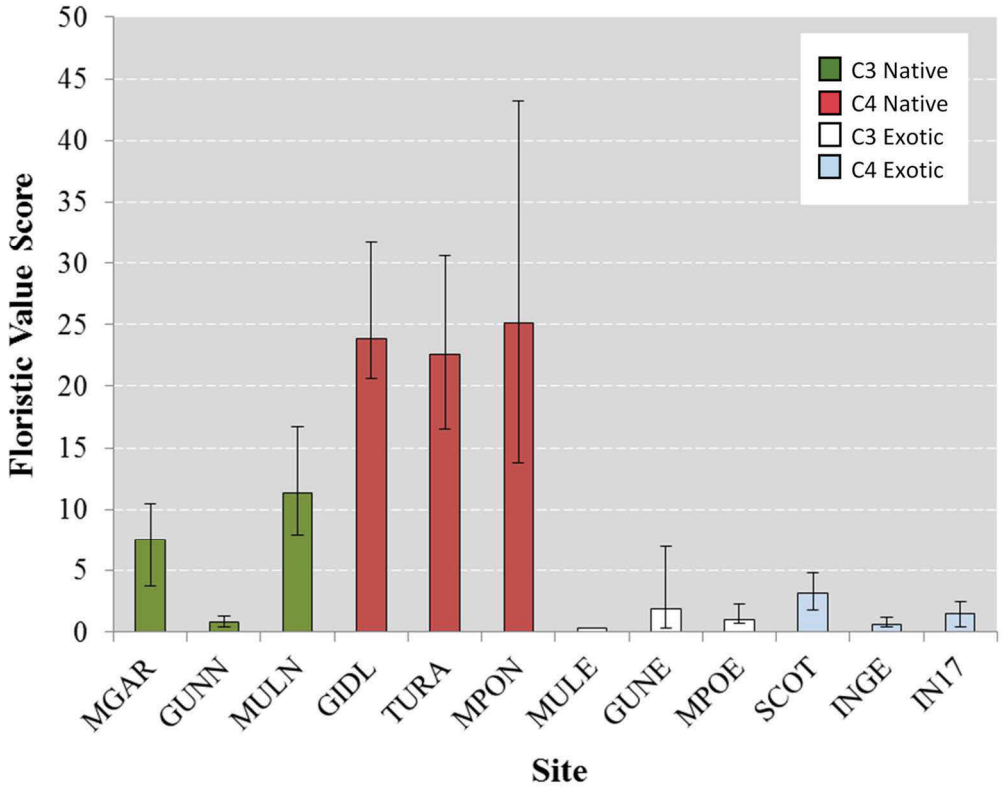

Figure 4.17. Mean annual Floristic Value Score for each site. Sites are grouped by functional type: C_3 native-dominated, C_4 native-dominated, C_3 exotic-dominated and C_4 exotic-dominated. Error bars represent the range of monthly values for each site.

The monthly FVS data for each site is shown in Table 4.8 and the score for each season is annotated to condition class in accordance with the thresholds in Table 4.4. With the exception of site MPON, all sites had their highest monthly FVS in the summer months of December, January or February. All native-dominated C_4 grasslands were classed as 'high condition' in all months. Two of the three native-dominated C_3 grasslands had an average FVS that placed them in the 'high condition' category but one of these (MULN) had lower scores in June and August that placed it as 'moderate condition' for these surveys. The third site (GUNN) was classed as 'low condition' for all months. All exotic-dominated sites had an average FVS that classed them as 'low condition' for most of the year. However, one exotic site recorded 'moderate condition' scores from June to August and another recorded a 'high condition' score in December.

Overall, 9 out of the 12 sites retained the same condition class throughout the year. Three sites changed condition class depending on the month that the survey was conducted; one of these (MGAR) fluctuated between ‘moderate condition’ and ‘high condition’, one (SCOT) fluctuated between ‘low condition’ and ‘moderate condition’, and one (GUNE) fluctuated between ‘low condition’ and ‘high condition’ with no ‘moderate condition’ periods.

Table 4.8. Mean Floristic Value Score for each site by season. Bold values represent the highest annual score for each site. Cells shaded in dark grey indicate 'high condition'. Cells shaded in light grey indicate 'moderate condition'. White cells indicate 'low condition'. Condition classes are outlined in Table 4.4.

	2014								2015				Annual Average
	May	June	Jul	Aug	Sep	Oct	Nov	Dec	Jan	Feb	Mar	Apr	
C3 Native-dominated Sites													
MGAR	6.6	3.7	7.1	6.1	9.4	9.7	6.9	8.3	**10.5**	7.5	7.2	7.8	7.6
GUNN	0.5	0.4	0.8	0.8	1	0.5	0.8	0.9	1.3	0.9	0.7	0.6	0.8
MULN	9.1	7.9	8.9	8.7	11.8	9.1	10.1	14	12.2	**16.7**	13.9	14.1	11.4
C4 Native-dominated Sites													
GIDL	20.6	21.2	20.9	22.2	22.3	25.7	30.2	**31.8**	25.1	21.7	22.7	22.4	23.9
TURA	19.5	16.5	17.8	18.4	16.9	20	28.2	29.6	**30.6**	27.8	22.5	23	22.6
MPON			13.8	20.5	28.3	**43.2**	31.5	28.6	26.6	19.3	17.5	21.7	25.1
C3 Exotic-dominated Sites													
MULE	0.3	0.3	0.3	0.3	0.3	0.3	0.3	0.3	0.3	0.3	0.3	0.3	0.3
GUNE	0.3	0.3	1.4	1.4	1.4	1.4	3.7	**7**	2.3	2	0.7	0.4	1.9
MPOE			0.7	0.7	0.7	0.7	0.8	0.8	1.8	**2.3**	1	0.8	1.0
C4 Exotic-dominated Sites													
SCOT	2.6	3.8	3.7	3.7	2.6	2.5	3.2	**4.8**	3.4	3	1.8	2.5	3.1
INGE	0.4	0.4	0.4	0.4	0.5	0.6	0.6	0.6	1.1	**1.2**	0.7	0.5	0.6
IN17		0.4	0.6	0.7	1.3	0.7	1	2.4	**2.5**	2.1	2.4	1.8	1.4

4.3.5 Tracking cover and phenophase of dominant species

The cumulative cover of dominant species at each site throughout the year is presented in Figure 4.18. It should be noted that this data does not consider the photosynthetic state of the vegetation; that is, the cover measurement is a mixture of photosynthetic and non-photosynthetic vegetation.

Native-dominated C_4 sites were highly consistent in vegetative cover throughout the year, maintaining cover of over 80%. Exotic-dominated C_3 sites also maintained a high consistent cover, though one site (INGE) was more variable.

C_3-dominated sites had a more variable cover throughout the year. In native-dominated C_3 sites, cover was maintained at maximum levels from May to October, and dropped during the warmer dryer months of November and December. January rain saw an increase in cover at four of the six sites.

Table 4.9 graphically shows the representative phenophase of each dominant species at each study site. Some species (e.g. *Themeda triandra* and *Eragrostis curvula*) have a predictable seasonal phenophase pattern that is consistent between sites, however others (e.g. forbs, *Rytidosperma* grasses) are driven more by climatic factors. These species may flower multiple times in one year, and can differ markedly in phenophase patterns from site to site. The dominant annual forbs found at some sites (e.g. *Trifolium* spp.) change markedly in phenophase and cover. These were absent during some surveys, typically during the summer months.

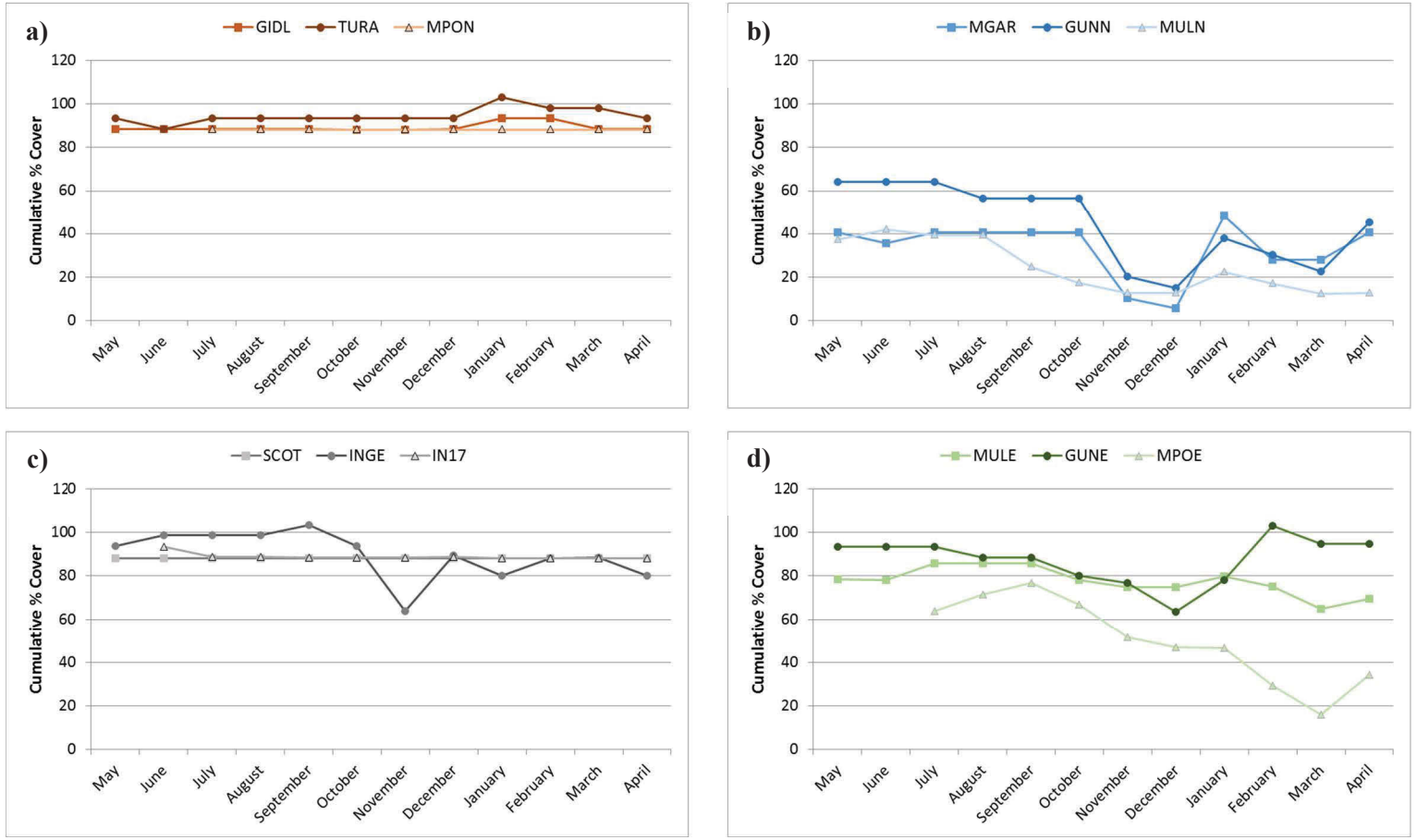

Figure 4.18. Cumulative percent cover of dominant species at each study site. Note that due to overlapping strata the maximum cover can exceed 100%. Sites are grouped by functional type: a) native-dominated C_4; b) native-dominated C_3; c) exotic-dominated C_4; d) exotic-dominated C_3.

Table 4.9. Phenophase of dominant species throughout the sampling period. Letters and shading indicate the representative phenophase throughout the site during that month (V = vegetative, Fl = flowering, Fr = fruiting, P = post-fruiting, S = senescent, X = not present. Blank cells were not surveyed).

		2014								2015			
Site	**Dominant Species**	**May**	**Jun**	**Jul**	**Aug**	**Sep**	**Oct**	**Nov**	**Dec**	**Jan**	**Feb**	**Mar**	**Apr**
C_4 Native-dominated sites													
GIDL	*Themeda triandra*	V	V	V	S	S	V	Fl	Fl	Fr	Fr	P	P
	Poa sieberiana	V	V	V	V	V	Fl	Fl	Fl	P	P	P	P
TURA	*Themeda triandra*	V	S	S	S	S	V	Fl	Fl	Fr	Fr	P	P
	Poa sieberiana	V	V	V	V	V	Fl	Fl	Fl	P	P	P	P
MPON	*Themeda triandra*			S	S	S	V	Fl	Fl	Fr	Fr	P	S
C_3 Native-dominated Sites													
MGAR	*Austrostipa scabra*	V	Fl	P	V	V	Fl	Fl	P	P	V	V	V
	Rytidosperma spp.	Fl	Fl	P	Fl	Fl	P	Fl	P	P	V	V	V
GUNN	*Austrostipa scabra*	V	Fl	Fl	V	V	V	Fl	Fr	P	P	V	V
	Trifolium spp.	V	Fl	V	V	Fl	Fl	S	X	X	V	V	V
MULN	*Trifolium* spp.	V	V	V	V	Fl	Fl	V	Fl	Fl	V	V	V
	Rytidosperma pallida	S	S	V	V	S	V	Fl	Fr	Fr	P	P	P
	Austrostipa bigeniculata	Fl	V	Fl	Fl	Fl	V	V	Fl	P	Fl	Fl	P
	Themeda triandra	P	P	P	S	S	V	Fl	Fl	Fl	Fr	P	P
	Rytidosperma spp.	Fl	Fl	Fr	Fr	Fr	V	V	Fl	Fl	Fl	Fr	P

		2014								2015			
Site	**Dominant Species**	**May**	**Jun**	**Jul**	**Aug**	**Sep**	**Oct**	**Nov**	**Dec**	**Jan**	**Feb**	**Mar**	**Apr**
C_4 Exotic-dominated Sites													
SCOT	*Eragrostis curvula*	P	P	S	S	S	S	V	Fl	Fl	Fr	P	P
INGE	*Eragrostis curvula*	P	S	S	S	S	V	Fl	Fl	Fr	P	P	V
	Trifolium spp.	V	V	V	V	V	Fl	Fl	V	X	X	X	V
IN17	*Eragrostis curvula*		S	S	S	S	V	Fl	Fl	Fr	P	P	S
	Trifolium spp.		V	V	V	V	V	Fl	V	X	X	X	X
C_3 Exotic-dominated Sites													
MULE	*Dactylis glomerata*	Fl	Fr	Fr	V	V	V	V	V	V	V	V	V
	Festuca sp.	Fr	P	V	V	V	V	Fl	Fl	Fl	Fl	Fl	Fl
	Medicago sativa	Fl	Fr	V	V	V	V	X	X	Fl	V	V	Fl
	Holcus sp.	P	P	V	V	V	V	V	Fl	Fl	Fl	Fl	V
	Phalaris aquatica	P	P	V	V	V	V	V	Fl	Fl	Fl	P	P
GUNE	*Phalaris aquatica*	V	V	V	V	V	V	Fl	Fl	Fr	P	P	P
	Juncus acutus	P	V	V	V	V	Fl	Fl	Fr	Fr	P	P	P
MPOE	*Festuca* sp.			V	V	V	Fl	Fl	P	P	P	P	P
	Trifolium spp.			V	V	V	Fl	Fl	V	V	V	X	V
	Holcus sp.			V	V	V	V	Fl	Fl	Fr	Fr	P	V
	Austrostipa spp.			V	V	S	V	Fl	Fl	P	Fl	P	V
	Phalaris aquatica			V	V	V	V	V	Fl	Fl	Fl	P	V

191

4.4 Discussion

4.4.1 Temperate grassland species richness

Monthly surveys of twelve grassland study sites recorded 192 grass and forb species throughout the year. Native-dominated sites tended to have higher average species richness than exotic-dominated sites, particularly for native forbs and grasses. There was less difference between native and exotic-dominated sites in richness of exotic species. This was not because native-dominated sites were infested with exotic species; rather that exotic-dominated sites comprised a small number of exotic species at high cover and native sites had a small number of exotic species at low cover.

Species richness changed from month to month as species with different life history and demographic strategies emerged, reproduced, and senesced. As a result, different species were present at each month, and most sites showed large differences in total species richness throughout the year. Across all sites, the highest species richness was in the summer months (December to February), with the lowest species richness from June to August. This is typical for this region, with most published grassland flora surveys designed to coincide with the period of highest diversity (e.g. Tremont and McIntyre 1994; Vivian and Baines 2014).

Species richness change over time is influenced by the native- or exotic-dominance of the vegetation, and by the functional type of each species. Particular difference in seasonal species richness patterns was observed in native-dominated vegetation, which has higher native species richness, particularly with respect to forbs. This was most apparent in grasslands dominated by *Themeda triandra*, which is known to be associated with high forb diversity (Cole and Lunt 2005, Rehwinkel 2007). Seasonal differences in richness patterns were particularly notable in native forbs; richness peaked two months later at exotic-dominated sites than native-dominated sites. A study in the northern tablelands of NSW also found a similar response in functional group patterns, albeit when examining grazed versus ungrazed landscapes instead of native-dominated versus exotic-dominated sites (Tremont 1994).

Exotic grass species richness is similar between exotic-dominated and native-dominated sites, but the per cent cover is markedly different. Exotic-dominated grasslands have a high cover of exotic grasses, between 70%–90% throughout the year, where native-dominated grasslands have a cover of exotic grasses below 10%. The inference from this data is that exotic grasses are present in native sites, but a high native cover restricts the establishment of exotic weeds (Eddy 2002, Robinson 2015). The species richness of exotic grasses peaks in November, consistent with the maturation of exotic annual species in this region.

Native-dominated sites had consistently high species richness, averaging above 35 species from October through to February. In contrast, exotic-dominated sites had a distinct peak in species richness in January. In this case, the shape of the curve, rather than the magnitude of species richness alone, is likely to represent a difference in ecosystem function and resilience between the two types.

The data shows that January is the optimum month for monitoring species richness in temperate Australian grasslands. Although surveys during January will detect the highest proportion of species, this equates to an average of 61% of the native forb species found at any individual site. In fact the average maximum detection for native forbs (regardless of month) is only 69% over all sites. Surveys conducted in the winter months of June–August will only detect approximately one-third of the total species. Consequently, if a monitoring objective is to detect more than 50% of the number of native species, surveys must be conducted between November and February. If the objective is to detect more than 50% of the number of native forbs, surveys must be conducted between December and February.

While the above recommendations for optimum sampling time (i.e. summer) are generally valid for temperate grasslands in the South Eastern Highlands bioregion, they are subject to seasonal constraints. For example, a summer with very low rainfall may not be conducive for conducting flora surveys as many plants will have wilted or died. Consideration must also be made of specific survey objectives; for example if there is a focus on early-flowering species or threatened species that have specific survey requirements (Office of Environment & Heritage 2016). This study shows that multiple surveys throughout the year are critical to identify more than 61% of the species. As a

minimum, two surveys per year should be conducted to capture both the early-flowering species (e.g. lilies and orchids), and summer-flowering species. Surveys conducted over multiple years are desirable for a complete species list (Sharp *et al.* 2015) but may not be compatible with monitoring budget or objectives.

Seasonal grassland surveys are not frequently undertaken, hence the true dynamics of grassland ecosystems are rarely revealed. This is often legitimately justified through gathering the most information at the optimal time of year (e.g. repeated surveys of Vivian and Baines 2014). The capability of using 'out of season' surveys to detect species not normally observed during summer has been highlighted in the past (Stuwe and Parsons 1977), and should be incorporated into surveys of temperate grasslands where accurate census data is required.

The variability in detection frequency is greater for forbs than it is for grasses. This may be explained by the nature of many graminoids to retain their dried inflorescence on the plant for long periods of time. Hence, these graminoid species can be located and identified long after flowering has occurred and sometimes after the plant has senesced. Forbs exhibit this characteristic only rarely, and in those cases tends to be only in common species (e.g. *Chrysocephalum apiculatum*, *Cirsium vulgare*).

The vegetative cover quantified in this chapter cannot be directly related to land phenology as it represents both photosynthetic and non-photosynthetic vegetation. This is the standard practice for collecting floristic data in NSW as it is relevant for other land capability assessments (Department of Environment Climate Change & Water 2011). The separation of photosynthetic and non-photosynthetic cover to enable comparison between remotely sensed land surface phenology and field data will be discussed in Chapter 5.

The proportion of different functional groups detected may be underpinned by the greater breadth of species at native sites. Exotic-dominated sites were observed to have a higher proportion of their native species detected in summer than native-dominated sites. A likely explanation of this is the increased quantity of annual grasses at exotic sites in spring results in increased competitive pressures for sensitive early-flowering species such as lilies and orchids. Hence, the majority of the native species that are

found in exotic sites are those that are summer-dominant. This is supported by the data: in native-dominated sites, September and October have approximately half of native species present. At exotic-dominated sites, only approximately one-quarter of native species are found during this time.

4.4.2 Grassland condition monitoring

The monitoring of grassland condition is essential for guiding management decisions in a range of contexts, such as grassland restoration, landscape degradation, and assessing the provision of ecosystem services (Sharp *et al.* 2015). While alternative methods for monitoring condition exist in temperate grasslands (Seddon *et al.* 2011), this study used the Floristic Value Score method as a surrogate for condition. The FVS gives a higher consideration to the abundance, richness and sensitivity of native forbs than other methods. This gives an ecologically sound estimate of condition, as the presence of high-value forbs on a site is consistent with one that has been managed sustainably and for conservation purposes. As high-value forbs are preferentially grazed from a pasture by domestic livestock, their presence is a good indication of historically low grazing pressures (Prober and Thiele 1995).

The results of this study found large seasonal difference in floristic value scores for many sites. Most sites (11 of 12) recorded their highest FVS between December and February. The exception was the native site MPON, which had its highest FVS in October. This site is unique in having a large proportion of its flora as high-value species that germinate and flower in spring (e.g. *Bulbine bulbosa, Drosera peltata, Microtis unifolia*). This site's FVS of 43.2 represents the highest score recorded in this study. This site is grazed by sheep at low intensity, and its high condition score relative to similar ungrazed sites (e.g. TURA) lends support to the ecological theory that intermediate disturbance of grassy ecosystems subtends higher species diversity (Grime 1973). This has been supported in some Australian grassy ecosystems (Prober and Thiele 1995) but not others (Fensham 1998).

Condition class changed despite the seasonal flexibility built into the method (i.e. favourable versus non-favourable time of year). Three sites changed class—including one exotic-dominated site that jumped from 'low' to 'high' condition class during

December due to the presence of high-value forbs. A justification could be made that the presence of these forbs at this time meant that this site is truly high-value, despite falling into the 'low condition' category at almost all times. However, the implication is that unless that site is surveyed thoroughly in a narrow time-window, it will be classified as 'low condition'. Low condition grasslands are not afforded the same conservation protection under Australian legislation, hence the importance of this classification system. Another exotic-dominated site was elevated into 'moderate condition' in the winter months, despite the trend that native richness (and consequently FVS) tends to be lower during this time of year. Conversely, July and August surveys saw a native-dominated site fall into the lower 'moderate condition' category.

The shift in condition class for some sites suggests that the thresholds for the 'non-favourable' time of year are inconsistent with those for the 'favourable' time of year. This presents the unintended outcome that a grassland may fall into a different class if sampled at a different time of year. Clearly, this has practical implications on conservation priorities and, conversely, development processes. Unless specific direction is provided by authorities, there is the potential for 'gaming' this method by surveying at the specific time that produces the most beneficial outcome.

In NSW, the timing of ecological assessment is restricted by season for some purposes, such as detecting the presence of certain threatened flora (Office of Environment & Heritage 2016). Indeed, for grassland assessment, the seasonal requirements for survey timing is clearly specified (Rehwinkel 2007). However, restricting assessments of vegetation condition to one time of year increases the time taken for development approvals, hence some jurisdictions have implemented 'out-of-season' thresholds, such as those used here (Department of Environment 2016). This study demonstrates the importance of maintaining consistency within a monitoring program. Further research should examine how out-of-season thresholds should best be applied before this philosophy is expanded to other vegetation types.

While suitable for this study, the Floristic Value Score is but one method for estimating condition, and requires *a priori* knowledge of the conservation value of all species. This requires significant investment. However, there are no other published methods that take into account the greater value of sensitive forbs. The FVS does have limitations—

in particular, the discovery of a single sensitive species can dramatically change the classification. In addition, the threshold values that determine the condition class are expert-derived rather than data-derived, and may not be appropriate for all regions or grassland communities.

Depending on the monitoring question, alternative methods for monitoring grassland condition may be considered, such as novel visual techniques (Morgan 2015) or using indicator species (e.g. Dorrough 2008). However, regardless of which method is used to estimate condition, it is essential to incorporate seasonal variability into the program design.

4.4.3 Cover and phenophase change

Sites that have one species with clear dominance (i.e. greater than 75% cover) tend to have relatively straightforward trends in vegetative cover. In our cases, these tended to be the C_4-dominated sites that had a consistent cover of either *Themeda triandra* (native sites) or *Eragrostis curvula* (exotic sites). With the exception of one site (INGE), these sites had a consistent cover of the dominant species above 80%. This can be readily explained by the perennial native of these grasses that retain dead material on the plant for several years (Morgan and Lunt 1999, Morgan 2015). The variation in INGE occurred in November, when a large number of cattle were released into the paddock. However, in these cases, the total cover does not explain any potential variation in land surface phenology as it does not take into consideration any changes in photosynthetic and non-photosynthetic vegetation, the proportions of which significantly impact visual and near infra-red vegetation indices (Asner 1998, Nagler *et al.* 2003).

In the sites with clear dominance of one species, the sequence of phenophase was consistent between sites of the same type. In native-dominated C_4 sites, the vegetative growth stage of *Themeda triandra* corresponded with higher temperatures in October, followed by flowering in November and December. Inflorescences were retained on the vegetative plant until April and the plants were senescent from June to September. In exotic-dominated C_4 sites, *Eragrostis curvula* followed almost identical patterns.

At these sites, the phenophase will be closely related to land surface phenology signature because a) overall cover remains constant, and b) species composition of dominant species is steady.

For the remainder of sites, the occurrence of co-dominant species resulted in a more variable range of cover throughout the year. These sites were much more responsive to dry periods at the end of spring (November) and summer (March) and showed a significant drop in cover. Native-dominated C_3 sites were dominated by *Rytidosperma* and *Austrostipa* grasses, which are regarded as non-climax communities. These species dominate some grasslands as a result of grazing and other disturbances (Austin *et al.* 1981, Dorrough *et al.* 2011, Sinclair *et al.* 2014). Native-dominated C_3 sites had a high population of native herbivores which would have further decreased the vegetative cover during these drier periods. Exotic-dominated C_3 sites tended to occur in lower parts of the landscape such as floodplains so were less susceptible to moisture stress during November and March. The exception to this was MULE, which exhibited a similar pattern to the native-dominated C_3 sites.

Examination of phenophase at these sites is more complex, as each site has several co-dominant species to consider. Exotic C_3 pasture grasses tend to follow similar phenophase, but native grasses and exotic forbs exhibit different patterns. While many annual and perennial species tend to sequentially follow the phases in Table 4.5, species that flower prolifically throughout the year (e.g. *Hypochaeris radicata*) or in response to rainfall, such as occur in some *Rytidosperma* species (Waters *et al.* 2008), may have a less predictable pattern.

While the vegetative stage can be legitimately viewed as the main predictor of land surface phenology, flowering time of dominant species can also impact remotely sensed phenology; typically producing non photosynthetic vegetation that is retained on the plant for several months once flowering is complete. The post-flowering designation used in this study implies that dead stalks or seed heads were retained on the plant. As many species have inflorescences that are retained for many months, this may lead to lagged impacts on land surface phenology. This will have a greater impact on sensors that collect imagery obliquely rather than from nadir sources.

It should also be acknowledged that some annual species germinate, flower, fruit and senesce over a relatively short time span. As such, multiple phenophases may pass between monthly sampling events. It is also a common reproductive strategy for plant species to have overlapping phenophases to increase the probability of successful fertilisation and seed dispersal (Davila and Wardle 2007). This increases the difficultly in correctly attributing phenophase class across the whole population.

4.4.4 Implications for land surface phenology

The results from this study highlight the magnitude of vegetative dynamics throughout the year, and the complexity of quantifying these vegetation changes in the context of land surface phenology. An understanding of how species change over time, and how the biophysical characteristics of those species change, is essential to avoid making incorrect inferences from remotely sensed data. Knowledge of ecology of the subject area is therefore essential for land surface phenology interpretation, and is the driver behind this chapter's research aims.

In temperate grasslands, grasses dominate the landscape but are relatively invariant in their species richness and cover throughout the year. In fact, the only prominent change in grass characteristics was in the species richness of exotic grasses. This peak of exotic grass richness in November coincided with the maturation timing of spring-growing annual grasses. Although no peak in the cover of exotic grass was observed in this month, exotic annual grasses have the potential to increase vegetation indices during the late spring when they are in the active growth period. They also have the potential to decrease vegetation indices after this period due to their abundance of mature (non-photosynthetic) inflorescences.

Overall grass cover was found to be relatively invariant throughout the year because most dominant grasses are perennial, and retain live and dead material on the plant, even when not in a phase of active growth (Morgan 2015). However, the phenophase and relative fractions of photosynthetic and non-photosynthetic vegetation is critical to remote sensing interpretation (Asner 1998, Guerschman *et al.* 2009). In this study, C_4 grasslands showed a consistent and predictable phenophase change that correspond with: increased photosynthetic fraction in late spring/summer; flowering and fruiting in

summer, which increases non-photosynthetic fraction as inflorescences mature; and senescence to minimal photosynthetic fraction in winter. The C_3 grasslands were more complex: they tended to have several dominant species that varied in relative abundance throughout the year and frequently had diverging or overlapping phenophases. For native sites, this may be an illustration of grassland dynamics in a non-climax vegetation type. In this scenario, multiple species occupy different ecological niches within different climatic conditions (Suttle *et al.* 2007). For exotic sites, species dynamics are more likely to be influenced by pasture management and in some cases grazing management. In either case, the task of coupling site ecological conditions with land surface phenology interpretation will be more difficult for sites with multiple dominant species that have differential phenophase.

The greatest floristic change throughout the year was in forb diversity. While forbs represent 70% of the total species, their contribution to the vegetative cover is typically low. Native forbs in particular recorded an average cover of 2% throughout the year and despite their importance floristically and ecologically are unlikely to have major implications on land surface phenology. However, some undisturbed temperate grasslands can support native forb cover at much greater quantities, so consideration of this potential is required.

Exotic forbs exhibited large changes in cover and richness throughout the year. These have a much greater potential to dominate landscapes and impact land surface phenology. In this study, pasture species were the only exotic forbs that met the definition of 'dominant' (greater than 5%–25% cover class). However, there is a strong potential for many regionally-specific weeds to impact land surface phenology measures. Many exotic forbs in this region are broad-leafed and form large rosettes (Richardson *et al.* 2011), structural characteristics that are more readily captured by remote sensing means than, say, the erect habit of grasses (Asner 1998).

4.4.4.1 Ecological interactions

Section 4.1.4 introduced the three factors that contribute to variation in land surface phenology: phenophase and environmental drivers, which impact the biophysical characteristics of individual species, and species composition which determines the

proportional influence of each species. However, these three factors do not act in isolation—in fact they are inherently linked. The land surface phenology response of temperate grasslands, as measured by satellite or ground-based sensors, is dictated by the relationships between these three factors, which may result in complex responses that are difficult to resolve.

Environmental Drivers and Community Composition

For some communities, environmental drivers will produce differential species responses. In this study, we observed that exotic forbs were unable to sustain vegetative cover during hot, dry conditions whereas native grasses maintained a reasonable cover, albeit with a reduced photosynthetic fraction. The ecological niche vacated by the exotic forbs may be occupied by another species, thereby changing the composition. Similarly, when rainfall follows drought events, some plants—typically exotic species—are better able to take advantage of this moisture, and grow, develop and reproduce more quickly than others (Baker 1974).

Some environmental drivers promote faster changes in community composition. Grazing animals will preferentially favour certain species over others, particularly inter-tussock forbs (McDougall and Walsh 2007), which has been shown to reduce in the cover and abundance of native forbs in grassland systems (Tremont 1994). Grazing animals can have other direct and indirect impacts on grassy ecosystems, including introducing exotic species, compacting soil and altering nutrient regimes (Eldridge *et al.* 2016). Other environmental drivers that were not observed in this study may include fire or chemical fertilisation. All of these factors can result in short and long-term modification of an ecological community.

Environmental Drivers and Species Phenophase

Climate has obvious impacts on individual plant phenophase. Rainfall can induce vegetation growth or flowering, and lack of rainfall can prevent flowering or even force the wilting and death of foliage. Cold temperatures can accelerate vegetation senescence, as was widespread in our C_4-dominated grasslands in winter. At C_4-dominated sites, warm weather usually induces leaf expansion and flowering.

Dormancy and germination in native forbs is primarily driven by seasonal conditions, though can also be influenced by unpredictable environmental changes such as soil wetting and changes in soil temperature (Tremont and McIntyre 1994). The cues that drive this may act differently between native and exotic species.

Species Phenophase and Community Composition

Phenophase can interact with community composition through population dynamics and life history strategies. Competitive advantage can be increased for species that germinate and grow earlier than others, particularly following disturbance (Li *et al.* 2006). Indeed, this is how many exotic species become so widespread, particularly annual species (Baker 1974). Species that are able to delay senescence will have more resources in storage for the following growing season. Alternatively, plants that flower earlier and more frequently than competitors can provide a greater representation in the seed bank and more individuals in the future (Brown and Venable 1986). The majority of these interactions will result in inter-annual changes, so were not directly observed in this study.

The complexity of these interactions suggests that a thorough knowledge of site ecology is required to fully explain remotely-generated phenology estimates. In dynamic systems it promotes the need for field validation at more regular intervals than may normally be considered. Technologies such as high-definition phenocams (Brown *et al.* 2011) or automated drones may soon be a viable approach for frequent observations of sites, however it is difficult to envisage a scenario where field observations become obsolete.

4.4.5 Study limitations

Grassland flora surveys are recognised as being difficult to conduct accurately. Particularly in sites that have high biomass, grass tussocks tend to obscure the smaller forbs (Garrard *et al.* 2008, 2013). In the current study, all C_4-dominated sites had high biomass that could feasibly increase the difficulty of detecting species and consequently underestimate the species richness and the cover/abundance scores of individual species. As there was only one observer in this study, imperfect detection is likely, despite the level of botanical experience of the surveyor and field training received from

expert grassland botanists. Ideally in future research, multiple surveyors should be used to increase the efficiency of the survey and improve the confidence that a site species list is complete.

As an extension of this theme, the number of survey replicates should be increased in future surveys. The number of plots were determined in accordance with the Office of Environment and Heritage method for homogenous vegetation zones (Department of Environment Climate Change & Water 2011). However, the definition of 'homogenous' is more accurate for some grasslands than others, and the concept of vegetation zones can be subjective to apply. Appropriate numbers of quadrats for a vegetation survey are best calculated based on analysis of repeated quadrats (e.g. species accumulation curves), however in this case was dictated by time, budget and expert opinion. The number of field sites in this study was commensurate with resourcing, but given the diversity within each grassland type, replication could be increased in future work.

The Braun-Blanquet method for assessing the relative cover/abundance of a species has been a common tool in vegetation studies for many decades (Poore 1955), not least of all due to its ease of use (Moore *et al.* 1970). However it has been criticised for its categorical scale that renders any sophisticated analysis or cumulative groupings impossible (Podani 2006). In the current study, these weaknesses were addressed by using a transformation of original Braun-Blanquet data. Several transformation methods exist (van der Maarel 1979, 2007, McNellie *et al.* 2017), and have been shown to result in good agreement with both field measures and theoretical models. While not implicitly stated in the assumptions of these transformations, they may be more accurate for large samples than the relatively small samples used in this study. In this project, a small difference in estimate can result in a relatively large difference in transformed data. For example, an original estimate of 4% cover gives a Braun-Blanquet score of 1. This results in a 'transformed cover' of 0.5%. As such, transformed values should be treated cautiously.

Further, visual estimates of vegetative cover are known to be significant sources of error (Klimeš 2003).The use of cover classes such as Braun-Blanquet improve this source of error but does not eliminate it entirely (Cheal 2008). Point-transect assessments may be a solution to estimate cover and abundance of each species in a more objective and

precise manner (Prober *et al.* 2007, Godínez-Alvarez *et al.* 2009) though the benefits of this must be weighed against the additional effort required for data collection.

In dynamic systems, it can be difficult to representatively allocate phenophase across a whole paddock. Small microclimates can yield difference in flowering or fruiting patterns, and the resultant attribution is subjective in some cases. It would also be advantageous to survey more regularly than once per month to capture rapid changes in abundance, cover and phenophase.

The influence of grazing on phenophase was not incorporated into this study, however is important to consider under some management practices. Particularly at exotic-dominated sites with a high density of livestock, grazing can obscure phenophase trends by removal or trampling of reproductive structures.

4.5 Conclusion

This study conducted monthly flora surveys at twelve temperate grassland sites to monitor species richness and phenophase change throughout the year. Native-dominated sites tallied a total of 152 species recorded throughout the year, while exotic-dominated sites recorded 115 species.

The species that are present in any given grassland changes throughout the year as a function of species life history, ecological interactions, climate and grazing effects. In general, more species are present in the summer months, and fewer species present in the winter months, though plant functional group directed this pattern. Exotic species were most readily detected in November (late spring). Whether a grassland was exotic- or native-dominated influenced the seasonal patterns of different functional groups of plants; for example, cover of exotic forbs peaked in November at native-dominated sites, and in January at exotic-dominated sites.

In addition, the proportion of species detectable in temperate grasslands changes from month to month. Native species are most readily detected in the summer months, with January having the highest proportion detected. The lowest proportion of native species

is found in the winter, with only around one-third of the total species being present during this time.

The timing of grassland flora surveys can have a major impact on the number of species detected, particularly if decisions are reliant on a single survey. Even at the optimum survey time, less than two-thirds of native species were detected. It is clear that multiple surveys are required per year in order to adequately assess the complete range of native species in temperate grasslands. Climatic conditions must also be integrated into the consideration of survey timing.

Consequently, assessments of grassland condition states are also influenced by the timing of survey. In this case we use the Floristic Value Score, a method that estimates condition by the cover and abundance of differently-valued native species. FVS varied through the year, particularly in native-dominated sites. This variation is mostly influenced by the presence of high-value forbs rather than by large changes in cover/abundance in any of the dominant species. Although most of the sites remained in the same condition class throughout the year, those that were close to threshold values changed classes depending on the month sampled. This inherent variation must be considered when interpreting long-term monitoring of grassland condition, and the utility of seasonal benchmarks.

The vegetative cover of dominant species at each site changed through the year, which impacts phenology patterns measured from near-surface and satellite sources. The complexity of integrating ground-based measures of cover and phenology is particularly illustrated by sites that have multiple dominant species that vary in their seasonal patterns at the same site. For sites with one dominant species that follows predictable phenological stages, integration of ground-based phenology with remotely sensed phenology may be more straightforward.

Overall, this study quantifies the dynamics of temperate grasslands at a floristic level, and highlights the importance of how seasonal changes in different plant functional groups can impact larger-scale estimates of land surface phenology. However, methods that quantify phenology—particularly vegetative phenology—at smaller time fractions may be necessary to enable direct comparisons with remotely sensed phenology data.

Chapter 5: Assessing phenology of C_3 and C_4 grasslands using near-surface and satellite remote sensing coupled with field measurements

5.1 Introduction

5.1.1 Different grassland functional types

Grasslands represent one of the most dynamic and widespread biomes on earth (Scurlock and Hall 1998). They occupy a broad range of ecological niches and are dominant ecosystems in a variety of climatic conditions. However, despite their importance in grazing systems and their acknowledged provision of ecosystem services, historical and current land management practices have degraded grasslands throughout the world (Ceballos *et al.* 2010). This is particularly true for temperate grasslands, which are facing many threats to their sustainable future (Peart 2008).

In Australia, 37% of the continent is classified as grasslands (Lymburner *et al.* 2011). Hummock grasslands of the arid and semi-arid interior are widespread and relatively undisturbed, whereas grasslands in the temperate zones are disturbed, fragmented and degraded. As such, the interior hummock grasslands are relatively secure, while native temperate grasslands represent some of the most threatened communities in the country (NSW Natural Resources Advisory Council 2010). These grasslands differ greatly in their composition, structure and functional attributes. Being able to classify grasslands based on these attributes is the first step in being able to direct their management, whether this is for an ecological or economic aim.

There are 60 recognised native grassland communities classified in the state of New South Wales (NSW), obtained from a range of vegetation classification programs (NSW Office of Environment & Heritage 2014). In addition to this are grasslands dominated by non-native (exotic) pasture grasses or weeds, and a continuum of intermediate states with both native and exotic components. Distinguishing native from exotic grasses is important from an agricultural productivity perspective—such as determining stocking

rates—but is also essential for detecting weed incursions into pastures or conservation areas.

Vegetation classification in Australia is important for land management, ecosystem inventory, habitat assessment, and a wide range of other purposes. Geoscience Australia has classified 32 land cover categories at 250 m spatial resolution, including elements such as trees, shrubs, crops, wetlands and grasses (Lymburner *et al.* 2011). Grasslands occupy 8 of these 32 categories. These broad classifications are based on structural and spectral attributes as well as phenological distinction; they separate grassland types such as 'closed tussock grasses' and 'scattered hummock grasses', but ultimately lack the fine detail required for discrimination of grassland communities required for ecological management.

One of the more fundamental distinctions in vegetation function is that of C_3 or C_4 photosynthetic type (Still *et al.* 2003). The nature of C_3 or C_4 dominance dictates patterns of growth and productivity during different times of the year; C_3 species are more productive in cooler, mesic climates, whereas C_4 species have a greater advantage in warmer, drier regions (Wand *et al.* 1999, Baldocchi 2011). Differentiating C_3-dominant grasslands from C_4-dominant grasslands has been a prominent theme in remote sensing research because of their distinct seasonal productivity patterns. This research has been driven by the potential impact of future climate scenarios on agricultural productivity (Winslow *et al.* 2003, Howden *et al.* 2008, Cullen *et al.* 2009, Pau *et al.* 2013). There has been debate in the scientific literature as to how C_3 and C_4 vegetation generally, and grasses specifically, will respond to increased CO_2 concentration, increased temperatures and modified moisture regimes of a changing climate (Baldocchi 2011), particularly as grasses are expected to be highly responsive to rising CO_2 levels (Sala 2001). Rising temperatures and lower available moisture are expected to favour C_4 grasses, while higher CO_2 concentrations should favour C_3 grasses (Morgan *et al.* 2011). However, the interactive effects between climate variables are likely to be complex and dependent on thresholds; for example C_3 plants may be favoured under certain moisture regimes and C_4 grasses may be favoured under others (Morgan *et al.* 2011). Research continues to separate out the likely trends for different species and ecosystems around the world, but it is clear that and competitive advantage granted to one photosynthetic group will drive a series of unpredictable

ecological cascades (Poorter and Navas 2003, Körner 2006). This change in composition on a global scale will in turn create large-scale feedbacks to climate systems and ecosystem services (Richardson *et al.* 2013). Understanding changes in this composition is therefore critical for ecosystem forecasting and better modelling of global climate models (Potter *et al.* 2007).

In Australia, most grasses in the tropical, arid and semi-arid zones utilise the C_4 photosynthetic pathway. The temperate south-east of the country comprises some areas where C_3 grasses dominate, some areas where C_4 grasses dominate, and some grasslands where C_3 and C_4 grasses co-exist (Hattersley 1983). Much of the grassland composition depends as much on disturbance factors as climate; in fact it is suggested that the C_4 grass *Themeda triandra* would dominate many undisturbed landscapes in the south-east if domestic stock grazing was eliminated (Wimbush and Costin 1979, Benson 1994). This is contrary to general opinion that C_4 grasses are predominantly adapted to areas of low rainfall or high temperatures (Pau *et al.* 2013).

5.1.2 Need for identification and monitoring of grasslands

In temperate NSW, native grasslands occur on flat, productive land which has resulted in extensive habitat destruction and modification for cropping and grazing agriculture. Many native grassland types occupy a very small fraction of their pre-European range (Benson 1994, McDougall and Kirkpatrick 1994), and eight grassland communities are listed as 'endangered' or 'critically endangered' under State and Commonwealth legislation (NSW Natural Resources Advisory Council 2010). Their conservation and restoration has been recognised as a priority, however the need to balance conservation and agriculture in this region is acute. Failure to adequately protect high conservation value grasslands will almost certainly result in increased fragmentation and further degradation. Conversely, overprotection of low conservation value grasslands can frustrate agricultural landholders who may become disengaged with conservation measures. This can result in further impediments to meaningful conservation on private land—a critical point, given that a large proportion of remnant native grassland in temperate Australia is known to be on private land (NSW Natural Resources Advisory Council 2010). Identification of remnant areas is important to quantify the area of native grasslands and strategically manage them at a landscape scale. However, identifying

these through traditional field methods is difficult due to the time and cost of travel and in many cases the difficulty in obtaining access to private property.

Monitoring is an important component of grassland management, particularly when determining the success of restoration or the consequences of degradation (Sharp *et al.* 2015). However, field monitoring has practical difficulties due to variability in species presence and vegetative cover throughout the seasons, as well as the intensity of survey workload that this requires (refer to Chapter 4).

Consequently, remote sensing has been suggested as a practical approach to identify grassland types and condition. Efforts to separate grassland communities worldwide have had some success in the spectral domain (e.g. Price, Guo and Stiles 2002), but in temperate Australia the unique properties of grassland vegetation have generally confounded attempts to achieve fine-scale classification of grassland or time-series monitoring of condition. Specifically, this is due to their dynamic, heterogeneous nature (Hill 2013), habit of retaining dead material on the plant (Tremont and McIntyre 1994, Morgan and Lunt 1999), unique shading issues that grasslands present (Shimada *et al*. 2012) and the continuum between disturbed and undisturbed condition states (Psomas 2008).

The use of phenological signatures—annual patterns in green vegetation change—for discriminating vegetation types has been successful in vegetation types globally (Hmimina *et al.* 2013), including the separation of C_3 and C_4 grassland types (Wang *et al.* 2013, Dye *et al.* 2016). This phenological approach has yet to be trialled in Australian temperate grasslands. The use of phenological methods to monitor vegetation in Australia is currently limited to the arid and semi-arid zones where changes in vegetation between seasons are driven by rainfall and are highly pronounced (Ma *et al.* 2013, Petus *et al.* 2013). Furthermore, many of the methods used for discrimination of vegetation functional types are based on northern hemisphere unimodal systems (e.g. Davidson and Csillag 2003; Wang *et al.* 2013) where common phenology metrics such as ‘start of season’ and ‘length of season’ are appropriate and meaningful. As has been found in semi-arid and arid parts of the country (Zhang *et al.* 2006, Broich *et al.* 2015), these approaches are not applicable to temperate Australian grasslands, which are more complex in their seasonal dynamics.

There are multiple challenges involved in the separation of grassland communities via remote sensing. Using phenological characteristics to improve the identification of native-dominated grasslands from exotic-dominated grasslands, and C_3-dominance from C_4-dominance is a research avenue that can improve the set of tools available for this challenge.

5.1.3 Phenology: methods of data collection

Chapter 1 introduced the potential of using land surface phenology to identify or separate different vegetation types. However, in Chapter 4 we learned that the ecology of the vegetation is critical to interpretation of land surface phenology and that understanding of field-scale detail is important to inform remote sensing data. As such, it is important that research investigating land surface phenology examines information that both fine-scale and broad-scale approaches can provide.

Vegetative phenology is fundamentally associated with the biophysical properties of the vegetation, such as leaf area index (LAI), phytomass, chlorophyll content, and fraction of absorbed radiation (Lu *et al.* 2003). These biophysical parameters are often highly related to the quantity and quality of green vegetation, but are also is impacted by the quantity and nature of non-photosynthetic vegetation (van Leeuwen and Huete 1996, Nagler *et al.* 2000, Watson *et al.* 2013). Several methods are used in contemporary research to capture these changes in biophysical characteristics to extract phenological information, and are discussed in this section.

Satellite data is now a prominent source of information on vegetation dynamics across the globe. Land surface phenology tools characterise the greening and browning patterns of vegetation types across continental scales (Broich *et al.* 2015). Typically, these tools use spectral reflectance converted to a vegetation index (VI) such as the Normalized Difference Vegetation Index (NDVI; Rouse *et al*. 1974; Tucker 1979) or the Enhanced Vegetation Index (EVI; Huete, Justice and Liu 1994). Different VIs calculated from satellite sensors have been shown to reliably estimate biophysical parameters for a range of vegetation types (Weiser *et al.* 1986, Huete *et al.* 2002). Satellite data has the advantage of being able to capture large areas consistently, and

provide different types of vegetation information through the use of varied spectral domains. However, satellite application to land surface phenology is limited by temporal resolution (i.e. time of satellite re-visit) and spatial resolution (i.e. size of pixel). The quality of satellite data is also impacted by atmospheric effects (Chuvieco and Huete 2009), and illumination effects (Saleska *et al.* 2007, Bhandari *et al.* 2011), many of which are incompletely understood. Satellite-based studies on vegetation phenology are extensive, with many covering grassland vegetation types (Justice and Hiernaux 1986, Fontana *et al.* 2008, Cui *et al.* 2012, Horion *et al.* 2013, Wang *et al.* 2013).The majority of these focus on northern hemisphere grasslands that, unlike Australian grasslands, have phenology strongly driven by temperature.

Time-lapse fixed cameras or 'phenocams' have shown great promise in capturing phenological information in an increasing range of biomes (Brown *et al.* 2016), including northern hemisphere broadleaf forest (Ahrends *et al.* 2008, Richardson *et al.* 2009, Nagai *et al.* 2011, Mizunuma *et al.* 2013), Brazilian cerrado (Alberton *et al.* 2014), European alpine grasslands (Migliavacca *et al.* 2011, Julitta *et al.* 2014), Malaysian tropical forest (Nagai *et al.* 2016) and grasslands in Japan (Inoue *et al.* 2015). In Australia, Moore provides an overview of phenocam imagery captured at specific locations, including tropical rainforest, tropical savannah and temperate evergreen forest (Moore *et al.* 2016).

Phenocams generally have a smaller spatial capture area than satellites and lack the spectral resolution of modern satellite sensors. However, they have the advantage of being able to capture high frequency (sub-daily) imagery, they can be positioned to directly monitor the vegetation of interest, atmospheric effects are rarely a concern, and users can visually examine imagery to explain observed patterns or anomalies in the data. Phenocam imagery is typically converted to a vegetation index such as Excess Green (Woebbecke *et al.* 1995) or Green Chromatic Coordinate (gcc; Gillespie, Kahle and Walker 1987; Sonnentag *et al*. 2012) through manipulation of the red, green and blue brightness values. Unlike satellite sensors, phenocams typically only use the visible part of the electromagnetic spectrum, although some have attempted to use the near infra-red (Nijland *et al.* 2014). Data generated from phenocam imagery has shown a good correspondence of phenophase timing with eddy-covariance towers, satellite imagery and field data (Richardson *et al.* 2007, Migliavacca *et al.* 2011, Nagai *et al.*

2011, Mizunuma *et al.* 2013, Toomey *et al.* 2015, Moore *et al.* 2017), albeit with quantifiable time lags or restrictions to certain times of year.

While early phenocam studies tended towards more expensive fixed cameras, advances in technology have led to smaller, more affordable phenocams being used. This allows researchers to deploy several inexpensive devices as opposed to one expensive camera. It also expands the number of potential locations that cameras can be placed, as the risk of losing a camera through vandalism becomes a lot less impactful on the overall project. The quality of data generated by inexpensive phenocams has been shown to be equivalent to that of higher cost hardware (Sonnentag *et al.* 2012).

Ideally, phenological data collected using remote sensing methods such as satellite sensors and phenocams should be complemented with concomitant field measurements of the vegetation properties. In some ecosystems, such as forests, appropriate field data can be difficult to gather due to error in estimates (Bréda 2003) but also because of the difficulty in adequately sampling tree biomass. In grasslands, obtaining representative biomass samples or estimates of vegetative cover can be more straightforward because of their ground-layer canopy, though LAI is difficult to interpret when there is significant non-photosynthetic material (White, Asner, *et al.* 2000). Much of the field-based data collection methods are based on agricultural methods for estimating productivity, and include canopy height, fractional cover and aboveground biomass harvesting.

Field based data is essential for validating remote data, but for decades has been used as a method for estimating vegetative phenology as seasonal productivity for agricultural research in its own right (e.g. Epstein *et al*. 1997; Lauenroth *et al*. 1986; Singh and Yadava 1974). Canopy height has been used to assess grassland condition (Gilgen and Buchmann 2009) and is routinely used in the field as a proxy for estimating aboveground biomass (Lopez Diaz and Gonzalez Rodriguez 2003). Aboveground biomass is fundamental characteristic of vegetation as it directly represents productivity (Scurlock *et al.* 2002). As such, biomass measures are frequently used in conjunction with grassland remote sensing research (Mutanga and Skidmore 2004b, Shen *et al.* 2008, Psomas *et al.* 2011). Fractional cover relates to the proportion of ground surface covered by photosynthetic (‘green’) vegetation, non-photosynthetic (‘brown’)

vegetation and background, or bare soil. It is an important variable in the context of grasslands as proportional variations are reflective of community structure (Li *et al.* 2005) as well as wider-reaching factors such as nutrient dynamics, fire risk, soil erosion and heat exchange (Guerschman *et al.* 2009). Fractional cover has also been used in remote sensing studies (Guerschman *et al.* 2009, Hill *et al.* 2011, Hufkens *et al.* 2016).

5.1.4 Phenology data collected at different scales

Many long-term phenological records, such as leafing-out or flowering time, are from visual observations collected from an individual plant, or small patch of plants (Sparks and Carey 1995, Aono and Kazui 2008). Visual observations of phenophase have been used for large-scale and long-term data sets to enable the evaluation of climate change on phenology across continents (Menzel *et al.* 2006). Citizen science programs to monitor phenology (e.g. Betancourt *et al*. 2007) are currently flourishing and use a similar approach. However, the limitations of visual observations are well recognised: many observations are necessarily subjective in nature, particularly when attempting to estimate a set proportion of a specific phenophase (e.g. 50% of leaf expansion). Attempting to compare data collected across large scales is challenging due to the lack of standardised data collection protocols, though this is changing thanks to greater awareness and promotion of this issue (Moore *et al.* 2016) and the proactivity by some organisations (e.g. US National Phenology Network). Given the phenological variability within any given species, the question of point-source representativeness is often raised (Siljamo *et al.* 2008), particularly in urban areas that have different climatic conditions to the ambient environment (Fisher and Mustard 2007). The validity of point-source studies to be used in phenological meta-analyses is also questioned (Parmesan and Yohe 2003). Further, the type of statistical analysis resulting from visual observations is still in its infancy, and more sophisticated approaches to analysis are in need of development (Keatley and Hudson 2010).

The alternative approach to point-source observations is that of land surface phenology, a remote sensing term that captures an integrated area of vegetation rather than a single plant (de Beurs and Henebry 2004). Land surface phenology is being more routinely estimated by satellites and phenocams tracking changes in vegetation indices. While not explicit in its definition, land surface phenology tends to concentrate on vegetative

phenology rather than flowering or fruiting phenology, due to the large body of work in the remote sensing sciences that explores the relationship of green vegetation to spectral reflectance. Concentration on the vegetative component is also a practical matter: reproductive structures usually contribute a relatively small proportion to the overall vegetation signal. Pragmatically, the spectral signature of green vegetation is relatively consistent, whereas flowers and fruits vary significantly in colour, size and surface characteristics, hence their utility in an integrated land surface phenology approach is limited.

As the comparison of remote sensing and field data is important, some authors have provided recommendations on how best to coordinate these elements (Rienke and Jones 2006). Field data and remotely-sensed data are very different in their fundamental approaches and are often used in conjunction to validate one another (Zhang *et al.* 2006, Liang *et al.* 2011). Although scaling from ground to satellite has been deemed a success in some research projects (Fisher and Mustard 2007, Studer *et al.* 2007), several studies have highlighted the often weak relationship between ground and satellite observations (Badeck *et al.* 2004, Ahl *et al.* 2006, Soudani *et al.* 2012). As a result, one of the pressing questions in phenological research is how phenological estimates taken at different scales compare to one another (Friedl *et al.* 1994, Reed *et al.* 2009). This is particularly relevant for grasslands, where variability in spatial scales of field measurements can be problematic (Klimeš 2003).

5.1.5 Aims

This study uses a combination of monthly field measurements and remote data sources to capture information on grassland land surface phenology. It aims to:

- identify changes in biophysical characteristics that cause changes to grassland land surface phenology;
- identify key phenological features of temperate grassland types, particularly C_3 and C_4 grasslands;
- compare ground-based methods and remote-sensing methods of capturing vegetation dynamics;
- explore the differentiation of grassland study types based on remote sensing; and
- evaluate the utility of phenocams for capturing vegetation dynamics in a temperate grassland system.

5.2 MATERIALS AND METHODS

5.2.1 Experimental design and study sites

The twelve sites used for this study are described in detail in Chapter 4, and represent a range of grassland functional types found throughout the temperate region. Their fundamental characteristics are reproduced in Table 5.1, and their location presented as Figure 5.1. Three sites are represented from each functional type: grasslands dominated by C_4 native grasses ('C_4 Native'), C_3 native grasses ('C_3 Native'), C_4 exotic grasses ('C_4 Exotic') and C_3 exotic grasses ('C_3 Exotic'). It should be noted that each grassland type contains minor but dynamic components of species outside the functional group. For example, C_4 Native sites may contain a minor fraction of C_3 native grasses and exotic species. C_3 forbs occur in most grasslands but usually represent a minor fraction of the total vegetation cover.

Most sites were sampled each month from May 2014 to April 2015, however three sites (IN17, MPON and MPOE) did not commence until July 2014 due to access issues.

Table 5.1. Summary of temperate grassland field sites. Full details of these sites (including floristic composition) are presented in Chapter 4.

Field Site Name	Field Site Code	Grass Dominance	C_3/C_4 Dominance
Mullunggari Nature Reserve	MGAR	Native	C_3
Gungaderra Grassland Reserve (native paddock)	GUNN	Native	C_3
Mulloon Creek Natural Farms (native paddock)	MULN	Native	C_3
Gidleigh Travelling Stock Reserve	GIDL	Native	C_4
Turallo Nature Reserve	TURA	Native	C_4
Millpost Farm (native paddock)	MPON	Native	C_4
Mulloon Creek Natural Farms (exotic paddock)	MULE	Exotic	C_3
Gungaderra Grassland Reserve (exotic paddock)	GUNE	Exotic	C_3
Millpost Farm (exotic paddock)	MPOE	Exotic	C_3
Scottsdale Bush Heritage Reserve	SCOT	Exotic	C_4
Ingelara Farm	INGE	Exotic	C_4
Ingelara Paddock 17	IN17	Exotic	C_4

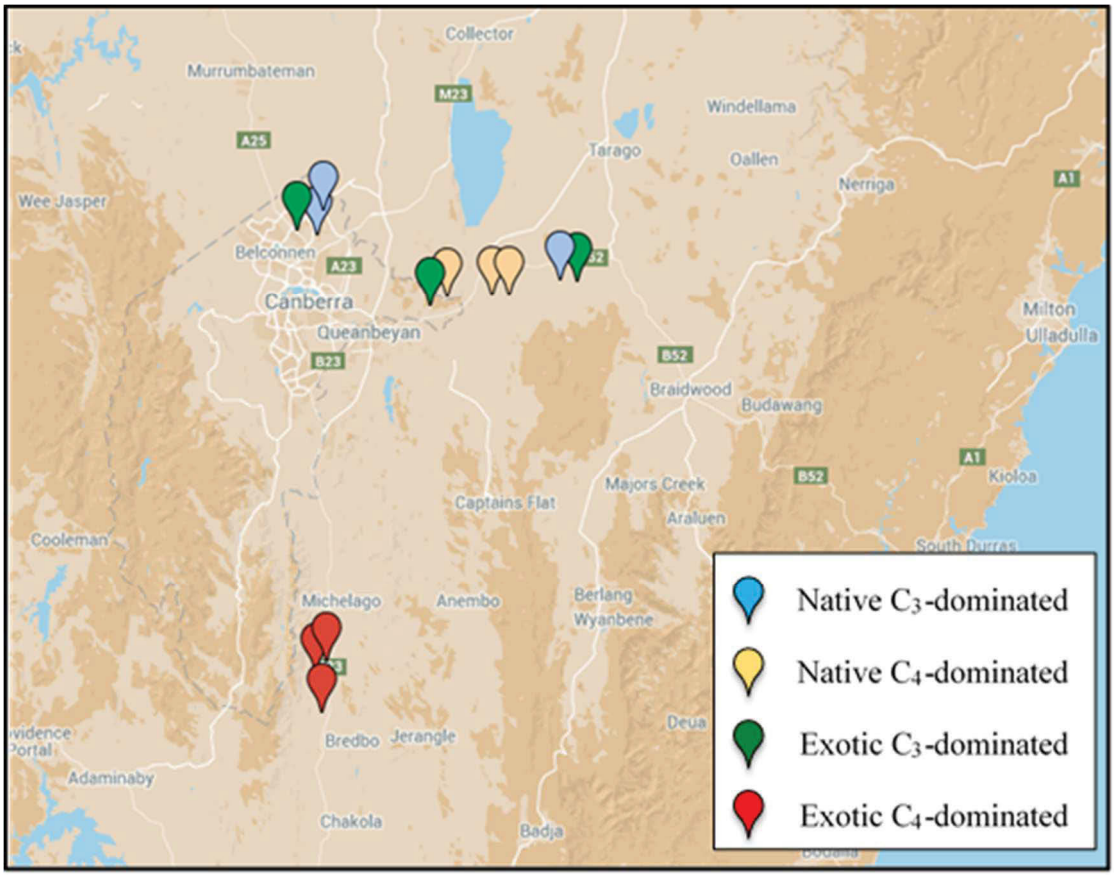

Figure 5.1. Location of grassland study sites in the South Eastern Highlands region of NSW.

5.2.2 Satellite phenology data sources

Satellite data was obtained from three sources: the MODIS (MODerate resolution Imaging Spectrometer) sensor aboard the Terra satellite, the Operational Land Imager (OLI) sensor aboard Landsat 8, and the Enhanced Thematic Mapper Plus (ETM+) sensor on Landsat 7.

The Terra MODIS 16-day composite NDVI (MOD13Q1) at 250 m spatial resolution was downloaded from the NASA Land Processes Distributed Active Archive Centre (http://e4ftl01.cr.usgs.gov/). The data were filtered based on the quality assurance (QA) flags provided in the quality control (QC) layers of the product. The MOD13Q1 product is a 16-day maximum composite NDVI for the period May 1, 2014 to April 30, 2015. This product is processed for atmospheric effects and BRDF (Bidirectional Reflectance Distribution Function) to standardise differences due to viewing and illumination angles. The 16-day composite data reduces impact of cloud cover on long-term data

sets, though at the expense of higher temporal resolution. Due to the relatively small size of most grassland patches, one pixel (250 m x 250 m) was used for analysis. Pilot studies determined NDVI to be the most appropriate vegetation index for this vegetation type, as many of the limitations attributed to NDVI (e.g. saturation, soil effects) do not apply to temperate Australian grasslands. NDVI was calculated as per Equation 6.1, using the bands specified in Table 5.2.

$$NDVI = \frac{\rho RED - \rho NIR}{\rho RED + \rho NIR} \quad (5.1)$$

Landsat data was obtained from the Climate Data Record (CDR) surface reflectance from the Science Processing Architecture System of USGS Earth Resources Observation and Science (EROS) Centre (http://espa.cr.usgs.gov/). This data is also corrected for atmospheric effects and BRDF. Landsat 7 and 8 data is collected at a nominal 16-day frequency, however this is subject to effects of clouds that can reduce or eliminate the usability of parts of an image. As such, temporal resolution frequently extends beyond 16 days. To capture a similar area as MODIS data sources, a 5 x 5 grid of Landsat pixels was used (each 30 m x 30 m) resulting in a total area of 150 m x 150 m. NDVI was calculated as per Equation 5.1, using the bands specified in Table 5.2. Landsat 7 and Landsat 8 data was combined into the one NDVI time series.

Table 5.2. Satellite sensor spectral bands used for the calculation of NDVI.

Sensor	Satellite	Red (RED)	Near Infrared (NIR)
MODIS	Terra	Band 1 (620–670 nm)	Band 2 (841–876 nm)
OLI	Landsat 8	Band 4 (640–670 nm)	Band 5: (850–880 nm)
ETM+	Landsat 7	Band 3 (630–690 nm)	Band 4 (770–900 nm)

5.2.3 Time-lapse digital photography

At each site, a Wingscapes™ time-lapse RGB camera ('phenocam') was installed to capture the changes to the vegetation at a high temporal capacity. These cameras are contained in a weatherproof housing and have favourably compared with more sophisticated phenocam systems (Sonnentag *et al.* 2012). The phenocam was mounted on a post 2.3 m above ground level and was angled approximately 15 degrees from

horizontal (refer to Figure 5.2). The ideal field-of-view (FOV) included the horizon in the picture but only a small quantity of sky, i.e. the majority of the scene was the target area of grassland. This FOV captured an area of between 2 and 4 hectares, with the precise area being dependent on the topography of the study site. Each phenocam was positioned to face south to reduce variability between sites and to minimise the impacts of sun glint on the images.

At two sites, phenocams were mounted in nadir-viewing positions to compare the effect of camera angle on visual greenness indices.

Figure 5.2. Positioning of phenocam 2.3 m above ground level, angled approximately 15 degrees from horizontal.

While the camera manufacturer claims the phenocam to be weatherproof, further waterproofing modifications were made, including a plastic rain shelter and the addition of silica gel within the camera housing to absorb moisture. Phenocams were installed with a supplementary solar panel, however the battery life was generally sufficient for the length of the study. Images were collected from the camera at monthly intervals. Although vandalism was considered to be a potential concern, no vandalism occurred throughout the study period.

The phenocams were programmed to take one photograph at hourly intervals between 9:00 and 15:00 Australian Eastern Standard Time. Pilot studies suggested that images captured outside this period were either too dark or too variable to be utilised for phenology purposes. No standardisation of colour was used through the use of reference cards as can be found in similar studies (Ahrends *et al.* 2008, Richardson *et al.* 2009, Sonnentag *et al.* 2012) due to the practical limitations of the equipment configuration: the card would not be in the same plane as the target; preventing the card from becoming contaminated through dust and rainfall was impractical; and the card could not be mounted from the camera without interfering with the image collection. Instead it was assumed that because the cameras were all from the same manufacturing batch, the sensors within each camera were equivalent. Therefore, any colour balance drift or sensor degradation would occur at the same rate. Colour balance drift has been reported in a study using phenocams (Ide and Oguma 2010) however this only became apparent after two years of use. As such, no significant colour balance drift is assumed for this study.

5.2.4 Field measurements

Field measurements were collected monthly from each study site. These measurements included pasture height and vegetative fractional cover using non-destructive methods, and aboveground biomass using destructive harvesting.

5.2.4.1 Pasture height

Pasture height is a measure of the growth of the dominant grass species, and has been strongly correlated with biomass and vegetation indices in grassland ecosystems (Lopez

Diaz and Gonzalez Rodriguez 2003). Monthly pasture height was collected using the falling plate method (Frame 1993, Rayburn and Rayburn 1998). A 100 m transect was established at each location and height measures taken every 5 m, resulting in 20 measurements. The average of these height measurements was used in calculations.

5.2.4.2 Fractional cover

Fractional cover refers to the proportion of the ground surface covered by photosynthetic ('green') vegetation (f_{PV}); non-photosynthetic ('brown') vegetation, (f_{NPV}) or background material such as soil (f_{BG}). Each component of fractional cover is represented as a percentage. Temperate Australian grasslands tend to retain a high proportion of standing litter (Tremont and McIntyre 1994), so f_{BG} is generally quite low unless disturbance has removed all vegetation (e.g. fire or vegetation clearing).

Monthly measures of fractional cover were taken using a step-toe method (NSW Catchment Management Authority 2005). During each measurement event, one 100 m transect was established across a representative part of the study site. The transect was traversed at 1 m intervals, and the fractional cover status at that point was noted. Summing the total resulted in a proportional fractional cover for each component. For quality control purposes, a duplicate transect was measured at least once during each sampling run (i.e. 1 duplicate for every 12 transects). If the duplicate was found to be within 10% of the original, the average of the two was applied. If the duplicate exceeded this threshold, a third transect was to be measured. However for all sampling events the duplicate was within 10% of the original, implying confidence in the repeatability of this method.

5.2.4.3 Biomass harvesting

Vegetative biomass is representative of an ecosystem's productivity; that is, the amount of carbon fixed through photosynthesis (Lauenroth *et al.* 1986). Monitoring of aboveground biomass through destructive harvesting is a routine method for determining productivity and validating estimates made through non-direct methods. (Brummer *et al.* 1994, Lopez Diaz and Gonzalez Rodriguez 2003).

At each site, total biomass was harvested by clipping all vegetation within six replicates of 1 m^2 quadrats to approximately 1 cm above ground level. The location of each quadrat was randomly selected at each visit, with GPS locations recorded at each time to ensure subsequent samples were not taken from the same place. These samples were stored in a plastic bag in a cool environment (a cooler in the field and a refrigerator in the laboratory) prior to processing to ensure that degradation of the vegetation did not occur. Processing was completed within 5 days of collection.

5.2.5 Processing and analysis

5.2.5.1 Biomass processing

Biomass samples were subsampled at 25% (i.e. one quarter of the original sample) to allow timely processing of all samples and minimise chlorophyll and structural degradation within tissues. Vegetation was separated into four components: photosynthetic graminoids ('live grass') photosynthetic forbs ('live forbs'), non-photosynthetic graminoids ('dead grass') and non-photosynthetic forbs ('dead forbs'). These components were placed in paper bags and oven-dried at 60 ºC for 72 hours. Dry vegetation was weighed to 3 decimal places and converted to kg/ha.

5.2.5.2 Statistical analysis

Data processing and analysis was conducted using the R software package (R Core Team 2013). Raw time-series data were suitable for comparison and analysis, however curves were fitted to some data using non-parametric Locally Weighted Scatterplot Smoothing (LOESS) to assist in visualisation of trends (Cleveland 1979). For comparison and correlation of different data sources, data was subset to the coarsest frequency (i.e. monthly).

5.2.6 Phenocam processing and analysis

Viable images were processed using ImageJ image processing software. Each image was decomposed into nine 'regions of interest' (ROIs) that represented three from the foreground, three from the midground and three from the background of the image grassland component (refer to Figure 5.3).

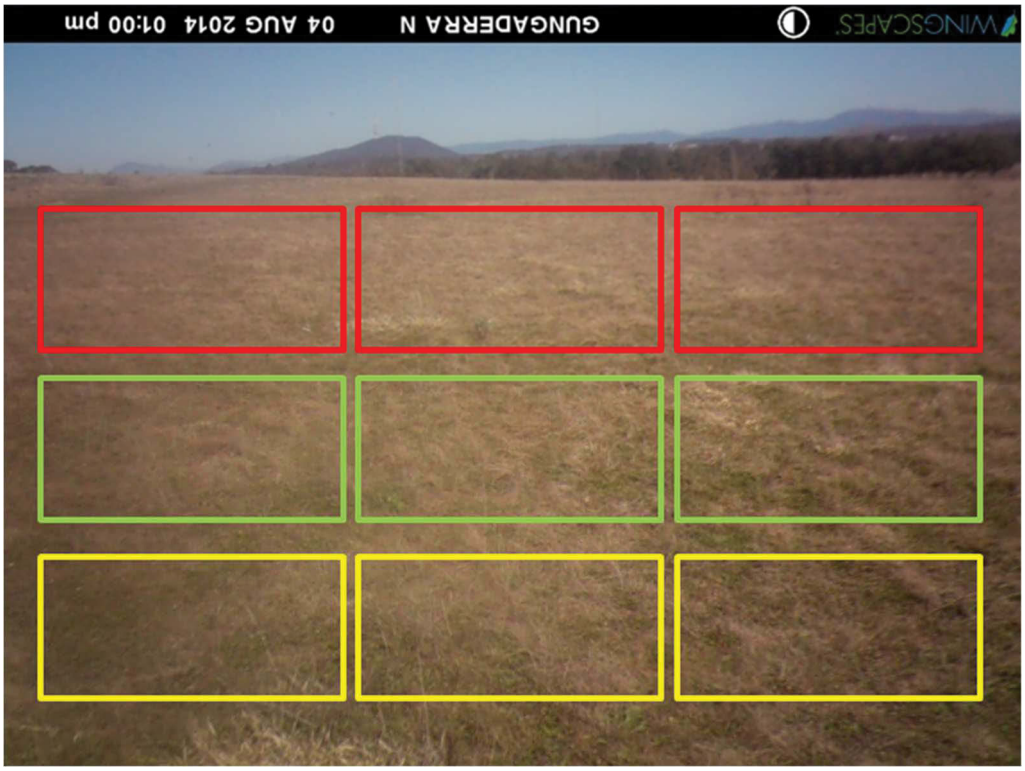

Figure 5.3. Representative phenocam image showing nine regions of interest (ROIs) used for image analysis. ROIs are separated into background (red), midground (green) and foreground (yellow).

This study used the Green Chromatic Coordinate (g_{CC}) as a vegetation index to monitor plot greenness. The g_{CC} is presented as equation 5.2 and is the relative brightness of the green fraction compared to the sum of the green, red and blue fractions (Gillespie *et al.* 1987, Sonnentag *et al.* 2012). The g_{CC} is a unitless index that pilot studies suggest ranges between 0.25 (no green vegetation) and 0.5 (abundant green vegetation) in temperate grassland systems. A variety of phenocam-based studies have preferentially used this index because of its dynamic response to changes in plant biophysical variables. The g_{CC} also shows robustness to variations in image brightness due to sky conditions, time of day or shadowing (Ide and Oguma 2010, Sonnentag *et al.* 2012, Julitta *et al.* 2014).

$$g_{CC} = \frac{G}{R + G + B} \tag{5.2}$$

(Gillespie *et al.* 1987, Sonnentag *et al.* 2012)

To generate the g_{CC} for each region, images were separated into their red, green and blue channels, and the pixel brightness of each channel was computed. The average pixel brightness was generated for each ROI.

Data summary and graphical interpretation was conducted with the R software package (R Core Team 2013). The g_{CC} values were calculated for each ROI. The mean g_{CC} was used for each hourly data point and was used to establish a daily time series, known as a phenology profile.

During pilot studies it was noted that the magnitude of g_{CC} was likely to be impacted by illumination effects and the camera angle. Appendix D illustrates the effect that time-of-day has on g_{CC}. Phenology profiles of foreground, midground and background ROIs are presented as Appendix E to compare the effect of camera angle on the g_{CC}.

5.2.7 Separation of grassland functional types through phenology data

Although many methods exist for the separation of vegetation types via phenological characteristics (e.g. de Beurs and Henebry 2010; Davidson and Csillag 2003; Wang *et al*. 2013), these utilise phenology metrics that are unsuitable for use in Australian temperate systems. As such, an alternative method was explored using the segmentation of mean g_{CC} phenocam data into seasonal datasets. The variability of climate in temperate Australia means that greening-up periods often occur with a large temporal window, rather than at a predictable time of year, hence the use of seasonal statistics may capture these changes more reliably.

Mean daily phenocam g_{CC} for each site was separated into the following seasons:

- Autumn (May 2014, March 2015, April 2015)
- Winter (June–August 2014)
- Spring (September–November 2014)
- Summer (December 2014–February 2015)

Several statistical parameters based on traditional phenological metrics were assessed. For each seasonal g_{CC} dataset, the mean, maximum, minimum, amplitude and variance were calculated. These values were ordinally grouped to determine if separation between groups could be identified that corresponded to biologically explicit changes. In addition, principal component analysis (PCA) was performed on these groupings and statistics.

5.3 RESULTS

5.3.1 Biomass breakdown

Monthly biomass measurement of live grass, dead grass, live forbs and dead forbs is presented in Figure 5.4. Live biomass (i.e. the sum of live grass and live forbs) were combined by grassland functional type and is presented in Figure 5.5.

Live grass biomass varied considerably between sites and between months at the same site. Exotic sites tended to have the greater quantity of mean live biomass, with GUNE (maximum = 2,769 kg/ha), IN17 (2,870 kg/ha) and INGE (2,284 kg/ha) recording the highest values.

The mean live biomass for C_4 Native sites never exceeded 1000 kg/ha, and C_3 Native sites never exceeded 500 kg/ha. C_4 Exotic sites had higher live biomass during the summer months than the winter months. C_3 Exotic sites fluctuated throughout the year in response to grazing pressures and seasonal drivers, particularly periods of low rainfall. Sites that were dominated by C_4 species had low quantities of live biomass during the winter months to a mean minimum of 134 kg/ha, though notably this was still above zero. The key features of the C_3 biomass pattern are an increase in September which reaches a peak in November (mean live biomass 1,536 kg/ha for exotic; 586 kg/ha for native). The C_4 sites commenced green-up a month later, in October, and reached a peak in December which was sustained through the summer (1,438 kg/ha exotic; 922 kg/ha native). C_4 Exotic sites showed an additional peak in late summer (February; mean live biomass 2026 kg/ha) though this was largely driven by one site and the associated standard deviation is very large.

Dead biomass (Figure 5.6) was greatest in C_4-dominated sites, particularly SCOT (exotic; peak dead biomass of 9,240 kg/ha), GIDL (native; 4,893 kg/ha) and TURA (native; 6,233 kg/ha). This accumulation of dead material is driven by minimal grazing at these sites and little other disturbance. C_4-dominated sites tended to have a higher biomass during the winter months but exhibited a very high variability between sites and replicates. C_3 Native sites had a consistent quantity of dead biomass throughout the

year, but C_3 Exotic sites were more variable. In C_4-dominated sites the dead biomass was much greater than live biomass throughout the year.

Live forbs and dead forbs contributed a very minor proportion of the overall biomass. On a site-by-site basis however, live forbs contributed a reasonable proportion of the total biomass on occasions where exotic forbs (e.g. *Trifolium* spp.) were abundant and grass coverage was low.

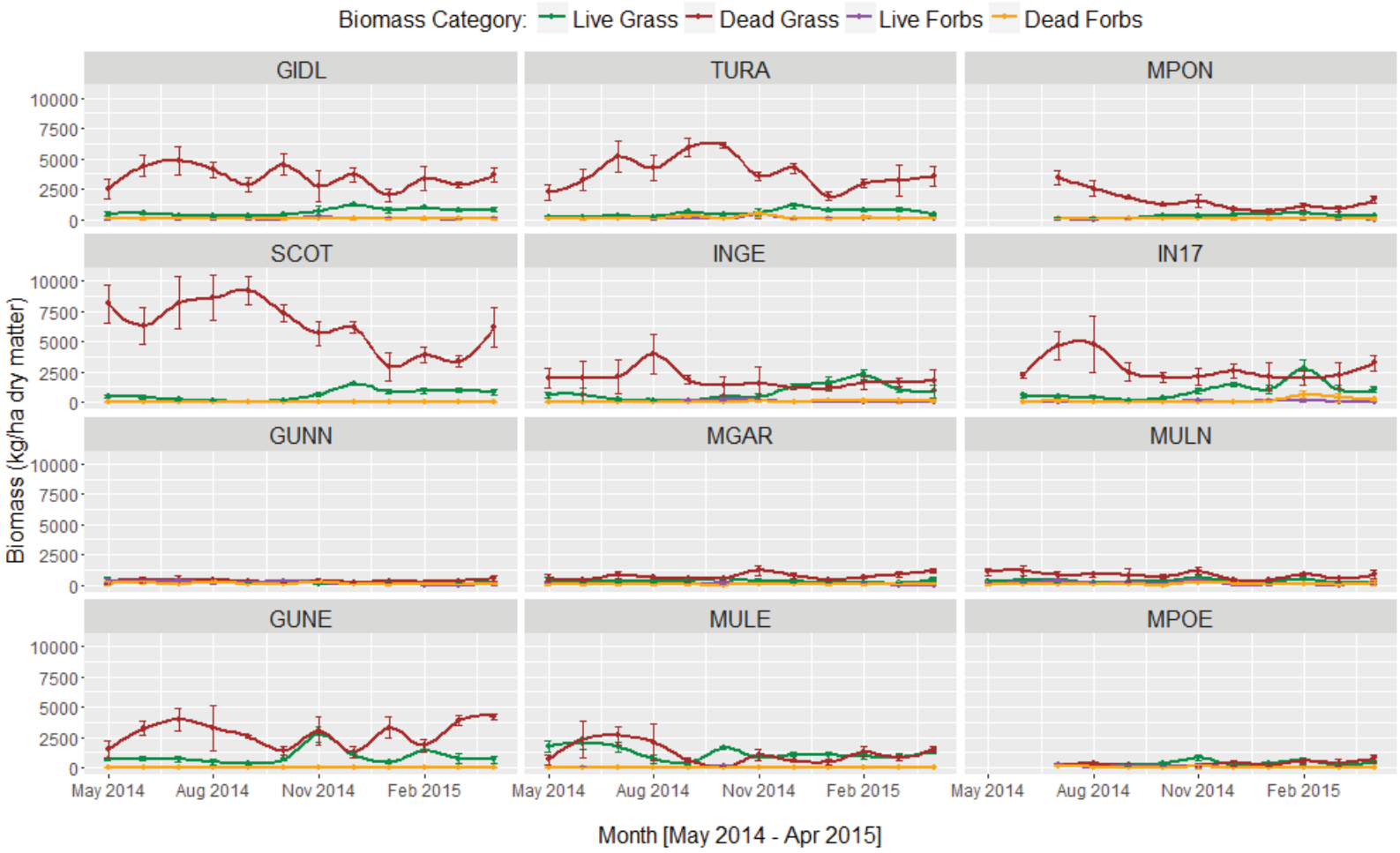

Figure 5.4. Mean monthly dry biomass (kg/ha; n = 6) at each location, separated into live grass, dead grass, live forbs and dead forbs (± s.d.).

228

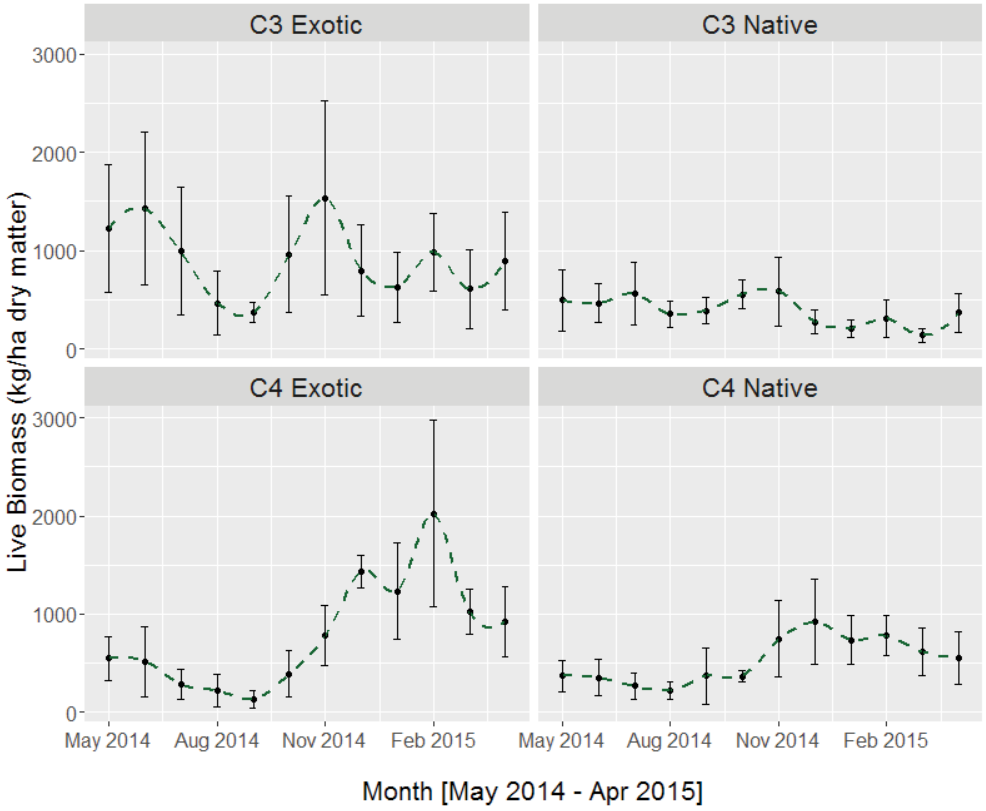

Figure 5.5. Mean monthly live biomass (kg/ha ± s.d.; n = 18) by functional type.

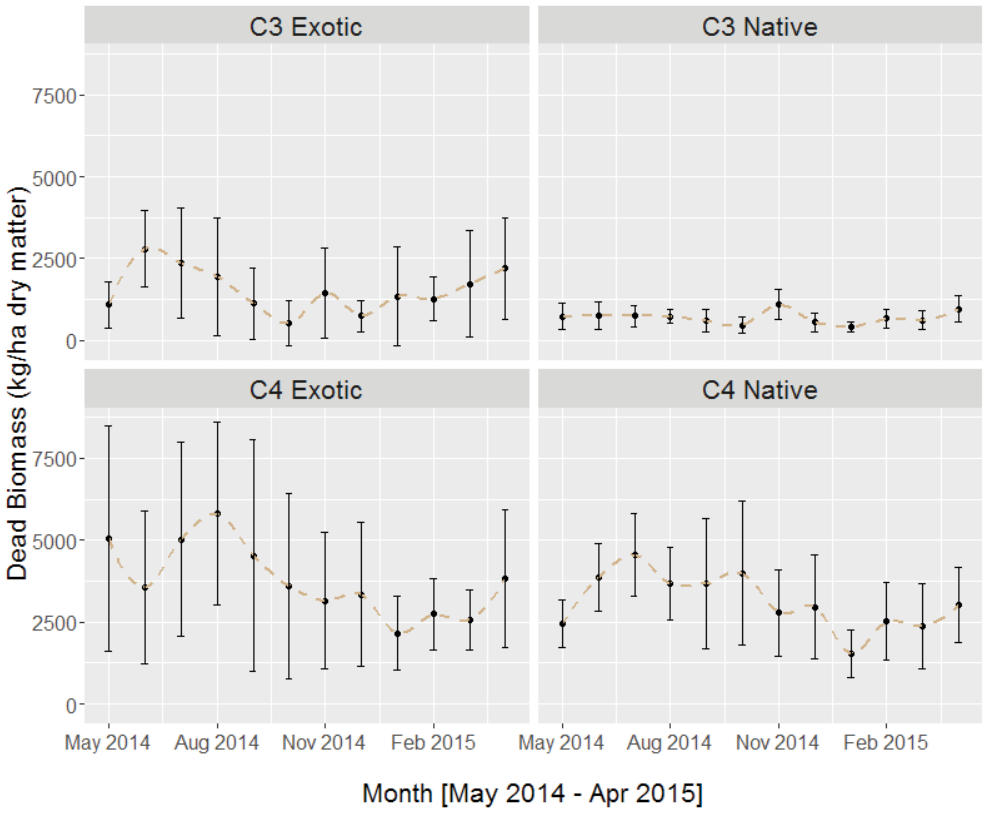

Figure 5.6. Monthly dead biomass (kg/ha ± s.d.; n = 18) by functional type.

5.3.2 Grassland height

Figure 5.7 shows the patterns of mean monthly height by functional group. Figure 5.8 represents the mean monthly height for the twelve sites included in this study. Patterns of pasture height were extremely variable between sites. Some sites though, particularly native-dominated, were consistent throughout the year. C_3 Native sites ranged between 10 cm and 20 cm height, and C_4 Native sites measured between 18 cm and 30 cm height. Exotic sites exhibited much more variation throughout the year and between sites. Exotic grasslands were typically taller: the maximum mean height of 60 cm was measured at GUNE in February 2015. However this was not always the case, with one C_3 Exotic site (MPOE) much shorter than the others (mean maximum of 20 cm).

Overall patterns showed C_3 Exotic sites to attain maximum height in January (mean height of 48 cm), however inter-site variability was extremely high. C_3 Native heights peaked in December (mean height of 12 cm). C_4 Exotic sites peaked in December (30.5 cm) but retained that height throughout the summer. C_4 Native sites had a peak height in February (mean maximum = 21 cm).

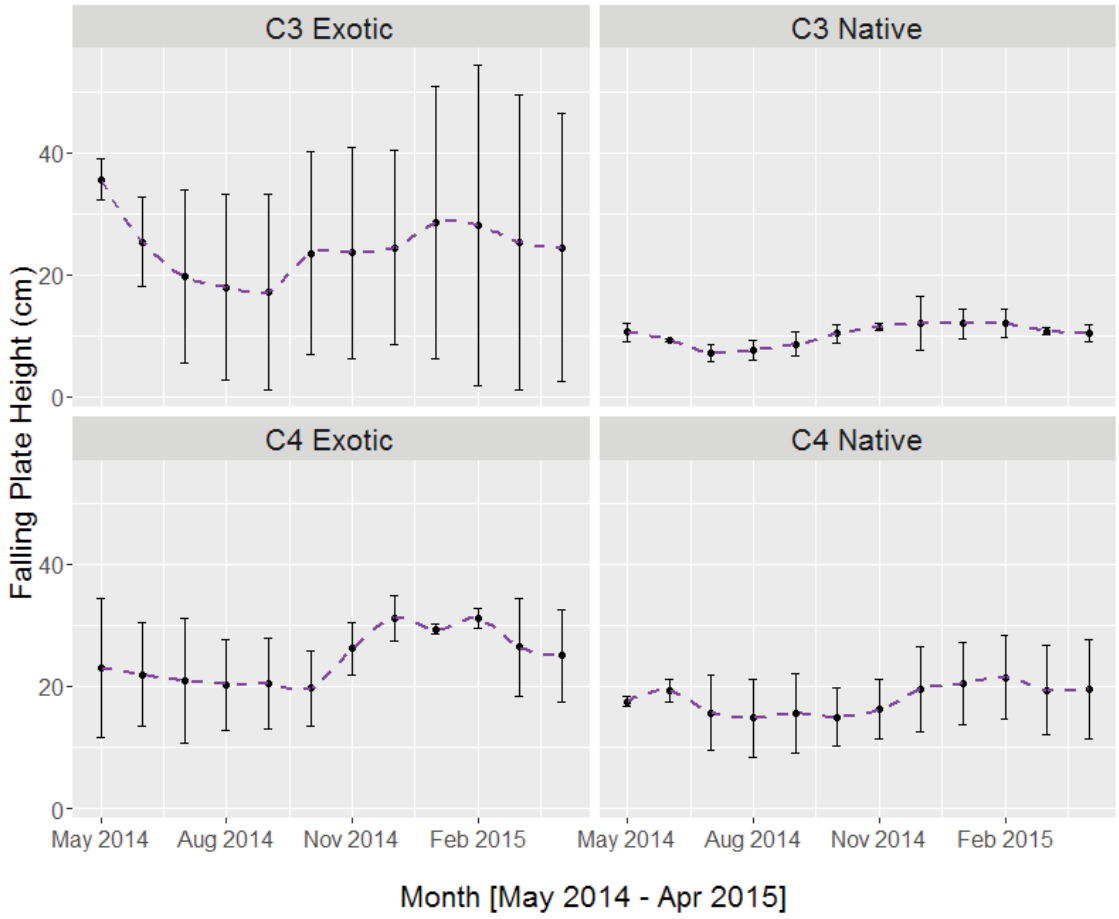

Figure 5.7. Mean monthly pasture height (cm of falling plate height ± s.d.; n = 60), by grassland functional type.

5.3.3 Fractional cover

All sites showed distinct changes in fractional cover throughout the year, as illustrated by Figure 5.9, with periods of high f_{PV} cover and periods of high f_{NPV} cover. The contribution of the background substrate was negligible at all sites. As such, the f_{NPV} represents the inverse of the f_{PV}.

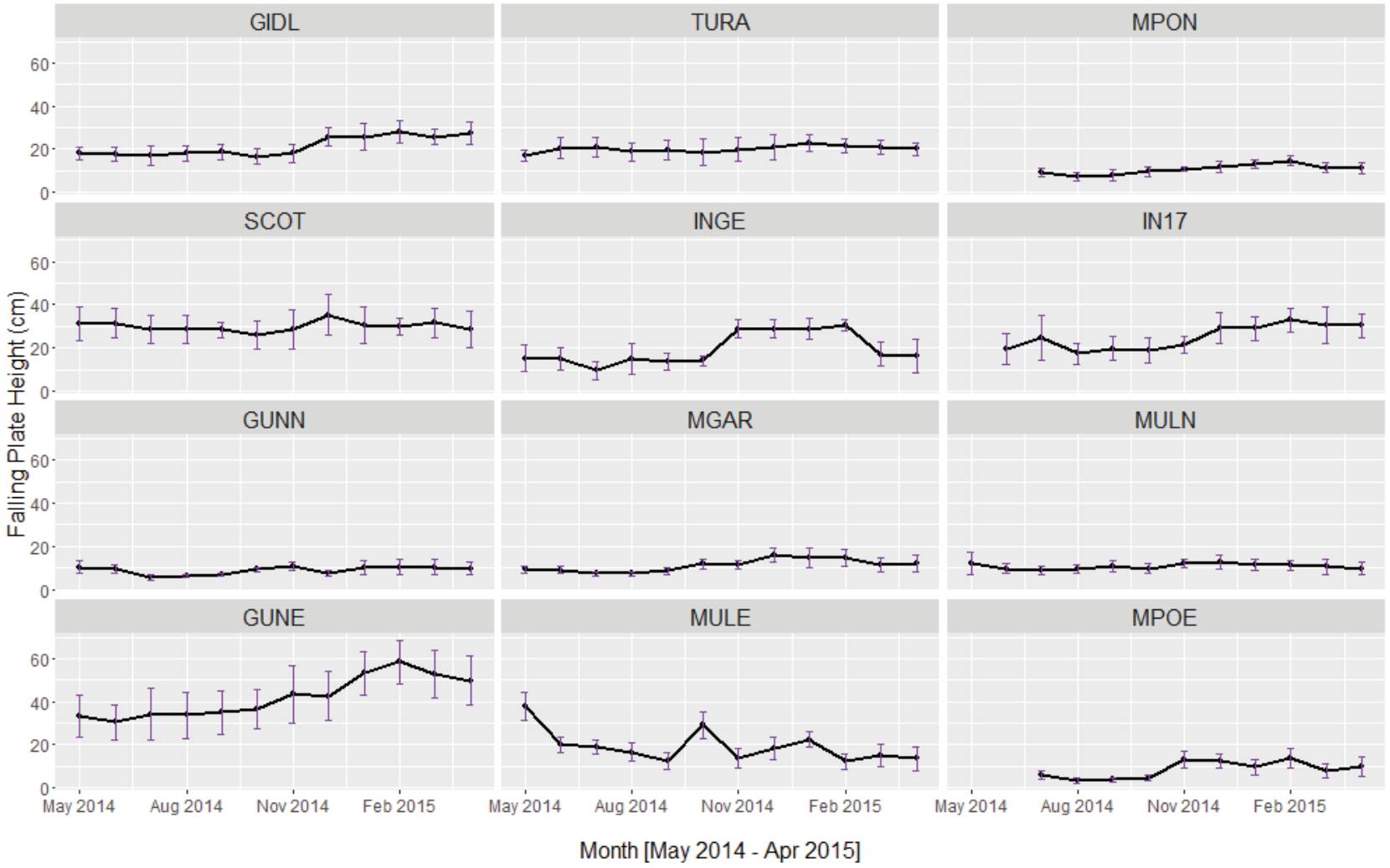

Figure 5.8. Mean monthly grassland height (cm of falling plate height; n = 20) at 12 grassland locations.

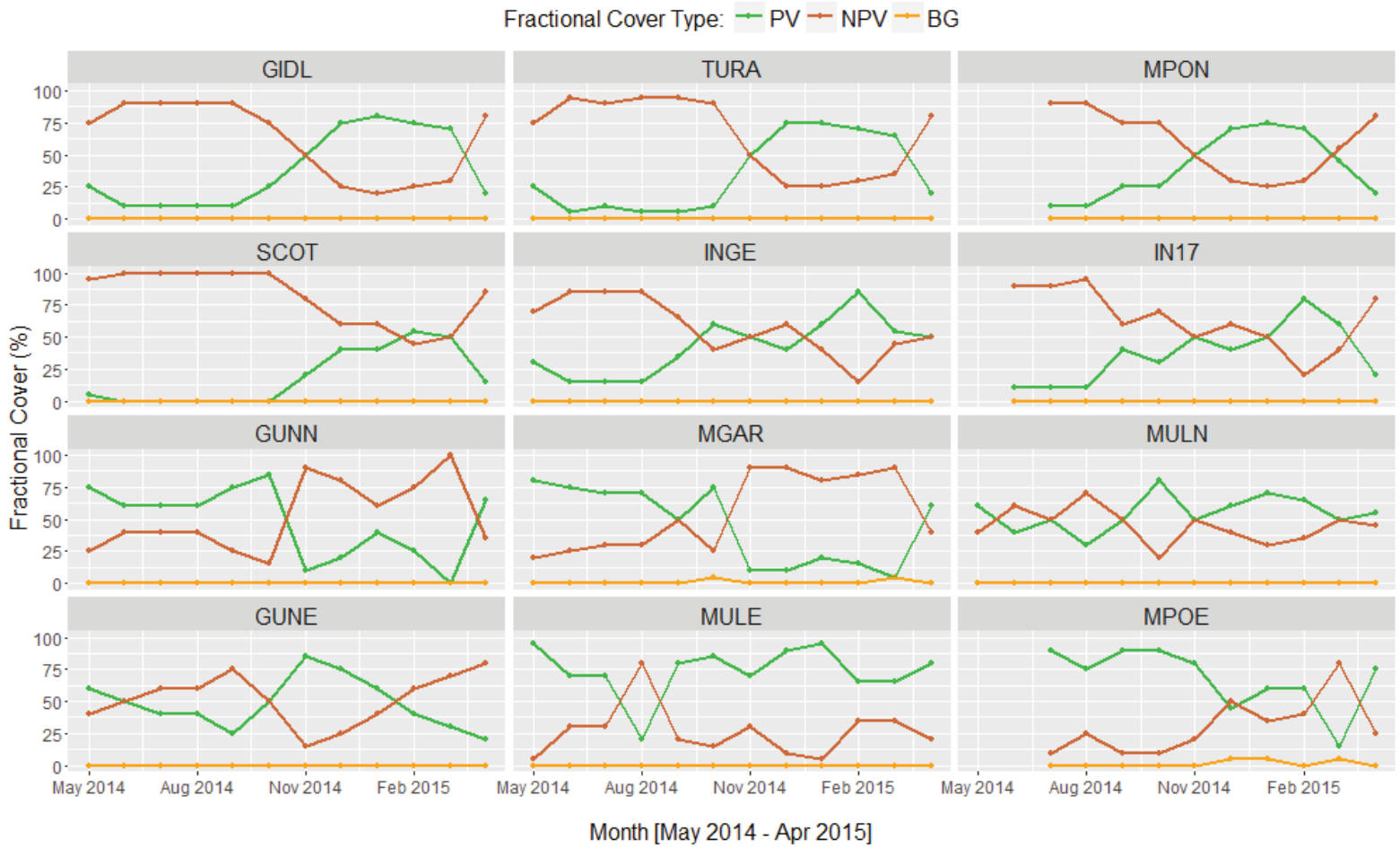

Figure 5.9. Monthly fractional cover (%), presented by site. Fractional cover is separated into photosynthetic vegetation fraction (f_{PV}), non-photosynthetic vegetation fraction (f_{NPV}) and background fraction (f_{BG}).

Figure 5.10 illustrates the mean f_{PV} for each functional type. C_4 Native sites demonstrate particularly distinctive and predictable patterns, with low f_{PV} during the winter months, rapid greening in October, and a peak of 75% f_{PV} maintained from December to February. After March, the f_{PV} decreases quickly to 20%. Variation within C_4 Native sites is low. C_4 Exotic grasslands have a similar pattern, though with greater variation between sites; low f_{PV} (approximately 10%) through winter, green-up starting in August with a steady increase to November, and a rapid rise to a peak of 75% in February. Similar to live biomass patterns for this group, this apparent 'double peak' is driven by different patterns within the group. C_3 Native sites show a high variability throughout the year, with a peak of 80% f_{PV} in October and minima in November and March corresponding with high temperatures and low rainfall. C_3 Exotic sites show less variability than C_3 Native sites, suggesting that they more robust to environmental changes. Peak f_{PV} is in November (76%) though high f_{PV} is maintained from September through January. The minimum f_{PV} occurs in March for C_3 Native and C_3 Exotic groups.

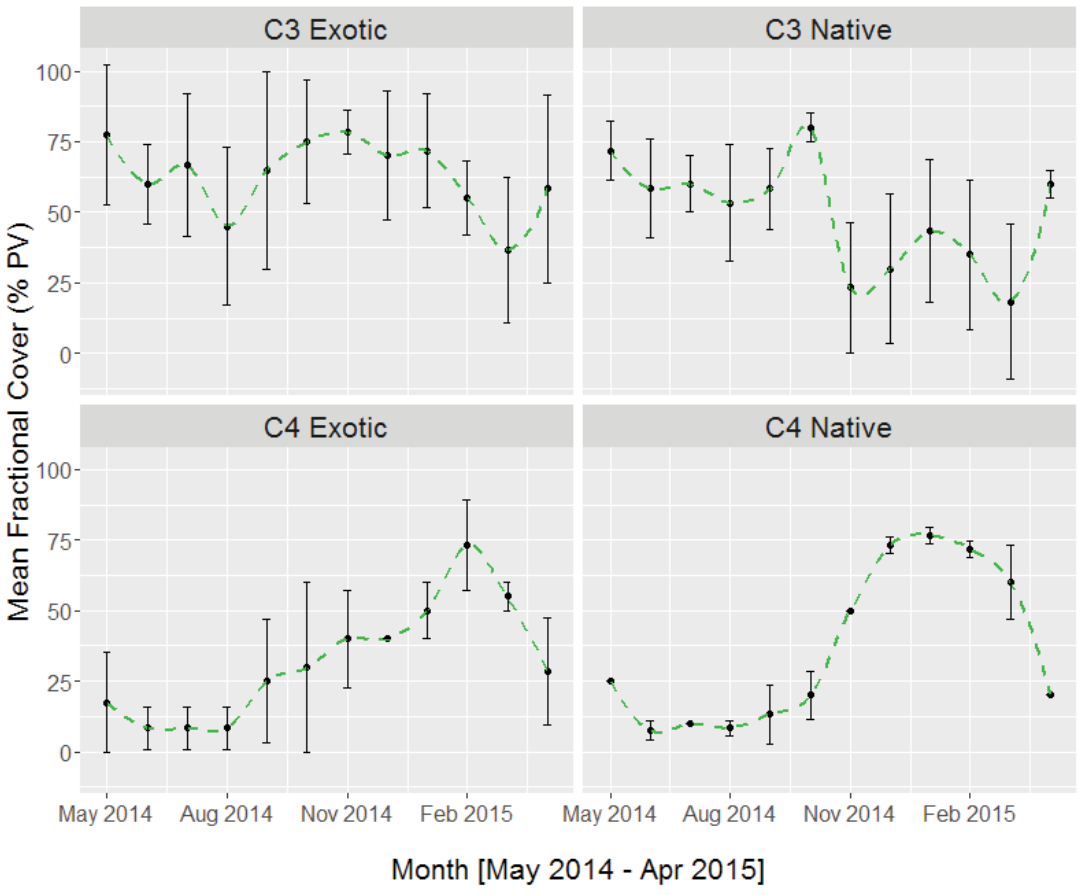

Figure 5.10. Monthly mean photosynthetic fraction (f_{PV}, n = 3), presented by grassland functional type.

5.3.4 Phenocams

5.3.4.1 Evaluation of phenocam data

Overall, the quality of the phenocam images and the reliability of the hardware were considered suitable for the objectives of this project. The cameras were found to be vulnerable to water ingress and lens fogging, particularly during the winter months. This required all images to undergo a comprehensive quality control procedure prior to processing and analysis. Issues with image quality arose when:

- the FOV was obscured by rain, animals or objects;
- the FOV was altered due to the camera having moved. This was usually minor and caused by wind or soil subsidence, though occasionally was major due to animals rubbing against the support post;
- weather conditions prevented the vegetation being viewed throughout the FOV, specifically fog, frost or smoke;
- unusual lighting was present; either as a result of the image being too dark (e.g. during thunderstorms or late in winter), where too much diffuse sky was visible in the image, or through excessive shadowing.
- the camera lens was fogged from the inside. This was typical following water ingress, and was most apparent in early-morning images.

Occasional hardware or power failure also resulted in data gaps in the image time series. Of the 29,295 potential images, a total of 23,512 images were retained for analysis. This represents a capture success rate of 80.2%.

Table 5.3 shows the percentage of days for each site that had viable images used for analysis. Across all sites, 64.9% of days had at least one viable image.

Table 5.3. Phenocam data availability for each site, based on the proportion of days that had viable imagery.

Site	Days Recorded	Number of days with viable image(s)	Percentage of days with viable images
MGAR	364	286	78.6
GUNN	364	219	60.2
MULN	362	217	59.9
GIDL	360	263	73.06
TURA	363	224	61.7
MPON	295	225	76.3
MULE	363	290	79.9
GUNE	364	219	60.2
MPOE	295	234	79.3
SCOT	364	164	45.1
INGE	364	201	55.2
IN17	297	156	52.6
TOTAL	**4155**	**2698**	**64.9**

Differences in illumination condition caused by local weather conditions and time of day are known to impact the RGB digital numbers (Inoue *et al.* 2015). However, due to the robust nature of the g_{CC} index to variations in illumination, the magnitude of differences due to time of day was found to be minor. One example phenology profile separating data by time of day is presented as Figure 5.11. Other sites are explored further in Appendix D.

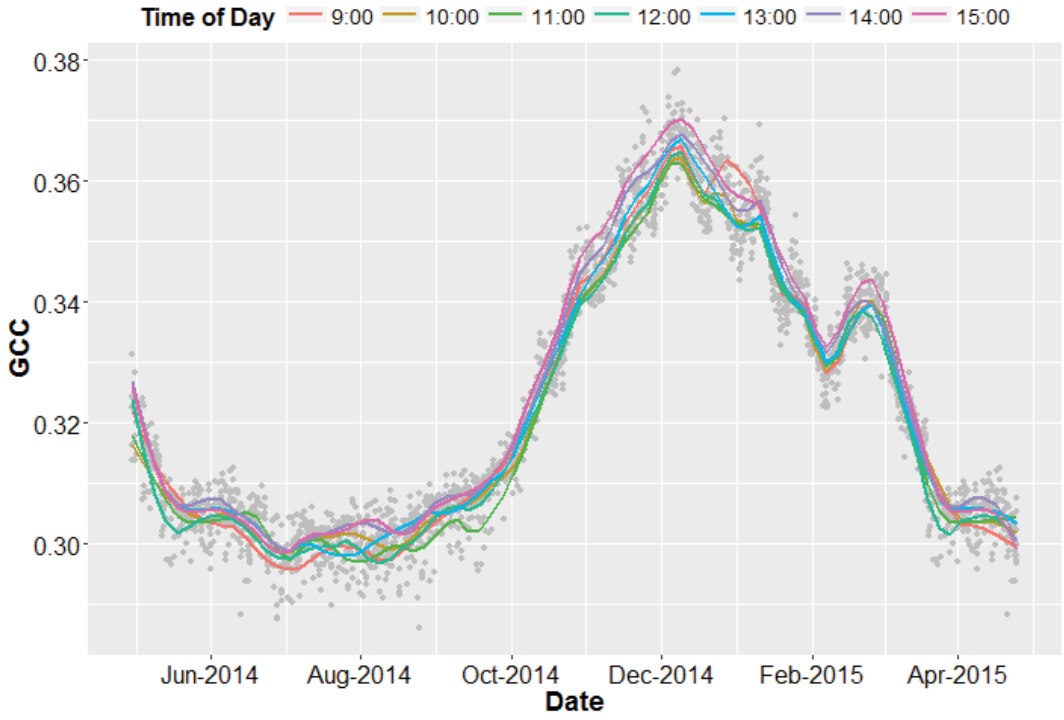

Figure 5.11. Comparison phenology profile of mean time-of-day g_{CC} from site GIDL (C_4 Native). The trend lines are LOESS fitted curves (span = 0.1) for visual comparison of the grouped temporal trends. Each data point is the mean value of 9 ROIs per image.

Differences in relative angle between the camera and the target have rarely been explored in the phenocam literature. This has the potential to be more confounding on RGB digital numbers and greenness indices than illumination effects. Though only minor differences in relative angle were present during this study, preliminary assessment suggests that, like similar studies in the satellite domain, relative view angle does impact the magnitude of g_{CC}. However, the timing and general trends of the curve remain the same. One example of this phenomenon is presented in Figure 5.12; the remainder of sites are explored further in Appendix E.

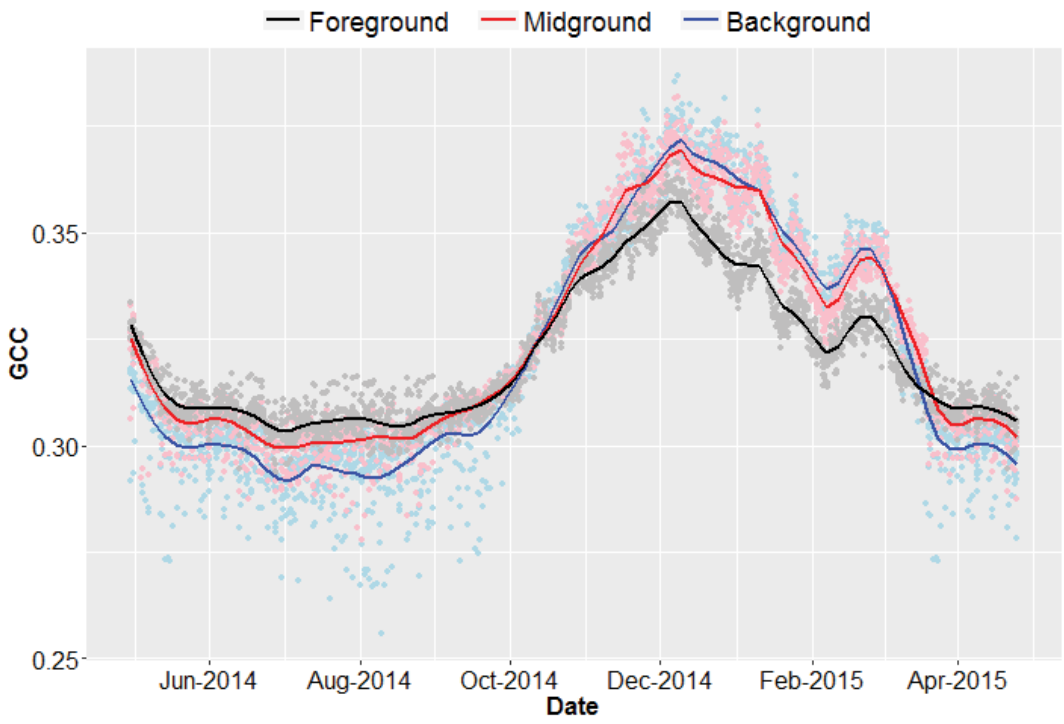

Figure 5.12. Comparison phenology profile of foreground (black), midground (red) and background (blue) g_{CC} from site GIDL (C_4 Native). The trend lines are LOESS fitted curves (span = 0.1) for visual comparison of the grouped temporal trends.

5.3.4.2 Phenology profiles of grassland sites

The series Figure 5.13 to Figure 5.16 show the g_{CC} phenology profiles for the grassland functional groups: C_4 Native, C_4 Exotic, C_3 Native, and C_3 Exotic. In all figures, individual hourly data points are presented. The sub-daily collection of g_{CC} data results in fine-detail phenology profiles that capture rapid changes in greenness.

C_4 Native phenology profiles (Figure 5.13) show a relatively consistent group of profiles, which is comparable to biomass and fractional cover seasonal patterns. All sites have low g_{CC} from May to August, with an indistinct inflection point in late August marking the start of a gradual greening. The sites are variable in their peak timing; MPON is the earliest (late October), while GIDL and TURA are in early December. GIDL has a more distinct peak than the other sites, but all maintain a relatively high g_{CC} through January. A characteristic drop in g_{CC} occurs in February, followed by a short greening period and steady g_{CC} decrease through April.

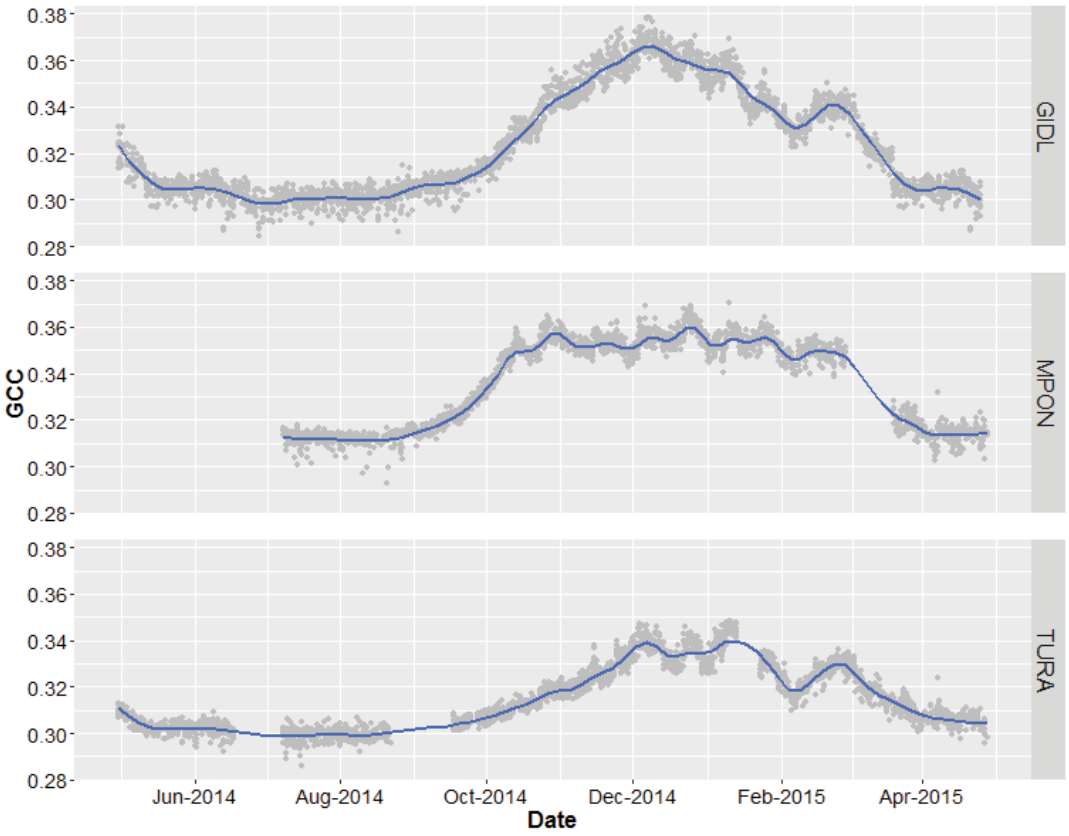

Figure 5.13. Annual g_{CC} phenology profiles at C_4 Native sites GIDL, MPON and TURA. Grey dots represent hourly data points. The blue line is a LOESS fitted curve (span = 0.1) for visual assistance of the temporal trends.

C_4 Exotic profiles (Figure 5.14) show some consistent signatures, but exhibit variability contingent on individual species compositional and structural characteristics. The g_{CC} values tend very low through the winter months, but each site showed a different pattern during spring. IN17 had a steady greening period, consistent with expectations and field measurements for C_4 sites. The IN17 curve is less well pronounced due to the more oblique camera angle with a greater proportion of sky, however has a consistently high g_{CC} throughout the summer, punctuated by minor greening and browning fluctuations. INGE displayed a sharp peak in October typical of C_3 vegetation, however demonstrated more consistent C_4 patterns through the summer. SCOT showed a delayed but very rapid increase in g_{CC}, commencing in November and lagging behind biomass-measured greening by two months. The greenness levels remained consistently high throughout the summer, with minor greening and browning fluctuations in response to environmental conditions. These summer fluctuations have identical timing in all C_4 Exotic profiles.

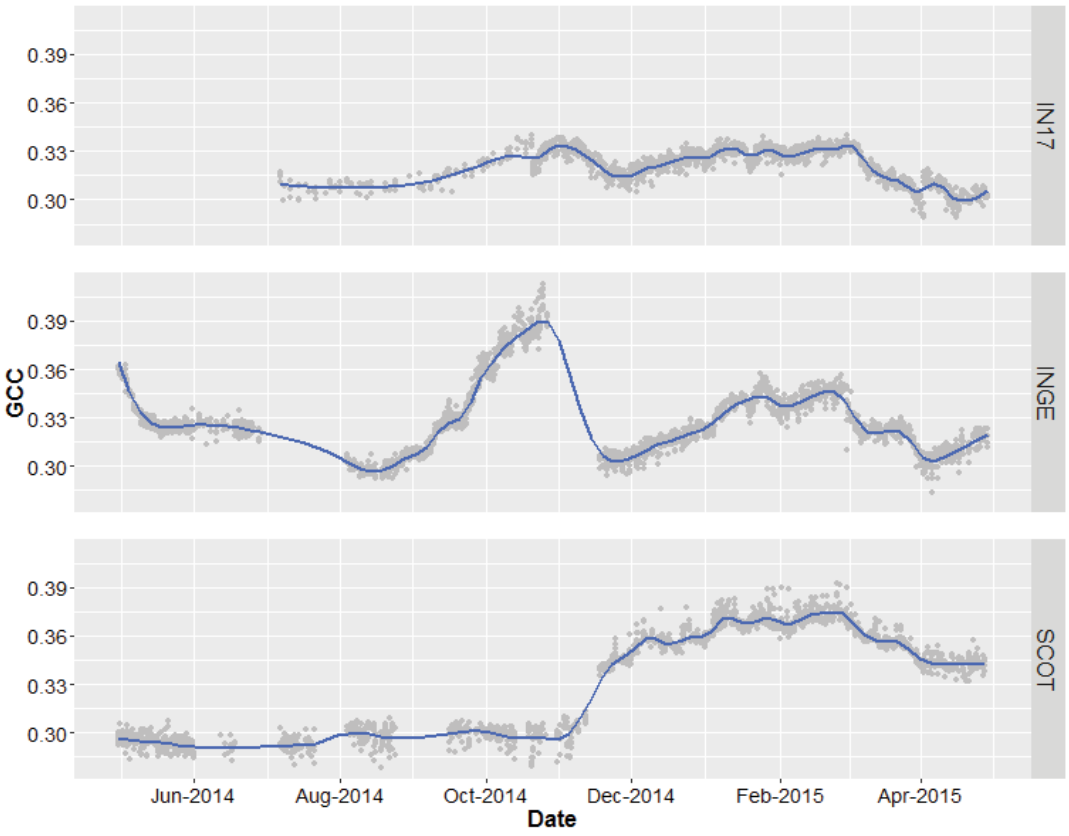

Figure 5.14. Annual g_{CC} phenology profiles at C_4 Exotic sites IN17, INGE and SCOT. Grey dots represent hourly data points. The blue line is a LOESS fitted curve (span = 0.1) for visual assistance of the temporal trends.

C_3 Native profiles (Figure 5.15) show consistency between the sites, with some minor variation reflective of differences in species composition and environmental drivers. All sites demonstrated a gradual decline of g_{CC} from May through to August, though GUNN was more difficult to describe due to extensive data gaps during this period. All sites showed a characteristic 'saw-tooth' greening commencing in August and reaching a peak in late October. The g_{CC} then abruptly decreased in November. Patterns changed marginally between the sites from this point; GUNN showed periods of greening and browning through the summer, whereas MGAR had only one small greening period. However, both showed a steady decline in g_{CC} through February to a minimum in March. MULN had partial elements of a C_4 signature in summer, with a low wide peak from December and reaching a minimum in late March. All C_3 Native sites exhibited a characteristic g_{CC} increase in April.

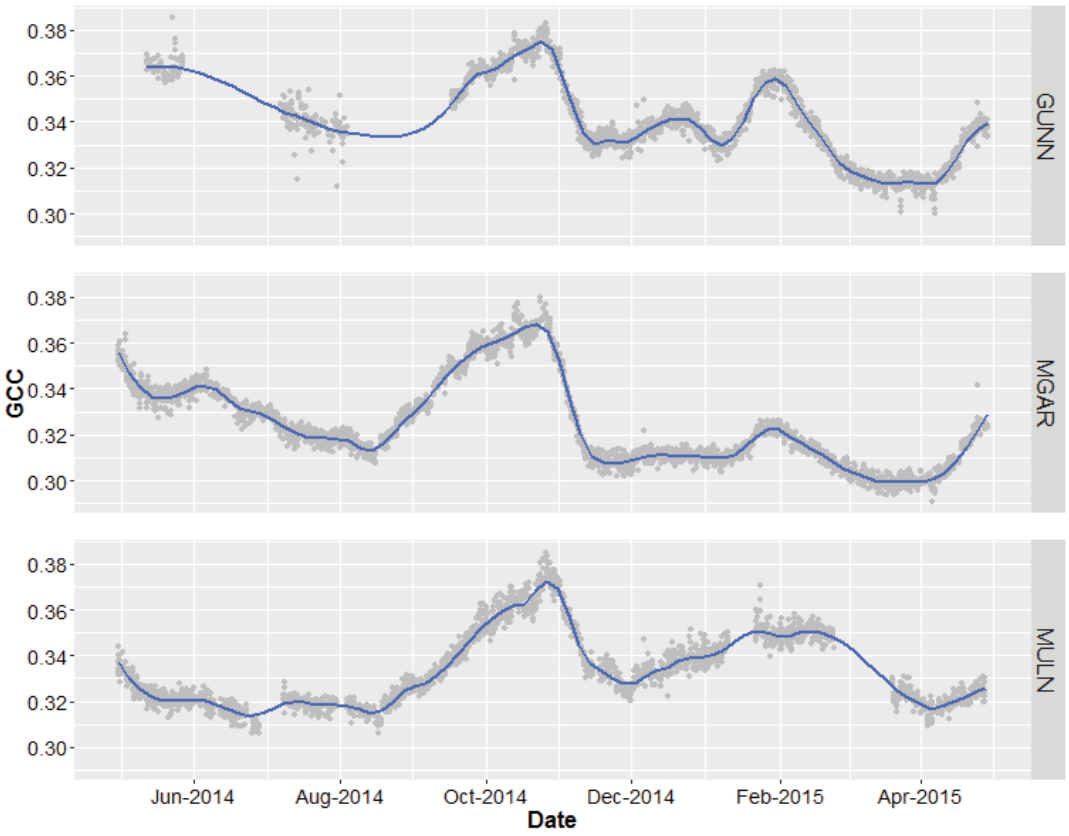

Figure 5.15. Annual g_{CC} phenology profiles at C_3 Native sites GUNN, MGAR and MULN. Grey dots represent hourly data points. The blue line is a LOESS fitted curve (span = 0.1) for visual assistance of the temporal trends.

C_3 Exotic profiles (Figure 5.16) exhibited the most profile variation of the functional groups. GUNE had an almost unimodal profile, increasing in g_{CC} from September, reaching a peak in November, and steadily decreasing to the baseline in January. MPOE had a similar profile to the C_3 Native sites: commencing green-up in August and steadily climbing to a peak in late October, before decreasing in December. Multiple small increases in g_{CC} occur until February, followed by a steady decline through March. MULE shows a steady decline through autumn and winter, with the greening period commencing late August and reaching a peak in mid-October. The sharp decline in November is followed by an increase and consistently high g_{CC} through the summer. The greenness decreases rapidly in February and increases again in April.

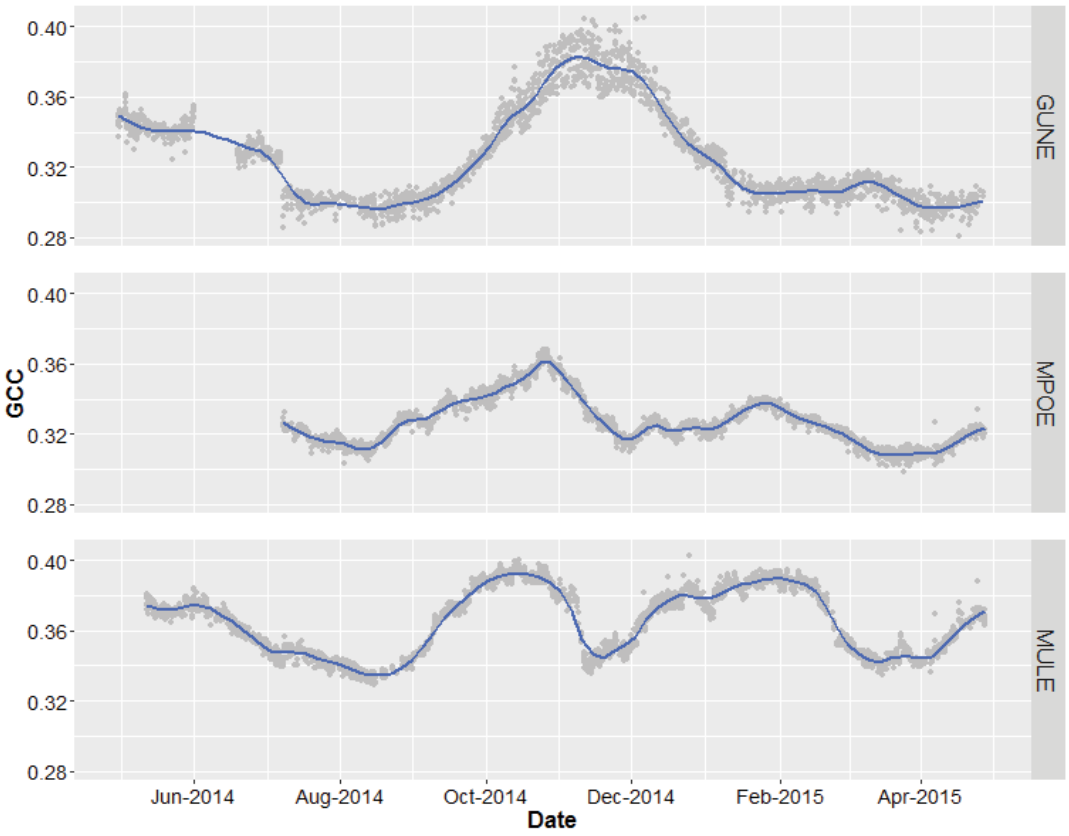

Figure 5.16. Annual g_{CC} phenology profiles at C_3 Exotic sites GUNE, MPOE and MULE. Grey dots represent hourly data points. The blue line is a LOESS fitted curve (span = 0.1) for visual assistance of the temporal trends.

All sites group by function type are presented as Figure 5.17. This allows the comparison of all sites within the one figure and visualisation of the variation within functional types.

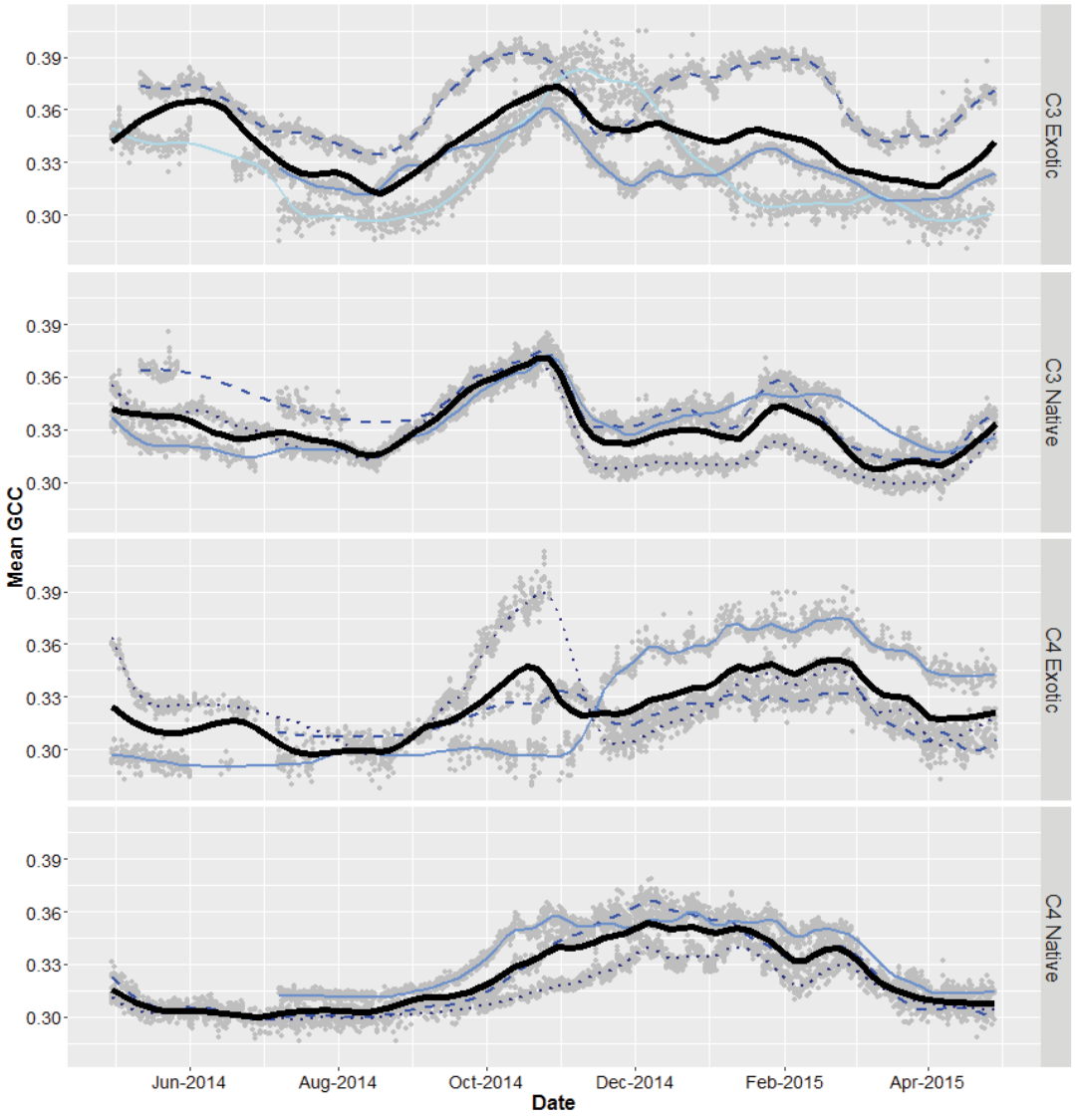

Figure 5.17. Annual combined g_{CC} phenology profiles for all sites, grouped by functional type. Grey dots represent hourly data points. Blue lines represent individual sites. The thick black line of each panel is a LOESS fitted curve (span = 0.1) for each functional type.

5.3.5 Satellite data

5.3.5.1 Data evaluation

An average of 19.2 data points (range: 18–20) was available per site for MODIS data and an average of 17.3 data points (range: 15–19) for Landsat data. Some large gaps were evident in this data series; up to 126 days for Landsat data and 48 days for MODIS data. This was particularly apparent from January 2015 onwards, where cloudy

conditions were prevalent. As MODIS data was a 16-day maximum composite of daily data, it was more robust to the cloudy periods, hence more data was available.

5.3.5.2 NDVI temporal trends

Overall, the coarser data collection frequency of satellite imagery results in temporal patterns that are more difficult to directly link to causal drivers. Nevertheless, some patterns from satellite data are evident that are consistent with patterns collected from other data sources.

Figure 5.18 shows the temporal NDVI pattern for MODIS and Landsat data for C_4 Native sites. Landsat and MODIS data show broadly the same trends though deviate substantially in magnitude at MPON and to a lesser extent at TURA. The paucity of Landsat data beyond January 2015 makes comparison difficult.

The resolution of a temporal C_4 Native pattern is much less clear in satellite data than in other data sources. GIDL and TURA site both show a consistently low NDVI below 0.5 throughout the autumn and winter months until green up commences in September 2014. After a peak in October, satellite data shows a decrease in greenness towards late November that is not apparent in other data sources. NDVI then increases bimodally throughout the remainder of the summer months to a maximum of 0.62 and then slowly tails off towards the winter baseline. MPON however is much more variable throughout the data series, although the primary NDVI peaks are still evident in October and January.

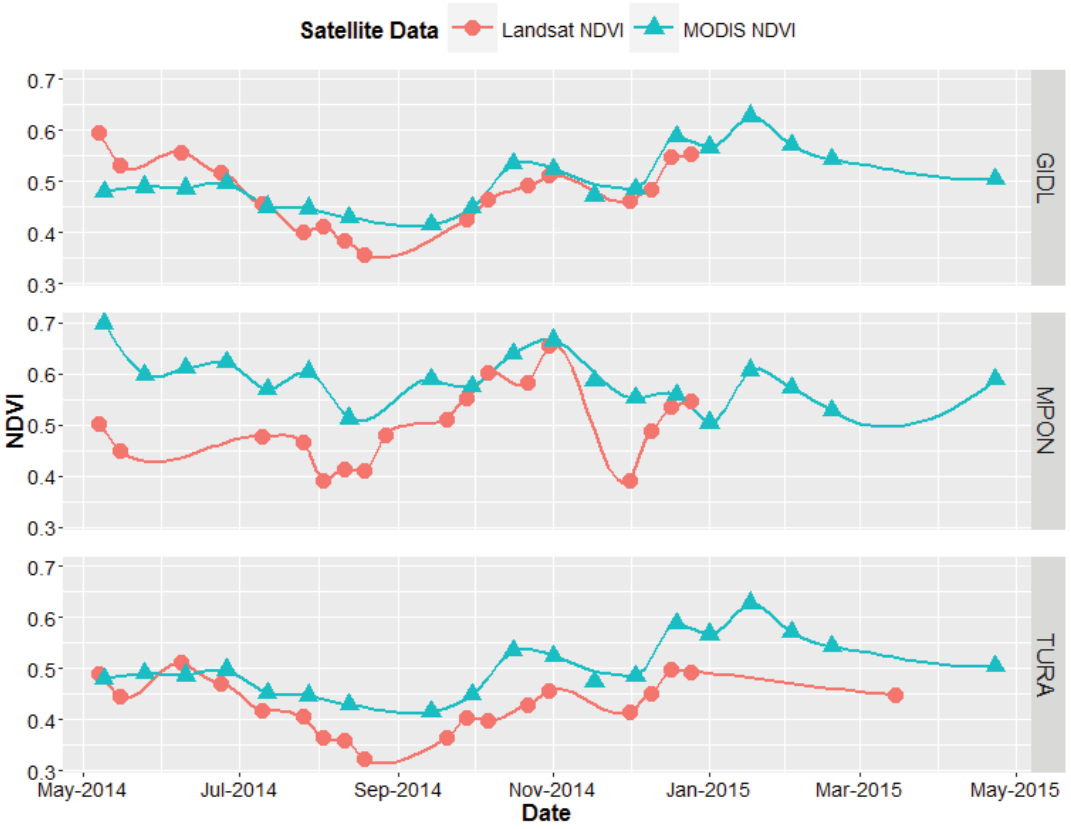

Figure 5.18. Terra MODIS (▲) and Landsat OLI/ETM+ (●) NDVI data for 1 May 2014–30 April 2015 at C_4 Native sites.

Satellite data for C_4 Exotic sites is presented as Figure 5.19. Overall, Landsat data was much more consistent than MODIS data, exhibiting smooth trends where MODIS fluctuated. This was particularly apparent at INGE and SCOT.

IN17 showed the most consistency between the two satellite data sources. From a typically low greenness during winter, NDVI started to increase in August to an October peak of 0.6. After a small browning period, NDVI remained relatively high during the summer and decreased to 0.49 by late August. Landsat data for INGE showed a more prominent peak on October (NDVI = 0.65), whereas MODIS data showed no major NDVI increase from May through November. The primary MODIS peak was apparent in February. Landsat data at SCOT showed low NDVI during the winter (NDVI < 0.3) with a long, gradual increase from late August to late December which contrasts with the rapid increase in g_{CC} observed in the phenocam data. MODIS data at SCOT showed a much more variable signal, with the only clear peak occurring in October and a high NDVI being maintained throughout summer.

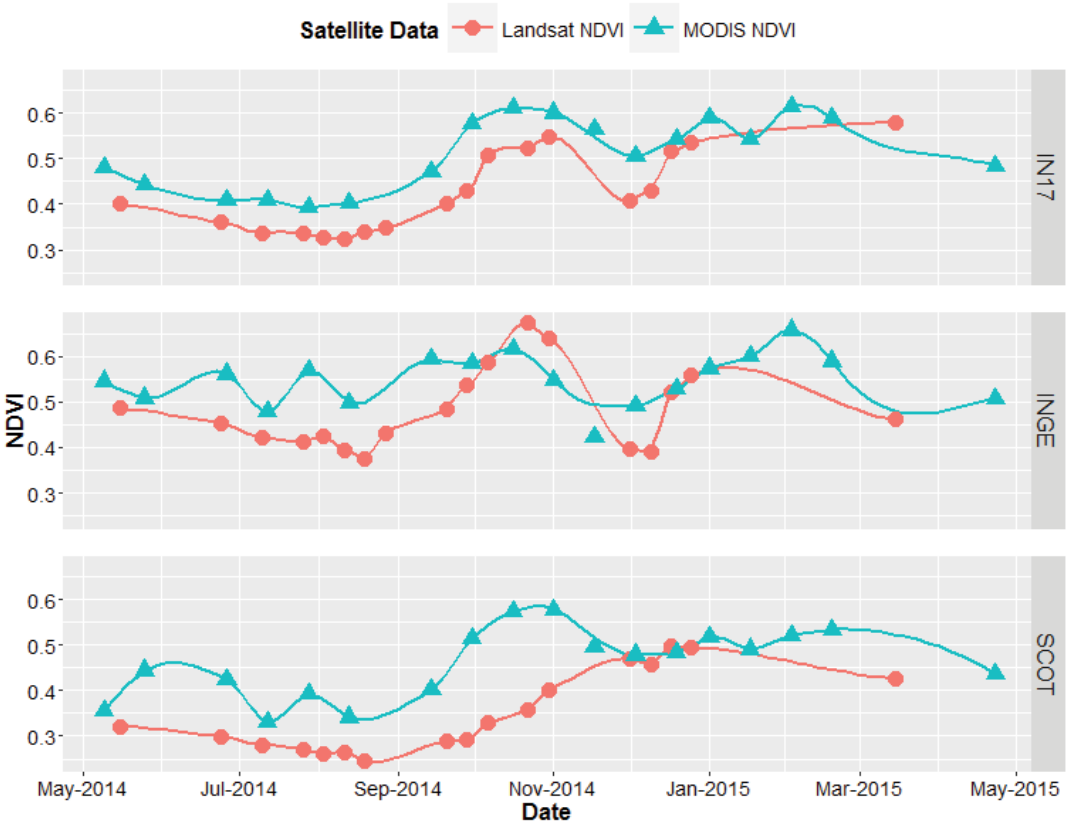

Figure 5.19. Terra MODIS (▲) and Landsat OLI/ETM+ (●) NDVI data for 1 May 2014–30 April 2015 at C_4 Exotic sites.

The satellite NDVI data for C_3 Native sites are presented in Figure 5.20. MODIS and Landsat data are extremely comparable, both in NDVI magnitude and trend. Some anomalies occur in Landsat data that are consistent between sites (e.g. September 20) for GUNN and MULN. Most of the inconsistent data points can be attributed to data gaps.

MODIS data shows consistent temporal patterns at all three sites that correspond well with phenocam and biomass trends. NDVI decreases from May to August, with the primary greening up period commencing mid-August and peaking in early October (NDVI ~ 0.75). A rapid decrease in NDVI occurs through to November to a low of 0.35–0.5, followed by two additional minor greening periods in February and May.

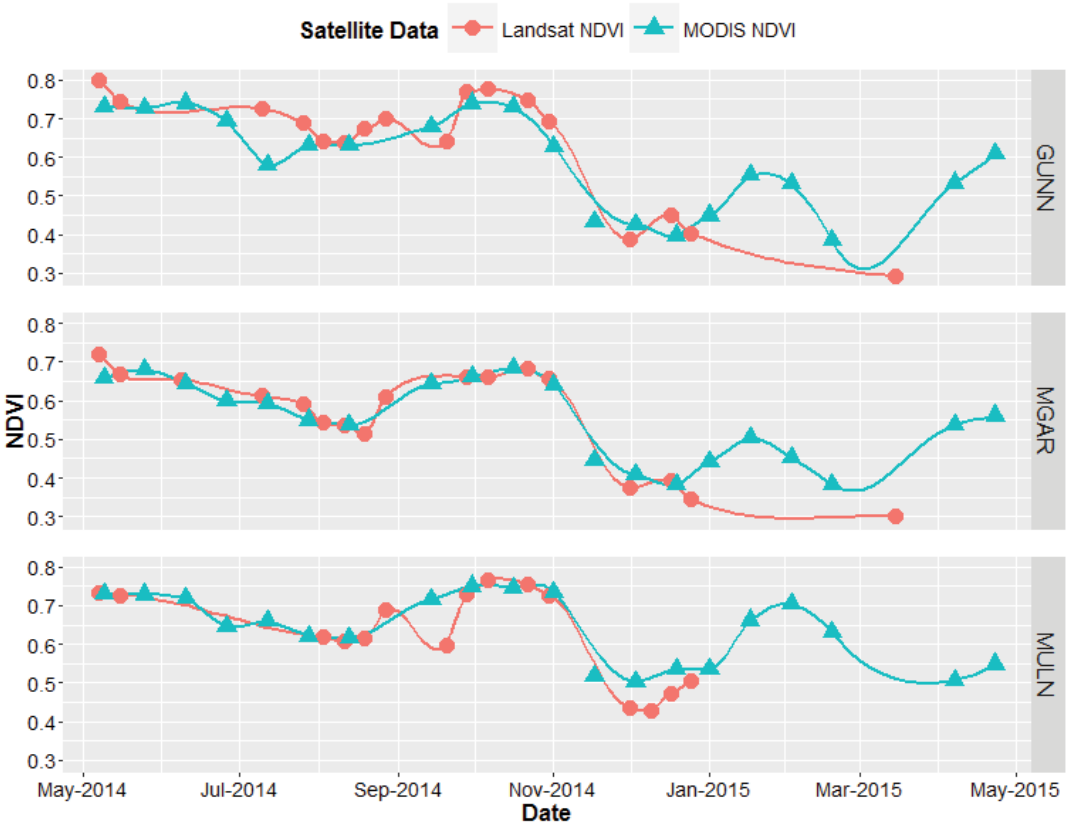

Figure 5.20. Terra MODIS (▲) and Landsat OLI/ETM+ (●) NDVI data for 1 May 2014–30 April 2015 at C_3 Native sites.

Temporal satellite patterns for C_3 Exotic sites are presented as Figure 5.21. Trends of Landsat and MODIS NDVI corresponded well for these sites, though deviations in magnitude were particularly evident at GUNE. Like other functional groups, the lack of Landsat data beyond December 2014 made comparisons difficult.

In general, patterns consistent with C_3 expectations were shown within the satellite data. All three sites showed greening commencing in July–August with a peak in October, and multiple additional peaks in February and April. Two of the C_3 Exotic sites had very high NDVI values, with MPOE having a maximum NDVI of 0.8 and MULE peaking at 0.88.

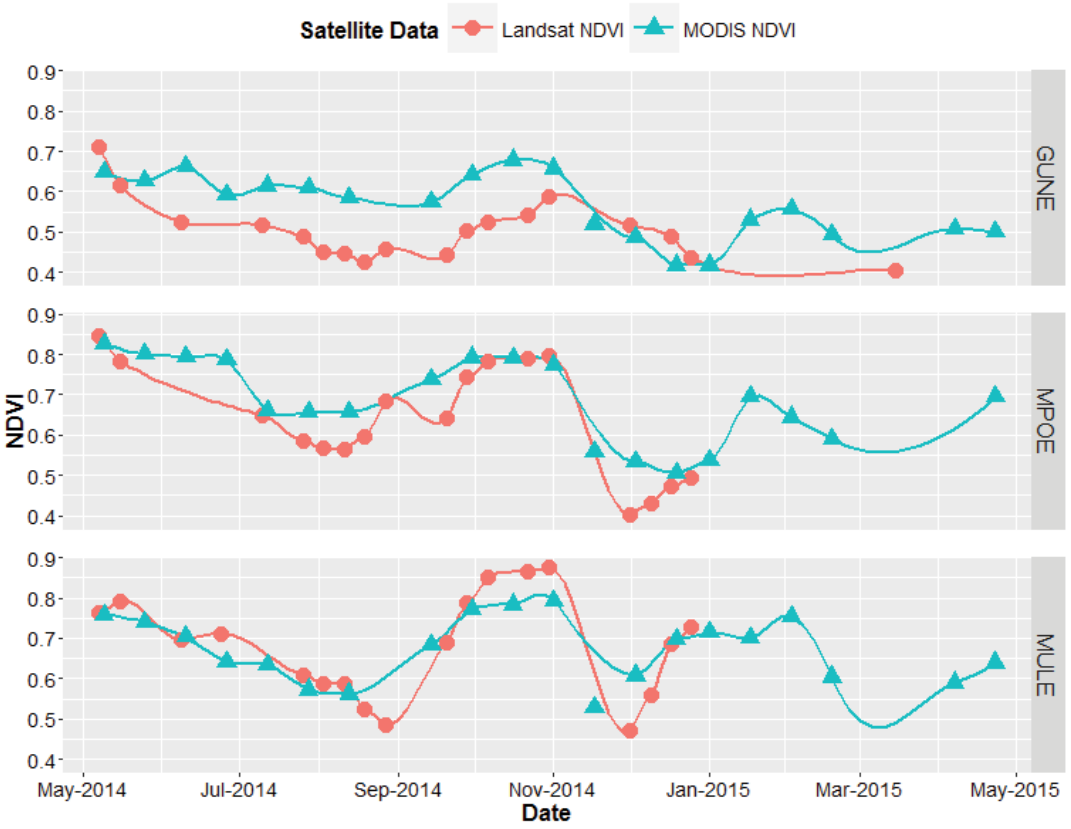

Figure 5.21. Terra MODIS (▲) and Landsat OLI/ETM+ (●) NDVI data for 1 May 2014–30 April 2015 at C_3 Exotic sites.

5.3.6 Relationship between remotely-sensed and biophysical variables

Variables were identified that were expected to be related to the quantity and quality of green vegetation: live grass biomass, live biomass, total biomass (i.e. live and dead grass and forbs), fraction of photosynthetic vegetation, fraction of non-photosynthetic vegetation, pasture height, phenocam g_{CC}, MODIS NDVI and Landsat NDVI. Initially, these variables were plotted with one another to enable qualitative comparison; identifying similarities and differences in the phenology profile trends throughout the year. An example of this graphical comparison at one site is presented in Figure 5.22; the remainder of sites are presented in Appendix F.

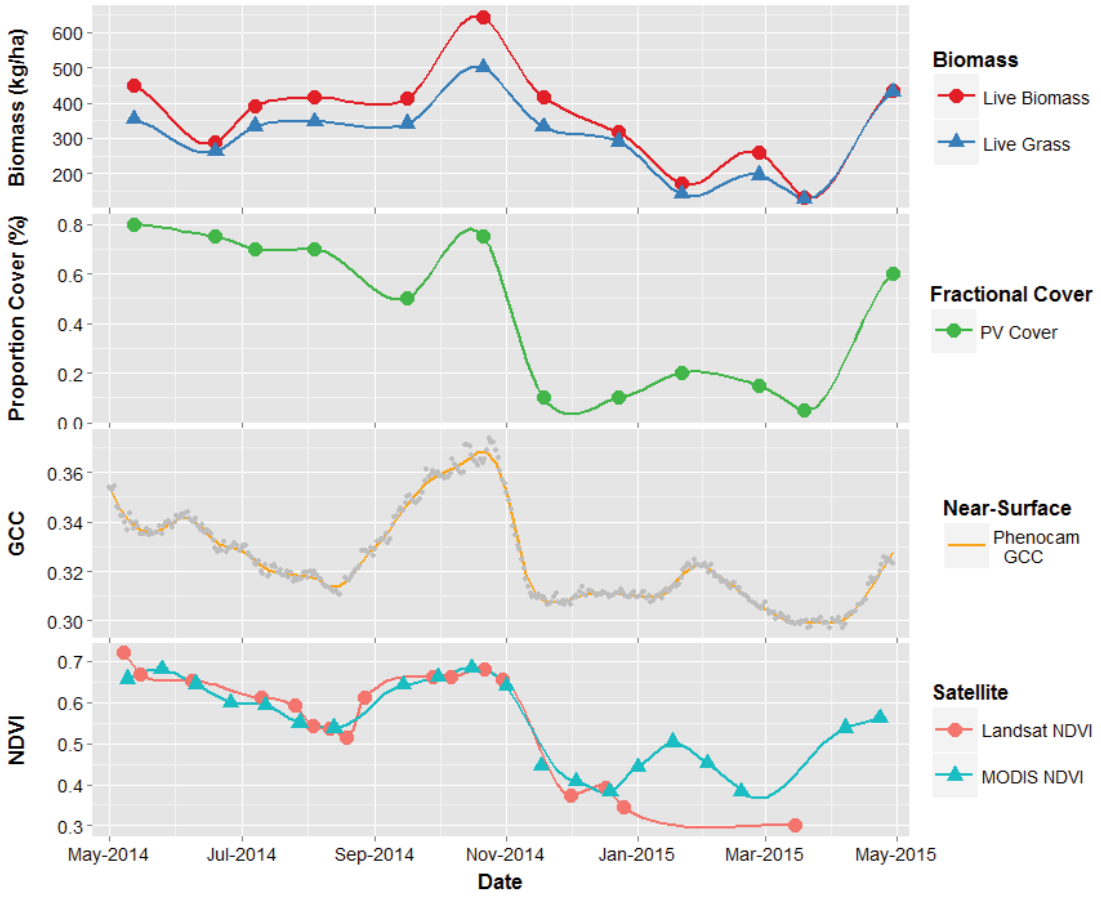

Figure 5.22. Multi-scale phenology for 1 May 2014—30 April 2015 at MGAR (C3 Native). From top to bottom panel: total live biomass (●) and live grass biomass (▲) in kg/ha; green (PV) fractional cover (%); phenocam 13:00 daily $g_{CC;}$ Terra MODIS (▲) and Landsat OLI/ETM+ (●) NDVI.

For quantitative analysis, data points from satellite and phenocam time-series were selected that were closest to the field sampling dates. Pearson's correlations were conducted across all sites between the identified variables. A correlation matrix was prepared (Figure 5.23), where coloured squares represent significant correlations between two variables and the numerical value represents the Pearson's correlation coefficient of determination (*r*). Positive values indicate a positive correlation whereas negative values indicate a negative correlation at a threshold of $p < 0.05$. Only the most relevant relationships are discussed.

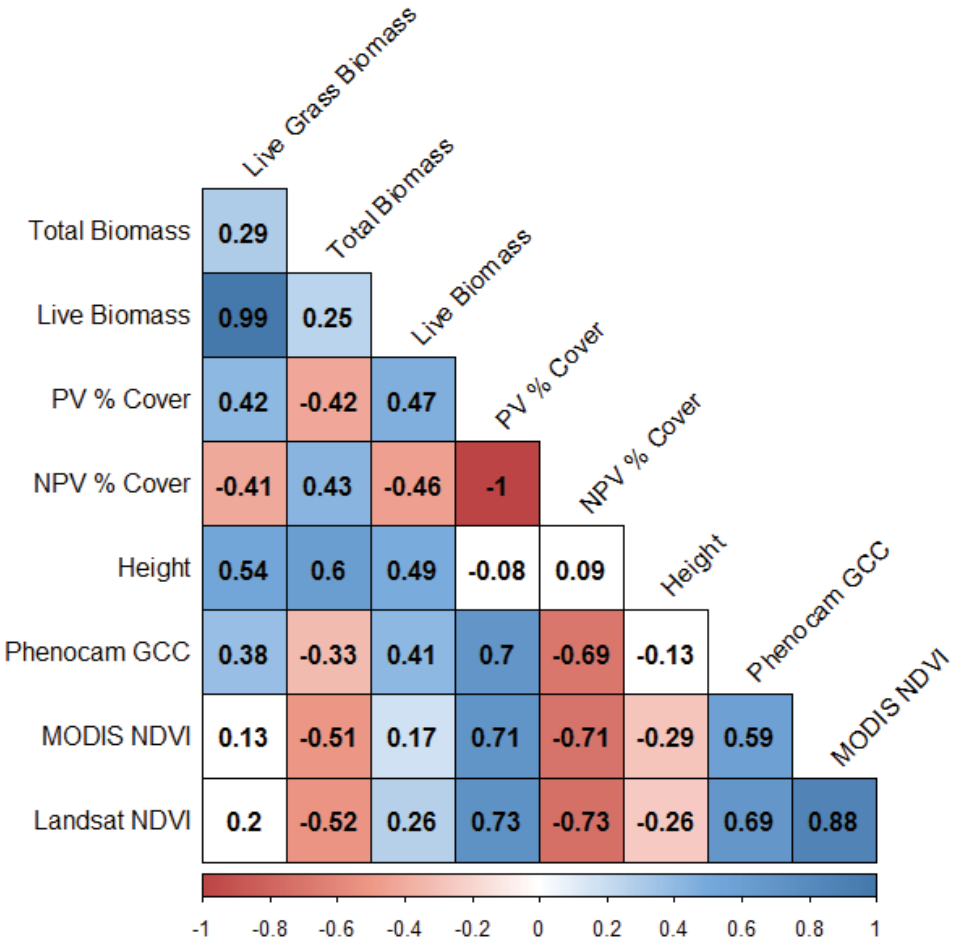

Figure 5.23. Pearson's correlation plot of variables across all sites that are relative to quality and quantity of green vegetation. Shaded values represent significant correlation at p = 0.05. Values are Pearson's correlation coefficient (*r*). Negative values (red) indicate a negative correlation; positive values (blue) indicate a positive correlation.

Across all sites, live biomass was strongly and significantly correlated with total biomass ($r = 0.99$, $p < 0.001$). This demonstrates that across all sites, the live biomass vegetation signal is dominated by the influence of grass rather than forbs. Live biomass, however was poorly-correlated with total biomass ($r = 0.25$), indicating that the contribution of the non-photosynthetic biomass component has a larger impact on the overall biomass.

Live biomass is not strongly correlated with satellite estimates of NDVI (MODIS NDVI $r = 0.17$; Landsat NDVI $r = 0.26$). Phenocam g_{CC} is more strongly correlated with live biomass than satellite NDVI, however the relationship is still not particularly strong ($r = 0.41$).

Height is poorly correlated with all remotely sensed NDVI and g_{CC} variables (Phenocam g_{CC} $r = 0.13$, MODIS NDVI $r = 0.29$, Landsat NDVI $r = 0.26$). It is more strongly correlated with biomass variables, such as total biomass ($r = 0.6$).

Phenocam g_{CC} has a stronger relationship to the fraction of photosynthetic cover ($r = 0.7$) than its relationship with any of the biomass variables (live biomass $r = 0.41$; live grass biomass $r = 0.38$). This suggests that phenocam data may be more appropriate in estimating cover rather than biomass in these systems. This same relationship between remote data sources and f_{PV} is true for Landsat NDVI ($r = 0.71$) and MODIS ($r = 0.73$), with satellite data also having a stronger correlation to green cover than to live biomass.

In terms of satellite similarity, MODIS and Landsat NDVI values are strongly and significantly correlated with one another ($r = 0.88$, $p < 0.001$). The correlation between phenocam g_{CC} and Landsat NDVI ($r = 0.69$) is stronger than that between g_{CC} and MODIS NDVI ($r = 0.59$).

To further explore relationships between these variables at different sites, similar Pearson's correlation matrices were created for each of the four functional groups (Figure 5.24). With a smaller sample size, the statistical power of each analysis was reduced, however still provides valuable input into circumstances where exceptions to conclusions from the overall data may apply.

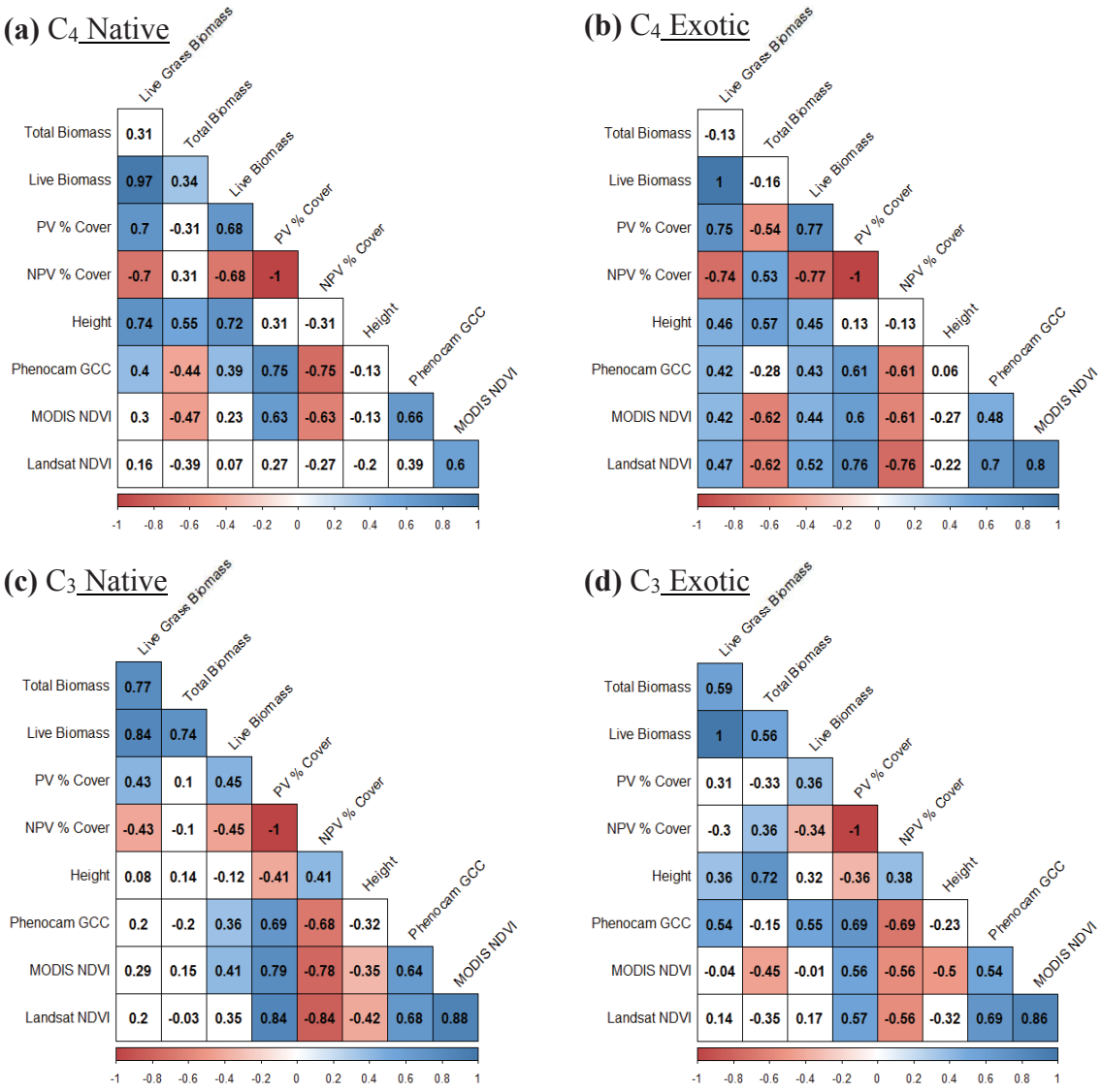

Figure 5.24. Pearson's correlation grids, separated by site type: (a) C_4 Native; (b) C_4 Exotic, (c) C_3 Native, (d) C_3 Exotic. Shaded cells represent significant correlations at p = 0.05. Shaded values indicate the strength of the correlation. Values are Pearson's correlation coefficient (*r*).

Across the whole dataset, live biomass is not well correlated with total biomass. However while C_4 Native and C4 Exotic sites do not show a significant relationship between live biomass and total biomass, C_3 Native and C3 Exotic sites do (C_3 Native $r = 0.77$; C_3 Exotic $r = 0.59$). However the overall relationship of live biomass being strongly and significantly correlated with live grass biomass is true for all groups.

Phenocam g_{CC} values show a better correlation with Landsat NDVI than MODIS NDVI when examined over all sites. When separated into functional groups, this relationship

holds true for all groups, but further shows that the g_{CC} at C_4 Native sites is the only group that is not significantly correlated with Landsat NDVI.

Across all sites, g_{CC} outperforms satellite NDVI in predicting live biomass, although this significant relationship is only moderately correlated ($r = 0.41$). However for some functional groups, satellite NDVI outperforms g_{CC} in predicting live biomass: MODIS NDVI for C_3 Native and both Landsat and MODIS NDVI for C_4 Exotic.

5.3.7 Separation of functional types by seasonal statistic

In order to separate grassland functional types into C_3 and C_4 or Native and Exotic, the phenological time series of g_{CC} data was segmented into seasons detailed in Section 5.2.7. For each season, data was calculated based on the minimum, maximum, mean, amplitude and variance of g_{CC} values, making a total of 20 statistical summaries.

Despite key common features in the C_3 and C_4 g_{CC} profiles, no seasonal statistic was able to distinguish all C_4- from C_3-dominated sites. The most promising combinations are presented in Table 5.4. The seasonal statistics of Winter variance, Spring mean, Spring maximum and Winter amplitude showed relatively low values for C_4 sites, with the exception of site INGE. This site is anomalous from a C_4 perspective as it contains a distinct spring peak more typical of C_3 grassland due to a strong spring flush of annual exotic grasses. The sites that had the three lowest winter variances were all C_4 Native sites. There were no ordinal groupings for C_3 sites that separated native from exotic types.

Table 5.4. Most useful seasonal g_{CC} statistics in separating C_3/C_4 grassland functional types. Shaded cells represent ordinal groupings (highest values).

C_3/C_4	Native Status	Location	Seasonal g_{CC} Statistic			
			Winter variance	Spring mean	Spring max.	Winter amplitude
C_4	Native	GIDL	8.1E-06	0.330	0.366	0.015
		MPON	2.9E-06	0.341	0.362	0.009
		TURA	3.5E-06	0.316	0.336	0.010
	Exotic	INGE	1.5E-04	0.341	0.405	0.034
		IN17	1.1E-05	0.323	0.336	0.015
		SCOT	2.3E-05	0.309	0.353	0.017
C_3	Native	GUNN	2.5E-05	0.354	0.379	0.021
		MULN	1.4E-05	0.348	0.378	0.020
		MGAR	8.0E-05	0.343	0.373	0.033
	Exotic	GUNE	2.0E-04	0.348	0.395	0.061
		MPOE	3.2E-05	0.340	0.365	0.021
		MULE	1.6E-04	0.372	0.397	0.047

To further develop this approach, and to reduce potential impact of g_{CC} magnitude between sites (refer to Appendix E), each seasonal statistic was divided by each other to create a seasonal statistic ratio. A total of 190 combinations resulted. Twenty-five of these successfully separated out one functional type (e.g. C_4 Native/ C_4 Exotic/ C_3 Native/ C_3 Exotic) using simple ordinal grouping, but no metric was able to completely split C_3 from C_4 nor Native from Exotic.

Like the basic seasonal statistics, none of the examined ratios were able to successfully separate the six C_4-domainated grasslands from the six C_3-dominated grasslands. The most promising ratios to develop as a 'C_4 index' were those that utilised the consistently low winter mean g_{CC}, amplitude or variance to contrast with a proportionally higher value from spring or summer. There were 35 such combinations that grouped all C_4 sites with the exception of the anomalous INGE site.

Principal Component Analysis (PCA) was used to assist in visualising the seasonal data. This multivariate statistical method reduces the dimensionality of the data to uncorrelated principal components (or 'dimensions'). The first two principal components characterise the most variation amongst the data (70%), and are used to display the groupings of sites in Figure 5.25 to Figure 5.27. Sites that are closely

clustered display low variance between one another based, whereas sites that are further apart display higher variation.

The PCA plot of sites grouped by functional type is presented as Figure 5.25. The C_4 Native sites are closely clustered, as are the C_3 Native sites. However the exotic-dominated sites are more separated, particularly C_3 Exotic, suggesting that seasonal variation of g_{CC} statistics (i.e. phenology profile characteristics) within this group is high. The seasonal statistics that contributed the highest weightings to these principal components were Winter mean, Winter minimum, Autumn minimum, Spring mean and Spring minimum.

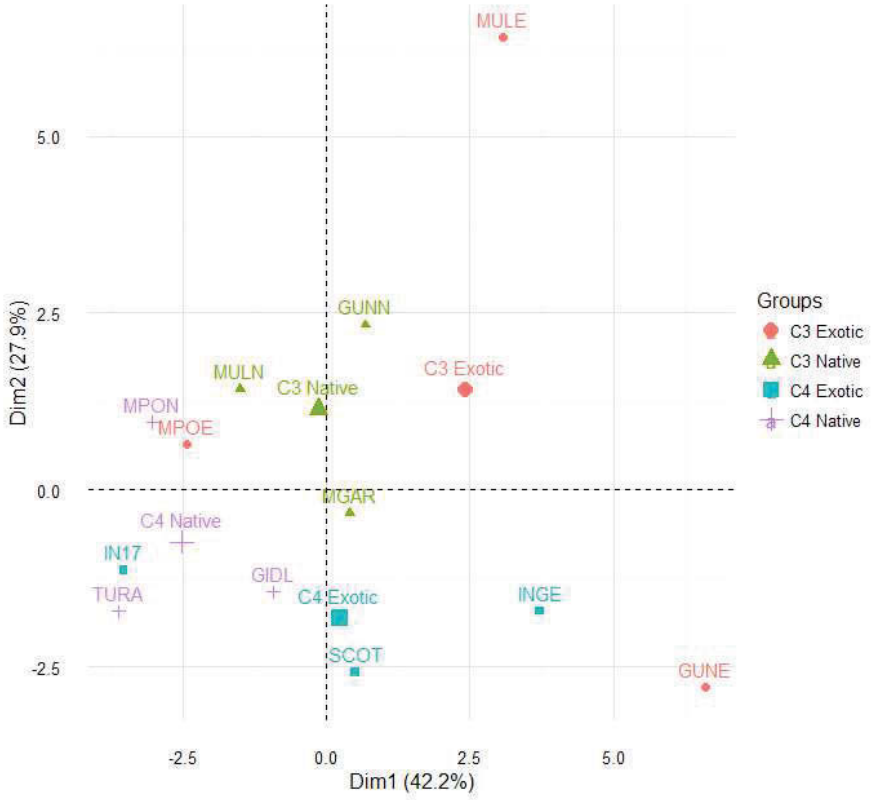

Figure 5.25. PCA plot of individual study sites, separated by functional type (C_4 Native, C_4 Exotic, C_3 Native, C_3 Exotic).

Figure 5.26 illustrates the study sites grouped by C_3- or C_4-dominance on the two principal component axes. The high variation demonstrated by the C_3-domainated sites hinders the discrimination between the groups. In contrast, the C_4-dominated sites are closely grouped, with INGE being the furthest outlier. Table 5.4 showed INGE to be the most anomalous C_4-dominated site for several seasonal statistics.

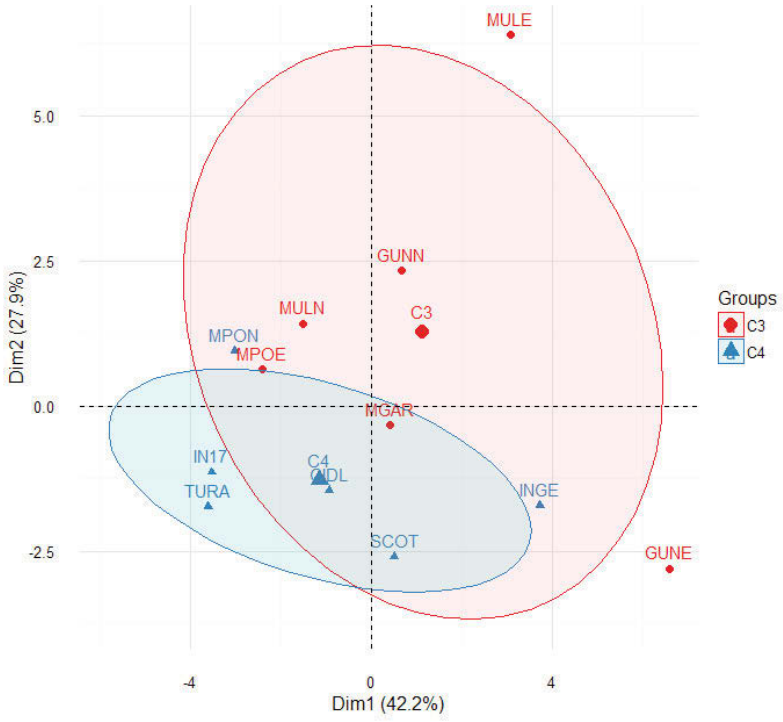

Figure 5.26. PCA plot comparing C3-dominant and C4-dominant sites, plotted on the two principal component axes.

Figure 5.27 clearly illustrates the difficulty in discriminating native-dominated from exotic-dominated sites using seasonal g_{CC} methods. Exotic-dominated sites displayed a large variance that covered the majority of the co-ordinate system. The native-dominant sites occurred in close proximity relative to the two principal components, but the high variation of exotic sites prevented useful clustering.

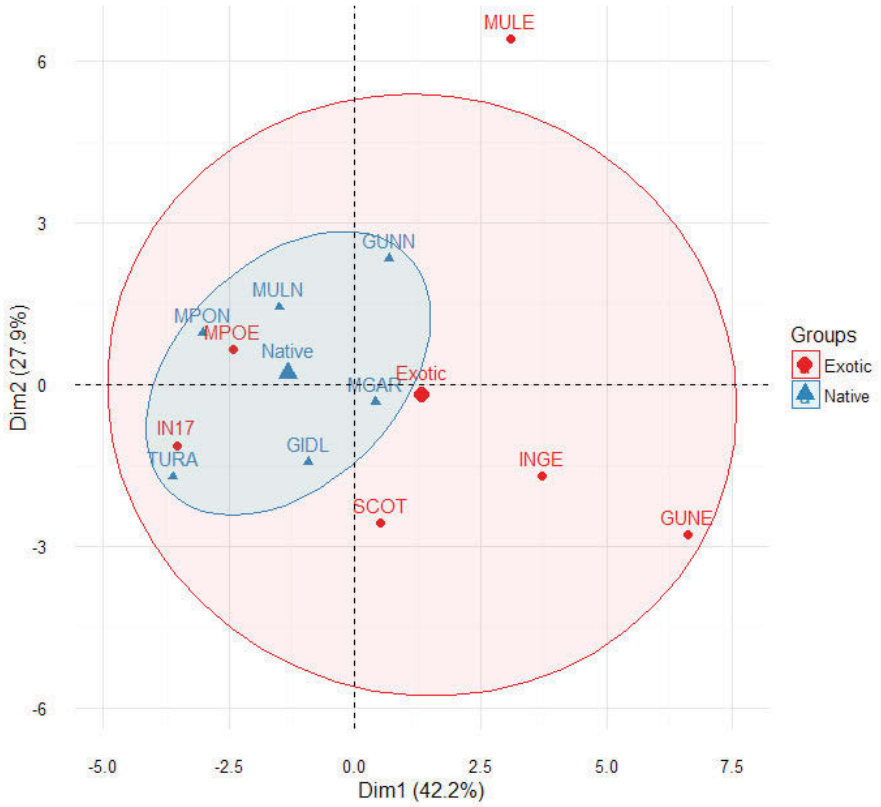

Figure 5.27. PCA plot comparing native-dominated and exotic-dominated sites, plotted on the two principal component axes.

5.4 Discussion

5.4.1 The C_3/C_4 phenological response

This study used field, near-surface and satellite measures to estimate vegetative phenology at different scales. Despite variability within method and within functional groups, several key phenological features were identified for C_3- and C_4-dominated grasslands. Some of these features are most prominent in the higher temporal frequency methods.

C_3-dominated grasslands showed a steady decline in green vegetation from May to August. A relatively sharp greening commenced in late August, reaching a peak in late October to early November as green leaf expansion was at its maximum. An abrupt decline in greenness followed, which is attributed to low rainfall and higher-than-

average temperatures. An additional peak in greenness is seen in late January followed by a steady decline to March. Greenness again increases during April.

In contrast, C_4-dominated grasslands demonstrated a consistently low quantity of green vegetation from May to August. Green-up commenced in September, and tended to be at a slower rate than the C_3 greening. Major C_4 vegetation greening in October resulted in either a single peak in December or—more often—consistently high greenness from December through February with minor fluctuations. There was a slight dip in greenness early February that was consistent between sites but only detected in phenocam data, followed by a gradual return to low levels in April. Generally the patterns of growth were much more distinct in C_4 grasslands, consistent with the botanical and phenological findings of Chapter 4.

Despite attempts to select similar homogenous sites for this project, the nature of temperate grasslands in NSW meant that variability was inevitable. The C_3 Exotic functional group showed the highest within-group variability. While all contained *Phalaris* as the dominant species, GUNE was ungrazed by domestic stock, and was in a seasonally wet position in the landscape. MPOE was moderately grazed by sheep and was extremely variable in composition. At times, it had a moderate native component, at other times a major exotic forb component, and the g_{CC} profile more resembled a typical native C_3 profile. MULE was a combination of similar pasture grasses (all within the C_3 Exotic functional group) but was periodically 'crash-grazed' by cattle. It was positioned on a floodplain so would be relatively resilient to rainfall shortages. These subtle differences between sites, though unintentional, can actually help in identifying reasons for greening differences.

Other sites demonstrated unexpected changes throughout the year. The site INGE contained predominantly C_4 exotic grasses. However climatic conditions in winter and early spring resulted in a flush of C_3 annual pasture grasses and forbs that is observed as a characteristic C_3 peak in early spring and confounds attempts to group C4-dominated sites. The C_3 Native site MULN was found to have a higher composition of C_4 grasses in the summer than was expected, hence exhibited a higher and more consistent greenness between December and February compared with other C_3-dominated locations. The main greening period of the C_4 Exotic site SCOT was later and more

rapid than other C_4-dominated sites, driven by the extremely high quantity of standing litter that obscured the growing leaves.

While it is difficult to predict inter-annual compositional changes in dynamic grasslands, the inclusion of more study sites would result in a greater set of sites where 'expected' phenology profiles occur. However, these anomalous sites also provide a valuable role in linking remotely sensed variables to observed species composition by forcing us to question the drivers that underpin this variation.

5.4.2 Separation of grassland functional groups

The temporal segregation between C_3 and C_4 grass growth patterns in some parts of the world have made the classification and detection of C_3- and C_4-dominated grasslands relatively simple in the remote sensing domain, including multispectral (Goodin and Henebry 1997, Tieszen *et al.* 1997, Davidson and Csillag 2003) and hyperspectral methods (Liu and Cheng 2011). Most of this success has occurred in northern hemisphere temperate systems that are temperature-limited with greening and browning periods that are both distinct and predictable. However, while this task is relatively straightforward, the need to improve methods for estimating groundcover variables has been identified as essential in order to improve remote sensing calibration and validation (Davidson and Csillag 2003).

Separating C_3 from C_4 grasslands proved to be more challenging in temperate Australia, with a more subtle temporal separation between the two groups. According to high-resolution phenocam data, C_3-dominated grasslands started the main greening period only one month earlier than C_4-dominated grasslands. The difference in peak timing was also approximately one month, hence these two functional groups do not exhibit as much temporal segregation as found elsewhere. In fact, this difference can easily be obscured when using satellite data sources that have lower temporal resolution. In temperate Australia, vegetation systems are influenced by both water and temperature and demonstrate a complex, multi-modal phenological profile. As such, traditional phenological metrics and separation techniques such as temporal trajectory indices (Goodin and Henebry 1997) cannot be applied and alternative approaches need to be

explored. This is not only true for Australian grasslands, but for any system where C_3/C_4 variability is not only controlled by seasonal drivers (Adjorlolo *et al.* 2012).

Using g_{CC} seasonal statistics was of limited effectiveness in isolating a specific seasonal statistic or a seasonal-based ratio to separate C_3 from C_4 types. Five out of six C_4 sites were grouped together, with the excluded site having anomalous annual C_3 grass species present at one time of the year. However, while anomalous in this instance, incursions of unusual species are typical in dynamic grasslands, and this anomaly needs to be accounted for in any classification method. The statistical groupings with the highest potential utilised the characteristic of C_4-dominated sites to have proportionally lower variance, amplitude and value of the winter g_{CC} component, as well as proportionally lower maximum and mean of spring g_{CC}. Principal component analysis was able to graphically demonstrate outliers and illustrate the difficulty in discriminating functional types. The analysis similarly found that the winter variability and autumn/spring minima contributed the highest weighting to the top two principal components. The consistency of these characteristics should be assessed on a wider range of sites.

We separated the year into seasonal windows in order to allow for the natural variability in phenological timing that the interaction between temperature and rainfall can present. Spring rains are variable in timing and quantity, and the vegetation will respond quickly and proportionally. As such, it is not feasible to use 'monthly' patterns in the profile. Seasonal profiles are more likely to incorporate key phenological drivers at somewhat consistent timeframes. In addition, missing data is not as critical; it does not restrict the use of seasonal data as much as, say, monthly data. A more effective approach may be to modify the traditional seasons to ecologically-meaningful periods—an broad approach that has been suggested by some botanical authorities (Entwistle 2014). Segmentation of the year into 'seasons' more appropriate for temperate Australia may improve the capacity to capture vegetation response in relevant temporal windows.

Unlike other methods that estimate the proportions of C_3 to C_4 grass composition (e.g. metric threshold and temporal trajectory indices), this approach uses binary separation into C_3- or C_4-dominated grassland. Given that several of the grassland types in this study contained a varied mix of C_3 and C_4 species at different times of the year, this

may skew the decision rules over what may have been developed with 'pure' C_3 and C_4 grassland types. As grasslands can change species composition dynamically, a binary tool may not be practical to implement. An alternative approach may be to use existing data to develop an 'idealised' C_4 grassland curve for a range of climatic variables, and determine how much measured phenology statistics deviate from that curve. The quantity of this deviation would indicate the proportion of C_3 and C_4 vegetative cover. This would need to be conducted at many sites over several years to ensure robustness in different geographical and climatic conditions.

Evaluation of this separation method was made possible through the high temporal capacity of phenocam imagery. It is unlikely that the satellite data used within this project could provide the temporal resolution required, as several sites contained seasons with low numbers of data points. Newer technologies that are becoming available, such as the Sentinel-2 satellites with high spatial resolution and a higher revisit time, may be an appropriate avenue for this line of investigation (Drusch *et al.* 2012). The potential for these sensors to detect grassland biophysical parameters has already been assessed using simulated data (Sakowska *et al.* 2016).

The caveat that applies to all conclusions from this study is that these findings are representative of only one year of data collection. Given the natural variation in south-eastern Australia's climate, trial of this method under additional climate variability should be undertaken. It is likely that during climatically different years that alternative metrics could be used for optimal differentiation.

It was not possible to separate native and exotic sites within the same C_3/C_4 group using the methods in this trial. There was a tendency for C_3 Exotic sites to have a higher maximum greenness though this was not universal. The most likely avenue for native/exotic separation in C_4 grasslands is through the propensity of native C_4-dominated sites to have very low winter variance. This however will need to be confirmed with further field trials at a larger number of sites.

5.4.3 Phenocams: limitations and variation

The data from this section is presented in Appendix D and E, but is discussed briefly here as it is of direct relevance to this chapter. It also contributes to the aim of evaluating the effectiveness of phenocams to monitor Australian temperate grasslands.

5.4.3.1 Viewing angle

The comparison of foreground, midground and background images at all sites showed a clear pattern of more distant targets (higher camera angle from vertical) providing an exaggerated g_{CC} than at closer targets (lower camera angle from vertical). As such distant targets appear greener during peak greening periods but browner during senescent periods. This demonstrates that relative viewing angle impacts the magnitude of g_{CC}, and consequently the magnitude of change throughout the year. However, where the foreground, midground and background capture the same vegetation type, the trend of the g_{CC} and the timing of key events are equivalent.

While only two comparisons were able to be made between nadir and oblique imagery, nadir images generally had a lower g_{CC} at any given point in time. This resulted from a greater contribution from background material—occasionally bare soil but usually litter. These results should be interpreted with caution due to the inherent differences in land surface phenology analysis and the different target areas that are involved, i.e. the nadir image captures approximately 2 m^2. Future studies involving Unmanned Aerial Vehicles (UAVs, or 'drones') collecting images at different heights and angles could provide more confirmatory data on the relationship between view angle and visual indices. This has historically been conducted in the spectral domain using goniometer studies (e.g. Coburn and Peddle 2006), but is already being trialled with UAVs (Grenzdorffer and Niemeyer 2011). As phenocam use in ecological applications continues to grow, further research into the effects of camera angle on vegetation indices should be conducted in a variety of different biomes with different structural and spectral characteristics.

5.4.3.2 Illumination effects

Diurnal g_{CC} patterns varied with time of year and site. This is likely due to different seasonal patterns of illumination and consequent differences in shadowing. Although g_{CC} has been shown to be robust to changes in illumination, shadows are known to have some impact on vegetation indices (Ide and Oguma 2013).The effect of overcast versus sunny days was not tested, but other illumination effects were investigated (see Appendix D).

Where researchers in other biomes have found that daily g_{CC} values are too variable, they have used a moving window approach or a smoothing spline to further minimise the influence of changes in scene illumination (Migliavacca *et al.* 2011, Sonnentag *et al.* 2012). However, this does come at a cost of temporal resolution, reducing the usable image frequency to once every three days. Extreme effects on daily g_{CC} data were not encountered here, due to manual filtering of the image archive prior to analysis. As such, this study opts to retain the original temporal frequency rather than applying a smoothing algorithm, as temperate grasslands show a much faster rate of change than broadleaved forests.

5.4.3.3 General quality issues

In the current study, the grassland subject was located relatively close to the camera, unlike some other studies where the target may be several hundreds of metres distant (e.g. Ide and Oguma 2010). As such, the images do not experience variation from changes in atmospheric conditions, which is known to impact phenocam performance (Inoue *et al.* 2015). Fog and bushfire smoke were apparent in some images, albeit rarely, and were filtered from the data.

Substantial effort was made to manually filter images of unacceptable quality. This labour intensive approach is contrary to the alternative approach: retain all images regardless of quality and allow a smoothing filter to buffer any outliers (Bradley *et al.* 2007, Migliavacca *et al.* 2011). While a manual filtering approach has some subjectivity and may be impractical for projects with larger scope, it results in a defensible dataset that maintains its temporal integrity. An intermediate solution may be to filter, or at

least manually examine, any images with a vegetation index outside prescribed thresholds.

The potential for camera sensors to undergo colour balance drift after several years of use has been identified (Ide and Oguma 2010). For a short-term study such as this, with cameras obtained from the same batch, it is assumed that the stability of the measured signal is high. However researchers should be aware that this issue does exist for longer-term studies. A reference panel is one method typically used to check and calibrate colour balance (Migliavacca *et al.* 2011). In some cases where reference panels are not appropriate, invariant alternatives such as freshly fallen snow have been used (Ide and Oguma 2010). In the current study, no reference panel was used due to the practical limitations of the equipment configuration: the card would not be in the same plane as the target; preventing the card from becoming contaminated through dust and rainfall was impractical; and the card could not be mounted from the camera without interfering with the image collection. Custom-made reference panels, protected from the elements and mounted vertically, might be a suitable option for long-term grassland phenocam research.

5.4.3.4 Weather conditions and shadows

As other researchers have suggested, the impact of shadows on phenocam images should be minimised (Ide and Oguma 2013, Toomey *et al.* 2015). In grasslands, much of the inter-tussock and intra-tussock space can be heavily shadowed, hence this requirement is difficult to implement and should be acknowledged as an inherent form of variability in these systems.

Unfortunately, the positioning of the camera facing south means that some shadowing is inevitable on sunny days, and selecting images that only have diffuse light (i.e. no shadows) would remove the advantage of high temporal data collection. However given the robustness of g_{CC} to shadows, this configuration is preferred to one where sun glints are present in the images. Three locations in this study also used trees as 'camouflage' for reducing vandalism; either mounting the phenocams directly on trees or locating them between saplings. It is acknowledged that the potential reduction in vandalism is a trade-off with more shadows impacting data quality.

Efforts should be taken to limit the quantity of sky in the image to less than 20% of the image area. The presence of the horizon within the FOV is useful for setting context, but a greater contribution of sky means that white balance is impacted by changes in atmospheric effects and sky conditions. This is particularly relevant for phenocams such as the Wingscapes model used in this study that do not allow manual control of white balance and other settings.

5.4.3.5 Additional advantages of time-lapse imagery

The use of phenocam imagery highlighted several advantages that may be useful to support vegetation studies in the future.

In some cases, flowering phenophase was able to be clearly observed (Figure 5.28). This phenophase has the potential to be quantified for some species, either through manual means or automated image processing. The response of flowering phenology to climate change is frequently examined due to its importance to pollinators and population demographics (Hovenden 2007, Caradonna *et al.* 2014). However, this has potential only for species that have conspicuous and abundant flowers.

Figure 5.28. Phenocam used to monitor flowering phenophase of *Hypochaeris radicata*. The upper image shows commencement of flowering (22 January 2015); the lower image shows peak flowering (30 January 2015).

Time-lapse imagery has potential to be used to monitor and quantify grazing pressures. Researchers from the ACT government studying kangaroo populations on one of the reserves used in the current study asked to review the phenocam images to correlate kangaroo numbers with their own census data (D. Fletcher, pers. comm.). When using photographs for this purpose, users should consider how representative the FOV is for the overall habitat. In the case of a phenocam mounted to a large tree, kangaroos would

be expected to use the shade of the tree for thermoregulation in the summer, hence would likely be more numerous near the tree than elsewhere on the reserve. The impact of domestic stock grazing was also used in this study to confirm g_{CC} trends. In the case of one site, the cause of an unexpected drop in g_{CC} was confirmed by reviewing the imagery and identifying that stock had been accidentally released into the paddock.

Finally, the regular frequency of image collection—in our case, every hour—led to photographic capture of both native wildlife and feral animals, including mammals, birds and reptiles. Although it is not the primary purpose of this imagery, these photos provide value-added information to local land management agencies or landholders that may foster support for similar projects and engage the broader community with scientific research.

5.4.3.6 Overall evaluation of phenocams and recommendations

Phenocams provide an excellent fine temporal resolution method for assessing vegetation dynamics in Australian temperate grasslands, and are particularly responsive to fast vegetation growth following rainfall. The ideal positioning of phenocams is south-facing (in the southern hemisphere), with maximal coverage of the target vegetation. In this environment, g_{CC} proved to be a suitable index for detecting vegetation dynamics. However, resultant g_{CC} phenology profiles do not lend themselves to traditional phenology metrics and smoothing methods; their strength is in fine-scale rapid greening and browning responses.

It is recommended that the relative angle between the camera and the target be standardised across locations to enable comparison of magnitude of g_{CC} change between sites. Correction of g_{CC} 'baseline' (i.e. where green vegetation cover approaches zero) may be another method of normalising g_{CC} data but would be contingent on the concomitant collection of field data and requires green cover to reach zero at some stage throughout the time-series.

The presence of shadows in phenocam images should be minimised to standardise the diurnal g_{CC} patterns. However it is recognised that the south-facing requirement does necessitate some shadowing from the camera infrastructure. It should also be

highlighted that seasonal changes in shadowing occur; hence the amount of shadowing will change throughout the year.

Ongoing uses of phenocams and similar technology will no doubt identify further opportunities for this technology in ecological research. The need to standardise the collection and analysis of phenological imagery has been highlighted by a recent review (Brown *et al.* 2016). In addition, standardised archiving of phenocam imagery will enable future developments in image analysis to be retroactively applied to historical phenocam studies.

5.4.4 Comparison of field and remotely sensed methods

This study collected monthly field data on variables that were readily measured in the field and reasonably expected to be related to the quality and quantity of photosynthetic vegetation: aboveground live biomass, green fractional cover and pasture height. Near-surface and satellite remote sensing methods for estimating greenness of vegetation were collected through the use of phenocam g_{CC} and NDVI data collected by Landsat OLI/ETM+ (30 m spatial resolution) and Terra MODIS (250 m spatial resolution) satellite sensors. The relationship between these variables was analysed using linear correlation using the entire data set, as well as separation into individual functional groups. This approach is similar to that of other researchers, who have compared field data with remote sensing data in an attempt to understand the effects on spatial scale on phenological estimates (e.g. Zhang *et al.* 2003).

5.4.4.1 Field measurement comparisons

The results show that live biomass is not well correlated with total biomass, which results from the proportionally high contribution of standing litter in temperate grassland systems. However, when examined by functional type, this relationship only holds for C_4 grassland types, as C_3 grasslands typically have much less standing litter present throughout the year. The very strong correlation of live biomass to live grass across the dataset illustrates the importance of the grass component: although forbs comprise a large component of grassland species richness (Wimbush and Costin 1979,

Tremont and McIntyre 1994), they only contribute a small fraction of the overall vegetative biomass.

Pasture height is significantly and strongly correlated with total biomass, more so than live biomass. This is consistent with expectations, because particularly at C_4-dominated sites the dead biomass is the tallest layer for much of the year. Pasture height is poorly correlated with vegetative fractional cover and remotely-sensed measures of greenness. This suggests that while height measurements are a common field tool for quickly estimating biomass, they should not be used as a proxy in temperate grasslands for validating remote sensing methods.

Green fractional cover is only moderately correlated with live biomass ($r = 0.43$) but is negatively correlated with total biomass. Again, this illustrates the influence that standing litter has in this biome: the greater the total biomass, the lower the proportion of green cover. This is particularly significant at C_4 Exotic sites.

5.4.4.2 Biomass and cover versus remote sensing

Like other grassland studies (e.g. Inoue *et al*. 2015; Migliavacca *et al*. 2011; Paruelo, Lauenroth and Roset 2000), we found a significant relationship between phenocam indices and live biomass ($r = 0.41$, $p < 0.001$) and between phenocam indices and satellite NDVI (Landsat $r = 0.69$, $p < 0.001$). However the strength and significance of these relationships varied between grassland functional types. It has been highlighted in the past that VI estimations of fractional cover in mixed species systems should be regarded as approximates, given that the cover:VI relationship varies between species (Glenn *et al.* 2008).

Live biomass was not strongly correlated with satellite NDVI ($r = 0.26$ and 0.17 for Landsat and MODIS, respectively). This is a significant finding as some grassland studies find a strong correlation between these variables (Migliavacca *et al.* 2011). This poorer correlation is likely due to the abundance of standing litter in many of the study sites. Non-photosynthetic vegetation not only obscures green vegetation, but it reflects more light in the red wavelengths, reducing the NDVI signal (Watson *et al.* 2013). Until the precise effect of litter is quantified in a variety of grassland types, the ability of

satellites to predict biophysical variables of Australian temperate grasslands may be limited.

This study found live biomass to be more strongly correlated with g_{CC} than satellite NDVI. This finding gives some strength to the theory that it is the NIR component confounding the relationship, as g_{CC} does not incorporate NIR. An alternative explanation for poorer satellite NDVI performance is that the signal noise from atmospheric effects increases the residual error and lowers the strength of the relationship. There may also be instances of spatial registration error: the phenocam is configured to view the specific area of grassland, however the satellites may capture small fractions of surrounding land use types, or slightly different grassland areas that degrade the strength of the NDVI:biomass relationship.

Phenocam-derived g_{CC} is more strongly correlated with green fractional cover than live biomass. This suggests that phenocam data may be more appropriate in estimating cover rather than biomass in these systems. This echoes results from research in the USA (Vanamburg *et al.* 2006) that suggest digital camera-based estimates of grassland biomass are limited in usefulness. However, in alpine grasslands, Migliavacca and colleagues found that their Greenness Index (equivalent to g_{CC}) was significantly correlated with green biomass as well as visual greenness estimates (Migliavacca *et al.* 2011). Clearly there are biophysical differences between the grassland types that result in this inconsistency. It should also be acknowledged that in our case, using g_{CC} magnitude as a comparison may be influenced by the issue of relative view angles (Appendix E).

The relatively weak correlation between satellite and ground variables may also be due to data gaps in the satellite time series. We used the nearest satellite data point to the monthly field sample (within 30 days), which may have been several days or weeks after the field measurement and may represent a large change in greenness state. This temporal registration could be improved by better coordinating field campaigns to coincide with cloud-free satellite revisit dates. Particularly for Landsat, however, this may result in unacceptably large gaps during cloudy seasons.

5.4.4.3 Remote sensing method comparisons

Although Landsat and MODIS NDVI data were highly correlated across the whole dataset, there was little consistency in this relationship between sites. For some sites (e.g. MGAR) they followed identical magnitudes and trajectories, whereas at others they deviated substantially (e.g. SCOT). While difficult to test statistically, it appears that the largest differences in NDVI magnitude between the two sensors occur at sites with the highest proportion of standing litter. This difference could be an artefact of the MODIS composite process that takes the maximum value recorded over the 16-day window; hence MODIS values are more likely to be greater than Landsat. The cause of this difference may also be that the error is within the natural variability of grassland as the two sensors are measuring slightly different view angles, spatial footprints and spectral wavebands. Other studies attempting to compare MODIS and Landsat data sources conclude similarly: overall, the datasets are comparable but particular regions exhibit discrepancies (Huete *et al.* 1997, Price 2003). Buheaosier and colleagues suggest that the MODIS NDVI value is greater than the ETM NDVI value over several land cover types and attribute this to the coarser spatial resolution (Buheaosier *et al.* 2003).

Overall, phenocam g_{CC} is better correlated with Landsat NDVI than MODIS NDVI. This may be due to the smaller Landsat footprint and highlights the importance of sampling equivalent size plots for different methods (Rienke and Jones 2006). Although phenocams are sampling an area of several hectares, proportionally more signal comes from the smaller area of the foreground of the image. Modification of the shape and size of the ROIs in the background, midground and foreground may correct for this.

One of the weaknesses with satellite data in a phenological context is the presence of data gaps that result from cloud cover (Stow *et al.* 2004). Because this satellite data was collected less regularly than phenocam imagery, errors due to data gaps can have stronger impacts on conclusions. As an example, data gaps can cause greenness peaks to be missed entirely, or a rapid green-up can appear to happen more gradually if data near the greening commencement is absent. Of the two satellite data sets, MODIS seemed to be more variable than Landsat, but that may be a legacy of having more data points available and having a larger spatial resolution.

Despite the reasonable correlation between satellite and field data, ultimately the 16-day satellite revisit time is too coarse to quantify the changes that occur in a dynamic grassland system, particularly given that cloud cover impacts often extend this data frequency (Stow *et al.* 2004). Other studies have indicated that a nominal 16-day revisit time is insufficient to detect key phenological dates (Westergaard-Nielsen *et al.* 2013). More regular data collection from MODIS is possible (Narasimhan and Stow 2010) but with an increase in temporal resolution comes a trade-off with data quality and consistency.

In this study, we combined data from Landsat 8 OLI and Landsat 7 ETM+ to improve the temporal coverage of Landsat NDVI. While Landsat ETM+ and OLI were shown to be quite comparable in analysis of crop biophysical variables (Li *et al.* 2014, Ahmadian *et al.* 2016) subtle differences are apparent, due in part to the difference in spectral band widths of the two sensors. In this case it can be argued that any minor differences between the two Landsat sensors are offset by the advantages provided by the higher temporal resolution.

The commonplace use of NDVI as a primary vegetation index in phenological studies has been criticised (Foody and Dash 2010, Wang *et al.* 2010) with the suggestion that further effort should be invested in developing phenologically-appropriate vegetation indices. In this temperate grassland scenario however, NDVI was found to be valuable in showing appropriate responses to vegetative dynamics throughout the study period.

5.4.4.4 Method and scale comparability

The comparability of vegetation variables measured at different scales has been identified as a challenge for decades (Friedl *et al.* 1995). While some studies have reported success in this regard (e.g. Fisher *et al.* 2006, Fisher and Mustard 2007), other authors caution that there are still major challenges in scaling field measures to satellites (Huete *et al.* 2002, Soudani *et al.* 2012). Often, it is the fundamental relationships between the measured variables that are key to understanding the limitations of scaling. For comparative studies, it is essential to establish field sites that are appropriate to

compare with remote sensing methods. This study used many of the methods recommended by one research group (Rienke and Jones 2006), including:

- utilising homogenous area of vegetation;
- selecting plots away from boundaries of other vegetation types to minimise spectral mixing;
- contemporaneous data collection;
- ensuring a suitable distance to the edge of the vegetation patch; and
- designing a plot size appropriate to pixel size.

As phenocams are a recent innovation, there are relatively few studies that compare phenocam estimates of phenology variables to ground or satellite scales.
An early assessment of comparing leaf area index in grasslands using digital photographs and ground estimates concluded that the contribution of non-photosynthetic vegetation and background soil in the image reduced the accuracy of the camera, and that further calibration techniques would be required to resolve these issues (Przeszlowska *et al.* 2006). More recently in a temperate hardwood forest in the north-eastern USA, Keenan and colleagues found that spring and autumn transition dates are well captured by phenocams, though LAI and leaf physiology lag behind projected greenness (Keenan, Darby, *et al.* 2014). A visual comparison of phenology was made in a Swiss mixed beech forest, finding that leaf emergence matched closely between visual estimates and green levels (Ahrends *et al.* 2008).

The earliest phenocams were often found in conjunction with eddy-covariance towers, hence several studies compare the gross primary productivity (GPP) with phenocam vegetation indices. A strong relationship was found between phenocam-estimated greenness indices and GPP in an alpine grassland (Migliavacca *et al.* 2011); this study also strongly linked phenocam greenness and common spectral vegetation indices such as NDVI. Similar success was found in an eddy-covariance flux tower study in an Australian tropical savannah (Moore *et al.* 2017), which used phenocams monitoring both understory and overstory vegetation to differentiate the tree and grass contribution to overall productivity. In an arctic wetland, modelled GPP from flux data significantly

correlated with several greenness indices in multiple locations (Westergaard-Nielsen *et al.* 2013). This study also found a significant correlation between g_{CC} and NDVI from the high-resolution WorldView-2 satellite.

Hufkens and colleagues note that estimates of phenology indices from a logistic model and MODIS vegetation indices show 'significant agreement', but estimation of timing metrics varies by approximately two weeks (Hufkens *et al.* 2012). Their findings caution that issues of scale and representation strongly influence the relationship between near surface and satellite remote sensing measures of phenology. A phenocam-based study in a Japanese grassland reported the strongest correlation between phenocam greenness and biomass measures (Inoue *et al.* 2015). This experiment focused on a small area (20 m x 20 m) of relatively homogenous grassland, and it is unlikely that such strong relationships would hold across a larger, more heterogeneous scale.

In the current study, linear correlation was used to compare the different methods. This analytical technique has been suggested by some authors to be overly simplistic, particularly when conducted on scaled variables (Keatley and Hudson 2010). This is certainly true; in the current study the correlation coefficient tells only a small part of how one variable compares to another, and qualitative differences between methods are necessary to provide further insights. However, linear correlation represents a quantitative starting point for investigating possible sources of variation between scales. Once hypotheses are made on preliminary trends, more sophisticated analytical techniques may be used to examine these further.

Scale transferability remains a major challenge despite decades of research in this field (Eisfelder *et al.* 2016). A fundamental difficulty in comparison studies is that there is often no single point of truth. This study compared alternative methods of measuring similar vegetation response. However, it is essential to acknowledge that each method provides slightly different information (Hufkens *et al.* 2012) but also different uncertainties and errors (Hill *et al.* 2006). In phenology studies, as in agricultural studies, plant biomass is often considered the standard. However vegetation sampling is subject to its own sources of uncertainty (Brummer *et al.* 1994). Productivity studies are replete with comparison studies of their own: investigating the effect of harvesting

frequency, dead material, and herbivory on how biomass and productivity can be accurately measured (Singh *et al.* 1975, Long *et al.* 1989, Scurlock *et al.* 2002). If this single point of truth cannot be known, then research needs to focus on understanding the drivers behind what is being measured, rather than determining which method is 'more correct'.

5.4.5 Sources of uncertainty and divergence in field measurements

The methods used within this project were developed in consultation with grassland field experts, conservation managers and agricultural practitioners to maximise the practical application of the findings. The methods were also designed to optimise data collection given the resources that were available. Pilot studies were conducted to ensure that, for example, biomass could be collected and processed in a timely fashion to ensure no tissue degradation. Grassland sites were selected for consistency and monitored for up to six months prior to project commencement to ensure the species composition was relatively consistent. However during the course of the field campaign, several areas of uncertainty were identified that relate to the variability of natural systems. While these do not reduce the applicability of the findings, they provide an opportunity for future studies to improve upon these methods.

The C_4 Native grasslands show the most consistent pattern within the functional groups. This group has the most homogenous grass cover, dominated by one climax species, *Themeda triandra*, and sites have comparable levels of grazing and other external disturbances. However all other functional groups demonstrated unwanted variability mostly due to unexpected species groups becoming common at different times of the year. Section 5.4.1 provides specific details of these changes. These 'unwanted' species are difficult to control in natural dynamic systems. Exotic pasture grasses are ubiquitous in low numbers in native pastures (Moore and Perry 1970), but can flourish if conditions are optimal. Subtle seasonal changes in grazing or environmental conditions can tip the thresholds, making certain microclimates more suitable for different species. This makes grasslands a challenge for classification—where species groups can be abundant one year, and rare the next (Vivian and Baines 2014). This can blur the boundaries between experimental units, in the case of the current study, grassland functional type.

Forbs were identified as contributing minimally to the overall biomass of grasslands, but may contribute proportionally more to measures of fractional cover and vegetation indices. Forbs may be under-represented in biomass assessment because common prostrate herbs (e.g. *Trifolium* spp., *Hypochaeris radicata*) are not as readily collected; most of their biomass occurs below the 1 cm harvesting threshold. When high numbers of these forbs occur, there may be a poorer correlation between biomass and remotely sensed indices. The canopy architecture and leaf morphology of these planophile forbs intercept and reflect more light than erectophile grasses (Jackson and Pinter 1986) and have a low proportion of dead vegetation. As such they have the potential to contribute proportionally higher to vegetation indices which may diverge from biomass data.

It was apparent during the collection process that the measured pasture height was unlikely to strongly correlate with live biomass. Particularly in the spring and summer, a large number of flowering spikes resulted in the falling plate 'hanging up' on seed heads above the grass leaves and giving an inflated height value. This was particularly true for sites dominated by *Phalaris aquatica* and *Themeda triandra* which have tall inflorescences that are retained on the plant for many months after flowering has occurred. This observation is supported by the height data: the timing of maximum height did not correspond with the timing of maximum biomass, as would be expected.

The flowering spikes can also change the relationship between photosynthetic and non-photosynthetic vegetation as they mature and dry. For C_4 grasslands, the maturation of flower spikes resulted in a peak in dead biomass which is not shown in the fractional cover data. This is also likely responsible for a decrease in g_{CC} that occurs at this time, as the phenocam oblique viewing angle is more sensitive to the tall, dense seed heads. However such trends are not observed in the fractional cover data or satellite NDVI, methods that use observations that are closer to nadir.

Issues with uncertainty can also result directly from grazing. On several occasions, the vegetation was trampled by domestic stock during grazing. This changes the architecture of the vegetation canopy, which in turn impacts the spectral reflectance properties and satellite vegetation indices (Mutanga *et al.* 2005). As the phenocam g_{CC}

is more responsive to changes in cover than biomass, this may represent a divergence in responses between near-surface and satellite methods.

The assessment of fractional cover introduced an element of subjectivity. The attribution of a leaf as either photosynthetic or non-photosynthetic does not account for the range of states dictated by physiology, chlorophyll content and other pigments. It requires the observer to select a colour threshold, above which is determined 'photosynthetic' and below which is determined 'non-photosynthetic'. For studies with multiple observers, additional subjectivity will result. Objective measures of canopy chlorophyll content are necessary to quantify the contribution of chlorophyll change to overall cover estimates. This may include colour charts (Hamill and Camlin 1984), chlorophyll meters (Víg *et al.* 2012), or chemical analysis.

Throughout this chapter, and indeed throughout this thesis, significant attention has been given to the impact that standing litter has on vegetation indices and phenology estimates. One key feature that has yet to be discussed occurs in sites with high volumes of standing dead litter. From the perspective of phenocams, satellites and cover estimates, the growth of new green leaves takes longer to emerge through the standing litter than a site with no litter. This is demonstrated by the data: live biomass data is recorded even when the VI curve is at its lowest and green cover data shows 0% f_{PV}. Particularly in the case of phenocams, the oblique angles of the cameras further suppress this. Hence the timing of greening estimated from phenocams is likely to be delayed where high quantities of litter are present.

5.4.6 Study limitations

The effects of grazing were noted throughout the study but were not controlled. Grazing reduces biomass and has been shown to decrease VI measures (Wylie *et al.* 2002, Yang and Guo 2011). Our sites show a variety of grazing pressures from known grazers—notably domestic stock and conspicuous native grazing animals (kangaroos)—but also will have grazing effects from other herbivores (e.g. rabbits, invertebrates). As such, grazing is a difficult variable to control on a large scale. However, phenocam g_{CC} shows that, within the same functional group, sites with constant grazing pressures have phenology curves consistent in shape with less heavily grazed sites. This is illustrated

for C_3 Native sites: GUNN and MGAR are heavily grazed but MULN is lightly grazed, yet the phenological profiles do not diverge. Similar responses occur for C4 Native sites: GIDL and TURA (ungrazed) show similar phenological response to MPON (moderately grazed). In each case, the more heavily grazed site has a consistently lower biomass. However it is feasible that while grazing removes biomass, it has little influence on fractional cover. Since we have shown g_{CC} to be more closely correlated with cover than biomass in these temperate grasslands, grazing may have less of an effect on g_{CC} than it does on other indices.

Data gaps in phenocam data have the potential to obscure trends if they are of significant duration (Hmimina *et al.* 2013). The main gaps in the phenocam data were as a result of lens fogging (particularly during cooler months), and technical failure due to moisture incursion. This was particularly prevalent in the early stages of the study before additional waterproofing was conducted. Efforts to eliminate data gaps in future phenocam studies will be rewarded with greater statistical power. More sophisticated phenocams (as described in Sonnentag *et al*. 2012) may assist in this endeavour, but come with the trade-off of greater cost and power requirements.

In the grasslands that were studied, and the conditions that occurred during the study period, the background soil contribution to the total cover was negligible. This is typical in Australian temperate grasslands—particularly native communities—as they retain dead material on the plant which covers any exposed soil (Morgan and Lunt 1999). However, in some situations, such as in drought, the background soil may contribute a significant proportion of fractional cover. The impact of this should be incorporated in studies where significant bare soil is likely to be present.

One factor that was not incorporated into this study was collecting phenological attributes that are comparable between scales (Rienke and Jones 2006). Unlike similar studies that have compared radiometric properties of vegetation at field versus remote scales (Westergaard-Nielsen *et al.* 2013, Inoue *et al.* 2015), the current study aimed to use commonly measured field biophysical parameters as the basis for ground-scale comparison. However, adding a field level spectral assessment would increase the ability to compare scales for estimating phenology (Garrity *et al.* 2011, Hmimina *et al.*

2013). Given the resources required for field spectral campaigns, this would need to be in the scope of a more focused research project.

The number of field biomass replicates represents another opportunity for improvement. While six 1 m^2 quadrats for sampling biomass seemed adequate based on homogeneous vegetation cover—and indeed was at the limit of what could be sampled and processed with available resources—further sampling would certainly have reduced the variability around the mean values (Brummer *et al.* 1994). Field sampling is known to have limited spatial applicability (White, Asner, *et al.* 2000) hence it is important to maximise samples where resources allow.

The most important limitation of this study is that conclusions have been drawn from only one year of monitoring. Given the inter-annual variability of south-eastern Australia's climate, several more years of monitoring would be worthwhile in confirming these trends. Several stakeholders from the project understand the value of this and have committed to continuing monitoring phenology variables to improve their understanding of how their vegetation changes from season-to-season and year-to-year.

5.4.7 Assessment of phenocams for monitoring temperate grasslands

This research found that the sub-daily image capture available through phenocams allows for the detection of fine-resolution changes in greenness that other methods could not match. Some researchers in other biomes incorporate moving-window averages to smooth fluctuations and remove error. However in Australian temperate systems these fluctuations indicate rapid responses to rainfall and temperature, and add enormous value in interpreting the dynamics of grassland vegetation. Although a smoothing line has been used in many of the figures within this thesis to interpolate data gaps and visually guide the reader, at times it is of insufficient resolution to discriminate these fine-scale changes.

The temporal scale collected by phenocams allow for the discrimination of phenology metrics at a time scale that is suitable to detect dynamic change. Changes in phenology due to climate trends typically report differences in scales of days per decade (Parmesan and Yohe 2003, Badeck *et al.* 2004, Graham *et al.* 2009). In many cases, satellite data

collected coarser than daily frequency will render changes under a certain threshold undetectable. Collecting data at daily frequency also has the capacity to resolve very subtle trends driven by community composition and environmental drivers that are not possible to resolve using other means.

The findings of this study suggest that the g_{CC} is a suitable vegetation index for capturing the dynamics of temperate grasslands. Like other studies (Sonnentag *et al.* 2012), this index was found to be invariant to changes in illumination, particularly where the camera field-of-view was appropriately positioned (i.e. with minimal sky in the frame). Overall the g_{CC} proved a consistent and repeatable index that matched visual interpretation.

Phenocams currently lack the spectral resolution shown by many satellites, and cannot match the large spatial coverage that satellite sensors capture easily. Nevertheless, technology in this field is advancing quickly, and will no doubt accelerate more as further research utilises these advantages. Phenocams have enormous potential as tools to support ecological monitoring, but should continue to be trialled in all biomes to develop image capture and analysis methods that can incorporate the enormous variation in global vegetation properties. As the knowledge in this field develops, there is a growing need to quantify illumination and camera angle effects on RBG indices, and to promote the standardisation of methodology to enable cross-continental phenological comparisons (Brown *et al.* 2016).

There may be an opportunity for large scale phenocam deployment outside the ecological sphere. It is clear from this research that phenocams could provide a distinct advantage to the agricultural industry, in determining appropriate times for pasture stocking, mowing or other management actions. On a larger scale, a network of phenocams could be established to quantify or forecast pasture yields or report on drought impacts—items that are always of relevance to Australian agriculture. As other phenocam networks have shown, this would require the development of novel methods to store, classify and analyse phenological information (Richardson *et al.* 2007, Nasahara and Nagai 2015). These is also significant scope for advances in statistical methods to characterise and analyse time-series imagery (Gray and Song 2013).

5.5 CONCLUSION

Australian temperate grasslands represent a continuum from highly productive exotic pastures to fragmented native grasslands. The need to identify and manage different grassland types is essential from an agricultural perspective to maximise grazing productivity under uncertain future climates. It is no less critical from a conservation perspective to identify the location of high conservation value native grasslands and monitor the recovery or degradation of these ecosystems. Remote sensing offers the capability to conduct this using land surface phenology of different grassland types, but an understanding of the biophysical and ecological principles underpinning phenology drivers is essential.

C_3 grasslands showed moderate greenness in autumn and winter, rapidly increasing to a peak greenness in October, and fluctuating greenness throughout the summer. They responded quickly to high temperatures and low rainfall during summer periods. C_4 grasslands exhibited very low green levels in the winter, began steadily greening from September to a December peak and maintained relatively high values until autumn. C_4 grassland phenology was influenced by the large quantities of standing litter that most sites contained.

Correlations between phenocam greenness, biomass estimates and satellite vegetation indices were significant across the data set and fall within the range of agreement found in similar cross-scalar studies. However, the use of additional field variables elicited further information, given that each data source provides a slightly varied contribution to land surface phenology. The significance and strength of these relationships was found to differ between grassland functional types. Imperfect correlations between measured variables occur due to different structural, spatial and spectral differences in the variables being measured. Differences in the remote-sensing response are exacerbated by differences in viewing angle: oblique viewing angles will be more affected by erectophile vegetation than nadir angles. The opposite effect is true for the emergence of broadleaved (planophile) forbs in spring: they may not be detected by oblique-viewing phenocams, but satellite remote sensing will be more responsive.

In Australian temperate grassland systems, remote sensing systems (satellite NDVI and phenocam g_{CC}) are more effective at estimating vegetation cover than biomass. Across all sites, satellites and phenocam are similar at predicting green cover. However, high frequency phenocam data elicits more immediate greening and browning events. Scaling measures between field and satellite level is dependent on understanding the variables being measured. As no variable represents a single point of truth, acknowledging that each measurement technique provides different information about the vegetation, but also represents different sources of error, is essential.

Differentiation of C_3-dominant grasslands from C_4-dominant grasslands is less straightforward than northern hemisphere biomes, as the dynamic nature of Australian temperate grassland renders standard methods inapplicable. This study attempted classification through seasonal segmentation of phenocam g_{CC} data, a method which takes advantage of the consistently low g_{CC} that C_4 grasslands exhibit during winter senescence and contrasts it with higher g_{CC} parameters at other times of year. This resulted in incomplete classification due to anomalous species mixes in certain functional groups. Further assessment of this method should be undertaken on a greater number of grasslands—preferably C_4-dominant, C_3-dominant, and mixed C_3/C_4—to assess the applicability of this method.

There are multiple challenges involved in the separation of grassland communities via remote sensing. Using phenological characteristics to improve the identification of native-dominated grasslands from exotic-dominated grasslands, and C_3-dominance from C_4-dominance is a research avenue that can improve the set of tools available for this challenge. Phenocams offer the advantage of high temporal capacity, which is necessary for highly dynamic systems.

Evaluation of the use of phenocams to monitor temperate grassland dynamics concluded that they are acceptable for capturing dynamic changes in greening and browning trends. However, standardisation of relative camera angle is essential for comparison between locations. They also provide value-added services such as monitoring of grazing densities, flowering phenology and providing records of wildlife and feral animals

Chapter 6: Synthesis and future research

Each chapter of this thesis presents the conclusions for that body of work. This section does not aim to reproduce that, but rather to synthesise the findings of multiple projects into major themes that also incorporate opportunities for future research.

6.1 Phenocams: Current Successes and Future Opportunities

In a short space of time, phenocams have moved from being a novel addition in ecological research to forming a major component of monitoring and research projects. As part of the current study, phenocams were used for the first time to quantify changes between experimental grassland treatments (Chapter 3). They were also used in the more conventional manner of quantifying vegetative phenology in observational research, and comparing the results to other methods of phenology estimation (Chapter 5). In both cases, the sub-daily temporal collection frequency combined with the robust g_{CC} vegetation index provided an excellent representation of vegetation dynamics. These patterns clearly coincided with known timing of rainfall, harvesting or disturbance and demonstrate confidence that phenocams provide accurate assessments of grassland dynamics at both the small scales of the experimental treatments and the large scales of the field research. This aligns with the conclusions of other researchers who have emphasised similar benefits of using phenocams (Sonnentag *et al.* 2012, Ide and Oguma 2013, Keenan, Darby, *et al.* 2014, Brown *et al.* 2016, Moore *et al.* 2016). Based on the success of this study, phenocams are likely to be used more commonly in controlled experiments and increase their standing in ecological monitoring projects.

From a technical perspective, phenocams demonstrated some weaknesses. The frequent loss of images through lens fogging or water ingress is undesirable in a method that cites high temporal capacity as a benefit. While there are more expensive phenocams available that would address these issues, budget constraints would reduce the number of experimental replicates and the power of any analysis. It would be more cost-effective to engineer waterproofing methods prior to camera deployment, and to maintain cameras regularly. Incorporation of a reference object to standardise colour measurements is an important addition to phenocam project, particularly when using

cameras that have limited manual control. However, the benefits of phenocams far outweighed the shortcomings.

Despite the success of phenocams in this domain, there is more research to be conducted as phenocams continue to be integrated into ecological studies. Chapter 5 and Appendix E provide an assessment of how camera angles impact the magnitude of visual indices. There is the potential to quantify view angle assessment more accurately using UAVs (e.g. multicopters) that can acquire imagery at multiple angles near-contemporaneously. Similarly, drone-based technology has potential to develop the effect of spatial scale on RGB and spectral indices. There is also scope for improving the accuracy of phenocam measurements through further investigation of illumination effects and shadowing.

The results from Chapter 3 suggest that valuable application exists in the agricultural sector for tracking pasture quality over time and conducting phenological forecasting. However, for this to be viable, further research is needed to confirm empirical relationships between RGB vegetation indices and vegetative productivity.

It seems likely that as the use of phenocams becomes widespread, technology will develop to provide researchers with new opportunities. To enable consistent global phenology comparisons, the primary challenge for researchers will be to design systematic methods for conducting, installing and archiving phenocam data in an environment of constantly-improving technology.

6.2 The Present and Future of Australian Temperate Grasslands

Temperate grasslands continue to be under threat, both within Australia and around the world (Henwood 2010, Williams and Morgan 2015). Since this project commenced, three additional temperate grassland communities have been added to Australia's listing of Critically Endangered Ecological Communities. While there have been advances in restoration techniques and laudable rates of community engagement in grassland conservation, the need to be able to identify and monitor temperate grasslands at a landscape scale remains key to the long-term sustainability of these communities. Likewise, from a grazing perspective, regional monitoring is important to maintain food

security and stability of the grazing sector in the context of a changing climate. Remote sensing still remains the most appropriate avenue to meet this challenge, but it is likely that the 'solution' is multi-faceted and best approached by advancement in several remote sensing techniques. This research highlights the potential of phenology as one such approach, but improvements in hyperspectral sensing, chlorophyll fluorescence, and other time-series based methods may provide other approaches.

The phenology of Australian temperate grassland systems is more complex than the well-studied northern hemisphere systems. Temperature, rainfall, ecology and land management have all been shown in this study to have an impact on land surface phenology. This complexity should be acknowledged by future researchers in this field; an *a priori* understanding that experimental settings may change as the grasslands themselves do. Experimental research that aims to control grazing or other land management may provide further information in this arena.

The requirements for successful grassland restoration are still not fully understood (Lunt and Morgan 1999). However effective methods for monitoring the success of restoration projects and experimental trials are essential to improve our knowledge. Monitoring projects must heed the requirement for floral surveys to be conducted at several times per year such that a full species census can be undertaken. Likewise, condition assessments must be cognisant of how seasonality can impact condition scores—particularly in grasslands that are close to condition thresholds.

Monitoring of species diversity is currently in the domain of botanical experts but may have its future in remote sensing technologies. The remote detection of individual species seems aspirational but is not beyond reach of current technology; indeed it has been possible for many years where the target species is conspicuous (e.g. Dehaan *et al.* 2007). Chapter 5 shows that the phenocams used in the current study, although boasting only a modest pixel resolution, can be used to detect the flowering of conspicuous species. Phenocams have also demonstrated the potential to identify regions of an image that demonstrate different phenology signatures. Like approaches in other grassland biomes (Julitta *et al.* 2014), pixel-level phenology metrics may be generated to present a surrogate for diversity: the higher the phenological variability, the higher the species

diversity. Remote technologies may not be able to identify all species as humans can currently do, but some of these applications are worth experimental development.

The use of phenocams and remote sensing will be key in future grassland monitoring as automated methods become standardised and more commonplace. Phenocams are already being used in broad-scale monitoring networks to track changes in vegetative cover, often used as a surrogate for condition (Hufkens *et al.* 2016). Phenocams are also being integrated in citizen science projects for phenology monitoring (Kosmala *et al.* 2016). Commercial applications for mobile devices have been developed that incorporate RGB greenness indices to estimate vegetative condition.

The role of ecological interactions between grassland species is a complex one that was not addressed in the controlled experiment of Chapter 2. As well as incorporating additional species, controlled experiments should incorporate mixtures of species to assist in developing spectral mixed models. This will assist in the disentangling of this issue in the field, where multiple species present a factor that is extremely difficult to control. The development of species-specific hyperspectral indices could be incorporated with PV/NPV mixture models to quantify the contribution of key grass species in a mixed system. Specialised indices are particularly required for non-photosynthetic vegetation, which was poorly characterised using the indices tested in these studies.

6.3 C_3 AND C_4 VEGETATION

The response of C_3 and C_4 vegetation to climatic changes in coming decades will be critical to ecological interactions, agricultural production and refinement of global climate models. This thesis examined empirical differences between phenology of some C_3 and C_4 species in the laboratory (Chapter 2) and how this translated into remotely-sensed phenology of known field sites (Chapter 5). From the laboratory perspective, future studies should assess phenological variability from a range of C_3 and C_4 species, and use more sophisticated treatments (e.g. higher temperatures, controlled watering regimes) to assess within-species variation. Field studies should focus on quantification of C_3/C_4 contribution to overall productivity. Ideally, this would include the integration of controlled and field experiments: planting areas of 'pure' C_3 and C_4 species mixes,

and comparing with mixed C_3/C_4 grasslands in the same region. In order to allow satellite remote sensing, this would have to be conducted at a larger spatial scale than any current research in Australia. The growing sector of native grassland restoration may help facilitate suitable research areas in the future.

Understanding the C_3/C_4 response under increased temperatures, enriched CO_2 and modified rainfall is still incomplete. Field studies of dynamic vegetation types present logistical and experimental difficulties, as researchers are dealing with a 'moving target' that can change unexpectedly throughout the course of an experiment. Significant investment is required into this field of research to enable the development of meaningful and realistic climate change adaptation strategies.

6.4 Remote Sensing of Phenology: Temporal and Spatial Scales

Observable changes in monthly grassland flora species and phenophase highlight that data collection must be frequent to accurately capture grassland dynamics. Satellite collection frequencies are often sub-optimal due to cloud cover resulting in extended data gaps. As satellites with different capabilities are launched, there is the opportunity to improve some temporal, spatial and spectral factors. However, while visual and near infrared bands of the spectrum continue to be most prominently used, cloud impacts will thwart efforts to improve and maintain consistent data collection.

The current research into multi-scale land surface phenology shows that measurements taken at different scales will fundamentally measure different parameters. They provide different sources of information and likewise have different sources of error. The relationship between the spatial scales differs as species composition and vegetation dynamics change, resulting in a practical challenge for researchers. As others have suggested (Rienke and Jones 2006), collection of comparable data contemporaneously is the best approach to achieve meaningful comparison.

The multi-scale comparisons in this study used relatively straightforward statistics as a first step in investigating these relationships in Australian temperate grasslands. Development of more robust statistical methods has been identified as a necessary step

for advancement of phenology (Keatley and Hudson 2010, Gray and Song 2013), and will be pivotal to maintaining analytical rigour as the phenology field grows.

6.5 Validation of Grassland Remote Sensing

It is broadly acknowledged that the integration of field validation is important in remote sensing studies. One of the lessons learned throughout this research is that dynamic systems such as grassland must also be validated dynamically; that is, conducted at several times throughout the year. Relationships between variables change depending on the season, and this needs to be considered throughout the experimental process. Chapter 4 demonstrated that grassland composition changes throughout the year, so multiple validation periods are required to capture this. Without rigorous validation, critical information to explain phenological variation of future studies may be lost.

The validation component of any project should be embedded into the study design to ensure that the timing, measurements and areas are all consistent with the remote component. As standing litter has been found to be an important factor in grassland remote sensing and phenological variation, validation efforts should incorporate some assessment of this variable, rather than focus on photosynthetic vegetation only.

Remote sensing studies have an implied paradigm that increased greenness equates to an improvement in condition. The findings of Chapter 3; that the post-drought increase in g_{CC} are due to an increase in herbaceous weeds, aligns with findings that increases in greenness do not necessarily correspond with increases in vegetation condition (Herrmann and Tappan 2013, Karnieli *et al.* 2013). Under more variable climates, weed invasions are likely to be more common (Scott *et al.* 2014) and ecological trophic cascades likely to be more pronounced (Suttle *et al.* 2007). Future remote sensing studies have to be cognisant of that element: validation should be conducted accordingly and anomalous results treated with a degree of caution.

6.6 Extensions of Current Research and Aspirational Studies

Each of the four research projects within this thesis represents an initial investigation into these research questions. Given the climatic variability in temperate Australia, the

key limitation of these findings is that they were derived from relatively short periods of data collection. An extension of this study is important to determine if these results are consistent under different climatic conditions.

The use of long-term satellite data sets is now becoming more feasible due to the substantial efforts of some organisations to make these consistent and publicly accessible. A logical next step is to investigate the long-term phenological trends of known grassland sites. For retrospective studies, the selection of sites that have historical records of vegetation (e.g. agricultural research stations, farms with good records, national parks, etc.) is critical to allow an element of historical validation. There is also opportunity to expand this work into the spatial domain by developing phenologically-based mapping products for temperate grasslands at an appropriately small scale.

The research within this thesis has improved our understanding of non-conventional phenology, which is a known knowledge gap in the phenology field (Adjorlolo *et al.* 2012). Further research into the phenology of different biomes is critical to accurately classify phenology at a global scale. Studies of phenology in Australia have been highlighted as a key limitation; hence our knowledge of Australian phenology can only improve with additional research in Australian biomes.

An aspirational research project to integrate the elements within this thesis would need to be both long-term and large scale. An appropriate facility would include the development of 'experimental grassland fields': plots of several hectares comprising sown native and exotic grasslands to be used for concomitant satellite, phenocam, spectroradiometer and ecological studies. Subsections of these fields could be used for large-scale climate manipulation experiments, incorporating rainfall, temperate and carbon enrichment factors. Results from these semi-natural plots are more readily compared with nearby native and exotic grasslands to better understand how the dynamics of natural grasslands responds to change. At the same time, fundamental investigations into scale, viewing geometry and image illumination would be undertaken with multi-angle phenocams and drone-mounted sensors. Ideally the whole facility would be covered with a small network of very high resolution phenocams such as those proposed by Brown and colleagues (2011). Critically, such a facility would

need to be transdisciplinary and collaborative, including researchers from a variety of fields (e.g. plant physiology, engineering, agricultural scientists) to develop applicable and practical solutions to grassland management issues, and convey these to the wider community.

Climate change presents an increased factor of uncertainty for the future of temperate grasslands, whether from the perspective of ecology and conservation, or from the perspective of economic growth and food security. The primary challenge for future researchers is to develop novel and innovative approaches to tackle the complex and uncertain future that Australian temperate grasslands—and other Australian ecosystems—are likely to face in coming decades. As the DRI-grass project and similar research continues to provide novel insights into the impacts of climate change, the importance of such research facilities may be realised. The advancement of our understanding depends on support for research in this country: an appetite for strategic investment in relevant scientific research is necessary to foster our knowledge of climate change impacts and the development of useful adaptation strategies.

Chapter 7: References

Abràmoff, M.D., Magalhães, P.J., and Ram, S.J., 2004. Image processing with imageJ. *Biophotonics International*, 11, 36–41.

ACT Territory & Municipal Services, 2010. *ACT kangaroo management plan*. ACT TAMS, Canberra: ACT TAMS.

Adamsen, A.F.J., Barnes, E.M., Kimball, B.A., Lamorte, R.L., Leavitt, S.W., and Pinter, P.J.J., 1999. Measuring wheat senescence with a digital camera. *Crop Science*, 39 (3), 719.

Adjorlolo, C., Mutanga, O., Cho, M., and Ismail, R., 2012. Challenges and opportunities in the use of remote sensing for C3 and C4 grass species discrimination and mapping. *African Journal of Range & Forage Science*, 29 (2), 47–61.

Agrecon, 2004. *Remote sensing mapping of grassy ecosystems in the Monaro*. Canberra: Report to the New South Wales Department of Environment and Conservation, Agricultural Reconnaisance Technologies Inc.

Agrecon, 2005. *Remote sensing mapping of grassy ecosystems in the upper catchment of the Shoalhaven River (Southern Tablelands section)*. Report to the New South Wales Department of Environment and Conservation, Agricultural Reconnaisance Technologies Inc.

Ahl, D.E., Gower, S.T., Burrows, S.N., Shabanov, N. V, Myneni, R.B., and Knyazikhin, Y., 2006. Monitoring spring canopy phenology of a deciduous broadleaf forest using MODIS. *Remote Sensing of Environment*, 104, 88–95.

Ahmadian, N., Ghasemi, S., Wigneron, J.-P., and Zölitz, R., 2016. Comprehensive study of the biophysical parameters of agricultural crops based on assessing Landsat 8 OLI and Landsat 7 ETM + vegetation indices. *GIScience & Remote Sensing*, 53 (3), 337–359.

Ahrends, H.E., Bräugger, R., Stöckli, R., Schenk, J., Michna, P., Jeanneret, F., Wanner, H., and Eugster, W., 2008. Quantitative phenological observations of a mixed beech forest in northern Switzerland with digital photography. *Journal of Geophysical Research: Biogeosciences*, 113 (G4).

Aiken, J., 2004. Redeveloping soil mapping key descriptors from generic soil series profiles for University of Western Sydney Hawkesbury campus soils. *In*: *3rd Australian & New Zealand Soils Conference*. Sydney, Australia: The Regional Institute Online Publishing.

Akiyama, T. and Kawamura, K., 2007. Grassland degradation in China: methods of monitoring, management and restoration. *Grassland Science*, 53, 1–17.

Alberton, B., Almeida, J., Helm, R., Torres, R., Menzel, A., and Morellato, L.P.C., 2014. Using phenological cameras to track the green up in a cerrado savanna and its on-the-ground validation. *Ecological Informatics*, 19, 62–70.

Allen, V.G., Batello, C., Berretta, E.J., Hodgson, J., Kothmann, M., Li, X., McIvor, J., Milne, J., Morris, C., Peeters, A., and Sanderson, M., 2011. An international terminology for grazing lands and grazing animals. *Grass and Forage Science*, 66, 2–28.

Analytical Spectral Devices, 1999. *Analytical Spectral Devices (ASD) technical guide*. Boulder, Colorado.

Anderegg, W.R.L., Plavcová, L., Anderegg, L.D.L., Hacke, U.G., Berry, J.A., and Field, C.B., 2013. Drought's legacy: multiyear hydraulic deterioration underlies widespread aspen forest die-off and portends increased future risk. *Global Change Biology*, 19 (4), 1188–1196.

Andrew, M.E. and Ustin, S.L., 2008. The role of environmental context in mapping invasive plants with hyperspectral image data. *Remote Sensing of Environment*, 112 (12), 4301–4317.

Aono, Y. and Kazui, K., 2008. Phenological data series of cherry tree flowering in Kyoto, Japan, and its application to reconstruction of springtime temperatures since the 9th century. *International Journal of Climatology*, 28, 905–914.

Asner, G.P., 1998. Biophysical and biochemical sources of variability in canopy reflectance. *Remote Sensing of Environment*, 64, 234–253.

Asner, G.P., Braswell, B.H., Schimel, D.S., and Wessman, C.A., 1998. Ecological research needs from multiangle remote sensing data. *Remote Sensing of Environment*, 63, 155–165.

Asner, G.P., Jones, M.O., Martin, R.E., Knapp, D.E., and Hughes, R.F., 2008. Remote sensing of native and invasive species in Hawaiian forests. *Remote Sensing of Environment*, 112, 1912–1926.

Austin, M.P., Williams, O.B., and Belbin, L., 1981. Grassland dynamics under sheep grazing in an Australian Mediterranean type climate. *Vegetatio*, 47, 201–211.

Australian Bureau of Agricultural and Resource Economics and Sciences, 2013. *Agricultural commodity statistics 2013*. Canberra: ABARES.

Australian Bureau of Statistics, 2014. *Agricultural commodities, Australia 2012-2013, Catalogue 7121.0*. Canberra: ABS.

Badeck, F.-W., Bondeau, A., Bottcher, K., Doktor, D., Lucht, W., Schaber, J., and Sitch, S., 2004. Responses of spring phenology to climate change. *New Phytologist*, 162, 295–309.

Baker, H.G., 1974. The evolution of weeds. *Annual Review of Ecology and Systematics*, 4, 1–24.

Baldocchi, D.D., 2011. The grass response. *Nature*, 476, 160–161.

Barlow, T., 1998. *Grassy Guidelines: how to manage native grasslands and grassy woodlands on your property*. Melbourne, Australia: Trust For Nature (Victoria).

Bater, C.W., Coops, N.C., Wulder, M.A., Hilker, T., Nielsen, S.E., McDermid, G., and Stenhouse, G.B., 2011. Using digital time-lapse cameras to monitor species-specific understorey and overstorey phenology in support of wildlife habitat assessment. *Environmental Monitoring and Assessment*, 180, 1–13.

Bates, J.D., Svejcar, T., Miller, R.F., and Angell, R.A., 2006. The effects of precipitation timing on sagebrush steppe vegetation. *Journal of Arid Environments*, 64, 670–697.

Beaumont, L.J., McAllan, I.A.W., and Hughes, L., 2006. A matter of timing: changes in the first date of arrival and last date of departure of Australian migratory birds. *Global Change Biology*, 12, 1339–1354.

Beier, C., Beierkuhnlein, C., Wohlgemuth, T., Penuelas, J., Emmett, B., Körner, C., de Boeck, H., Christensen, J.H., Leuzinger, S., Janssens, I.A., and Hansen, K., 2012. Precipitation manipulation experiments - challenges and recommendations for the future. *Ecology Letters*, 15 (8), 899–911.

Benson, J.S., 1994. The native grasslands of the Monaro region: Southern Tablelands of NSW. *Cunninghamia*, 3 (3), 609–650.

Benson, J.S., Ashby, E.M., and Porteners, M.F., 1997. The native grasslands of the Riverine Plain, New South Wales. *Cunninghamia*, 5 (1), 1–48.

Betancourt, J., Schwartz, M.D., Breshears, D.D., Brewer, C.A., Frazer, G., Gross, J.E., Mazer, S.J., Reed, B.C., and Wilson, B.E., 2007. Evolving plans for the USA National Phenology Network. *Eos*, 88 (19), 211.

de Beurs, K.M. and Henebry, G.M., 2004. Land surface phenology, climatic variation, and institutional change: analyzing agricultural land cover change in Kazakhstan. *Remote Sensing of Environment*, 89, 497–509.

de Beurs, K.M. and Henebry, G.M., 2005. A statistical framework for the analysis of long image time series. *International Journal of Remote Sensing*, 26 (8), 1551–1573.

de Beurs, K.M. and Henebry, G.M., 2010. Spatio-temporal statistical methods for modelling land surface phenology. *In*: I.L. Hudson and M.R. Keatley, eds. *Phenological research*. Dordrecht: Springer Netherlands, 177–208.

Bhandari, S., Phinn, S., and Gill, T., 2011. Assessing viewing and illumination geometry effects on the MODIS vegetation index (MOD13Q1) time series: implications for monitoring phenology and disturbances in forest communities in Queensland, Australia. *International Journal of Remote Sensing*, 32 (22), 7513–7538.

Biddiscombe, E.F., Cuthbertson, E.G., and Hutchings, R.J., 1953. Autecology of some natural pasture species at Trangie, NSW. *Australian Journal of Botany*, 2, 69–98.

Blackburn, G.A., 2007. Hyperspectral remote sensing of plant pigments. *Journal of Experimental Botany*, 58 (4), 855–867.

Bradley, B.A., Jacob, R.W., Hermance, J.F., and Mustard, J.F., 2007. A curve fitting procedure to derive inter-annual phenologies from time series of noisy satellite NDVI data. *Remote Sensing of Environment*, 106, 137–145.

Bradley, B.A. and Mustard, J.F., 2008. Comparison of phenology trends by land cover class: a case study in the Great Basin, USA. *Global Change Biology*, 14, 334–346.

Bréda, N.J.J., 2003. Ground-based measurements of leaf area index: a review of methods, instruments and current controversies. *Journal of Experimental Botany*, 54 (392), 2403–2417.

Brinkmann, K., Dickhoefer, U., Schlecht, E., and Buerkert, A., 2011. Quantification of aboveground rangeland productivity and anthropogenic degradation on the Arabian Peninsula using Landsat imagery and field inventory data. *Remote Sensing of Environment*, 115 (2), 465–474.

Broich, M., Huete, A., Paget, M., Ma, X., Tulbure, M., Restrepo, N., Evans, B., Beringer, J., Devadas, R., Davies, K., and Held, A., 2015. A spatially explicit land surface phenology data product for science, monitoring and natural resources management applications. *Environmental Modelling and Software*, 64, 191–204.

Brown, J.S. and Venable, D.L., 1986. Evolutionary ecology of seed-bank annuals in temporally varying environments. *The American Naturalist*, 127 (1), 31–47.

Brown, T., Zimmermann, C., Panneton, W., Noah, N., and Borevitz, J., 2011. High-resolution, time-lapse imaging for ecosystem-scale phenotyping in the field. *In*: J. Normanly, ed. *High throughput phenotyping in plants: methods in molecular biology*. New York: Springer, 71–96.

Brown, T.B., Hultine, K.R., Steltzer, H., Denny, E.G., Denslow, M.W., Granados, J., Henderson, S., Moore, D., Nagai, S., Sanclements, M., Sánchez-Azofeifa, A., Sonnentag, O., Tazik, D., and Richardson, A.D., 2016. Using phenocams to monitor our changing Earth: toward a global phenocam network. *Frontiers in Ecology and the Environment*, 14

(2), 84–93.

Brummer, J.E., Nichols, J.T., Engel, K., and Kent, M., 1994. Efficiency of different quadrat sizes and shapes for sampling standing crop. *Journal of Range Management*, 47, 84–89.

Buheaosier, Tsuchiya, S., Kaneko, M., and Sung, S.J., 2003. Comparison of image data acquired with AVHRR, MODIS, ETM+ and ASTER over Hokkaido, Japan. *Advances in Space Research*, 32 (11), 2211–2216.

Cai, W., Cowan, T., Briggs, P., and Raupach, M., 2009. Rising temperature depletes soil moisture and exacerbates severe drought conditions across southeast Australia. *Geophysical Research Letters*, 36 (21), doi:10.1029/2009GL040334.

Campbell, B., Stafford Smith, D., and McKeon, G., 1997. Elevated CO_2 and water supply interactions in grasslands: a pastures and rangelands management perspective. *Global Change Biology*, 3, 177–187.

Campbell, P.K.E., Middleton, E.M., McMurtrey, J.E., Corp, L.A., and Chappelle, E.W., 2007. Assessment of vegetation stress using reflectance or fluorescence measurements. *Journal of Environmental Quality*, 36 (3), 832–845.

Caradonna, P.J., Iler, A.M., and Inouye, D.W., 2014. Shifts in flowering phenology reshape a subalpine plant community. *Proceedings of the National Academy of Sciences of the United States of America*, 111 (13), 4916–4921.

Ceballos, G., Davidson, A., List, R., Pacheco, J., Manzano-Fischer, P., Santos-Barrera, G., and Cruzado, J., 2010. Rapid decline of a grassland system and its ecological and conservation implications. *PloS one*, 5 (1), e8562.

Chambers, L.E., 2008. Trends in timing of migration of south-western Australian birds and their relationship to climate. *Emu*, 108, 1–14.

Chambers, L.E., 2009. Evidence of climate related shifts in Australian phenology. *In*: *18th World IMACS/MODSIM Congress, 13-17 July 2009*. Cairns, Australia, 2597–2603.

Chambers, L.E., Gibbs, H., Weston, M.A., and Ehmke, G.C., 2008. Spatial and temporal variation in the breeding of Masked Lapwings (*Vanellus miles*) in Australia. *Emu*, 108, 115–124.

Chan, C.W., 1980. Natural grasslands in Canberra: their distribution, phenology and effects of mowing. Unpublished MSc Thesis, Australian National University.

Chandola, V., Hui, D., Gu, L., Bhaduri, B., and Vatsavai, R.R., 2010. Using time series segmentation for deriving vegetation phenology indices from MODIS NDVI data. *In*: *2010 IEEE International Conference on Data Mining Workshops*. Sydney, Australia, 202–

208.

Cheal, D., 2008. Repeatability of cover estimates? *Ecological Management and Restoration*, 9 (1), 67–68.

Cheng, Y., Gamon, J., Fuentes, D., Mao, Z., Sims, D., Qiu, H., Claudio, H., Huete, A.R., and Rahman, A., 2006. A multi-scale analysis of dynamic optical signals in a Southern California chaparral ecosystem: a comparison of field, AVIRIS and MODIS data. *Remote Sensing of Environment*, 103, 369–378.

Churkina, G. and Running, S.W., 1998. Contrasting climatic controls on the estimated productivity of global terrestrial biomes. *Ecosystems*, 1 (2), 206–215.

Chuvieco, E. and Huete, A.R., 2009. Physical principles of remote sensing. *In*: E. Chuvieco and A.R. Huete, eds. *Fundamentals of satellite remote sensing*. Boca Raton, Florida: CRC Press, 21–62.

Cleland, E.E., Chuine, I., Menzel, A., Mooney, H.A., and Schwartz, M.D., 2007. Shifting plant phenology in response to global change. *Trends in Ecology & Evolution*, 22 (7), 357–365.

Clements, B., Ayres, L., Langford, C., McGarva, L., Simpson, P., Hennessey, G., Keys, M., Upjohn, B., and Leech, F., 2003. *Grazier's guide to pastures: sowing and managing profitable pastures in the Central and Southern Tablelands, Monaro and Upper South West Slopes of New South Wales*. Dubbo: NSW Agriculture.

Cleveland, W.S., 1979. Robust locally weighted regression and smoothing scatterplots. *Journal of the American Statistical Association*, 74 (368), 829–836.

Coburn, C.A. and Peddle, D.R., 2006. A low-cost field and laboratory goniometer system for estimating hyperspectral bidirectional reflectance. *Canadian Journal of Remote Sensing*, 32 (3), 244–253.

Cole, I. and Lunt, I.D., 2005. Restoring Kangaroo Grass (*Themeda triandra*) to grassland and woodland understoreys: a review of establishment requirements and restoration exercises in south-east Australia. *Ecological Management and Restoration*, 6 (1), 28–33.

Coops, N.C., Stone, C., Culvenor, D.S., and Chisholm, L., 2004. Assessment of crown condition in eucalypt vegetation by remotely sensed optical indices. *Journal of Environmental Quality*, 33 (3), 956–964.

Coughenor, M.B., 1985. Graminoid responses to grazing by large herbivores: adaptations, exaptations and interacting processes. *Annals of the Missouri Botanic Garden*, 72, 852–863.

Crimmins, M.A. and Crimmins, T.M., 2008. Monitoring plant phenology using digital repeat

photography. *Environmental Management*, 41 (6), 949–958.

Crimmins, T.M., Crimmins, M.A., Bertelsen, D., and Balmat, J., 2008. Relationships between alpha diversity of plant species in bloom and climatic variables across an elevation gradient. *International Journal of Biometeorology*, 52, 353–366.

Cristiano, P.M., Posse, G., Di Bella, C.M., and Boca, T., 2012. Influence of contrasting availabilities of water and nutrients on the radiation use efficiency in C3 and C4 grasses. *Austral Ecology*, 37, 323–329.

Cristiano, P.M., Posse, G., Di Bella, C.M., and Jaimes, F.R., 2010. Uncertainties in fPAR estimation of grass canopies under different stress situations and differences in architecture. *International Journal of Remote Sensing*, 31 (15), 4095–4109.

Crosthwaite, J., 1995. *Economic benefits for native grassland on farms*. Canberra, Australia: Environment Australia.

CSIRO, 2011. *Climate change: science and solutions for Australia*. Collingwood, Victoria: CSIRO Publishing.

CSIRO and Bureau of Meteorology, 2015. *Climate change in Australia: information for Australia's natural resource management regions*. Canberra: CSIRO and Bureau of Meteorology.

Cui, X., Guo, Z.G., Liang, T.G., Shen, Y.Y., Liu, X.Y., and Liu, Y., 2012. Classification management for grassland using MODIS data: a case study in the Gannan region, China. *International Journal of Remote Sensing*, 33 (10), 3156–3175.

Cullen, B., Eckard, R., Johnson, I., Lodge, G., Walker, R., Rawnsley, R., Dassanayake, K., Christie, K., McCaskill, M., Clark, S., Sanford, P., Browne, N., Sinclair, K., Chapman, D., Leiffering, M., Snow, V., Hovenden, M., and Perring, M., 2008. *Climate change impacts on Australian grazing systems: whole farming systems analysis and tools for the Australian and New Zealand grazing industries project report*. Melbourne: University of Melbourne.

Cullen, B.R., Johnson, I.R., Eckard, R.J., Lodge, G.M., Walker, R.G., Rawnsley, R.P., and McCaskill, M.R., 2009. Climate change effects on pasture systems in south-eastern Australia. *Crop and Pasture Science*, 60, 933–942.

Dardel, C., Kergoat, L., Hiernaux, P., Mougin, E., Grippa, M., and Tucker, C.J., 2014. Re-greening Sahel: 30 years of remote sensing data and field observations (Mali, Niger). *Remote Sensing of Environment*, 140, 350–364.

Datt, B., 1998. Remote sensing of chlorophyll a, chlorophyll b, chlorophyll a&b, and total

carotenoid content in Eucalyptus leaves. *Remote Sensing of Environment*, 66, 111–121.

Daughtry, C.S.T., Biehl, L.L., and Ranson, K.J., 1989. A new technique to measure the spectral properties of conifer needles. *Remote Sensing of Environment*, 27, 81–91.

Daughtry, C.S.T., McMurtrey, J.E., Nagler, P.L., Kim, M.S., and Chappelle E W, 1996. Spectral reflectance of soils and crop residues. *In*: A.M.C. Davies and P. Williams, eds. *Near infrared spectroscopy: the future waves*. Chichester, UK: NIR Publications, 505–511.

Davidson, A. and Csillag, F., 2003. A comparison of three approaches for predicting C4 species cover of northern mixed grass prairie. *Remote Sensing of Environment*, 86, 70–82.

Davila, Y.C. and Wardle, G.M., 2007. Bee boys and fly girls: do pollinators prefer male or female umbels in protandrous parsnip, *Trachymene incisa* (Apiaceae)? *Austral Ecology*, 32, 798–807.

Dawson, T.P. and Curran, P.J., 1998. A new technique for interpolating the reflectance red edge position. *International Journal of Remote Sensing*, 19 (11), 2133–2139.

Dehaan, R., Louis, J., Wilson, A., Hall, A., and Rumbachs, R., 2007. Discrimination of blackberry (*Rubus fruticosus* sp. agg.) using hyperspectral imagery in Kosciuszko National Park, NSW, Australia. *ISPRS Journal of Photogrammetry and Remote Sensing*, 62, 13–24.

Department of Environment, 2016. *Natural temperate grassland of the South Eastern Highlands: a nationally protected ecological community*. Canberra: Commonwealth of Australia.

Department of Environment Climate Change & Water, 2011. *Operational Manual for BioMetric 3.1*. Sydney, Australia.

Department of the Environment, 2016. *Approved conservation advice (including listing advice) for natural temperate grassland of the South Eastern Highlands [effective from 6 Apr 2016]*. Canberra: Commonwealth of Australia.

Dilley, A.C., Millie, S., O'Brien, D.M., and Edwards, M., 2004. The relation between Normalized Difference Vegetation Index and vegetation moisture content at three grassland locations in Victoria, Australia. *International Journal of Remote Sensing*, 25 (19), 3913–3928.

Donald, G.E., Gherardi, S.G., Edirisinghe, A., Gittins, S.P., Henry, D.A., and Mata, G., 2010. Using MODIS imagery, climate and soil data to estimate pasture growth rates on farms in the south-west of Western Australia. *Animal Production Science*, 50, 611–615.

Donohue, R.J., McVicar, T.R., and Roderick, M.L., 2009. Climate-related trends in Australian

vegetation cover as inferred from satellite observations, 1981-2006. *Global Change Biology*, 15 (4), 1025–1039.

Dorrough, J., McIntyre, S., and Scroggie, M.P., 2011. Individual plant species responses to phosphorus and livestock grazing. *Australian Journal of Botany*, 59 (7), 669–680.

Dorrough, J.W., 2008. Broad-scale management of biodiversity in temperate grazing lands and implications for productivity and profitability. *In*: C. Waters and D. Gordon, eds. *Proceedings of the 25th Annual Conference of The Grasslands Society of NSW*. Sydney, 16–23.

Dostálek, J. and Frantík, T., 2011. Response of dry grassland vegetation to fluctuations in weather conditions: a 9-year case study in Prague (Czech Republic). *Biologia*, 66 (5), 837–847.

Drusch, M., Bello, U. Del, Carlier, S., Colin, O., Fernandez, V., Gascon, F., Hoersch, B., Isola, C., Laberinti, P., Martimort, P., Meygret, A., Spoto, F., Sy, O., Marchese, F., and Bargellini, P., 2012. Sentinel-2: ESA's optical high-resolution mission for GMES operational services. *Remote Sensing of Environment*, 120, 25–36.

Dudney, J., Hallett, L.M., Larios, L., Farrer, E.C., Erica, N., Stein, C., and Suding, K.N., 2016. Lagging behind: have we overlooked previous-year rainfall effects in annual grasslands? *Journal of Ecology*, 1–12.

Dunin, F.X., Aston, A.R., and Reyenga, W., 1978. Evaporation from a Themeda grassland. II: resistance model of plant evaporation. *Journal of Applied Ecology*, 15, 847–858.

Dunlop, M. and Brown, P.R., 2008. *Implications of climate change for Australia's national reserve system: a preliminary assessment. Report to the Department of Climate Change, February 2008*. Canberra: Department of Climate Change.

Dye, D.G., Middleton, B.R., Vogel, J.M., Wu, Z., and Velasco, M., 2016. Exploiting differential vegetation phenology for satellite-based mapping of semiarid grass vegetation in the Southwestern United States. *Remote Sensing*, 8 (11), doi:10.3390/rs8110889.

Easterling, D.R., Meehl, G.A., Parmesan, C., Changnon, S.A., Karl, T.R., and Mearns, L.O., 2000. Climate extremes: observations, modeling, and impacts. *Science*, 289, 2068–2074.

Eco Logical Australia, 2009. *The native grasslands of New South Wales: environmental, indigenous and agricultural values and sustainable management*. Project No. 227-001: Prepared for National Resources Advisory Council.

Eddy, D., 2002. *Managing native grassland: a guide to management for conservation, production and landscape protection*. Sydney: WWF Australia.

Ehleringer, J.R., Cerling, T.E., and Helliker, B.R., 1997. C4 photosynthesis, atmospheric CO_2, and climate. *Oecologia*, 112 (3), 285–299.

Eisfelder, C., Kuenzer, C., Dech, S., Eisfelder, C., Kuenzer, C., and Dech, S., 2016. Derivation of biomass information for semi-arid areas using remote-sensing data. *International Journal of Remote Sensing*, 33 (9), 2937–2984.

Eldridge, D.J., Poore, A.G.B., Ruiz-Colmenero, M., Letnic, M., and Soliveres, S., 2016. Ecosystem structure, function, and composition in rangelands are negatively affected by livestock grazing. *Ecological Applications*, 26 (4), 1273–1283.

Entwistle, T.J., 2014. *Sprinter and sprummer: Australia's changing seasons*. Collingwood, Victoria: CSIRO Publishing.

Environmental Research & Information Consortium, 2001. *Remote sensing detection of native grasslands using multi-image spectral analysis*. Prepared for NSW National Parks and Wildlife Service.

Epstein, H., Lauenroth, W., and Burke, I., 1997. Effects of temperature and soil texture on ANPP in the U.S. Great Plains. *Ecology*, 78 (8), 2628–2631.

Epstein, H.E., Lauenroth, W.K., Burke, I.C., and Coffin, D.P., 1997. Productivity patterns of C3 and C4 functional types in the U.S. Great Plains. *Ecological Society of America*, 78 (3), 722–731.

Fang, J., Piao, S., Zhou, L., He, J., Wei, F., Myneni, R.B., Tucker, C.J., and Tan, K., 2005. Precipitation patterns alter growth of temperate vegetation. *Geophysical Research Letters*, 32 (21).

Fay, P.A., Carlisle, J.D., Knapp, A.K., Blair, J.M., and Collins, S.L., 2003. Productivity responses to altered rainfall patterns in a C4-dominated grassland. *Oecologia*, 137, 245–251.

Fay, P.A., Kaufman, D.M., Nippert, J.B., Carlisle, J.D., and Harper, C.W., 2008. Changes in grassland ecosystem function due to extreme rainfall events: implications for responses to climate change. *Global Change Biology*, 14, 1600–1608.

Fensham, R.J., 1998. The grassy vegetation of the Darling Downs, south-eastern Queensland, Australia. Floristics and grazing effects. *Biological Conservation*, 84 (3), 301–310.

Fischer, B.U., Frehner, M., Hebeisen, T., Zanetti, S., Stadelmann, F., Luscher, A., Hartwig, U.A., Hendrey, G.R., Blum, H., and Nosberger, J., 1997. Source-sink relations in *Lolium perenne* L. as reflected by carbohydrate concentrations in leaves and pseudo-stems during regrowth in a free air carbon dioxide enrichment (FACE) experiment. *Plant, Cell and*

Environment, 20, 945–952.

Fisher, J.I. and Mustard, J.F., 2007. Cross-scalar satellite phenology from ground, Landsat, and MODIS data. *Remote Sensing of Environment*, 109, 261–273.

Fisher, J.I., Mustard, J.F., and Vadeboncoeur, M.A., 2006. Green leaf phenology at Landsat resolution: scaling from the field to the satellite. *Remote Sensing of Environment*, 100, 265–279.

Fitter, A. and Fitter, R., 2002. Rapid changes in flowering time in British plants. *Science*, 296, 1689–1691.

Flanagan, L.B., 2009. Phenology of plant production in the northwestern Great Plains: relationships with carbon isotope discrimination, net ecosystem productivity and ecosystem respiration. *In*: A. Noormets, ed. *Phenology of ecosystem processes: applications in global change research*. New York: Springer, 169–185.

Fontana, F., Rixen, C., Jones, T., Aberegg, G., and Wunderle, S., 2008. Alpine grassland phenology as seen in AVHRR, VEGETATION and MODIS NDVI time series - a comparison with in situ measurements. *Sensors*, 8, 2833–2853.

Foody, G.M. and Dash, J., 2010. Estimating the relative abundance of C3 and C4 grasses in the Great Plains from multi-temporal MTCI data: issues of compositing period and spatial generalizability. *International Journal of Remote Sensing*, 31 (2), 351–362.

Foran, B.D., 1987. Detection of yearly cover change with Landsat MSS on pastoral landscapes in Central Australia. *Remote Sensing of Environment*, 23, 333–350.

Frame, J., 1993. Herbage mass. *In*: A. Davies, R.D. Baker, S.A. Grant, and A.S. Laidlaw, eds. *Sward measurement handbook*. British Grassland Society, 59–63.

Friedl, M.A., Davis, F.W., Michaelsen, J., and Moritz, M.A., 1995. Scaling and uncertainty in the relationship between the NDVI and land surface biophysical variables: an analysis using a scene simulation model and data from FIFE. *Remote Sensing of Environment*, 54, 233–246.

Friedl, M.A., Schimel, D.S., Michaelsen, J., Davis, F.W., and Walker, H., 1994. Estimating grassland biomass and leaf area index using ground and satellite data. *International Journal of Remote Sensing*, 15 (7), 1401–1420.

Fry, E.L., Manning, P., Allen, D.G.P., Hurst, A., Everwand, G., Rimmler, M., and Power, S.A., 2013. Plant functional group composition modifies the effects of precipitation change on grassland ecosystem function. *PloS one*, 8 (2), e57027.

Fry, E.L., Manning, P., and Power, S.A., 2014. Ecosystem functions are resistant to extreme

changes to rainfall regimes in a mesotrophic grassland. *Plant and Soil*, 381, 351–365.

Gallagher, R. V., Hughes, L., and Leishman, M.R., 2009. Phenological trends among Australian alpine species: Using herbarium records to identify climate-change indicators. *Australian Journal of Botany*, 57 (1), 1–9.

Gammage, B., 2011. *The biggest estate on Earth*. Melbourne: Allen & Unwin Sydney.

Gao, J., 2006. Quantification of grassland properties: how it can benefit from geoinformatic technologies? *International Journal of Remote Sensing*, 27 (7), 1351–1365.

Garbulsky, M.F., Peñuelas, J., Gamon, J., Inoue, Y., and Filella, I., 2011. The photochemical reflectance index (PRI) and the remote sensing of leaf, canopy and ecosystem radiation use efficiencies A review and meta-analysis. *Remote Sensing of Environment*, 115, 281–297.

Garrard, G.E., Bekessy, S.A., Mccarthy, M.A., and Wintle, B.A., 2008. When have we looked hard enough? A novel method for setting minimum survey effort protocols for flora surveys. *Austral Ecology*, 33, 986–998.

Garrard, G.E., McCarthy, M.A., Williams, N.S.G., Bekessy, S.A., and Wintle, B.A., 2013. A general model of detectability using species traits. *Methods in Ecology and Evolution*, 4, 45–52.

Garrity, S.R., Bohrer, G., Maurer, K.D., Mueller, K.L., Vogel, C.S., and Curtis, P.S., 2011. A comparison of multiple phenology data sources for estimating seasonal transitions in deciduous forest carbon exchange. *Agricultural and Forest Meteorology*, 151 (12), 1741–1752.

Gavier-Pizarro, G.I., Kuemmerle, T., Hoyos, L.E., Stewart, S.I., Huebner, C.D., Keuler, N.S., and Radeloff, V.C., 2012. Monitoring the invasion of an exotic tree (Ligustrum lucidum) from 1983 to 2006 with Landsat TM/ETM+ satellite data and Support Vector Machines in Córdoba, Argentina. *Remote Sensing of Environment*, 122, 134–145.

Geerken, R., Zaitchik, B., and Evans, J.P., 2005. Classifying rangeland vegetation type and coverage from NDVI time series using Fourier Filtered Cycle Similarity. *International Journal of Remote Sensing*, 26 (24), 5535–5554.

Ghannoum, O., Evans, J., and von Caemmerer, S., 2011. Nitrogen and water use efficiency of C4 plants. *In*: A.S. Raghavendra and R.F. Sage, eds. *C4 photosynthesis and related CO_2 concentrating mechanisms*. Springer Netherlands, 129–146.

Gibbs, H., 2007. Climatic variation and breeding in the Australian Magpie (*Gymnorhina tibicen*): a case study using existing data. *Emu*, 107, 284–293.

Gibson, D.J., 2009. *Grasses and grassland ecology*. New York: Oxford University Press.

Gilgen, A.K. and Buchmann, N., 2009. Response of temperate grasslands at different altitudes to simulated summer drought differed but scaled with annual precipitation. *Biogeosciences Discussions*, 6 (3), 5217–5250.

Gillespie, A.R., Kahle, A.B., and Walker, R.E., 1987. Color enhancement of highly correlated images. II. Channel ratio and 'chromaticity' transformation techniques. *Remote Sensing of Environment*, 22 (3), 343–365.

Gitelson, A.A., Gritz, Y., and Merzlyak, M.N., 2003. Relationships between leaf chlorophyll content and spectral reflectance and algorithms for non-destructive chlorophyll assessment in higher plant leaves. *Journal of Plant Physiology*, 160, 271–282.

Gitelson, A.A. and Merzlyak, M.N., 1994. Spectral reflectance changes associated with autumn senescence of *Aesculus hippocastanum* L. and *Acer platanoides* L. leaves. Spectral features and relation to chlorophyll estimation. *Journal of Plant Physiology*, 143, 286–292.

Glenn, E.P., Huete, A.R., Nagler, P.L., and Nelson, S.G., 2008. Relationship between remotely-sensed vegetation indices, canopy attributes, and plant physiological processes: what vegetation indices can and cannot tell us about the landscape. *Sensors*, 8, 2136–2160.

Glenn, N.F., Mundt, J.T., Weber, K.T., Prather, T.S., Lass, L.W., and Pettingill, J., 2005. Hyperspectral data processing for repeat detection of small infestations of leafy spurge. *Remote Sensing of Environment*, 95, 399–412.

Godínez-Alvarez, H., Herrick, J.E., Mattocks, M., Toledo, D., and Van Zee, J., 2009. Comparison of three vegetation monitoring methods: their relative utility for ecological assessment and monitoring. *Ecological Indicators*, 9 (2009), 1001–1008.

Goel, P.K., Prasher, S.O., Patel, R.M., Landry, J.A., Bonnell, R.B., and Viau, A.A., 2003. Classification of hyperspectral data by decision trees and artificial neural networks to identify weed stress and nitrogen status of corn. *Computers and Electronics in Agriculture*, 39, 67–93.

Goodin, D.G. and Henebry, G.M., 1997. A technique for monitoring ecological disturbance in tallgrass prairie using seasonal NDVI trajectories and a discriminant function mixture model. *Remote Sensing of Environment*, 61, 270–278.

Goodwin, N., Turner, R., and Merton, R., 2005. Classifying *Eucalyptus* forests with high spatial and spectral resolution imagery: an investigation of individual species and vegetation communities. *Australian Journal of Botany*, 53 (4), 337–345.

Gott, B., 1982. Ecology of root use by the Aborigines of southern Australia. *Archaeology in Oceania*, 17 (1), 59–67.

Gott, B., Williams, N.S.G., and Antos, M., 2015. Humans and grasslands - a social history. *In*: N.S.G. Williams, A. Marshall, and J.W. Morgan, eds. *Land of sweeping plains*. Clayton, Victoria: CSIRO Publishing, 6–26.

Govender, M., Chetty, K., and Bulcock, H., 2007. A review of hyperspectral remote sensing and its application in vegetation and water resource studies. *Water South Africa*, 33 (2), 145–152.

Goward, S.N., Tucker, C.J., and Dye, D.G., 1985. North American vegetation patterns observed with the NOAA-7 advanced very high resolution radiometer. *Vegetatio*, 64, 3–14.

Graham, E.A., Riordan, E.C., Yuen, E.M., Estrin, D., and Rundel, P.W., 2010. Public internet-connected cameras used as a cross-continental ground-based plant phenology monitoring system. *Global Change Biology*, 16, 3014–3023.

Graham, E.A., Yuen, E.M., Robertson, G.F., Kaiser, W.J., Hamilton, M.P., and Rundel, P.W., 2009. Budburst and leaf area expansion measured with a novel mobile camera system and simple color thresholding. *Environmental and Experimental Botany*, 65, 238–244.

Gray, J. and Song, C., 2013. Consistent classification of image time series with automatic adaptive signature generalization. *Remote Sensing of Environment*, 134, 333–341.

Greaves, B.L. and Spencer, R.D., 1993. An evaluation of spectroradiometry and multispectral scanning for differentiating forest communities. *Australian Forestry*, 56, 68–79.

Green, K., 2010. Alpine taxa exhibit differing responses to climate warming in the Snowy Mountains of Australia. *Journal of Mountain Science*, 7, 167–175.

Greenville, A.C., Dickman, C.R., Wardle, G.M., and Letnic, M., 2009. The fire history of an arid grassland: the influence of antecedent rainfall and ENSO. *International Journal of Wildland Fire*, 18, 631–639.

Grenzdorffer, G.J. and Niemeyer, F., 2011. UAV based BRDF-measurements of agricultural surfaces with PFIFFikus. *International Archives of the Photogrammetry, Remote Sensing and Spatial Information Sciences*, 38, 229–234.

Grime, J.P., 1973. Control of species density in herbaceous vegetation. *Journal of Environmental Management*, 1, 151–167.

Groves, R.H., 1965. Growth of *Themeda australis* tussock grassland at St. Albans, Victoria. *Australian Journal of Botany*, 13, 291–302.

Groves, R.H., 1979. The status and future of Australian grasslands. *New Zealand Journal of*

Ecology, 2, 76–81.

Groves, R.H., 1994. *Australian vegetation*. Second ed. Cambridge, UK: Cambridge University Press.

Groves, R.H. and Whalley, R.D.B., 2002. Grass and grassland ecology in Australia. *In*: K. Mallett and A.E. Orchard, eds. *Flora of Australia, Volume 43*. Canberra: Australian Biological Resources Study, 157–182.

Gu, Y., Wylie, B.K., and Bliss, N.B., 2013. Mapping grassland productivity with 250-m eMODIS NDVI and SSURGO database over the Greater Platte River Basin, USA. *Ecological Indicators*, 24, 31–36.

Guerschman, J.P., Hill, M.J., Renzullo, L.J., Barrett, D.J., Marks, A.S., and Botha, E.J., 2009. Estimating fractional cover of photosynthetic vegetation, non-photosynthetic vegetation and bare soil in the Australian tropical savanna region upscaling the EO-1 Hyperion and MODIS sensors. *Remote Sensing of Environment*, 113, 928–945.

Hamill, M. and Camlin, M.S., 1984. The measurement of leaf colour in grasses. *The Journal of Agricultural Science*, 103 (2), 387–393.

Hansen, P.M. and Schjoerring, J.K., 2003. Reflectance measurement of canopy biomass and nitrogen status in wheat crops using normalized difference vegetation indices and partial least squares regression. *Remote Sensing of Environment*, 86 (4), 542–553.

Harle, K.J., Howden, S.M., Hunt, L.P., and Dunlop, M., 2007. The potential impact of climate change on the Australian wool industry by 2030. *Agricultural Systems*, 93, 61–89.

Harper, C.W., Blair, J.M., Fay, P.A., Knapp, A.K., and Carlisle, J.D., 2005. Increased rainfall variability and reduced rainfall amount decreases soil CO_2 flux in a grassland ecosystem. *Global Change Biology*, 11 (2), 322–334.

Hattersley, P.W., 1983. The distribution of C3 and C4 grasses in Australia in relation to climate. *Oecologia*, 57 (1983), 113–128.

Heisler-White, J.L., Blair, J.M., Kelly, E.F., Harmoney, K., and Knapp, A.K., 2009. Contingent productivity responses to more extreme rainfall regimes across a grassland biome. *Global Change Biology*, 15, 2894–2904.

Heisler-White, J.L., Knapp, A.K., and Kelly, E.F., 2008. Increasing precipitation event size increases aboveground net primary productivity in a semi-arid grassland. *Oecologia*, 158, 129–140.

Henebry, G., 1993. Detecting change in grasslands using measures of spatial dependence with Landsat TM data. *Remote Sensing of Environment*, 46, 223–234.

Henneken, R., Dose, V., Schleip, C., and Menzel, A., 2013. Detecting plant seasonality from webcams using Bayesian multiple change point analysis. *Agricultural and Forest Meteorology*, 168, 177–185.

Hennessy, K., Fitzharris, B., Bates, B.C., Harvey, N., Howden, S.M., Hughes, L., Salinger, J., and Warrick, R., 2007. Australia and New Zealand. *In*: M.L. Parry, O.F. Canziani, J.P. Palutikof, P.J. van der Linden, and C.E. Hanson, eds. *Climate Change 2007: impacts, adaptation and vulnerability. Contribution of working group II to the Fourth Assessment Report of the Intergovernmental Panel on Climate Change*. Cambridge, UK: Cambridge University Press, 507–540.

Hennessy, K., J, P., Mcinnes, K., Walsh, K., Pittock, B., Bathols, J., and Suppiah, R., 2004. *Climate change in the Northern Territory*. Darwin, Australia: CSIRO.

Henwood, W.D., 2010. Toward a strategy for the conservation and protection of the world's temperate grasslands. *Great Plains Research*, 20 (1), 121–134.

Herrmann, S.M. and Tappan, G.G., 2013. Vegetation impoverishment despite greening: a case study from central Senegal. *Journal of Arid Environments*, 90, 55–66.

Hestir, E.L., Khanna, S., Andrew, M.E., Santos, M.J., Viers, J.H., Greenberg, J.A., Rajapakse, S.S., and Ustin, S.L., 2008. Identification of invasive vegetation using hyperspectral remote sensing in the California Delta ecosystem. *Remote Sensing of Environment*, 112 (11), 4034–4047.

Hill, M.J., 2013. Vegetation index suites as indicators of vegetation state in grassland and savanna: An analysis with simulated SENTINEL 2 data for a North American transect. *Remote Sensing of Environment*, 137, 94–111.

Hill, M.J., Donald, G.E., Hyder, M.W., and Smith, R.C.G., 2004. Estimation of pasture growth rate in the south west of Western Australia from AVHRR NDVI and climate data. *Remote Sensing of Environment*, 93, 528–545.

Hill, M.J., Román, M.O., Schaaf, C.B., Hutley, L., Brannstrom, C., Etter, A., and Hanan, N.P., 2011. Characterizing vegetation cover in global savannas with an annual foliage clumping index derived from the MODIS BRDF product. *Remote Sensing of Environment*, 115, 2008–2024.

Hill, M.J., Senarath, U., Lee, A., Zeppel, M., Nightingale, J.M., Williams, R.J., and McVicar, T.R., 2006. Assessment of the MODIS LAI product for Australian ecosystems. *Remote Sensing of Environment*, 101 (4), 495–518.

Hill, R.S., 2004. Origins of the southeastern Australian vegetation. *Philosophical Transactions of the Royal Society of London. Series B, Biological Sciences*, 359 (1450), 1537–1549.

Hmimina, G., Dufrêne, E., Pontailler, J.-Y., Delpierre, N., Aubinet, M., Caquet, B., de Grandcourt, A., Burban, B., Flechard, C., Granier, A., Gross, P., Heinesch, B., Longdoz, B., Moureaux, C., Ourcival, J.-M., Rambal, S., Saint André, L., and Soudani, K., 2013. Evaluation of the potential of MODIS satellite data to predict vegetation phenology in different biomes: An investigation using ground-based NDVI measurements. *Remote Sensing of Environment*, 132, 145–158.

Hnatuik, R., Thackway, R., and Walker, J., 2009. Vegetation. *In*: *Australian soil and land survey field handbook*. Collingwood, Victoria: CSIRO Publishing.

Hodgkinson, K.C., 2014. *Condition of selected natural temperate grassland sites in urban and peri-urban Canberra*. Final report to the Commissioner of Sustainability and the Environment, ACT.

Hodgkinson, K.C. and Miller, W.J., 2005. Death model for tussock perennial grasses: a rainfall threshold for survival and evidence for landscape control of death in drought. *The Rangeland Journal*, 27, 105–115.

Horion, S., Cornet, Y., Erpicum, M., and Tychon, B., 2013. Studying interactions between climate variability and vegetation dynamic using a phenology based approach. *International Journal of Applied Earth Observation and Geoinformation*, 20, 20–32.

Hovenden, M.J., 2007. Flowering phenology in a species-rich temperate grassland is sensitive to warming but not elevated CO_2. *New Phytologist*, 178, 815–823.

Hovenden, M.J., Williams, A.L., Pedersen, J.K., Vander Schoor, J.K., and Wills, K.E., 2008. Elevated CO_2 and warming impacts on flowering phenology in a southern Australian grassland are related to flowering time but not growth form, origin or longevity. *Australian Journal of Botany*, 56, 630–643.

Hovenden, M.J., Wills, K.E., Vander Schoor, J.K., Williams, A.L., and Newton, P.C.D., 2008. Flowering phenology in a species-rich temperate grassland is sensitive to warming but not elevated CO_2. *New Phytologist*, 178, 815–822.

Howden, M., Hughes, L., Dunlop, M., Zethoven, I., Hilbert, D., and Chilcott, C., 2003. *Climate change impacts on biodiversity in Australia, outcomes of a workshop sponsored by the Biological Diversity Advisory Committee, 1-2 October 2002*. Canberra: Commonwealth of Australia.

Howden, S., Crimp, S., and Stokes, C., 2008. Climate change and Australian livestock systems: impacts, research and policy issues. *Australian Journal of Experimental Agriculture*, 48, 780–788.

Howden, S.M., McKeon, G.M., Walker, L., Carter, J.O., Conroy, J.P., Day, K.A., Hall, W.B.,

Ash, A.J., and Ghannoum, O., 1999. Global change impacts on native pastures in south-east Queensland, Australia. *Environmental Modelling and Software*, 14, 307–316.

Huang, C.-Y. and Asner, G.P., 2009. Applications of remote sensing to alien invasive plant studies. *Sensors*, 9, 4869–4889.

Hudson, I.L., 2010. Meta-analysis and its application in phenological research: a review and new statistical approaches. *In*: I.L. Hudson and M.R. Keatley, eds. *Phenological research*. Dordrecht: Springer Netherlands, 463–509.

Huete, A.R., 1988. A Soil-Adjusted Vegetation Index (SAVI). *Remote Sensing of Environment*, 25, 295–309.

Huete, A.R., 2012. Vegetation indices, remote sensing and forest monitoring. *Geography Compass*, 6 (9), 513–532.

Huete, A.R., Didan, K., Miura, T., Rodriguez, E.P., Gao, X., and Ferreira, L.G., 2002. Overview of the radiometric and biophysical performance of the MODIS vegetation indices. *Remote Sensing of Environment*, 83, 195–213.

Huete, A.R. and Jackson, R.D., 1987. Suitability of spectral indices for evaluating vegetation characteristics on arid rangelands. *Remote Sensing of Environment*, 23, 213–232.

Huete, A.R., Justice, C., and Liu, H., 1994. Development of vegetation and soil indices for MODIS-EOS. *Remote Sensing of Environment*, 49 (3), 224–234.

Huete, A.R., Liu, H.Q., Batchily, K., and van Leeuwen, W., 1997. A comparison of vegetation indices over a global set of TM images for EOS-MODIS. *Remote Sensing of Environment*, 59, 440–451.

Huete, A.R., Restrepo-Coupe, N., Ratana, P., Didan, K., Saleska, S.R., Ichii, K., Panuthai, S., and Gamo, M., 2008. Multiple site tower flux and remote sensing comparisons of tropical forest dynamics in Monsoon Asia. *Agricultural and Forest Meteorology*, 148, 748–760.

Hufkens, K., Friedl, M., Sonnentag, O., Braswell, B.H., Milliman, T., and Richardson, A.D., 2012. Linking near-surface and satellite remote sensing measurements of deciduous broadleaf forest phenology. *Remote Sensing of Environment*, 117, 307–321.

Hufkens, K., Keenan, T.F., Flanagan, L.B., Scott, R.L., Bernacchi, C.J., Joo, E., Brunsell, N.A., Verfaillie, J., and Richardson, A.D., 2016. Productivity of North American grasslands is increased under future climate scenarios despite rising aridity. *Nature Climate Change*, 6, 710–714.

Hughes, L., 2000. Biological consequences of global warming: is the signal already apparent? *Trends in Ecology & Evolution*, 15 (2), 56–61.

Huxman, T.E., Cable, J.M., Ignace, D.D., Eilts, J.A., English, N.B., Weltzin, J., and Williams, D.G., 2004. Response of net ecosystem gas exchange to a simulated precipitation pulse in a semi-arid grassland: the role of native versus non-native grasses and soil texture. *Oecologia*, 141, 295–305.

Ide, R. and Oguma, H., 2010. Use of digital cameras for phenological observations. *Ecological Informatics*, 5 (5), 339–347.

Ide, R. and Oguma, H., 2013. A cost-effective monitoring method using digital time-lapse cameras for detecting temporal and spatial variations of snowmelt and vegetation phenology in alpine ecosystems. *Ecological Informatics*, 16, 25–34.

Inoue, T., Nagai, S., Kobayashi, H., and Koizumi, H., 2015. Utilization of ground-based digital photography for the evaluation of seasonal changes in the aboveground green biomass and foliage phenology in a grassland ecosystem. *Ecological Informatics*, 25, 1–9.

IPCC, 2014. *Climate Change 2014: impacts, adaptation, and vulnerability. Part A: gobal and sectorial aspects. Working Group II contribution to the Fifth Assessment Report of the Intergovernmental Panel on Climate Change*. Cambridge, UK and New York, NY, USA: Cambridge University Press.

Jackson, R.D. and Pinter, P.J., 1986. Spectral response of architecturally different wheat canopies. *Remote Sensing of Environment*, 20, 43–56.

Jenerette, G.D., Scott, R.L., and Huete, A.R., 2010. Functional differences between summer and winter season rain assessed with MODIS-derived phenology in a semi-arid region. *Journal of Vegetation Science*, 21, 16–30.

Jetz, W., Thomas, G.H., Joy, J.B., Redding, D.W., Harman, K., and Mooers, A.O., 2014. Global distribution and conservation of evolutionary distinctness in birds. *Current Biology*, 24, 1–12.

Jobbagy, E.G. and Sala, O.E., 2000. Controls of grass and shrub aboveground production in the Patagonian steppe. *Ecological Applications*, 10 (2), 541–549.

Jones, H. and Vaughan, R., 2010. *Remote sensing of vegetation: principles, techniques and applications*. New York: Oxford University Press.

Jones, M.B. and Donnelly, A., 2004. Carbon sequestration in temperate grassland ecosystems and the influence of management, climate and elevated CO_2. *New Phytologist*, 164 (3), 423–439.

Julitta, T., Cremonese, E., Migliavacca, M., Colombo, R., Galvagno, M., Siniscalco, C., Rossini, M., Fava, F., Cogliati, S., Morra, U., and Menzel, A., 2014. Using digital camera

images to analyse snowmelt and phenology of a subalpine grassland. *Agricultural and Forest Meteorology*, 198–199, 116–125.

Justice, C.O. and Hiernaux, P.H.Y., 1986. Monitoring the grasslands of the Sahel using NOAA AVHRR data: Niger 1983. *International Journal of Remote Sensing*, 7 (11), 1475–1497.

Kalapos, T., 1994. Leaf water potential - leaf water deficit relationship for ten species of a semiarid grassland community. *Plant and Soil*, 160, 105–112.

Kandwal, R., Jeganathan, C., Tolpekin, V., and Kushwaha, S.P.S., 2009. Discriminating the invasive species, 'Lantana' using vegetation indices. *Journal of Indian Remote Sensing*, 37, 275–290.

Karnieli, A., Bayarjargal, Y., Bayasgalan, M., Mandakh, B., Dugarjav, C., Burgheimer, J., Khudulmur, S., Bazha, S.N., and Gunin, P.D., 2013. Do vegetation indices provide a reliable indication of vegetation degradation? A case study in the Mongolian pastures. *International Journal of Remote Sensing*, 34 (17), 6243–6262.

Keatley, M.R., Fletcher, T.I.M.D., Hudson, I.L., and Ades, P.K., 2002. Phenological studies in Australia: potential application in historical and future climate analysis. *International Journal of Climatology*, 22, 1769–1780.

Keatley, M.R. and Hudson, I.L., 2010. *Phenological research: methods for environmental and climate change analysis*. Dordrecht: Springer Netherlands.

Keenan, T.F., Darby, B., Felts, E., Sonnentag, O., Friedl, M.A., Hufkens, K., O'Keefe, J., Klosterman, S.T., Munger, J.W., Toomey, M., and Richardson, A.D., 2014. Tracking forest phenology and seasonal physiology using digital repeat photography: a critical assessment. *Ecological Applications*, 24 (6), 1478–1489.

Keenan, T.F., Gray, J., Friedl, M.A., Toomey, M., Bohrer, G., Hollinger, D.Y., Munger, J.W., Keefe, J.O., Schmid, H.P., Wing, I.S., Yang, B., and Richardson, A.D., 2014. Net carbon uptake has increased through warming-induced changes in temperate forest phenology. *Nature Climate Change*, 4, 598–604.

Keith, D.A. and Gorrod, E., 2006. The meanings of vegetation condition. *Ecological Management and Restoration*, 7 (S1), S7–S9.

Kharin, V. V., Zwiers, F.W., Zhang, X., and Hegerl, G.C., 2007. Changes in temperature and precipitation extremes in the IPCC ensemble of global coupled model simulations. *Journal of Climate*, 20, 1419–1444.

Kirkpatrick, J.B., 1999. Grassy vegetation and subalpine communities. *In*: J.B. Reid, R.S. Hill, M.J. Brown, and M.J. Henenden, eds. *Vegetation of Tasmania*. Canberra: Australian

Biological Resources Study.

Kirono, D.G.C. and Kent, D.M., 2011. Assessment of rainfall and potential evaporation from global climate models and its implications for Australian regional drought projection. *International Journal of Climatology*, 31, 1295–1308.

Klimeš, L., 2003. Scale-dependent variation in visual estimates of grassland plant cover. *Journal of Vegetation Science*, 14, 815–821.

Klosterman, S.T., Hufkens, K., Gray, J.M., Melaas, E., Sonnentag, O., Lavine, I., Mitchell, L., Norman, R., Friedl, M.A., and Richardson, A.D., 2014. Evaluating remote sensing of deciduous forest phenology at multiple spatial scales using PhenoCam imagery. *Biogeosciences Discussions*, 11, 2305–2342.

Knapp, A.K., Beier, C., Briske, D.D., Classen, A.T., Luo, Y., Reichstein, M., Smith, M.D., Smith, S.D., Bell, J.E., Fay, P.A., Heisler, J.L., Leavitt, S.W., Sherry, R., Smith, B., and Weng, E., 2008. Consequences of more extreme precipitation regimes for terrestrial ecosystems. *BioScience*, 58 (9), 811–821.

Knapp, A.K., Briggs, J.M., and Koelliker, J.K., 2001. Frequency and extent of water limitation to primary production in a mesic temperate grassland. *Ecosystems*, 4 (1), 19–28.

Knapp, A.K., Fay, P.A., Blair, J.M., Collins, S.L., Smith, M.D., Carlisle, J.D., Harper, C.W., Danner, B.T., Lett, M.S., and McCarron, J.K., 2002. Rainfall variability, carbon cycling, and plant species diversity in a mesic grassland. *Science*, 298 (5601), 2202–5.

Knapp, A.K. and Smith, M.D., 2001. Variation among biomes in temporal dynamics of aboveground primary production. *Science*, 291 (5503), 481–484.

Koch, E., 2010. Global framework for data collection - data bases, data availability, future networks, online databases. *In*: I.L. Hudson and M.R. Keatley, eds. *Phenological research*. New York: Springer, 23–62.

Kokaly, R.F., Despain, D.G., Clark, R.N., and Livo, K.E., 2003. Mapping vegetation in Yellowstone National Park using spectral feature analysis of AVIRIS data. *Remote Sensing of Environment*, 84, 437–456.

Körner, C., 2006. Plant CO_2 responses: an issue of definition, time and resource supply. *New Phytologist*, 172, 393–411.

Kosmala, M., Crall, A., Cheng, R., Hufkens, K., Henderson, S., and Richardson, A., 2016. Season Spotter: using citizen science to validate and scale plant phenology from near-surface remote sensing. *Remote Sensing*, 8, doi:10.3390/rs8090726.

Kuhnell, C., Goulevitch, B., Danaher, T.J., and Harris, D., 1998. Mapping woody vegetation

cover over the state of Queensland using Landsat TM. *In*: *9th Australasian Remote Sensing and Photogrammetry Conference*. Sydney, Australia.

Kulmatiski, A. and Beard, K.H., 2013. Woody plant encroachment facilitated by increased precipitation intensity. *Nature Climate Change*, 3 (9), 833–837.

Kumar, L., 1998. Modelling forest resources using geographical information systems and hyperspectral remote sensing. Unpublished PhD Thesis, School of Geography, The University of New South Wales, Sydney.

Kurc, S.A. and Benton, L.M., 2010. Digital image-derived greenness links deep soil moisture to carbon uptake in a creosotebush-dominated shrubland. *Journal of Arid Environments*, 74, 585–594.

Lane, D., Coffin, D., and Lauenroth, W., 1998. Effects of soil texture and precipitation on above-ground net primary productivity and vegetation structure across the Central Grassland region of the United States. *Journal of Vegetation Science*, 9, 239–250.

Lauenroth, W., Hunt, H., Swift, D., and Singh, J., 1986. Estimating aboveground net primary production in grasslands: a simulation approach. *Ecological Modelling*, 33, 297–314.

Lawley, V., Lewis, M., Clarke, K., and Ostendorf, B., 2015. Site-based and remote sensing methods for monitoring indicators of vegetation condition: an Australian review. *Ecological Indicators*, 60, 1273–1283.

Lawrence, R.L., Wood, S.D., and Sheley, R.L., 2006. Mapping invasive plants using hyperspectral imagery and Breiman Cutler classifications (RandomForest). *Remote Sensing of Environment*, 100, 356–362.

Lazarides, M., 2002. Economic attributes of Australian grasses. *In*: K. Mallett and A.E. Orchard, eds. *Flora of Australia, Volume 43*. Canberra: Australian Biological Resources Study, 213–244.

van Leeuwen, W.J.D. and Huete, A.R., 1996. Effects of standing litter on the biophysical interpretation of plant canopies with spectral indices. *Remote Sensing of Environment*, 138, 123–138.

Levin, N.A., Levental, S.A., and Morag, H.A., 2012. The effect of wildfires on vegetation cover and dune activity in Australia's desert dunes: a multisensor analysis. *International Journal of Wildland Fire*, 21, 459–475.

Lewis, M., Jooste, V., and de Gasparis, A.A., 2001. Discrimination of arid vegetation with airborne multispectral scanner hyperspectral imagery. *IEEE Transactions on Geoscience and Remote Sensing*, 39 (7), 1471–1479.

Lhermitte, S., Verbesselt, J., Verstraeten, W.W., and Coppin, P., 2011. A comparison of time series similarity measures for classification and change detection of ecosystem dynamics. *Remote Sensing of Environment*, 115 (12), 3129–3152.

Li, J., Duggin, J.A., Loneragan, W.A., and Grant, C.D., 2006. Grassland responses to multiple disturbances on the New England Tablelands in NSW, Australia. *Plant Ecology*, 193 (1), 39–57.

Li, P., Jiang, L., and Feng, Z., 2014. Cross-comparison of vegetation indices derived from Landsat-7 Enhanced Thematic Mapper Plus (ETM+) and Landsat-8 Operational Land Imager (OLI) sensors. *Remote Sensing*, 6, 310–329.

Li, X.-B., Chen, Y.-H., Yang, H., and Zhang, Y.-X., 2005. Improvement, comparison, and application of field measurement methods for grassland vegetation fractional coverage. *Journal of Integrative Plant Biology*, 47 (9), 1074–1083.

Liang, L., Schwartz, M.D., and Fei, S., 2011. Validating satellite phenology through intensive ground observation and landscape scaling in a mixed seasonal forest. *Remote Sensing of Environment*, 115, 143–157.

Liu, L. and Cheng, Z., 2011. Mapping C3 and C4 plant functional types using separated solar-induced chlorophyll fluorescence from hyperspectral data. *International Journal of Remote Sensing*, 21 (24), 9171–9183.

Liu, Z.-Y., Huang, J.-F., Wu, X.-H., and Dong, Y.-P., 2007. Comparison of vegetation indices and red-edge parameters for estimating grassland cover from canopy reflectance data. *Journal of Integrative Plant Biology*, 49 (3), 299–306.

Long, S.P., Garcia Moya, E., Imbamba, S.K., Kamnalrut, A., Piedade, M.T.F., Scurlock, J.M.O., Shen, Y.K., and Hall, D.O., 1989. Primary productivity of natural grass ecosystems of the tropics: a reappraisal. *Plant and Soil*, 115 (2), 155–166.

Lopez Diaz, J.E. and Gonzalez Rodriguez, A., 2003. Measuring grass yield by non-destructive methods: a review. *In*: *Proceedings of the 12th Symposium of the European Grassland Federation*. Pleven, Bulgaria.

Lu, H., Raupach, M.R., McVicar, T.R., and Barrett, D.J., 2003. Decomposition of vegetation cover into woody and herbaceous components using AVHRR NDVI time series. *Remote Sensing of Environment*, 86, 1–18.

Lunt, I.D., 1997. Effects of long-term vegetation management on remnant grassy forests and anthropogenic native grasslands in south-eastern Australia. *Biological Conservation*, 81, 287–297.

Lunt, I.D. and Morgan, J., 2002. The role of fire regimes in temperate lowland grasslands of southeastern Australia. *In*: R.A. Bradstock, J.E. Williams, and M.A. Gill, eds. *The fire regimes and biodiversity of a continent*. Cambridge: Cambridge University Press, 177–196.

Lunt, I.D. and Morgan, J.W., 1999. Vegetation changes after 10 years of grazing exclusion and intermittent burning in a *Themeda triandra* (Poaceae) grassland reserve in south-eastern Australia. *Australian Journal of Botany*, 47 (4), 537–552.

Lymburner, L., Tan, P., Mueller, N., Thackway, R., Lewis, A., Thankappan, M., Randall, L., Islam, A., and Senarath, U., 2011. *The national dynamic land cover dataset, Record 2011/31*. Canberra: Geoscience Australia.

Ma, X., Huete, A., Yu, Q., Coupe, N.R., Davies, K., Broich, M., Ratana, P., Beringer, J., Hutley, L.B., Cleverly, J., Boulain, N., and Eamus, D., 2013. Spatial patterns and temporal dynamics in savanna vegetation phenology across the North Australian Tropical Transect. *Remote Sensing of Environment*, 139, 97–115.

van der Maarel, E., 1979. Transformation of cover-abundance values in phytosociology and its effects on community similarity. *Vegetatio*, 39 (2), 97–114.

van der Maarel, E., 2007. Transformation of cover-abundance values for appropriate numerical treatment – alternatives to the proposals by Podani. *Journal of Vegetation Science*, 18, 767–770.

MacPhail, M.K. and Hill, R.S., 2002. Paleobotany of the Poaceae. *In*: K. Mallett and A.E. Orchard, eds. *Flora of Australia, Volume 43*. Canberra: Australian Biological Resources Study, 37–70.

Maguire, O., Armstrong, R.C., Benson, J.S., Streeter, R., Paterson, C., McDonald, P., Salter, N., East, M., Webster, M., Sheahan, M., and Young, D., 2012. Using high resolution digital aerial imagery interpreted in a 3-D digital GIS environment to map predefined plant communities in central-southern New South Wales. *Cunninghamia*, 12 (4), 247–266.

Martin, D., Grant, I., Jones, S., and Anderson, S., 2009. Development of satellite vegetation indices to assess grassland curing across Australia and New Zealand. *In*: S. Jones and K. Reinke, eds. *Innovations in Remote Sensing and Photogrammetry*. Berlin: Springer-Verlag, 211–227.

Matesanz, S., Brooker, R.W., Valladares, F., and Klotz, S., 2009. Temporal dynamics of marginal steppic vegetation over a 26-year period of substantial environmental change. *Journal of Vegetation Science*, 20, 299–310.

McAlpine, C.A., Syktus, J., Ryan, J.G., Deo, R.C., Mckeon, G.M., Mcgowan, H.A., and Phinn,

S.R., 2009. A continent under stress: interactions, feedbacks and risks associated with impact of modified land cover on Australia's climate. *Global Change Biology*, 15 (9), 2206–2223.

McDougall, K.L. and Kirkpatrick, J., 1994. *Conservation of lowland native grasslands in south-eastern Australia*. Sydney: World Wide Fund for Nature (Australia).

McDougall, K.L. and Walsh, N.G., 2007. Treeless vegetation of the Australian Alps. *Cunninghamia*, 10 (1), 1–57.

McIntyre, S. and Martin, T.G., 2002. Managing intensive and extensive land uses to conserve grassland plants in sub-tropical eucalypt woodlands. *Biological Conservation*, 107, 241–252.

McNellie, M., Dorrough, J.W., and Oliver, I., 2017. Using skewed species abundance distribution to underpin and inform ordinal cover-abundance transformation. *(in preparation)*.

Menzel, A., 2002. Phenology: its importance to the global change community. *Climatic Change*, 54, 379–385.

Menzel, A., Sparks, T.H., Estrella, N., Koch, E., Aasa, A., Ahas, R., Alm-Kübler, K., Bissolli, P., Braslavská, O., Briede, A., Chmielewski, F.M., Crepinsek, Z., Curnel, Y., Dahl, Å., Defila, C., Donnelly, A., Filella, Y., Jatczak, K., Måge, F., Mestre, A., Nordli, Ø., Peñuelas, J., Pirinen, P., Remišová, V., Scheifinger, H., Striz, M., Susnik, A., Van Vliet, A.J.H., Wielgolaski, F.-E., Zach, S., and Zust, A., 2006. European phenological response to climate change matches the warming pattern. *Global Change Biology*, 12 (10), 1969–1976.

Migliavacca, M., Galvagno, M., Cremonese, E., Rossini, M., Meroni, M., Sonnentag, O., Cogliati, S., Manca, G., Diotri, F., Busetto, L., Cescatti, A., Colombo, R., Fava, F., Morra di Cella, U., Pari, E., Siniscalco, C., and Richardson, A.D., 2011. Using digital repeat photography and eddy covariance data to model grassland phenology and photosynthetic CO_2 uptake. *Agricultural and Forest Meteorology*, 151 (10), 1325–1337.

Min, S.-K., Zhang, X., Zwiers, F.W., and Hegerl, G.C., 2011. Human contribution to more-intense precipitation extremes. *Nature*, 470, 378–381.

Miranda, J. de D., Padilla, F.M., and Pugnaire, F.I., 2009. Response of a Mediterranean semiarid community to changing patterns of water supply. *Perspectives in Plant Ecology, Evolution and Systematics*, 11 (4), 255–266.

Misson, L., Degueldre, D., Collin, C., Rodriguez, R., Rocheteau, A., Ourcival, J.-M., and Rambal, S., 2011. Phenological responses to extreme droughts in a Mediterranean forest.

Global Change Biology, 17 (2), 1036–1048.

Mizunuma, T., Wilkinson, M., L. Eaton, E., Mencuccini, M., I. L. Morison, J., and Grace, J., 2013. The relationship between carbon dioxide uptake and canopy colour from two camera systems in a deciduous forest in southern England. *Functional Ecology*, 27, 196–207.

Moore, C.E., Beringer, J., Evans, B., Hutley, L.B., and Tapper, N.J., 2017. Tree-grass phenology information improves light use efficiency modelling of gross primary productivity for an Australian tropical savanna. *Biogeosciences Discussions*, 14, 111–129.

Moore, C.E., Brown, T., Keenan, T.F., Duursma, R.A., Van Dijk, A.I.J.M., Beringer, J., Culvenor, D., Evans, B., Huete, A., Hutley, L.B., Maier, S., Restrepo-Coupe, N., Sonnentag, O., Specht, A., Taylor, J.R., Van Gorsel, E., and Liddell, M.J., 2016. Reviews and syntheses: Australian vegetation phenology: new insights from satellite remote sensing and digital repeat photography. *Biogeosciences*, 13, 5085–5102.

Moore, J.J., Fitzsimons, S.J.P., Lambe, E., and White, J., 1970. A comparison and evaluation of some phytosociological techniques. *Vegetatio*, 20 (1–4), 1–20.

Moore, R., 1970. *Australian grasslands*. Canberra: Australian National University Press.

Moore, R.M. and Perry, R.A., 1970. Vegetation. *In*: *Australian grasslands*. Canberra: Australian National University Press, 59–73.

Moran, M.S., Ponce Campos, G.E., Huete, A., McClaran, M.P., Zhang, Y., Hamerlynck, E.P., Augustine, D.J., Gunter, S.A., Kitchen, S.G., Peters, D.P.C., Starks, P.J., and Hernandez, M., 2014. Functional response of U.S. grasslands to the early 21st-century drought. *Ecology*, 95 (8), 2121–2133.

Moran, M.S., Zhang, Y., Ponce, G., Huete, A.R., Mcclaran, M.P., Denton, R.G., Kitchen, S.G., Morgan, J.A., and Peters, D., 2011. Response of southwestern grasslands to precipitation and temperature extremes of the early 21st century drought. *In*: *The Fourth Interagency Conference on Research in the Watersheds, 26-30 September 2011*. Fairbanks, Alaska, 26–30.

Morecroft, M.D., Masters, G.J., Brown, V.K., Clarke, I.P., Taylor, M.E., and Whitehouse, A.T., 2004. Changing precipitation patterns alter plant community dynamics and succession in an ex-arable grassland. *Functional Ecology*, 18 (5), 648–655.

Morgan, J.A., LeCain, D.R., Pendall, E., Blumenthal, D.M., Kimball, B.A., Carrillo, Y., Williams, D.G., Heisler-White, J., Dijkstra, F.A., and West, M., 2011. C4 grasses prosper as carbon dioxide eliminates desiccation in warmed semi-arid grassland. *Nature*, 476 (7359), 202–205.

Morgan, J.A., Pataki, D.E., Körner, C., Clark, H., Del Grosso, S.J., Grünzweig, J.M., Knapp, A.K., Mosier, A.R., Newton, P.C.D., Niklaus, P.A., Nippert, J.B., Nowak, R.S., Parton, W.J., Polley, H.W., and Shaw, M.R., 2004. Water relations in grassland and desert ecosystems exposed to elevated atmospheric CO_2. *Oecologia*, 140, 11–25.

Morgan, J.W., 2015. Biomass management in native grasslands. *In*: N.S.G. Williams, A. Marshall, and J.W. Morgan, eds. *Land of sweeping plains*. Clayton, Victoria: CSIRO Publishing, 202–222.

Morgan, J.W. and Lunt, I.D., 1999. Effects of time-since-fire on the tussock dynamics of a dominant grass (*Themeda triandra*) in a temperate Australian grassland. *Biological Conservation*, 88, 379–386.

Morgan, J.W. and Williams, N.S.G., 2015. The ecology and dynamics of temperate native grasslands in southeastern Australia. *In*: N.S.G. Williams, A. Marshall, and J.W. Morgan, eds. *Land of sweeping plains*. Clayton, Victoria: CSIRO Publishing, 61–85.

Morisette, J.T., Richardson, A.D., Knapp, A.K., Fisher, J.I., Graham, E.A., Abatzoglou, J., Wilson, B.E., Breshears, D.D., Henebry, G.M., Hanes, J.M., and Liang, L., 2009. Tracking the rhythm of the seasons in the face of global change: phenological research in the 21st century. *Frontiers in Ecology and the Environment*, 7 (5), 253–260.

Mpelasoka, F., Hennessy, K., Jones, R., and Bates, B., 2008. Comparison of suitable drought indices for climate change impacts assessment over Australia towards resource management. *International Journal of Climatology*, 28, 1283–1292.

Murphy, B.F. and Timbal, B., 2008. A review of recent climate variability and climate change in southeastern Australia. *International Journal of Climatology*, 28, 859–879.

Murphy, B.P. and Bowman, D.M.J.S., 2007. Seasonal water availability predicts the relative abundance of C3 and C4 grasses in Australia. *Global Ecology and Biogeography*, 16, 160–169.

Mutanga, O. and Skidmore, A., 2004a. Integrating imaging spectroscopy and neural networks to map grass quality in the Kruger National Park, South Africa. *Remote Sensing of Environment*, 90, 104–115.

Mutanga, O. and Skidmore, A.K., 2004b. Narrow band vegetation indices overcome the saturation problem in biomass estimation. *International Journal of Remote Sensing*, 25 (19), 3999–4014.

Mutanga, O., Skidmore, A.K., Kumar, L., and Ferwerda, J., 2005. Estimating tropical pasture quality at canopy level using band depth analysis with continuum removal in the visible domain. *International Journal of Remote Sensing*, 26 (6), 1093–1108.

Nagai, S., Ichie, T., Yoneyama, A., Kobayashi, H., Inoue, T., and Ishii, R., 2016. Usability of time-lapse digital camera images to detect characteristics of tree phenology in a tropical rainforest. *Ecological Informatics*, 32, 91–106.

Nagai, S., Maeda, T., Gamo, M., Muraoka, H., Suzuki, R., and Nasahara, K.N., 2011. Using digital camera images to detect canopy condition of deciduous broad-leaved trees. *Plant Ecology & Diversity*, 4, 79–89.

Nagler, P.L., Brown, T., Hultine, K.R., van Riper, C., Bean, D.W., Dennison, P.E., Murray, R.S., and Glenn, E.P., 2012. Regional scale impacts of Tamarix leaf beetles (*Diorhabda carinulata*) on the water availability of western U.S. rivers as determined by multi-scale remote sensing methods. *Remote Sensing of Environment*, 118, 227–240.

Nagler, P.L., Daughtry, C.S.T., and Goward, S.N., 2000. Plant litter and soil reflectance. *Remote Sensing of Environment*, 215, 207–215.

Nagler, P.L., Inoue, Y., Glenn, E.P., Russ, A.L., and Daughtry, C.S.T., 2003. Cellulose absorption index (CAI) to quantify mixed soil–plant litter scenes. *Remote Sensing of Environment*, 87 (2), 310–325.

Narasimhan, R. and Stow, D., 2010. Daily MODIS products for analyzing early season vegetation dynamics across the North Slope of Alaska. *Remote Sensing of Environment*, 114 (6), 1251–1262.

Nasahara, K.N. and Nagai, S., 2015. Development of an in situ observation network for terrestrial ecological remote sensing: the Phenological Eyes Network (PEN). *Ecological Research*, 30, 211–223.

Nelson, J.A., Morgan, J.A., LeCain, D.R., Mosier, A.R., Milchunas, D.G., and Parton, B.A., 2004. Elevated CO_2 increases soil moisture and enhances plant water relations in a long-term field study in semi-arid shortgrass steppe of Colorado. *Plant and Soil*, 259, 169–179.

Nijland, W., de Jong, R., de Jong, S.M., Wulder, M.A., Bater, C.W., and Coops, N.C., 2014. Monitoring plant condition and phenology using infrared sensitive consumer grade digital cameras. *Agricultural and Forest Meteorology*, 184, 98–106.

Norment, C.J.A. and Green, K.B., 2004. Breeding ecology of Richard's Pipit (*Anthus novaeseelandiae*) in the Snowy Mountains. *Emu*, 104, 327–336.

Noy-Meir, I., 1973. Desert ecosystems: environment and producers. *Annual Review of Ecology and Systematics*, 4, 51–58.

NSW Catchment Management Authority, 2005. *Native Vegetation Regulation 2005 Clause 28 Policy - special provisions for long term environmental benefits*. NSW CMA.

NSW Natural Resources Advisory Council, 2010. *Understanding our native grasslands*. Sydney, Australia: State of NSW.

NSW Office of Environment & Heritage, 2014. VIS classification database v2.1 [online]. *VIS Classification Database Public User Manual*. Available from: http://www.environment.nsw.gov.au/research/Visclassification.htm [Accessed 1 Aug 2016].

O'Mara, F.P., 2012. The role of grasslands in food security and climate change. *Annals of Botany*, 110 (6), 1263–1270.

Odenweller, J.B. and Johnson, K.I., 1984. Crop identification using Landsat temporal-spectral profiles. *Remote Sensing of Environment*, 54, 39–54.

Office of Environment & Heritage, 2016. *NSW guide to surveying threatened plants*. Sydney, Australia: NSW OEH.

Owensby, C., Ham, J., Knapp, A., Bremer, D., and Auen, L.M., 1997. Water vapour fluxes and their impact under elevated CO_2 in a C4-tallgrass prairie. *Global Change Biology*, 3, 189–195.

Owensby, C.E., Coyne, P.I., Ham, J.M., Auen, L.M., and Knapp, A.K., 1993. Biomass production in a tallgrass prairie ecosystem exposed to ambient and elevated CO_2. *Production*, 3 (4), 644–653.

Owensby, C.E., Ham, J.M., Knapp, A.K., and Auen, L.M., 1999. Biomass production and species composition change in a tallgrass prairie ecosystem after long-term exposure to elevated atmospheric CO_2. *Global Change Biology*, 5, 497–506.

Paltridge, G.W. and Barber, J., 1988. Monitoring grassland dryness and fire potential in Australia with NOAA/AVHRR Data. *Remote Sensing of Environment*, 25, 381–394.

Parmesan, C. and Yohe, G., 2003. A globally coherent fingerprint of climate change impacts across natural systems. *Nature*, 421, 37–42.

Parton, W.J., Scurlock, J.M.O., Ojima, D.S., Schimel, D.S., and Hall, D.O., 1995. Impact of climate change on grassland production and soil carbon worldwide. *Global Change Biology*, 1 (1), 13–22.

Paruelo, J.M., Lauenroth, W.K., and Roset, P.A., 2000. Estimating aboveground plant biomass using a photographic technique. *Journal of Range Management*, 53, 190–193.

Pau, S., Edwards, E.J., and Still, C.J., 2013. Improving our understanding of environmental controls on the distribution of C3 and C4 grasses. *Global Change Biology*, 19, 184–196.

Pearson, M. and Lennon, J., 2010. *Pastoral Australia: fortunes, failures and hard yakka: a*

historical overview 1788-1967. Melbourne: CSIRO Publishing.

Peart, B., 2008. *Life in a working landscape: towards a conservation strategy for the world's temperate grasslands*. A record of the World Temperate Grasslands Conservation Initiative Workshop, Hohhot, China, June 28 & 29.

Pech, R. and Davis, A.W., 1987. Reflectance modeling of semiarid woodlands. *Remote Sensing of Environment*, 23, 365–377.

Pekin, B. and Macfarlane, C., 2009. Measurement of crown cover and leaf area index using digital cover photography and its application to remote sensing. *Remote Sensing*, 1, 1298–1320.

Pengra, B.W., Johnston, C.A., and Loveland, T.R., 2007. Mapping an invasive plant, *Phragmites australis*, in coastal wetlands using the EO-1 Hyperion hyperspectral sensor. *Remote Sensing of Environment*, 108, 74–81.

Peñuelas, J., Filella, I., Zhang, X., Llorens, L., Ogaya, R., Lloret, F., Comas, P., Estiarte, M., and Terradas, J., 2004. Complex spatiotemporal phenological shifts as a response to rainfall changes. *New Phytologist*, 161, 837–846.

Peñuelas, J., Rutishauser, T., and Filella, I., 2009. Phenology feedbacks on climate change. *Science*, 324, 887–888.

Peterson, D.L., Price, K.P., and Martinko, E.A., 2002. Discriminating between cool season and warm season grassland cover types in northeastern Kansas. *International Journal of Remote Sensing*, 23 (23), 5015–5030.

Petherick, L., Bostock, H., Cohen, T.J., Fitzsimmons, K., Tibby, J., Fletcher, M.S., Moss, P., Reeves, J., Mooney, S., Barrows, T., Kemp, J., Jansen, J., Nanson, G., and Dosseto, A., 2013. Climatic records over the past 30ka from temperate Australia - a synthesis from the Oz-INTIMATE workgroup. *Quaternary Science Reviews*, 74, 58–77.

Petrie, M.D., Brunsell, N.A., and Nippert, J.B., 2011. Climate change alters growing season flux dynamics in mesic grasslands. *Theoretical and Applied Climatology*, 107, 427–440.

Pettorelli, N., Vik, J.O., Mysterud, A., Gaillard, J.-M., Tucker, C.J., and Stenseth, N.C., 2005. Using the satellite-derived NDVI to assess ecological responses to environmental change. *Trends in Ecology & Evolution*, 20 (9), 503–510.

Petus, C., Lewis, M., and White, D., 2013. Monitoring temporal dynamics of Great Artesian Basin wetland vegetation, Australia, using MODIS NDVI. *Ecological Indicators*, 34, 41–52.

Pitman, A.J., Narisma, G.T., and McAneney, J., 2007. The impact of climate change on the risk

of forest and grassland fires in Australia. *Climatic Change*, 84, 383–401.

Podani, J., 2006. Braun-Blanquet's legacy and data analysis in vegetation science. *Journal of Vegetation Science*, 17, 113–117.

Poore, M., 1955. The use of phytosociological methods in ecological investigations I. The Braun-Blanquet system. *Journal of Ecology*, 43 (1), 226–244.

Poorter, H. and Navas, M.-L., 2003. Plant growth and competition at elevated CO*2*: on winners, losers and functional groups. *New Phytologist*, 157, 175–198.

Potter, C., Klooster, S., Huete, A.R., and Genovese, V., 2007. Terrestrial carbon sinks for the United States predicted from MODIS satellite data and ecosystem modeling. *Earth Interactions*, 11, 1–21.

Power, S.A., Barnett, K.L., Ochoa-Hueso, R., Facey, S.L., Gibson-forty, E.V.J., Hartley, S.E., Nielsen, U.N., Tissue, D.T., and Johnson, S.N., 2016. DRI-Grass: a new experimental platform for addressing grassland ecosystem responses to future precipitation scenarios in south-east Australia. *Frontiers in Plant Science*, 7, 10.3389/fpls.2016.01373.

Price, J.C., 2003. Comparing MODIS and ETM+ data for regional and global land classification. *Remote Sensing of Environment*, 86, 491–499.

Price, K.P., Guo, X., and Stiles, J.M., 2002. Optimal Landsat TM band combinations and vegetation indices for discrimination of six grassland types in eastern Kansas. *International Journal of Remote Sensing*, 23 (23), 5031–5042.

Prioul, J., Brangeon, J., and Reyss, A., 1980. Interaction between external and internal conditions in the development of photosynthetic features in a grass leaf. *Plant Physiology*, 66, 762–769.

Prober, S. and Thiele, K., 1995. Conservation of the grassy white box woodlands: relative contributions of size and disturbance to floristic composition and diversity of remnants. *Australian Journal of Botany*, 43 (4), 349–366.

Prober, S.M., Thiele, K.R., and Lunt, I.D., 2007. Fire frequency regulates tussock grass composition, structure and resilience in endangered temperate woodlands. *Austral Ecology*, 32 (7), 808–824.

Przeszlowska, A., Trlica, M.J., and Weltz, M.A., 2006. Near-ground remote sensing of green area index on the shortgrass prairie. *Rangeland Ecology & Management*, 59, 422–430.

Psomas, A., 2008. Hyperspectral remote sensing for ecological analyses of grassland ecosystems. Unpublished PhD Thesis. Universitat Zurich.

Psomas, A., Kneubühler, M., Huber, S., and Itten, K., 2011. Hyperspectral remote sensing for

estimating aboveground biomass and for exploring species richness patterns of grassland habitats. *International Journal of Remote Sensing*, 32 (24), 9007–9031.

Purevdoj, T., Tateishi, R., Ishiyama, T., and Honda, Y., 1998. Relationships between percent vegetation cover and vegetation indices. *International Journal of Remote Sensing*, 19 (18), 3519–3535.

Qi, J., Cabot, F., Moran, M.S., and Dedieu, G., 1995. Biophysical parameter estimations using multidirectional spectral measurements. *Remote Sensing of Environment*, 54, 71–83.

R Core Team, 2013. *R: A language and environment for statistical computing*. Vienna, Austria: R Foundation for Statistical Computing.

Rahman, A.F., Gamon, J.A., Sims, D.A., and Schmidts, M., 2003. Optimum pixel size for hyperspectral studies of ecosystem function in southern California chaparral and grassland. *Remote Sensing of Environment*, 84, 192–207.

Ratana, P., Huete, A.R., and Ferreira, L., 2005. Analysis of cerrado physiognomies and conversion in the MODIS seasonal–temporal domain. *Earth Interactions*, 9 (3), 1–22.

Rayburn, E. and Rayburn, S., 1998. A standardized plate meter for estimating pasture mass in on-farm research trials. *Agronomy Journal*, 90 (2), 238–241.

Reed, B.C., Brown, J.F., VanderZee, D., Loveland, T.R., Merchant, J.W., and Ohlen, D.O., 1994. Measuring phenological variability from satellite imagery. *Journal of Vegetation Science*, 5, 703–714.

Reed, B.C., Schwartz, M.D., and Xiao, X., 2009. Remote sensing phenology: status and the way forward. *In*: A. Noormets, ed. *Phenology of ecosystem processes: applications in global change research*. New York: Springer-Verlag, 231–246.

Rehwinkel, R., 2007. *A method to assess grassy ecosystem sites: using floristic information to assess a site's quality*. Sydney: NSW Department of Environment and Climate Change.

Rehwinkel, R., 2014. A revised floristic value scoring method to assess grassland condition. *In*: A. Milligan and H. Horton, eds. *Grass half full or grass half empty? Valuing native grassy landscapes. Proceedings of the Friends of Grasslands 20th anniversary forum, 30 October – 1 November 2014.* Canberra, Australia.

Reisinger, A., Kitching, R.L., Chiew, F., Hughes, L., Newton, P.C.D., Schuster, S.S., Tait, A., and Whetton, P., 2014. Australasia. *In*: C.B. Field, V.R. Barros, K.J. Dokken, K.J. Mach, M.D. Mastandrea, T.E. Bilir, M. Chatterjee, K.L. Ebi, Y.O. Estrada, R.C. Genova, B. Girma, E.S. Kissel, A.N. Levy, S. MacCracken, P.R. Mastrandrea, and L.L. White, eds. *Climate change 2014: impacts, adaptation and vulnerability. Part B: regional aspects.*

Contribution of Working Group II to the Fifth Assessment Report of the Intergovernmental Panel on Climate Change. Cambridge, UK and New York, NY, USA: Cambridge University Press, 1371–1438.

Reyer, C.P.O., Leuzinger, S., Rammig, A., Wolf, A., Bartholomeus, R.P., Bonfante, A., de Lorenzi, F., Dury, M., Gloning, P., Abou Jaoudé, R., Klein, T., Kuster, T.M., Martins, M., Niedrist, G., Riccardi, M., Wohlfahrt, G., de Angelis, P., de Dato, G., François, L., Menzel, A., and Pereira, M., 2013. A plant's perspective of extremes: terrestrial plant responses to changing climatic variability. *Global Change Biology*, 19 (1), 75–89.

Richardson, A.D., Anderson, R.S., Arain, M.A., Barr, A.G., Bohrer, G., Chen, G., Chen, J.M., Ciais, P., Davis, K.J., Desai, A.R., Dietze, M.C., Dragoni, D., Garrity, S.R., Gough, C.M., Grant, R., Hollinger, D.Y., Margolis, H. a., McCaughey, H., Migliavacca, M., Monson, R.K., Munger, J.W., Poulter, B., Raczka, B.M., Ricciuto, D.M., Sahoo, A.K., Schaefer, K., Tian, H., Vargas, R., Verbeeck, H., Xiao, J., and Xue, Y., 2012. Terrestrial biosphere models need better representation of vegetation phenology: results from the North American Carbon Program Site Synthesis. *Global Change Biology*, 18 (2), 566–584.

Richardson, A.D., Braswell, B.H., Hollinger, D.Y., Jenkins, J.P., and Ollinger, S. V., 2009. Near-surface remote sensing of spatial and temporal variation in canopy phenology. *Ecological Applications*, 19 (6), 1417–1428.

Richardson, A.D., Jenkins, J.P., Braswell, B.H., Hollinger, D.Y., Ollinger, S. V., and Smith, M.-L., 2007. Use of digital webcam images to track spring green-up in a deciduous broadleaf forest. *Oecologia*, 152, 323–334.

Richardson, A.D., Keenan, T.F., Migliavacca, M., Ryu, Y., Sonnentag, O., and Toomey, M., 2013. Climate change, phenology, and phenological control of vegetation feedbacks to the climate system. *Agricultural and Forest Meteorology*, 169, 156–173.

Richardson, F., Richardson, R., and Shepherd, R., 2011. *Weeds of the south-east: an identification guide for Australia*. Second Ed. Meredith, Victoria, Australia: CSIRO Publishing.

Rickards, L. and Howden, S.M., 2012. Transformational adaptation: agriculture and climate change. *Crop and Pasture Science*, 63, 240–250.

Ricotta, C. and Feoli, E., 2013. Does ordinal cover estimation offer reliable quality data structures in vegetation ecologicalstudies? *Folia Geobotanica*, 48 (2013), 437–447.

Rienke, K. and Jones, S., 2006. Integrating vegetation field surveys with remotely sensed data. *Ecological Management and Restoration*, 7 (S1), S18–S23.

Robertson, D., 1985. Interrelationships between kangaroos, fire and vegetation dynamics at

Gellibrand Hill Park, Victoria. Unpublished PhD Thesis, The University of Melbourne.

Robinson, G.G. and Archer, K.A., 1988. Agronomic potential of native grass species on the Northern Tablelands of New South Wales. I. Growth and herbage production. *Australian Journal of Agricultural Research*, 39, 415–423.

Robinson, R., 2015. Weed management in native grasslands. *In*: N.S.G. Williams, A. Marshall, and J.W. Morgan, eds. *Land of sweeping plains*. Clayton, Victoria: CSIRO Publishing, 224–252.

Rose, H. and Rose, C., 2012. *Grasses of coastal NSW*. Sydney, Australia: New South Wales Department of Primary Industries.

Ross, J., 1999. *Guide to best practice conservation of temperate native grasslands*. Sydney: World Wide Fund for Nature (Australia).

Rouse, J.W.J., Haas, R.H., Schell, J.A., and Deering, D.W., 1974. Monitoring vegetation systems in the Great Plains with ERTS. *In*: *Proceedings, Third Earth Resources Technology Satellite-1 Symposium*. Greenbelt: NASA SP-351, 301–317.

Royal Botanic Gardens and Domain Trust, 2016. PlantNET (The NSW plant information network system) [online]. Available from: http://plantnet.rbgsyd.nsw.gov.au/ [Accessed 31 Jul 2016].

Running, S.W. and Nemani, R.R., 1988. Relating seasonal patterns of the AVHRR vegetation index to simulated photosynthesis and transpiration of forests in different climates. *Remote Sensing of Environment*, 24, 347–367.

Sakamoto, T., Wardlow, B.D., Gitelson, A.A., Verma, S.B., Suyker, A.E., and Arkebauer, T.J., 2010. A two-step filtering approach for detecting maize and soybean phenology with time-series MODIS data. *Remote Sensing of Environment*, 114, 2146–2159.

Sakowska, K., Juszczak, R., and Gianelle, D., 2016. Remote sensing of grassland biophysical parameters in the context of the Sentinel-2 satellite mission. *Journal of Sensors*, doi: 10.1155/2016/4612809.

Sala, A.O.E., Lauenroth, W.K., and Parton, W.J., 1992. Long-term soil water dynamics in the shortgrass steppe. *Ecology*, 73 (4), 1175–1181.

Sala, O.E., 2001. Temperate grasslands. *In*: F.S. Chapin, O.E. Sala, and E. Huber-Sannwald, eds. *Global biodiversity in a changing environment: scenarios for the 21st century*. New York: Springer-Verlag, 121–137.

Sala, O.E., Parton, W.J., Joyce, L.A., and Lauenroth, W.K., 1988. Primary production of the central grassland region of the United States. *Ecology*, 69 (1), 40–45.

Saleska, S.R., Didan, K., Huete, A.R., and da Rocha, H.R., 2007. Amazon forests green-up during 2005 drought. *Science*, 318 (5850), 612.

Schmidt, M., Udelhoven, T., Gill, T., and Röder, A., 2012. Long term data fusion for a dense time series analysis with MODIS and Landsat imagery in an Australian Savanna. *Journal of Applied Remote Sensing*, 6, DOI: 10.1117/1.JRS.6.063512.

Schulmeister, J. and Lees, B., 1995. Pollen evidence from tropical Australia for the onset of an ENSO-dominated climate at c. 4000 BP. *The Holocene*, 5, 10–18.

Schwartz, M.D., 1999. Advancing to full bloom: planning phenological research for the 21st century. *International Journal of Biometeorology*, 42, 113–118.

Schwartz, M.D., Reed, B.C., and White, M.A., 2002. Assessing satellite-derived start-of-season measures in the conterminous USA. *International Journal of Climatology*, 22, 1793–1805.

Scott, A.J. and Morgan, J.W., 2012. Recovery of soil and vegetation in semi-arid Australian old fields. *Journal of Arid Environments*, 76, 61–71.

Scott, J.K., Webber, B.L., Murphy, H., Ota, N., Kriticos, D.J., and Loechel, B., 2014. *Weeds and climate change: supporting weed management adaptation*. Canberra: CSIRO.

Scott, R.L., Hamerlynck, E.P., Jenerette, G.D., Moran, M.S., and Barron-Gafford, G.A., 2010. Carbon dioxide exchange in a semidesert grassland through drought-induced vegetation change. *Journal of Geophysical Research*, 115 (G3), G03026.

Scurlock, J.M.O. and Hall, D.O., 1998. The global carbon sink: a grassland perspective. *Global Change Biology*, 4, 229–233.

Scurlock, J.M.O., Johnson, K., and Olson, R.J., 2002. Estimating net primary productivity from grassland biomass dynamics measurements. *Global Change Biology*, 8, 736–753.

Seddon, J., Bourne, M., Murphy, D., Doyle, S., and Briggs, S., 2011. Assessing vegetation condition in temperate montane grasslands. *Ecological Management and Restoration*, 12 (2), 141–144.

Seneviratne, S.I., Corti, T., Davin, E.L., Hirschi, M., Jaeger, E.B., Lehner, I., Orlowsky, B., and Teuling, A.J., 2010. Investigating soil moisture-climate interactions in a changing climate: a review. *Earth-Science Reviews*, 99, 125–161.

Sharp, S., 2006. Assessment of vegetation condition of grassy ecosystems in the Australian Capital Territory. *Ecological Management and Restoration*, 7 (S1), S63–S65.

Sharp, S., Garrard, G., and Wong, N., 2015. Planning, documenting and monitoring for grassland management. *In*: N.S.G. Williams, A. Marshall, and J.W. Morgan, eds. *Land of sweeping plains*. Clayton, Victoria: CSIRO Publishing, 115–162.

Shaw, M.R., Zavaleta, E.S., Chiariello, N.R., Cleland, E.E., Mooney, H.A., and Field, C.B., 2002. Grassland responses to global environmental changes suppressed by elevated CO_2. *Science*, 298, 1987–1990.

Shen, M., Tang, Y., Klein, J., Zhang, P., Gu, S., Shimono, A., and Chen, J., 2008. Estimation of aboveground biomass using in situ hyperspectral measurements in five major grassland ecosystems on the Tibetan Plateau. *Journal of Plant Ecology*, 1 (4), 247–257.

Sherry, R.A., Arnone III, J.A., Johnson, D.W., Schimel, D.S., Verburg, P.S., and Luo, Y., 2012. Carry over from previous year environmental conditions alters dominance hierarchy in a prairie plant community. *Journal of Plant Ecology*, 5 (2), 134–146.

Shimada, S., Matsumoto, J., Sekiyama, A., Aosier, B., and Yokohana, M., 2012. A new spectral index to detect Poaceae grass abundance in Mongolian grasslands. *Advances in Space Research*, 50, 1266–1273.

Si, Y., Schlerf, M., Zurita-Milla, R., Skidmore, A., and Wang, T., 2012. Mapping spatio-temporal variation of grassland quantity and quality using MERIS data and the PROSAIL model. *Remote Sensing of Environment*, 121, 415–425.

Siljamo, P., Sofiev, M., Ranta, H., Linkosalo, T., Kubin, E., Ahas, R., Genikhovich, E., Jatczak, K., Jato, V., Nekovar, J., Minin, A., Severova, E., and Shalaboda, V., 2008. Representativeness of point-wise phenological Betula data collected in different parts of Europe. *Global Ecology and Biogeography*, 17, 489–502.

Sims, D.A. and Gamon, J.A., 2002. Relationships between leaf pigment content and spectral reflectance across a wide range of species, leaf structures and developmental stages. *Remote Sensing of Environment*, 81 (2), 337–354.

Sinclair, S.J., Duncan, D.H., and Bruce, M.J., 2014. Mortality of native grasses after a summer fire in natural temperate grassland suggests ecosystem instability. *Ecological Management and Restoration*, 15 (1), 91–94.

Sinden, J., Jones, R., Hester, S., Odom, D., Kalisch, C., James, R., and Cacho, O., 2004. *The economic impact of weeds in Australia*. Armidale, Australia.

Singh, J.S., Lauenroth, W.K., and Steinhorst, R.K., 1975. Review and assessment of various techniques for estimating net aerial primary production in grasslands from harvest data. *Botanical Review*, 41 (2), 181–232.

Singh, J.S. and Yadava, P.S., 1974. Seasonal variation in composition, plant biomass and net primary productivity of a tropical grassland at Kurukshetra, India. *Ecological Monographs*, 44 (3), 351–376.

Sonnentag, O., Detto, M., Vargas, R., Ryu, Y., Runkle, B.R.K., Kelly, M., and Baldocchi, D.D., 2011. Tracking the structural and functional development of a perennial pepperweed (*Lepidium latifolium* L.) infestation using a multi-year archive of webcam imagery and eddy covariance measurements. *Agricultural and Forest Meteorology*, 151 (7), 916–926.

Sonnentag, O., Hufkens, K., Teshera-Sterne, C., Young, A.M., Friedl, M., Braswell, B.H., Milliman, T., O'Keefe, J., and Richardson, A.D., 2012. Digital repeat photography for phenological research in forest ecosystems. *Agricultural and Forest Meteorology*, 152, 159–177.

Soudani, K., François, C., le Maire, G., Le Dantec, V., and Dufrêne, E., 2006. Comparative analysis of IKONOS, SPOT, and ETM+ data for leaf area index estimation in temperate coniferous and deciduous forest stands. *Remote Sensing of Environment*, 102, 161–175.

Soudani, K., Hmimina, G., Delpierre, N., Pontailler, J.-Y., Aubinet, M., Bonal, D., Caquet, B., de Grandcourt, A., Burban, B., Flechard, C., Guyon, D., Granier, A., Gross, P., Heinish, B., Longdoz, B., Loustau, D., Moureaux, C., Ourcival, J.-M., Rambal, S., Saint André, L., and Dufrêne, E., 2012. Ground-based network of NDVI measurements for tracking temporal dynamics of canopy structure and vegetation phenology in different biomes. *Remote Sensing of Environment*, 123, 234–245.

Sparks, T.H. and Carey, P.D., 1995. The responses of species to climate over two centuries: analysis of the Marsham phenological record, 1736-1947. *Journal of Ecology*, 83, 321–329.

Specht, R.L., 1969. A comparison of schlerophyllous vegetation typical of Mediterranean type climates in France, California and southern Australia. *Australian Journal of Botany*, 17, 277–292.

Stafford Smith, D.M., McKeon, G.M., Watson, I.W., Henry, B.K., Stone, G.S., Hall, W.B., and Howden, S.M., 2007. Learning from episodes of degradation and recovery in variable Australian rangelands. *Proceedings of the National Academy of Sciences of the United States of America*, 104 (52), 20690–20695.

Stevens, M., Parraga, C.A., Cuthill, I.C., Partridge, J.C., and Troscianko, T.S., 2007. Using digital photography to study animal coloration. *Biological Journal of the Linnean Society*, 90 (2), 211–237.

Still, C.J., Berry, J.A., Collatz, G.J., and DeFries, R.S., 2003. Global distribution of C3 and C4 vegetation: carbon cycle implications. *Global Biogeochemical Cycles*, 17 (1), 6–14.

Stokes, C., Ash, A., and Howden, S., 2008. Climate change impacts on Australian rangelands. *Rangelands*, 3, 40–45.

Stokes, C. and Howden, S., eds., 2010. *Adapting agriculture to climate change: preparing Australian agriculture, forestry and fisheries for the future*. Melbourne, Australia: CSIRO Publishing.

Stow, D.A., Hope, A., Mcguire, D., Verbyla, D., Gamon, J., Huemmrich, F., Houston, S., Racine, C., Sturm, M., Tape, K., Hinzman, L., Yoshikawa, K., Tweedie, C., Noyle, B., Silapaswan, C., Douglas, D., Griffith, B., Jia, G., Epstein, H., Walker, D., Daeschner, S., Petersen, A., Zhou, L., and Myneni, R., 2004. Remote sensing of vegetation and land-cover change in Arctic Tundra Ecosystems. *Remote Sensing of Environment*, 89, 281–308.

Studer, S., Stöckli, R., Appenzeller, C., and Vidale, P.L., 2007. A comparative study of satellite and ground-based phenology. *International Journal of Biometeorology*, 51 (5), 405–414.

Stuwe, J. and Parsons, R.F., 1977. *Themeda australis* grasslands on the Basalt Plains, Victoria: floristics and management effects. *Australian Journal of Ecology*, 2, 467–476.

Suter, D., Frehner, M., Fischer, B.U., Nösberger, J., and Lüscher, A., 2002. Elevated CO_2, increases carbon allocation to the roots of *Lolium perenne* under free-air CO_2 enrichment but not in a controlled environment. *New Phytologist*, 154, 65–75.

Suttle, K.B., Thomsen, M.A., and Power, M.E., 2007. Species interactions reverse grassland responses to changing climate. *Science*, 315 (5812), 640–642.

Swemmer, A.M., Knapp, A.K., and Snyman, H.A., 2007. Intra-seasonal precipitation patterns and above-ground productivity in three perennial grasslands. *Journal of Ecology*, 95 (4), 780–788.

Tieszen, L.., Reed, B.C., Bliss, N.B., Wylie, B.K., and DeJong, D.D., 1997. NDVI, C3 and C4 production and distributions in Great Plains grassland cover classes. *Ecological Applications*, 7 (1), 59–78.

Toomey, M., Friedl, M.A., Frolking, S., Hufkens, K., Klosterman, S.T., Sonnentag, O., Baldocchi, D.D., Bernacchi, C.J., Biraud, S.C., Bohrer, G., Brzostek, E.R., Burns, S.P., Coursolle, C., Hollinger, D.Y., Margolis, H.A., McCaughey, H., Monson, R.K., Munger, J.W., Pallardy, S.G., Phillips, R.P., Torn, M.S., Wharton, S., Zeri, M., and Richardson, A.D., 2015. Greenness indices from digital cameras predict the timing and seasonal dynamics of canopy-scale photosynthesis. *Ecological Applications*, 25 (1), 99–115.

Tozer, M.G., Turner, K., Keith, D.A., Tindall, D., Pennay, C., Simpson, C., MacKenzie, B., Beukers, P., and Cox, S., 2010. Native vegetation of southeast NSW: a revised classification and map for the coast and eastern tablelands. *Cunninghamia*, 11 (3), 359–406.

Tremont, R., 1994. Life-history attributes of plants in grazed and ungrazed grasslands on the

Northern Tablelands of New South Wales. *Australian Journal of Botany*, 42, 511–530.

Tremont, R. and McIntyre, S., 1994. Natural grassy vegetation and native forbs in temperate Australia: structure, dynamics and life histories. *Australian Journal of Botany*, 42, 641–658.

Tuanmu, M., Viña, A., Bearer, S., Xu, W., Ouyang, Z., Zhang, H., and Liu, J., 2010. Mapping understory vegetation using phenological characteristics derived from remotely sensed data. *Remote Sensing of Environment*, 114, 1833–1844.

Tucker, C.J., 1979. Red and photographic infrared linear combinations for monitoring vegetation. *Remote Sensing of Environment*, 8, 127–150.

Tucker, C.J. and Sellers, P.J., 1986. Satellite remote sensing of primary production. *International Journal of Remote Sensing*, 7 (11), 1395–1416.

Underwood, E., Ustin, S.L., and Dipietro, D., 2003. Mapping nonnative plants using hyperspectral imagery. *Remote Sensing of Environment*, 86, 150–161.

United Nations Environment Programme, 2008. *State of the world's protected areas: an annual review of global conservation progress*. Cambridge, UK: UNEP-WCMC.

Ustin, S.L., Roberts, D.A., Gamon, J.A., Asner, G.P., and Green, R.O., 2004. Using imaging spectroscopy to study ecosystem processes and properties. *Bioscience*, 54 (6), 523–534.

Vanamburg, L.K., Trlica, M.J., Hoffer, R.M., Weltz, M.A., Trlica, M.J., Hoffer, R.M., and Ground, M.A.W., 2006. Ground based digital imagery for grassland biomass estimation. *International Journal of Remote Sensing*, 27 (5), 939–50.

Verbesselt, J., Hyndman, R., Newnham, G., and Culvenor, D.S., 2010. Detecting trend and seasonal changes in satellite image time series. *Remote Sensing of Environment*, 114, 106–115.

Verbesselt, J., Hyndman, R., Zeileis, A., and Culvenor, D.S., 2010. Phenological change detection while accounting for abrupt and gradual trends in satellite image time series. *Remote Sensing of Environment*, 114, 2970–2980.

Verhoeven, G.J.J., 2010. It's all about the format – unleashing the power of RAW aerial photography. *International Journal of Remote Sensing*, 31 (8), 2009–2042.

Vickers, H., Gillespie, M., and Gravina, A., 2012. Assessing the development of rehabilitated grasslands on post-mined landforms in north west Queensland, Australia. *Agriculture, Ecosystems & Environment*, 163, 72–84.

Vickery, P.J., Hill, M.J., and Donald, G.E., 1997. Satellite derived maps of pasture growth status: association of classification with botanical composition. *Australian Journal of*

Experimental Agriculture, 37, 547–562.

Víg, R., Huzsvai, L., Dobos, A., and Nagy, J., 2012. Systematic measurement methods for the determination of the SPAD values of maize (*Zea mays* L.) canopy and potato (*Solanum tuberosum* L.). *Communications in Soil Science and Plant Analysis*, 43 (12), 1684–1693.

Vivian, L. and Baines, G., 2014. *Research update 2014/4: Longitudinal study of groundcover flora condition in select grassy ecosystem sites*. Environment and Planning Directorate, Canberra.

Vohland, M. and Jarmer, T., 2008. Estimating structural and biochemical parameters for grassland from spectroradiometer data by radiative transfer modelling (PROSPECT+SAIL). *International Journal of Remote Sensing*, 29 (1), 191–209.

Volder, A., Briske, D.D., and Tjoelker, M.G., 2013. Climate warming and precipitation redistribution modify tree-grass interactions and tree species establishment in a warm-temperate savanna. *Global Change Biology*, 19 (3), 843–857.

Volder, A., Tjoelker, M.G., and Briske, D.D., 2010. Contrasting physiological responsiveness of establishing trees and a C4 grass to rainfall events, intensified summer drought, and warming in oak savanna. *Global Change Biology*, 16 (12), 3349–3362.

Volk, M., Niklaus, P.A., and Korner, C., 2000. Soil moisture effects determine CO_2 responses of grassland species. *Oecologia*, 125, 380–388.

Walker, P., 1960. *A soil survey of the county of Cumberland, Sydney Region New South Wales. Soil survey unit bulletin No 2*. Sydney, Australia: New South Wales Department of Agriculture Chemist's Branch.

Waller, R. and Sale, P., 2001. Persistence and productivity of perennial ryegrass in sheep pastures in south-western Victoria: a review. *Australian Journal of Experimental Agriculture*, 41 (1), 117–144.

Wand, S.J.E., Midgley, G.F., Jones, M.H., and Curtis, P.S., 1999. Elevated atmospheric CO_2 concentration: a meta-analytic test of current theories and perceptions. *Global Change Biology*, 5, 723–741.

Wang, C., Hunt, E.R., Zhang, L., and Guo, H., 2013. Phenology-assisted classification of C3 and C4 grasses in the U.S. Great Plains and their climate dependency with MODIS time series. *Remote Sensing of Environment*, 138, 90–101.

Wang, C., Jamison, B.E., and Spicci, A.A., 2010. Trajectory-based warm season grassland mapping in Missouri prairies with multi-temporal ASTER imagery. *Remote Sensing of Environment*, 114, 531–539.

Waring, R.H., Coops, N.C., Fan, W., and Nightingale, J.M., 2006. MODIS enhanced vegetation index predicts tree species richness across forested ecoregions in the contiguous U.S.A. *Remote Sensing of Environment*, 103, 218–226.

Waters, C., Dear, B., Hackney, B., Jessop, P., and Melville, G., 2008. Trangie wallaby grass [(*Austrodanthonia caespitosa*) (Gaudich.) H.P. Linder]. *Australian Journal of Experimental Agriculture*, 48 (4), 575–577.

Watson, C.J., Restrepo Coupe, N., and Huete, A.R., 2013. Hyperspectral assessments of condition and species composition of Australian grasslands. *In*: *Proceedings of the 2013 IEEE International Geoscience & Remote Sensing Symposium*. Melbourne, Australia, 2770–2773.

Wearne, L.J. and Morgan, J.W., 2001. Recent forest encroachment into subalpine grasslands near Mount Hotham, Victoria, Australia. *Arctic, Antarctic and Alpine Research*, 33 (3), 369–377.

Webb, L.B., Whetton, P.H., and Barlow, E.W.R., 2011. Observed trends in winegrape maturity in Australia. *Global Change Biology*, 17 (8), 2707–2719.

Weiser, R.L., Asrar, G., Miller, G.P., and Kanemasu, E.T., 1986. Assessing grassland biophysical characteristics from spectral measurements. *Remote Sensing of Environment*, 20, 141–152.

Weltzin, J. and McPherson, G., 2003. *Terrestrial ecosystems: a North American perspective*. Tuscon, Arizona: University of Arizona Press.

Weltzin, J.F., Loik, M.E., Schwinning, S., Williams, D.G., Fay, P.A., Haddad, B.M., Harte, J., Huxman, T.E., Knapp, A.K., Lin, G., Pockman, W.T., Shaw, M.R., Small, E.E., Smith, M.D., Smith, S.D., Tissue, D.T., and Zak, J.C., 2003. Assessing the response of terrestrial ecosystems to potential changes in precipitation. *Bioscience*, 53 (10), 941–952.

Westergaard-Nielsen, A., Lund, M., Ulf, B., and Peter, M., 2013. Camera-derived vegetation greenness index as proxy for gross primary production in a low Arctic wetland area. *ISPRS Journal of Photogrammetry and Remote Sensing*, 86, 89–99.

White, M.A., Asner, G.P., Nemani, R.R., Privette, J.L., and Running, S.W., 2000. Measuring fractional cover and Leaf Area Index in arid ecosystems: digital camera, radiation transmittance, and laser altimetry methods. *Remote Sensing of Environment*, 74, 45–57.

White, M.A. and Nemani, R.R., 2006. Real-time monitoring and short-term forecasting of land surface phenology. *Remote Sensing of Environment*, 104, 43–49.

White, R., Murray, S., and Rohweder, M., 2000. *Pilot analysis of global ecosystems: grassland*

ecosystems. Washington, DC: World Resources Institute.

Williams, A.L., Wills, K.E., Janes, J.K., Schoor, J.K. Vander, Newton, P.C.D., and Hovenden, M.J., 2007. Warming and free-air CO_2 enrichment alter demographics in four co-occurring grassland species. *New Phytologist*, 176, 365–375.

Williams, N.S.G., Marshall, A., and Morgan, J.W., eds., 2015. *Land of sweeping plains*. Clayton, Victoria: CSIRO Publishing.

Williams, N.S.G., Marshall, A., Morgan, J.W., Delpratt, J., Gibson-Roy, P., and Wong, N., 2015. The future of south-eastern Australia's native temperate grasslands. *In*: N.S.G. Williams, A. Marshall, and J.W. Morgan, eds. *Land of sweeping plains*. Clayton, Victoria: CSIRO Publishing, 419–431.

Williams, N.S.G. and Morgan, J.W., 2015. The native temperate grasslands of south-eastern Australia. *In*: N.S.G. Williams, A. Marshall, and J.W. Morgan, eds. *Land of sweeping plains*. Clayton, Victoria: CSIRO Publishing, 27–59.

Williams, N.S.G., Morgan, J.W., McCarthy, M.A., and McDonnell, M.J., 2006. Local extinction of grassland plants: the landscape matrix is more important than patch attributes. *Ecology*, 87 (12), 3000–3006.

Williams, O.B., 1961. Studies in the ecology of the Riverine Plain III. Phenology of a *Danthonia caespitosa* Gaudich. grassland. *Australian Journal of Agricultural Research*, 12, 247–259.

Williams, R.J., Myers, B.A., Muller, W.J., Duff, G.A., and Eamus, D., 1997. Leaf phenology of woody species in a North Australian tropical savanna. *Ecology*, 78 (8), 2542–2558.

Wimbush, D. and Costin, A.B., 1979. Trends in vegetation at Kosciusko. II: subalpine range transects, 1959-1978. *Australian Journal of Botany*, 27, 789–831.

Winkler, E. and Klotz, S., 1997. Long-term control of species abundances in a dry grassland: a spatially explicit model. *Journal of Vegetation Science*, 8, 189–198.

Winslow, J.C., Hunt, E.R., and Piper, S.C., 2003. The influence of seasonal water availability on global C3 versus C4 grassland biomass and its implications for climate change research. *Ecological Modelling*, 163 (1), 153–173.

Woebbecke, D.M., Meyer, G.E., Von Bargen, K., and Mortensen, D.A., 1995. Color indices for weed identification under various soil, residue, and lighting conditions. *Transactions of the ASAE*, 38 (1), 259–269.

Wong, N. and Dorrough, J.W., 2015. Integrating grassland conservation into farming practice. *In*: N.S.G. Williams, A. Marshall, and J.W. Morgan, eds. *Land of sweeping plains*.

Clayton, Victoria: CSIRO Publishing, 253–284.

Wood, E.M., Pidgeon, A.M., Radeloff, V.C., and Keuler, N.S., 2012. Image texture as a remotely sensed measure of vegetation structure. *Remote Sensing of Environment*, 121, 516–526.

Wylie, B.K., Meyer, D.J., Tieszen, L.L., and Mannel, S., 2002. Satellite mapping of surface biophysical parameters at the biome scale over the North American grasslands - a case study. *Remote Sensing of Environment*, 79, 266–278.

Xiao, X., Zhang, J., Yan, H., Wu, W., and Biradar, C., 2009. Land surface phenology: convergence of satellite and CO_2 eddy flux observations. *In*: A. Noormets, ed. *Phenology of ecosystem processes*. New York: Springer-Verlag, 247–270.

Xie, Y., Sha, Z., and Yu, M., 2008. Remote sensing imagery in vegetation mapping: a review. *Journal of Plant Ecology*, 1 (1), 9–23.

Yang, L., Wylie, B.K., Tieszen, L.L., and Reed, B.C., 1998. An analysis of relationships among climate forcing and time-integrated NDVI of grasslands over the U.S. northern and central Great Plains. *Remote Sensing of Environment*, 65, 25–37.

Yang, X. and Guo, X., 2011. Investigating vegetation biophysical and spectral parameters for detecting light to moderate grazing effects: a case study in mixed grass prairie. *Central European Journal of Geosciences*, 3 (3), 336–348.

Youngentob, K.N., Roberts, D.A., Held, A.A., Dennison, P.E., Jia, X., and Lindenmayer, D.B., 2011. Mapping two Eucalyptus subgenera using multiple endmember spectral mixture analysis and continuum-removed imaging spectrometry data. *Remote Sensing of Environment*, 115, 1115–1128.

Zeppel, M.J.B., Wilks, J. V., and Lewis, J.D., 2014. Impacts of extreme precipitation and seasonal changes in precipitation on plants. *Biogeosciences*, 11 (11), 3083–3093.

Zerger, A., McIntyre, S., Gobbett, D., and Stol, J., 2011. Remote detection of grassland nutrient status for assessing ground layer vegetation condition and restoration potential of eucalypt grassy woodlands. *Landscape and Urban Planning*, 102, 226–233.

Zhang, X., Friedl, M.A., and Schaaf, C.B., 2006. Global vegetation phenology from Moderate Resolution Imaging Spectroradiometer (MODIS): Evaluation of global patterns and comparison with in situ measurements. *Journal of Geophysical Research*, 111 (G4), 1–14.

Zhang, X., Friedl, M.A., Schaaf, C.B., Strahler, A.H., Hodges, J.C.F., Gao, F., Reed, B.C., and Huete, A.R., 2003. Monitoring vegetation phenology using MODIS. *Remote Sensing of Environment*, 84, 471–475.

Zhang, Y., Smith, A.M., and Hill, M.J., 2009. Estimating fractional cover of grassland components from two satellite remote sensing sensors. *In*: *34th International Symposium on Remote Sensing of Environment, 10-15 April 2010*. Sydney, Australia, 2–5.

Zhang, Y., Susan Moran, M., Nearing, M.A., Ponce Campos, G.E., Huete, A.R., Buda, A.R., Bosch, D.D., Gunter, S.A., Kitchen, S.G., Henry McNab, W., Morgan, J.A., McClaran, M.P., Montoya, D.S., Peters, D.P.C., and Starks, P.J., 2013. Extreme precipitation patterns and reductions of terrestrial ecosystem production across biomes. *Journal of Geophysical Research: Biogeosciences*, 118 (1), 148–157.

Appendices

Appendix A PEARSON'S CORRELATION TABLE OF VEGETATION INDICES

This appendix presents a Pearson's correlation table (Table A.1) of the vegetation indices and cover estimates that were used for the research described in Chapter 2. These relationships can also be applied to other chapters throughout this thesis where comparison is made between cover, camera-based indices and spectral indices. Abbreviations used in this table include:

Fractional cover:

PV (photosynthetic vegetation)

NPV (non-photosynthetic vegetation)

Camera-based indices:

RGB (red-green-blue)

GCC (Green Chromatic Coordinate)

ExG (Excess Green)

Spectral Indices:

AVHRR (Advanced Very High Resolution Radiometer)

MODIS (MODerate resolution Imaging Spectroradiometer)

NDVI (Normalized Difference Vegetation Index)

EVI (Enhanced Vegetation Index)

SARVI (Soil and Atmosphere Resistant Vegetation Index)

CAI (Cellulose Absorption Index)

PRI (Photochemical Reflectance Index)

Table A.1 Pearson's correlation coefficient (*r*) of fractional cover estimates, RBG indices and spectral indices described in Chapter 2. Fractional cover was estimated using camera-based quantification of pixel colour. RGB indices were generated from integrated colour of digital images. Spectral indices were generated from an ASD spectroradiometer and include narrow-band indices used in hyperspectral studies and spectroradiometer simulations of common satellite-based VIs using the appropriate spectral bands. Relationships are significantly correlated at $p < 0.05$ (*), $p < 0.01$ (**) and $p < 0.001$ (***).

		PV % Cover	NPV % Cover	Camera GCC	Camera ExG	Camera Green:Red	ASD GCC	AVHRR NDVI	Landsat TM NDVI	MODIS NDVI	Narrow-band NDVI	MODIS Simple Rat io	Narrow-band Simple Rat io	MODIS EVI	MODIS SARVI	NDVI 705	MODIS CAI
Fractional Cover	PV % Cover																
	NPV % Cover	-0.36***															
RGBIndices	Camera GCC	0.88***	-0.26***														
	Camera ExG	0.90***	-0.27***	0.97***													
	Camera Green:Red	0.86***	-0.47***	0.78***	0.83***												
	ASD GCC	0.86***	-0.53***	0.78***	0.79***	0.76***											
Spectral Indices	AVHRR NDVI	0.75***	-0.17***	0.76***	0.75***	0.52***	0.65***										
	Landsat TM NDVI	0.84***	-0.20***	0.82***	0.83***	0.62***	0.76***	0.98***									
	MODIS NDVI	0.81***	-0.19***	0.80***	0.80***	0.59***	0.72***	0.99***	1.00***								
	Narrow-band NDVI	0.83***	-0.25***	0.81***	0.81***	0.61***	0.77***	0.98***	0.99***	0.99***							
	MODIS Simple Rat io	0.81***	-0.26***	0.83***	0.82***	0.63***	0.76***	0.95***	0.96***	0.96***	0.96***						
	Narrow-band Simple Rat io	0.84***	-0.32***	0.85***	0.85***	0.68***	0.83***	0.91***	0.94***	0.93***	0.95***	0.99***					
	MODIS EVI	0.61***	0.07	0.65***	0.65***	0.44***	0.47***	0.75***	0.75***	0.75***	0.74***	0.74***	0.71***				
	MODIS SARVI	0.56***	0.06	0.61***	0.61***	0.41***	0.43***	0.69***	0.69***	0.70***	0.68***	0.69***	0.67***	0.99***			
	NDVI 705	0.85***	-0.19***	0.83***	0.84***	0.65***	0.74***	0.97***	0.99***	0.99***	0.98***	0.96***	0.94***	0.77***	0.71***		
	MODIS CAI	-0.68***	0.62***	-0.59***	-0.60***	-0.59***	-0.82***	-0.59***	-0.65***	-0.62***	-0.68***	-0.64***	-0.68***	-0.21***	-0.17***	-0.62***	
	PRI	0.53***	-0.68***	0.38***	0.41***	0.58***	0.76***	0.18***	0.28***	0.25***	0.32***	0.30***	0.38***	0.09*	0.09*	0.27***	-0.65***

Appendix B ADDITIONAL TIME SEGMENTATION FROM DRI-GRASS PHENOCAM DATA

This appendix contains supplementary data to Chapter 3. Refer to Chapter 3 for details regarding methods used to generate this data.

Because phenocam data is taken at sub-daily frequency, the data can be split into segments of various lengths to compare different variables. In the main section of this chapter, we compare treatments by total data series, by season and by drought periods, as these results had the most relevant findings to the study. However, other meaningful groups were also considered and are presented here for completeness.

Segmentation by Mode

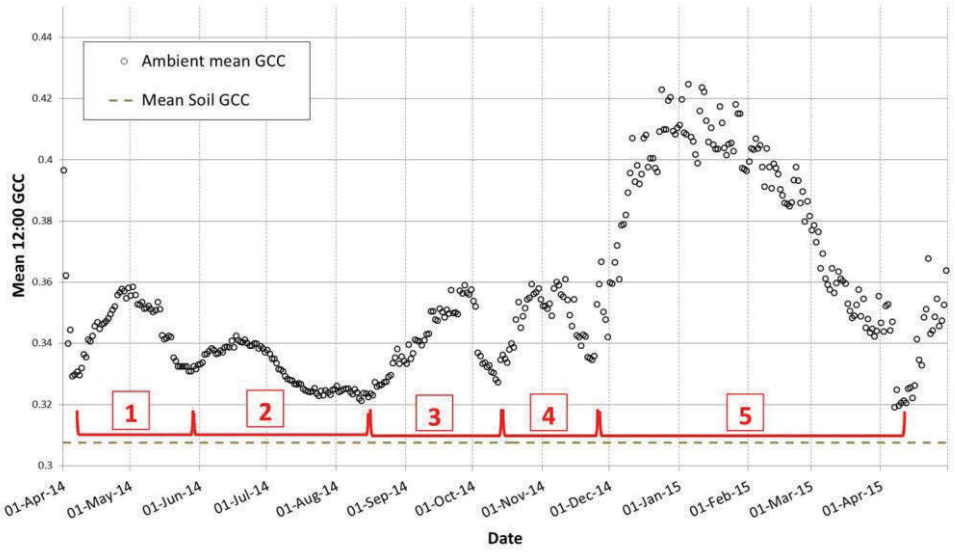

Figure B.1 Phenology profile of mean ambient treatment, separated into modes (discrete periods of greening/browning). The horizontal dashed line represents the mean soil g_{CC} value.

- Mode 1: 6 April 2014–29 May 2014
- Mode 2: 30 May 2014–15 August 2014
- Mode 3: 16 August 2014–10 October 2014
- Mode 4: 11 October 2014–22 November 2014
- Mode 5: 23 November 2014–7 April 2015

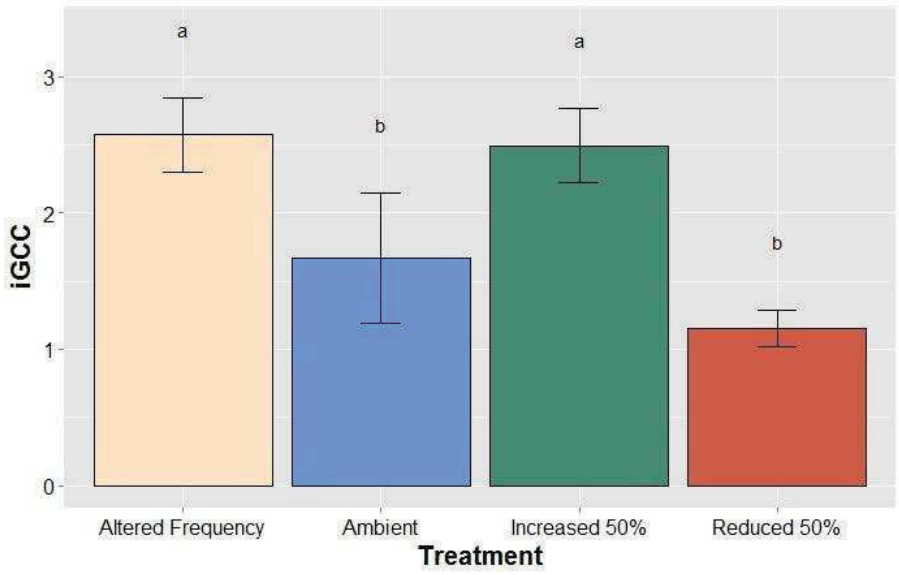

Figure B.2 Mean ig_{CC} (± 1 s.d.) by treatment for Mode 1 (6 April 2014–29 May 2014). Means with the same letter are not significantly different between each treatment (Dunn's post-hoc test $p < 0.05$).

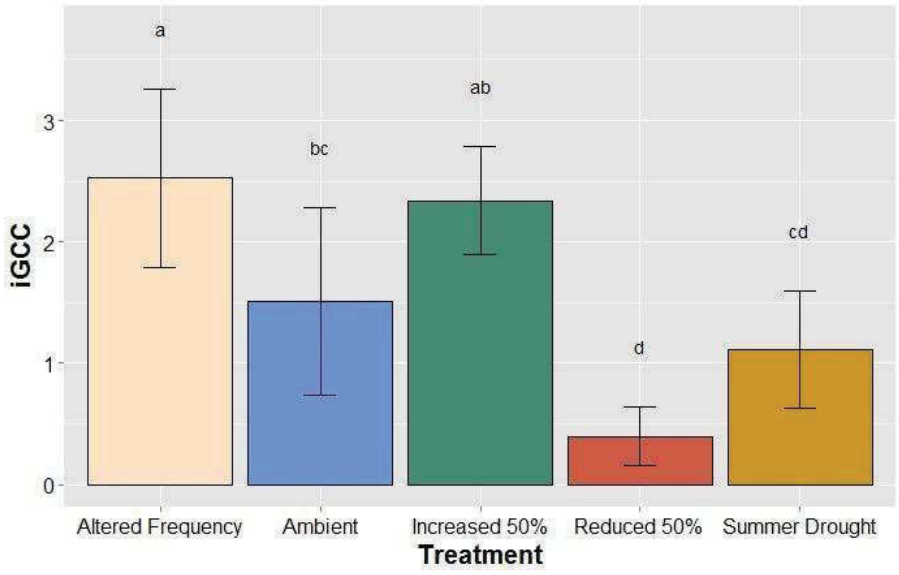

Figure B.3 Mean ig_{CC} (± 1 s.d.) by treatment for Mode 2 (30 May 2014–15 August 2014). Means with the same letter are not significantly different between each treatment (Dunn's post-hoc test $p < 0.05$).

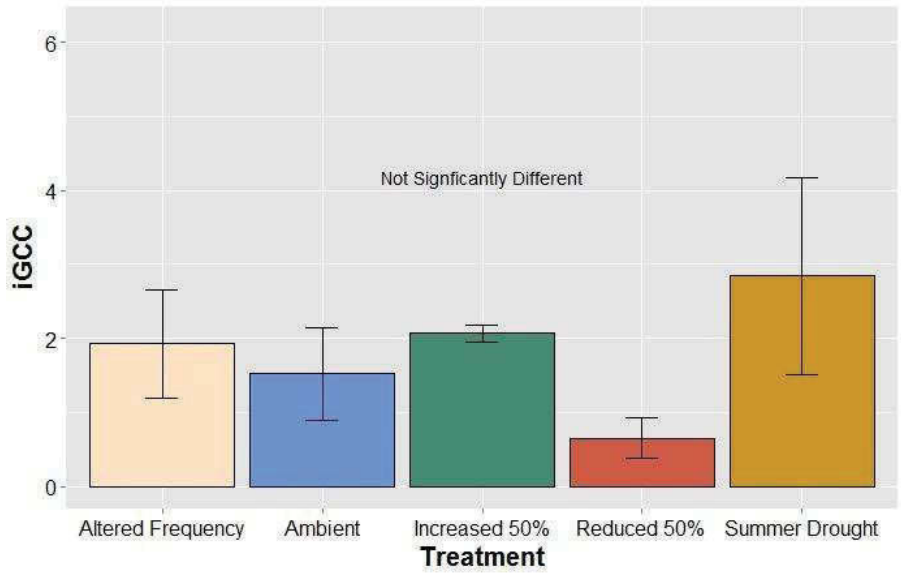

Figure B.4 Mean ig_{CC} (± 1 s.d.) by treatment for Mode 3 (16 August 2014–10 October 2014).

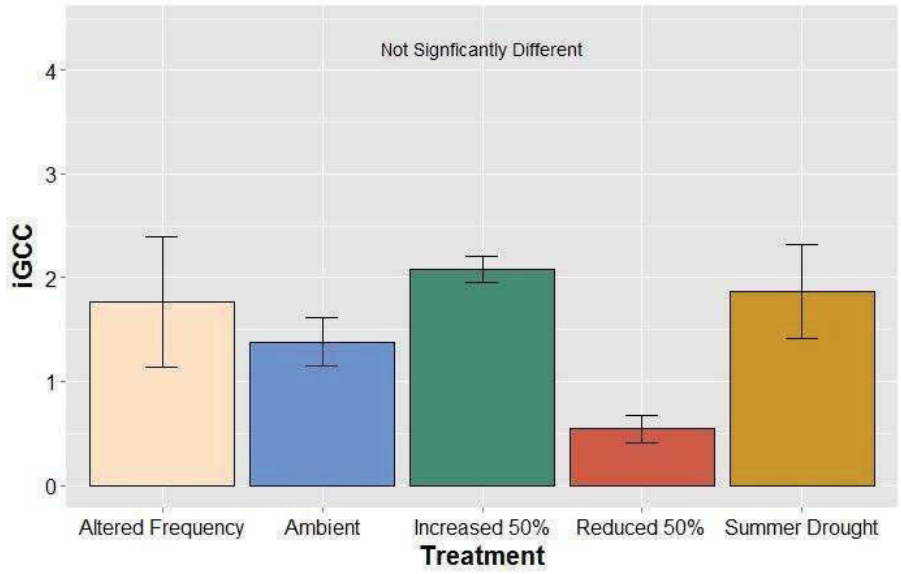

Figure B.5 Mean ig_{CC} (± 1 s.d.) by treatment for Mode 4 (11 October 2014–22 November 2014).

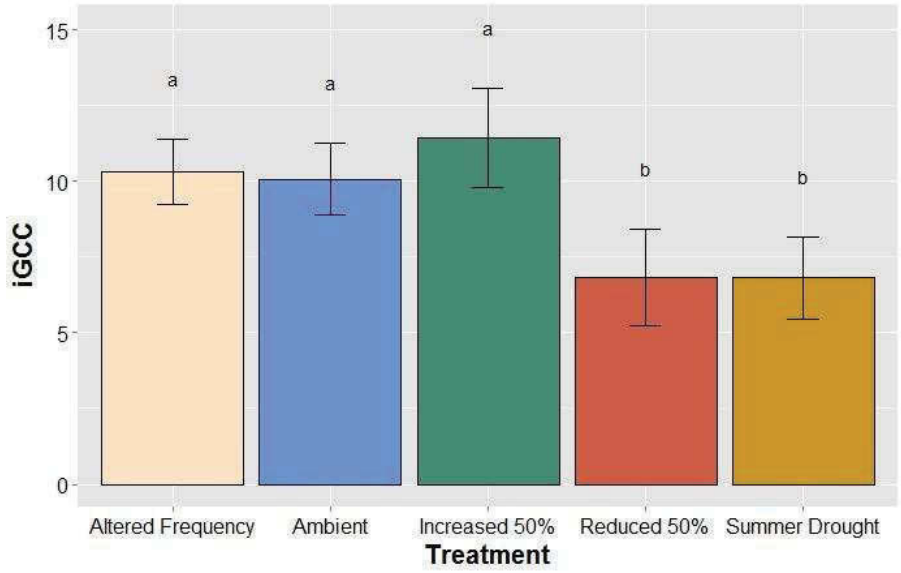

Figure B.6 Mean ig_{CC} (± 1 s.d.) by treatment for Mode 5 (23 November 2014–7 April 2015). Means with the same letter are not significantly different between each treatment (Dunn's post-hoc test $p < 0.05$).

Segmentation by harvest period

A destructive harvesting study was conducted orthogonal to this phenocam study. Harvesting occurred twice to capture growth from April 2014 to September 2014—autumn to early spring—and October 2014 to April 2015—spring to autumn (Figure B.7). The difference between treatments for the two harvest periods is illustrated in Figure B.8 and Figure B.9.

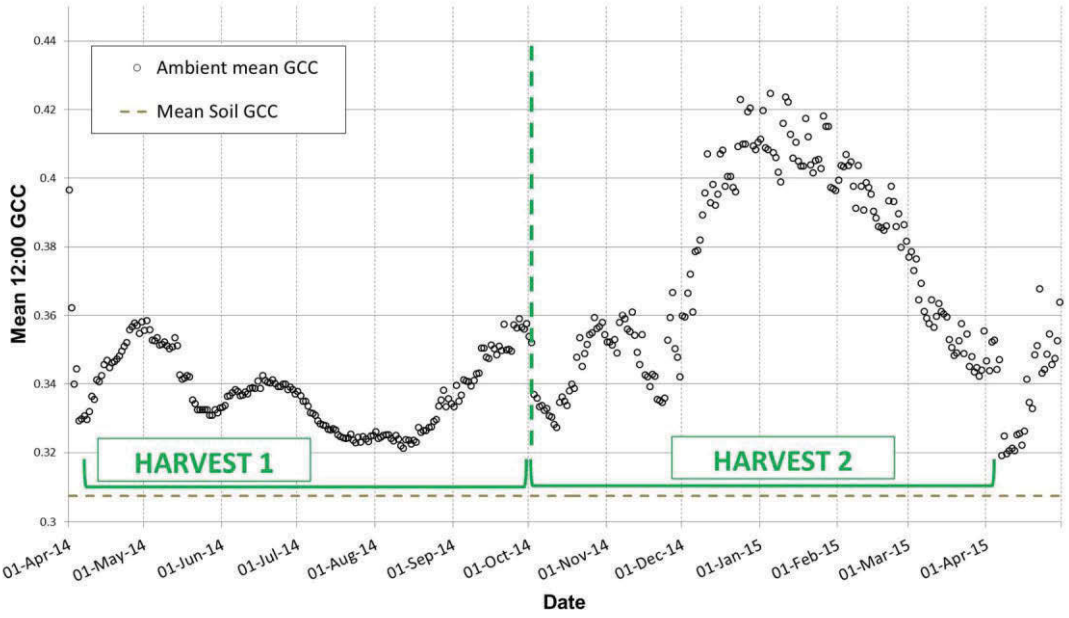

Figure B.7 Phenology profile of mean ambient treatment, separated into harvest periods. The horizontal dashed line represents the mean soil g_{CC} value.

- Harvest 1: 7 April 2014–4 October 2014
- Harvest 2: 5 October 2014–27 March 2015

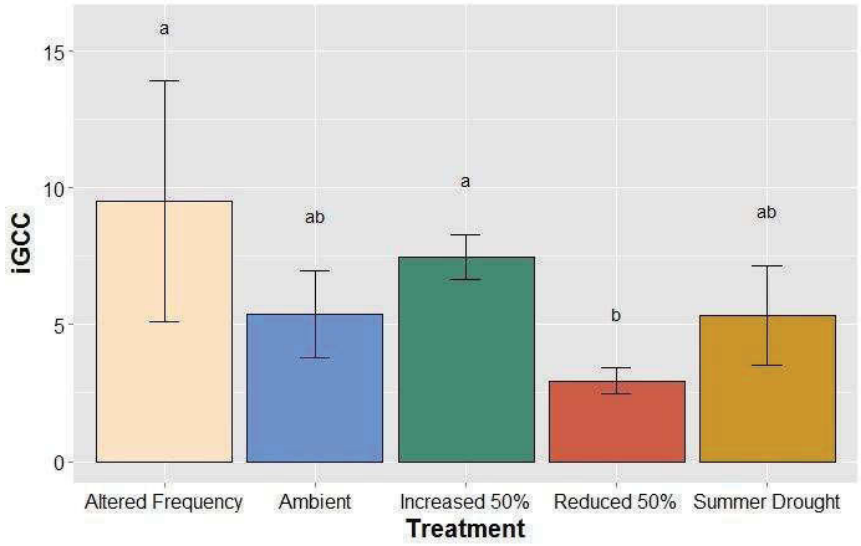

Figure B.8 Mean ig_{CC} (± 1 s.d.) by treatment for Harvest 1 (7 April 2014–4 October 2014; 180 days). Means with the same letter are not significantly different between each treatment (Dunn's post-hoc test $p < 0.05$).

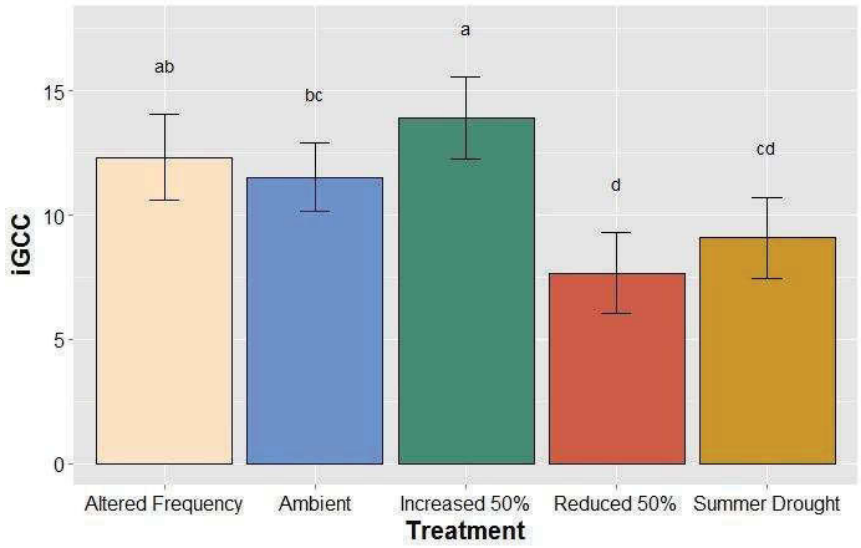

Figure B.9 Mean ig_{CC} (± 1 s.d.) by treatment for Harvest 2 (5 October 2014–27 March 2015; 173 days). Means with the same letter are not significantly different between each treatment (Dunn's post-hoc test $p < 0.05$).

Appendix C VASCULAR PLANT SPECIES LIST FOR ALL SITES

Table C.1 List of vascular plant species detected at each site during monthly monitoring over a one year period. Native status refers to either native (N) or exotic (E). Growth form refers to either graminoid (G) or forb (F). Plant names follow the Royal Botanic Gardens PlantNET database.

DIVISION	CLASS	FAMILY	SCIENTIFIC NAME	NATIVE STATUS	GROWTH FORM	SITE											
						MGAR	GUNN	MULN	GIDL	TURA	MPON	MULE	GUNE	MPOE	SCOT	INGE	IN17
Pteridophyta	Pteridopsida	PTERIDACEAE	*Cheilanthes austrotenuifolia*	N	F										X		
Magnoliophyta	Liliospida	ASPHODELACEAE	*Bulbine bulbosa*	N	F						X			X			
		COLCHICACEAE	*Wurmbea dioica*	N	F	X		X				X					
		CYPERACEAE	*Carex inversa*	N	G			X									
			Carex sp.	U	G								X				
			Carex sp. 2	U	G			X	X								
			Carex sp. 3	N	G					X							
			Cyperus eragrostis	E	G								X			X	
			Lepidosperma sp.	U	G			X									
			Schoenus apogon	N	G						X						
		HYPOXIDACEAE	*Hypoxis hygrometrica*	N	F					X	X						

DIVISION	CLASS	FAMILY	SCIENTIFIC NAME	NATIVE STATUS	GROWTH FORM	SITE											
						MGAR	GUNN	MULN	GIDL	TURA	MPON	MULE	GUNE	MPOE	SCOT	INGE	IN17
		JUNCACEAE	*Juncus acutus*	E	G		X	X	X	X	X		X	X			
			Juncus articulatus	E	G			X		X			X				
			Juncus bufonius	E	G										X	X	
			Juncus filicaulis	N	G	X		X	X	X	X						
			Luzula densiflora	N	G			X	X		X						
		LOMANDRACEAE	*Lomandra filiformis*	N	F	X		X	X	X	X				X		X
			Lomandra sp.	N	G						X						
		ORCHIDACEAE	*Diuris monticola*	N	F				X	X	X						
			Diuris sp.	N	F					X							
			Microtis unifolia	N	F	X				X	X						
		POACEAE	*Aira cupaniana*	E	G	X	X	X	X	X	X						
			Aira sp.	E	G					X							
			Aristida ramosa	N	G			X									
			Austrostipa bigeniculata	N	G	X		X		X							
			Austrostipa scabra	N	G	X	X									X	X
			Austrostipa sp.	N	G									X			
			Avena barbata	E	G	X	X	X		X						X	X
			Bothriochloa macra	N	G	X		X	X								
			Briza maxima	E	G		X		X								
			Briza minor	E	G			X	X	X	X						
			Bromus hordeaceus	E	G	X	X	X	X	X				X	X	X	X

DIVISION	CLASS	FAMILY	SCIENTIFIC NAME	NATIVE STATUS	GROWTH FORM	SITE											
						MGAR	GUNN	MULN	GIDL	TURA	MPON	MULE	GUNE	MPOE	SCOT	INGE	IN17
			Chloris truncata	N	G			X						X			
			Cynodon dactylon	N	G									X			
			Dactylis glomerata	E	G					X		X		X			
			Dichelachne crinita	N	G			X	X	X	X						
			Dichelachne sp.	N	G					X							
			Eleusine tristachya	E	G		X							X		X	
			Elymus scaber	N	G	X	X	X	X	X	X			X	X		
			Enneapogon nigricans	N	G						X						
			Eragrostis brownii	N	G			X		X				X			
			Eragrostis curvula	E	G			X						X	X	X	X
			Festuca arundinacea	E	G			X				X		X			
			Holcus lanatus	E	G	X		X				X	X	X			
			Hordeum leporinum	E	G		X							X		X	X
			Lolium perenne	E	G			X					X	X		X	
			Microlaena stipoides	N	G		X	X						X			
			Nassella neesiana	E	G	X											
			Nassella trichomata	E	G	X	X	X		X				X	X	X	X
			Panicum effusum	N	G	X		X	X	X	X						
			Paspalum dilatatum	E	G			X					X				
			Phalaris aquatica	E	G	X	X	X	X	X	X	X	X	X	X	X	X
			Poa labillardierei	N	G	X		X	X		X				X	X	

DIVISION	CLASS	FAMILY	SCIENTIFIC NAME	NATIVE STATUS	GROWTH FORM	SITE											
						MGAR	GUNN	MULN	GIDL	TURA	MPON	MULE	GUNE	MPOE	SCOT	INGE	IN17
			Poa sieberiana	N	G					X							
			Rytidosperma caespitosum	N	G	X	X	X	X	X	X		X	X	X	X	X
			Rytidosperma carphoides	N	G	X				X							
			Rytidosperma laeve	N	G	X		X	X	X							
			Rytidosperma pallidum	N	G			X									
			Rytidosperma racemosum	N	G	X		X									
			Rytidosperma tenuius	N	G					X							
			Sorghum leiocladum	N	G					X							
			Themeda triandra	N	G	X		X	X	X	X						
			Unknown (Poaceae)	U	G		X						X				
			Unknown graminoid (IN1714)	U	G												X
			Unknown graminoid (MGAR10)	U	G	X											
			Unknown graminoid (MULN31)	U	G			X									
			Vulpia myuros	E	G	X	X	X	X		X			X		X	X
	Magnoliopsida	ANTHERICACEAE	*Arthropodium milleflorum*	N	F	X		X	X	X	X						
			Dichopogon fimbriatus	N	F								X				
			Thysanotus tuberosus	N	F						X						
			Tricoryne elatior	N	F	X			X	X			X				
		APIACEAE	*Eryngium ovinum*	N	F				X	X							
			Hydrocotyle laxiflora	N	F			X	X	X	X			X			

DIVISION	CLASS	FAMILY	SCIENTIFIC NAME	NATIVE STATUS	GROWTH FORM	SITE											
						MGAR	GUNN	MULN	GIDL	TURA	MPON	MULE	GUNE	MPOE	SCOT	INGE	IN17
			Oreomyrrhis eriopoda	N	F			X									
		ASTERACEAE	*Arctotheca calendula*	E	F		X										
			Calocephalus citreus	N	F				X	X							
			Carthamus lanatus	E	F	X	X				X				X	X	X
			Chondrilla juncea	E	F	X	X								X	X	X
			Chrysocephalum apiculatum	N	F	X	X	X	X	X	X						X
			Chrysocephalum semipapposum	N	F										X		
			Cichorium intybus	E	F							X					
			Cirsium vulgare	E	F	X		X	X	X	X			X	X	X	X
			Conyza bonariensis	E	F			X			X				X	X	X
			Conyza sp.	E	F			X			X						
			Conyza sumatrensis	E	F	X		X	X	X					X	X	X
			Coronidium scorpioides	N	F			X									
			Craspedia variabilis	N	F						X						
			Crepis capillaris	E	F						X						
			Cymbonotus lawsonianus	N	F	X		X	X	X	X				X		X
			Euchiton japonicus	N	F	X		X								X	
			Euchiton sphaericus	N	F		X	X	X		X					X	X
			Gamochaeta coarctata	E	F												X
			Gamochaeta purpurea	E	F											X	X
			Hieracium pilosella	E	F										X		

DIVISION	CLASS	FAMILY	SCIENTIFIC NAME	NATIVE STATUS	GROWTH FORM	SITE											
						MGAR	GUNN	MULN	GIDL	TURA	MPON	MULE	GUNE	MPOE	SCOT	INGE	IN17
			Hypochaeris radicata	E	F	X	X	X	X	X	X	X	X	X	X	X	X
			Lactuca serriola	E	F		X	X			X				X	X	X
			Lapsana communis	E	F			X			X				X	X	X
			Leptorhynchos squamatus	N	F			X	X	X	X						
			Microseris lanceolata	N	F						X						
			Onopordum acanthium subsp. *acanthium*	E	F		X	X						X	X	X	X
			Senecio jacobaea	E	F		X							X			
			Senecio madagascariensis	E	F										X	X	X
			Senecio quadridentatus	N	F		X	X							X		
			Solenogyne dominii	N	F	X		X		X	X						
			Sonchus asper	E	F			X		X				X	X	X	
			Sonchus oleraceus	E	F	X	X	X		X					X		X
			Taraxacum sp.	E	F	X					X	X					
			Tolpis barbata	E	F			X			X				X	X	X
			Tragopogon dubius	E	F	X		X		X					X	X	X
			Triptilodiscus pygmaeus	N	F						X				X		
			Vittadinia cuneata	N	F	X	X	X		X							X
			Vittadinia muelleri	N	F	X		X		X	X				X		
		BORAGINACEAE	*Cynoglossum suaveolens*	N	F		X										
			Echium plantagineum	E	F	X	X	X	X						X	X	X

DIVISION	CLASS	FAMILY	SCIENTIFIC NAME	NATIVE STATUS	GROWTH FORM	SITE											
						MGAR	GUNN	MULN	GIDL	TURA	MPON	MULE	GUNE	MPOE	SCOT	INGE	IN17
			Echium vulgare	E	F		X	X							X	X	X
		BRASSICACEAE	*Capsella bursa-pastoris*	E	F	X	X								X	X	X
			Lepidium campestre	E	F												X
			Sisymbrium officinale	E	F							X				X	X
		CAMPANULACEAE	*Wahlenbergia communis*	N	F	X	X	X	X	X	X				X	X	X
			Wahlenbergia gracilis	N	F			X			X				X		
			Wahlenbergia sp.	N	F												X
		CARYOPHYLLACEAE	*Cerastium glomeratum*	E	F			X			X						
			Petrorhagia nanteuilii	E	F			X			X				X	X	X
		CHENOPODIACEAE	*Chenopodium album*	E	F									X			
			Dysphania pumilio	N	F									X		X	
		CLUSIACEAE	*Hypericum gramineum*	N	F			X	X	X	X						
			Hypericum perforatum	E	F	X	X		X	X	X		X		X		X
		CONVOLVULACEAE	*Convolvulus angustissimus*	N	F	X	X	X	X	X	X				X	X	X
			Dichondra repens	N	F			X									X
		DROSERACEAE	*Drosera peltata*	N	F				X	X	X						
		EUPHORBIACEAE	*Euphorbia maculata*	E	F			X									
		FABACEAE	*Cullen tenax*	N	F	X					X						
			Desmodium varians	N	F					X							
			Glycine clandestina	N	F					X					X		
			Medicago polymorpha	E	F							X					

DIVISION	CLASS	FAMILY	SCIENTIFIC NAME	NATIVE STATUS	GROWTH FORM	SITE											
						MGAR	GUNN	MULN	GIDL	TURA	MPON	MULE	GUNE	MPOE	SCOT	INGE	IN17
			Medicago sativa	E	F							X					
			Trifolium arvense	E	F	X		X	X	X	X				X	X	X
			Trifolium dubium	E	F	X		X	X	X	X				X	X	
			Trifolium repens	E	F		X	X		X		X		X	X	X	X
			Trifolium sp.	E	F		X					X			X		
			Trifolium subterraneum	E	F	X	X	X	X					X		X	
			Trifolium vesiculosum	E	F							X				X	
			Vicia sativa subsp. *nigra*	E	F			X									
			Vicia villosa	E	F			X									
		GENTIANACEAE	*Centaurium erythraea*	E	F	X		X	X	X	X		X		X		X
		GERANIACEAE	*Erodium botrys*	E	F							X		X		X	X
			Erodium crinitum	N	F	X	X										X
			Geranium dissectum	E	F				X								
			Geranium molle	E	F			X						X			
			Geranium solanderi	N	F			X			X			X			
		GOODENIACEAE	*Goodenia pinnatifida*	N	F				X	X							
			Velleia paradoxa	N	F			X	X		X						
		HALORAGACEAE	*Gonocarpus tetragynus*	N	F				X	X	X						
			Haloragis heterophylla	N	F	X		X	X	X	X		X				
		LAMIACEAE	*Salvia verbenaca*	E	F	X				X						X	X
		LYTHRACEAE	*Lythrum hyssopifolia*	N	F								X				

DIVISION	CLASS	FAMILY	SCIENTIFIC NAME	NATIVE STATUS	GROWTH FORM	SITE											
						MGAR	GUNN	MULN	GIDL	TURA	MPON	MULE	GUNE	MPOE	SCOT	INGE	IN17
		MYRSINACEAE	*Lysimachia arvensis*	E	F			X							X		
		ONAGRACEAE	*Epilobium billardierianum*	N	F	X		X		X	X		X		X		
			Epilobium ciliatum	E	F										X		
		OROBANCHACEAE	*Parentucellia latifolia*	E	F			X			X						
		OXALIDACEAE	*Oxalis perennans*	N	F	X	X	X	X	X	X				X		
			Oxalis sp.	U	F		X							X	X	X	X
		PLANTAGINACEAE	*Linaria pelisseriana*	E	F												
			Plantago gaudichaudii	N	F				X	X							
			Plantago lanceolata	E	F	X	X	X	X	X		X	X		X	X	X
			Plantago major	E	F			X									
			Plantago varia	N	F	X		X	X	X	X						
			Veronica sp.	E	F			X			X						
		POLYGONACEAE	*Acetosella vulgaris*	E	F	X	X	X	X	X	X			X	X	X	X
			Rumex brownii	N	F	X	X	X	X	X	X		X	X	X	X	X
			Rumex crispus	E	F							X	X				
			Rumex dumosus	N	F				X	X							
		RANUNCULACEAE	*Ranunculus lappaceus*	N	F						X						
		ROSACEAE	*Acaena ovina*	N	F	X		X	X	X	X			X	X	X	X
			Sanguisorba minor	E	F		X									X	
		RUBIACEAE	*Asperula conferta*	N	F	X		X	X	X	X						

DIVISION	CLASS	FAMILY	SCIENTIFIC NAME	NATIVE STATUS	GROWTH FORM	SITE											
						MGAR	GUNN	MULN	GIDL	TURA	MPON	MULE	GUNE	MPOE	SCOT	INGE	IN17
			Galium aparine	E	F										X		
		SCROPHULARIACEAE	*Verbascum thapsus* subsp. *thapsus*	E	F	X									X	X	X
			Verbascum virgatum	E	F	X											
		SOLANACEAE	*Solanum nigrum*	E	F		X										
		STACKHOUSIACEAE	*Stackhousia monogyna*	N	F				X	X							
		THYMELAEACEAE	*Pimelea curviflora*	N	F			X	X	X	X						
		VERBENACEAE	*Verbena* sp.	E	F										X		
		UNKNOWN	Unknown exotic forb (IN1715)	E	F												X
			Unknown exotic forb (MULE1)	E	F							X					
			Unknown exotic forb (MULE2)	E	F							X					
			Unknown forb (GIDL15)	U	F				X								
			Unknown forb (IN176)	U	F												X
			Unknown forb (MPOE3)	E	F									X			
			Unknown forb (MULN21)	U	F			X									
			Unknown forb (MULN36)	E	F			X									
			Unknown sp. (MPON17)	U	F						X						

Appendix D EFFECT OF TIME-OF-DAY ON PHENOCAM GCC PATTERNS

This appendix presents data on the effect of illumination as a result of time-of-day sun angle on the magnitude and patterns of phenocam g_{CC}. This is presented at each of the 12 study sites, details of which can be found in Chapter 4. Refer to Chapter 5, Section 5.2.3 for details on how the cameras were installed, and Section 5.2.6 for details on how images were analysed.

Figure D.1 to Figure D.12 present comparison phenology profiles of each site, where each coloured trend line represents g_{CC} at different times of day between 9:00 and 15:00 Australian Eastern Standard Time. The trend lines are LOESS fitted curves (span = 0.1) for visual comparison of the grouped temporal trends. Each data point is the mean value of 9 ROIs per image.

Differences in g_{CC} were generally invariant with time of day. Some sites (e.g. INGE, MGAR, GUNN) showed near identical phenology profile shapes and magnitude for each hourly dataset throughout the monitoring period. A few sites (GUNE, IN17, TURA) had minor deviation in g_{CC} magnitude; these were most apparent during periods of highest greenness.

Where there is minor discrepancy in the shape of the trend lines, data at 15:00 tends to be have the highest g_{CC}. Frequently this is only for a few months of the year, but this trend is not seasonally consistent within plots. Data points at 14:00 show the next highest g_{CC}. Conversely, 9:00 tended to have the lowest g_{CC}. The 9:00 data deviated a little from the others, however this is likely to be due to the lower numbers of 9:00 data points. Data from 9:00 had the highest number of images removed as part of the quality control process. The shape of the trend line is vulnerable to data gaps, hence the likelihood of more variation at 9:00.

Although the time-of-day differences were slight, 11:00 to 13:00 showed the least variability. While using all available data is preferred, if only one data point is used per day, it is suggested that be consistent through time, and within the 11:00 to 13:00 range.

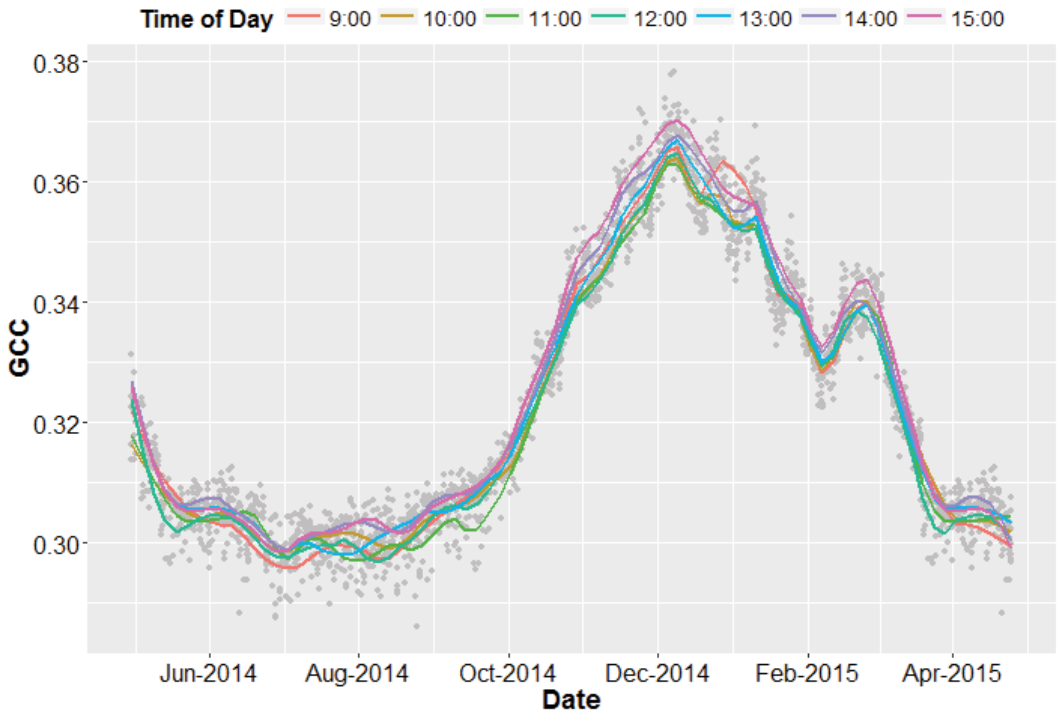

Figure D.1 Comparison phenology profile of mean time-of-day g_{CC} from site GIDL (C4 Native).

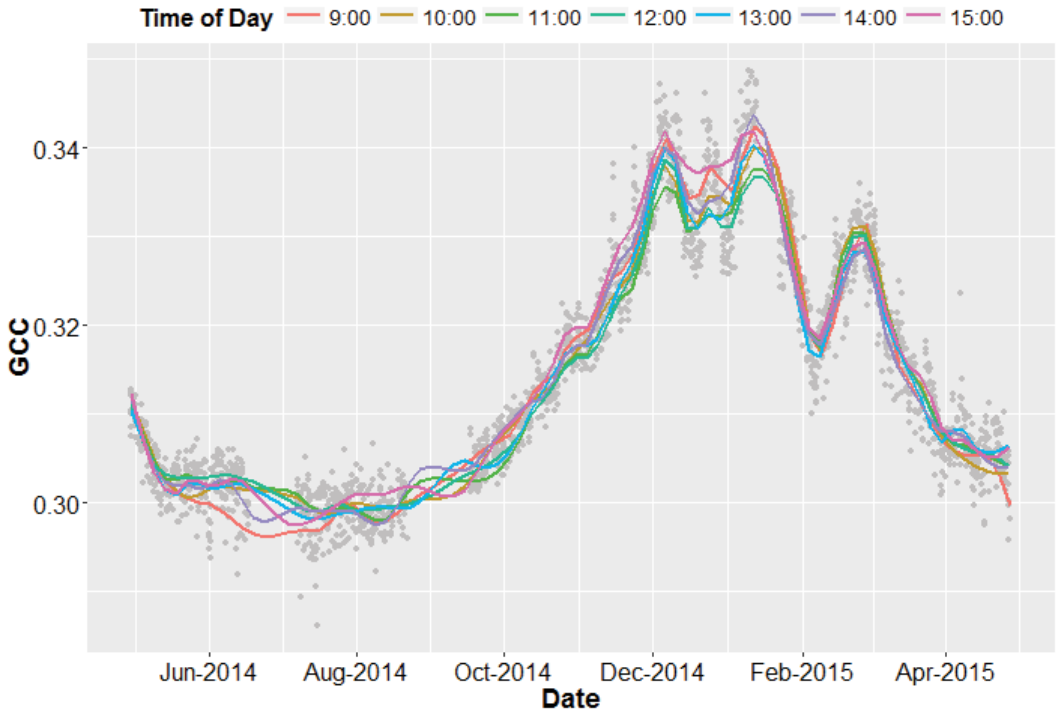

Figure D.2 Comparison phenology profile of mean time-of-day g_{CC} from site TURA (C4 Native).

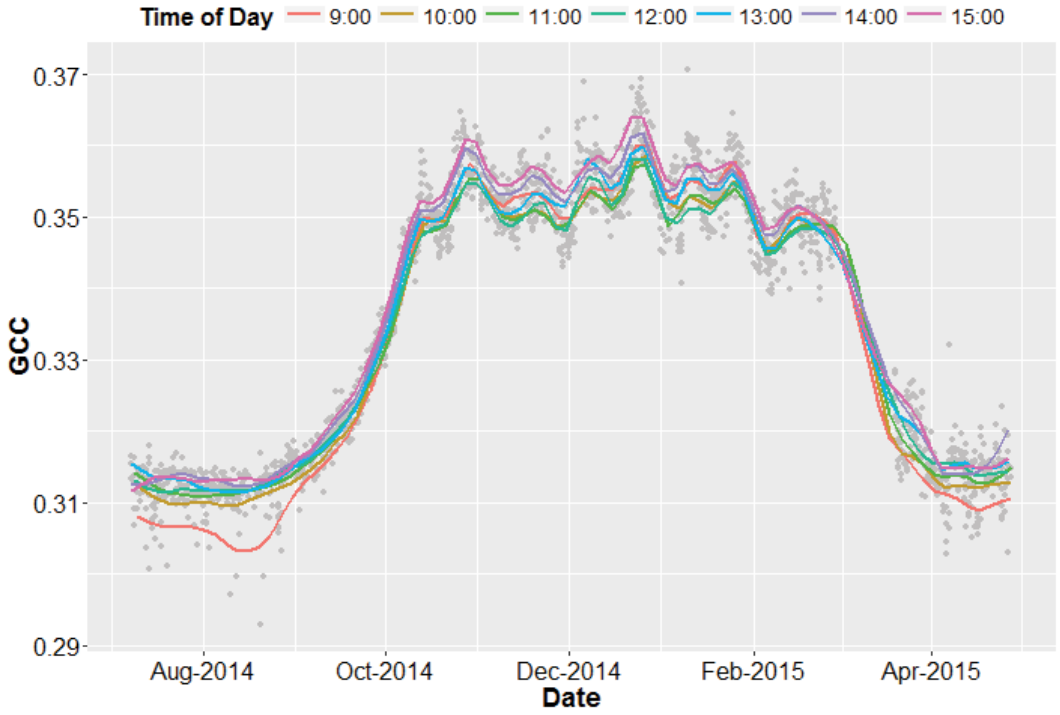

Figure D.3 Comparison phenology profile of mean time-of-day g_{CC} from site MPON (C4 Native).

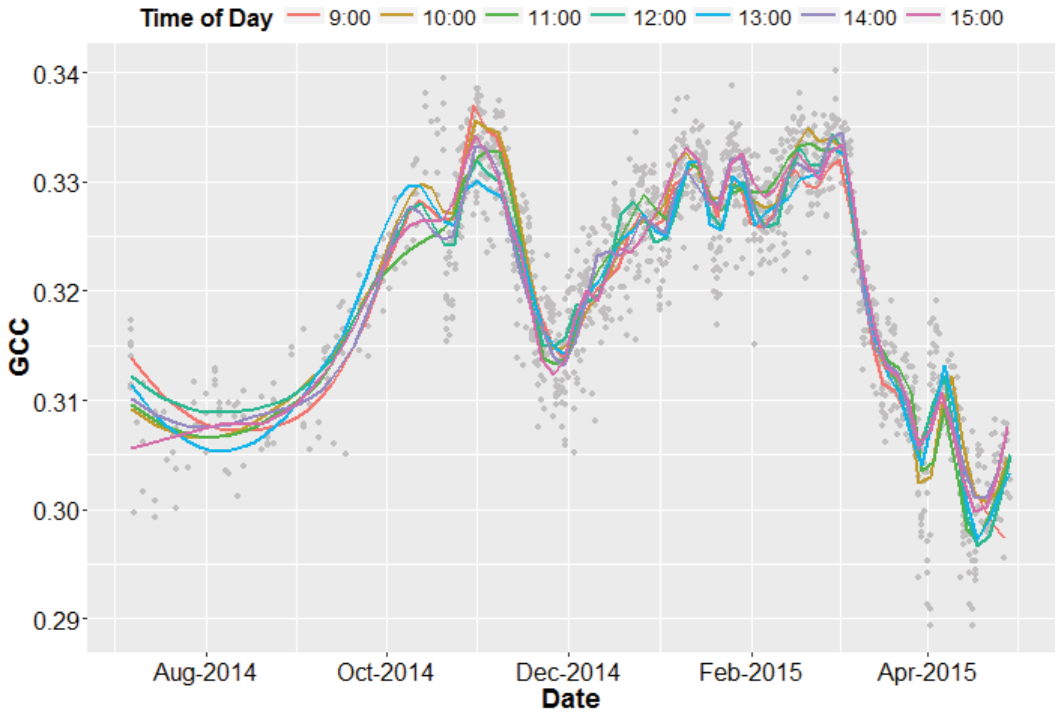

Figure D.4 Comparison phenology profile of mean time-of-day g_{CC} from site IN17 (C4 Exotic).

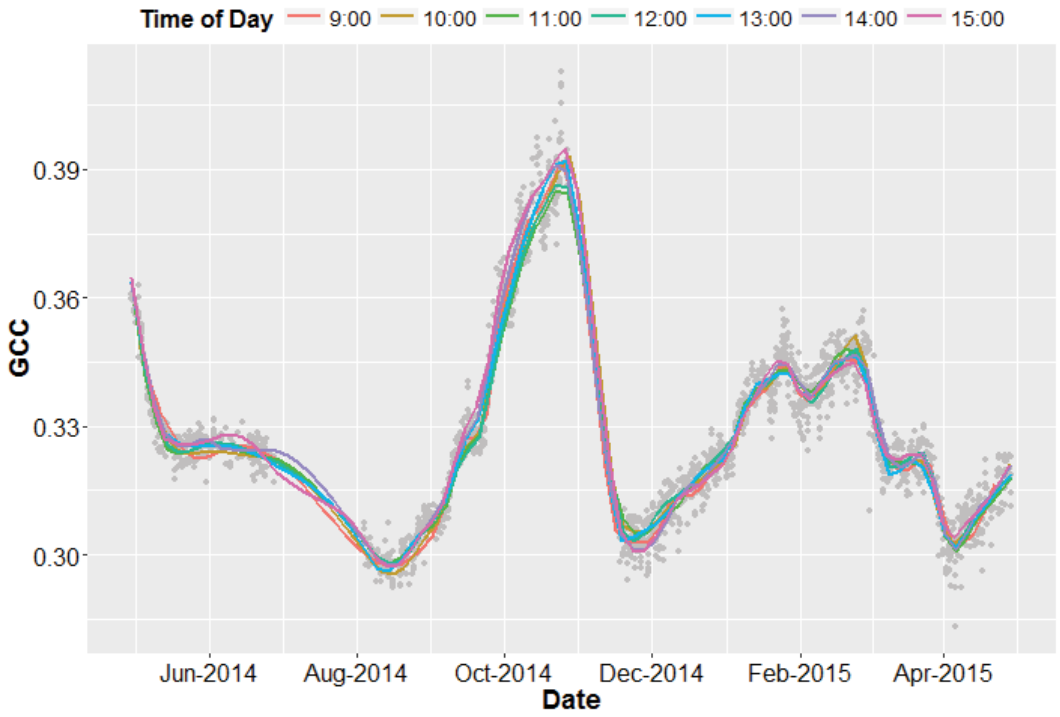

Figure D.5 Comparison phenology profile of mean time-of-day g_{CC} from site INGE (C4 Exotic).

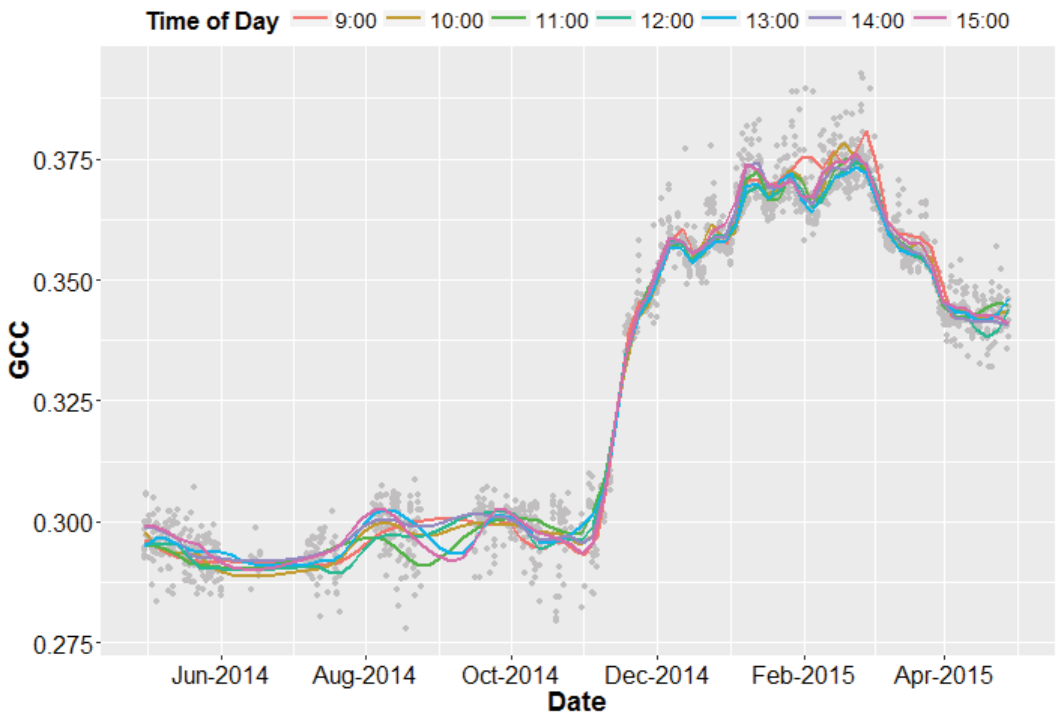

Figure D.6 Comparison phenology profile of mean time-of-day g_{CC} from site SCOT (C4 Exotic).

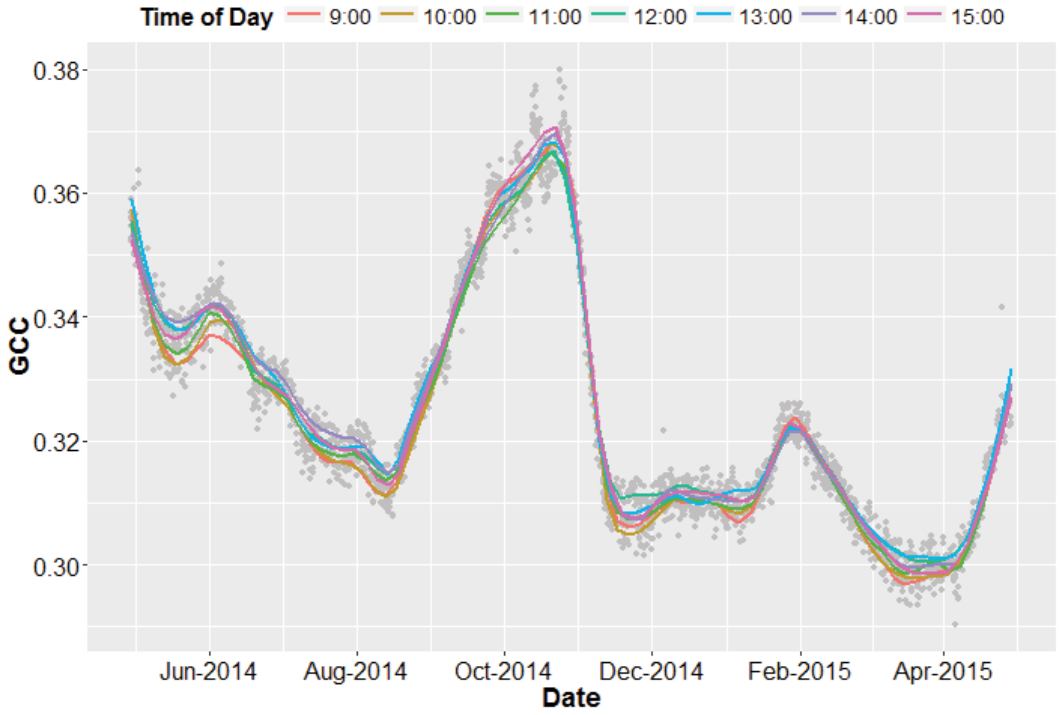

Figure D.7 Comparison phenology profile of mean time-of-day g_{CC} from site MGAR (C3 Native).

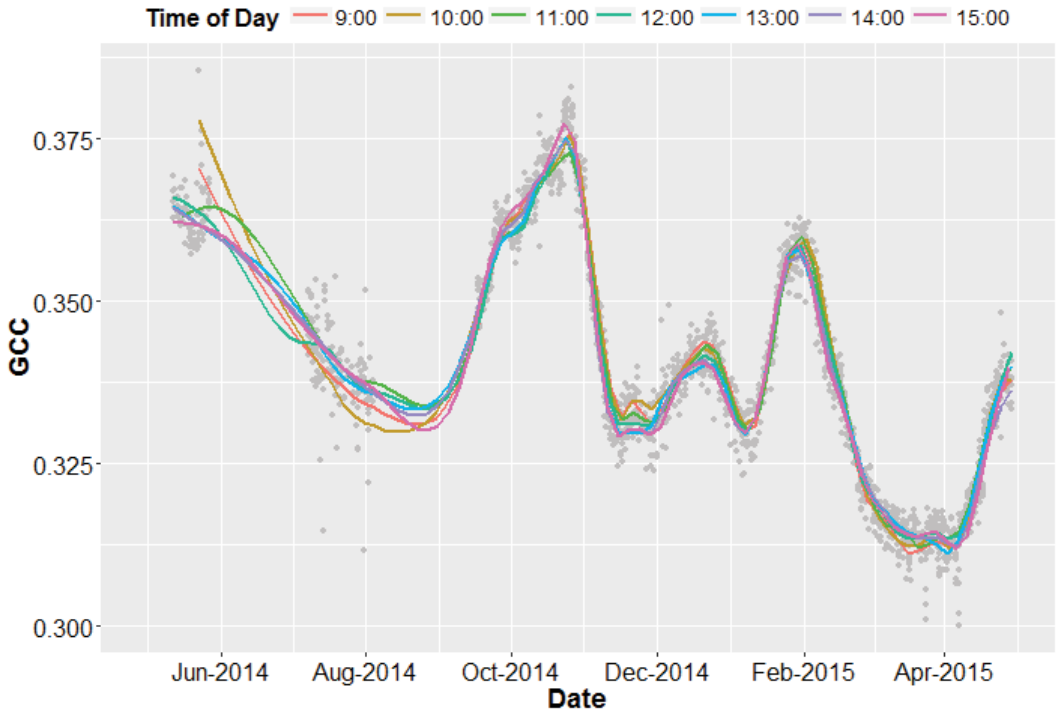

Figure D.8 Comparison phenology profile of mean time-of-day g_{CC} from site GUNN (C3 Native).

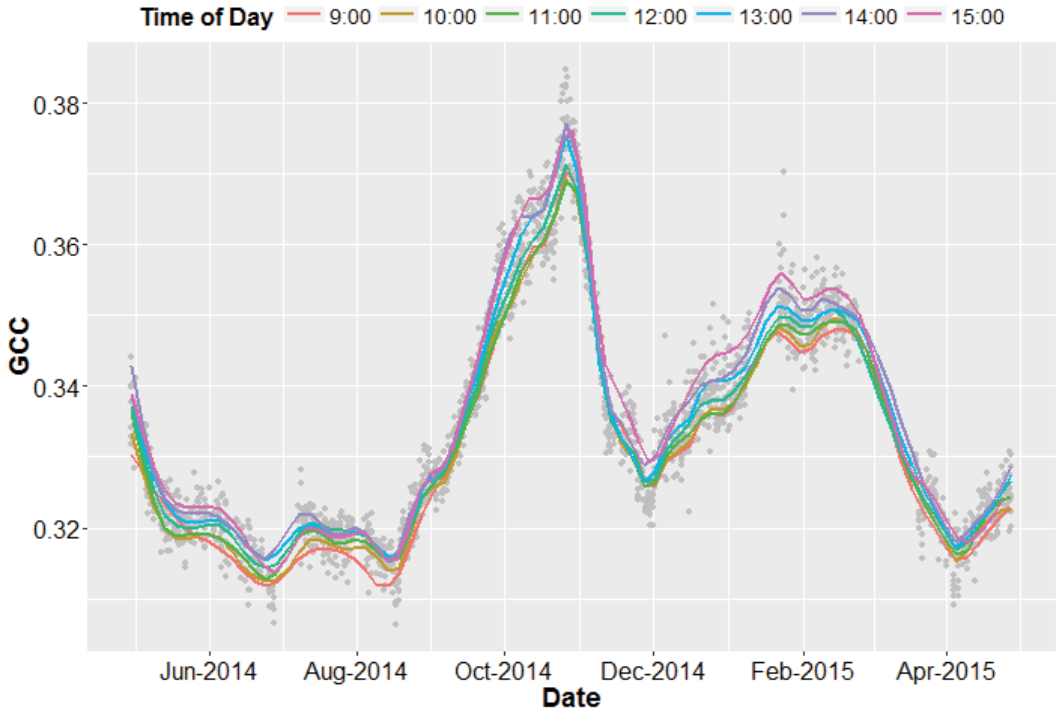

Figure D.9 Comparison phenology profile of mean time-of-day g_{CC} from site MULN (C3 Native).

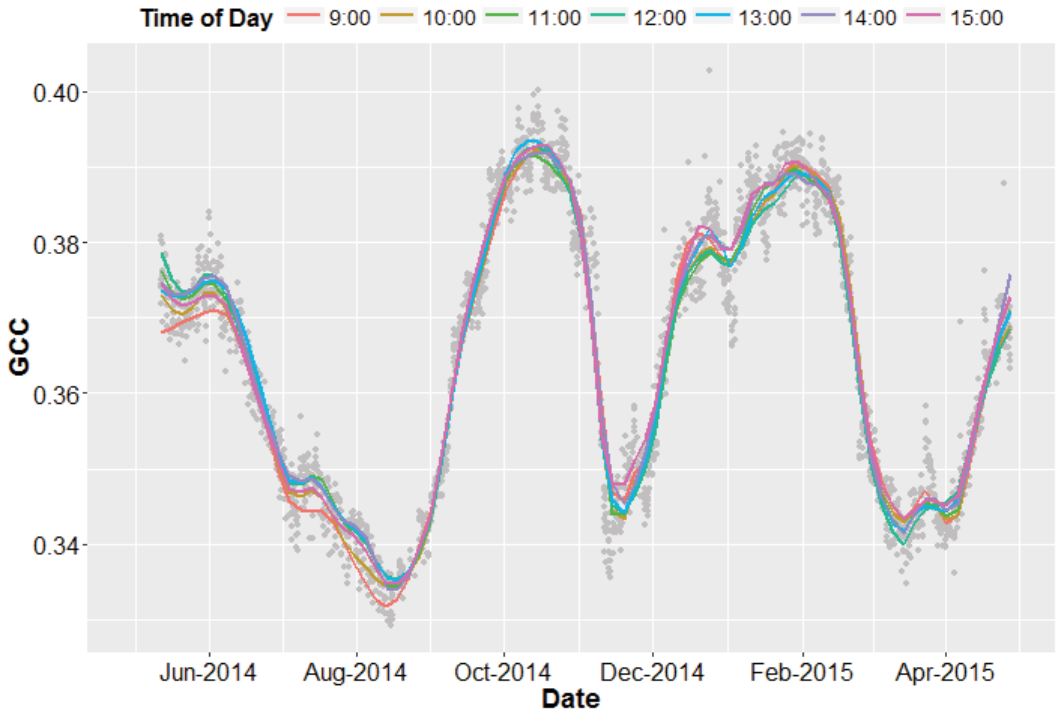

Figure D.10 Comparison phenology profile of mean time-of-day g_{CC} from site MULE (C3 Exotic).

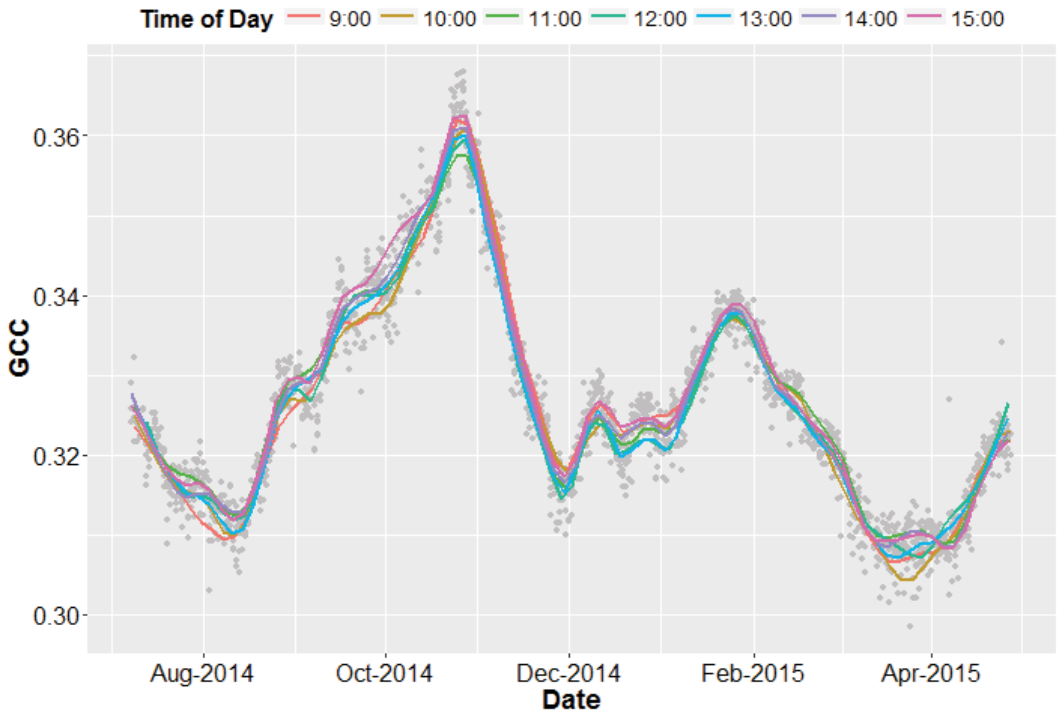

Figure D.11 Comparison phenology profile of mean time-of-day g_{CC} from site MPOE (C3 Exotic).

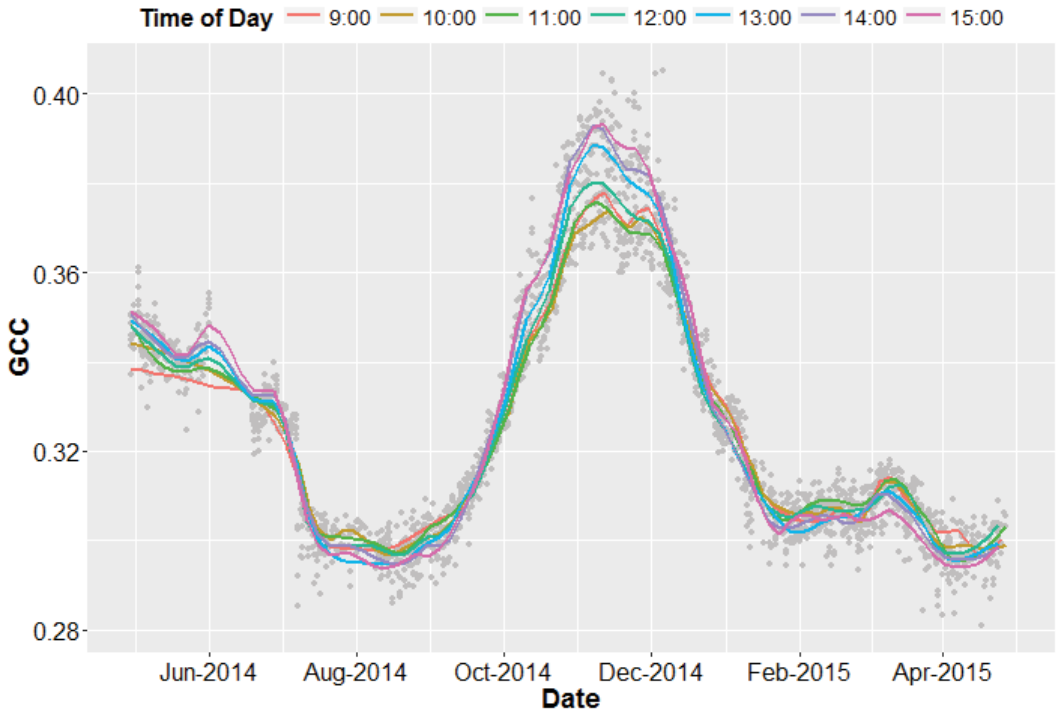

Figure D.12 Comparison phenology profile of mean time-of-day g_{CC} from site GUNE (C3 Exotic).

Appendix E EFFECT OF CAMERA ANGLE ON G_{CC} MAGNITUDE

This appendix presents data on the effect of phenocam camera angle on the magnitude of g_{CC} of each of the 12 study sites. Chapter 4 provides details of each site. Refer to Chapter 5, Section 5.2.3 for details on how the cameras were installed, and Section 5.2.6 for details on how different camera angles were analysed.

Figure E.1 to Figure E.14 present phenology profiles of each site, where different coloured data points and trend lines represent different camera angles. Figure E.2 (site GIDL) and Figure E.9 (site GUNN) show a comparison of nadir camera g_{CC} against the mean g_{CC} for each site's oblique camera. All other figures compare the g_{CC} at different regions of the camera's field-of-view (foreground, midground and background), representing relative camera angle. The trend lines are LOESS fitted curves (span = 0.1, except where indicated) for visual comparison of the grouped temporal trends.

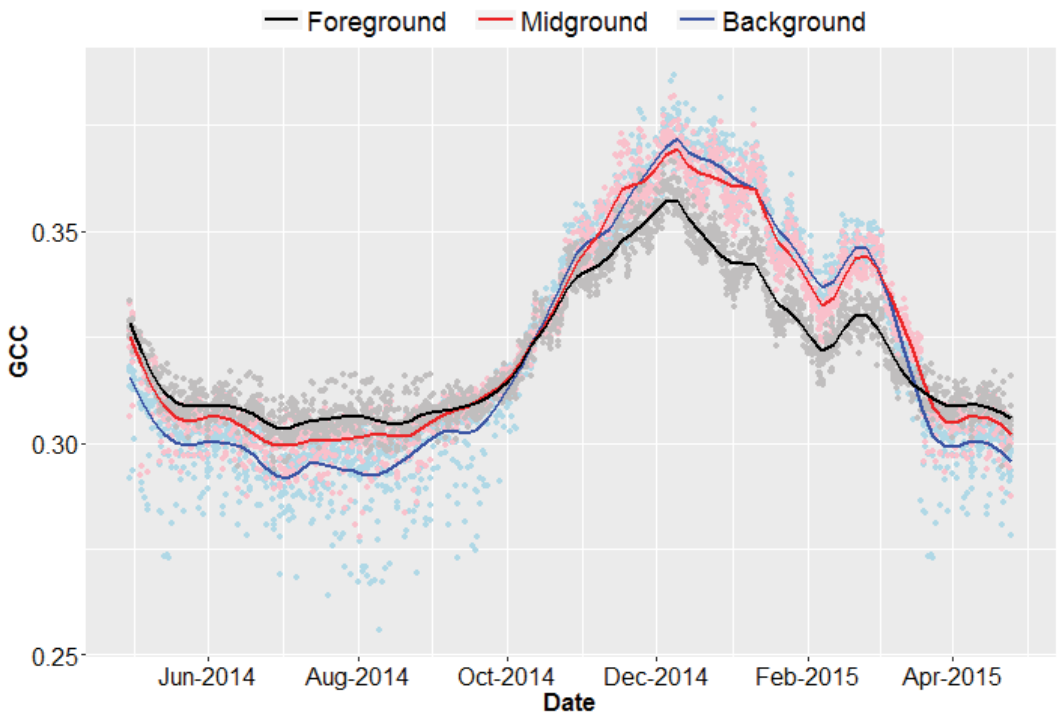

Figure E.1 Comparison phenology profile of foreground, midground and background g_{CC} from site GIDL (C4 Native).

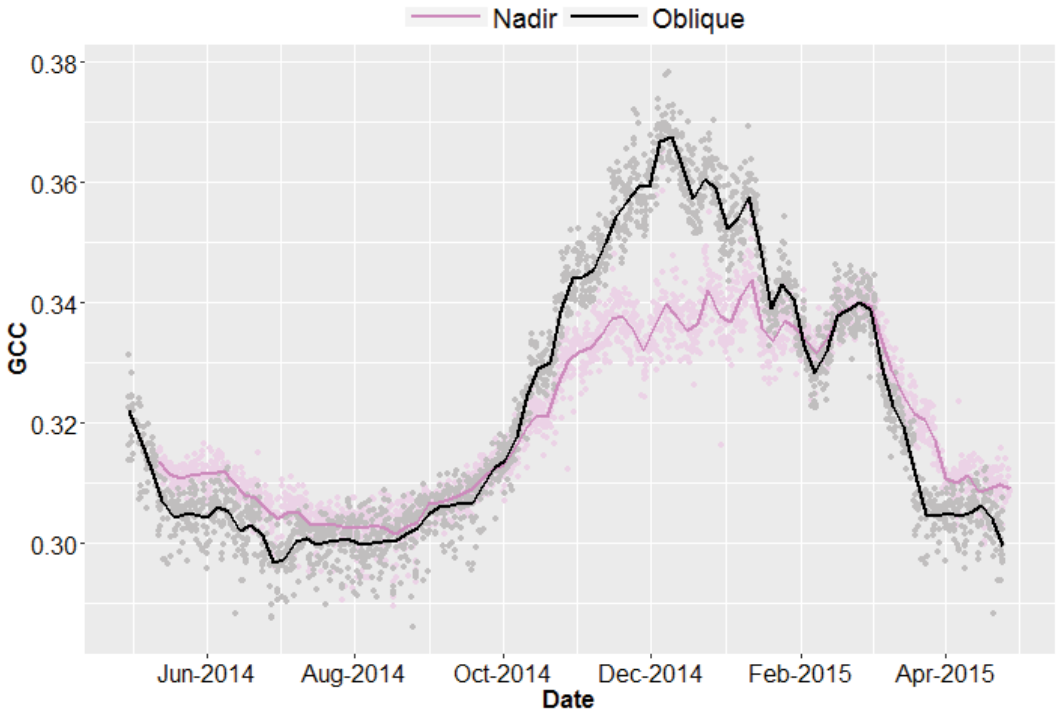

Figure E.2 Comparison phenology profile of oblique mean g_{CC} and nadir mean g_{CC} from site GIDL (C4 Native), with a LOESS span of 0.05.

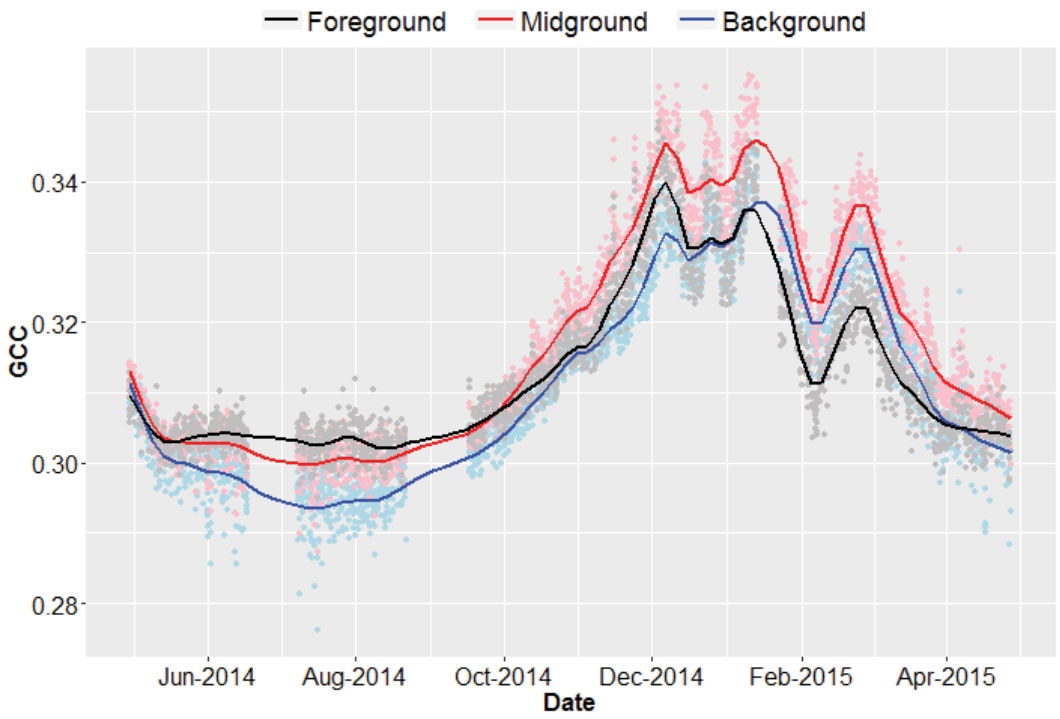

Figure E.3 Comparison phenology profile of foreground, midground and background g_{CC} from site TURA (C4 Native).

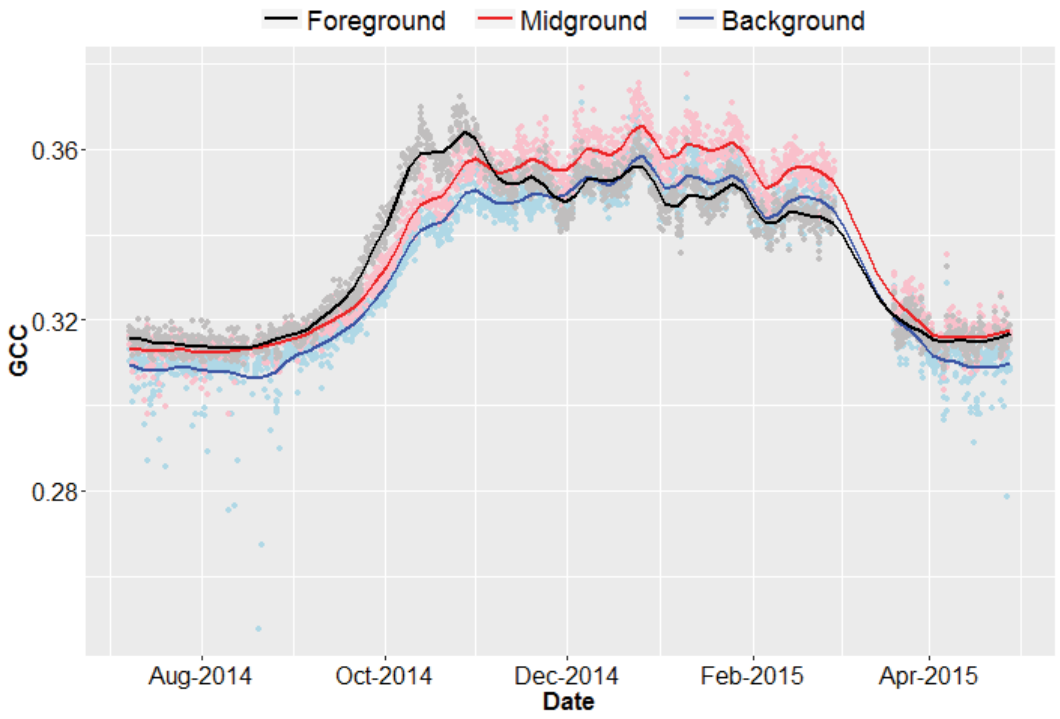

Figure E.4 Comparison phenology profile of foreground, midground and background g_{CC} from site MPON (C4 Native).

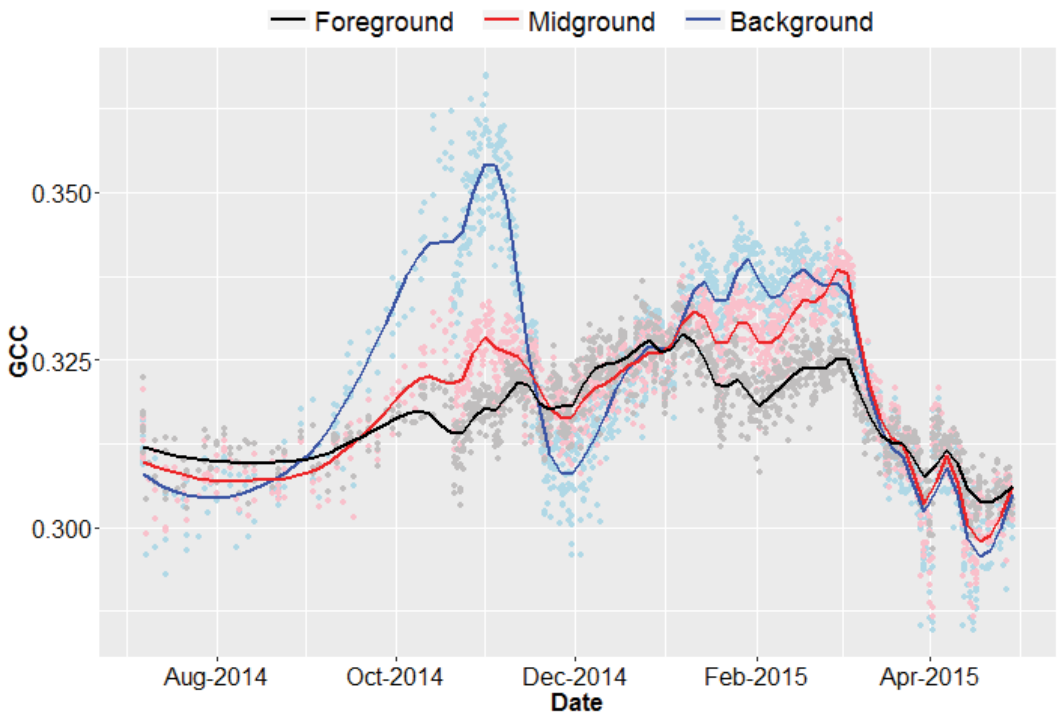

Figure E.5 Comparison phenology profile of foreground, midground and background g_{CC} from site IN17 (C4 Exotic).

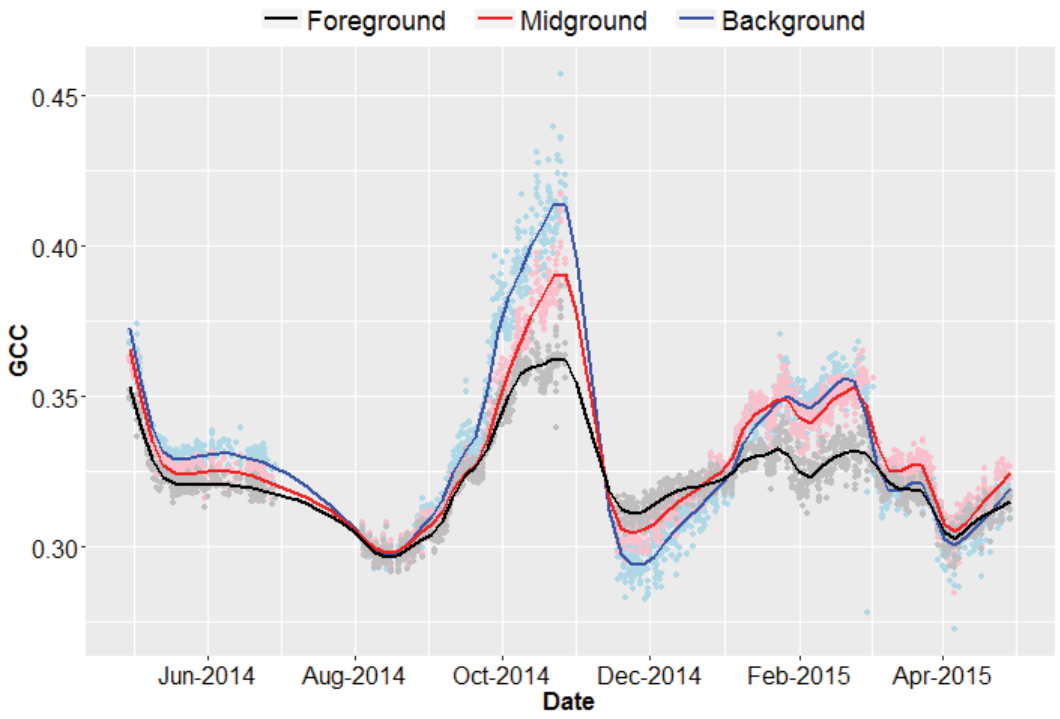

Figure E.6 Comparison phenology profile of foreground, midground and background g_{CC} from site INGE (C4 Exotic).

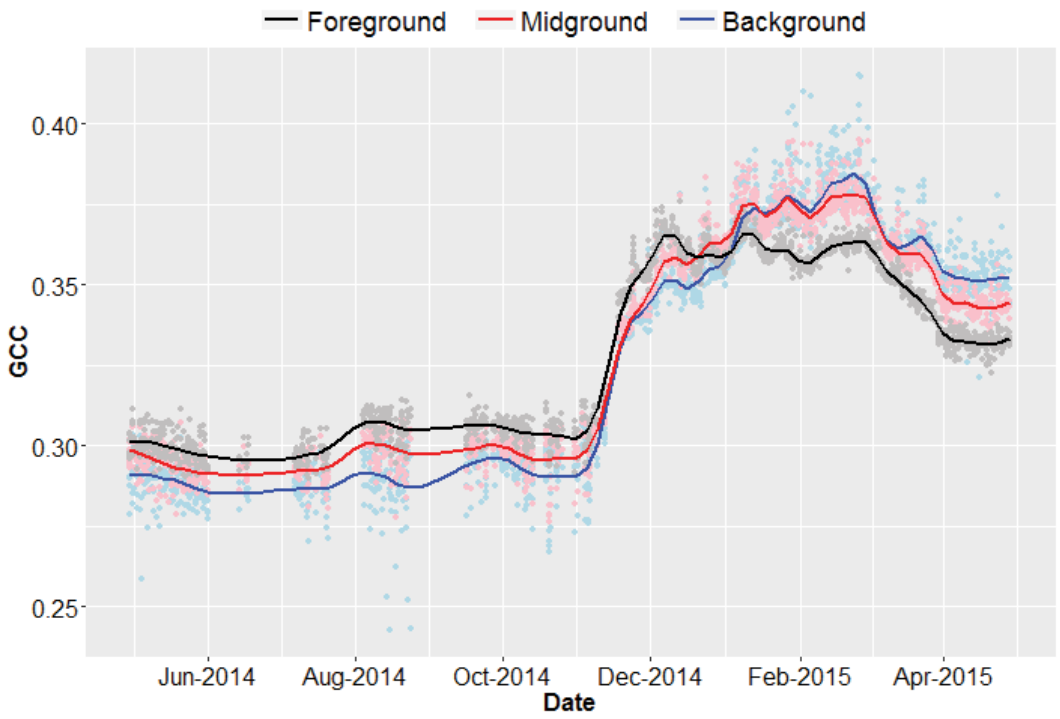

Figure E.7 Comparison phenology profile of foreground, midground and background g_{CC} from site SCOT (C4 Exotic).

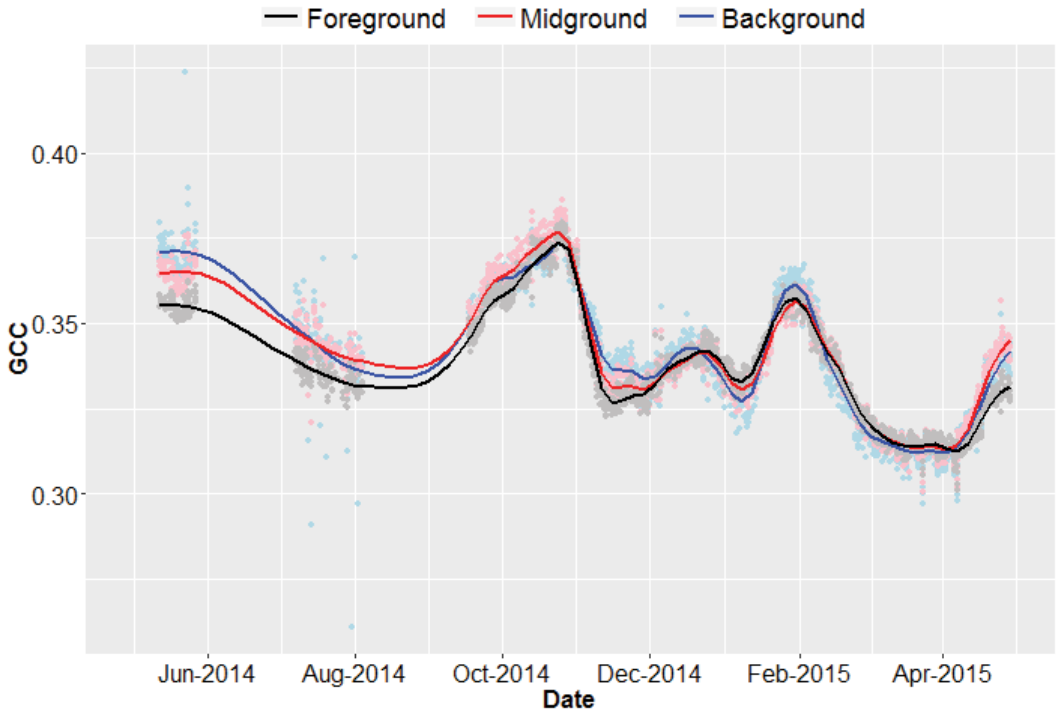

Figure E.8 Comparison phenology profile of foreground, midground and background g_{CC} from site GUNN (C3 Native).

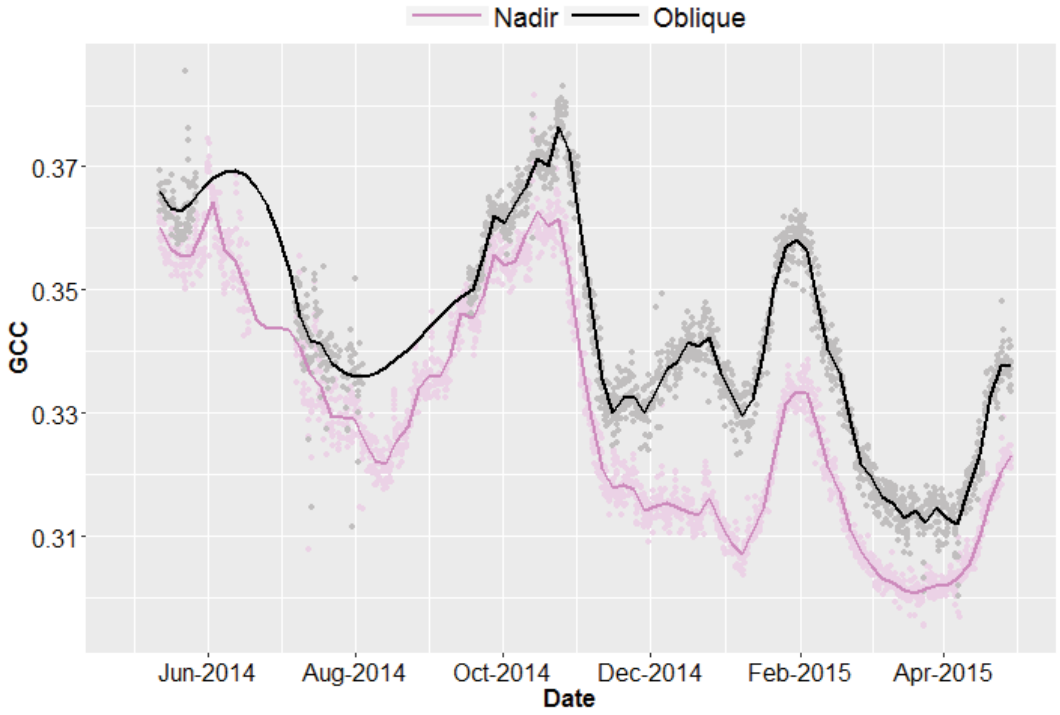

Figure E.9 Comparison phenology profile of oblique mean g_{CC} and nadir mean g_{CC} from site GUNN (C3 Native), with a LOESS span of 0.05.

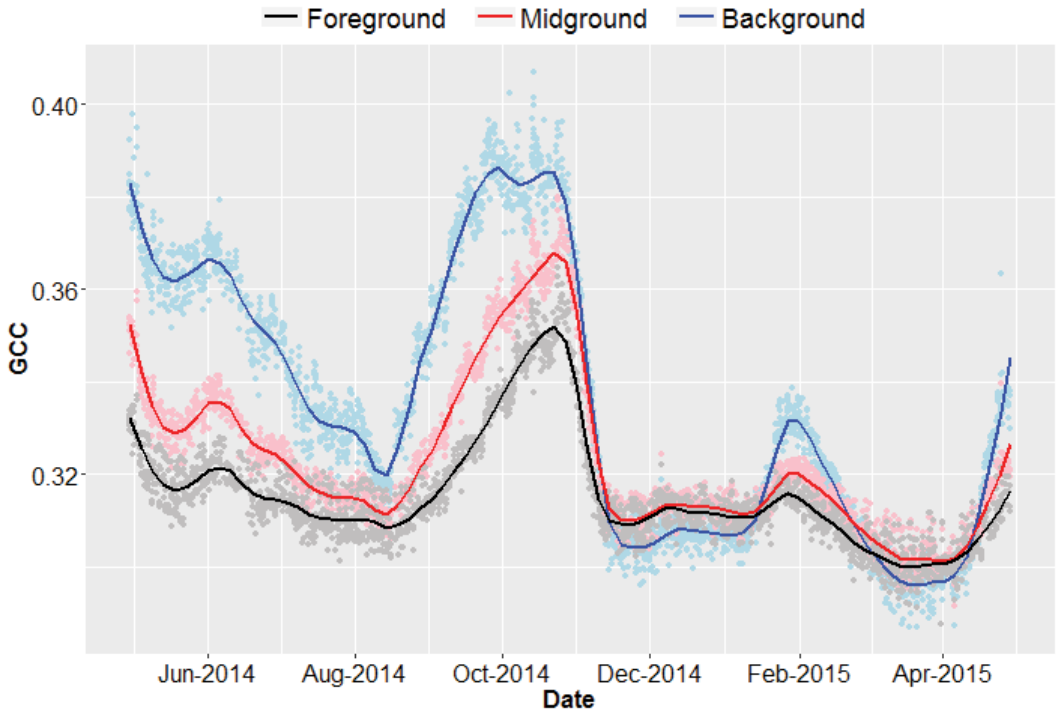

Figure E.10 Comparison phenology profile of foreground, midground and background g_{CC} from site MGAR (C3 Native).

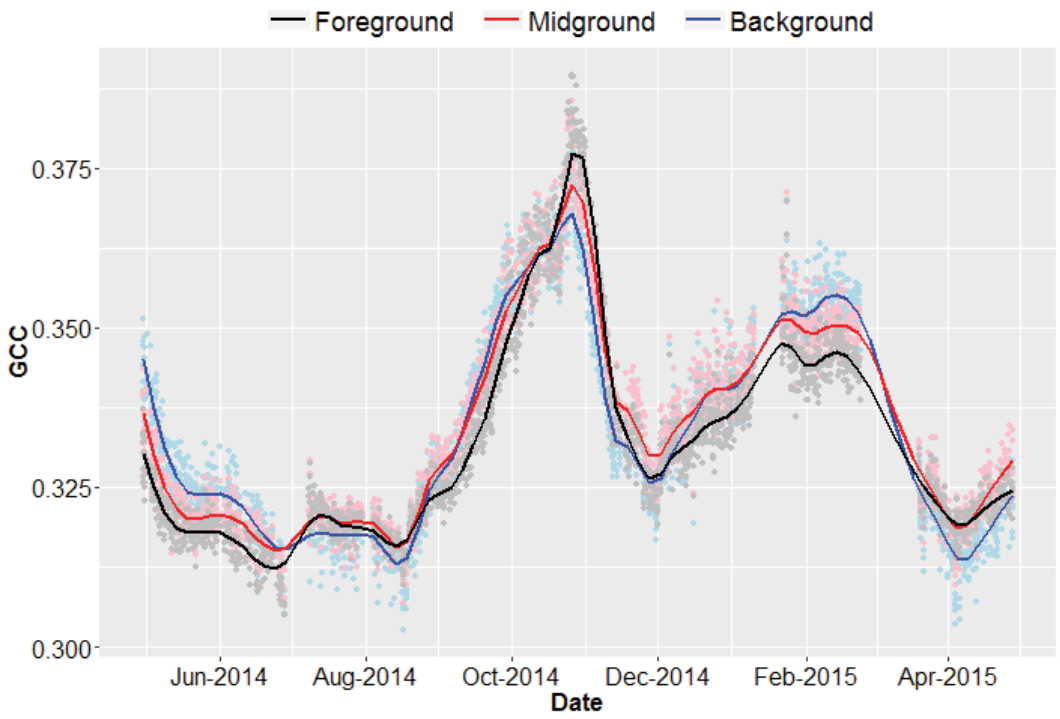

Figure E.11 Comparison phenology profile of foreground, midground and background g_{CC} from site MULN (C3 Native).

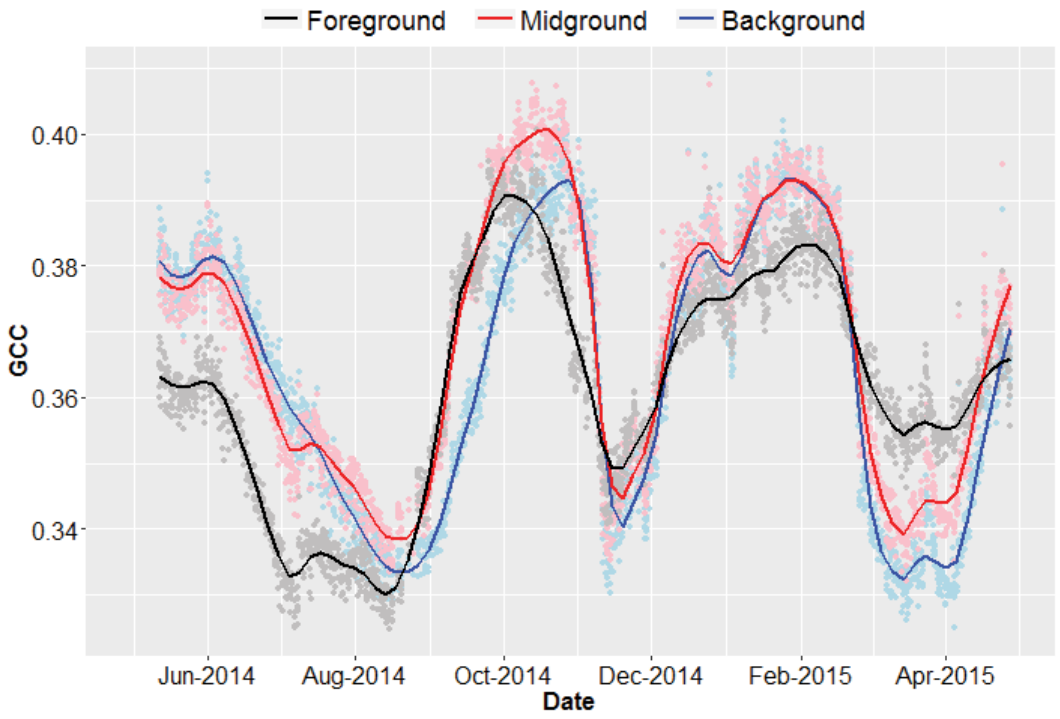

Figure E.12 Comparison phenology profile of foreground, midground and background g_{CC} from site MULE (C3 Exotic).

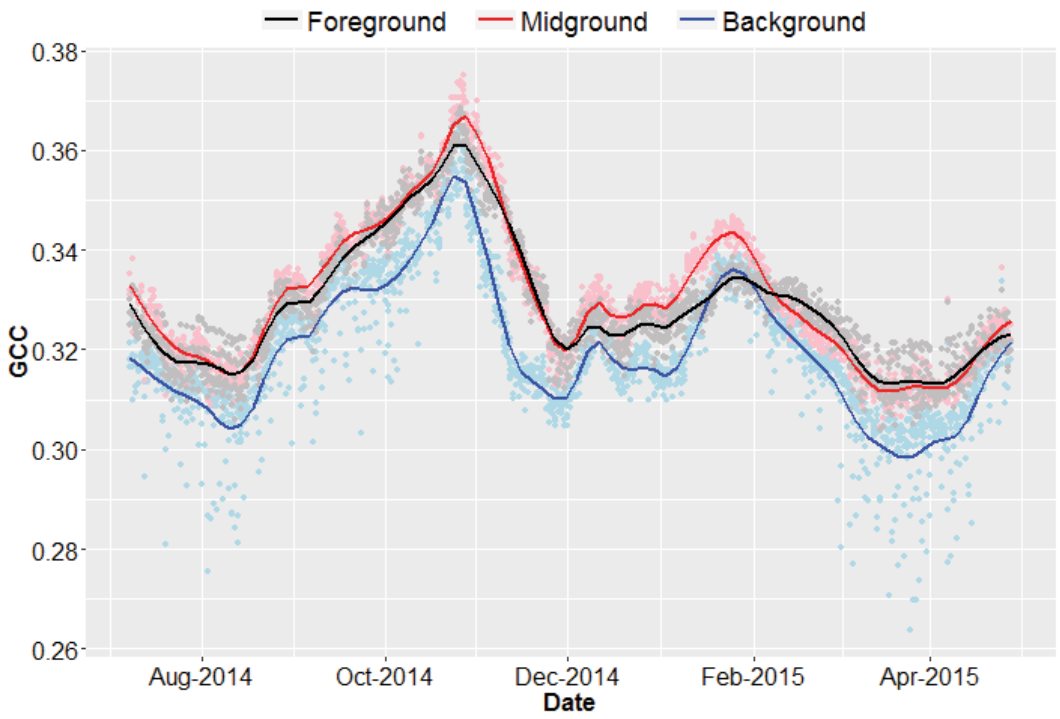

Figure E.13 Comparison phenology profile of foreground, midground and background g_{CC} from site MPOE (C3 Exotic).

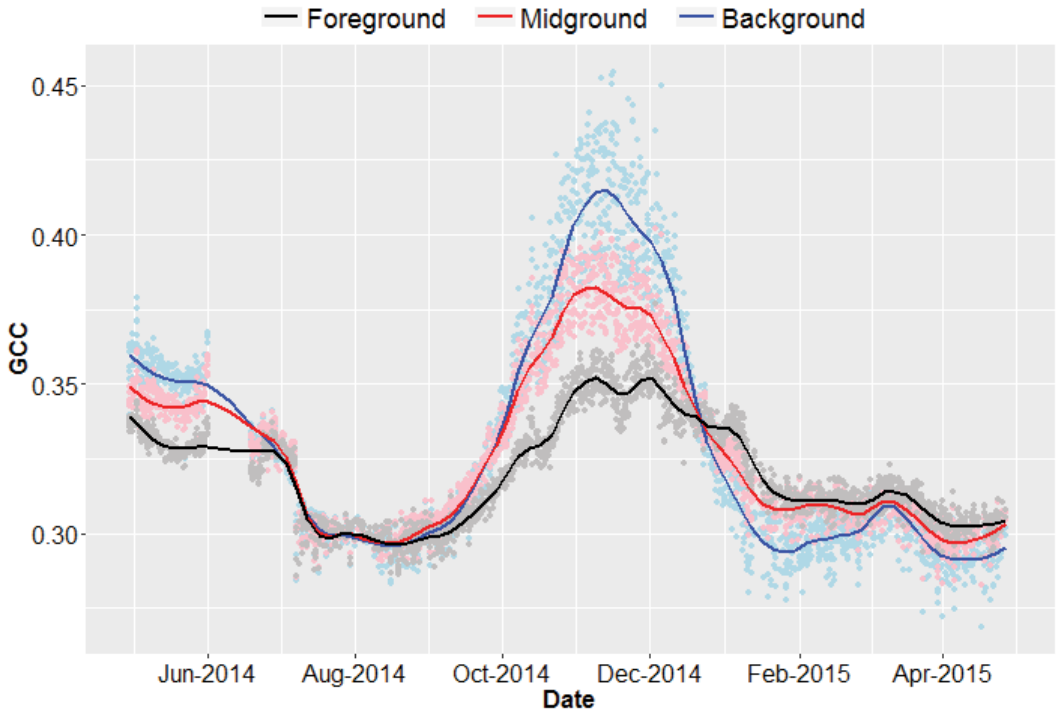

Figure E.14 Comparison phenology profile of foreground, midground and background g_{CC} from site GUNE (C4 Native).

The comparison phenology profiles demonstrate that the further the distance from the camera (or, the closer the relative angle to horizontal), the more exaggerated the g_{CC} response (i.e. greener during growth periods, browner during senescence periods). The background data points also showed higher variability than foreground data points, with more instances of high and low g_{CC} outliers. This may suggest that the background of the image is more subject to atmospheric effects such as fog or haze. This trend does not apply at all sites, and depends on the aspect of the field site and the orientation of the phenocam. For example, the site MULN slopes away from the phenocam, resulting in a smaller difference in relative angle between the three regions and corresponding smaller difference in g_{CC}. The largest apparent difference between the three image regions is consistently on the flattest landscapes (e.g. GIDL, GUNE, TURA). Regardless, the data shows that the magnitude of g_{CC} changes with camera angle.

The trends and timing of g_{CC} dynamics align regardless of camera angle. For the majority of sites, the commencement of greening, peak times of GCC and overall phenology profile shape match extremely closely. At sites where one region shows an anomalous phenology profile to the others (e.g. MULE, IN17), this indicates regions of the image where land surface phenology is different. In this case, it represented different species composition, but could also be used to identify different microclimates, soil types or regions of disturbance.

For the two comparisons between nadir and oblique imagery, nadir g_{CC} generally follows the same trends of the oblique, despite representing very different scales. The nadir camera captured 2 m^2, whereas the oblique camera captures 20,000–40,000 m^2. In one example (GUNN), the magnitude of g_{CC} was less for the nadir image than the oblique for the entire period. However, in the other (GIDL), a similar trend was observed to the foreground/midground/background phenology profiles: nadir showed a higher g_{CC} during green periods and a lower g_{CC} during less green periods.

Fundamentally, this shows that relative camera angle has an effect on the magnitude of g_{CC}, therefore inter-site comparisons of g_{CC} magnitude should not be made unless camera angles are standardised.

Appendix F COMPARISONS OF FIELD, NEAR-SURFACE AND SATELLITE PHENOLOGY

The figures in this appendix represent a graphical comparison of the methods used to represent vegetative phenology at different spatial and temporal scales. This is intended to assist the reader in viewing similarities and differences between the methods. As each method provides subtly different information about vegetation dynamics, these complement each other to explain the actual and apparent vegetative phenology at each location.

The methods used to derive each time-series dataset are presented in Chapter 5, Section 5.2. Each dataset represents changes in the quantity and quality of green vegetation from twelve grassland locations. Details of the field sites are included in Chapter 4. To account for the variation between functional groups, the y-axis varies between figures.

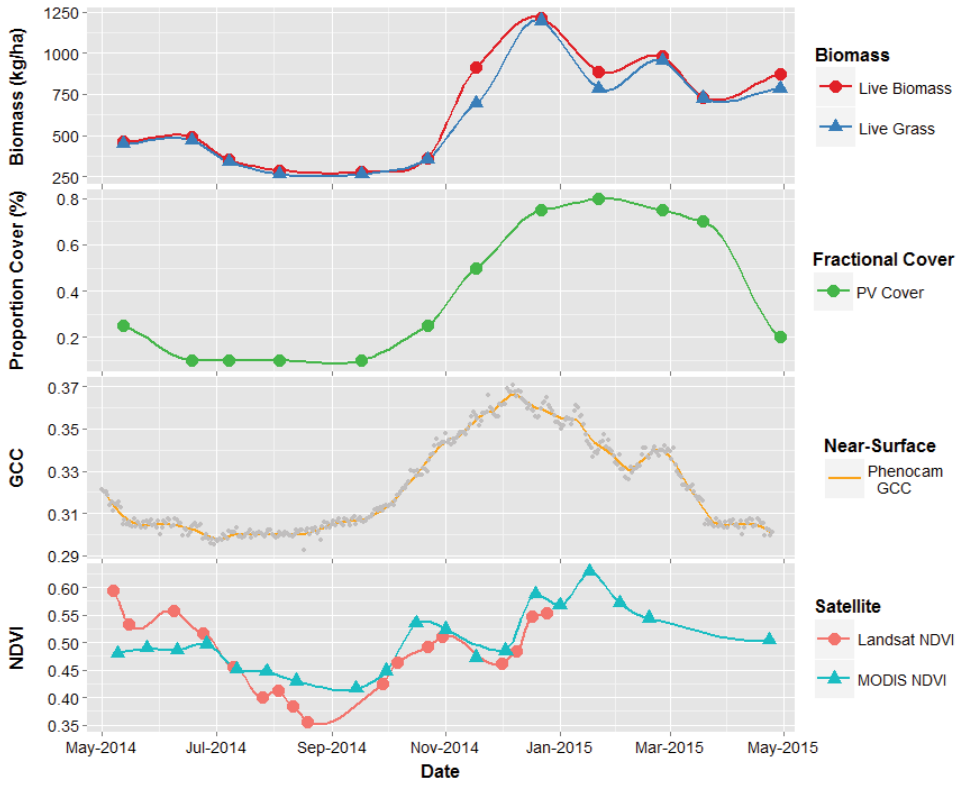

Figure F.1 Multi-scale phenology from 1 May 2014 to 30 April 2015 at GIDL (C4 Native). From top to bottom panel: total live biomass (●) and live grass biomass (▲) in kg/ha; green (PV) fractional cover (%); phenocam 13:00 daily $g_{CC;}$ Terra MODIS (▲) and Landsat OLI/ETM+ (●) NDVI.

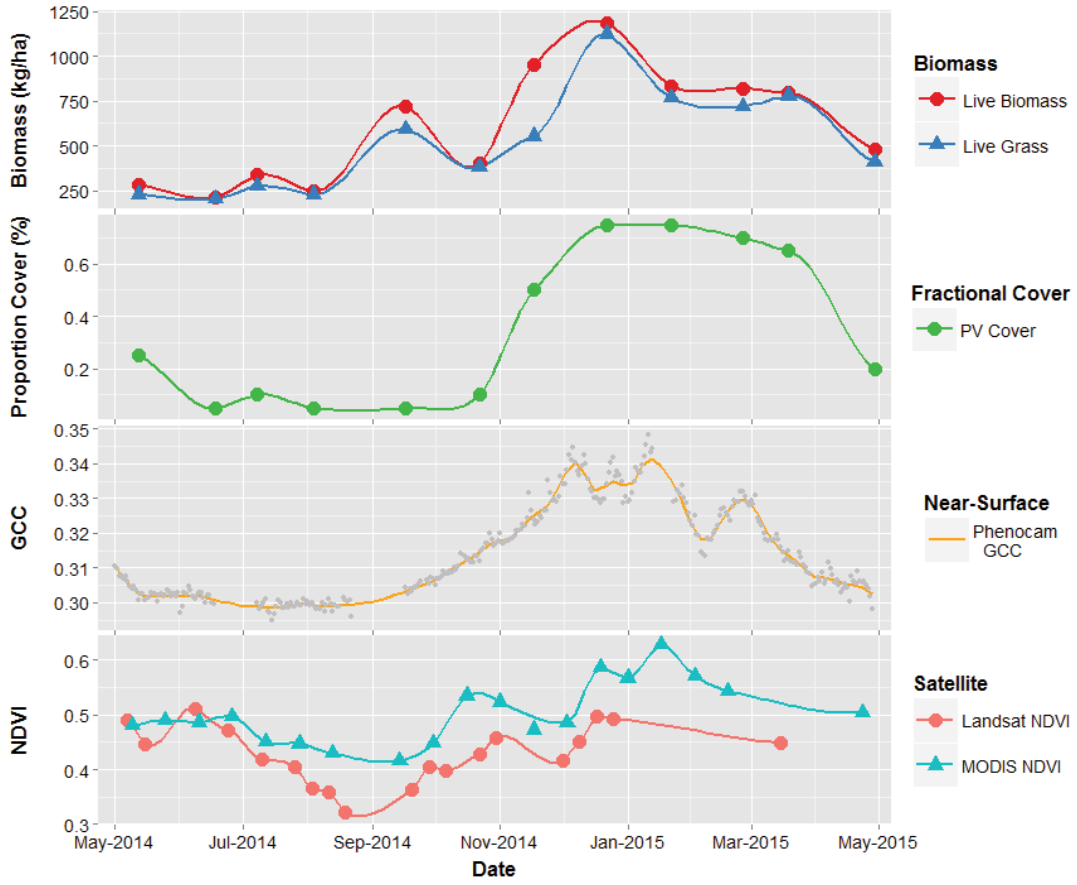

Figure F.2 Multi-scale phenology from 1 May 2014 to 30 April 2015 at TURA (C4 Native). From top to bottom panel: total live biomass (●) and live grass biomass (▲) in kg/ha; green (PV) fractional cover (%); phenocam 13:00 daily $g_{CC;}$ Terra MODIS (▲) and Landsat OLI/ETM+ (●) NDVI.

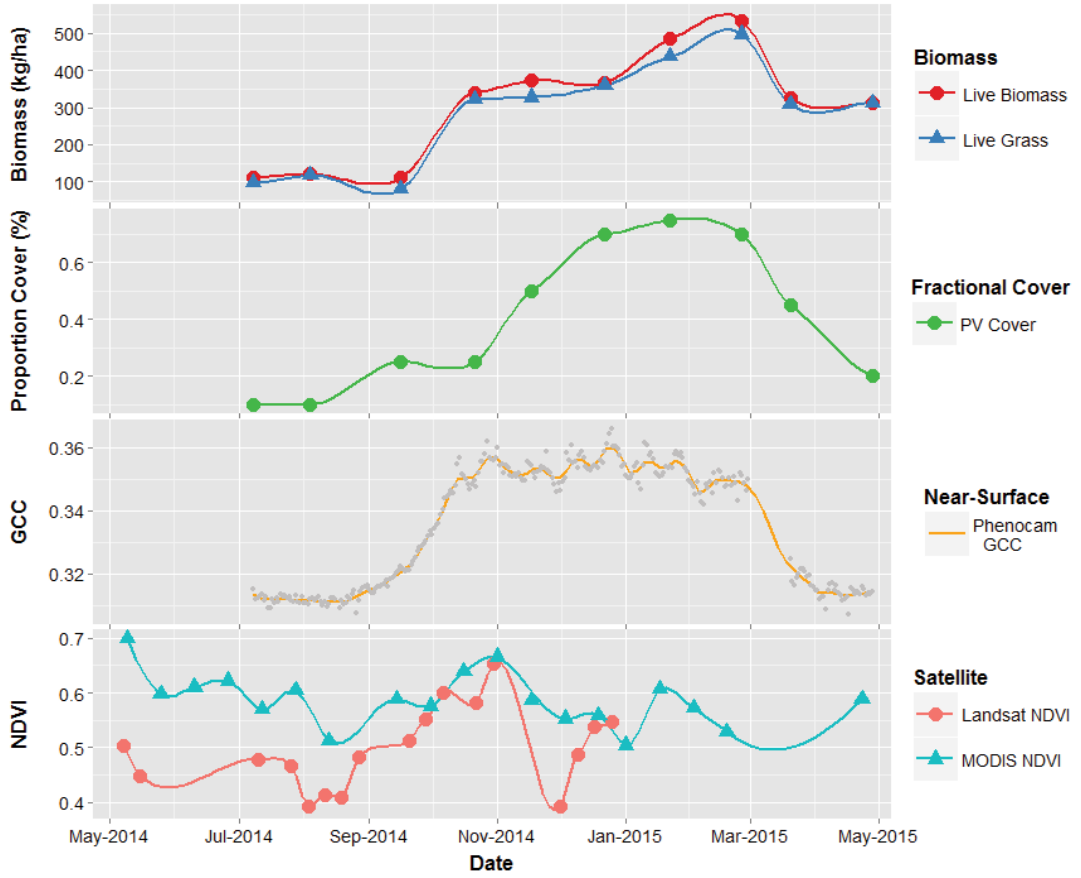

Figure F.3 Multi-scale phenology from 1 May 2014 to 30 April 2015 at MPON (C4 Native). From top to bottom panel: total live biomass (●) and live grass biomass (▲) in kg/ha; green (PV) fractional cover (%); phenocam 13:00 daily $g_{CC;}$ Terra MODIS (▲) and Landsat OLI/ETM+ (●) NDVI.

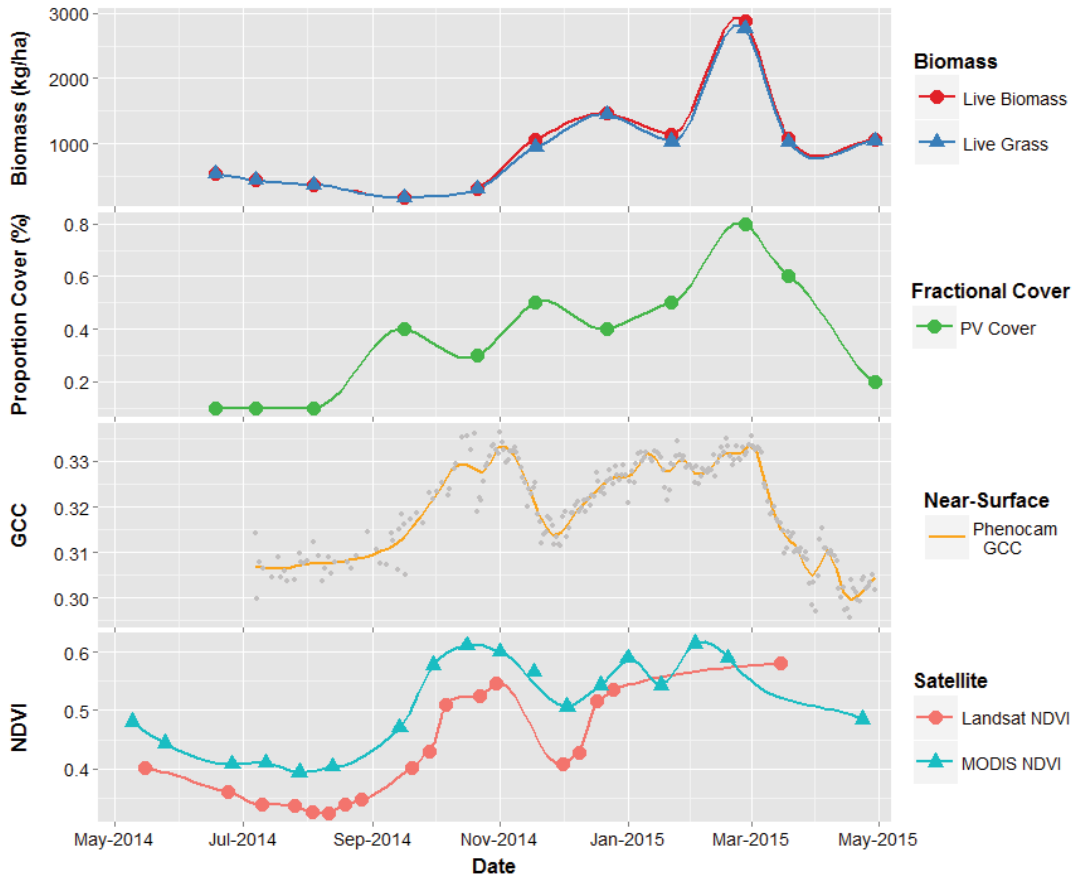

Figure F.4 Multi-scale phenology from 1 May 2014 to 30 April 2015 at IN17 (C4 Exotic). From top to bottom panel: total live biomass (●) and live grass biomass (▲) in kg/ha; green (PV) fractional cover (%); phenocam 13:00 daily $g_{CC;}$ Terra MODIS (▲) and Landsat OLI/ETM+ (●) NDVI.

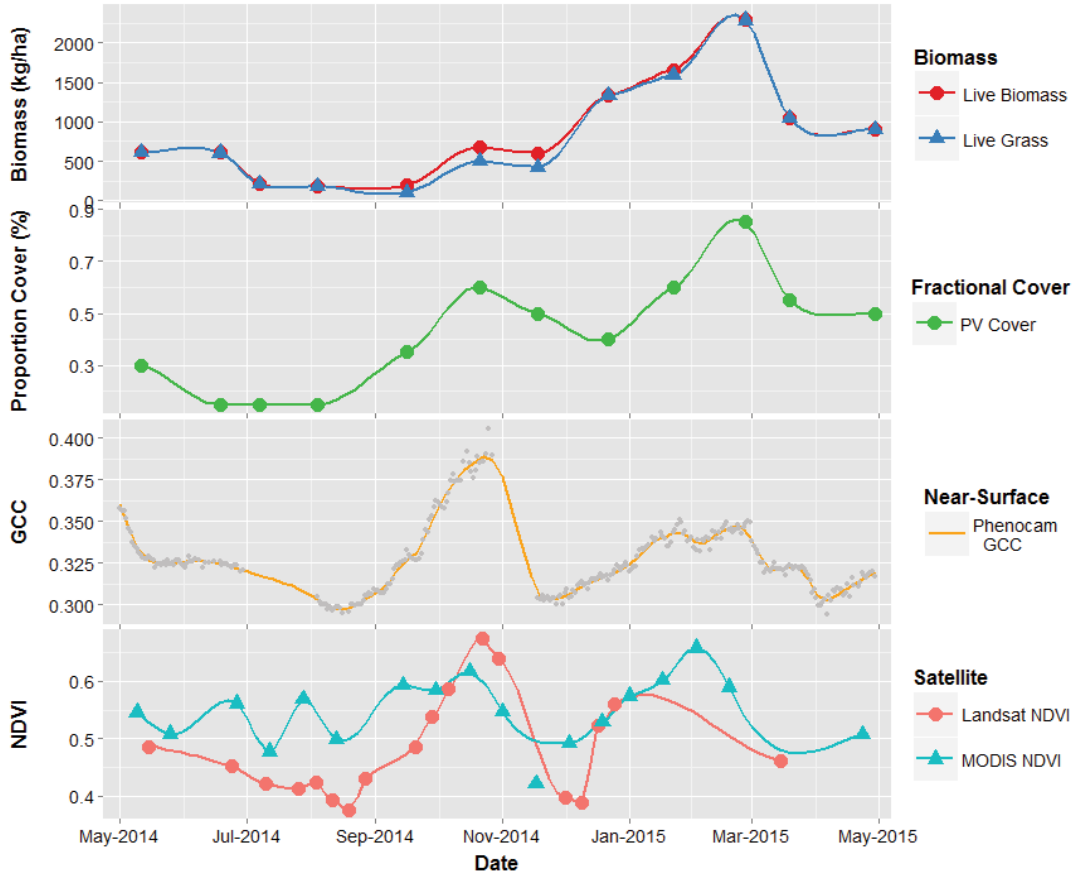

Figure F.5 Multi-scale phenology from 1 May 2014 to 30 April 2015 at INGE (C4 Exotic). From top to bottom panel: total live biomass (●) and live grass biomass (▲) in kg/ha; green (PV) fractional cover (%); phenocam 13:00 daily $g_{CC;}$ Terra MODIS (▲) and Landsat OLI/ETM+ (●) NDVI.

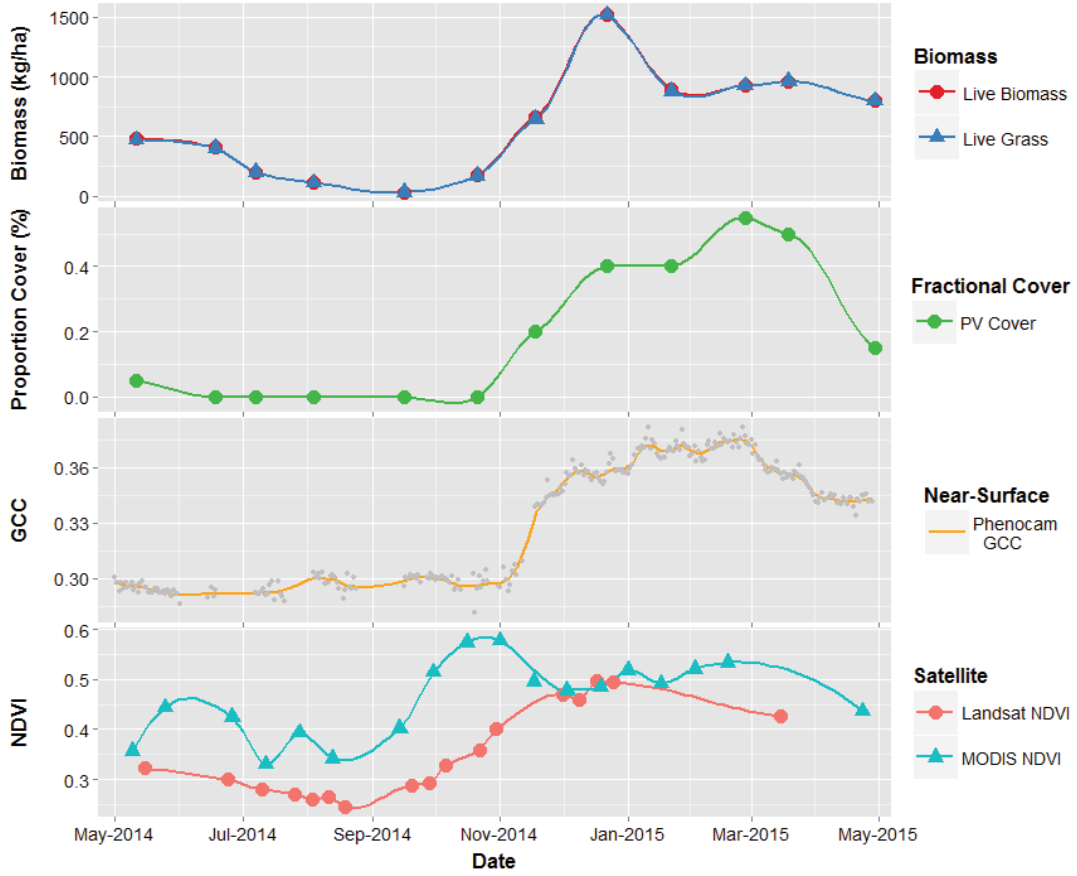

Figure F.6 Multi-scale phenology from 1 May 2014 to 30 April 2015 at SCOT (C4 Exotic). From top to bottom panel: total live biomass (●) and live grass biomass (▲) in kg/ha; green (PV) fractional cover (%); phenocam 13:00 daily $g_{CC;}$ Terra MODIS (▲) and Landsat OLI/ETM+ (●) NDVI.

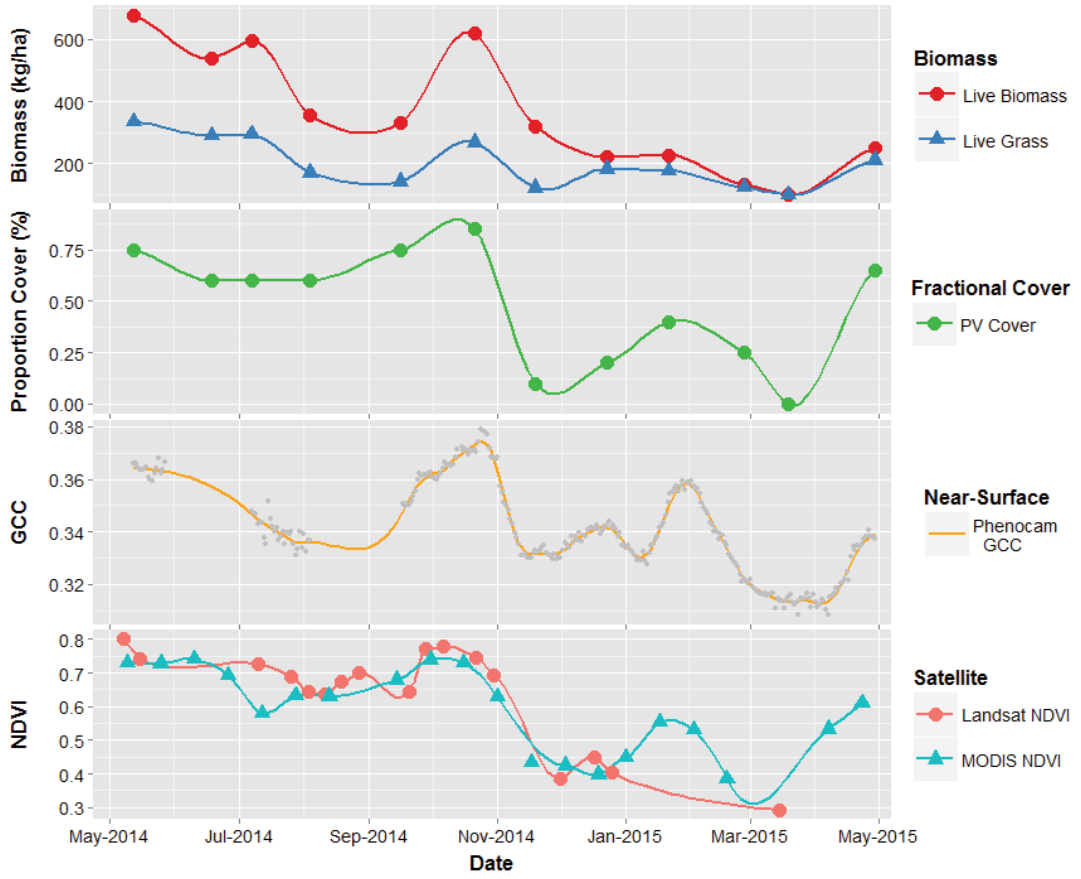

Figure F.7 Multi-scale phenology from 1 May 2014 to 30 April 2015 at GUNN (C3 Native). From top to bottom panel: total live biomass (●) and live grass biomass (▲) in kg/ha; green (PV) fractional cover (%); phenocam 13:00 daily $g_{CC;}$ Terra MODIS (▲) and Landsat OLI/ETM+ (●) NDVI.

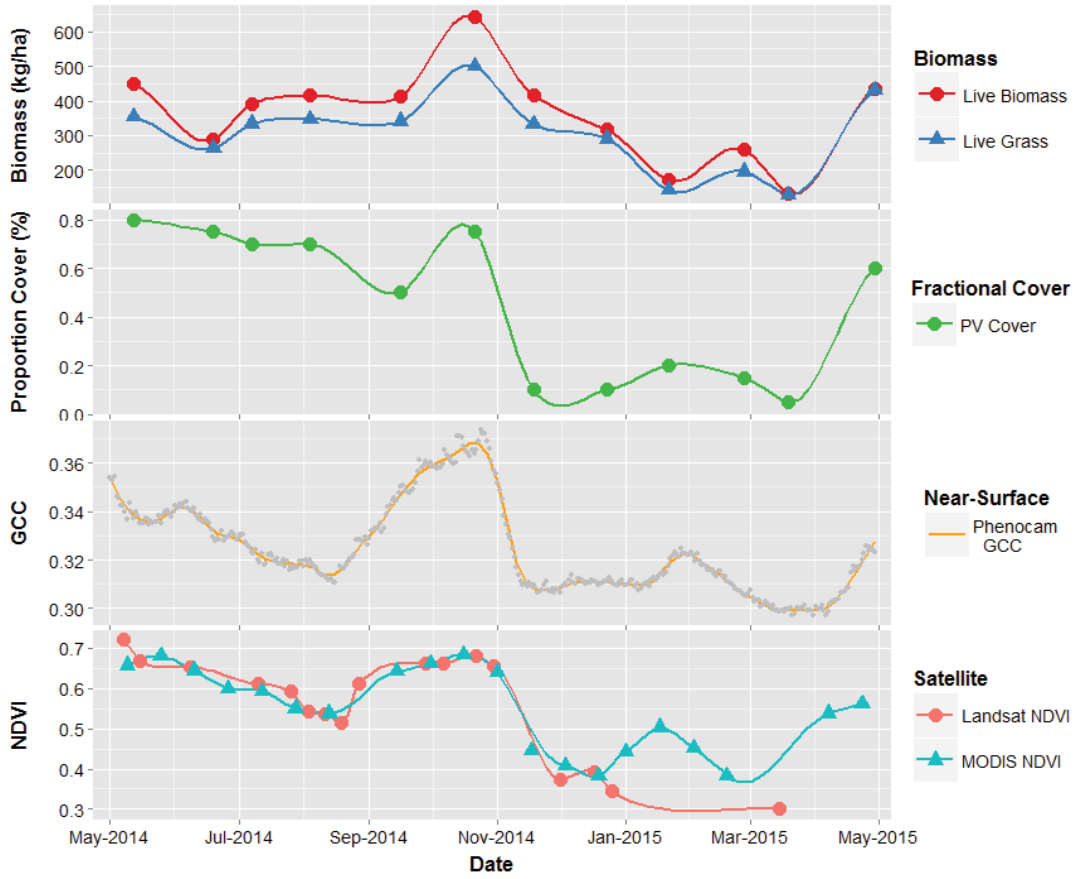

Figure F.8 Multi-scale phenology from 1 May 2014 to 30 April 2015 at MGAR (C3 Native). From top to bottom panel: total live biomass (●) and live grass biomass (▲) in kg/ha; green (PV) fractional cover (%); phenocam 13:00 daily $g_{CC;}$ Terra MODIS (▲) and Landsat OLI/ETM+ (●) NDVI.

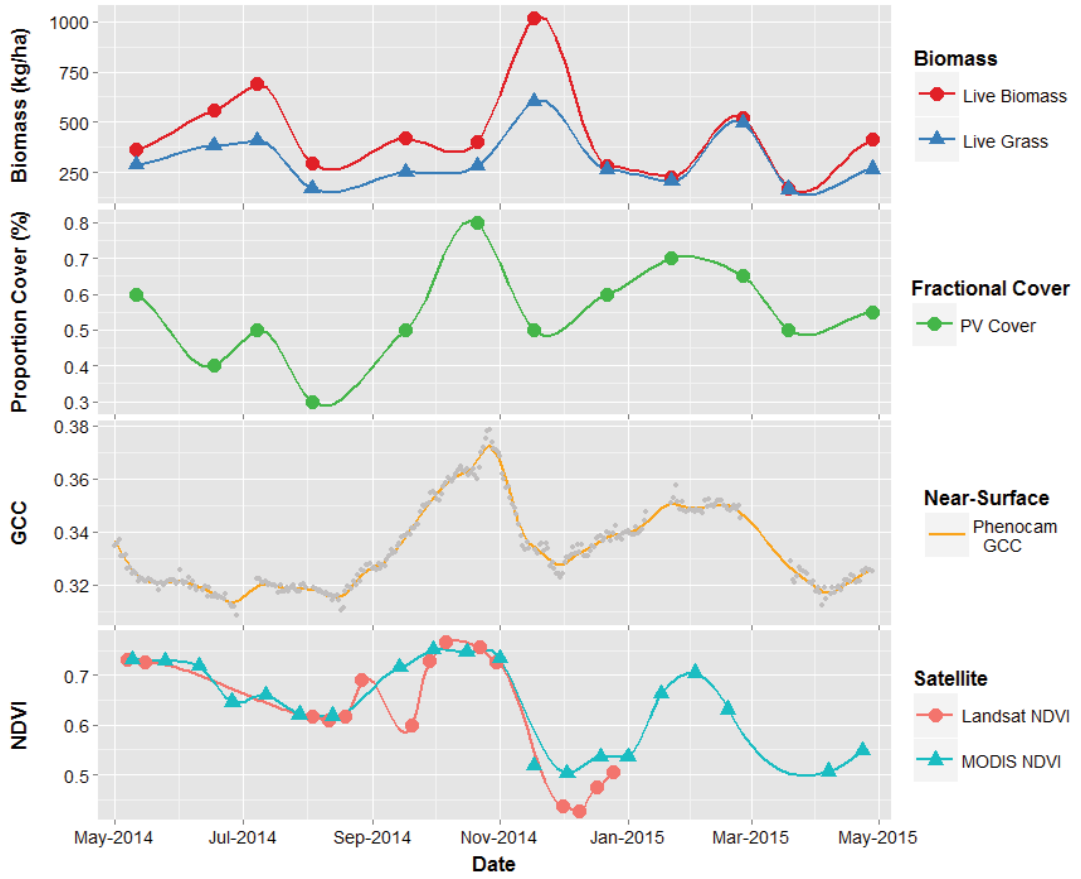

Figure F.9 Multi-scale phenology from 1 May 2014 to 30 April 2015 at MULN (C3 Native). From top to bottom panel: total live biomass (●) and live grass biomass (▲) in kg/ha; green (PV) fractional cover (%); phenocam 13:00 daily $g_{CC;}$ Terra MODIS (▲) and Landsat OLI/ETM+ (●) NDVI.

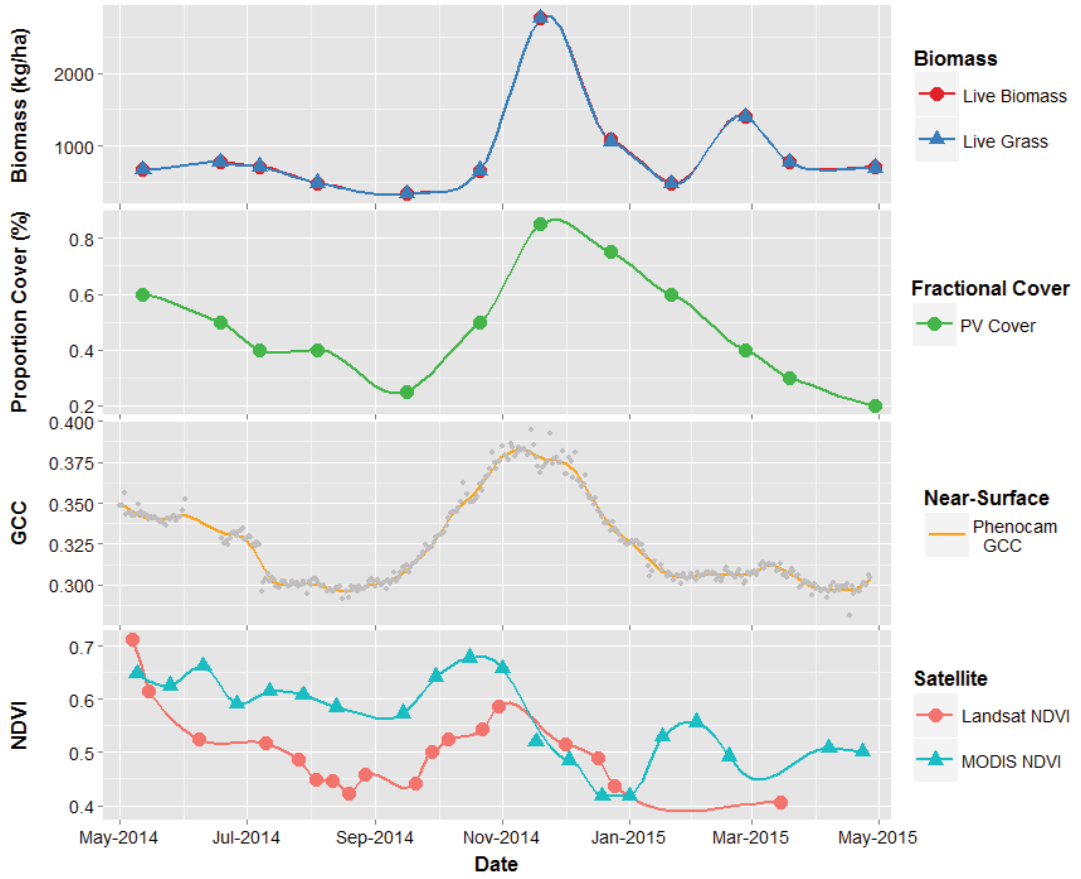

Figure F.10 Multi-scale phenology from 1 May 2014 to 30 April 2015 at GUNE (C3 Exotic). From top to bottom panel: total live biomass (●) and live grass biomass (▲) in kg/ha; green (PV) fractional cover (%); phenocam 13:00 daily $g_{CC;}$ Terra MODIS (▲) and Landsat OLI/ETM+ (●) NDVI.

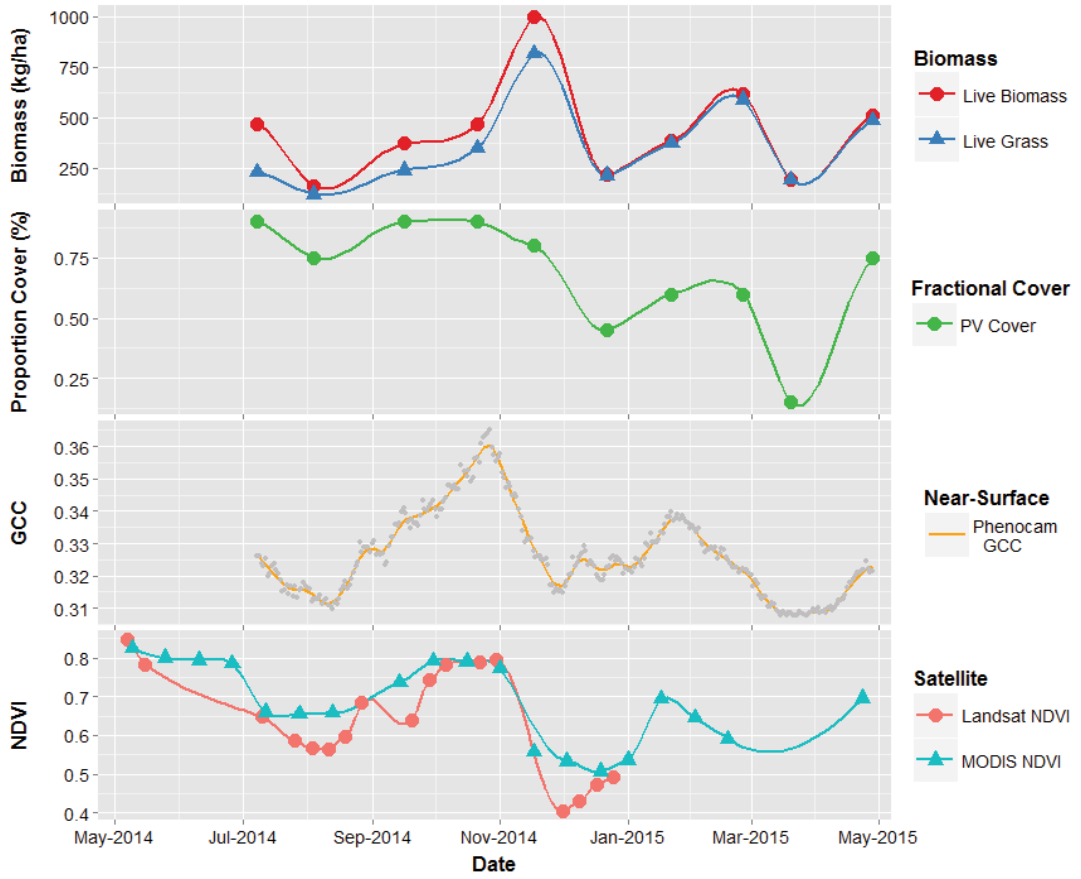

Figure F.11 Multi-scale phenology from 1 May 2014 to 30 April 2015 at MPOE (C3 Exotic). From top to bottom panel: total live biomass (●) and live grass biomass (▲) in kg/ha; green (PV) fractional cover (%); phenocam 13:00 daily $g_{CC;}$ Terra MODIS (▲) and Landsat OLI/ETM+ (●) NDVI.

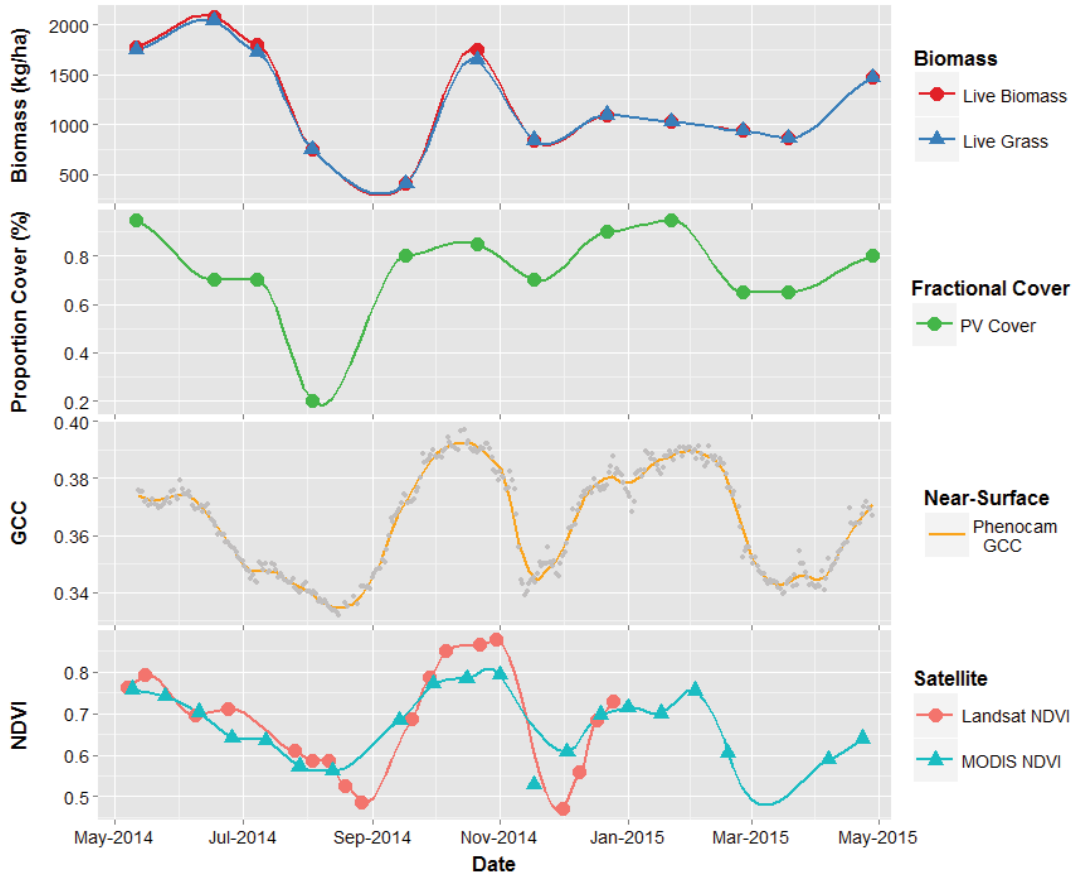

Figure F.12 Multi-scale phenology from 1 May 2014 to 30 April 2015 at MULE (C3 Exotic). From top to bottom panel: total live biomass (●) and live grass biomass (▲) in kg/ha; green (PV) fractional cover (%); phenocam 13:00 daily $g_{CC;}$ Terra MODIS (▲) and Landsat OLI/ETM+ (●) NDVI.